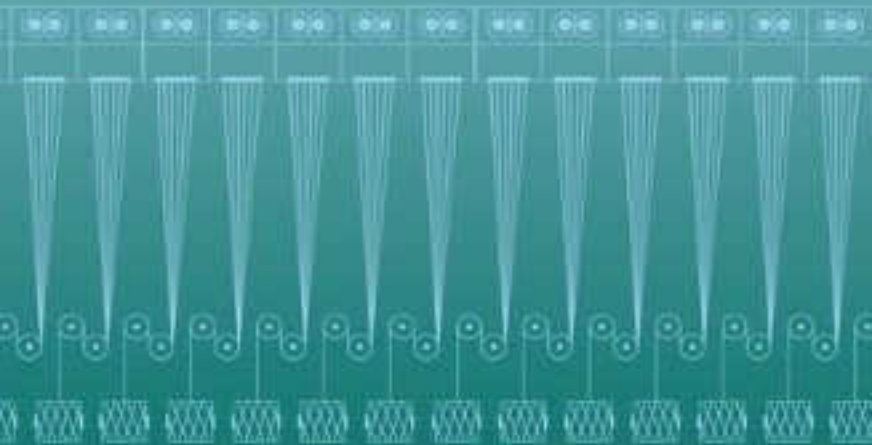# MANUFACTURED FIBRE TECHNOLOGY

EDITED BY

V.B. Gupta and V.K. Kothari

CHAPMAN & HALL

Manufactured Fibre Technology

Manufactured Fibre Technology

Edited by

V.B. Gupta and V.K. Kothari
Indian Institute of Technology, Delhi, India

SPRINGER-SCIENCE+BUSINESS MEDIA, B.V.

A catalogue record for this book is available from the British Library

Contents

Contributors

P. Bajaj
Professor,
Department of Textile Technology,
Indian Institute of Technology,
Hauz Khas, New Delhi – 110016,
India

Y.C. Bhuvanesh
Research Associate/Assistant
Professor,
School of Textiles, Fiber and
Polymer Science,
161 Sirrine Hall,
Clemson University,
Clemson, SC 29634-1307, USA

S.S. Cameotra
Vice President (Plant Operations),
Swadeshi Polytex Limited,
New Kavi Nagar,
Ghaziabad – 201002, India

B.L. Deopura
Professor,
Department of Textile Technology,
Indian Institute of Technology,
Hauz Khas, New Delhi – 110016,
India

B.C. Goswami
Professor,
School of Textiles,
Fiber and Polymer Science,
161 Sirrine Hall,
Clemson University,
Clemson, SC 29634-1307, USA

A.K. Gupta
Professor,
Centre for Polymer Science and
Engineering,
Indian Institute of Technology,
Hauz Khas, New Delhi – 110016,
India

V.B. Gupta
Professor,
Department of Textile Technology,
Indian Institute of Technology,
Hauz Khas, New Delhi – 110016,
India

V.K. Kothari
Professor,
Department of Textile Technology,
Indian Institute of Technology,
Hauz Khas, New Delhi – 110016,
India

Kushal Sen
Professor,
Department of Textile Technology,
Indian Institute of Technology,
Hauz Khas, New Delhi – 110016,
India

T. Manabe
Consultant,
Modipon Limited,
Modinagar – 201204, India

A.K. Mukherjee
Professor,
Department of Textile Technology,
Indian Institute of Technology,
Hauz Khas, New Delhi – 110016,
India

V.M. Nadkarni
Techcellence Consultancy Services
Pvt. Ltd,
10 Narendra Society,
Senapati Bapat Road,
Pune – 411016, India

Satish Kumar
Associate Professor,
School of Textile and Fiber
Engineering,
Georgia Institute of Technology,
Atlanta, GA 30332-0295, USA

A.K. Sengupta
Advisor,
Ahmedabad Textile Industry's
Research Association,
Ahmedabad – 380015, India

N.D. Sharma
Senior General Manager (R & D),
J.K. Synthetics Ltd (PSG Group),
Jakaynagar,
Kota – 324003, India

Preface

The need for a book on manufactured fibre technology has been felt by us for several years while teaching undergraduate and postgraduate students taking courses on or related to the subject. While there are excellent books dealing with the chemistry of fibre production or with the fundamentals of the spinning processes or with newer fibres, there is a dearth of books dealing with the subject in an integrated manner at an appropriate level and suitable for a course lasting one or two semesters. The present book has been designed to fulfil this need. It covers in considerable detail the two principal stages in the manufacture of fibre, namely the production of the fibre-forming polymers and their conversion to fibre. Adequate emphasis is laid on fundamental principles and newer developments without recourse to advanced mathematics.

That such a book will have a much wider base became clear to us while conducting a two-week continuing education programme organized in our department for teachers from textile colleges and technologists from industry. The faculty for this programme was drawn from academic institutions, industry and research laboratories. From our experience of running several such programmes, we feel that this book will also be useful to such teachers and to technologists in industry. In addition, it will provide the basic material to those interested in organizing and running intensive training courses on this topic.

The book has been designed with the following features:

- the treatment is at an undergraduate level for a course on fibre production; however, the needs of students taking a Master's level course have also been kept in mind;
- the treatment is intensive rather than extensive;
- the emphasis is on fundamental principles, wherever basic concepts are involved;

- the industrial practices obtaining on a global scale have been included, as far as possible;
- the information is up-to-date and state-of-the-art.

Emphasis on in-depth treatment of the subject required careful selection of the topics to be covered. In the present book, the various aspects of fibre production centre around 20 chapters as outlined below.

- *Processes*: the fibre production processes of melt-, wet- and dry-spinning, drawing and heat-setting are covered in detail in five chapters with adequate emphasis being placed on fundamentals.
- *Fibre types*: all important commodity fibres, namely polyester, polyamide, acrylic, polypropylene and viscose rayon, are treated in detail in five chapters. The vinyl fibres, namely polyvinyl alcohol, polyvinyl acetate and polyvinyl chloride, and the modified cellulosic fibres, namely cellulose diacetate and cellulose triacetate, have not been included.
- *Recent developments*: newer developments including high performance fibres and the techniques of dry-jet wet-spinning and gel-spinning, spunbonding and melt-blowing, computer simulation of melt-spinning and modification of fibres for value addition are covered in four chapters.
- *Characterization and testing*: the methods used for characterization of polymers and fibres and for testing fibres for both quality control and R&D are described in two chapters.
- *Others*: important industrial aspects relating to spin finishes and their application and of reuse of waste generated in the plant and elsewhere are covered in two chapters. One chapter is devoted to the development of basic structural concepts and the other is introductory in nature and traces the history of manufactured fibres and gives some statistics and typical applications.

The diverse topics listed above were handled by fifteen authors with basic background in one or more of the following subjects: physics, chemistry, materials science, textile technology and chemical engineering. They were drawn from academic institutes, research laboratories and industry and all have considerable expertise in various aspects of fibres and textile materials and processes. We have tried to retain the flavour of the author's experience and approach while ensuring an in-depth coverage of the different topics with a minimum overlap between the chapters. We hope that we have succeeded in meeting the objectives for which the book was designed and that the users will find it useful in teaching, research, production and applications.

A book of this magnitude is the joint effort of a number of persons and as editors we would like to express our gratitude to them. We

thank the authors for their contributions. The understanding shown and cooperation extended by them during the prolonged editorial exercise is gratefully acknowledged. We would also like to acknowledge with thanks the reviewers for their generous advice and comments. The editorial staff of the publishers, Chapman & Hall, deserve special thanks for the assistance rendered during different stages of publication. The generosity of several publishers and authors in permitting the reproduction of figures and tables (listed in a separate section) from their published work is gratefully acknowledged. We are indebted to Mr R.K. Arora for doing the entire word-processing work single-handed. We are thankful to Mr K.G. Padam for line sketches, Ms Sujata Caprihan and Mr T. Vineet for some artwork, and Mr K.P. Vetrival and Mr J.K. Sensarma for computer graphics. We would be failing in our duty if we did not thank the many generations of students whom we had the privilege to teach and whose association has been stimulating and educative for us.

Finally, we would like to thank our wives, Lata and Purnima, for support, patience and encouragement without which it would have been difficult to undertake this project.

New Delhi   V.B. Gupta
May, 1997   V.K. Kothari

Acknowledgements

SI units and symbols

The International System of Units (SI) divides units into three classes: base units, supplementary units and derived units. SI is based on seven well-defined base units (Table A) which by convention are regarded as dimensionally independent. There are two supplementary units – the radian and the steradian (Table A).

Derived units are formed by combining base units, supplementary units, and other derived units according to the algebraic relations linking the corresponding quantities. The symbols for derived units are obtained by means of the mathematical signs for multiplication, division, and use of exponents. For example, the SI unit for velocity is the metre per second (m/s or $m\,s^{-1}$), and that for angular velocity is the radian per second (rad/s or $rad\,s^{-1}$). Derived units are given in Table B. Table C gives the preferred SI units and conversion factors for some of the non-SI units used in this book.

Table A Base and supplementary SI units

Quantity	Unit	Symbol
Length	metre	m
Mass	kilogram	kg
Time	second	s
Electric current	ampere	A
Thermodynamic temperature	kelvin	K
Amount of substance	mole	mol
Luminous intensity	candela	cd
Plane angle[a]	radian	rad
Solid angle[a]	steradian	sr

[a] Supplementary units.

Table B Derived SI units with special names

Quantity	Unit	Symbol	Formula
Frequency (of a periodic phenomenon)	hertz	Hz	s^{-1}
Force	newton	N	$kg\,m\,s^{-2}$
Pressure, stress	pascal	Pa	$N\,m^{-2}$
Energy, work, quantity of heat	joule	J	$N\,m$
Power, radiant flux	watt	W	$J\,s^{-1}$
Electric charge	coulomb	C	$A\,s$
Electric potential, potential difference, electromotive force	volt	V	$W\,A^{-1}$
Electric capacitance	farad	F	$C\,V^{-1}$
Electric resistance	ohm	Ω	$V\,A^{-1}$
Electric conductance	siemens	S	$A\,V^{-1}$
Magnetic flux	weber	Wb	$V\,s$
Magnetic flux density	tesla	T	$Wb\,m^{-2}$
Inductance	henry	H	$Wb\,A^{-1}$
Celsius temperature	degree Celsius[a]	°C	[a]
Luminous flux	lumen	lm	$cd\,sr$
Illuminance	lux	lx	$lm\,m^{-2}$
Activity (of a radionuclide)	becquerel	Bq	s^{-1}
Absorbed dose	gray	Gy	$J\,kg^{-1}$
Dose equivalent	sievert	Sv	$J\,kg^{-1}$

[a] The SI unit of thermodynamic temperature is the kelvin (K), and this unit is properly used for expressing thermodynamic temperature and temperature intervals. Wide use is also made of the degree Celsius (°C), which is the SI unit used for expressing Celsius temperature and temperature intervals. The Celsius scale (formerly called centigrade) is related directly to thermodynamic temperature (kelvin) as follows:

The temperature interval one degree Celsius equals one kelvin exactly. Celsius temperature (t) is related to thermodynamic temperature (T) by the equation:

$$t = T - T_0$$

where $T_0 = 273.15\,K$ by definition.

Table C Units used in this book and conversion factor to obtain preferred SI unit[1]

Quantity	Unit used at some places in this book	Preferred SI unit	Conversion factor
Length	inch (in)	m	2.54×10^{-2}
		mm	25.4
		μm	2.54×10^4
Area	inch^2 (in^2)	m^2	6.4516×10^{-2}
Volume	cm^3	m^3	10^{-6}
	dl	m^3	10^{-4}
	l	m^3	10^{-3}
Density	g cm^{-3}	kg m^{-3}	10^3
Linear density	denier (den)	tex	0.1111
		dtex	1.1111
Tenacity	gf den^{-1}	N tex^{-1}	8.829×10^{-2}
(mass stress)	gf tex^{-1}	N tex^{-1}	9.81×10^{-3}
Surface tension	dyn cm^{-1}	N m^{-1}	10^{-3}
Viscosity	poise (P)	N s m^{-2}	10^{-1}
	centipoise (cP)	N s m^{-2}	10^{-3}
Specific heat	cal (g °C)$^{-1}$	J kg^{-1} K^{-1}	4.19×10^3
Force	gf	N	9.81×10^{-3}
	kgf	N	9.81
	dyne	N	10^{-5}
	lbf	N	4.44822
Stress/pressure	kgf mm^{-2}	N m^{-2} (Pa)	9.81×10^6
	kgf cm^{-2}	N m^{-2} (Pa)	9.81×10^4
	lbf in^{-2} (p.s.i./psi)	N m^{-2} (Pa)	6.89×10^3
Pressure	mmHg	N m^{-2} (Pa)	133.322
	atmosphere (atm)	N m^{-2} (Pa)	1.013×10^5
Energy	cal	N m^{-1} (J)	4.1868

[1] Conversion factors between various units of stress and mass stress are given in Table D.

Table D Conversion between various units commonly used for specifying fibre mechanical properties. To convert a quantity with a unit given in column I to a quantity with a unit given in the top row, multiply the former by the conversion factor given under the column containing the desired unit. ρ is the density of the fibre in g cm^{-3}. (Courtesy W.W. Adams and Hao Jiang, WL/MLPJ, WPAFB, OH 545333-7702)

Column I ↓	gf d^{-1}	gf tex^{-1}	kgf mm^{-2}	dyn cm^{-2}	Pa	lbf in^{-2}
gf d^{-1}	1	9	$\rho \times 9$	$\rho \times 8.83 \times 10^8$	$\rho \times 8.83 \times 10^7$	$\rho \times 1.28 \times 10^4$
gf tex^{-1}	0.111	1	ρ	$\rho \times 9.81 \times 10^7$	$\rho \times 9.81 \times 10^6$	$\rho \times 1.42 \times 10^3$
kgf mm^{-2}	$\dfrac{0.111}{\rho}$	$\dfrac{1}{\rho}$	1	9.81×10^7	9.81×10^6	1.42×10^3
dyn cm^{-2}	$\dfrac{1.13}{\rho} \times 10^{-9}$	$\dfrac{1.02}{\rho} \times 10^{-8}$	1.02×10^{-8}	1	0.1	1.45×10^{-5}
Pa	$\dfrac{1.13}{\rho} \times 10^{-8}$	$\dfrac{1.02}{\rho} \times 10^{-7}$	1.02×10^{-7}	10	1	1.45×10^{-4}
lbf in^{-2}	$\dfrac{7.81}{\rho} \times 10^{-5}$	$\dfrac{7.03}{\rho} \times 10^{-4}$	7.03×10^{-4}	6.90×10^4	6.90×10^3	1

Examples: In order to convert a mass stress in gf d^{-1} into a stress value in Pa, the gf d^{-1} value will have to be multiplied by $\rho \times 8.83 \times 10^7$. A stress value in kgf mm^{-2} can be converted into a mass stress in gf tex^{-1} by multiplying it by $1/\rho$.

Note on equivalence and equivalent weight

The concept of equivalence and its quantification in terms of equivalent weight has been used in Chapters 10, 12, 14 and 15 of this book to estimate the end group content in polymers or the amount of reactants in specific chemical reactions, e.g. the amount of water to be charged into caprolactam at the beginning of polymerization in a VK tube. Since different units have been used by different authors to denote equivalent weight, a brief description of the concept and the units that have been used is given below, mainly to facilitate conversion from one unit to another.

In chemical compounds, equivalent weight can be expressed as weight associated with unit functionality, where functionality is the number of reactive functional group(s) per molecule. 'Equivalent weight' for chemical compounds (or polymers) is thus defined as that weight which contains one gram equivalent weight of the component taking part in the reaction. It often happens that the same compound will possess different equivalent weights in different reactions. An example relevant to the use of this term in the present book is given below:

Consider a simple chemical compound, viz. pure hexamethylene diamine, $H_2N-(CH_2)_6-NH_2$, which has two amino groups and an approximate molecular weight of 116.2. The equivalence in terms of its reaction with acids may be expressed as

- equivalent weight $= 116.2/2 = 58.1$, expressed as a number,
- gram equivalent $= 58.1\,g$, expressed in grams.

Alternatively, the equivalence may also be expressed in terms of

- eq g^{-1} and related units: since $58.1\,g$ is the gram equivalent of one amino group in the compound, 1 gram will be the equivalent of $1/58.1$ amino group, which may be expressed as $1/58.1$ i.e. 17.2×10^{-3} eq g^{-1} or 17.2 milli eq g^{-1} or 17.2×10^2 milli eq kg^{-1} or 17.2×10^3 eq ton^{-1}.

- eq mole^{-1}: this can be obtained by multiplying equivalence in eq g^{-1} by molecular weight in g mole^{-1}, i.e., 17.2×10^{-3} eq g$^{-1} \times 116.2$ g mole$^{-1} = 2$ eq mole^{-1}.

Introduction 1

V.B. Gupta and V.K. Kothari

1.1 DEFINITION AND CLASSIFICATION

A textile fibre is a long thin object with a high ratio of length to thickness. It is characterized by a high degree of fineness and outstanding flexibility. In addition, it should have dimensional and thermal stability and minimum levels of strength and extensibility consistent with the end use. Fibres should also be capable of being converted into yarns and fabrics. There are a number of other requirements that a fibre must satisfy, but those noted above are relatively more significant.

The fibres that satisfy the requirements noted above are surprisingly small in number. They can be broadly considered as belonging to one of the following two classes: (a) natural, and (b) manufactured. Natural fibre is a class name for various genera of fibres of vegetable (e.g. cotton, flax), animal (e.g. wool, silk) or mineral (e.g. asbestos) origin produced by nature. Manufactured fibres is a class name for various genera of fibres produced from fibre-forming substances which may be (1) modified or transformed natural polymers, (2) wholly synthetic polymers, or (3) materials of inorganic origin. The principal manufactured fibres belonging to the above three classes are listed in Table 1.1. Fibres produced by nature are generally of relatively short length, say between 10 and 500 mm; these are called staple fibres. However, silk is produced by the silkworm in continuous lengths of around 2 km and is referred to as filament. Manufactured fibres are produced as continuous filaments but, when required in staple form, they are cut into short lengths.

Table 1.1 The principal manufactured fibres

Based on natural polymers	Based on wholly synthetic polymers	Based on inorganic materials

Cellulosics
  Viscose rayon
	Polyamides
	  Nylon 66
	  Nylon 6
	  Kevlar^{TM}
		Glass
		Ceramic

Modified cellulosics
  Cellulose acetate
  Cellulose triacetate
		Metallic

	Polyesters
	  Poly(ethylene terephthalate)
	  Poly(butylene terephthalate)	

	Polyacrylonitrile	

	Polyolefins
	  Polypropylene
	  Polyethylene	

	Polyurethane	
	Polyvinyl alcohol	

1.2 EVOLUTION OF MANUFACTURED FIBRES

The story of manufactured fibres may be traced to the accidental discovery of cellulose nitrate in 1846 by C.F. Schönbein, a Professor of Chemistry at the University of Basel in Switzerland. He observed that cotton may be converted into a soluble plastic substance by the action of a mixture of nitric and sulphuric acids. This solution was extruded into fine filaments by Hillaire de Chardonnet in 1884. The organic chemists gave a correct interpretation of the underlying chemical reaction by suggesting that the action of acid mixture on cellulose, a natural fibre-former, converted it into a derivative, i.e. cellulose nitrate. Unlike cellulose, cellulose nitrate was soluble in a mixed alcohol/ether solvent and therefore spinnable. The commercial production of viscose rayon fibre in the late nineteenth century through the intermediate product cellulose sodium xanthate, and of cellulose acetate fibre at the turn of this century, were based on a similar procedure.

The origins of wholly synthetic fibres can be traced to the pioneering work of W.H. Carothers in the USA. A number of systems were tried by Carothers and his group during the years 1928 to 1932; the first successful wholly synthetic fibre was produced commercially in 1938 from adipic acid and hexamethylene diamine. This fibre was called nylon 66. The filaments were pulled out from the melt and then stretched to give a useful fibre. Paul Schlack in Germany discovered polycaprolactam, or nylon 6, which came into production just as World War II started in 1939. Other synthetic fibres soon appeared, the most successful being

polyacrylonitrile in 1949, polyvinyl alcohol in 1950, poly(ethylene terephthalate) in 1953 and polypropylene in 1957. Aromatic polyamide and aromatic polyester fibres came in 1962 and 1972, respectively. The most recent addition is that of gel-spun, ultra high molecular weight, high density polyethylene fibres.

1.3 FIBRE-FORMING PROCESSES

Fibre manufacture involves the following two principal operations: (1) production of the polymer, and (2) conversion of the polymer into the fibre. For fibres based on raw materials derived from nature, step (1) is not involved.

1.3.1 PRODUCTION OF THE FIBRE-FORMING POLYMER

The two principal mechanisms suggested by Carothers [1] for synthesizing fibre-forming polymers are condensation (step growth) and addition (chain growth) polymerization. The synthesis of condensation polymers proceeds by the step-wise reactions of functional groups, each reaction proceeding with the elimination of a small molecule, usually water. The use of bifunctional monomers in condensation polymerization leads to linear condensation polymers, typical examples of which are the polyesters and polyamides. When the molecular weights of condensation polymers exceed 10 000, they can be drawn into tough fibres.

Addition polymers are formed by the addition of unsaturated monomers to the growing chain without the elimination of water or other small molecules. Consequently in the polymer the same number of elements are present as in the corresponding monomer. The synthesis of addition polymers from unsaturated monomers may proceed by either a free-radical or an ionic mechanism. The free-radical processes are characteristic of chain reactions and involve at least three processes, namely initiation, chain propagation and chain termination. Addition polymerization may also be either cationic or anionic, depending on the nature of the monomer and the catalyst employed.

1.3.2 CONVERSION OF THE POLYMER INTO FIBRE

The basic steps involved in the conversion of the polymer into a fibre are spinning or extrusion, and post-spinning operations which include drawing and heat-setting.

(a) Spinning of polymers into fibres

The fibre-forming polymers can be converted into filaments using two principal routes. The first, melt-spinning, involves extruding the

polymer melt through small capillary holes to form fibres, attenuated by an external force applied at the wind-up. The filament is cooled to its solid state by quenching as it emerges from the capillary holes. The second, solution-spinning, involves the extrusion of a solution to form fibres. The solvent is removed from the fluid filament by vaporization with hot gases in dry-spinning, or by coagulation in a non-solvent in wet-spinning.

(b) Post-spinning operations

In most cases the as-spun fibre does not have the properties required of a fibre and is therefore subjected to drawing. This aligns the molecules in the direction of the long axis of the filament and reinforces it with orientation and crystallinity. Drawing is followed by heat-setting to stabilize the fibre and make it dimensionally more stable. The stabilization that occurs during heat-setting is due to post-crystallization and stress relaxation in the fibre.

1.4 FIBRE PRODUCTS AND PROPERTIES

1.4.1 TYPES OF FIBRE PRODUCTS

Manufactured fibres are widely used by textile manufacturers for producing apparel and household textiles. Manufacturers of industrial fibrous products use fibres in such diverse applications as filter materials, protective clothing and as reinforcement for tyres, rubber goods and composites. Such a broad utilization of manufactured fibres has been achieved through many technical advances.

Manufactured fibres are used in various applications in a variety of forms. A bundle of continuous filaments forms a multifilament yarn with some or no additional twist. Textile fabrics woven from continuous filament yarns generally have a lustrous appearance, which is desirable for lining, hosiery, outerwear, home furnishing, etc.

There are considerable limitations with continuous filament yarns for textile purposes. These include the synthetic look, lack of bulkiness, and clothing discomfort due to poor water sorption. For this reason, as stated earlier, some fibres are cut into short lengths as staple fibres. Staple fibres can be spun like natural fibres to form a yarn. They can also be blended with other fibres to impart certain desirable characteristics to the resultant yarn. Alternatively, continuous filament yarns can be textured. These fibre products give textile fabrics the desired aesthetics, comfort, durability and feel.

Yang [2] has classified manufactured fibres into four categories based on their characteristics.

1. *Conventional fibres.* These comprise viscose rayon, cellulose acetate, nylon 66, nylon 6, poly(ethylene terephthalate), linear polyethylene, isotactic polypropylene and polyvinyl alcohol.
2. *Second generation fibres.* Yang's classification [2] describes second generation fibres as those whose properties have been improved as a result of physical modification (textured yarns, bicomponents) and chemical modification (high molecular weight, flame resistant, anti-static, easily dyeable, etc.).
3. *High temperature fibres.* This category comprises fibres used in many industrial, military and aerospace applications for extended periods of time at temperatures of 200–400 °C. High temperature fibres include aromatic polyamides and other similar fibres.
4. *High performance fibres.* The final category comprises those fibres with the necessary dimensional stability and light weight required for end uses that involve high temperatures, high tensile or compressive load and hostile environments. The high temperature fibres considered earlier may thus also be considered as high performance fibres. Aromatic systems based on polyamides, polyesters, polyimides and heterocyclic polymers come into this category. Linear ultra high molecular weight polyethylene fibres, carbon fibres, and inorganic fibres like boron, alumina and silicon carbide all come into this category of fibres. Glass fibre is not strictly a high performance fibre, but is used for various industrial applications.

1.4.2 FIBRE PROPERTIES

Some important properties of the principal manufactured fibres are listed in Table 1.2. For comparison, the properties of some natural fibres are also given. It is noteworthy that compared with the natural fibres, the manufactured fibres have a wider property spectrum. This is an important and useful feature of these fibres.

1.5 PRODUCTION TRENDS

Historically, manufactured fibres have been with us for over 100 years, but their rate of growth of production has witnessed a phenomenal increase during the past 25 years. The production of manufactured fibres at the beginning of the twentieth century was extremely small. Even until 1935, it remained below half a million tonnes and was confined mainly to regenerated cellulosic fibres. It was only after wholly synthetic fibres were introduced in 1938 that manufactured fibre production increased dramatically. Table 1.3 gives detailed world production statistics relating to both natural and manufactured fibres. Figure 1.1 shows the production figures for total natural fibres, total manufactured

Table 1.2 Properties of major textile fibres

Fibre	Density $(g\,cm^{-3})$	Moisture regain at 65% RH (%)	Tenacity $(gf\,tex^{-1})$	Breaking elongation (%)	Initial modulus $(gf\,tex^{-1})$
Polyester	1.34–1.38	0.4	25–54	12–55	600–1200
Nylon 66	1.14	2.8–5.0	32–65	16–65	200–300
Nylon 6	1.14	2.8–5.0	32–65	30–55	200–300
Acrylic	1.14–1.17	1.5	18–30	20–50	600–700
Polypropylene	0.90	0.04–0.10	35–80	15–35	225–900
Polyethylene	0.95	0	30–60	10–45	225–450
Viscose	1.46–1.54	11–13	20–51	8–20	500–800
Acetate	1.28–1.34	6.0–6.5	13	24	350
Triacetate	1.32	4	12	30	300
Cotton	1.50–1.55	7–8	19–46	5.6–7.1	400–740
Wool	1.30–1.32	14–16	11–14	29–43	210–310
Silk	1.34	10	39	23–24	750

fibres, and two main groups among the manufactured fibres separately over the past 100 years. In the late 1940s and 1950s many new synthetic fibres were introduced and in the late 1960s the total world production of synthetic fibres started to exceed that of regenerated cellulosic fibres. In the early stages of their introduction, the total production of filament yarns exceeded that of staple fibres for both cellulose-based and wholly synthetic fibres. However, for many years the total production of staple fibres has exceeded that of filament yarns. In 1995, 23.19 million tonnes of manufactured fibres were produced, accounting for almost 53% of the total (natural and manufactured) world fibre production of 43.651 million tonnes; nearly 87% of the total manufactured fibre production was from synthetic polymers.

Figure 1.2 gives the geographical breakdown of the world production of manufactured fibres. It can be seen that since 1980 the increase in the production of these fibres in the USA, Western Europe and Japan has been very slow, although in 1992 these regions still accounted for nearly 43% of the total manufactured fibres produced. Other countries, particularly Taiwan, China, South Korea and India, have shown strong expansion of manufactured fibre production since the mid 1980s. Figure 1.3 shows a detailed geographical breakdown of manufactured fibre production during 1994. Polyester, polyamide, acrylic and polypropylene account for 98% of synthetic fibre production. Capacities and production of these fibres in 1991 and their projected values up to the year 2001 are shown in Fig. 1.4. It can be seen that polyester is the predominant synthetic fibre; according to one estimate it accounted for 52% of total synthetic fibre production in 1995.

Table 1.3 World production of major fibres in thousand tonnes

Year	Cotton	Wool	Silk	Cellulosics			Synthetics			Total manufactured fibres	Grand total
				Filament	Staple	Total	Filament	Staple	Total		
1890	2715	727	12								3454
1900	3170	732	17	1		1				1	3920
1910	4318	805	23	8		8				8	5154
1920	4477	809	21	19		19				19	5326
1925	6174	914	47	85		85				85	7220
1930	5939	1005	59	205	3	208				208	7211
1935	6068	982	55	425	65	490				490	7595
1940	6985	1136	59	543	586	1129	1	4	5	1134	9314
1945	4677	1036	11	402	200	602	13	3	16	618	6342
1950	6661	1059	19	876	739	1615	55	15	70	1685	9424
1955	9512	1268	29	1045	1239	2284	184	83	267	2551	13 360
1960	10 129	1469	31	1133	1472	2605	418	286	704	3309	14 938
1965	11 629	1495	33	1377	1969	3346	1128	927	2055	5401	18 558
1970	11 782	1602	41	1393	2043	3436	2363	2337	4700	8136	21 561
1975	11 798	1487	48	1136	1842	2960	3765	3590	7355	10 315	23 648
1980	13 991	1607	56	1130	2392	3522	4854	5925	10 779	14 301	29 955
1985	16 565	1722	59	933	2301	3234	5792	7233	13 025	16 259	34 605
1990	18 714	1966	66	864	2351	3215	7528	8357	15 885	19 100	39 846
1991	18 650	1934	67	837	2220	3057	7821	8678	16 499	19 556	40 207
1992	18 758	1739	67	815	2207	3022	8159	9059	17 218	20 240	40 804
1993	18 494	1687	68	690	2088	2778	9057	8899	17 956	20 734	40 983
1994	18 394	1736	69	670	2211	2881	10 034	9623	19 657	22 538	42 737
1995	18 602	1767	92	698	2333	3031	10 692	9467	20 159	23 190	43 651
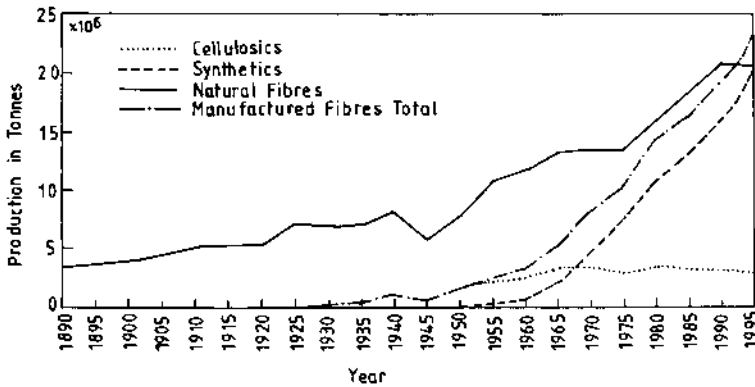
Fig. 1.1 Production of different fibres during the period 1890–1995.

1.6 APPLICATION AREAS

The application areas for textile products may be considered under the following three categories: (1) apparel, (2) household, and (3) industrial, technical and engineering. Manufactured fibres have made significant inroads into all three categories. Figure 1.5 shows the application areas of the principal synthetic fibres. Conventional and modified manufactured
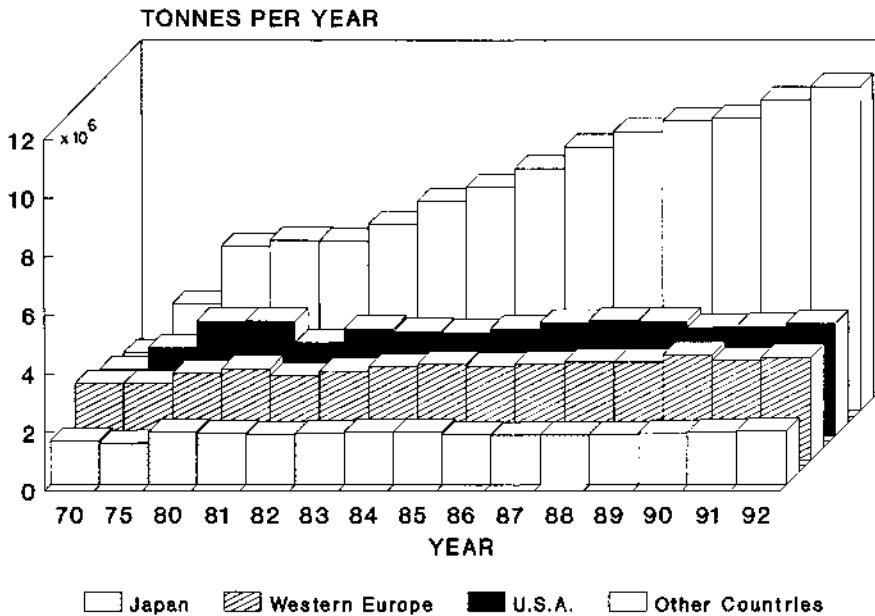
Fig. 1.2 Geographical breakdown of the world production of manufactured fibres during the period 1970–92.
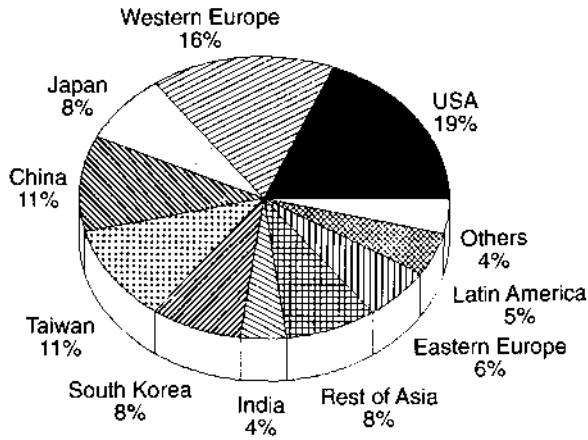
Fig. 1.3 Detailed geographical breakdown of the world production of manufactured fibres in 1994.

fibres are being increasingly used in apparel and household sectors owing to their durability, easy-care and many other desirable performance characteristics. These fibres, along with newer high temperature, high performance fibres, are also being used in a large number of industrial, technical and engineering applications. Manufactured fibres are used in woven, knitted as well as non-woven fabric structures, and their production and uses are steadily growing.

Poly(ethylene terephthalate) (PET) is the most widely used fibre in the world in its various forms. PET is a strong, dimensionally stable fibre
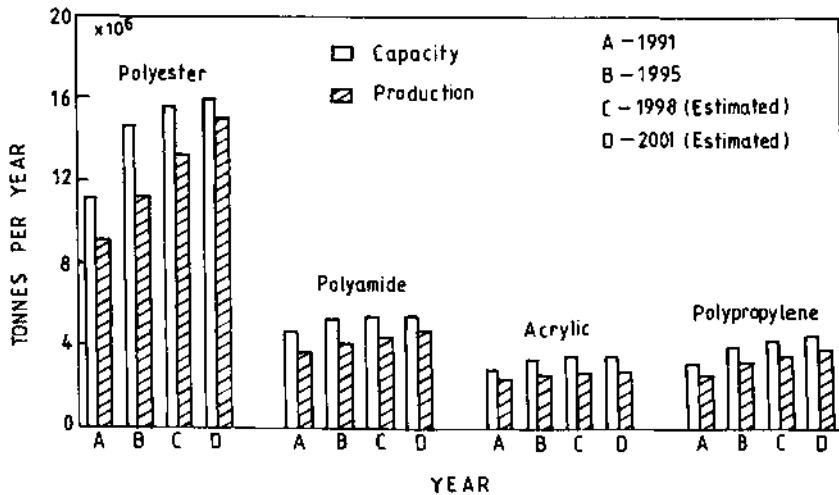
Fig. 1.4 Manufacturing capacity and production of the main synthetic fibres.
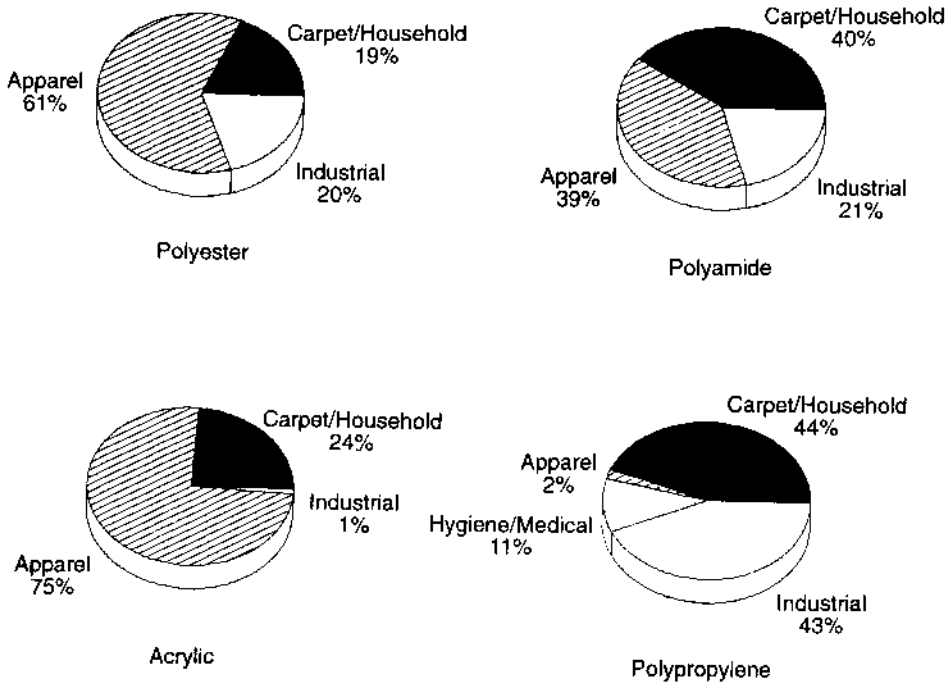
Fig. 1.5 Applications of synthetic fibres in 1992.

and is extensively used in both staple and filament forms. In the apparel area, which accounts for nearly 50% of the total fibre market, PET is used extensively both alone and in blends with cotton and viscose, mainly because it imparts easy-care characteristics, wrinkle resistance and durability to the fabrics. Comfort characteristics and dyeability of the fibre have been improved through modification techniques and PET multifilament yarns are also used extensively in the textured form. A large quantity of PET fibre is also used for both woven and non-woven fabrics meant for industrial and technical applications such as filtration and geotextiles.

Nylon 66 and nylon 6 were the first synthetic fibres to be introduced into the market and continue to be important. They are used in a wide range of applications including hosiery, stretch fabrics, sportswear, parachutes, tyre cords and conveyor belts. Nylon fibres perform well in applications that require high strength, light weight, abrasion resistance, and strong adhesion, impact and fatigue resistance. Some applications where these properties are desirable are luggage, truck covers, sleeping bags, tents, webbings, inflatables and carpets.

Acrylic fibres are used worldwide in a wide variety of applications including sweaters, children's wear, T-shirts, blankets and velvets.

Acrylic fibre has been extensively used in a number of industrial applications, for example as a precursor for carbon fibre, as a substitute for asbestos in fibre-reinforced cement, and in hot gas and wet filtration.

The use of polypropylene and other polyolefins in textile products now exceeds one million tonnes. Primary carpet backing for tufted carpets, sacks, bale wraps, flexible intermediate bulk containers, ropes, twines, and coverstock for disposable nappies (diapers) are some of the major uses of polypropylene fibre. Floor coverings and upholstery made from polypropylene have the merits of good wear resistance and easy stain removal. Clothing uses of polypropylene have not developed widely because its moisture sorption, dyeability and thermal resistance are poor. However, polypropylene spun yarns are used to some extent in knitwear while coarser fibres find use in heavier filtration fabrics, geotextiles, cement and concrete reinforcement, and sports surfaces.

Viscose rayon conducts heat more readily than silk, has a cooler feeling against the skin, and is highly absorbent, enhancing its value as a clothing material. It is often used for blending with other natural and synthetic fibres, contributing moisture absorption and other cellulosic characteristics to blends of viscose with stronger but less absorbent synthetic fibres. Viscose rayon in its many forms is highly versatile and is used in outerwear, underwear, furnishing and other household textiles, and in medical applications. Acetate and triacetate yarns have always been 'silk-like' in their pleasing appearance and handle. Their uses include linings, dresswear, lingerie, home furnishing fabrics including draperies and bed spreads, garment labels and ribbons.

Apart from the commodity manufactured fibres and their variants discussed above, a number of high temperature, high performance fibres are being used in limited quantities in the specialized applications of protective clothing, filter fabrics, engineering composites, etc. Industrial, technical and engineering applications of both commodity and high performance fibres is a vast and fast growing field for manufactured fibres. It is estimated that the 1995 share of 15–20% of total fibre uses in these applications will grow rapidly. The share of fibre uses in industrial, technical and engineering applications in countries like the USA and Japan is already one-third of the total fibre uses and it is predicted that world fibre uses in these applications will exceed their use in apparel by the year 2000. Manufactured fibres will continue to dominate in these increasingly important applications.

1.7 SCOPE OF THIS BOOK

This book has been designed to cover in detail the production technology of manufactured fibres, particularly commodity fibres. Structure,

properties, applications and other related areas are also described briefly to put the subject into its correct perspective and provide a comprehensive coverage. The first two chapters (Chapters 1 and 2) are introductory in nature. The present chapter (Chapter 1) gives a brief introduction to the fibre types and their production technology. Chapter 2 introduces the structural aspects of polymers and discusses such important factors as molecular weight, molecular interactions and glass transition temperature.

The next five chapters (Chapters 3–7) deal with the extrusion or spinning of polymers to produce filaments. Chapter 3 deals with the fundamentals of flow of melts and solutions through fine capillaries and along the spin lines. Chapter 4 discusses the melt-spinning process in terms of a number of variables and describes the various operations involved in melt-spinning. High speed spinning and spin-drawing are also briefly discussed. Chapter 5 considers the computer simulation of melt-spinning, particularly of poly(ethylene terephthalate), and the investigation of the various variables through sensitivity analysis. Chapter 6 deals with various aspects of the solution-spinning processes. Finally, in Chapter 7 the importance of the application of spin finish and various related aspects are brought out in detail.

In Chapters 8 and 9 two important post-spinning operations, namely drawing and heat-setting, are discussed. The technology is described and the effect of these operations on structure and properties of fibres is examined.

The next two chapters (Chapters 10 and 11) are devoted to characterization and testing. In Chapter 10, the characterization of polymers and fibres is briefly considered in terms of such important techniques as molecular weight determination, X-ray diffraction, infrared spectroscopy, microscopy and thermal techniques. Chapter 11 deals with testing of manufactured fibres with particular emphasis on the testing of fineness, tensile properties, evenness, frictional properties and shrinkage behaviour.

The next seven chapters (Chapters 12–18) deal with specific fibre families, namely poly(ethylene terephthalate), polyamides, speciality nylon and polyester yarns, acrylics, polypropylene, rayon and industrial fibres. The chemistry of polymer production is first discussed. This is followed by a discussion of the technology of the conversion of the polymer to a fibre, and finally a brief description of structure, properties and applications.

The last two chapters (Chapters 19 and 20) deal with direct fabric manufacturing techniques from manufactured fibres and reuse of polymer and fibre waste, respectively. In Chapter 19, spunbonding and melt-blowing technologies are discussed. In Chapter 20, the recycling and reuse of polymer and fibre waste is considered, both from the

point of view of the technology as well as from the consideration of application areas.

REFERENCES

1. Carothers, W.H. (1929) *J. Am. Chem. Soc.,* **51**, 2548.
2. Yang, H.H. (1989) *Aromatic High Strength Fibers,* John Wiley & Sons, New York, p. 15.

Structural principles of polymeric fibres

2

V.B. Gupta

2.1 INTRODUCTION

A fibre must ultimately satisfy the needs of the consumer. The consumer is not concerned with the method of production of the fibre, nor with its chemistry and physics; the consumer looks for durability, comfort, adequate dimensional stability and other useful properties in addition to aesthetic appeal. However, the fibre producer must have a good understanding of how fibre structure controls its properties so that the fibre can be 'engineered' by suitable choice of the polymer and its molecular weight, orientation, crystallinity, morphology, etc. By so doing, the fibre producer can expect to meet the needs of the consumer. The starting point to gain such an understanding is to consider the fibre-forming polymers against the backdrop of the available polymers so that the structural requirements for a useful fibre-forming polymer become clear. This is the primary purpose of this chapter. The emphasis is on a physical understanding of the structure–property relationships in very simple terms; the resulting loss of accuracy should not detract from the main theme that is developed.

Polymers in the form of fibres, rubbers and plastics have been known for a long time. The word polymer, meaning literally many parts (from the Greek *polus*, many; and *meros*, parts, segments), is used to include all those materials whose molecules are made up of many units; these units consist more usually of a small group of atoms in a state of chemical combination. Polymers in the form of natural fibres, which may be of either plant (cotton and jute) or animal (silk and wool) origin have been

known to be used as clothing and for other textile applications for centuries; there is evidence that cotton was in use over 5000 years ago. However, it was only in the late 1920s that Staudinger's idea that polymers were formed from long molecules was considered with some degree of seriousness by the scientific community. It was around the same time that it was appreciated that, in addition to high molecular weight, the fibres had good orientation with varying degrees of crystallinity. These observations were possible because of developments in viscometry, X-ray diffraction and electron microscopy. These ideas, supported by experimental techniques, were in no small measure responsible for the synthesis and development of a large number of polymers, including fibre-forming polymers; nylon 66 and nylon 6 were developed before 1940 and poly(ethylene terephthalate) (PET) and acrylics after 1940.

2.2 MOLECULAR SIZE AND INTERACTION

Although characteristics of individual units in a polymer molecule can have a considerable influence on properties (this aspect is considered later), the role of molecular size is of paramount importance. This is illustrated by the examples in Table 2.1, where the properties of some low molecular weight compounds are compared with compounds built up of an increasingly large number of similar units [1]. On the left-hand side, the nature of the intermolecular forces remains the same but the size of the molecule is progressively increased, while on the right-hand side, the main difference between the various compounds shown is with

Table 2.1 Effect of molecular weight and intermolecular forces on melting points of some compounds [1]

Equi-intermolecular forces: substances with increasing molecular weights			Equi-molecular weight substances exhibiting increasing intermolecular forces		
Chemical name	Structure	Melting point (°C)	Chemical name	Structure	Melting point (°C)
Butane	C_4H_{10}	−138	Hexanol	$C_6H_{13}OH$	−56
Octane	C_8H_{18}	−57	Hexane-1-amine	$C_6H_{13}NH_2$	−19
Dodecane	$C_{12}H_{26}$	−10	Hexanoic acid	$C_5H_{11}CO_2H$	−2
Octadecane	$C_{18}H_{38}$	+28	Hexamethylene glycol	$C_6H_{12}(OH)_2$	+41
Tricontane	$C_{30}H_{62}$	+65	Hexamethylene diamine	$C_6H_{12}(NH_2)_2$	+43
Polyethylene	C_nH_{n+2} $(n > 500)$	+137	Adipic acid	$C_4H_8(CO_2H)_2$	+153

respect to intermolecular forces. Although in both cases there is a gradual change from gas to liquid to high melting point solid, only the high molecular weight substances (e.g. polyethylene) possess adequate mechanical properties. It is this type of observation that makes one realize the importance of macromolecular (or polymer) systems in materials engineering.

The dependence of glass transition temperature (T_g) on molecular weight will be considered later and it will be shown that to qualify as a high polymer, a high molecular weight is necessary. For many synthetic polyamides and polyesters, fibre formation becomes possible at a molecular weight of about $5000 \, g \, mol^{-1}$, and at values above about $10\,000 \, g \, mol^{-1}$, commercial fibres can be made. The larger the molecule, the more difficult it will be for chain segments to separate from their neighbours, and therefore the higher the fracture resistance.

The long chain contributes what could be considered to be a very important requirement in an oriented fibre at and around room temperature, namely finite extensibility of 5–10% on application of a load and recovery on release of the load. The extension results from secondary bond deformation and hindered rotation around the single covalent bonds in those regions of the fibre which are not highly ordered. The fibre goes back to its original state once the applied stress is removed with interatomic forces, entanglements and crystallites acting as cross-link points. The continuity provided by the valence bonds between atoms constituting the chain molecules also provides a mechanism for large-scale deformation in rubbers. It also confers spinnability to fibre-forming polymer systems, which allows them to be converted to filaments.

The internal rotation has been studied extensively in the case of low molecular mass organic compounds, in which most rotational modes have frequencies of over $10^{10} \, s^{-1}$. Similar rotational motions of small pendant groups also occur in high polymers around single bonds. However, deformation of polymers involves movement of chain segments. The rate of movement of a polymer segment is not equal to the bond rotation rate, but is some small fraction of it. Segmental motion is illustrated in Fig. 2.1 and involves the simultaneous co-operation of several bond rotations, both within the moving segment and within neighbouring segments which have to co-operate in the motion. It is believed that at the glass transition temperature, segments of about 25 carbon atoms in length are involved in rotation with a time constant of say about 10s per rotation. This may be compared with the much more vigorous thermal motion in the polymer melt in which the segmental motion may occur at the rate of $10^6 \, s^{-1}$. There have been significant developments which have enhanced our understanding of molecular motion during flow; some of these are reviewed in Chapter 3.
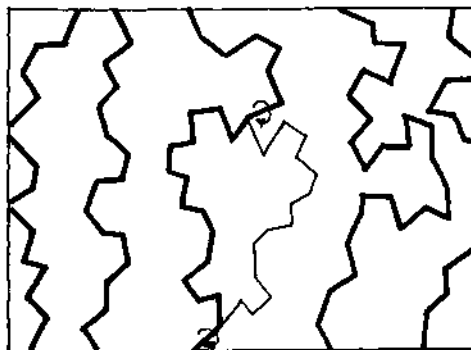
Fig. 2.1 Segmental motion in a polymer by rotation of about two carbon–carbon bonds in a chain molecule. The new position occupied by the segment is shown in light shade. The hole which provided room for this jump is displaced to the left as a consequence.

2.3 MOLECULAR ORIENTATION AND CRYSTALLINITY IN FIBRES

High molecular weight alone will not ensure desirable mechanical properties. The degree of orientation of the fibre is also crucial; higher orientation means greater resistance to deformation, greater breaking load and relatively lower extension to break. These attributes render the fibre more suitable for the desired uses.

The role of molecular orientation of the long polymer chains in enhancing intermolecular cohesion is of considerable importance in fibres. Most simple compounds can form crystals in which individual molecules are arranged in a regular fashion. So, too, many polymers can crystallize, but with the important difference that instead of entire molecules, only parts of molecules are incorporated into crystalline regions. This is shown schematically for a typical fibre in Fig. 2.2. It is obvious that longer chains would thread through more crystallites compared with shorter chains and would also be more entangled in amorphous regions; both these factors would contribute to enhancement of some mechanical properties.

Crystallization is only one aspect of orientation. Molecular orientation may not always result in crystallization but in an enhancement of order when the various types of bonds such as hydrogen bonds and other weak interatomic forces can contribute to property enhancement. Individually each bond may be quite weak, but if many weak bonds connect a single long chain to its neighbours then the total force holding that chain in place will be high.

Amongst the three principal industries based on polymers, namely fibres, plastics and rubbers, anisotropy (having different properties in

Fig. 2.2 A single molecule may form part of several ordered regions in a fibre.

different directions) is of most importance in fibres. It should be empha-
sized that the polymer chain is highly anisotropic in two respects: first,
in terms of geometrical dimensions (a typical chain of polyethylene may
be 12 000 Å long and 3–4 Å wide, thus having a length-to-diameter ratio
of around 4000), and second, in terms of bonding forces (the stronger
covalent bonds along the molecular chain axis have a dissociation
energy of the order of 100 kcal mol^{-1} and the weaker physical bonds in
the transverse direction have a dissociation energy of 5 kcal mol^{-1}). This
highly anisotropic nature of the polymer chain has two important
consequences [2]. First, as a result of the anisotropy of dimensions,
stretching or flow processes result in a tendency for the molecular
chains to line up relative to each other. Second, the anisotropy in terms
of mechanical strength is the basis of fibre formation.

2.4 POLYMERS AS FIBRES, PLASTICS AND RUBBERS

2.4.1 POLYMERS AS FIBRES

The fact that only a limited number of synthetic polymers (PET,
nylon 66, nylon 6 and acrylics) have succeeded as large-tonnage fibre-
forming polymers (polypropylene has also started making its mark) can
be explained on two fronts. The first is the technological angle, which
has been partly developed in this chapter as an interplay of an optimum
molecular weight with adequate intermolecular force and the capacity
for orientational reinforcement of the structure through molecular align-
ment. In cases where the intermolecular forces are weak, a stiff backbone
containing rigid units, such as ring structures, and the capacity to orient

will be assets. Such is the case with PET fibres. Second, the economic considerations of producing large-tonnage materials give the established fibre-forming polymers a tremendous advantage over newer materials because of their tested usefulness in terms of long years of use and the availability of R&D data that has been generated over these years.

It is interesting to note that nature prefers to build fibres with very high molecular weights, e.g. cotton cellulose may reach a molecular weight greater than $1\,500\,000\,\mathrm{g\,mol^{-1}}$. When cellulose is converted by man into viscose fibre, the molecular weight is less than one-tenth this value. With polyamides and polyesters, the molecular weight is kept at between $18\,000$ and $24\,000\,\mathrm{g\,mol^{-1}}$. This large difference will be discussed in more detail later. Here it will only be pointed out that, in natural fibres, the necessary alignment or arrangement of the polymer molecules along the direction of the length of the fibre is laid down during the actual process of growth. In conventional synthetic fibres, the filaments, as originally produced from the melt at conventional speeds, have limited molecular orientation and an additional stretching or drawing operation becomes necessary to achieve molecular alignment. At higher speeds of spinning, significant orientation can be introduced in the fibre during spinning itself; however, further drawing to a limited extent is still required in most cases to achieve the desired properties.

2.4.2 POLYMERS AS PLASTICS

The large-tonnage plastics encompass a wide range of polymers, e.g. polyethylene (PE), polypropylene (PP), polyvinyl chloride (PVC), polystyrene, polymethyl methacrylate (PMMA), phenol formaldehyde, polyester and epoxy resins, etc., and form the basis of a large industry. It may be stated that the distinction between fibres, plastics and rubbers, which is made mainly on the basis of their physical properties, is rather artificial and is with reference to room temperature. In general, polymers are capable of showing both glass-like and rubber-like behaviour as a function of temperature or strain rate.

In a large number of applications, the plastics products are isotropic (properties not changing with direction) and in these products anisotropy (introduced during processing) is often detrimental to properties and is removed by annealing the sample (for example by a suitable heat treatment). In some plastics products, uniaxial orientation (chair cane) or biaxial orientation (film) is introduced to enhance the properties in one or two directions, as desired. Plastics can be crystalline or amorphous (Greek *a*, without; *morphe*, form). The amorphous polymers used as plastics are generally glassy at room temperature (T_g above room temperature) but can be made rubber-like (T_g below room temperature), for
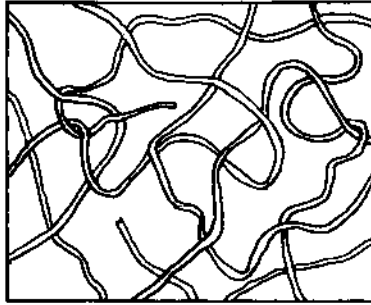
Fig. 2.3 Structure of an unoriented amorphous polymer.

example by adding plasticizers to PVC. The glassy amorphous polymers (PMMA, polystyrene, PVC) have molecules with rather large pendant groups which result in steric hindrance and lead to a glassy structure. The semicrystalline polymers (PE, PP) have more flexible chains which are stiffened by crystallization. Schematic representations of a glassy amorphous thermoplastic and a semicrystalline thermoplastic – both in the isotropic state – appear in Figs 2.3 and 2.4, respectively. The polymers used as plastics generally have a higher molecular weight than polymers used as fibres; this point will be considered later. There is another class of polymers used as plastics – these are the three-dimensional networks with different degrees of crosslinking. 'Bakelite' (phenol formaldehyde) and cured epoxy resins are two examples of this important class of thermosetting plastics. A schematic sketch of a thermosetting polymer is shown in Fig. 2.5.

2.4.3 POLYMERS AS RUBBERS

Rubbers are required to be very flexible, undergoing large deformation under small stresses and showing good elastic recovery when unloaded.
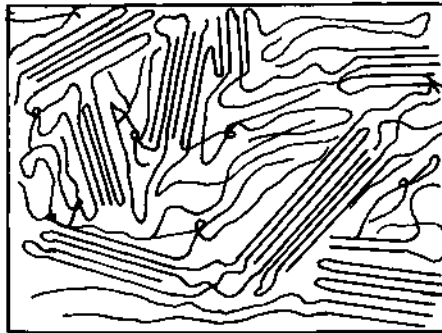
Fig. 2.4 Structure of an unoriented semicrystalline polymer.
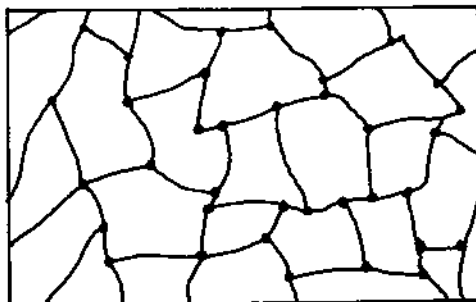
Fig. 2.5 A highly crosslinked polymer has a three-dimensional network.

Three conditions must be satisfied if a material is to show rubber-like properties.

1. It must be composed of long-chain molecules possessing freely rotating links.
2. The forces between the molecules must be weak, as in a liquid.
3. The molecules must be joined together or 'crosslinked' at certain points along the length.

A schematic sketch of vulcanized rubber is shown in Fig. 2.6. The requirements listed above for such polymers illustrate the important role played by the arrangement of the molecular structure in space. The isoprene unit $\{C_5H_8\}_n$ of the polyisoprene molecules has two isomeric forms, namely *trans* and *cis*, as shown in Fig. 2.7 [3]. In *cis*-polyisoprene or natural rubber, the two single C—C bonds lie on the same side of the non-rotating double bond; consequently chain straightening and crystallization are restricted. Thus the chain of natural rubber cannot be linear
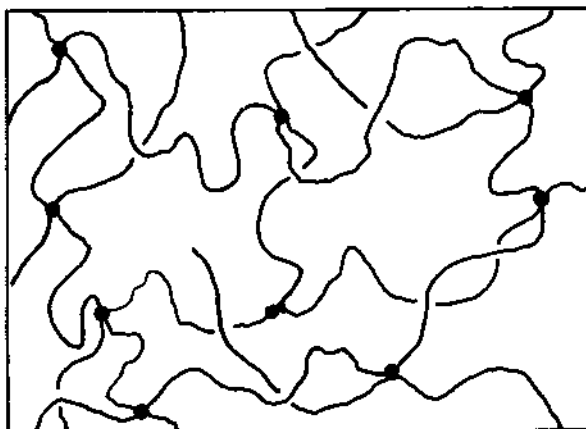
Fig. 2.6 Structure of a lightly crosslinked rubber.
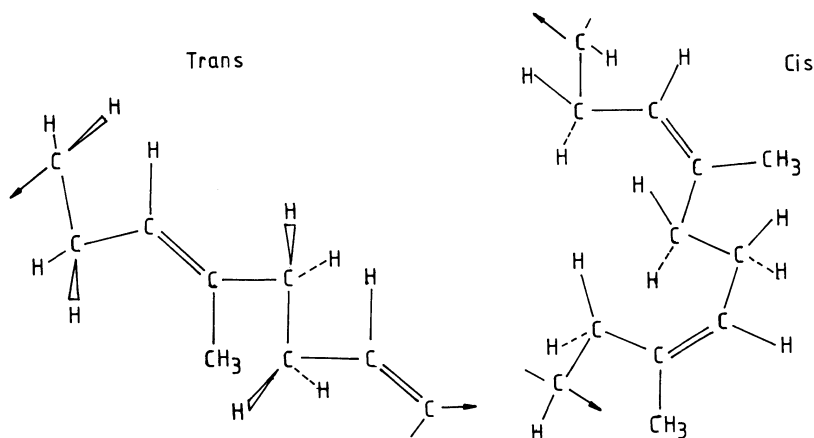
Fig. 2.7 The two isomeric forms of polyisoprene, *trans* and *cis*, in which all the carbon atoms in the backbone lie in one plane (adapted from reference [3]).

whilst also keeping the backbone atoms in one plane [3]. It consequently adopts a random geometry and large deformations are possible as the ends of the chain are pulled apart under stress. In *trans*-polyisoprene or gutta percha, on the other hand, the two single C—C bonds are on opposite sides of the double bond and the chains are in linear extended form. Consequently the resultant crystalline material is rigid and brittle. In contrast to fibres, rubbers are not normally crystalline (they can crystallize on stretching) but are amorphous. It is this rather loose structure which gives rubbers (natural rubber or *cis*-polyisoprene, butadiene rubber, styrene-butadiene rubber, butyl rubber, etc.) their softness and flexibility. The molecular weight of uncrosslinked rubber is very high and the crosslink density of vulcanized rubber is much less than that of crosslinked thermosetting plastics. The crosslinks in rubber are responsible for their recovery from large strains. A schematic sketch of a lightly crosslinked rubber is shown in Fig. 2.6. It may be noted that the presence of double bonds in the chains allows the crosslinks to be created subsequently. It has also been pointed out [4] that a double bond between two carbon atoms which are located on the chain backbone, with the double bond itself not located inside a ring, causes inefficiency of packing, which enhances molecular mobility.

2.4.4 MOLECULAR WEIGHT DIFFERENCES BETWEEN FIBRES AND PLASTICS

As stated earlier, nature prefers to design fibres of very high molecular weight. Natural rubber, which is tapped from a rubber tree, also has

extremely high molecular weight. This has to be reduced by milling before the rubber can be processed.

When a polymer is synthesized for use both by the plastics industry and the fibre industry, the molecular weight is generally relatively low in the case of polymer to be used as a fibre. The actual limits of molecular weight are determined on the basis of property requirements. In the case of polyamides, which are hydrogen-bonded, a molecular weight of $18\,000\,\mathrm{g\,mol^{-1}}$ is adequate for fibres for apparel use. For tyre cord, a molecular weight of $24\,000\,\mathrm{g\,mol^{-1}}$ or above is preferred. The same polymer used for moulded products will have a molecular weight of $75\,000\,\mathrm{g\,mol^{-1}}$ or so. In the case of polypropylene, where the intermolecular bonding is of the weak van der Waals type, the fibre-grade polymer will have a molecular weight of $60\,000\,\mathrm{g\,mol^{-1}}$ or so, while for mouldings, the molecular weight may be about $150\,000\,\mathrm{g\,mol^{-1}}$. While the property requirement is the prime determinant, processability requirements also play a very important part. The most important structural variable determining the flow properties of polymers is molecular weight or chain length $\langle z \rangle$; the melt viscosity is related to $\langle z \rangle^{3.4}$. Thus low molecular weight ensures a melt of low viscosity which is easier to handle. Further advantages of low molecular weight are the ease of orientation and the higher crystallization rate. Finally, at very high molecular weights, the spinnability can be poor and fibre breaks during spinning can become significant. However, polymers with higher molecular weights can be spun by solution- or gel-spinning. It has been reported [5] that ultra high molecular weight, high density polyethylene, which is unprocessable by the standard melt-spinning process, shows minimum viscosity over a very narrow temperature window (150–152 °C) in which it forms a highly mobile hexagonal crystalline mesophase. This opens the possibility of using the liquid crystal spinning technique with this flexible system.

2.5 FIBRE MORPHOLOGY

Flexible chain, semicrystalline thermoplastics form the basis of a number of important commodity plastics and fibre-forming polymers. These are converted to plastics products and manufactured fibres mostly through melt-processing but sometimes through solution-processing. Under quiescent conditions, spherulites containing lamellar ribbons are formed as the melt cools; these are unoriented in the macroscopic sense but are not homogeneous at a molecular level. The solutions, on the other hand, give rise to different morphologies depending upon polymer concentration. Very dilute solutions lead to folded chain lamellae; with increasing concentration, multilamellar structures form, ultimately resulting in a spherulite.
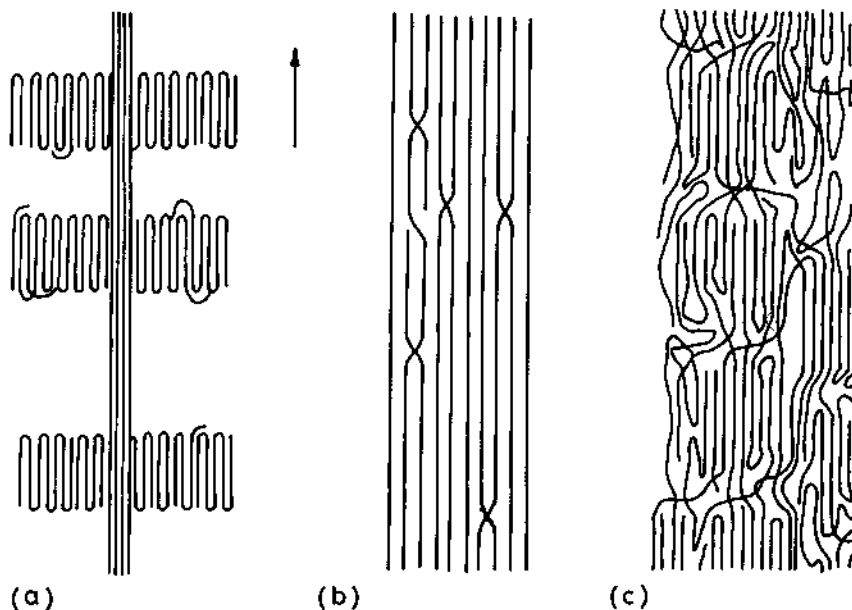
Fig. 2.8 The morphologies of some oriented products: (a) shish kebab, (b) gel-spun and drawn high density polyethylene fibre, and (c) nylon 6 fibre (Fig. 2.8(c) adapted from reference [6]).

For crystallization to occur in the fibrous form, the chains have to be stretched first. This may be achieved in different ways. If a dilute polymer solution is agitated by stirring, the elongational flow field stretches the longest molecules preferentially and around these nuclei lamellar chain-folded crystals form during cooling; such structures are called shish kebab (Fig. 2.8(a)). The second route to such anisotropic products is through the spinning of a gel and then drawing the gel-spun filament. The resultant product has a structure composed predominantly of extended molecules (Fig. 2.8(b)). The third method of producing oriented products is the conventional melt- or solution-spinning of flexible chain polymers by extruding a melt or a solution in an elongational field and then, in a subsequent operation, drawing the spun filament in the solid state; the resultant morphology is schematically illustrated in Fig. 2.8(c) [6]. It may be noted that there are significant differences in molecular organization between the above models and they lead to very significant differences in physical properties. Though the model shown in Fig. 2.8(c) is for nylon 6 fibres, a number of other important manufactured fibres like PET, nylon 66 and polypropylene, which are melt-spun, have broadly speaking similar morphology; all of them are semicrystalline with different degrees of crystallinity. The properties of all these fibres

are generally interpreted in terms of two-phase models. The structure shown in Fig. 2.8(b) is representative of ultra high molecular weight, high density polyethylene fibre made by drawing of gel-spun fibre. Kevlar^{TM} fibre has a similar morphology. Both Kevlar and nylon 6 are high performance fibres and their moduli and strengths are much higher than those of conventional fibres. The shish kebab structure shown in Fig. 2.8(a) has too few extended molecules and very limited chain continuity along the fibre axis; it has therefore little practical use-fulness due to its poor mechanical properties [7]. The differences in properties are mainly related to the roles played by the two phases; in products represented by Fig. 2.8(b), the crystalline phase plays a pre-dominant role while the amorphous phase plays a more significant role in products represented by Fig. 2.8(c).

  In a semicrystalline polymeric fibre, the crystallites make a significant contribution to the macroscopic stiffness, strength, durability, thermal resistance and stability of the fibre. The amorphous phase is more loosely packed compared with the crystalline phase and contributes mainly to the extensibility, pliability, recovery, moisture uptake and dyeability.

  The various fibre-forming polymers crystallize at very different rates, poly(ethylene terephthalate) crystallizing very slowly while polyamides and polypropylene crystallize very rapidly. The two stages of crystalliza-tion involve first the local ordering of chains (nucleation), followed by addition of other chains (growth). The rate of crystallization increases with increased supercooling but is retarded by the increasing viscosity as the temperature is reduced. There is, therefore, a maximum in the rate–temperature curve which is about midway between the glass transi-tion temperature and the melting point [8].

2.6 THERMAL TRANSITIONS

The two important thermal transitions in a semicrystalline polymer are the glass transition and melting; the respective temperatures of these transitions are denoted by T_g, which is characteristic of the amorphous phase, and T_m, which relates to the crystalline phase. While T_m is a primary transition involving change of phase from a solid to a liquid, T_g is a secondary transition; the molecules are glass-like below T_g because of very limited molecular mobility and rubber-like above T_g when large segments of the molecule become mobile. Thermal transi-tions can be mapped with the help of a dilatometer, which measures the volume expansion of the polymer as a function of temperature. The dependence of specific volume of an amorphous and a semicrystalline polymer on temperature is shown in Figs 2.9(a) and (b), respectively. In both cases the specific volume increases with increase in temperature.
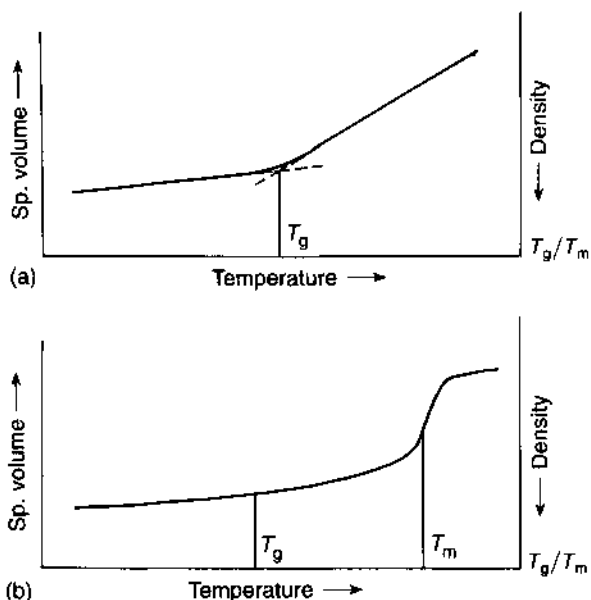
Fig. 2.9 Specific volume–temperature curves for (a) amorphous and (b) semicrystalline polymer.

However, in the case of the amorphous polymer (Fig. 2.9(a)), the rate of change of specific volume increases quite noticeably above T_g and the polymer continues to be rubber-like. In the case of the semicrystalline polymer (Fig. 2.9(b)), the amorphous portions 'melt' or 'soften' at T_g [4] while the crystalline portions remain 'solid'. Consequently the change of slope at T_g is not so great but there is a discontinuity in specific volume at the melting point. An amorphous polymer does not have a conventional melting point; on progressive heating it passes from a brittle solid to a rubber-like solid which then becomes a highly viscous liquid.

2.6.1 GLASS TRANSITION TEMPERATURE

A very simple explanation of the glass transition temperature is given in Fig. 2.10 in terms of the free volume theory, where the free volume is assumed to be the difference between the total volume and the occupied volume; the latter is assumed to be independent of temperature (this assumption is not strictly correct since, because of local thermal vibrations, the occupied volume also increases with temperature). On this model, above T_g enough free volume becomes available for rotation of molecular segments about 25 carbon atoms long, leading to a more rapid increase of specific volume. This makes the polymer soft and flexible.
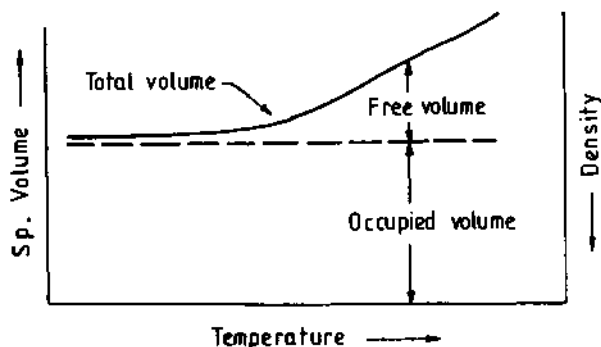
Fig. 2.10 Free volume explanation of the specific volume–temperature curve.

We next consider the transition from the rubber-like state to the glassy state as the sample is cooled. This transition is more relevant to the behaviour of the amorphous phase in the fibre during its manufacture. As the temperature of the polymer in the rubbery state is lowered, the equilibrium state corresponding to a new temperature is attained after some time during which the kinetic units of the polymer occupy the new equilibrium state. These relaxation processes are accomplished only if sufficient time is given to the polymer in the new state. Moreover, as the temperature is lowered, the increase in relaxation time, being generally governed by an exponential law, is very large. Near T_g the relaxation time becomes so large that, under normal cooling rates, the equilibrium state of the polymer and the corresponding structure are rarely achieved. The glassy state is thus generally a metastable state in which the polymer may exist for an infinitely long time. The cooling rate effect with polystyrene is as follows: at a cooling rate of $1\,°\text{C}\,\text{min}^{-1}$, T_g is found to be $105\,°\text{C}$, while at a cooling rate of $1\,°\text{C}\,\text{day}^{-1}$, it is $100\,°\text{C}$ [9]. This effect also manifests itself when T_g is measured by different methods. For example, the T_g of PMMA has been reported as follows: thermal method (time $10^4\,\text{s}$) $100\,°\text{C}$; penetrometry ($10^2\,\text{s}$) $120\,°\text{C}$; and rebound elasticity ($10^{-5}\,\text{s}$) $160\,°\text{C}$ [10]. The T_g of a textile fibre is frequently reported as the temperature of the mechanical loss tangent peak, although it is significantly greater than the equilibrium T_g. The theories of T_g invariably treat the observed value of T_g as a kinetic (rate-dependent) manifestation of an underlying thermodynamic phenomenon [4].

The T_g and T_m (melting point) values of some polymers are given in Table 2.2. Elastomeric or rubbery materials have a T_g or softening temperature below room temperature, whereas brittle, rigid materials have a T_g above room temperature.

With few exceptions, polymer structure affects the glass transition (T_g) and the melting point (T_m) similarly. This is not unexpected, since

Table 2.2 Values of T_g and T_m for some polymers

Polymer	T_g (°C)	T_m (°C)
Polyethylene	−120	137
Isotactic polypropylene	−10	176
Polybutadiene	−85	−
cis-Polyisoprene (natural rubber)	−73	−
Atactic polystyrene (amorphous)	100	−
Isotactic polystyrene (semicrystalline)	100	240
Polyvinyl chloride (isotactic)	87	227
Poly(ethylene terephthalate)	69	265
Nylon 6	50	220
Polyacrylonitrile	100	320[a]

[a] Estimated.

similar considerations of cohesive energy and molecular packing apply to both the amorphous and crystalline regions. T_m and T_g are rather simply related for many polymers, depending on symmetry; T_g (K) is approximately one-half to two-thirds of T_m (K). There are, however, some exceptions to the general rule.

The effect of structural factors on T_g can be considered in terms of the observation that the thermal energy supplied to the polymer overcomes two types of resistance to large-scale motions of its components, namely the cohesive forces holding the components together and the inherent inflexibility of the chain segments [4]. The intrachain effect is more important than the interchain effect in determining the value of T_g. The simplest approach to understanding the structural dependence of T_g considers the glass transition temperature in terms of the free volume concept discussed earlier. Both chemical and physical factors affect T_g and by and large the factors which enhance free volume lower the T_g of the polymer, and vice versa. The presence of highly polar groups along the polymer chains has the effect of increasing the intermolecular forces, bringing the chains closer together; this reduces the free volume. Polar polymers therefore have relatively high T_g values. However, a more important factor is the steric effect of the chain substituent groups. Stiff and bulky side groups, which inhibit the free rotation of the chain segments, increase T_g, whereas flexible side groups, which tend to hold the chains apart, free their motions and decrease T_g.

Chain flexibility and symmetry lower T_g while crosslinking raises T_g. The glass transition temperature is also affected by molecular weight, crystallinity, orientation, morphology and additives. Molecular weight has only a small effect within the range in which polymers become useful. The general dependence can be depicted as shown in Fig. 2.11. At low molecular weight the effect is dramatic, but in the range when it is a useful polymer the effect is relatively small. The effect of crystallinity
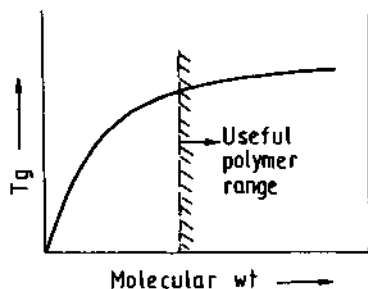
Fig. 2.11 The dependence of T_g on molecular weight.

and orientation may be illustrated with respect to PET fibre. The as-spun fibre is amorphous and unoriented and has a T_g of 67 °C. If it is heat-set in this state, it crystallizes in a random form and the T_g rises to about 100 °C. If the spun filament is first stretched and then heat-set, the oriented and crystalline PET filament has a T_g of 125 °C.

2.6.2 THE MELTING PHENOMENON

At the melting point, equilibrium exists between the liquid and crystal phases. The equilibrium melting point of a crystal is given by ΔH_m (enthalpy of melting)/ΔS_m (entropy of melting). This definition only applies to crystals of infinite size (no surface effects) which contain only equilibrium defects, if any. In reality the crystals in the fibres are meta-stable and contain non-equilibrium defects. The melting point of a fibre may, however, also be considered in terms of the thermodynamic relationship given above. The simplest approaches identify large heat of fusion with strong intermolecular forces. It has been pointed out that attempts to correlate the melting points of polymers with intermolecular interactions, utilizing the cohesive energy density of the repeating units as a measure of these interactions, have been notably unsuccessful. No simple correlation is observed between melting point and ΔH_m, as is clear from the extensive data available in the literature. It was therefore thought that ΔS_m is more likely to be of prime importance in establishing the value of the melting point.

In the thermodynamic equation the heats and entropies of fusion represent the differences in enthalpy and entropy between the liquid and crystalline states; it is therefore necessary that both these states of matter should be considered in any interpretation of the melting point. On this basis the high melting point of polyamides is due to the low entropy of the liquid phase (perhaps due to the presence of hydrogen bonds), while the low melting point of aliphatic polyesters results chiefly from a low heat of fusion.

In melting and many other physical characteristics of typical fibres, the concepts developed by polymer physicists [8, 11] provide the basic framework. The application of these ideas to polymeric fibres in a suitable manner allows a more comprehensive understanding not only of their physical properties, but also of their structure and morphology.

REFERENCES

1. Mascia, L. (1982) *Thermoplastics: Materials Engineering*, Applied Science Publishers, London, p. 14.
2. Sharples, A. (1966) *Introduction to Polymer Crystallization*, Edward Arnold (Publishers) Ltd., London, p. 119.
3. Campbell, I.M. (1994) *Introduction to Synthetic Polymers*, Oxford University Press, Oxford.
4. Bicerano, J. (1993) *Prediction of Polymer Properties*, Marcel Dekker Inc., New York.
5. Waddon, A.J. and Keller, A. (1990) *J. Polym. Sci., Polym. Phys. Ed.*, **28**, 1063.
6. Murthy, N.S., Reimschuessel, A.C. and Kramer, V. (1990) *J. Appl. Polym. Sci.*, **40**, 249.
7. Frank, F.C. (1970) *Proc. Roy. Soc.*, **A319**, 127.
8. Birley, A.W., Haworth, B. and Batchelor, J. (1991) *Physics of Plastics*, Hanser Publishers, Munich,.
9. Bueche, F. (1962) *Physical Properties of Polymers*, Wiley-Interscience, New York, p. 100.
10. Elias, H.G. (1984) *Macromolecules I*, 2nd edn, Plenum Press, New York, p. 412.
11. Gedde, U.W. (1995) *Polymer Physics*, Chapman & Hall, London.

Basic principles of fluid flow during fibre spinning

3

V.B. Gupta and Y.C. Bhuvanesh

3.1 INTRODUCTION

The inspiration and the knowledge needed to develop the spinning techniques used for fibre manufacture were provided by the spider and the silkworm. These creatures showed that the following steps were required for extruding thin continuous filaments: (1) acquisition of spinnable liquid, (2) jet formation, and (3) jet hardening. Add to this bobbin winding, and we get manufactured fibres in the spun state. The manufactured fibres may need further drawing so that they have adequate properties.

In the manufacture of polymeric fibres, the polymer in the form of a melt or a solution is squirted under pressure through capillaries having diameters typically in the range of 0.002 to 0.04 cm and lengths either equal to or three to four times the diameter. The fluid comes out of the capillary as a thread. It is pulled rapidly onto a winder as it is attenuated and solidified to a thin filament generally of gradually reducing cross-section, which ultimately acquires a uniform final cross-sectional shape or a constant diameter (a typical final diameter is 0.002 cm or 20 μm).

The first spinnable fluids were solutions of cellulose nitrate (celluloid) in a mixture of alcohol/ether solvent, the solidification of the jet being achieved by solvent evaporation.

The second method of fibre production to be developed was the viscose process, in which a solution of cellulose was solidified by chemical coagulation. Polyacrylonitrile that is largely atactic is often spun by this method.

The third method arrived with the development of a melt-stable material (nylon 66) and used jet solidification by freezing it. Poly(ethylene terephthalate) (PET), nylon 66, nylon 6 and isotactic polypropylene are all spun by this technique.

The first, second and third methods referred to above are now well-established techniques and are known as dry-spinning, wet-spinning, and melt-spinning, respectively. Melt-spinning is the youngest and most economical of the three processes.

Melt-spinning is also the simplest and technologically the most elegant method of producing filaments. Solidification of the melt thread involves only heat transfer, whereas in dry-spinning it also involves one-way mass transfer and in wet-spinning two-way mass transfer. The result is that fast production rates become possible and the melt-spun filaments are smooth and circular. Thermal stability of the polymer melt is a prerequisite for melt-spinning. Polymers that do not give a stable melt are sometimes spun by blending them with volatile or extractable plasticizers before spinning. However, this method is not as widely used as spinning from solutions. The choice between dry- and wet-spinning is made on the basis of a number of factors which are described in Chapter 6. The manufactured fibres produced by the different spinning methods are listed in Table 3.1. Though aromatic polyamides have been included in the wet-spinning (coagulation) category, they are produced by the dry-jet wet-spinning method using liquid crystal spinning technology. Similarly, although polyethylene filaments from fibre-grade polyethylene are produced by melt-spinning, ultra high molecular weight, high density polyethylene is converted to high performance fibres using the gel-spinning technique. These special techniques of fibre manufacture will be described in Chapter 18.

Table 3.1 Manufactured fibres produced by the different spinning methods

Melt-spinning	Solution spinning		
	Dry-spinning	Wet-spinning: direct solvent	Wet-spinning: derivative-based
Nylon 66	Cellulose diacetate	Acrylic (e.g. Courtelle^{TM}, Acrilan^{TM})	Viscose rayon
Nylon 6	Cellulose triacetate Acrylic (e.g. Orlon^{TM})	Modacrylic Rayon (Tancel^{TM})	
PET	Polyurethane (e.g. Lycra^{TM})	Polyurethane (e.g. Vyrene^{TM})	
Polypropylene	Polyvinyl chloride	Polyvinyl alcohol	
Polyethylene	Chlorinated PVC	Aromatic polyamide	

The quality of the spun filament determines its subsequent behaviour – if the spun filament is uniform and homogeneous, the drawn, treated commercial filament will also be uniform and homogeneous. Its properties, e.g. mechanical properties and dyeability characteristics, will also be uniform, which is a highly desirable feature. If the spun filament is not uniform and homogeneous, the final filament will show regions of weakness and its dye absorption will be non-uniform, putting it at a disadvantage and making it uncompetitive.

The spinning processes described above involve the flow of polymer fluids, namely melts and solutions, and a brief consideration of fluids as materials and the mechanism of fluid flow will therefore be in order at this stage. It is well known that substances can exist in three states of aggregation: as gas, liquid and solid. The state of aggregation of a substance is determined by the relation between the average kinetic energy and the average potential energy of interaction between molecules of the substance [1]. In gases, the average kinetic energy is much higher than the average potential energy of interaction between molecules. On the other hand, in solids the absolute value of the average potential energy of molecular interaction is much higher than the average kinetic energy. In liquids these values are nearly equal. A consequence of this is that the liquid state shows short-range order but no long-range order, unlike the solid state, which is characterized by both short-range and long-range order, or the gaseous state, which shows no order. It must be emphasized that this categorization is not unambiguous as a material like pitch can behave as a solid or a liquid at different time scales.

In low molecular weight fluids at rest, there is a continuous change of neighbours as molecules jump from one position to another. In polymeric fluids, on the other hand, the change of neighbours may involve, according to a widely accepted model described later, rotatory segmental jumps, as illustrated in Fig. 2.1. Since in the quiescent state the number of jumps in any one direction is the same as the number of jumps in other directions, there is no net transport of the liquid in any direction. This phenomenon is known as self-diffusion. If, however, the liquid is subjected to an external stress, there is preferential movement in the direction of the stress and we get flow. This is known as viscous flow. The ease with which a given molecule may change its neighbours is related to an important property of a liquid, namely its viscosity. According to this model, flow becomes possible when the molecules acquire the necessary 'activation energy' to break away from the attractive forces which bind them to their neighbours. The activation energy for flow was determined by Kauzmann and Eyring [2] for a series of hydrocarbons of the paraffin type with various chain lengths. In Fig. 3.1 the resulting values of the activation energy are plotted against the number of carbon atoms in the chain [2]. It can be seen that the activation
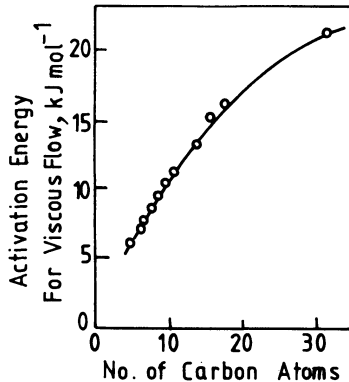
Fig. 3.1 Dependence of the activation energy for viscous flow of paraffins on the number of carbon atoms in the chain [2].

energy first increases almost in proportion to the number of carbon atoms, but with further increase in chain length the rate of increase of the activation energy becomes slower, approaching a limit for a chain length of about 25 carbon atoms. This suggests that the unit which moves during flow is not the whole molecule but a short segment of the chain. A similar observation was made by Flory [3], who measured the viscosity at constant temperature and pressure of a wide range of polydecamethylene adipates. He found that the activation energy of viscous flow levels off to a constant value; the size of the jumping segment overcoming the barrier is approximately the same for the various samples. Recently there have been significant developments in our understanding of the molecular basis of fluid flow; some of the models are reviewed in Section 3.4.

The production of all spun filaments involves fluid flow and therefore it is important to first describe the basic underlying principles relating to the flow of fluids in the spinneret channel and then in the spinline. In this chapter an attempt has been made to deal briefly with these two aspects. In addition a brief review is made of the molecular theories of flow and the concept of spinnability. The problems of flow instabilities are also considered.

3.2 SHEAR FLOW

3.2.1 VISCOUS FLOW AND NEWTONIAN FLUIDS

The response of a liquid to an externally applied force can be illustrated with the help of Fig. 3.2, which shows a block of fluid contained between two parallel planes, each of area A cm^2, and h cm apart (Fig. 3.2). When a
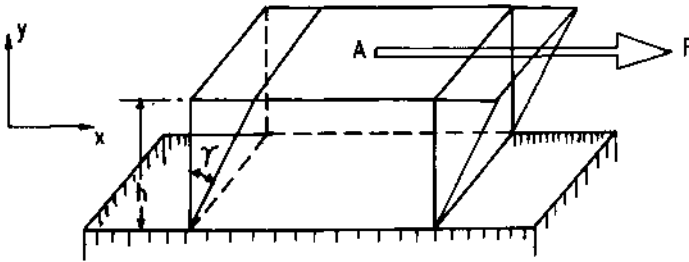
Fig. 3.2 Deformation of a block of fluid subjected to a shear force.

force of F dyn is applied to the upper plane, the shear stress τ acting on this plane (F/A dyn cm^{-2}) causes it to move with a certain velocity relative to the lower plane. This flow is called streamline or laminar flow and is visualized as one set of parallel material planes sliding over another. The angle γ is a measure of shear strain.

In Fig. 3.3, C and D represent two streamline layers of the liquid flowing under steady conditions. The two light particles P and Q, placed in the layers C and D respectively, are a distance δy apart at a time t such that the line joining them is at right angles to the parallel streamlines (Fig. 3.3), that is along the direction y. The speed of liquid flow will be slightly different along the two streamlines so that after a further time δt, particle P has moved to P' while particle Q has moved to Q'. The line joining P'Q' is at an angle $\delta\gamma$ to the y axis, which is a measure of shear strain. The rate of shear is $\delta\gamma/\mathrm{d}t$.

If the velocity of liquid flow along streamline C is u, and that along D is $u + (\mathrm{d}u/\mathrm{d}y)\,\delta y$, where δy is along the y axis, then in time δt the particle P moves a distance $u.\delta t$, while particle Q moves a distance $[u + (\mathrm{d}u/\mathrm{d}y)\,\delta y]\,\delta t$. Now

$$\delta\gamma = \frac{\left[u + \dfrac{\mathrm{d}u}{\mathrm{d}y}\delta y\right]\delta t - u\,\delta t}{\delta y} = \frac{\mathrm{d}u}{\mathrm{d}y}\delta t. \tag{3.1}$$
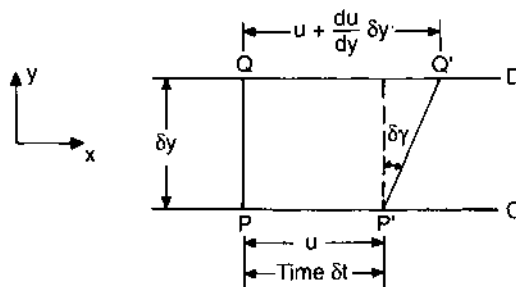
Fig. 3.3 The flow of streamline layers of a fluid under steady conditions.

So, in the limit,

$$\frac{d\gamma}{dt} = \frac{du}{dy}. \tag{3.2}$$

Thus the rate of shear of the liquid is equal to the velocity gradient normal to the direction of flow.

For a number of liquids undergoing laminar flow, Newton observed that the shear stress acting over surfaces parallel to the direction of flow needed to maintain a given shear rate is proportional to the shear rate. Thus

$$\tau \propto d\gamma/dt \quad \text{or} \quad \tau = \eta \, d\gamma/dt, \tag{3.3}$$

where η is a constant for a given liquid at a given temperature and pressure. A liquid for which the above relationship holds is termed 'Newtonian' and η is known as the coefficient of viscosity or shear viscosity.

It may be noted that the unit of shear rate is reciprocal second (s^{-1}) and that of viscosity is $N\,s\,m^{-2}$ or $Pa\,s$ in SI units, or $dyn\,s\,cm^{-2}$ in the CGS system. If a force of 1 dyn acting on $1\,cm^2$ area results in a shear rate of $1\,s^{-1}$, then the viscosity is $1\,dyn\,s\,cm^{-2}$ or $0.1\,Pa\,s$ (or 1 poise).

3.2.2 CAPILLARY FLOW

In a spinning head the melt or solution has to pass through a capillary where it takes the shape of a fibre. The law governing fluid flow through a capillary was first derived by Poiseuille. He assumed a steady flow of liquid through a cylindrical narrow tube of circular cross-section under a pressure gradient. The flow is assumed to be streamline and the pressure constant over any cross-section, that is no radial flow occurs. In a liquid in which the flow is laminar, adjacent layers of liquid travel with different speeds. The layer immediately in contact with the wall is adsorbed to that surface and is therefore, from a macroscopic point of view, at rest relative to the surface. This adsorbed layer is in dynamic equilibrium, as molecules are continually being removed as a result of collision with other molecules, and different molecules take their place.

The construction shown in Fig. 3.4 helps us to set up an equation to describe the flow of an incompressible, Newtonian liquid of density ρ and viscosity η through a capillary of radius R and length L. The velocity of the liquid in contact with the wall may be taken as zero, assuming no slip. Symmetry considerations indicate that the velocity distribution in the capillary will be symmetrical about the axis of the tube and have its maximum value on this axis, as shown in Fig. 3.5. Let the velocity of the layer at a distance r from the axis be V. Consider the forces acting on the liquid in a cylindrical element of radius r, coaxial with the tube (Fig. 3.4).
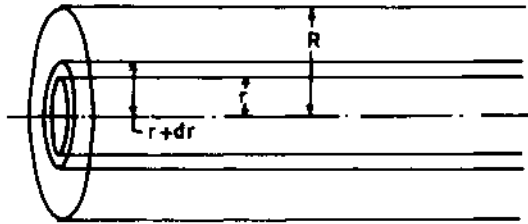
Fig. 3.4 Construction for deriving Poiseuille's equation.

If P is the applied pressure (or more strictly the applied pressure difference between the inlet and outlet of the capillary), the accelerating force acting on the liquid cylinder of radius r is $P\pi r^2$. The viscous drag or retarding viscous force exerted on the surface of this liquid cylinder by the remainder of the liquid is $\tau \times 2\pi r L$, where τ is the shear stress ($\tau = \eta\, dV/dr$, assuming the fluid to be Newtonian) acting on a fluid layer at a distance r from the axis. When the conditions are steady, these two forces must be equal and opposite, i.e.

$$P\pi r^2 = -\tau \times 2\pi r L = -\eta\left(\frac{dV}{dr}\right) \times 2\pi r L \quad \text{or} \quad \frac{dV}{dr} = -r\frac{P}{2\eta L}. \quad (3.4)$$

The velocity gradient or shear rate is thus proportional to r, the distance from the axis of the tube, and vanishes at the axis.

The shear stress τ across the capillary is given by $\tau = -Pr/2L$ and is thus a maximum at the capillary walls and zero at the axis of the capillary.

At the wall of the tube $r = R$ and velocity $V = 0$. Integrating equation (3.4) from $r = R$ to $r = r$, we have

$$R^2 - r^2 = \frac{4\eta L V}{P} \quad \text{or} \quad V = \frac{P}{4\eta L}(R^2 - r^2). \quad (3.5)$$

The profile of the advancing liquid is therefore a parabola.

The volume of the liquid, dQ, flowing through the tube per second is

$$dQ = 2\pi r V\, dV. \quad (3.6)$$
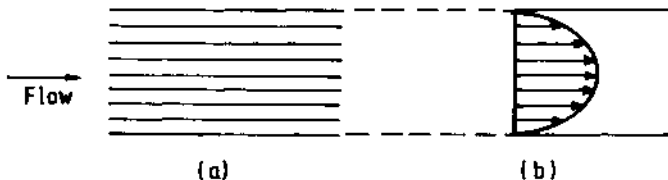
Fig. 3.5 Fluid flow through a capillary: (a) laminar flow, (b) parabolic velocity profile.

Hence the total volume of liquid flowing through the tube per second, is

$$Q = \int_0^R \frac{P\pi}{2\eta L}(R^2 - r^2)r\,dr = \frac{\pi PR^4}{8\eta L}. \tag{3.7a}$$

We may rearrange this as

$$\eta = \frac{\pi PR^4}{8QL}. \tag{3.7b}$$

Equation (3.7b) is known as Poiseuille's equation. The volume of liquid flowing out of the capillary per second, Q, is seen from equation (3.7a) to be directly proportional to the applied pressure and depends on the fourth power of the capillary radius. Thus the capillary radius is a very important parameter in fluid flow. The treatment so far is based on two assumptions: first, that the liquid is Newtonian, and second, that all the energy supplied to push the liquid through the capillary is used to overcome the viscous drag or internal friction or rheological force. Neither of these assumptions is valid for molten polymers and polymer solutions which are non-Newtonian and viscoelastic. It is therefore necessary to take account of these two factors when computing viscosity.

3.2.3 NON-NEWTONIAN FLUIDS

Water, simple organic liquids, true solutions, dilute suspensions and emulsions and gases are in general Newtonian in character. For them a plot of rate of shear, $d\gamma/dt$ or $\dot{\gamma}$, against shear stress, τ, is a straight line passing through the origin, provided that flow is laminar. Many materials of interest to fibre manufacturers, such as polymer melts and solutions, do not exhibit the simple characteristics of a Newtonian fluid. Non-Newtonian behaviour may be considered under two categories: time-independent fluids and time-dependent fluids.

Time-independent fluids, like Newtonian fluids, are fluids in which the rate of shear is a function of the shearing stress. Time-dependent fluids are more complex systems in which shear stress–shear rate relationships depend on how the fluid has been sheared and on its previous history. The rheological characteristics of these two types of fluids are briefly described here.

(a) Time-independent fluids

The shear stress–shear rate curves for four kinds of time-independent fluids are shown in Fig. 3.6 (note that as per convention the shear stress is plotted on the x axis and the rate of shear on the y axis). Line A represents the behaviour shown by a Newtonian fluid, as discussed earlier. In this case, it is only necessary to make one determination at a single rate
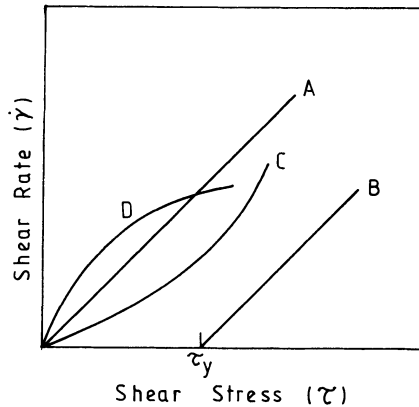
Fig. 3.6 The shear stress–shear rate curves for different categories of fluids (see text).

of shear. Line B is a representation of an idealized Bingham body which is considered to have a connected internal structure that collapses above a yield stress, τ_y. Above the yield stress, the shear rate increases linearly with shear stress, i.e.

$$\eta\dot{\gamma} = (\tau - \tau_y), \qquad \text{where} \qquad \tau \geq \tau_y. \tag{3.8}$$

Pottery clay, chocolate, toothpaste, butter and putty approximate in their behaviour to Bingham bodies, although the τ–$\dot{\gamma}$ relationship above may be non-linear in some cases, mostly pseudoplastic (like curve C) with a yield value (not shown in the figure).

Curve C represents pseudoplastic flow; it commences at the origin, is linear at low shear rates and then becomes convex to the stress axis. Polymeric fluids are generally of this type. As shown in Fig. 3.7, the viscosity, which is defined as the ratio $\tau/(d\gamma/dt)$ and designated apparent viscosity, is no longer a constant but decreases as the rate of shear is increased. Since the slope of the line OP_2 (which is equal to fluidity or reciprocal of viscosity) is greater than that of OP_1, it follows that $\eta_2 < \eta_1$. An alternative method of estimating apparent viscosity is to take the local slope of the τ–$\dot{\gamma}$ plot at the required shear rate; however, the former method is more often used to characterize viscosity. This type of behaviour is termed 'pseudoplastic' or 'shear-thinning'. Many industrial materials including polymer melts and solutions, natural resins, rubbers, bitumens and heavy oils exhibit pseudoplastic behaviour. The reduction in viscosity with an increasing rate of shear implies that the stresses required to produce high rates of flow are not as high as would be expected from measurements of viscosity at low shear rates. The decrease in viscosity is really an advantage because it reduces the power requirements for processing to a considerable extent.
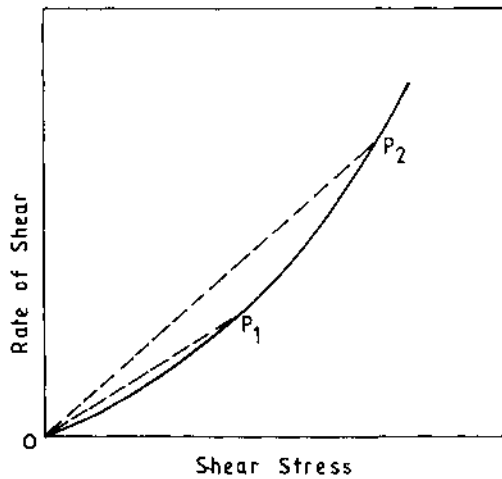
Fig. 3.7 Estimation of viscosity of a pseudoplastic fluid.

The shear-thinning behaviour of polymeric fluids is attributed to the extensively entangled and randomly oriented nature of the long-chain molecules (Fig. 3.8). As the shear rate increases, the molecules tend to become aligned and points of entanglements are reduced. The rate of loss of existing entanglements is higher but not the rate of generating new ones, so that the number of entanglements in a given volume of material has lower equilibrium values at larger shear rates. Consequently the frictional resistance between adjacent layers of the laminar fluid decreases. The fluid thus exhibits a 'shear-thinning' effect and the viscosity decreases. At very high shear rates, the orientation of the molecules may be complete and in this range near-Newtonian behaviour may be observed, as in the very low shear rate region.
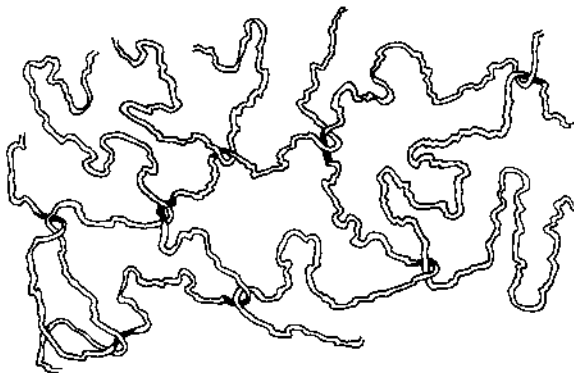
Fig. 3.8 An entangled molecular network.

A number of empirical equations have been proposed [4] to describe pseudoplastic fluids. The equation that has found very wide acceptance is the power-law equation, also known as the Ostwald–de Waele equation. This takes the form:

$$\tau = k(\dot{\gamma})^n \tag{3.9}$$

where k and n are constant, n being less than unity for pseudoplastic fluids. Sometimes this relationship is written as

$$\dot{\gamma} = A\tau^p. \tag{3.10}$$

If we put $p = 1/n$ and $A = (1/k)^{1/n}$, the two equations are seen to be equivalent.

Equation (3.9) may be written in logarithmic form as

$$\log \tau = \log k + n \log \dot{\gamma}. \tag{3.11}$$

Thus it would be expected that a plot of $\log \tau$ against $\log \dot{\gamma}$ should give a straight line with positive slope from which the constants k and n can be found. For polymer melts, such plots give straight lines over a few decades of shear rate but depart from linearity at higher shear rates.

For a pseudoplastic fluid, the apparent viscosity can thus be written as

$$\eta_{\mathrm{app}} = \tau/\dot{\gamma} = k(\dot{\gamma})^{n-1}. \tag{3.12}$$

Sometimes the following approach is taken to eliminate k. If η_{app} is the apparent viscosity at some shear rate $\dot{\gamma}$ and η'_{app} is the apparent viscosity at some arbitrary reference shear rate $\dot{\gamma}'$, then it follows that

$$\eta_{\mathrm{app}}/\eta'_{\mathrm{app}} = (\dot{\gamma}/\dot{\gamma}')^{n-1}. \tag{3.13}$$

If $\dot{\gamma}'$ is put equal to $1\,\mathrm{s}^{-1}$, equation (3.13) simplifies to

$$\eta_{\mathrm{app}} = \eta'_{\mathrm{app}}(\dot{\gamma})^{n-1}, \tag{3.14}$$

where η'_{app} is the approximate viscosity at a shear rate of $1\,\mathrm{s}^{-1}$. This approach is elaborated upon further in Chapter 14.

The next category of flow is dilatant flow, shown by curve D in Fig. 3.6. The behaviour is characterized by a curve which passes through the origin, remains linear at low shear rates and then shows non-linear increase, becoming concave to the stress axis. Dilatant materials thus show an increase in apparent viscosity with an increase in shear rate. This type of behaviour has led them to be designated as 'shear-thickening' fluids.

Dilatancy is often exhibited by highly concentrated suspensions, particularly PVC pastes. The irregularly shaped particles are closely packed with minimum voids in the stress-free state. At low shear rates the solid particles do not make much contact while at high shear rates the particles do not pack easily and the rubbing friction enhances the resistance

to flow. Such behaviour has also been observed in sand–water suspensions, clay suspensions and printing inks.

The power-law equation $\tau = k(\dot{\gamma})^n$, with $n > 1$, is the equation most used to represent dilatant behaviour.

(b) Time-dependent fluids

When the shear stress changes in Newtonian, dilatant or pseudoplastic liquids, as well as in Bingham fluids above the flow limit, the corresponding shear rate or the corresponding viscosity is reached almost instantaneously. In some liquids viscosity depends on time. If at a constant shear stress or constant shear rate the viscosity falls as time increases, then the liquid is termed thixotropic. If the apparent viscosity increases with time, the liquid is termed rheopectic. Thixotropy is interpreted as a time-dependent collapse of ordered structure which breaks down to a lower apparent viscosity when sheared.

Most formal studies on time-dependent behaviour have been concerned with reversible effects. A thixotropic fluid rebuilds itself in time if allowed to rest. Paints, shaving cream, margarine, printing ink, etc. are examples of thixotropic materials. A rheopectic material shows time-dependent behaviour in the opposite direction.

3.2.4 VISCOELASTIC FLUIDS

Polymeric fluids are not ideally viscous. This means that not all of the energy supplied to make them flow is used to overcome the resistance to flow due to internal friction; some of it may be stored as elastic energy which relaxes at an appropriate time. The expansion of liquid thread on emerging from the spinneret (Fig. 3.9) is known as 'dieswell'. The amount of expansion is found to be a function of the length of the capillary up to a certain length, beyond which it becomes constant. In polymer melts and solutions, the source of elasticity is believed to be the orientation of molecules that is induced on stressing; this can relax when the load is released. The phenomenon of dieswell is discussed in greater detail later.

3.2.5 APPARENT AND TRUE VISCOSITY

The viscosity that is determined from Poiseuille's equation is called the 'apparent viscosity', and may be very different from the 'true viscosity', which takes the non-Newtonian and viscoelastic nature of the fluid into account.

The viscoelastic nature of the fluid will be considered first. The simplest approach to account for the viscoelastic nature of the fluid in
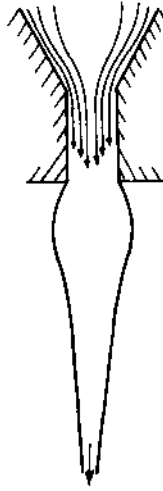
Fig. 3.9 Expansion of the liquid thread on emerging from the spinneret.

capillary flow is that of Bagley [5], illustrated in Fig. 3.10. It is based on the assumption that the effective pressure which is responsible for Poiseuille flow is less than the total applied pressure; some of the applied energy is stored as elastic energy and released as the dieswell effect at the exit of the capillary. If the effective length of the capillary is greater, the transit time of the fluid is higher and the elastic effects can become negligible. A number of dies of different length-to-radius ratios are taken and flow curves are obtained. On plotting pressure against L/R for fixed shear rates, straight lines are obtained (Fig. 3.10) which, on
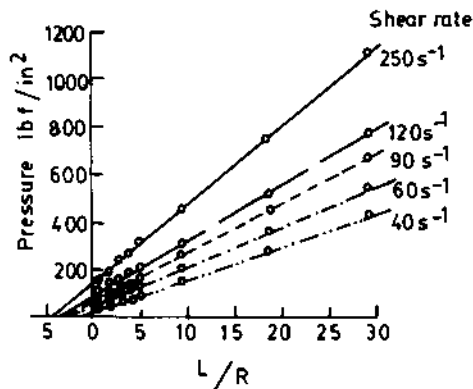
Fig. 3.10 Plot of pressure vs. L/R (length/radius) of the capillary for a polyethylene melt of melt flow index 2.9 for a range of shear rates from 40 to $250\,s^{-1}$. The end correction is given by the negative intercept on the L/R axis [5].

extrapolation, converge to a single point. Taking the effective capillary length as $L + bR$, we have

$$\text{True shear stress} = \frac{PR}{2(L + bR)} = \frac{P}{2[(L/R) + b]}. \quad (3.15)$$

Now at $P = 0$, $b = -L/R$. Hence the Bagley factor b can be read off from the negative intercept and the true stress computed.

The non-Newtonian nature of the fluid is accounted for by making use of equation (3.9), that is

$$\tau = k(d\gamma/dt)^n,$$

which may be rewritten as

$$\tau^{1/n} = \tau^{n'} = k'(d\gamma/dt) \quad (3.16)$$

where $n' = 1/n$. Since $\tau = -Pr/2L$, we get

$$-(Pr/2L)^{n'} = k'(d\gamma/dt). \quad (3.17)$$

Now since $d\gamma/dt = dV/dr$, we may write

$$-(Pr/2L)^{n'} = k'(dV/dr). \quad (3.18)$$

By integration of equation (3.18), the velocity V is obtained and then the flow rate Q comes out to be

$$Q = \frac{\pi R^{n'+3}}{(n'+3)} (P/2L)^{n'}. \quad (3.19)$$

This introduces a correction in the shear rate. The true shear rate $(d\gamma/dt)_{\text{true}}$ comes out to be equal to $[(d\gamma/dt)_{\text{Newtonian}} \times (3 + n')/4]$, where n' is the slope of the double logarithmic plot of shear rate against shear stress.

3.2.6 SOLUTION VISCOSITY

It is common industrial practice to characterize viscosity in a quick and arbitrary manner. The method adopted is to prepare a solution of the polymer in a suitable solvent. The solution is then passed through a capillary and the time (t) needed to flow between two marks is noted. The time of flow for solvent is then measured and noted (t_0). A term relative viscosity is then defined as $\eta_r = \eta/\eta_0 = t/t_0$, where η is the viscosity of the solution and η_0 the viscosity of the solvent. Other viscosity terms are defined as follows:

$$\text{Specific viscosity } \eta_{\text{sp}} = \eta_r - 1$$

and

$$\text{Intrinsic viscosity } [\eta] = (\eta_{\text{sp}}/c)_{c \to 0},$$

where c is the concentration of the solution. Intrinsic viscosity of a polymer solution is determined with the help of a viscometer like the Ubbelohde viscometer, using polymer solution of concentrations up to about 2%.

It may be noted that while Poiseuille's equation allows an absolute measurement of viscosity, the solution methods described above lead to a relative measure which must be calibrated with fluids of known viscosity to obtain the absolute value.

3.2.7 FACTORS AFFECTING SHEAR VISCOSITY

The influence of temperature, molecular weight, shear rate and shear history, molecular structure, and pressure on viscosity will now be considered.

(a) Effect of temperature

The flow behaviour of Newtonian fluids as a function of temperature can generally be described by the Arrhenius equation:

$$\eta_{(T)} = \text{constant} \times \exp\left(E_\eta/RT\right), \tag{3.20}$$

where $\eta_{(T)}$ is the viscosity at temperature T, E_η is the activation energy for flow and R the gas constant.

Inorganic glasses and metals show close to Newtonian behaviour in the fluid-like state. For these fluids plots of $\log \eta_{(T)}$ against $1/T$ give straight lines. The activation energy, E_η, can be estimated from the slopes of these lines.

For polymeric fluids, the linearity in plots of $\log \eta$ against $1/T$ is restricted to a very narrow temperature range, thus indicating that these fluids show a non-Arrhenius type of behaviour. For a wider temperature range, the relationship is non-linear and the apparent activation energy, E_{app}, decreases as temperature increases. This observation may be explained on the basis that viscosity is sensitive to the extra free volume made available by the kinetic agitation as well as by thermal expansion. The temperature dependence of melt viscosity can accordingly be represented by an empirical relationship proposed by Williams, Landel and Ferry [6], which may be expressed in the following form:

$$\log\left(\eta_T/\eta_{T_g}\right) = \frac{-17.44(T - T_g)}{51.6 + (T - T_g)}, \tag{3.21}$$

where T_g is the reference temperature. For a reference temperature T_s, which has a unique value of $T_g + 50\,°C$ [7], the following form of the

Williams, Landel and Ferry (WLF) equation holds:

$$\log(\eta_T/\eta_T) = -\frac{8.86(T - T_s)}{(101.6 + T - T_s)}. \tag{3.22}$$

The variable activation energy for flow, E_η, may be expressed as

$$E_\eta = \frac{4120T^2}{(101.6 + T - T_s)^2}. \tag{3.23}$$

It is noteworthy that equations (3.21) to (3.23) can be derived using an empirical relation proposed by Doolittle [8] for the variation of viscosity with free volume, that is

$$\eta = A\exp(B/v_f), \tag{3.24}$$

where A and B are constants and v_f is the free volume fraction.

The fact that in a polymer the temperature dependence of the viscosity, and the activation energy derived from it, are both independent of the chain length does not mean that the actual value of viscosity is similarly independent of the chain length [9]. Indeed, this is far from being the case. The value of the viscosity is determined by the resultant motion of the molecule as a whole. This resultant motion depends not only on the rate of jumping of individual segments, but also on the way these segmental jumps are related to one another in direction. Because of the complicated form of the molecule in space and the mutual entanglements between molecules, the resultant displacement needs to be carefully estimated.

(b) Effect of molecular weight

The molecular weight dependence in the case of polymer solutions is given by the following empirical relationship:

$$[\eta] = kM^\alpha, \tag{3.25}$$

where $[\eta]$ is the intrinsic viscosity (at infinite dilution), k and α are constants and M is the molecular weight.

For concentrated polymer solutions, when double logarithmic plots of viscosity against concentration are examined, the data appear to fit two straight lines of differing slopes (Fig. 3.11). The straight lines intersect at a critical concentration, C_{crit}. This critical concentration is interpreted as the concentration at which polymer chain entangles and/or close packing of molecular segments first occurs [10]. A critical molar mass is also found in the case of polymer melts (Fig. 3.12). Below the critical molecular weight, the zero shear melt viscosity (η_0) is directly proportional to the weight average molecular weight ($\bar{M}_w$):

$$\eta_0 = k\bar{M}_w. \tag{3.26}$$
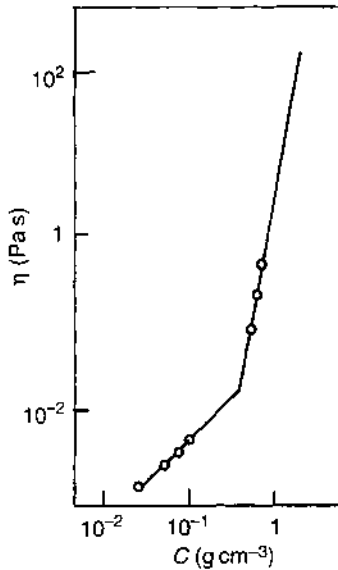
Fig. 3.11 Viscosity of solutions of polyisobutylene of molar mass 40 600 g in toluene at 25 °C as a function of concentration, C (data of J. Schurz and H. Hochberger taken from reference [10]).

In contrast, the viscosity above the critical molecular weight is given by

$$\eta_0 = k' \bar{M}_w^{3.4}. \tag{3.27}$$

Entanglements can only occur when the molecular chains are sufficiently long, that is, when a sufficiently large number, N_{crit}, of chain
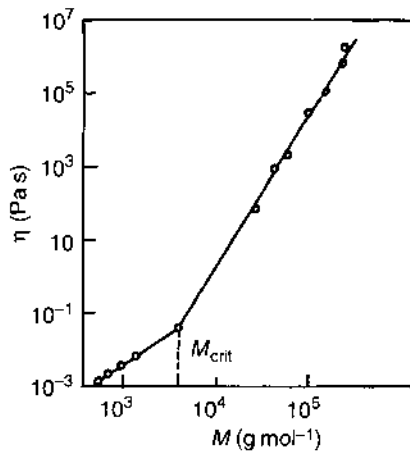
Fig. 3.12 Zero shear rate melt viscosity of unbranched polyethylenes as a function of molar mass M at 190 °C (data of H.P. Schreiber, E.B. Bagley and D.C. West taken from reference [10]). M_{crit} occurs at $\log M = 3.6$.

Table 3.2 Critical chain link number, N_{crit}, of various polymers [10]

Polymer	N_{crit}
Polyethylene	286
1,4-cis-Polyisoprene	296
Atactic polyvinyl acetate	570
Polyisobutylene	609
Atactic polystyrene	730
Polydimethylsiloxane	784

links is present [10]. The tendency to entangle increases with decreasing stiffness of the macromolecule (Table 3.2).

(c) Effect of shear rate and shear history

The shear-thinning nature of polymer fluids and the time-dependent effects have already been described. Irreversible effects due to the shear history of the sample are best illustrated when natural rubber is masticated and are attributed to chain scission or crosslinking which are caused by oxidation or mechano-chemical processes. If the extrudate collected from a capillary viscometer is re-extruded, a reduction in viscosity by a factor of two can occur, provided the shear rate is above the critical shear rate for elastic turbulence to occur [11].

Thus in viscosity measurements, the shear history of the sample can play a significant role and it is advisable to ensure that comparison of flow properties is made between samples having similar shear and heat histories.

(d) Effect of molecular structure

As a general guide, it may be said that the stiffer the polymer chain, the greater the melt viscosity at some reference temperature [12]. This observation is consistent with the WLF equation (3.21), according to which the higher the value of T_g, the higher the viscosity. It follows therefore that those structural factors which affect T_g (these are listed in Chapter 2), and which include chain stiffness, will in general increase the melt viscosity.

(e) Effect of pressure

Since viscosity is related to the distance between molecules [12] and since an increase in pressure will decrease this distance, it might be

expected that viscosity will increase with increase in pressure. It has been reported [13] that the viscosity of polystyrene at 25 000 psi is 100 times the viscosity at 2000 psi, while in the case of high density polyethylene, the increase is five times.

At high pressures crystallization may be induced, which stiffens the material and may result in the shear-thinning fluid becoming shear-thickening at very high shear stresses.

3.2.8 MEASUREMENT OF SHEAR VISCOSITY

The viscosity of polymeric fluids varies from 1 poise to greater than 10^{12} poise. To investigate the entire range experimentally, many methods have been devised to study the flow properties of polymer solutions and melts; some of the commonly used methods are listed in Table 3.3 [14]. The most frequently used methods involve rotational and capillary devices.

Rotational viscometers are available with several different geometries, including concentric cylinders, two cones of different angles, a cone and a plate, or combinations of these.

Capillary flow has been the most popular method for measuring viscosity of fibre-forming polymers. The small diameter capillary minimizes the effect of viscous heating, which is a significant problem with rotational devices. The flow is generally pressure-driven and pressure gradients are unavoidable. As the driving pressure is increased to allow the study of higher shear rates, a point is reached where the variation of viscosity with pressure cannot be neglected [15]. The experimental conditions must be limited to situations in which the pressure effect is negligible; the easiest way to judge this is to see that the Bagley plot (Fig. 3.10) is linear. Some high molecular weight polymers can undergo mechanically induced degradation at high shear rates.

Table 3.3 Methods for determining viscosity [14]

Method	Approximate useful viscosity range (P)
Capillary pipette	$10^{-2}-10^3$
Falling sphere	$1-10^5$
Capillary extrusion	$1-10^8$
Parallel plate	10^4-10^9
Falling coaxial cylinder	10^5-10^{11}
Stress relaxation	10^3-10^{10}
Rotating cylinder	$1-10^{12}$
Tensile creep	$10^5->10^{12}$

3.3 ELONGATIONAL FLOW

3.3.1 THE NATURE OF ELONGATIONAL FLOW

So far, the emphasis has been on shear flow of a fluid through a capillary. In the manufacture of fibres, after passing through the capillary, the fluid emerges from the orifice into air or some fluid much less viscous than the liquid of the jet and is stretched by a force at a fixed point some distance downstream of the orifice. As the fluid thread moves down, the cross-sectional area decreases and its velocity increases, though all these quantities at any point in space are independent of time [16].

It has been pointed out by Petrie [16] that Ziabicki [17] appears to have been the first person to make the distinction between shear flow and elongational flow in terms of the velocity gradient which is transverse in shear flow (Fig. 3.13(a)) and longitudinal in elongational flow (Fig. 3.13(b)). Within the capillary, the fluid is confined during shear flow. As the fluid leaves the orifice, there is a transition from shearing to elongational flow and from a confined to a free-surface flow. From the earlier discussion on laminar flow, it would be expected that if a molecule gets extended in shear, it is oriented parallel to the streamlines and
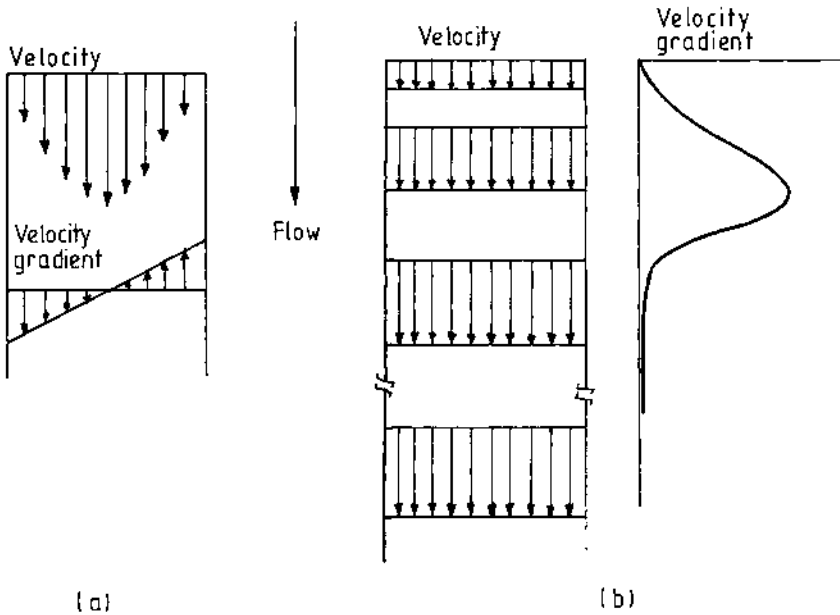
Fig. 3.13 The velocity gradient in (a) shear flow in a capillary, and (b) elongational flow in a spinline (the corresponding velocity profiles are also shown).

lies more or less in a fluid of uniform velocity as the velocity does not change along the streamlines. Thus the motion of the fluid is not greatly affected by the molecule. In elongation, the velocity changes along the streamlines as shown in Fig. 3.13(b) and the ends of a molecule will experience an increasingly different velocity. Thus there is likely to be a change from the coiled to the extended form which will affect the motion significantly.

The first place in the spinning equipment where the polymer molecules could be oriented is the spinneret channel. It has been pointed out by Ziabicki [18] that although in principle shear flow is capable of orienting macromolecules along the flow direction, two facts make this mechanism ineffective in melt-spinning:

1. the residence (transit) time, i.e. the time of action of the shear field, is rather short; and
2. the polymer jet leaving the spinneret channel is subject to relaxation indicated by the dieswell phenomenon. The orientation, if any, produced within the channel is therefore relaxed to a large extent just below the spinneret.

A number of studies have since shown quite clearly that spinning orientation develops gradually along the spinning path. It results from elongational flow of the spinning line and is determined by the local velocity or the local tensile stress. Though it is now recognized that in fibre manufacture the principally important technological state is not the shear flow but extension or jet drawing, a detailed understanding of extensional flow is yet to emerge.

Elongational flow was first studied by Trouton [19] with pitch and waxes. He observed that the ratio of tensile stress, σ, to elongation rate, $d\varepsilon/dt$ or $\dot{\varepsilon}$ (the coefficient of viscous traction or elongational viscosity), was three times the shear coefficient of viscosity. In the range of very low deformation rates (below $1\,s^{-1}$), isothermal elongational viscosity hardly differs from the 3η value predicted by the Newtonian model.

3.3.2 FACTORS AFFECTING ELONGATIONAL VISCOSITY

For a model elastic liquid system, theoretical analysis by Lodge [20] showed that while shear viscosity is independent of shear rate, the elongational or traction viscosity will increase sharply with elongation rate. It is only when the curves are taken to zero strain rate that the elongational viscosity is equal to three times the shear viscosity. Under these conditions, the material may be described as Troutonian.

When the elongational viscosity of a polymer fluid is actually measured at higher elongation rates, the following three types of behaviour are observed [12].

1. The material appears to be Troutonian at all measurable elongation rates.
2. The material is Troutonian over a range of elongation rates but a critical elongation rate is eventually reached when the traction viscosity decreases with increased tension. The term tension-thinning (analogous to the term shear-thinning used earlier) is sometimes used for such materials.
3. The material becomes non-Troutonian at quite low stresses but in this case the traction viscosity increases with stress. Such a material might be referred to as tension-stiffening.

The studies made by Vinogradov et al. [21] on polystyrene and by Münstedt and Luan [22] on low density polyethylene over a wide range of shear and strain rates illustrate the types of behaviour listed above. Vinogradov et al. made measurements of the shear viscosity of poly-styrene and its elongational viscosity at 130 and 150 °C respectively; the data are shown in Fig. 3.14.

It was observed that while the shear viscosity of polystyrene showed typical behaviour expected of a shear-thinning fluid at both tempera-tures, the elongational viscosity showed Trouton-like behaviour at 150 °C but tension-stiffening was observed when the extensional flow was studied at 130 °C. These results were explained by Vinogradov et al. [23] as follows: At both temperatures, the elongational viscosity shows Troutonian behaviour at very low rates of extension since the network-like fluid structure is regenerated fast enough so that the material is still isotropic and results in steady flow. At higher strain rates, the deformation can no longer be considered to be purely viscous, particularly at relatively low temperatures. There is a transition from flow
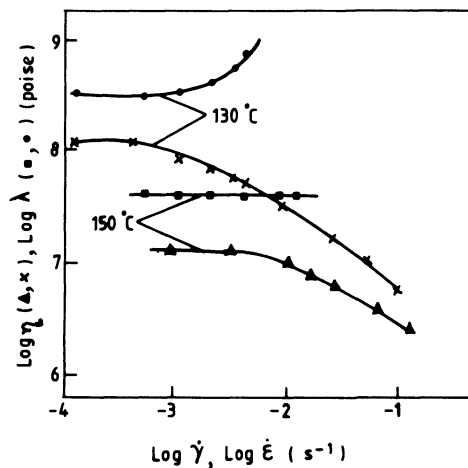
Fig. 3.14 Shear and elongational viscosity data for polystyrene [21].
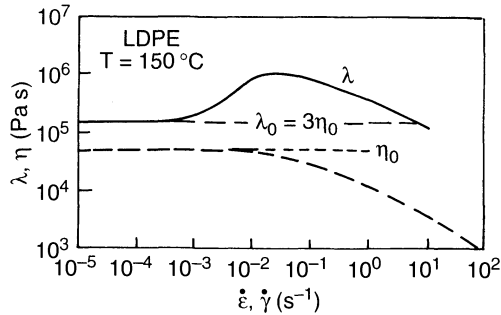
Fig. 3.15 Shear and elongational viscosity data for low density polyethylene at 150 °C [22].

to viscoelastic strain and the material partly loses its capacity to undergo irreversible deformation. A considerable amount of reversible deformation (elasticity) is accumulated and the material tends to retract, leading to an increased resistance to flow, thus giving rise to tension-stiffening.

The studies on low density polyethylene by Münstedt and Luan [22] were made at 150 °C over seven decades of shear rate and strain rate. As shown in Fig. 3.15, these studies show shear-thinning behaviour typical of a pseudoplastic material when shear viscosity is measured but show three regimes of flow behaviour in tension. While the existence of the first two regimes may be understood in terms of the explanation given above, the third regime in which the extensional viscosity drops at the highest strain rates may be because the network-like structure is itself destroyed and the molecules are oriented side-by-side, thus giving rise to a drop in elongational viscosity. A similar behaviour was observed at all temperatures between 120 and 180 °C.

It must be emphasized that it may not always be possible to strictly observe and differentiate between the three regimes of flow. One or all of the three types of behaviour may be observed, depending on the polymer, its molecular weight, molecular weight distribution, presence of side branches and the amount and conditions of deformation (temperature, rate of deformation, etc.).

The effect of molecular weight distribution on apparent elongational viscosity (λ) of high density polyethylene has been studied by Ishizuka and Koyama [24]. The results for two samples with differing distributions are shown as plots of λ against distance from spinneret exit (Fig. 3.16(a)) and of λ against $1/T$ (Fig. 3.16(b)); in both cases the take-up velocity was 8 m min^{-1}. It is noteworthy that the broad distribution sample A with a polydispersity of 43 (polydispersity is the ratio of weight average molecular weight, $\bar{M}_w$, to number average molecular weight, $\bar{M}_n$) shows a minimum in λ in both the plots, while for the narrow distribution sample B (polydispersity = 6.9) the viscosity behaviour is the same as
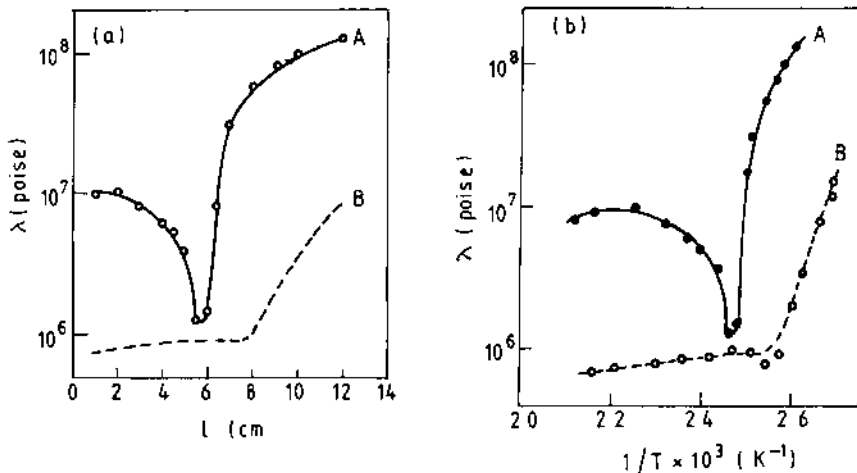
Fig. 3.16 Apparent elongational viscosity of two polyethylene spinlines as a function of (a) distance from spinneret exit and (b) $1/T$. For curve A, $\bar{M}_w/\bar{M}_n$ is 6.9, and for curve B it is 43 [24].

that of many other polymers, namely an increase of viscosity with decrease of temperature. While the latter behaviour is an expected result, the fall in viscosity as the temperature decreases from 160 to 130 °C is unexpected. The authors conclude that the wide distribution of molecular strain rates in broad molecular weight distribution samples is possibly responsible for the abrupt decrease in elongational viscosity in melt-spinning. An alternative explanation postulates that over this temperature range liquid crystal formation can result and lead to this anomaly. It is interesting to recall, as pointed out in Chapter 2, that such an effect has actually been observed in very high molecular weight, high density polyethylene; liquid crystal formation was suggested to explain it.

3.3.3 MEASUREMENT OF ELONGATIONAL VISCOSITY

As pointed out by Ziabicki [25], fibre spinning is generally considered to be steady-state but non-uniform flow, which, as stated earlier, implies that the velocity, deformation rate, etc. at point x on the spinning line are constants. However, from the point of view of a small particle of polymer moving along the spinning line, deformation is time-dependent and the particle experiences different strain rates as it moves along its trajectory. During the elongational flow of molten polymer, transient viscoelastic effects bring about a transition from steady-state flow to rapid deformation which can lead to fracture. Large relaxation times and deformation rates result in pronounced viscoelastic effects. While
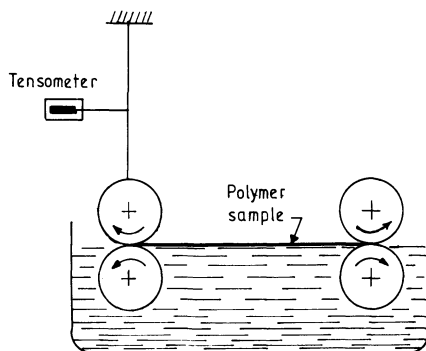
Fig. 3.17 Meissner's method for measuring elongational viscosity.

the behaviour at low elongation rates may be approximated to steady viscous flow, elastic, reversible deformation is involved at high rates and relaxation effects therefore play an important role in elongational flow. Hence elongational viscosity measured under non-steady-state or non-uniform elongational conditions may show major deviations from steady-state characteristics. For this reason, elongational viscosities obtained from spinning experiments, which are non-isothermal in nature, do not adequately characterize elongational flow.

However, steady-state conditions are extremely difficult to achieve with elongational flows since a steady-state value of recoverable strain has to be reached. The most commonly used method to measure elonga-tional viscosity is that due to Meissner [26, 27], which involves stretching the rod-like polymer between two rotating nips formed by two pairs of rollers. These rollers rotate at constant speed over a fluid bath of silicone oil placed horizontally to compensate for gravity (Fig. 3.17). The strain rate is estimated from the measurement of velocity or diameter and the tension is measured to obtain the stress. Other measurement devices have been reviewed by Ziabicki [18].

3.4 MOLECULAR THEORIES OF FLUID FLOW

Molecular theories of flow allow a better understanding to be achieved of the relationship between molecular parameters and rheological prop-erties. In concentrated polymer solutions and polymer melts, there is a strong interaction between the molecular chains. Starting with the classical work of Eyring and his colleagues [28] in the early 1940s which involved a molecular segment as the unit of flow, the molecular theory was refined by Rouse [29] to take into account the coordinated move-ment of the molecular chain segments. The innovative idea of reptation, in which a molecular chain is confined within a tube defined by its
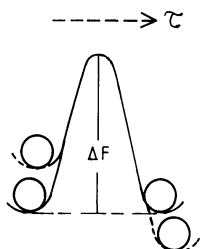
Fig. 3.18 Potential energy barrier for flow.

neighbours and moves by wriggling along a tortuous path, was conceived by de Gennes [30] and translated into a quantitative theory of polymer chain dynamics by Doi and Edwards [31]. Finally Curtiss and Bird [32] developed a kinetic theory for polymer melts and were able to predict the correct dependence of the zero shear viscosity on molecular weight. The Doi–Edwards theory was shown to be a limiting case of the Curtiss–Bird theory. These theories will now be briefly described.

3.4.1 THE EYRING MODEL

One of the earliest theories of fluid flow is that due to Eyring and co-workers [28], briefly referred to above. Eyring considered a liquid to be close to a disordered solid, comprising flow units which could be segments of chain molecules or chain molecules themselves. In the stress-free state, the flow units are assumed to lie in a potential well (Fig. 3.18), which represents the position of minimum potential energy; the potential energy barrier which the flow unit has to overcome is ΔF and represents the energy of activation for diffusion to occur. Eyring applied the 'transition state' theory of chemical rate processes to the molecular jump and the jump frequency, ν, as

$$\nu = \frac{KT}{h}\exp(-\Delta F/RT) \qquad (3.28)$$

where K is Boltzmann's constant, h is Planck's constant, ΔF the height of free energy barrier and R the universal gas constant.

The application of a stress to the system modifies the shapes of the potential wells, as shown in Fig. 3.18, so that jumps in the forward direction involve a lower energy barrier than jumps in the reverse direction. The chance of a molecule jumping forwards into a hole under stress is thus greater than the chance of one jumping back, and so a net movement occurs in the stress application direction.

Meares [33] has pointed out that Eyring's model neatly reconciles the two viewpoints that are generally taken to explain viscosity. The first theory is based on the premise that fluidity (i.e. the reciprocal of

viscosity) is a function solely of the free volume of the liquid. The alternative view considers viscous flow to be an activated process with an activation energy which is concerned only with raising the flowing molecules over the potential energy barrier between one equilibrium position and the next. The activation energy was shown by Eyring to be made up from two contributions, namely the work required to make a hole for the molecule to jump into and the work required to free the molecule of its immediate environment to enable it to jump, the former being higher than the latter for simple and relatively non-polar liquids. As stated earlier, the flowing units are not whole molecules but molecular segments around 25 carbon atoms long.

The type of deformation that occurs in viscous polymeric fluids has been visualized by Meares [33] to be as follows. Under stress, breakdown of chain entanglements may take place, while in the stress-free state, new entanglements may form. Simultaneously the relatively free chain segments diffuse in the stress direction by a preponderance of micro-Brownian jumps. Thus the chains are able to progress as a whole without ever departing far from an equilibrium distribution of configurations consistent with the random chain theory.

A shortcoming of the Eyring approach is that it refers only to localized mobility of submolecules and does not include the effect of molecular weight on flow.

3.4.2 THE MODELS OF ROUSE AND BUECHE

Rouse [29] considered the polymer molecule divided into a number of equal segments, each of which contains enough chain units for its end-to-end distance to be governed by a Gaussian probability distribution. Each segment thus behaves as an elastic spring, as required by the theory of rubber elasticity. A friction factor f_0 of a segment is assumed which arises from the fact that the segment is surrounded by the neighbouring polymer segments and the solvent. The relaxation spectrum for a dilute solution is essentially a straight line and is quite closely predicted by the Rouse theory. More concentrated solutions or polymer melts show a horizontal region or a plateau which becomes more prominent as the concentration and molecular weight increase (Fig. 3.19). Atkinson [7] has pointed out that this plateau region is an expression of entanglements between the chains of contiguous polymer molecules. Such entanglements would be more common in concentrated solutions of polymer of high molecular weight, and could be expected to affect those relaxation modes which involve longer portions of the molecular chains, by increasing their relaxation times. Rouse's theory is still applicable to the shorter relaxation time region with a somewhat increased value of f_0. The long relaxation time end of the spectrum can only be
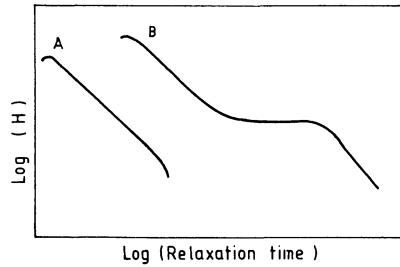
Fig. 3.19 Relaxation spectra for polymer solutions of (A) low and (B) high concentration (adapted from reference [7]).

fitted to the theory if the friction factor is increased considerably. Bueche [34] has shown that the entanglements between the polymer chains can cause such an increase in the apparent friction factor.

3.4.3 THE THEORIES OF YAMAMOTO AND LODGE

Yamamoto [35] considered the network to be in a state of constant flux in which the junction points (physical entanglements) are constantly being broken and re-formed under the action of thermal forces at equilibrium. When the network is deformed, there is an increase in the end-to-end distance in accordance with affine deformation. Yamamoto considered the rate of deformation to be slower than both the rate of micro-Brownian motion of the segments and the rate of breakage and re-formation of junctions, so that the system was in equilibrium at any instance.

Lodge [20] developed a continuum theory for entangled polymer fluids based upon the molecular ideas manifest in the theory of rubber elasticity and some features of Yamamoto's molecular theory. Lodge considered flow as a quasistatic deformation of the network and the attainment of thermodynamic equilibrium was taken to be instantaneous. Thus it was assumed that there was no change in the number of entanglements on deformation and that the entanglements re-formed in the same positions. The breakdown and re-formation of entanglements resulted in the dissipation of energy which was taken to be responsible for the relaxational response. The most important contribution of the theory was that it explained the origin of anomalous effects shown by polymeric fluids such as normal stresses, etc.

3.4.4 THE MODELS OF de GENNES AND DOI AND EDWARDS

The model of de Gennes [30] considered an idealized single polymeric chain trapped inside a three-dimensional network (Fig. 3.20), such as a polymeric gel. The surrounding molecules act as fixed obstacles and the
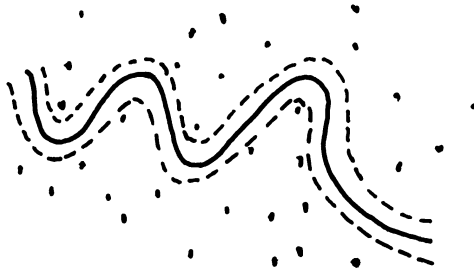
Fig. 3.20 Idealized single polymer chain trapped inside a three-dimensional network, as visualized by de Gennes. The dots represent chain cross-sections.

chain is not allowed to cross any of these obstacles. Consequently the lateral movement of the molecular chain is impeded. A tubular element surrounding the molecular chain to limit its lateral fluidity was therefore introduced into the model. Movement of the molecular chain through a snake-like translational motion of each chain parallel to its own contour or through creeping along such a tube was termed 'reptation'. The reptation motion results in a forward movement and the end of the chain can then assume various new orientations. Using scaling concepts, de Gennes found that the diffusion coefficient of a chain in a gel is inversely proportional to the square of the molecular weight, and the relaxation time is proportional to the cube of the molecular weight. Both of these theoretical relationships have been shown to hold in a number of polymeric systems.

Doi and Edwards [31] generalized and extended the de Gennes model for flow. They assumed that the chains pass through fixed sliplinks and have a net tension along the chain which disallows free slippage of the chain through the links.

3.4.5 THE MODEL OF CURTISS AND BIRD

Curtiss and Bird [32] used the concept of reptational motion of a chain but introduced an empirical chain constraint parameter β, which depended not only on the density of surrounding molecules, but also on the length of the chain itself. The Curtiss and Bird model predicts the correct type of relationships for a number of flow parameters, as is shown in the next subsection.

3.4.6 COMPARISON OF THE VARIOUS MOLECULAR THEORIES

The molecular theories briefly described above will now be compared in terms of their ability to predict (1) the general form of the dependence of longitudinal viscosity on strain rate, and (2) the $\bar{M}_w^{3.4}$ dependence of zero shear viscosity.
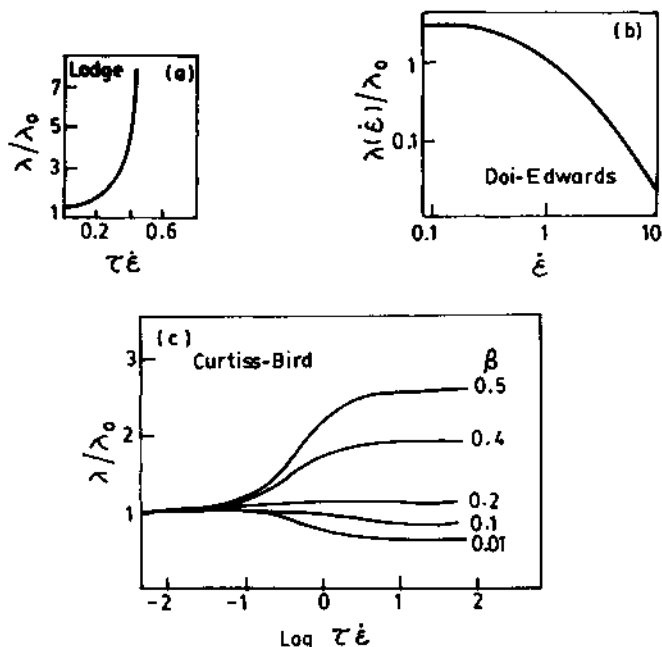
Fig. 3.21 Normalized longitudinal viscosity, λ/λ_0, vs. strain rate according to (a) Lodge's theory, (b) Doi–Edwards theory and (c) Curtiss–Bird theory [32].

The normalized longitudinal viscosity λ/λ_0 increases with strain rate according to Lodge's theory (Fig. 3.21(a)), while according to the Doi–Edwards theory it decreases (Fig. 3.21(b)). This is because in Lodge's theory there is no restriction to lateral mobility as there is in the Doi–Edwards theory. As shown earlier, both these types of behaviour have been observed experimentally for different polymer fluids. The Curtiss–Bird theory can predict both a decrease and an increase of normalized longitudinal viscosity, as shown in Fig. 3.21(c), depending on the lateral mobility parameter. It is thus seen that the Curtiss–Bird molecular theory is more general; it has been shown that the Doi–Edwards theory is a special case of the Curtiss–Bird theory. The experimentally observed $\bar{M}_w^{3.4}$ dependence of zero shear viscosity is also predicted by the Curtiss–Bird theory. The Doi–Edwards theory predicts an $\bar{M}_w^3$ dependence. The other models do not consider molecular weight as a factor.

3.5 SPINNABILITY AND FLOW INSTABILITIES

3.5.1 SPINNABILITY OF FLUIDS

A fluid is spinnable under given deformation conditions if steady-state, continuous elongation of the fluid jet proceeds without a break of any

kind [18]. One of the earlier studies on spinnability was that of Nitsch-mann and Schrade [36], who suggested that elongational viscosity should increase with strain rate to stabilize the filament. This is essential because in industrial spinning the stress increases as the filament moves away from the spinneret. In the absence of such an increase in viscosity, a localized defect could get drawn endlessly, leading to catastrophic ductile failure. Such failures are generally observed on isothermal stretching of polymer melts. As stated in Section 3.3.3, the viscoelastic nature of the fluids can result in the accumulation of recoverable defor-mation in which the elasticity of the fluid plays an important role. An ideally viscous, incompressible Newtonian fluid would deform end-lessly with instantaneous dissipation of the deformation energy. In a viscoelastic fluid, a part of the deformation energy is stored; if it reaches some limiting value, cohesive, brittle fracture occurs. The deformation rate and the relaxational characteristics of the viscoelastic fluid are the two important parameters. Relaxation of the stored energy reduces the chances of failure. Relaxation times of spinning fluids range from several milliseconds (solutions used in wet-spinning) to 1 s or more (high molecular weight polyolefin melts). Thus cohesive fracture is more frequent with fibre-grade polyolefins with $\bar{M}_n \geq 60\,000\,\mathrm{g\,mol}^{-1}$ which have relaxation times of 1–10 s at the processing temperatures. Such effects are much less in PET, nylon 6 and nylon 66 with $\bar{M}_n$ in the range 18 000 to 24 000 g mol^{-1} and relaxation times of 0.01–0.1 s. Melt-spinning is a non-isothermal process and the elongational viscosity increases along the spinline due to cooling of the filament; this enhances the stability of the spinline. High speed spinning of polycondensates at speeds up to 5000 m min^{-1} and with high spin draw ratio thus becomes possible.

The stability of semi-melt-spinning procedures, solution dry-spinning and wet-spinning are also largely dominated by cohesive fracture. It has been shown that in the wet-spinning of acrylic fibres, the maximum take-up velocities are high for solutions of low polymer concentration in the spinning dope and increase with the temperature of the spinning bath, both effects being associated with relaxation time.

Besides cohesive fracture, the other possible process of breaking fluid threads is associated with surface tension and the formation of capillary waves on the free surface of a liquid jet [18] leading to the break-up of the jet into drops. The initial distortions of amplitude of the order of 10–100 μm are generated in the extrusion die as a result of pressure or density fluctuations. As the capillary waves proceed from the exit of the spinneret along the filament, the growing amplitude of the capillary wave ultimately splits the jet into individual drops through the cohesive fracture mechanism. Too low a viscosity and too high a surface tension of the polymer fluid result in too high a ratio of surface tension to

viscosity which promotes the break-up of the spinning line. Compared with condensation polymers, polyolefins have a higher fluid viscosity but similar surface tension; thus the condensation polymers are more susceptible to capillary break-up. In dry-spinning solutions, the surface tension is not very different from that for melt-spinning but the solution viscosity is much lower. As a result the dry-spun fibres may also show such breakage.

In wet-spun polymer solutions, viscosities are rather low, but so also is the interface tension. Under industrial conditions, breaks due to this mechanism are not likely.

The above approach, advocated by Ziabicki [18], has been criticized by Walczak [37], who questioned the assumption that viscosity, surface tension and density are constant. However, Ziabicki has presented considerable evidence in support of his approach. He has found that the cohesive mechanism of thread breakage seems to operate across a wide range of spinning conditions. In industrial practice, the instability due to cohesive fracture determines the upper limit of take-up velocity and spin draw ratio above which no spinning is possible.

3.5.2 FLOW INSTABILITIES

One of the primary concerns of the fibre industry is to produce filaments with uniform diameter or cross-section. Flow instabilities can introduce non-uniformities and are therefore to be avoided. The main flow instabilities that arise during fibre spinning can be considered under two headings. The first has its origin in the spinneret channel – the two instabilities under this category are dieswell and melt fracture. The second type of flow instability occurs when the spin draw ratio reaches a critical value and is termed draw resonance. These will now be briefly discussed.

(a) Dieswell and melt fracture

Dieswell appears as a bulge in the extruded filament at the spinneret exit (Fig. 3.9) while melt fracture refers to distortion of the extrudate surface, with the severity ranging from simple roughness to helical indentations. Both these flow instabilities are believed to result mainly from the elastic energy stored in the viscoelastic fluid during its passage through the spinneret orifice. If the relaxation rate of the fluid molecules is fast, significant relaxation of the stored elastic energy can take place, as illustrated by the data on cuprammonium solution presented in Table 3.4 [38]. It is noteworthy that the elastic energy is comparable with, and for short capillaries even larger than, the energy dissipated in steady shear (Poiseuille) flow. In shorter capillaries, a large proportion of the elastic

Table 3.4 Energy contributions for spinneret flow of a cuprammonium cellulose solution (8% cellulose) [38]

Channel length L (cm)	0.015	0.030	0.075	0.150	0.300	0.600
L/R ratio	1	2	5	10	20	40
Transit time (ms)	21	42	104	208	416	832
Total energy supplied (erg s^{-1})	150	193	321.5	536	965	1823
Energy dissipated in steady Poiseuille flow (erg s^{-1})	43	86	214.5	429	868	1716
Energy of elastic deformation (erg s^{-1})	107	107	107	107	107	107
Transformation of elastic energy (erg s^{-1})						
(a) Dissipation (heat)	21.5	33	54.8	65.6	75.8	76.6
(b) Dieswell	85.5	74	52.2	41.4	31.2	30.4

Channel radius, $R = 0.015$ cm; temperature $T = 30\,°C$; output, $Q = 5.09 \times 110^{-4}$ cm^3 s^{-1}.

energy is stored and affects swelling of the extrudate. The other part relaxes during the transit time.

When the extrudate fluid leaves the capillary, the boundary conditions are changed abruptly. Within the capillary, the velocity of the fluid at the wall is zero, while outside the capillary there is no limitation of the velocity on the surface of the emerging jet. The extent of the dieswell will depend on the stored elastic energy. The degree of swelling (often called the dieswell ratio; maximal diameter of extrudate/diameter of capillary) depends on the conditions of extrusion temperature and geometry of the extrusion die. The significance of dieswell in fibre formation technology has several aspects; dieswell is governed by the same viscoelastic factors as, and is therefore correlated with, the instability in the exit zone known as melt fracture. In extreme conditions (very low temperatures, very high shear rates, etc.) dieswell itself may be a source of unstable or irregular spinning. Therefore extrusion conditions and the geometry of the spinneret orifices become important variables of the spinning process.

Dieswell, indicative of the elasticity of melts, is commonly observed in the absence of an external tensile force. The dieswell ratio in melt spinning of polyamides and polyesters is not large, except for temperatures close to the solidification point where relaxation time increases rapidly. Nylon 6, for example, shows a dieswell of 7.9 at an extrusion temperature of 220 °C and the maximum diameter appears at a distance several millimetres from the exit of the spinneret. At normal extrusion temperatures, the dieswell does not exceed 1.2–1.5 [39].

Melt fracture seldom disturbs spinning of polycondensate polymers. Critical shear rate for the onset of melt fracture in nylon 66 is 10^5 s^{-1} at a

temperature of 275 °C, while maximum shear rates in spinneret flow do not usually exceed $10^4\,s^{-1}$. However, in the case of nylon 6, irregular flow was observed at $5 \times 10^2\,s^{-1}$ when spinneret temperature was 220 °C.

The dependence of maximum extrudate diameter on the length-to-diameter (L/D) ratio of the capillary and shear rate has been investigated for polypropylene. The higher the L/D ratio of the capillary, the lower is the dieswell. Also the lower the shear rate, the lower is the dieswell. This supports the earlier observation that dieswell is related to relaxation phenomena. Since the effective deformation gradient and the relaxation characteristics are very sensitive to temperature distribution along the spinning line, the cooling process is often slowed down by the application of heated cells below the spinneret to achieve stability.

In solution spinning, the dieswell ratio usually increases with increase in viscosity and elasticity of the dope and increase in polymer concentration and molecular weight; it however decreases with increase in extrusion temperature. Take-up tension (and velocity) is found to reduce the dieswell effect considerably. A very important effect in wet-spinning is due to the nature of the precipitation bath. Mass transfer and phase transition phenomena occurring in the bath reduce swelling of the jet. One can suppose that the formation of a rigid precipitated layer on the outside of the jet (skin) suppresses expansion and reduces the maximum degree of swelling. The skin mechanism has been confirmed by studies on acrylic copolymer where a reduction in dieswell was observed with an increasing rate of coagulation. Various studies have suggested that minimum dieswell corresponds to maximum spinnability.

Walczak [37] has shown that dieswelling in extrusion is much more complex than has been assumed and that fluid elasticity may not be the only factor affecting it. Molecular entanglements can create network structures and these depend on the thermal and shear history of the melt. They can also affect dieswell effects.

(b) Draw resonance

Periodic fluctuations in the thread diameter have been observed during melt spinning. This is referred to as 'draw resonance'. The interesting feature is that draw resonance occurs only when the spin draw ratio reaches a certain critical value. In the case of isothermal melt-spinning of a Newtonian fluid, the critical spin draw ratio is around 20 [40].

Jinan Cao [40] has shown that for a power-law fluid the appearance of draw resonance for isothermal melt-spinning depends on the draw mode. For a power-law exponent less than one (tension thinning situation), the application of tension on a non-uniformity results in the amplification of the non-uniformity. The critical spin draw ratio for resonance to appear is very low (Fig. 3.22). For a power-law exponent greater than
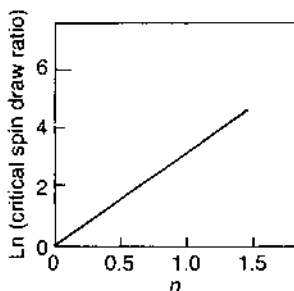
Fig. 3.22 The logarithm of the critical spin draw ratio vs. power-law index (*n*) in isothermal and uniform tension melt-spinning [40].

one (tension stiffening), the non-uniformity is stabilized since the thinner sections will offer greater resistance to deformation. This can happen when the polymer fluids develop orientation or crystallization during spinning. Furthermore, the non-isothermal nature of actual melt-spinning increases the critical draw ratio further.

Polymers like low density polyethylene which are tension-stiffening rarely produce draw resonance. Polypropylene and high density polyethylene are tension-thinning beyond a critical stress and draw resonance is quite common during melt-spinning of these polymers.

It is generally believed that draw resonance is closely related to the spinning conditions. In the presence of stretching and either melt inhomogeneity or frictional heating (due to molecules sliding past one another), draw resonance can occur [41].

REFERENCES

1. Mateev, A.N. (1985) *Molecular Physics*, Mir Publishers, Moscow, p. 18.
2. Kauzmann, W. and Eyring, H. (1940) *J. Am. Chem. Soc.*, **62**, 3113.
3. Flory, P.J. (1940) *J. Am. Chem. Soc.*, **62**, 1057.
4. Rosen, M.R. (1979) *Polym. Plast. Technol. Eng.*, **12**(1), 1–42.
5. Bagley, E.B. (1957) *J. Appl. Phys.*, **28**, 626.
6. Williams, M.L., Landel, R.F. and Ferry, J.D. (1955) *J. Am. Chem. Soc.*, **77**, 3701.
7. Atkinson, E.B. (1965) Molten polymers and concentrated polymer solutions, in *Physics of Plastics* (ed. P.D. Ritchie), Plastics Institute (Illife Books Ltd, London and D. Van Nostrand Co., Princeton), pp. 248–284.
8. Doolittle, A.K. (1951) *J. Appl. Phys.*, **22**, 1471.
9. Treloar, L.R.G. (1970) *Introduction to Polymer Science*, Wykeham Publication Ltd, London, p. 173.
10. Elias, Hans-Georg (1984) *Macromolecules-I: Structure and Properties*, 2nd edn, Plenum Press, New York.
11. Howells, E.R. and Benbow, J.J. (1962) *Trans. Plastics*, **30**, 240.
12. Brydson, J.A. (1970) *Flow Properties of Polymer Melts*, Plastics Institute, Iliffe Books, London, p. 59.
13. Westover, R.F. (1966) *Polym Eng. Sci.*, **6**, 83.

14. Billmeyer, Jr, Fred W. (1971) *Textbook of Polymer Science*, 2nd edn, John Wiley & Sons Inc., New York, p. 187.
15. Dealy, John M. (1982) *Rheometers for Molten Plastics*, Van Nostrand Reinhold Co., New York.
16. Petrie, C.J.S. (1979) *Elongational Flows*, Pitman, London.
17. Ziabicki, A. (1959) *J. Appl. Polym. Sci.*, **2**, 24–31.
18. Ziabicki, A. (1976) *Fundamentals of Fibre Formation. The Science of Fibre Spinning and Drawing*, Wiley-Interscience, London.
19. Trouton, F. (1906) *Proc. Roy. Soc.*, **A77**, 426.
20. Lodge, A. (1964) *Elastic Liquids*, Academic Press, New York.
21. Vinogradov, G.V., Fikhman, V.D., Radushkevich, B.V. and Ya Malkin, A. (1970) *J. Polym. Sci.*, **A28**, 657.
22. Münstedt, H. and Luan, H.M. (1978) *Rheol. Acta*, 17, 415.
23. Vinogradov, G.V., Dreval, V.E., Borisenkova, E.K., Burbanaliev, M.K. and Shalganova, V.G. (1981) *Rheol. Acta*, **20**, 433.
24. Ishizuka, O. and Koyama, K. (1985) In *High Speed Fibre Spinning* (eds A. Ziabicki and H. Kawai), John Wiley & Sons, New York.
25. Ziabicki, A. (1985) In *High Speed Fibre Spinning* (eds A. Ziabicki and H. Kawai), John Wiley & Sons, New York.
26. Meissner, J. (1969) *Rheol. Acta*, **8**, 78.
27. Meissner, J. (1971) *Rheol. Acta*, **10**, 230.
28. Glasstone, S., Laidler, K.J. and Eyring, H. (1941) *Theory of Rate Processes*, McGraw Hill, New York.
29. Rouse, Jr, P.E. (1953) *J. Chem. Phys.*, **21**, 1272.
30. de Gennes, P.G. (1971) *J. Chem. Phys.*, **55**, 572.
31. Doi, M. and Edwards, S.F. (1978) *J. Chem. Soc. Faraday Trans II*, **74**, 1789, 1802, 1818.
32. Curtiss, C.F. and Bird, R.B. (1981) *J. Chem. Phys.*, **74**, 2016, 2026.
33. Meares, P. (1985) *Polymers: Structure and Bulk Properties*, D. Van Nostrand Co., London.
34. Bueche, F. (1954) *J. Chem. Phys.*, **22**, 603.
35. Yamamoto, M. (1956) *J. Phys. Soc. Japan*, **11**, 413; *Idem* (1957) *ibid.* **12**, 1148; *Idem* (1958) *ibid.* **13**, 1200.
36. Nitschmann, H. and Schrade, J. (1948) *Helv. Chim. Acta*, **31**, 297.
37. Walczak, Z.K. (1977) *Formation of Synthetic Fibres*, Gordon and Breach, Science Publishers, London.
38. Kast, W. (1963) *Kolloid-Z*, **187**, 89.
39. Ziabicki, A. (1967) In *Man-made Fibers: Science and Technology*, Vol. I (eds H.F. Mark, S.M. Atlas and E. Cernia), Interscience, New York.
40. Cao, Jinan (1991) *J. Appl. Polym. Sci.*, **42**, 143.
41. Han, C.D., Lamonte, R.R. and Shah, Y.T. (1972) *J. Appl. Polym. Sci.*, **16**, 3307.

Melt-spinning processes

4

V.B. Gupta

4.1 INTRODUCTION

As stated in the previous chapter, melt-spinning is the simplest method of fibre manufacture, mainly because it does not involve problems associated with the use of solvents. It is therefore the preferred method, provided the polymer gives a stable melt. When polymer granules or chips form the starting material for melt-spinning, they are first dried and then melted in the extruder. The homogenized and filtered melt is squirted through narrow channels into a quench chamber where solidification of the fluid filament bundles is achieved (Fig. 4.1). Finally, spin finish is applied before the filament bundles are wound on tube rolls. In larger modern plants, polyester and nylon are produced in continuous polymerization units in which the melt is directly transported from the final polymerizer to the melt-spinning unit. In the case of polypropylene, since polymerization leads to a solid product, it is separate from the spinning process.

A major development in the area of melt-spinning was the transition in the 1970s from conventional spinning at wind-up speeds of around $1000 \, \text{m} \, \text{min}^{-1}$ to high speed spinning at speeds of $3000 \, \text{m} \, \text{min}^{-1}$ and above. As far back as 1975, more than half of the textured yarn in the world was based on yarn produced using this technology. However, monofilaments continue to be produced at relatively low spinning speeds because of the problem of heat removal. The chronology of techniques used for fibre manufacture based on melt-spinning is as follows [1].
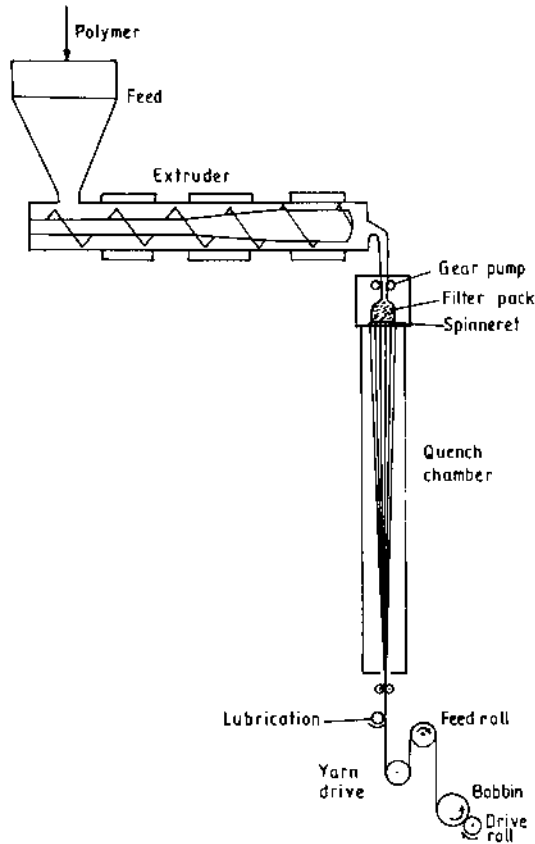
Fig. 4.1 A typical melt-spinning line.

1. *Conventional process*: spinning at 600–1500 m min⁻¹. The spun yarn is then drawn at 400–1000 m min⁻¹ to a draw ratio of between 3 and 4.5 generally.

2. *Direct spin–draw process*: in this integrated process, which couples spinning and drawing in one continuous operation, ultimate wind-up speeds may be as high as 6000 m min⁻¹, but the spinning speed is unlikely to exceed 4000 m min⁻¹.

3. *High speed spinning process*: spinning at 3000–4000 m min⁻¹ to get partially oriented yarn (POY), to which a further draw of up to 2 can be applied during sequential/simultaneous draw texturing.

4. *Super high speed spinning process*: spinning at 4000 to over 6000 m min⁻¹. For filament spun at 5500 m min⁻¹, a further slight draw has still to be applied.

The general nomenclature for wind-up speeds up to 6000 m min⁻¹ is high speed spinning, and super high speed spinning refers to speeds in

excess of $6000 \, \text{m} \, \text{min}^{-1}$. It is noteworthy that techniques (2), (3) and (4) are all based on high speed spinning. In this chapter various aspects of the melt-spinning process operating at different speeds will be considered, and the direct spin–draw process will also be briefly described.

4.2 THE MELT-SPINNING LINE

4.2.1 GENERAL FEATURES

A melt-spinning line is shown schematically in Fig. 4.1. Strictly speaking, the line sketch is representative of melt-spinning at relatively low speeds using polymer chips as the starting material. There are two departures from this line that need to be noted. First, in the direct spinning process, the homogeneous and spinnable melt produced by polymerization may be directly passed to the spinning machine at the gear pump stage. Second, when the winding speeds are high, the yarn may be directly dropped to the wind-up device with no godets being used. An industrial melt-spinning unit without godets is shown in Fig. 4.2(a), while Fig. 4.2(b) shows the lower part of the unit with godets. The latter version allows the yarn tension on the take-up machines to be controlled using S-shaped wraps around cold godets.

When polymer chips form the starting material, chips from several polymerization reactors are mixed to minimize batch-to-batch variation. The chips are dried (moisture content should not exceed 0.05% by weight for nylon 6 and 0.005% for PET) and then melted. In the majority of contemporary processes, melting is carried out continuously in screw melters as these deliver a more homogenized and uniform melt. The polymer melt is transported under pressure to spinning blocks where an exact metering pump, e.g. a gear pump, maintains a highly even issue of the melt. The polymer melt is then forced through a fine filter (a pack of sand particles of 20–80 μm size, a series of stainless steel wire gauzes of different mesh sizes, etc.). Filtration of the molten polymer before it enters the spinneret further homogenizes the melt and removes solid impurities such as metal pieces and semisolid degraded polymer gel, and also eliminates gaseous bubbles. Efficient filtration brings down the breakage rate to below six breaks per 1000 kg production and also reduces the frequency of nubs or undrawn portions in the spun filament.

After filtration, the melt is forced through capillaries in a plate, called the spinneret, and in this way an endless, fine stream of fluid is formed. The molten polymer, on emerging from the spinneret, bulges slightly due to release of elastic energy stored during shear flow through the narrow channels. This is known as the dieswell effect and has been discussed in Chapter 3. The filaments are then quenched and solidified in the quench chamber while being drawn off from the bottom. The
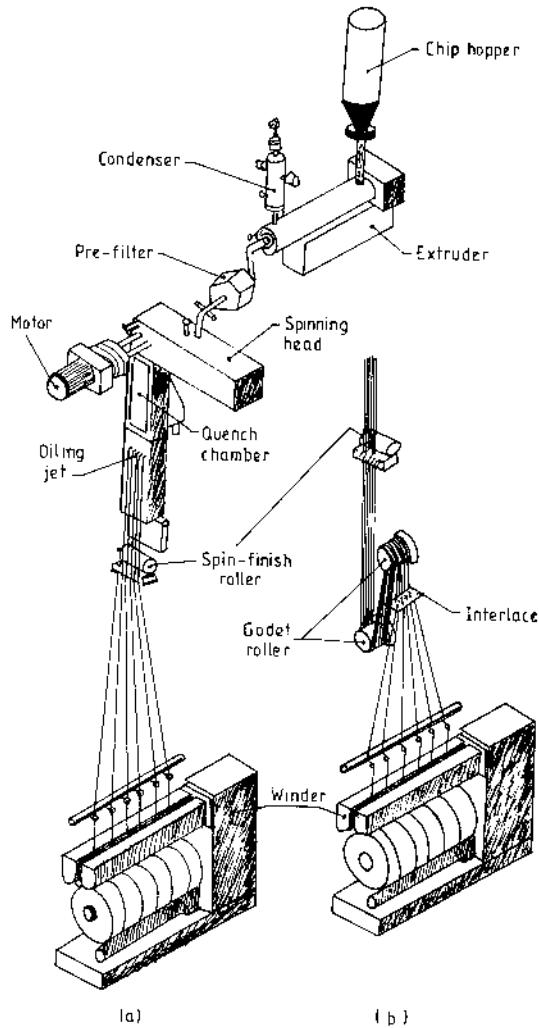
Fig. 4.2 An industrial melt-spinning unit: (a) without godets, (b) with godets.

filament diameter reduces and a number of these filaments are then made to converge into a bundle with the help of two guides. A spin finish is applied before the bundles are wound up on a tube roll, which is often friction-driven by a roller.

4.2.2 THE EXTRUDER

In the past, the granules were melted on grids consisting of a large heating area in the form of ribs and coils heated from inside. However,
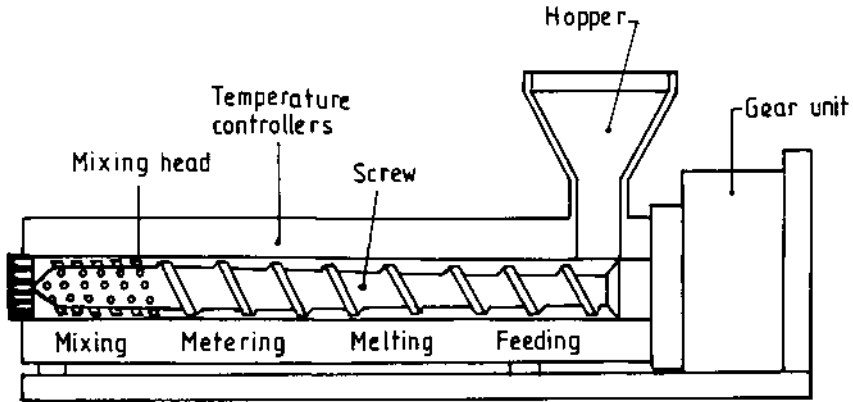
Fig. 4.3 The functional parts of a typical extruder.

because screw melters or extruders offer the advantages of much higher melting rate, large capacity, short residence time, pressure build-up, greater homogenization and delivery of a metered quantity of the melt, they have now replaced grid melters. The functional parts of a typical extruder are shown in Fig. 4.3, while the details of a typical screw appear in Fig. 4.4. The extruders [2–4] consist essentially of a cylindrical barrel within which rotates one or more close-fitting screws (only single screw extrudes will be considered here). Screws with diameter of 45–300 mm are, for example, used for polypropylene with melting capacity of 50–2000 kg h^{-1}. The screw length for polypropylene is larger than for polyester and polyamide, with the length normally being 28–33 times the diameter. The barrel is heated along its length by oil or electricity. The chips are fed to one end of the screw from a feed hopper and are then
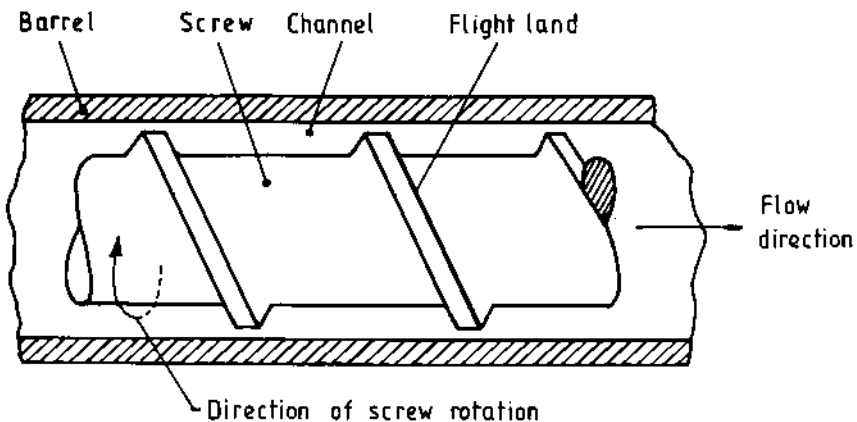
Fig. 4.4 Details of an extruder screw.

forced forward through the barrel by the rotating screw; the rotation is achieved at the base of the machine. As the polymer moves forward, it is softened partly by conducted heat from the barrel walls and partly by frictional heat developed as a result of mechanical shearing of the polymer by the action of the screw. When it reaches the end of the screw, the molten and homogenized melt is guided through a changeable filter pack into a gear pump which meters a desired throughput into the spinneret through another filter assembly.

To visualize how mixing and homogenization of the melt occurs, it is worth noting that if the polymer sticks to the screw and slips at the barrel surface, there would be no output from the extruder because the material will rotate with the screw without being pushed forward. On the other hand, if the polymer sticks to the wall and slips at the screw, the rotational speed of the material will be less than that of the screw and as a result the material is forced along the extruder by the leading edge of the flight.

Generally, single screw extruders can be considered as operating with the following distinct regions as one travels along the length of the screw starting from the hopper.

1. *The feed section or the solids transport zone*: this section lies just beneath the hopper.
2. *The compression and melting zone*: the solid polymer chips undergo compression in this zone because of reduced volume of the screw flights. The chips start melting at the point where the first liquid film forms at the barrel wall, which is heated, and melting can extend along a considerable length to the point where all the polymer in the cross-section of the channel is in molten form.
3. *The metering zone*: in this zone the pressure builds up and the melt is transported and homogenized. Three flow components can be distinguished in this zone:
   (a) forward or drag flow, which is the unrestricted flow caused by contact effects between the material and the barrel and screw surfaces;
   (b) a pressure flow due to the pressure that is built up at the exit of the extruder due to the constriction or die. The direction of this flow is opposite to that of the drag flow so that overall output is reduced;
   (c) a leakage flow through the gap between the barrel and the flight of the screw. This reverse flow is normally very small and may be neglected.

   In a typical extruder, the volumetric flow rate is predominantly governed by the drag flow and the contributions of back flow and leakage flow are very small.

4. *The mixing zone*: the feedstock at this stage may not be entirely homogeneous and the close-clearance mixing section (Fig. 4.3) is incorporated to promote intensive mixing.

4.2.3 THE SPINNING MANIFOLD

The design and heating conditions of the spinning manifold have a significant effect on the filament quality and therefore need careful consideration. In a typical spinning unit, the polymer fluid may be conveyed from the last polycondensation vessel in the case of direct spinning, or from the extruder in the case of batch processing, to the spinning head via double-jacketed tubes. These tubes are generally heated by circulation of Dowtherm^{TM}. The polymer fluid is delivered to a number of spinnerets, each equipped with a spinning pump. There are two important requirements: first, all melt paths before reaching the spinneret orifice must be of exactly the same length to ensure equality of pressure, which in turn ensures that the same quantity of material reaches each orifice; and second, the melt streams and the spinneret must have identical temperature profiles. To ensure melt homogeneity and a uniform temperature profile, static mixers are installed in front of the metering pumps.

4.2.4 THE SPIN PACK AND THE SPINNERET

The polymer melt is transported under pressure to spinning heads where an exact metering pump, e.g. a gear pump, maintains a highly even issue of the melt. As shown in Fig. 4.5, the spinning head [5] has a polymer inlet through which the molten polymer enters into the pump block and a metered quantity of the melt is then led through it into the spin pack (not labelled in Fig. 4.5). The gear pump consists of three surface-ground steel plates [6]: a base, a central and a cover plate, which are firmly screwed to one another. The central plate has two gear wheels (not shown in the figure), the shafts of which lie in the base and cover plate. Pumps are made of high grade steel containing molybdenum and vanadium. Conveyance of the melt is effected as follows: the engaged teeth of both gear wheels open opposing gaps when they turn. These are filled with melt arriving from the feed channel which is seized by both gear wheels. When the two wheels mesh, the melt is again pressed out of the gaps in the gear wheel by opposite teeth and reaches the spinneret via the built-in filtering device. Spinning of fine filaments normally requires spinning pumps of 1–4 cm^3 capacity per revolution and 10–35 rev min^{-1}. The spinning of coarse filaments or staple fibre requires pumps with a considerably greater capacity of about 20 cm^3 per revolution and more.
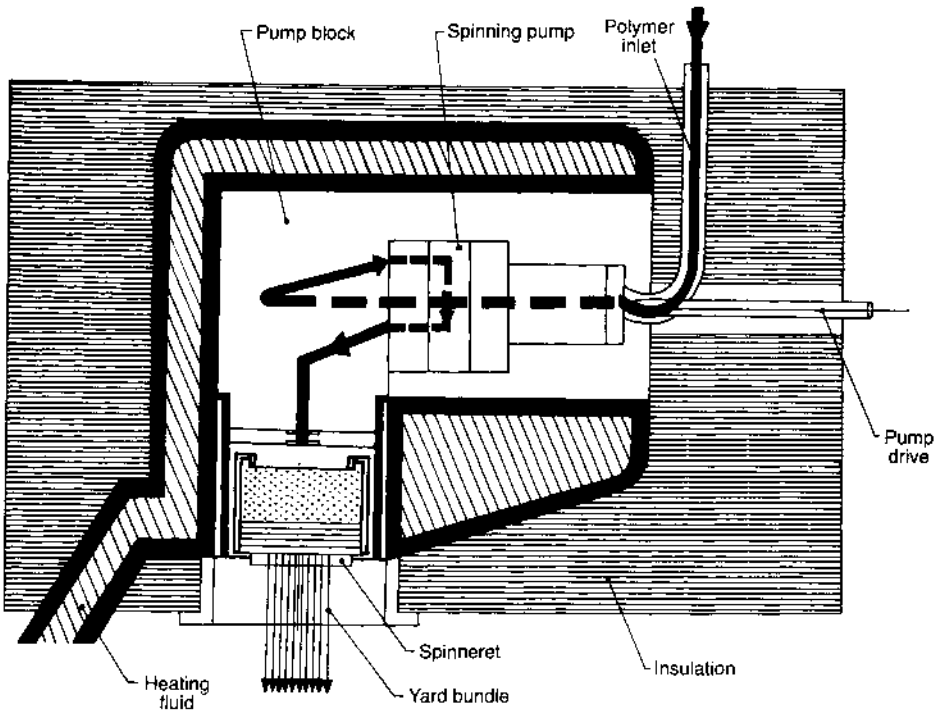
Fig. 4.5 A spinning head (adapted from reference [5]).

The metering pumps must be capable of feeding against high back pressures of 20–200 bars without change of feed rate and with a precision of ±3%.

For filtration, graded fine sand or alumina held in place by metal screens or sintered metal disks is employed [7]. The sieves and the filter sand are in a device which supports the filtration system; this also accommodates the spinneret plate and the bracket plate. Filtration removes large solid or gel particles. Smaller particles, such as delustrants, are not retained by the filter. The filters also influence the rheological behaviour by providing shearing action. The spinnerets are made of stainless steel 3–30 mm thick and contain holes of diameter 100–500 μm. Many different arrangements of holes are available such as concentric circles, parallel rows and scatter patterns. The holes are relatively wide and cylindrical at the inlet end and eventually narrow conically to their ultimate diameter which is maintained for a length of only one to five diameters. The number of holes varies from two to four for monofilaments to up to 60 000 for heads contributing to a staple tow.

The combined filter and spinneret assembly, or pack, is removable and is exchanged at intervals to avoid development of unduly high pack pressures or hole blockages.

The heated pack body sometimes extends a few centimetres below and around the edge of the spinneret to form a shroud that provides a heated zone around the initially extruded yarn. A blanket of hot gas around the threadline allows a spun yarn of low orientation but high orientation potential to be produced, which can be converted to high tenacity yarn.

4.2.5 THE COOLING SYSTEM

Between 1937 and 1940 the first melt-spun fibre, nylon 66, was extruded through spinneret holes at 285 °C and cooled by natural convection down to 40–80 °C before reaching the first contact points (finish application rolls, godets, etc.). For the cooling, a distance of 5–6 m at take-up speeds of 600–800 m min^{-1} was necessary, corresponding to a cooling time of approximately 0.7 s. The boundary layer of air formed by air friction on the filament caused poor heat convection and a certain instability in the thread path. A 1939 Du Pont patent claimed that the boundary layer could be made as small as possible by providing a cross-flow of air, thus reducing the thread cooling path to 1.5 m, corresponding to a cooling time of about 0.5 s. Many important developments in later years have reduced the cooling time to 0.05 s for fine yarns. The following types of quenching systems [5] are in use (for schematic representation, see Figs 4.6(a), (b) and (c)):

1. cross-flow quench;
2. in-flow quench;
3. out-flow quench.

Cross-flow quench is a universally used method for fine and large deniers and for round and rectangular spin packs. With in-flow quench, air from outside streams radially and symmetrically through the filaments which must be arranged in a ring shape. Together with the filaments, the air then streams downwards. Out-flow quench is used for filament yarns of high deniers and for spinning of staple fibres. In this system, much air can be blown uniformly through a bundle of many, densely arranged filaments. For this type of quench, larger spinneret diameters and distances between the spinnerets are necessary than for the first two methods. Each quench system comprises turbulent air streams but the degree of turbulence is kept to a minimum for production of uniform filament yarns. One disadvantage inherent in cross-flow quench is the fact that not all filaments of the yarn bundle
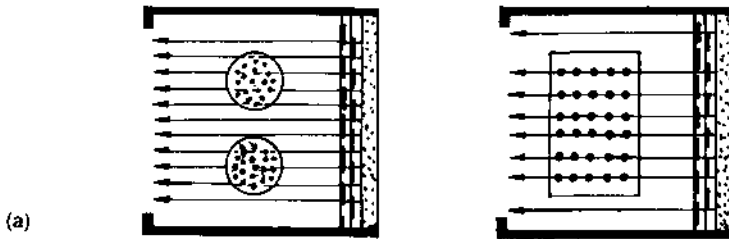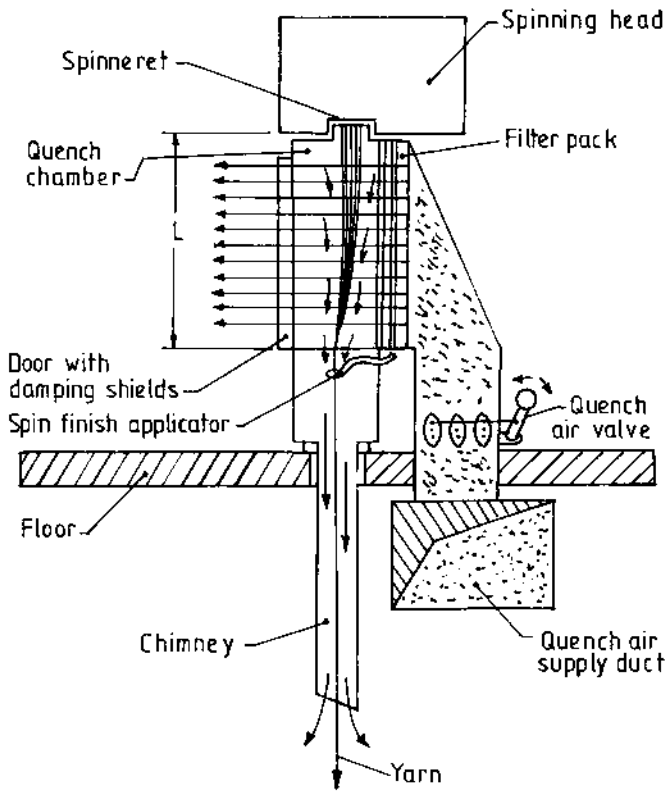
Fig. 4.6 Quench systems for synthetic filament yarns: (a) cross-flow quench, round and rectangular spinnerets; (b) in-flow quench; (c) out-flow quench [5].

Spinneret

Quench chamber

Filter candle

Quench air stream

Ring spinneret

Quench chamber

Chimney

Air stream candle

Filament bundle

Air supply

Counter weight

Yarn bundle

(b)

Fig. 4.6 Continued.

(c)
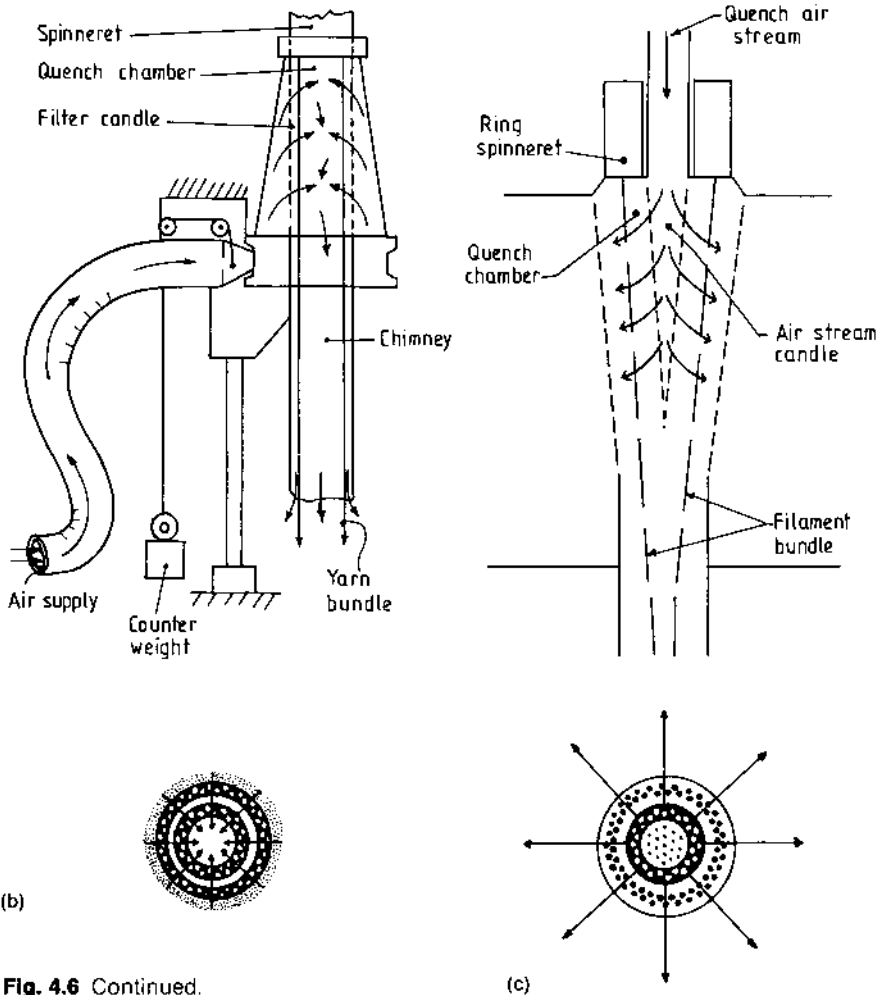
are uniformly provided with air. Quench types with radial air stream are advantageous in this respect. In the in-flow quench system, air streams through a porous tube radially to the centre on to filaments which are arranged in a ring shape. A quench length of about 60 cm is sufficient in this case.

The threadline is sometimes protected from strong draughts by enclosing it in a protective chimney below the quench chamber. In the case of polyamides, some processes include a steam-filled conditioning tube to improve the dimensional stability of the filaments, so that they do not slough off the bobbin during storage due to moisture absorption and further crystallization.

4.2.6 SPIN FINISH APPLICATION

The next step is spin finish application. Conventionally, lubricating systems are mounted at the bottom of the quench duct but there are several advantages in moving the application point at a variable height inside the quench duct, particularly when the speeds of spinning are high. This aspect of fibre production is covered in detail in Chapter 7.

4.2.7 THE WIND-UP DEVICE

The take-up device lies horizontally below the appropriate spinneret. To attain uniform speed, the tube roll is friction-driven by a roller; this ensures that the requirement of constant take-up speed is complied with when the diameter of the wrap increases. Generally the yarn passes through two godets before reaching the package winder. In order to lay the filament satisfactorily around the package, it is grasped by the forked thread guide and moved equally to the left and the right by a traverse guide. In high speed spinning, godets are generally dispensed with and a grooved roller is used in conjunction with tube rolls. An alternative driving mechanism is based on the spindle drive in which the speed of rotation of the spindle is controlled by a signal from an on-line tension pick-up device.

4.3 MELT-SPINNING VARIABLES AND CONDITIONS FOR CONTINUOUS SPINNING

4.3.1 MELT-SPINNING VARIABLES

There are many state variables involved in melt-spinning which determine the course of fibre formation and the resulting fibre dimensions and properties. Ziabicki [8] has divided these variables into three groups:

1. Independent or primary variables, which uniquely determine the course of the spinning process and the resulting fibre structure and properties.
2. Secondary variables, which are related to primary variables through simple geometrical relationships and are useful in defining spinning conditions.
3. Resulting variables, which are determined by the independent variables through the fundamental laws of spinning kinetics.

These groups can be subdivided as follows.

1. *Independent (primary) variables*
   (a) Polymer material;
   (b) Extrusion temperature (T_0);

   (c) Spinneret channel dimensions (d_0, diameter; l_0, length);
   (d) Number of filaments in the spinning line (n);
   (e) Mass output rate (W);
   (f) Spinning path length (L);
   (g) Take-up velocity (V_L);
   (h) Cooling conditions (cooling medium, its temperature and flow rate).

2. *Secondary variables*
   (a) Average extrusion velocity,

$$V_0 = \frac{4W}{n\rho_0\pi d_0^2},$$

   where ρ_0 is the density of the melt.
   (b) Equivalent diameter of a single filament at $x = L$,

$$d_L = 2\left[\frac{W}{n\pi\rho_L V_L}\right]^{1/2}.$$

   (c) Denier of the filament $= 9000[W(\mathrm{g\,min^{-1}})/V_L(\mathrm{m\,min^{-1}})]$.
   (d) Deformation ratio or melt–draw ratio, $S = V_L/V_0 = d_0^2/d_L^2$.

3. *Resulting variables*
   (a) Tensile force at take-up device, F_{ext};
   (b) Tensile stress at take-up device, $\sigma_L = 4F_{ext}/n\pi d_L^2$;
   (c) Temperature of filament at $x = L$, T_L;
   (d) Filament structure (orientation, crystallinity, morphology).

Walczak considers the above division into primary, secondary and resulting variables to be artificial and superfluous [9]. He divides the variables into two types: independent and dependent. According to Walczak those variables which may be changed directly within a technologically reasonable and possible range, e.g. molecular weight, extrusion temperature, length of quench zone, draw ratio, etc., are independent variables. Such properties, conditions or states which do have an influence on the course or result of the process of fibre formation but cannot be regulated independently are taken as dependent variables. A change of every independent variable causes change in at least one dependent variable. The dependent variables, on the other hand, are usually affected by changes of more than one of the independent variables.

4.3.2 CONDITIONS FOR SPINNING WITHOUT A BREAK

Ziabicki has considered the mechanical aspects of fibre spinning [10] and postulated that two general conditions should be fulfilled if spinning without a break is to be accomplished:

1. Continuity of flow:

$$AV\rho = \text{constant} = W,$$

   where A is the cross-sectional area of the spinning line at any inter-
   mediate point, V the linear stream (fibre) velocity and ρ the density.
   W is the mass output rate (mass extruded in unit time through the
   spinneret orifice and therefore equal to $Q\rho$).

2. The tensile stress on the melt stream must never exceed the tensile
   strength of the filament.

4.4 SPECIAL FEATURES OF HIGH SPEED SPINNING

4.4.1 THE PROCESS AND THE PRODUCT

A typical high speed spinning plant was shown in Fig. 4.2. The higher
the output and the higher the spinning speed, the greater are the
demands on the quality of the melts fed to the spinneret. This increased
quality requirement applies not only to the polymer feed with respect to
viscosity, homogeneity, freedom from dust, etc., but also to the proces-
sing conditions, involving proper drying and optimum melting condi-
tions in the extruder. The propulsion and distribution of the melt to the
individual spinning positions, including mixing and filtering, require
more attention. To deliver a perfectly homogeneous polymer melt,
static mixers for distributive mixing are installed between the extruder
and the metering pumps [11]. The mixing elements consist of a lattice
made up of cross-wise interlocking webs which are at an oblique angle
to the pipe axis and are incorporated in the pipework of the spinning
system. Another area that needs special attention is the quenching of
the filaments. When spinning at super high speeds, as the quench air
flow rate is increased, the number of broken filaments passes through a
minimum (optimum) value [5]; this phenomenon is not usually observed
at conventional spinning speeds. Greater shear forces generated by the
special spinneret will provide a surface temperature high enough to
compensate for the extensive quenching of the threadline that is needed
to obtain adequate cooling at these super high speeds. The heat from
crystallization will also add to this. Control of thread tension in the
wind-up zone becomes more difficult with increasing spinning speed.
In contrast to conventional spinning, wind-up in high speed spinning is
often carried out without godets, as shown earlier in Fig. 4.2(a). The
absence of godets reduces capital costs and makes thread string-up
simpler. However, the advantage of godets in that they allow the adjust-
ment of wind-up thread tension by the speed difference between godets
and wind ups, regardless of the thread tension exerted by drawing from
the spinneret, is lost. When spinning without godets, the wind-up

mechanism itself assumes the role of drawing-off from the spinneret. The thread tension is consequently the wind-up thread tension.

In addition to controlling thread tension as discussed above, the following requirements are also imposed on high speed winding devices: stability in operation, the possibility of winding two or more packages on a single working position, preparation of packages of weight not less than 10 kg, a low noise level, and simple to use, repair and maintain. With the increase in the weight of the packages, mechanized or automated package removal devices (so-called 'auto-doffers') have also been developed.

In the conventional process of melt-spinning, which was in use for a very long time, spinning was done at 600–1500 m min^{-1}. The spun yarn was then drawn at 400–1000 m min^{-1} to draw ratios of between 3 and 4.5.

The production of fibres at speeds higher than conventional speeds will now be considered in more detail.

4.4.2 SPINNING AT MODERATELY HIGH SPEEDS

When filaments are produced at speeds of up to 1800 m min^{-1} they are known as low oriented yarn (LOY). Speeds between 1800 and 2800 m min^{-1} lead to the formation of medium oriented yarn (MOY). Polyester yarns spun in these speed ranges have limited storage and transport capabilities.

Filaments spun at 2800–4000 m min^{-1} give rise to partially oriented yarn (POY). For polyester (PET), POY for draw-texturing is produced at speeds of 2800–3500 m min^{-1}. This ensures cost-effective operation in the spinning line as well as high quality subsequent processing in the texturing plant. The packages can be transported with ease and can be stored for months. For polyamide POY, speeds of 2500–4500 m min^{-1} have been used [13] but speeds of 4200–5000 m min^{-1} have become customary so that spinning can be more cost-effective for the fine deniers. For subsequent processing of the POY packages to flat yarn by draw-twisting or recently also by draw-warping, these packages are used with great success because of their transport and storage stability and their excellent take-off performance at high speeds. Two reasons have been given [12] for the relatively lower speeds used for polyester (PET) POY production compared with those used for polyamide POY. First, polyester is more highly sensitive to mechanical strain than polyamides; for example, in ring spinning, polyester gives a far greater amount of fibre rubbing (snow) than in polyamides, so problems are found to arise at a much earlier stage. Second, the throughput vs. spinning speed curve (Fig. 4.7) shows [13] that polyester performance curve flattens remarkably so that speeds have to be increased to over 4000 m min^{-1} in order to achieve a rise in throughput as speeds are
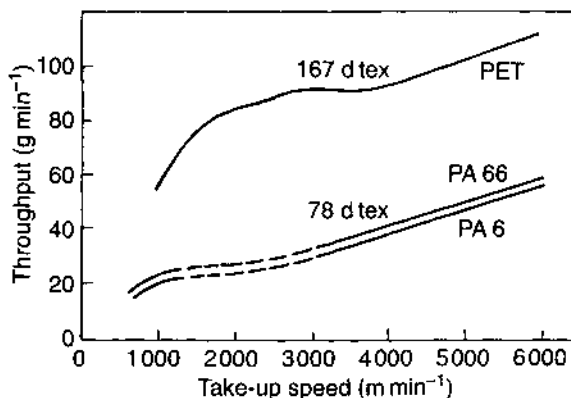
Fig. 4.7 Throughput vs. spinning speed [13].

raised. By contrast, polyamide throughput rises almost linearly as speed increases. Polypropylene POY is produced at speeds of $4000 \, \mathrm{m \, min^{-1}}$ and then draw-textured for making knitted goods. The normal polypropylene grades have a polydispersity $(\bar{M}_w / \bar{M}_n)$ of 7; for POY production a narrow molecular weight distribution with polydispersity of 3 is recommended. One benefit is that the strength of the filament is greater than $3.5 \, \mathrm{g \, den^{-1}}$ in the narrow distribution case compared with $2-2.5 \, \mathrm{g \, den^{-1}}$ for the wide distribution sample.

4.4.3 SPINNING AT VERY HIGH SPEEDS

From the industrial point of view, a one-step process based on high speed spinning is very attractive to fibre producers. High speed winders up to $6000 \, \mathrm{m \, min^{-1}}$ were developed in 1978 and high speed spinning machinery became available in 1981.

Yarn made at speeds of $4000-6000 \, \mathrm{m \, min^{-1}}$ is called highly oriented yarn (HOY). It is not fully oriented and has elongation-to-break values of between 40 and 60%. In order to obtain fully oriented yarn (FOY) by a one-step process, with elongation-to-break values of 20–30%, spinning speeds of well over $6000 \, \mathrm{m \, min^{-1}}$ would be needed. This is presently not viable either economically or technologically. However, research in this area continues and it has been reported that in the case of PET the use of a heated sleeve near the spinneret face and a liquid isothermal bath around 100 cm below the spinneret allows a filament to be produced in one step having structure and properties identical to those of a two-step process [14]. Alternatively, the spin–draw method described in Section 4.7 is already established.

There are currently two possibilities for making use of one-step process yarns, that is either to use them as they are or to modify these yarns

so that they have properties closer to those of a fully drawn yarn made by the conventional two-step process. Both these possibilities have been tried.

4.4.4 THE CURRENT STATUS OF HIGH SPEED SPINNING

In the usual melt-spinning technology, the increase in wind-up speed from 1000–1500 m min^{-1} to 4000 m min^{-1} has now become accepted and wind-up speeds up to 4000 m min^{-1} are widely used. High speed spin–draw and highly oriented yarn (HOY) technologies at speeds of around 6000 m min^{-1} are now being used to some extent. Speeds above 6000 m min^{-1} have only been used to a very slight extent and the yarns produced are seen to have properties different from the yarns produced using existing, more common techniques. Research and development work is going on to develop new application fields for these yarns.

4.5 THE ROLE OF SOME CRITICAL PARAMETERS AND THEIR VARIATION ALONG THE SPINLINE

The fibre manufacturer controls the basic spatial arrangement of molecules in the spun fibres, and thus the properties of the fibre, through the various state variables listed earlier. While the role of the various spinning parameters in controlling the structure and properties of the spun fibre is considered in some detail in the next chapter, two basic features, namely the various components of tensile force and the variation of some critical state variables along the spinline, will be briefly considered in this section.

4.5.1 THE TENSILE FORCE

The extensional force produced by the winding drum of the take-up device (F_{ext}) and the force due to gravity (F_{grav}) are balanced by the rheological frictional force which arises because of the friction between molecules (F_{rheo}), the aerodynamic force (F_{aero}) which is due to the drag exerted by the ambient gaseous medium on the moving stream, the inertial force (F_{inert}) and the surface tension force (F_{surf}). Thus, we may write [8]:

$$F_{ext} + F_{grav} = F_{rheo} + F_{aero} + F_{inert} + F_{surf}.$$

The data of Ziabicki [8] on nylon 6 spun at a winding velocity of 656 m min^{-1} showed that it is reasonable to assume that the force is constant along the spinline.

The assumption of constant force along the spinline is not valid at higher spinning speeds, as is clear from Ziabicki's calculations of the
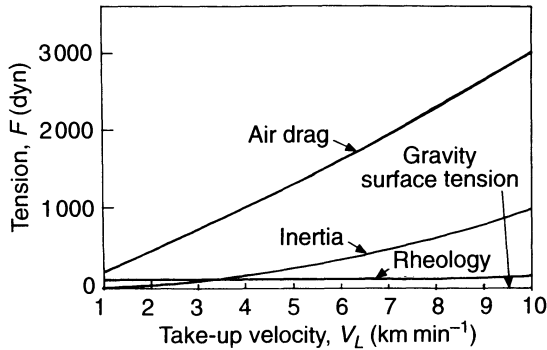
Fig. 4.8 Individual contributions to take-up force for PET fibres.

individual tension contributions to the total take-up tension from the analysis of spinning dynamics [15]; the results are shown in Fig. 4.8. For low velocities (up to 1000–2000 m min^{-1}), spinning dynamics is considerably affected by the rheological force, i.e. the rheological resistance of the extruded polymer melt to applied stress. For high velocities, the dominant role is played by the air drag force. The air resistance can be lowered by forming the filaments into a bundle as near to the spinneret as possible or by providing a flow of compressed air in the spinning direction. It has also been suggested that the thread can be formed into bundles by an electrostatic field.

4.5.2 THE NATURE OF VARIATION OF SOME PARAMETERS ALONG THE SPINLINE

Some state variables for two melt-spinning threadlines of PET produced at wind-up speeds of 1218 m min^{-1} [16] and 6000 m min^{-1} [17], respectively, are shown in Figs 4.9(a) and (b). As expected, the 6000 m min^{-1} threadline develops much higher birefringence compared with the 1218 m min^{-1} threadline, apparently due to the much higher stress at the higher speed. It is also interesting to note that in both cases the velocity gradient along the spinline first increases to a maximum and then decreases; the peak appears at a distance of 30–40 cm from the spinneret exit for the low speed spun PET yarn and 110–120 cm from the spinneret exit for the high speed yarn. However, such a simple comparison of the data in terms of the effect of only one state variable, namely take-up speed, can be misleading for the following reasons: first, as indicated, the throughput rates in the two cases are different; second, while at the low spinning speed the material remains amorphous, at the higher spinning speed it crystallizes; and third, the other state variables in the two cases such as quench air temperature and flow rate may not be
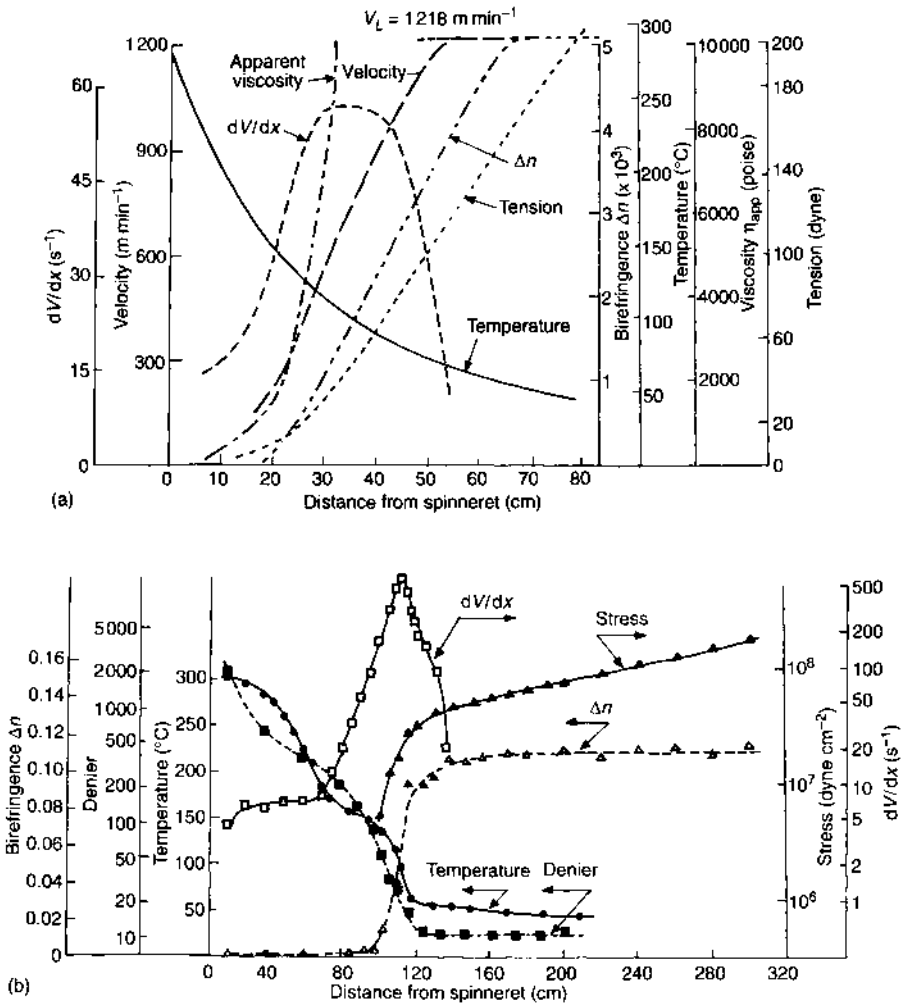
Fig. 4.9 Some state variables for PET melt-spinning threadlines for wind-up speeds of (a) 1218 m min^{-1} [16] and (b) 6000 m min^{-1} [17].

identical. The effects of the first two factors will now be considered. The effects of various other state variables are considered in Chapter 5.

(a) The effects of variable throughput rate [18]

To gain a clear understanding of the effects of variable throughput rate, we need to be aware of the way in which variable winding speed affects key state variables at *constant* throughput rate. Figures 4.10(a) and (b) show the effect of variable winding speed at constant throughput rate
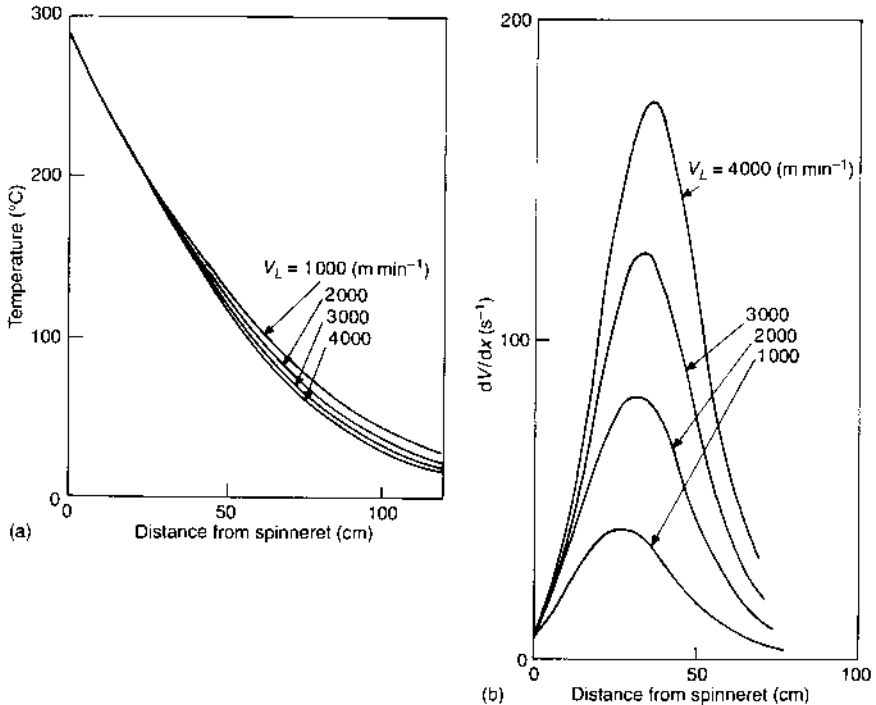
Fig. 4.10 Calculated average temperature profiles (a) and velocity gradient distributions (b) for different winding speeds at a constant throughput rate of 2.70 g min^{-1} per hole [18].

on temperature and velocity gradient (dV/dx) along the spinline. Now keeping the winding rate constant, Figs 4.11(a) and (b) show the effect of *variable* throughput rate on temperature and velocity gradient along the spinline. In both cases, under the conditions used, PET cannot crystallize during spinning so the effect of crystallization need not be taken into account. It should also be noted that the results presented on temperature and velocity gradient distribution are based on simulation using the energy balance equation and the constitutive equation, respectively.

It can be seen that, at constant throughput rate, the effects of take-up velocity on the temperature profile (Fig. 4.10(a)) and the velocity gradient distribution (Fig. 4.10(b)) are small. Thus the solidification point is mainly dependent on the extrusion rate. However, the variation of throughput rate at constant take-up velocity results in significant changes in the temperature profile and also in the velocity gradient distribution (Fig. 4.11). Assuming that the solidification point is T_g (70 °C), the position of the solidification point is seen to change from 60 cm to 145 cm from the spinneret with increasing extrusion rate [18].
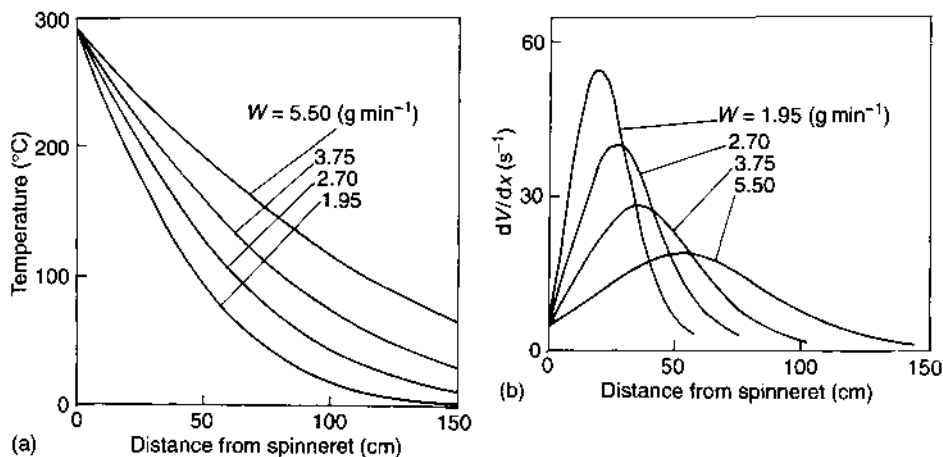
Fig. 4.11 Calculated average temperature profiles (a) and velocity gradient distributions (b) for different throughput rates at a constant winding velocity of $1000\,\mathrm{m\,min^{-1}}$ [18].

(b) The consequences of crystallization

The crystallization of the threadline during spinning occurs in the case of PET at wind-up speeds of $5000\,\mathrm{m\,min^{-1}}$ and above. The velocity profiles for melt-spun PET for a range of take-up speeds ($3000\text{--}6000\,\mathrm{m\,min^{-1}}$) at constant throughput rate are shown in Fig. 4.12 [19]. The data on deformation rate or velocity gradient distribution in PET spinlines for wind-up speeds of $4000\text{--}10\,000\,\mathrm{m\,min^{-1}}$, taken from another source [20], are shown in Fig. 4.13. The data in the two figures are for different throughput rates but some wind-up speeds are common.

The velocity and velocity gradient profiles for amorphous spinlines are seen to be significantly different compared with those for crystallizing spinlines. In the amorphous spinline, there is a gradual build-up of velocity which gives rise to a broad velocity gradient distribution. In this particular case, since the throughput rate is high, the velocity gradient peak at a wind-up speed of $4000\,\mathrm{m\,min^{-1}}$ is far removed from the spinneret exit. At higher speeds the induced crystallinity results in an abrupt rise of velocity, suggesting an almost instantaneous change from a viscous melt to a semicrystalline solid; this is consistent with the observed necking of the spinline. It is also noteworthy that with an increase in spinning speed, the maximum of the velocity gradient moves closer to the spinneret. This is apparently because at higher speeds stress-induced crystallization can occur and shift the peaks to higher temperatures, thus moving the dV/dx peak closer to the spinneret exit.

It may be noted that conditions such as higher temperature of extrusion and higher throughput rate slow the process of cooling. This
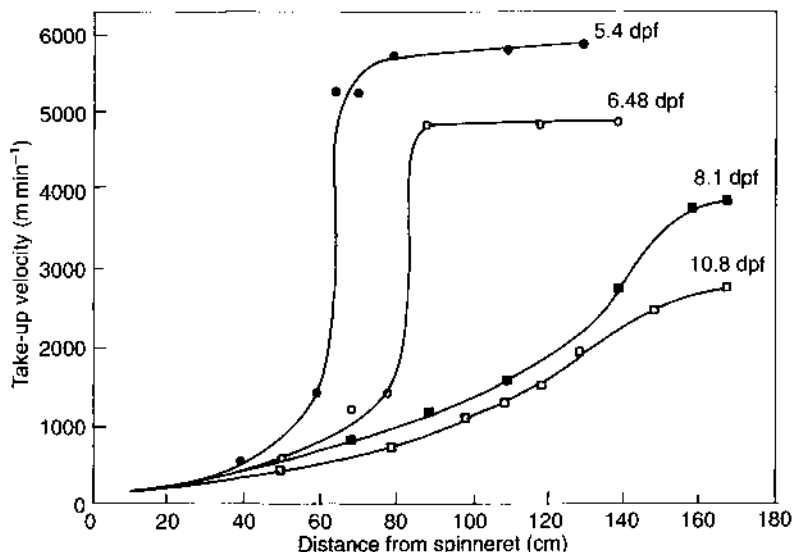
Fig. 4.12 Measured velocity profiles for melt-spun PET yarns at a range of take-up speeds at a constant throughput of $3.6\,g\,min^{-1}$ per hole (denier per filament, dpf, indicated) [19].

reduces the peak value of the velocity gradient, as well as shifting the location further away from the spinneret exit. This is not surprising because now the deformation can take place over a large distance, since the location of the freeze line is also farther from the spinneret exit.

In the above discussion, considerable importance has been attached to velocity gradient profile or the rate of filament thinning which is
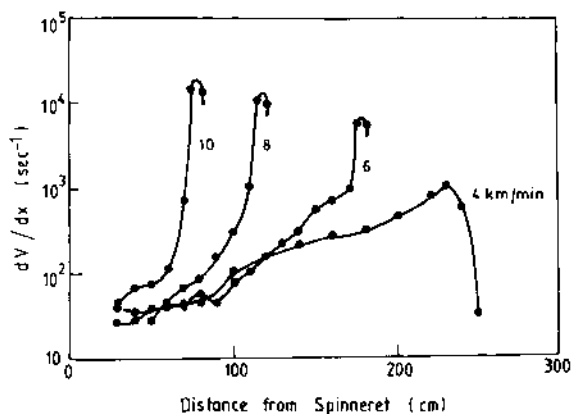
Fig. 4.13 The variation of deformation rate along the spinline for a range of take-up speeds as indicated at a constant throughput of $6.2\,g\,min^{-1}$ per hole [20].

determined by the deformation of filaments under stress. This is because this state variable, together with temperature, which depends mainly on convective heat transfer by the air used for quenching, have been identified as the two state variables that predominantly affect changes in fibre properties during spinning [21]. The temperature profile and the velocity gradient profile are both related to the location of the freeze line. Ziabicki has shown [22] that the condition for the point of inflexion in velocity gradient is an increase in elongational viscosity along the axis, no matter how it depends on the velocity gradient. The data given in Fig. 4.9(a) show that the exponential rise in apparent shear velocity coincides with the point of inflexion. Since the shear viscosity (η) has been estimated from the elongational viscosity (λ) assuming that $\lambda = 3\eta$, Ziabicki's basic postulate is confirmed. To that extent the point of inflexion relates to a structural transition involving initiation of 'solidification'.

4.5.3 THE COUPLING OF STATE VARIABLES

In considering the roles of different state variables, the interaction between them should also be taken into account. In particular, it must be noted that for a given denier product, the spinning parameters are coupled. As an illustration, two primary state variables, namely throughput rate and take-up velocity, may be considered. For a constant throughput rate, increase in take-up velocity increases orientation due to enhanced spin draw in the spinline. For a constant take-up velocity, however, orientation reduces as the throughput rate is increased. This is because the filament denier increases rapidly with the throughput rate even though the spinline tension actually decreases marginally. The net effect, therefore, is a reduction in spinline stress as throughput rate is increased. Thus to produce products over a range of denier and tenacity, the throughput rate and take-up speed have to be jointly manipulated.

4.5.4 MINIMIZATION OF PRODUCT VARIABILITY

To ensure product uniformity the state variables must be controlled within very narrow limits. Even a variation of 1% in extrusion temperature, for example, can result in a 10% variation in spinline stress, which in turn can give rise to a significant increase in the coefficient of variation of filament denier. Thus accurate temperature control and monitoring of spinline pack temperature are critical.

A number of factors contribute to filament non-uniformity. Take-up tension variation due to slight fluctuation in temperature has already been mentioned as a possible cause. Some of the other factors are: heterogeneity of the spinning melt; instability of flow within the spinneret channel, non-uniform channel dimension in the spinneret; time

variation of technical process variables like temperature and throughput rate, flow rate of cooling medium in the quench chamber, etc. To ensure steady-state spinning so that filaments of the required uniformity are produced, it is essential to exercise strict control on the polymer, melt homogeneity and the various state variables and other factors mentioned above, so that variation in filament dimensions is kept to a minimum.

4.6 STRUCTURE FORMATION DURING SPINNING

4.6.1 STRUCTURE DEVELOPMENT AT LOW SPEEDS

(a) Molecular orientation

Molecular orientation arises from parallelization of the molecular chains along the fibre axis in both the crystalline and non-crystalline regions of the fibre. In polymers exhibiting very low crystallization rates, e.g. PET, the orientation produced by spinning at low speeds involves amorphous regions alone. On the other hand, rapidly crystallizing polyolefins and polyamides show some orientation of crystallites accompanying that of amorphous regions. In ordinary low molecular weight molecules, thermal agitation is normally fast enough to counteract completely the tendency of the flow to deform and orient the molecules. In macro-molecules, the relaxation time is several orders of magnitude larger and grows rapidly with molecular weight, entanglements and the need for co-operative motion. The chain conformations can thus rearrange with the possibility of development of significant orientation.

The development of molecular orientation during spinning may be considered in two stages: first, in the spinneret channel, and then during the elongation of the fluid filament. When the fluid is forced through the channel, the macromolecules are aligned in the direction of flow. As the filaments emerge from the spinneret exit, they are pulled rapidly towards the winding mechanism and the tensile force results in molecular alignment. Molecular alignment in the spinneret channel contributes very little to orientation because the aligned molecules become disoriented on coming out of the channel. The orientation due to elongation of the filament contributes the main part of the spin orientation. This is evident from Fig. 4.14 [23], where the birefringence of the spinning line of PET is plotted against distance from the spinneret. This suggests that the spinning orientation results from extensional flow and the factors which are important in the spinning line are the parallel velocity gradient, the relaxation time distribution of the fluid and the elapsed time. The spin orientation increases with heat transfer coefficient of the filament (the higher the rate of heat removal from the filament, the more effective the freezing of orientation on filament quenching), take-up
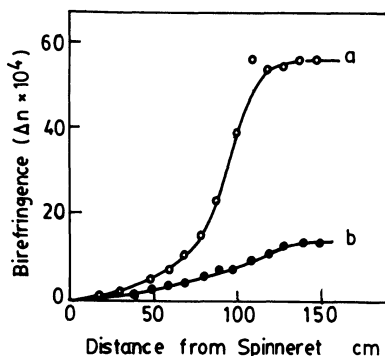
Fig. 4.14 Birefringence of melt-spun PET fibres vs. distance from the spinneret for two take-up velocities: (a) 1000 m min^{-1}, (b) 400 m min^{-1} [22].

velocity, extrudate viscosity (the higher the viscosity, the greater the relaxation time and therefore the higher the retained orientation) and reciprocal outflow intensity or $1/W$ (low mass output means more efficient quenching). The effect of spin draw ratio is of secondary importance (when filament thickness and take-up velocity remain unchanged), which distinguishes this process from cold drawing where draw ratio is the most important factor.

(b) Crystallinity and morphology

Formation of crystallites, like molecular orientation, plays a very important role in melt-spinning. Non-isothermal and oriented crystallization of the filament is very sensitive to spinning conditions. Since spinning is done above the melting point and the fibre cools along the spinline, somewhere along the spinline crystallization commences. However, where this happens differs from polymer to polymer. Crystallization is almost zero for rapidly solidified, slowly crystallizing polymers like melt-spun polyethylene terephthalate, intermediate for rapidly solidified but fast crystallizing polymers like melt-spun polyamides, and high for very fast crystallizing polymers like polypropylene and polyethylene.

It is well known that polymers crystallize faster under strain. The residence time of the polymer from spinneret to take-up rollers is 0.10–10 s. For unoriented PET the maximum crystallization rate is 0.025 s^{-1}, while for oriented PET it is 10^2–10^6 s^{-1}.

Crystallinity, unlike orientation, is found to decrease with an increase in heat transfer coefficient and increases with an increase in filament (spin-line) radius. This is because slow cooling gives more time for molecules to form crystallites. Increasing cooling rate decreases crystallization rate for the same reason.

Information on the effect of spinning conditions on the crystallinity of as-spun fibres is rather scanty. Often the crystallinity of as-spun fibres is characterized in terms of density. It should be noted that macroscopic density fails as a quantitative measure of crystallinity when many structural modifications with different densities are involved, or when micro- or macro-voids are present.

It has been shown [24] that when a polymer crystallizes under axial deformation, the nuclei are formed along the stress direction and grow in the form of platelets perpendicular to this direction; this is known as row nucleation and is believed to occur in both melts and solutions. During spinning, a large number of molecules become extended and form a bundle. Such a string forms a nucleus from which molecules crystallize radially. Platelets, consisting of lamellae of folded crystals longitudinally tied by the string-like row nucleus, form perpendicular to it. This morphological entity is believed to be formed during the spinning of crystallizable fibres. Fibrillar structures have been observed in melt-spun PET. Spherulites appear only sporadically in some melt-spun fibres, in particular when thick filaments are spun at low speeds.

4.6.2 STRUCTURE DEVELOPMENT AT HIGH SPEEDS

(a) PET filaments

It has been pointed out [25] that the tensile stress reaches a level of $10^7 \, \mathrm{dyn \, cm^{-2}}$ at the take-up point. This level of stress is in the range of yield stress required for hot drawing of PET fibres (the stress level required for cold drawing is around $5 \times 10^9 \, \mathrm{dyn \, cm^{-2}}$). These observations led Shimizu, Okui and Kikutani [26] to propose a scheme for the development of fibre structure along the spinline (Fig. 4.15), according to which the fibre diameter decreases from the molten state in which the molecules have random orientation. With a further decrease in fibre diameter, an oriented mesophase is formed. At a certain point along the spinline, neck-like deformation appears. After the neck-like deformation has been completed, the diameter does not change and a high degree of crystallinity and a high molecular orientation are achieved.

Thus at take-up speed of 3000–4000 m min⁻¹, the as-spun filaments of PET (called POY), show a relatively high molecular orientation but almost no crystallinity, the maximum velocity gradient along the spinline being $120 \, \mathrm{s^{-1}}$. Above 5000 m min⁻¹, the velocity gradient is $1000 \, \mathrm{s^{-1}}$ and high orientation and high crystallinity are obtained. At such a high take-up speed, the time required for passage through a 10 cm length in the spinline is only about 1 ms and the temperature at the position of abrupt thinning is 100–150 °C. Therefore, compared with the conventional two-stage PET yarn, the crystals in high speed spun filaments are
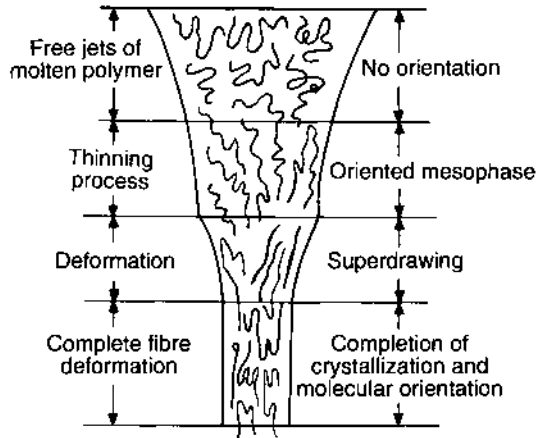
Fig. 4.15 The development of fibre structure in the spinline at high spinning speeds [25].

larger and more perfect. Also crystallinity and crystal orientation are high but amorphous orientation is low.

(b) Nylon 6 yarns

In the case of nylon 6 polymer, high speed spinning leads to yarns containing mixtures of two-crystal modifications: α and γ.

The studies reported by Heuvel and Huisman [27] were made on nylon 6 yarns spun from chips at 290 °C with spinneret hole diameter 250 μm and winding speeds of 700–5500 m min^{-1}. X-ray studies were made on both dry (unconditioned) and conditioned (at 20 °C, 60% relative humidity, RH) yarns. In the dry, unconditioned sample, the crystallization process did not reach completion during spinning when the yarns were spun at speeds lower than 3000 m min^{-1}. At higher winding speeds, crystallization reaches completion. In this respect, nylon 6 shows a clear analogy with the behaviour of PET yarns. With respect to the conditioned yarn, it should be emphasized that a large difference between nylon 6 and PET is that conditioned nylon 6 is above its T_g under normal conditions in the winding room. This permits a continuation of the crystallization process under winding room conditions. It follows that the structure present in conditioned yarns spun at lower speed is mainly due to crystallization after moisture pick-up, while the crystals in the yarns wound at speeds higher than 3000 m min^{-1} are already generated during the spinning process. Also orientation-induced crystallization promotes the γ phase. These seem to form from orientation-induced nuclei.

When the as-spun yarn is subjected to further drawing or to heat-setting, the γ crystal phase changes into the more stable α form.

4.7 INTEGRATED SPIN–DRAW PROCESS

Though patents for high speed spinning were registered by Du Pont in the USA as early as 1952 (for example, see reference [28]), its commercial exploitation had to await the availability of high speed winders at an economic price; this happened in the early 1970s. Around 1960 a new process was introduced into commercial production, in which spinning and drawing were combined into a coupled spin–drawing (SD) process. A British patent was filed in 1958 and a US patent in 1961. This process has assumed significance in tyre cord production but its development on a commercial scale was also linked to the availability of high speed winders. Draw winders, which are based on side winding and introduce no twist (as opposed to draw-twisters, which introduce a small amount of twist into the yarn at wind-up by end-winding using a ring and traveller system), can operate commercially at up to about $6000 \, \text{m min}^{-1}$ and are therefore much more productive. To make the yarn coherent in subsequent processes, it is usually necessary to introduce some substitute for twist; the most generally used methods depend upon physical intermingling of the individual filaments by passing them through an air or stream jet intermingler just before they are wound up. A typical spin–draw attachment for production of nylon 66 tyre yarn is shown in Fig. 4.16. Here the spinning speed is low and the yarn is drawn in two stages in a coupled SD process; the final winding speed is high. The entanglement jet shown in the figure intermingles the filament, giving them cohesion.

An interesting use of SD technique is the production of bulked continuous filament (BCF) yarn. After spinning and drawing in a single process, the fully drawn filament yarn is conveyed to a stuffer box by hot air or steam, where filaments buckle under the influence of the heat.

The equipment and energy costs for the three principal processes are compared in Table 4.1 [28]. The numbers shown in this table are examples of the calculated costs for spin–draw and one-step processes, assuming the cost of the conventional two-step process to be 100. Here the one-step process is assumed to be an ideal simple spinning process without any additional heating or annealing equipment; consequently it appears in the table as the most economical industrial process.

In the conventional two-step process, the draw-twisted yarn may be highly stressed during twisting and there may exist large variations in winding tension and orientation differences associated with the traverse.
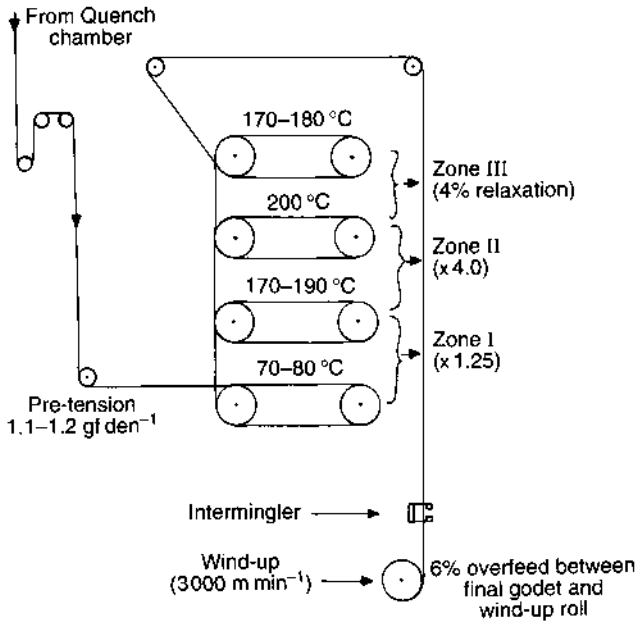
Fig. 4.16 A spin–draw attachment.

The price of draw-twisted yarn is high and the packages are relatively small, while the longitudinal shrinkage may exhibit variations.

Conventional methods of spinning and draw-twisting are now being replaced by more modern improved technology. While the use of POY is established for textured yarn production, the spin–draw process has gained wide acceptance for tyre yarn production. The strength and elongation-at-break values obtained with this process are normally adequate for most end uses. The problem of residual shrinkage is generally under control and the SD yarn has greater dimensional stability due to less heat shrinkage. The final yarn speed in most cases is in the range $3000–4000\,\mathrm{m\,min}^{-1}$.

Table 4.1 Comparison of production cost in the three spinning processes [28]

Method	Cost (arbitrary units)	
	Equipment	Energy
Conventional	100	100
Spin–draw	86	75
One-step high speed spinning	50	45

4.8 OTHER TECHNIQUES TO PRODUCE FIBROUS STRUCTURES

Besides the melt-spinning techniques described here, several other techniques have been utilized [29] to produce fibrous structures. These include solid state extrusion (cold extrusion or hydrostatic extrusion of a polymer billet by application of high pressure), ultra-drawing (melt-spinning of relatively low molecular weight polymer with a specified distribution and then stretching it to very high draw ratios at slow speeds), crystallization from stirred solution (polymer solution is stirred with a counter-rotating device to give a shish kebab type fibrous structure) and high pressure crystallization (e.g. in the capillary of a melt rheometer). Scaling-up of some of these processes on a large scale is being attempted and their potential to provide high speed technology tested.

REFERENCES

1. Ihm, D.W. and Cuculo, J.A. (1984) *J. Macromol. Sci., Rev. Macromol. Chem. Phys.*, **C24**(1), 419–496.
2. Rauwendaal, C. (1986) *Polymer Extrusion*, Hanser Publishers, Munich.
3. Birley, A.W., Haworth, B. and Batchelor, J. (1991) *Physics of Plastics*, Hanser Publishers, Munich, p. 98.
4. McCrum, N.G., Buckley, C.P. and Bucknall, C.B. (1990) *Principles of Polymer Engineering*, Oxford University Press, Oxford, p. 255.
5. Bauer, K. (1987) *Man-made Fiber Year Book*, Chemiefasern & Textilindustrie, Frankfurt.
6. Ludewig, H. (1964) *Polyester Fibers: Chemistry and Technology*, Wiley-Interscience, New York.
7. McIntyre, J.E. (1985) Polyester fibers, in *Fiber Chemistry* (eds M. Lewin and E.M. Pearce), Marcel Dekker, New York.
8. Ziabicki, A. (1967) Principles of melt-spinning, in *Man-made Fibers: Science & Technology*, Vol. I (eds H.F. Mark, S.M. Atlas and E. Cernia), Interscience Publishers, New York, p. 169.
9. Walczak, Z.K. (1977) *Formation of Synthetic Fibers*, Gordon and Breach, New York, p. 210.
10. Ziabicki, A. (1967) Physical properties of fiber spinning processes, in *Man-made Fibers: Science and Technology*, Vol. I (eds H.F. Mark, S.M. Atlas and E. Cernia), Interscience Publishers, New York, p. 13.
11. Schneider, G. (1986) *Man-made Fiber Year Book*, Chemiefasern & Textilindustrie, Frankfurt, p. 27.
12. Reimschuessel, H. (1985) In *Fiber Chemistry* (eds M. Lewin and E.M. Pearce), Marcel Dekker, New York.
13. Treptow, H. (1986) In *Man-made Fiber Year Book*, Chemiefasern & Textilindustrie, Frankfurt; Riehl, L. (1986) *ibid.*, p. 38.
14. Wu, G., Zhou, Q., Chen, J.-Y., Hotter, J.F., Tucker, P.A. and Cuculo, J.A. (1995) *J. Appl. Polym. Sci.*, **55**, 1275.
15. Ziabicki, A. (1985) In *High Speed Fiber Spinning* (eds A. Ziabicki and H. Kawai), Wiley-Interscience, New York, p. 26.

16. Thompson, A.B. (1962) In *Fibre Structure* (eds J.W.S. Hearle and R.H. Peters), Butterworth and The Textile Institute, Manchester, p. 486.
17. Matsui, M. (1985) In *High Speed Fiber Spinning* (eds A. Ziabicki and H. Kawai), Wiley-Interscience, New York, p. 141.
18. Shimizu, J., Okui, N. and Kikutani, T.K. (1985) In *High Speed Fiber Spinning* (eds A. Ziabicki and H. Kawai), Wiley-Interscience, New York, p. 173.
19. George, H.H. (1985) In *High Speed Fiber Spinning* (eds A. Ziabicki and H. Kawai), Wiley-Interscience, New York, p. 271.
20. Murase, Y. and Nagai, A. (1994) In *Advanced Fibre Spinning Technology* (eds K. Kajiwara and J.E. McIntyre), Woodhead Publishing Ltd, Cambridge, UK, p. 25.
21. Prevorsek, D.C. and Oswald, H.J. (1990) In *Solid State Behaviour of Linear Polyesters and Polyamides* (eds J.M. Schultz and S. Fakirov), Prentice Hall, Englewood Cliffs, NJ, p. 131.
22. Ziabicki, A. (1976) *Fundamentals of Fibre Formation*, John Wiley & Sons, London, p. 72.
23. Ziabicki, A. (1976) *Fundamentals of Fibre Formation*, John Wiley & Sons, London, p. 103.
24. Keller, A. (1955) *J. Polym. Sci.*, **31**, 31.
25. Ziabicki, A. (1976) *Fundamentals of Fibre Formation*, John Wiley & Sons, London, p. 207.
26. Shimizu, J., Okui, N. and Kikutani, T. (1985) In *High Speed Fiber Spinning* (eds A. Ziabicki and H. Kawai), Wiley-Interscience, New York, p. 441.
27. Heuvel, H.M. and Huisman, R. (1985) In *High Speed Fiber Spinning* (eds A. Ziabicki and H. Kawai), Wiley-Interscience, New York, p. 295.
28. Kawaguchi, R. (1985) Chapter I, in *High Speed Fiber Spinning* (eds A. Ziabicki and H. Kawai), Wiley-Interscience, New York, p. 15.
29. Ward, I.M. (1985) *Advances in Polymer Science*, Springer-Verlag, Berlin, **70**, 1.

Computer simulation of melt-spinning

5

V.M. Nadkarni

NOTATIONS

A cross-sectional area, m^2
A_L final cross-sectional area, m^2
A_0 initial cross-sectional area, m^2
C stress optical coefficient, Pa^{-1}
C_p specific heat, $J\,kg^{-1}\,{}^\circ C^{-1}$
F spinline tension, N
F_s initial guess for F, N
h heat transfer coefficient, $J\,s^{-1}\,m^{-2}\,{}^\circ C^{-1}$
IV melt intrinsic viscosity, $dl\,g^{-1}$
L freeze line location, m
Q_a volumetric quench air flow rate, $m^3\,h^{-1}$
T temperature, $^\circ C$
T_a quench air temperature, $^\circ C$
T_E extrusion temperature, $^\circ C$
T_g glass transition temperature, $^\circ C$
T_0 spinneret exit temperature, $^\circ C$
V velocity, $m\,s^{-1}$
V_a quench air velocity, $m\,s^{-1}$
W melt flow rate, $kg\,s^{-1}$
x distance from spinneret, m
Δn birefringence
η_0 shear viscosity of PET, Pa s

ρ melt density, $kg\,m^{-3}$

σ spinline stress, Pa

σ_L stress at the freeze line, Pa

5.1 INTRODUCTION

The production of poly(ethylene terephthalate) (PET), nylon and poly-propylene (PP) fibres or filaments involves melt-spinning of the molten polymer followed by solid state drawing and annealing. The final fibre properties such as tensile strength, elongation, shrinkage and dyeability are determined by structural parameters such as orientation and crystallinity. The fibre morphology is the result of the combined influence of the spinning, drawing and annealing steps. Although the desired orientation and crystallinity are achieved primarily through the control of process parameters in the drawing and annealing steps, the fibre line processability in terms of drawability and level of broken and fused filaments is determined by the orientation and uniformity of the as-spun fibres. Also the final product quality para-meters such as the coefficient of variation of fibre denier and tenacity, level of over-length fibres, etc. are influenced mainly by the spinning process variables. This is because the basic spatial arrangement of the polymer molecules with respect to the fibre axis is determined in the melt-spinning step.

The orientation developed in the spinning threadline is the result of tensile deformation under stress in the flowing melt. The net orientation in the flowing melt is determined by the relative rates of extensional flow and the disorienting thermal relaxation phenomena. These rates are governed by the velocity and temperature variation along the threadline. Figure 5.1 is a schematic representation of the melt-spinning process. Molten polymer is extruded through a spinneret into a quench air stream blowing across the spinline. The spinline, so formed, cools and finally solidifies at a distance from the spinneret known as the 'freeze line'. The solidified filament is then wound on take-up rolls at a speed significantly greater than the extrusion velocity. This difference in speed causes stretching of the filament and the final cross-sectional area is con-siderably smaller (about 100–200 times) than the initial extruded area. In the absence of crystallization in the spinline, the orientation of the soli-dified filament represents the orientation in the spinning threadline frozen at or near the glass transition temperature of the polymer. The as-spun orientation is therefore governed by the stress level at the freeze line and controlled via process variables such as extrusion temperature, extrusion velocity, take-up speed, quench air velocity and temperature, etc. The uniformity of the fibre quality is influenced by the fibreline stress.
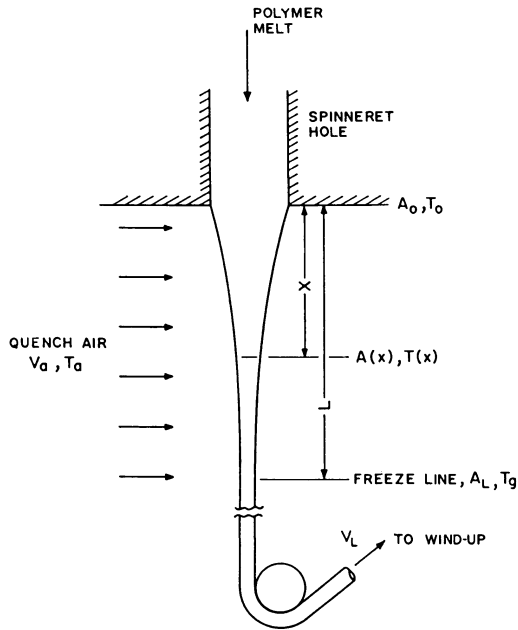
Fig. 5.1 The melt-spinning process.

The development of processing–structure–property correlations in melt-spinning involves establishing mathematical equations for estimating the fibreline stress from readily measurable process variables on the one hand, and quantitative correlations between the fibreline stress and a structural parameter of the solidified fibre on the other. As mentioned earlier, the spinning stage converts the molten polymer to as-spun filaments.

The spinning process represents a non-isothermal, uniaxial elongational flow situation, which is readily amenable to mathematical analysis provided certain simplifying assumptions are made. The initial work on the mathematical formulation of the flow dynamics in melt-spinning was carried out by Kase and Matsuo [1, 2]. This was further improved upon by other research groups [3, 4]. The mathematical equations that have been derived can then be used for computer simulation of the melt-spinning process to illustrate the variation of the fibreline stress with changes in the process variables, such as melt temperature, take-up speed, extrusion velocity, etc. [5–7].

The significant influence of the elongational flow in melt-spinning on the orientation level of the as-spun fibres was first demonstrated by Ziabicki and co-workers for both addition polymers [8] and condensation polymers [9]. The relationship between the orientation and fibreline

stress in vitrified polymers was investigated by White and co-workers [10]. The molecular orientation in the as-spun filaments is the combined effect of extensional deformation and cooling. Thus, the orientation is expected to vary across the cross-section of the filament because of the varying cooling rates across the filament. Such orientation distribution can be predicted by using the simulation approach [5].

Aspects of structure development and the effect of structure on mechanical properties have been reported for nylon 6 [11], isotactic polypropylene [12], nylon 66 [13] and poly(butylene terephthalate) [14].

Among the various synthetic fibres, PET fibres and filaments represent a commercially very important product group. Although parametric studies of PET melt-spinning have been reported in the literature [1,2,5,6,15], the information regarding the sensitivity of the as-spun filament quality to changes in operating conditions and melt properties is not readily discernible from them. This knowledge, however, is of considerable importance for commercial processes as the critical variables need to be controlled carefully. Failure to do so may result in a number of downstream operational problems like poor drawability, unacceptable broken filament count, unacceptable textile processability and increased product non-uniformity (coefficient of variation, CV, of denier). Dutta and Nadkarni [16] have reported on the identification of critical process variables in PET melt-spinning by following a simulation approach based on a constant force model. This approach has been further refined recently by using a variable spinline force model [17]. A majority of the simulation studies have been carried out on a single filament model, whereas the actual commercial process involves multiple filament spinning. In a multifilament bundle, the quench conditions seen by the different filaments are different; Dutta has proposed a simulation approach for the multifilament PET spinning [18].

In this chapter, a simple quantitative procedure is presented for identifying critical operating conditions and material properties for the melt-spinning of PET. The method is based on the experimental observation that for vitrified polymers like polystyrene and PET spun at speeds below $3000\,\mathrm{m\,min^{-1}}$, the molecular orientation of the as-spun filament is uniquely determined by σ_L, the spinline stress at the glass transition temperature (the freeze line). Using a constant tension model which predicts σ_L for a single filament, a sensitivity analysis of the filament orientation to changes in process variables is investigated. Finally, the use of the simulation approach for process optimization and product development is illustrated with the help of commercially relevant case studies [19,20].

For further detailed information on computer simulation of melt-spinning, the reader is referred to recent reviews on the subject [21,22].

5.2 THEORETICAL BACKGROUND

Mathematical analysis of the melt-spinning process has received considerable attention in the literature and therefore will not be dealt with in detail here. Instead, the basic assumptions shall be briefly postulated, the relevant governing equations stated, and the solution technique outlined. Clearly, the spinning stage represents a non-isothermal, uniaxial elongational flow situation with variable physical properties. In order to develop the governing equations, the following assumptions are necessary.

1. The process is operating under steady state conditions.
2. The temperature and velocity field are independent of radial position.
3. The elongational viscosity is independent of extension rate and is equal to the Trouton viscosity.
4. All the molecular motions are 'frozen-in' at temperatures less than the glass transition temperature, T_g.
5. The effects of inertia, gravity, surface tension and air drag are negligible.
6. Dieswell effects are small.

Figure 5.1 shows the coordinate system used for the analysis. Based on the above assumptions, the governing equations can be written as:

$$W = \rho A V \tag{5.1}$$

$$\sigma = \frac{F}{A} = 3\eta_0 \frac{\mathrm{d}V}{\mathrm{d}x} \tag{5.2}$$

or alternatively

$$\frac{\mathrm{d}A}{\mathrm{d}x} = -\frac{\rho F A}{3W\eta_0} \tag{5.3a}$$

and

$$\frac{\mathrm{d}T}{\mathrm{d}x} = \frac{-2(\pi A)^{1/2}}{WC_p} h(T - T_a). \tag{5.3b}$$

The appropriate boundary conditions are

$$\text{at } x = 0, \quad A = A_0, \quad T = T_0 \tag{5.4a}$$

$$\text{at } x = L, \quad A = A_L, \quad T = T_g \tag{5.4b}$$

where L is the distance of the freeze line from the spinneret. The temperature, $T(x)$, the velocity $V(x)$, and the spinline tension F, are obtained by solving equations (5.2) and (5.3) subject to the conditions represented by equations (5.4). In order to accomplish that, however, correlations for the temperature dependence of physical properties (ρ, C_p, η_0) and the heat transfer coefficient, h, need to be provided.
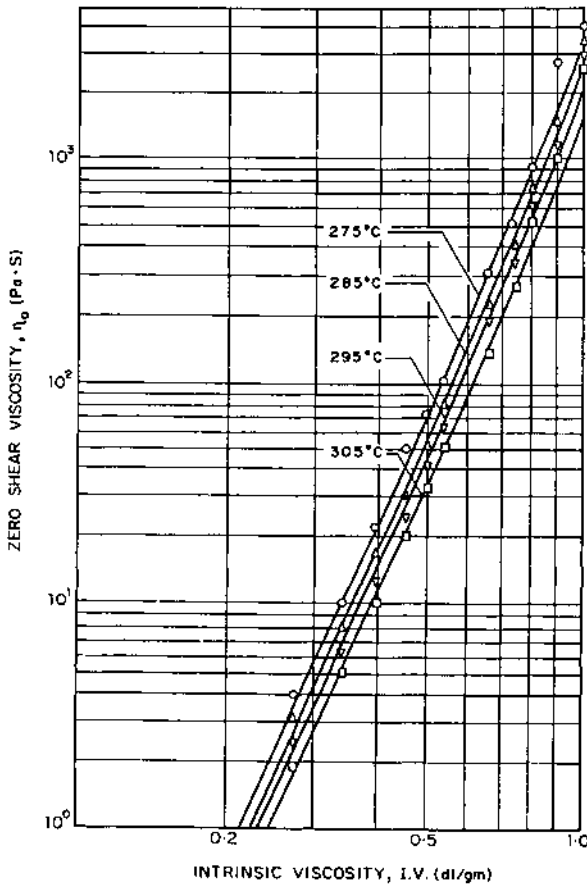
Fig. 5.2 PET shear viscosity as a function of intrinsic viscosity and temperature (V.M. Nadkarni, personal communication). Symbols: $\bigcirc = 275\,°C$; $\triangle = 285\,°C$; $\nabla = 295\,°C$; $\square = 305\,°C$; solid lines represent equation (5.5).

Rheological measurements of the shear viscosity of PET indicate that it behaves like a Newtonian liquid for shear rates up to about $200\,s^{-1}$. Thus the assumption of Newtonian behaviour may not be too inappropriate for PET. The variation of zero shear viscosity of PET, η_0, as a function of intrinsic viscosity (IV) for different temperatures is shown in Fig. 5.2. Experimental data (V.M. Nadkarni, private communication) suggest the following expression for the zero shear viscosity,

$$\eta_0 = 9.76 \times 10^{-3} (IV)^{5.2893} \exp\left[(6923.7)/(T + 273)\right]. \tag{5.5}$$

A similar expression for shear viscosity of PET has also been provided by Gregory [23]. It can be seen that equation (5.5) adequately represents the data over a wide range of IV or molecular weight. Only for IV greater

than 0.9, equation (5.5) underpredicts the shear viscosity. However, since the intrinsic viscosities for fibre-grade PET are generally between 0.5 and 0.65, the equation is valid for a spinning simulation.

For density and specific heat, we assume the following linear variations with temperature [7]:

$$\rho = 1.375 \times 10^{-3} - 0.75T \tag{5.6a}$$

$$C_p = 9.95 \times 10^2 + 3.875T. \tag{5.6b}$$

For the heat transfer coefficient, the best available correlation is that due to Kase and Matsuo [2], which is given as

$$h = 1.98A^{-1/3}[(W/\rho A)^2 + (8V_a)^2]^{1/6}. \tag{5.7}$$

Employing the above correlations, equations (5.2) and (5.3) can be solved using the fourth-order Runge–Kutta technique. Since the spinline tension F is not known *a priori*, an initial guess is necessary for the value of F. Based on the guessed value, the problem is solved as an initial value problem and the solution is checked for satisfactory agreement of the boundary conditions (5.4b). This iterative procedure is continued until a value of F is chosen that makes the solution satisfy all the conditions given by equation (5.4). A proper choice of F is crucial for smooth operation of the numerical procedure; a fairly good starting estimate can be obtained from the following equation:

$$F_s = 10.635 \frac{\displaystyle\int_{A_0}^{A_L} hA^{-1/2} \, dA}{\displaystyle\int_{T_0}^{T_s} \frac{\rho C_p \, dT}{\eta_0(T - T_a)}}, \tag{5.8}$$

provided the density is assumed to be constant while evaluating h from equation (5.7).

5.3 SPINLINE ORIENTATION

At intermediate take-up speeds ($\sim 3000 \, \text{m min}^{-1}$), melt-spinning of PET results in almost entirely amorphous as-spun fibres. Therefore, the molecular orientation of the as-spun fibre is expected to represent the 'frozen-in' stress in the spinline. The mechanical properties like tenacity, per cent elongation at break, initial modulus, and also drawability, are all unique functions of the molecular orientation as measured by the birefringence. Thus, if the birefringence can be quantitatively related to the process variables, then a link can be established between the latter and the as-spun fibre properties.

For amorphous polystyrene, Oda, White and Clark [10] investigated the relationship between molecular orientation and the principal stress
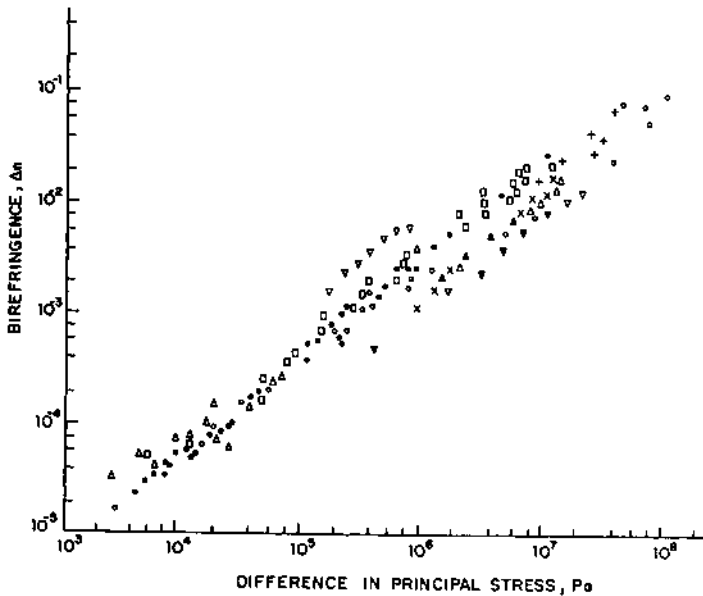
Fig. 5.3 Variation of birefringence with principal stress difference. Symbols represent data collected from various sources for polystyrene (PS) and PET. Spinning data: △ = atactic PS-BW [9]; ▼ = atactic PS-3 [9]; □ = atactic PS [10]; ⊙ = atactic PS, on-line [10]; + = PET, $\bar{M}_n \approx 24\,000$ (V.M. Nadkarni, personal communication); ○ = PET, $\bar{M}_n$ 17 000 (V.M. Nadkarni, personal communication); × = PET, $\bar{M}_n$ 15 000 [8]; ▽ = PET, on-line [3]. Elongation: ● = atactic PS [10]. Shear: ▲ = atactic PS [10].

difference. They found that the orientation as measured by the birefringence is directly proportional to the principal stress difference independent of the deformation mode. Figure 5.3 depicts literature data obtained from melt-spinning, uniaxial extension and shear deformation of polystyrene [9, 10]. It is clear that the birefringence varies linearly with the principal stress difference, which for melt-spinning implies that

$$\Delta n = C\sigma = C(F/A) \qquad (5.9)$$

C being the stress optical coefficient. At intermediate take-up speeds, melt-spun PET fibres are amorphous owing to the slow crystallization behaviour of PET. Hence, like polystyrene, a linear relationship between Δn and σ is also expected for PET fibres. Experimental data (V.M. Nadkarni, private communication) for melt-spun PET fibres under different process conditions are also shown in Fig. 5.3. It is evident that the birefringence is directly proportional to the spinline stress for PET. It is also of interest to note that in spite of the scatter in the data collected from various sources, both PET and polystyrene appear to follow a linear behaviour with C varying between 1×10^{-9} and 8×10^{-9} Pa^{-1}. Interestingly, similar behaviour has been reported for semicrystalline

polymers (like isotactic polypropylene) [12]. It has been observed that, irrespective of the spinning conditions, a unique relationship exists between the as-spun orientation and the spinline stress for polypropylenes of different grades. Unlike amorphous polymers, however, this relationship is non-linear with the stress optical coefficient, C, being a function of the spinline stress.

Referring to Fig. 5.3, the slopes of the lines for the different polymers are comparable although the lines are shifted parallel to each other, depending on the molecular weight (PET). This suggests that the incremental mechanical energy input needed for a specific increase in the orientation level is unique for all glassy polymers, although the absolute stress needed to achieve a specific orientation is governed by the molecular weight. It implies that at an equivalent degree of polymerization, there is a unique relationship between the applied stress and the resulting molecular orientation in the absence of crystallization. The differences in the chemical structure of the glassy polymers would be expected to affect the molecular packing and the intermolecular forces. However, at the high temperatures of melt processing, these factors are insignificant and only the physical structural parameters such as the degree of entanglement (influenced mainly by the molecular weight and its distribution) might affect the orientation–stress relationship through changes in the relaxation rate. A lower stress (and hence take-up speed) is therefore needed to reach a desired orientation for a high molecular weight polymer.

In the foregoing it has been demonstrated that for the melt-spinning of PET, the birefringence depends on the (experimentally measured) spinline stress only. George [7] has investigated the relationship between the as-spun fibre birefringence and the calculated stress at the freeze line, σ_L. Here again, a linear variation was obtained with $C \sim 6 \times 10^{-9}$ to 9×10^{-9} Pa^{-1}, which compares quite favourably with the values obtained by different experimental techniques. A value of $C \sim 6.55 \times 10^{-9}$ Pa^{-1} was also reported by Yasuda, Sugiyama and Yanagawa [5] for the correlation between birefringence and σ_L, where σ_L is taken to be the spinline stress at which the velocity is 95% of the take-up velocity. Thus it is clear that σ_L controls the orientation of the as-spun fibre, which in turn determines the mechanical properties and fibreline processability. The sensitivity of the as-spun fibre properties is therefore directly related to the sensitivity of σ_L to the changes in process variables. σ_L, on the other hand, can readily be obtained from the process simulation calculations, provided the operating conditions and the melt properties are available.

5.4 SENSITIVITY ANALYSIS

From the preceding discussion it follows that the critical process variables are those that will significantly affect σ_L, the stress at the freeze

Table 5.1 Process variables for PET in a typical melt-spinning operation

Variable	Value
Melt intrinsic viscosity	$0.611\,dl\,g^{-1}$
Extrusion temperature	$285\,°C$
Glass transition temperature	$67\,°C$
Ambient air temperature	$25\,°C$
Spinneret hole diameter	$3.8 \times 10^{-4}\,m$
Mass flow rate	$10^{-3}\,kg\,min^{-1}$
Quench air velocity	$48\,m\,min^{-1}$
Take-up velocity	$1500\,m\,min^{-1}$
Spinline tension[a]	$9.72 \times 10^{-4}\,N$
Freeze line location from spinneret[a]	$0.37\,m$

[a] Calculated value.

line. Quantitative information can be obtained by considering a typical PET spinning process summarized in Table 5.1, and calculating σ_L for different operating conditions and melt properties. The results are shown in Figs 5.4 and 5.5. The slope of the curves provides a measure of the sensitivity of σ_L to process variable changes. As can be seen, σ_L is very strongly affected by changes in extrusion temperature, melt IV, take-up velocity and the melt throughput rate. In comparison, σ_L is moderately sensitive to changes in quench air velocity and relatively insensitive to alterations in the quench air temperature. Thus, the process variables, if arranged in descending order of their influence on σ_L, will be: extrusion temperature, intrinsic melt viscosity, melt flow rate, quench air velocity, and quench air temperature. Since the as-spun fibre quality is uniquely determined by its birefringence, which in turn is directly related to σ_L, the degree of sensitivity of the as-spun fibre properties to changes in these process variables will be the same as that of σ_L.

So far we have only considered the effect of operating variables on the orientation. Another variable that also deserves consideration, however, is the location of the freeze line L. Certainly, care must be taken to ensure that the spinline length is greater than L such that the filament is solidified before it is wound. Figure 5.6 illustrates the sensitivity of L to changes in process conditions. In comparison with the σ_L behaviour, L is more sensitive to changes in the throughput rate as well as the extrusion temperature and is relatively unperturbed by changes in the melt IV. Changes in the other operating conditions, however, exert only moderate influence in determining the freeze line location. In general, therefore, the extrusion temperature, the throughput rate and the intrinsic melt viscosity require very careful control for maintaining the desired as-spun fibre quality. For typical processes, where changes in these
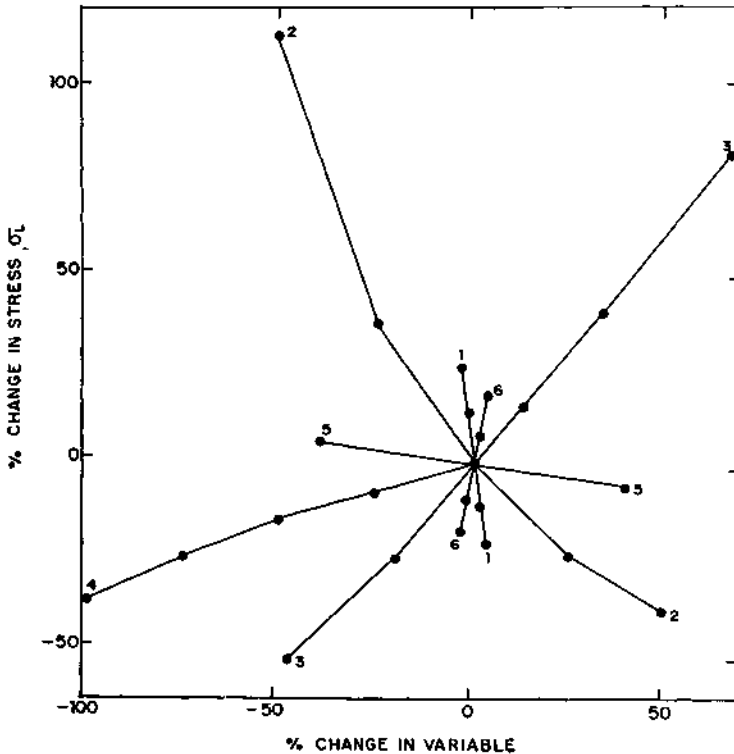
Fig. 5.4 Sensitivity plot for stress at the freeze line. The various curves are for changes in (1) extrusion temperature, (2) melt flow rate, (3) take-up velocity, (4) quench air velocity, (5) quench air temperature, and (6) melt intrinsic viscosity. Symbols represent calculated values.

variables are not desirable or possible, the fibre properties can still be adjusted to a certain degree by appropriate alterations in the take-up velocity.

5.5 PROCESS IMPLICATIONS

The sensitivity analysis described above gives valuable insights into making effective changes in the process parameters for trouble-shooting and product quality improvement. For controlling the as-spun filament orientation, the extrusion temperature, the intrinsic viscosity of the polymer melt (that is, the average molecular weight), the take-up velocity and the melt flow rate are identified as the critical process variables. An increase in temperature and/or a decrease in melt IV will result in reduced spinline stress, thereby adversely affecting the stretchability.
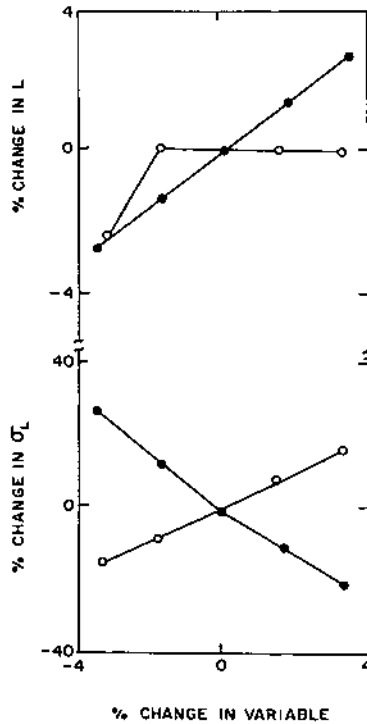
Fig. 5.5 Expanded sensitivity plot for extrusion temperature (●) and intrinsic viscosity (○).

The high sensitivity of the spinline stress to extrusion temperature has important implications for maintaining uniform product quality in a multiposition commercial plant with each position carrying multiple hole spinnerets. A variation of about 3 °C in the end-to-end temperature profile of the spinneret represents a 1% change in the extrusion temperature, but could result in about 10% variation in the spinline stress (Fig. 5.5), thereby increasing the CV of elongation. Accurate temperature control and monitoring of spin pack temperature are therefore critical. The use of static mixers upstream of the spin pack is desirable for delivering a thermally homogeneous melt to the spinnerets.

In batch processes, control of moisture content of the chips is of considerable importance because of the strong dependence of as-spun fibre quality on polymer IV. In order to minimize hydrolytic degradation, the moisture content of the melt must be maintained at less than 0.005 wt %. A moisture level of 0.01% could lower the polymer IV from 0.6 to 0.56. Although this represents only a 7% change in IV, it leads to a 35% change in spinline stress, thereby affecting spinnability and product quality.
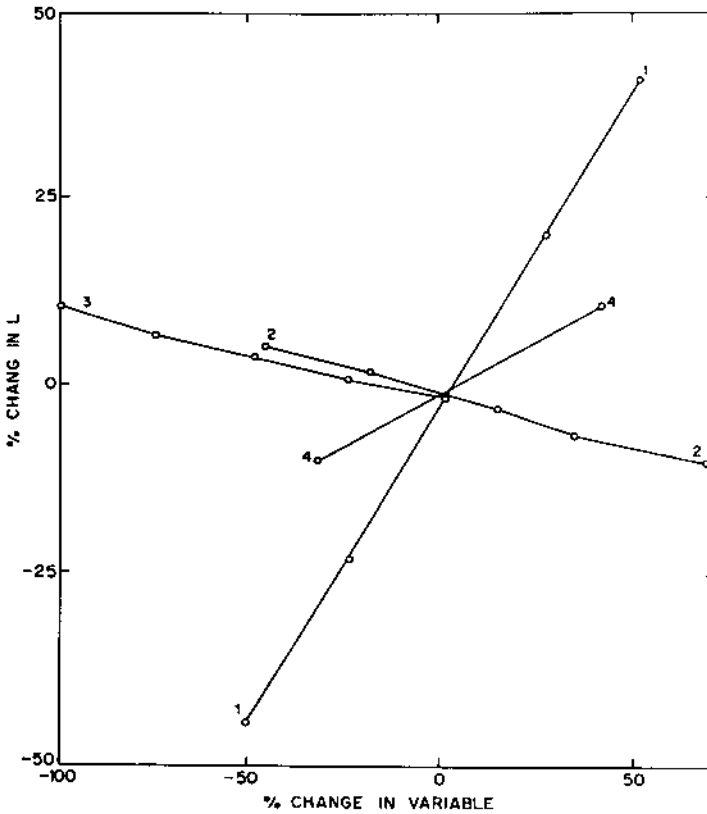
Fig. 5.6 Sensitivity plot for freeze line location. The various curves are for changes in (1) melt flow rate, (2) take-up velocity, (3) quench air velocity, and (4) quench air temperature. Symbols represent calculated values.

In plants with continuous polymerization, variation in polymer IV may also result from reactor perturbation. For example, level fluctuations in the polycondensation reactor (finisher) are often due to vacuum fluctuations or flow perturbations. Since the control level (at 20% of the reactor height) is critical for effective surface contact, any disturbance in the level will be manifested by changes in polymer IV. A sudden drop in polymer IV may cause the melt to stick to the spinneret, thereby disturbing process continuity. Therefore, incorporation of an on-line viscometer to monitor the melt quality is likely to be a necessary instrumentation.

Both the melt flow rate and the take-up velocity influence the as-spun filament quality. For a constant flow rate, increase in take-up velocity increases orientation due to enhanced stretching. For a constant take-up velocity, however, orientation reduces as the flow rate is enhanced. This is because the filament denier increases rapidly with the flow rate even though the spinline tension actually decreases marginally. The net effect,

therefore, is a reduction in spinline stress as throughput is increased. Nevertheless, by manipulating the melt flow rate and the take-up speed, it is possible to produce products over a range of denier and tenacity. It should be emphasized, however, that for a given denier product, the throughput and take-up speed are coupled. Thus, for increasing production rate of a particular denier product by say 30%, both the throughput and the take-up velocity need to be increased proportionately. This, in turn, would result in an increase of about 15% in the spinline stress, leading to higher orientation in the as-spun fibre bundle. The fibreline conditions may have to be modified accordingly in order to maintain product quality and textile processability. A preferred option for upgrading productivity under these circumstances would be to increase the number of holes in the spinneret by 30%, if possible as per hole layout guidelines. No changes in throughput and take-up speed are then involved and the basic physical aspects of the fibre formation remain practically unaltered.

The location of the freeze line, although not important for as-spun fibre orientation, has critical practical implications for spinline stability and product uniformity in multifilament spinning. It is necessary to design the quench chamber in such a fashion as to avoid any air turbulence in the vicinity of the freeze line. The fibreline is the weakest in terms of its load-bearing ability upstream of the freeze line. Air turbulence in this region can lead to filament breakage and/or fused filaments resulting in process interruptions and poor product quality. The quench air temperature, though not a very useful process parameter for controlling orientation, can be used effectively for stabilizing the spinline. Reducing the quench air temperature from 25 to 15°C (40% change) does not affect orientation significantly, yet would make the filaments more stable by moving the freeze line closer to the spinneret, thereby making it less susceptible to air turbulence.

Barring throughput, neither the extrusion temperature nor the melt IV can be changed readily to alter the as-spun fibre properties in commercial plants with a continuous polymerization unit. Since throughput controls the production rate and therefore generally is not flexible, the operating variable that is most readily amenable for controlling orientation is the take-up velocity. This is in spite of the fact that the take-up velocity is not the most dominant controlling variable for orientation development (Fig. 5.4). This leads us to the question of whether high strength PET filaments can be directly spun by suitably adjusting the take-up speed, thereby eliminating the cumbersome drawing stage. For obtaining an answer to this question, the calculated spinline stress at high spinning speeds would have to be compared with the melt strength of the spinline. The aspect of further stress build-up due to flow-induced crystallization beyond $4000 \, \text{m min}^{-1}$ also needs to be considered.

Table 5.2 Parametric space covered (taken from actual industrial data)

Parameters	Range	No. of variable points
Extrusion temperature (°C)	275–290	2
Quench air temperature (°C)	15–25	3
Quench air velocity (cm s⁻¹)	30–130	7
Spinneret hole diameter (mm)	0.2–0.3	3
Take-up velocity (m min⁻¹)	500–1250	11
Throughput rate (g hole⁻¹ min⁻¹)	0.5–1.0	9
Intrinsic viscosity (dl g⁻¹)	0.6–0.65	2
Filament denier	4.0–12.0	11

5.6 STRESS–ORIENTATION RELATIONSHIP FOR PET

In order to be able to use the computer simulation for spinning process optimization, it is essential to develop a quantitative correlation between the spinline stress and the as-spun filament orientation, and to confirm its validity over the relevant parametric space employed in industrial operations. The PET spinning process parameters from three different plants in India, representing 19 different sets of process conditions, were used for computing the spinline stress, σ_L, by using the Dutta–Nadkarni simulation package. Table 5.2 summarizes the industrial data used; only the broad range of the variables and the number of data points in each range have been indicated in order to protect proprietary information. The birefringences, Δn, of the as-spun filaments from the different industrial runs were measured experimentally. These data (filled points), along with other published data [3], are shown in Fig. 5.7.

A straight line fit between Δn and σ_L on the log–log plot in Fig. 5.7 is apparent. A linear regression analysis was used to fit the data and the following correlation is obtained with a correlation coefficient of 0.96 for fitting 37 data points:

$$\sigma_L = 2.526 \times 10^{-9}(\Delta n^{1.265}). \tag{5.10}$$

It should be noted that σ_L in this correlation would be obtained in pascals (Pa). Development of equation (5.10) also confirms that though the sources of data, the equipment involved and the process parameters are different, there exists a unique relationship between Δn and σ_L for the melt-spinning of PET at speeds up to 3000 m min⁻¹. Hence, equation (5.10) can be used with confidence for process optimization.

5.7 CASE STUDY FOR PROCESS OPTIMIZATION

The use of equation (5.10), together with the computer simulation package, can be illustrated with a case study in which it is desired to increase
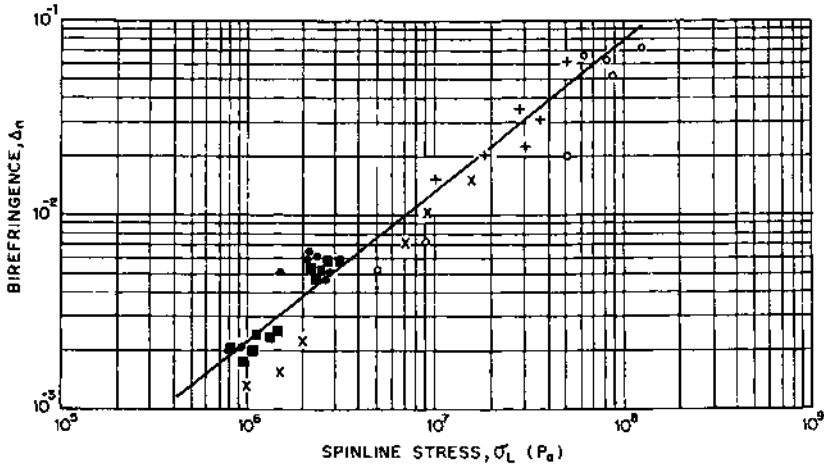
Fig. 5.7 Variation of birefringence with principal normal stress difference at the freeze line. Filled symbols represent data collected from various industrial operations from India while the other symbols represent other published data.

the production rate in spinning without affecting the fibreline processing conditions of the as-spun filaments. In order to avoid downstream process optimization at the higher productivity, it is necessary to maintain the denier and the orientation of the as-spun filaments at the reference levels. This means that for a given denier product, the throughput (melt flow) rate and the take-up speed have to be increased proportionally, coupled with other process changes that would maintain the orientation at its original value.

Since it is not desirable to change the polymer viscosity, the process parameters available for manipulation are the spinning or extrusion temperature, quench air velocity and quench air temperature. From the process sensitivity analysis, it is known that the orientation of the as-spun filaments, as measured by birefringence Δn, is very sensitive to changes in the spinning temperature. As the orientation is uniquely determined by the freeze line stress σ_L, the spinning temperature is to be changed so that the freeze line stress σ_L and spinline tension F are maintained at the original values.

Although the quench air velocity and temperature do not significantly affect the spinline stress, they influence the freeze line location, that is the distance from the spinneret at which the spinline temperature is equal to the glass transition temperature of PET. It is important to maintain the freeze line location unaffected in order to ensure stability of the spinline. Instability or fluttering of the spinning filaments could lead to unacceptable values of uster and denier variation.

The production rate can also be improved by a proportional increase in the number of spinneret holes. In this approach, no changes in the

Table 5.3 Effect of changes in productivity on spinline stress, tension and location of the freeze line

Parameters	Original condition	Increase in W, V_L		
		10%	20%	30%
Intrinsic viscosity, IV (dl g^{-1})	0.60	0.60	0.60	0.60
Extrusion temperature, T_E (°C)	280	280	280	280
Quench air temperature, T_a (°C)	20	20	20	20
Quench air velocity, V_a (cm s^{-1})	100	100	100	100
Spinneret hole diameter, d_0 (mm)	0.2	0.2	0.2	0.2
Take-up velocity, V_L (m min^{-1})	1000	1100	1200	1300
Throughput rate, W (g hole^{-1} min^{-1})	0.5	0.55	0.6	0.65
Spinline stress, σ_L (10^7 dyn cm^{-2})	2.18	2.32	2.46	2.60
Spinline tension, F (dyn)	82.8	87.5	93.8	98.0
Freeze line location, L (cm)	26.4	28.0	30.8	33.0

throughput per hole, take-up speed and spinning temperature will have to be made. The quench air parameters will have to be suitably manipulated to compensate for the additional heat load. However, this option would involve capital investment for new spinnerets. Hence, it would be preferable to upgrade the productivity via only 'software' changes, if feasible.

The reference process parameters of a spinline whose productivity is to be improved are summarized in Table 5.3, along with the process conditions determined for production rate increases of 10, 20 and 30%. The process variables provided in this table are representative of values used in a typical spinning operation, as averaged out from within the ranges given in Table 5.2. The computer simulation of Dutta and Nadkarni was used for determining the changes in the process variables when the throughput rate, W, and the take-up speed are proportionally increased by 10, 20 and 30%. The effect on the response parameters, such as the spinline stress σ_L, spinline tension F and freeze line location L for increased productivity is shown in Fig. 5.8. It is seen that σ_L, F and L all increase proportionally with increased W and V_L. Thus, it is observed that for a 10% increase in W and V_L, there is about a 6% increase in σ_L, F and L. In order to maintain the molecular orientation level and the downstream process variables constant it is essential to bring down the values of σ_L, F and L through proper adjustment of the other process variables.

The sensitivity analysis indicates that increasing the extrusion temperature decreases the spinline stress and the spinline tension but extends the freeze line location. Figure 5.9 shows the effect of increasing the extrusion temperature by 1 to 4%. The extrusion temperature, T_E, is
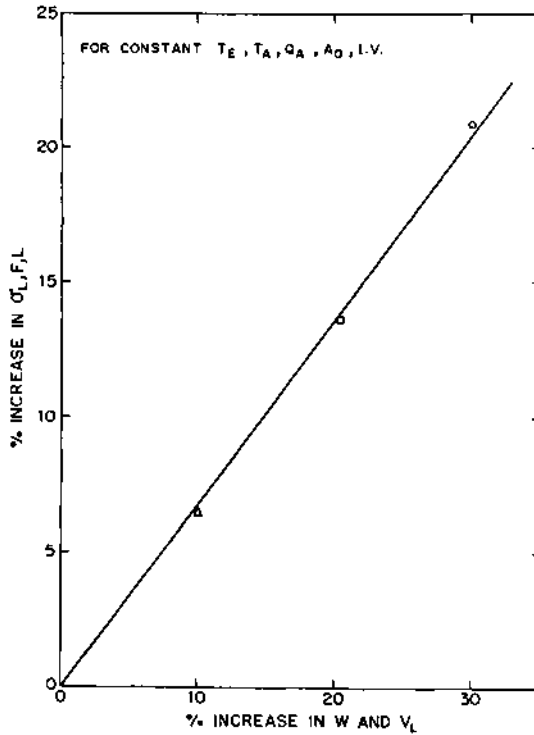
Fig. 5.8 Effect of percentage increase in throughput and take-up velocity on the spinline stress, spinline tension and freeze line location.

assumed to be equal to the spinneret exit temperature, T_0. In the present case, a 1.87% increase in temperature corresponds to an extrusion temperature T_E increase from 280 to 285 °C and a 3.74% increase corresponds to an increase from 280 to 290 °C. Figure 5.9 shows the effect of the increase in extrusion temperature on σ_L, F and L for each of the three cases of 10, 20 and 30% increase in W and V_L. It is seen that even for different throughput rates, the effect of increase in extrusion temperature on σ_L, F and L is of nearly the same magnitude. It is seen that for a 10% increase in productivity, in order to return the spinline stress and tension from a 6% increase to the original level, the increase in the extrusion temperature should be approximately 1.87%. However, a 1.87% increase in T_E would result in a further 1.75% increase in L. The freeze line location is thus sensitive to the combined changes in throughput rate and extrusion temperature.

Referring to Table 5.4, although the spinline stress and tension can be brought back to the original values by a change in the extrusion temperature, the freeze line location remains different from the original
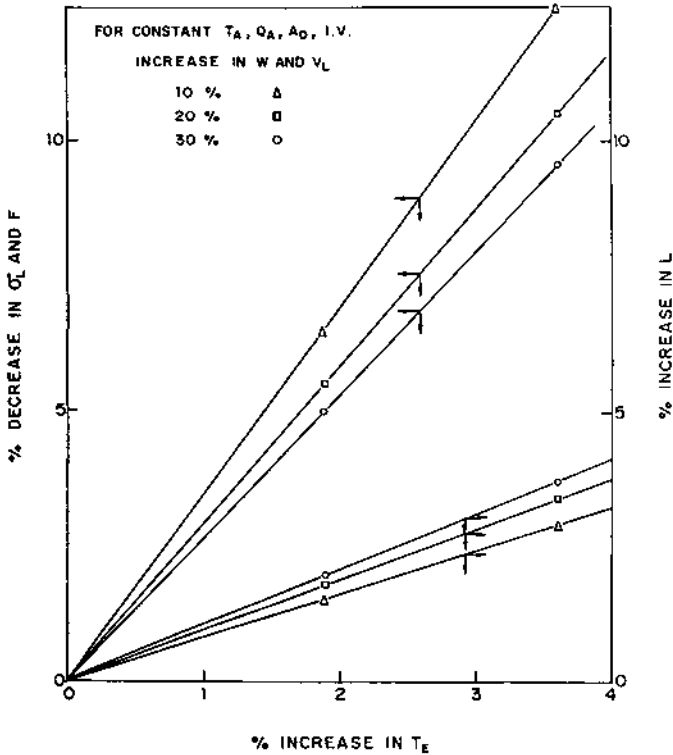
Fig. 5.9 Effect of percentage increase of extrusion temperature on the spinline stress, spinline tension and freeze line location for each of the three cases of 10%, 20% and 30% increase in throughput and take-up velocity.

value by about 9.5%. The location of the freeze line has a definitive effect on the spinline stability and product uniformity, and hence its retention at the original value is desirable. A process variable is to be sought which would move the location of the freeze line closer to the spinneret without any significant changes in either σ_L or F. The quench air temperature, T_a, is known to influence L to a greater extent relative to F and σ_L, and can be effectively used for stabilizing the spinline. Figure 5.10 shows the effect on the response parameters (F, σ_L, L) for 0 to 60% decrease in quench air temperature. It is seen that to move the freeze line location by about 8.0%, the quench air temperature has to be decreased by about 45%. Furthermore, the effect of this process change on σ_L and F is insignificant. The entire exercise is summarized in Table 5.4, which indicates the changes in process variables required to increase productivity while maintaining the denier, orientation and stability of the spinline.

Table 5.4 Summary of process changes required to obtain a 10% productivity increase while product quality is maintained constant

Parameters	Original condition	10% increase in W, L	1.9% increase in T_E	45% decrease in T_a
Intrinsic viscosity, IV (dl g^{-1})	0.60	0.60	0.60	0.60
Extrusion temperature, T_E (°C)	280[a]	280	285	285[a]
Quench air temperature, T_a (°C)	20[a]	20	20	11[a]
Quench air velocity, V_a (cm s^{-1})	100	100	100	100
Spinneret hole diameter, d_0 (mm)	0.2	0.2	0.2	0.2
Take-up velocity, V_L (m min^{-1})	1000[a]	1100	1100	1100[a]
Throughput rate, W (g hole^{-1} min^{-1})	0.5[a]	0.55	0.55	0.55[a]
Spinline stress, σ_L (10^7 dyn cm^{-2})	2.18[b]	2.32	2.20	2.19[b]
Spinline tension, F (dyn)	82.8[b]	87.9	83.3	82.9[b]
Freeze line location, L (cm)	26.4[b]	28.0	28.9	26.8[b]

[a] Parametric values changed to achieve a 10% increase in productivity for constant product quality
[b] Values held constant to maintain product quality.

5.8 CASE STUDIES FOR PRODUCT DEVELOPMENT

5.8.1 SUBDENIER FIBRES

The first case study considers the development of subdenier fibres, which provide better comfort for clothing in tropical countries. The most common fibre deniers used for shirting and ladies' dress fabrics are 1.5 denier in Western countries and 1.2 denier in the Indian textile industry. For producing subdenier drawn fibres, it is necessary to start with a lower spun denier, since the maximum possible draw ratios that can be achieved without inducing fibre breakage at commercial line speeds are in the range 3.5–4. The reference parameter values of the spinning process which is to be modified to obtain lower spun denier are given in the first column of Table 5.5.

In view of the upper limitation on the spin stretch factor (ratio of take-up speed to jet velocity) for ensuring spinning continuity without filament breakage, the use of a smaller diameter capillary is required to obtain lower spun denier. It is also desirable to maintain the orientation level of the lower denier as-spun filaments at the original value so as to retain their drawability and minimize changes in the fibreline process. This can
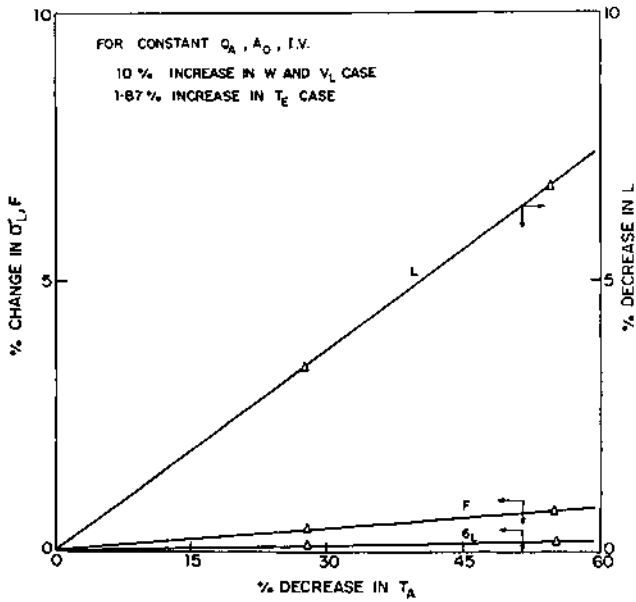
Fig. 5.10 Effect of percentage decrease in quench air temperature on spinline stress, spinline tension and freeze line location for the specific case of 10% increase in throughput and take-up velocity.

be achieved if the freeze line stress remains unchanged under the modified spinning conditions. It is also important to maintain the freeze line location in order to ensure spinline stability. The objective of the simulation exercise is thus to specify spinning process changes to produce lower denier as-spun filaments, while maintaining the freeze line stress and location constant. A fibre product denier of 0.8–0.9 would certainly provide better comfort in tropical climates. From the viewpoint of commercial production, it would be useful to determine the feasibility of producing such a premium grade fibre on an existing spinning line without any major hardware changes. In the following, it will be demonstrated how the spinning variables need to be manipulated in order to obtain a low-spun denier necessary for producing subdenier drawn fibres.

In the reference case, the spinneret hole diameter of 0.375 mm is used. For the development of subdenier fibres of 0.8–0.9 denier, a spinneret hole diameter of 0.2 mm (8 mil) has been chosen. The computer simulation is now used for determining the new spinline stress value and the freeze line location due to this change under conditions equivalent to the reference case. It is seen from Table 5.5 that the spinline stress drops while the freeze line location shifts away from the spinneret. A further restriction is now imposed that the draw ratio should remain unchanged from the value of 3.75. This would mean the as-spun denier would have

Table 5.5 Summary of process changes required to obtain subdenier fibres without affecting downstream variables

Parameters	Reference condition (capillary diameter = 15 mils)	0.85 denier fibre				0.8 denier fibre	
		47% decrease in capillary diameter	40% increase in V_L and 0.8% decrease in W	3.5% increase in T_E	50% decrease in T_a	13% decrease in W	0.7% increase in T_E
Intrinsic viscosity, IV (dl g^{-1})	0.60	0.60	0.60	0.60	0.60	0.60	0.60
Extrusion temperature, T_E (°C)	280[a]	280	280	290	290[a]	290	292[a]
Quench air temperature, T_a (°C)	20[a]	20	20	20	10[a]	10	10[a]
Quench air velocity, V_a (cm s^{-1})	100	100	100	100	100	100	100
Spinneret hole diameter, d_0 (mm)	0.375[a]	0.2	0.2	0.2	0.2[a]	0.2	0.2[a]
Take-up velocity, V_L (m min^{-1})	1000[a]	1000	1400	1400	1400[a]	1400	1400
Throughput rate, W (g hole^{-1} min^{-1})	0.5[a]	0.5	0.496	0.496	0.496[a]	0.467	0.467[a]
Spinline stress, σ_L (10^7 dyn cm^{-2})	3.18[b]	2.18	3.6	3.13	3.18[b]	3.33	3.29[a]
Spinline tension, F (dyn)	119.0[a]	82.8	96.0	85.2	84.7[a]	84.1	83.0[a]
Freeze line location, L (cm)	25.2[b]	26.4	26.6	27.7	25.2[b]	24.2	24.4[a]
As-spun fibre denier	4.5[a]	4.5	3.1875	3.1875	3.1875	3.0	3.0[a]
Drawn fibre denier	1.2[a]	1.2	0.85	0.85	0.85	0.8	0.8[a]
Draw ratio	3.75[b]	3.75	3.75	3.75	3.75[b]	3.75	3.75[b]

[a] Parametric values changed to achieve the new subdenier fibre product.
[b] Values held constant to maintain the downstream process variables at constant values.

to be between 3.0 and 3.375 in order to develop a fibre with a drawn denier of 0.8–0.9. Increasing the take-up velocity would help in this respect as well as enhancing the spinline stress. These changes result in an increase in spinline stress to a level beyond the required value of 3.18×10^7 dyn cm^{-2}, as can be seen from Table 5.5. It has been shown that increasing the extrusion temperature helps in decreasing the spinline stress value. But this would also lead to further shifting of the freeze line location away from the spinneret. The most sensitive parameter for adjusting the freeze line location without significantly affecting the spinline stress has been identified as the quench air temperature. Thus, decreasing the value of the quench air temperature from 20 to 10 °C establishes the conditions for obtaining fibres of 0.85 denier, as shown in Table 5.5. If it is desirable to obtain a 0.8 denier fibre, the throughput rate would have to be decreased by about 8%. However, it is seen from the last two columns of Table 5.5 that the spinline stress increases considerably and cannot be readjusted to the original value even by raising the extrusion temperature to 292 °C. It must be noted that the extrusion temperature of 292 °C would be the limiting value beyond which degradation of the molten polymer is likely to take place faster. Thus, for the given reference conditions and under the imposed constraints, it is possible to adjust the processing conditions to obtain 0.85 denier fibre without any hardware changes other than the spinneret. It is interesting to note that in adjusting the processing parameters, the final conditions result in a higher value of take-up velocity, as can be seen from Table 5.5, and hence higher productivity, which is the added bonus in this new product development.

5.8.2 LOW PILL FIBRES

The second case study considers the development of low pill fibres. Pilling is a common phenomenon that occurs at the collars and cuffs of mens' shirts made of polyester/cotton blends. The higher strength of the PET fibre in comparison with the cotton fibre does not allow free fall of fibres disentangled from the fabric due to friction at the collars and cuffs. The loose fibres therefore curl up in small balls hanging on the fabric. One way of preventing pill formation is to lower the fibre strength. This may be achieved by lowering the intrinsic viscosity (IV), that is, by using a base polymer of lower molecular weight. Unlike in the earlier case, the present study would prefer to maintain the product denier at its original value of 1.2. However, the draw ratio would have to be lower than that used for the reference case in order to prevent fibre breakage in downstream processing. Thus, a constraint could be imposed to reduce the draw ratio to a value of 3.5. This would restrict the as-spun denier to 4.2 instead of its original value of 4.5 in the reference case, as seen in Table 5.6.

Table 5.6 Summary of process changes required to obtain low pill fibres without affecting downstream variables

Parameter	Reference condition (IV = 0.6)	8.3% decrease in IV	22.5% increase in V_L; 14.2% increase in W	1.8% decrease in T_E	50% decrease in T_a
Intrinsic viscosity, IV (dl g⁻¹)	0.6[a]	0.55	0.55	0.55	0.55[a]
Extrusion temperature, T_E (°C)	280[a]	280	280	275	275[a]
Quench air temperature, T_a (°C)	20[a]	20	20	20	10[a]
Quench air velocity, V_a (cm s⁻¹)	100	100	100	100	100
Spinneret hole diameter, d_0 (mm)	0.2	0.2	0.2	0.2	0.2
Take-up velocity, V_L (m min⁻¹)	1000[a]	1000	1225	1225	1225[a]
Throughput rate, W (g hole⁻¹ min⁻¹)	0.5[a]	0.5	0.571	0.571	0.571[a]
Spinline stress, σ_L (10⁷ dyn cm⁻²)	2.18[b]	1.63	2.05	2.16	2.18[b]
Spinline tension, F (dyn)	82.8[a]	61.8	72.5	76.6	76.9[a]
Freeze line location, L (cm)	26.4[b]	26.3	29.6	29.3	26.5[b]
As-spun fibre denier	4.5[a]	4.5	4.2	4.2	4.2[a]
Drawn fibre denier	1.2[b]	1.2	1.2	1.2	1.2[b]
Draw ratio	3.75[a]	3.75	3.5	3.5	3.5[a]

[a] Parametric values changed to achieve low pill fibre product.
[b] Values held constant to maintain the downstream process variables at constant values.

The new low pill fibre product development is done for the IV value of 0.55 as opposed to the original value of 0.60 (8.3% change). This change results in a drastic decrease in the spinline stress and spinline tension which could make the melt unspinnable (Table 5.6). One way to increase the spinline stress is to increase the take-up velocity and the throughput rate. In the present case, the take-up velocity and the throughput rate are adjusted to new values so that the as-spun denier is controlled at a value of 4.2. This was found to be achieved by increasing the take-up velocity by 22.5% and the throughput rate by 14.2%, as shown in Table 5.6. In order to achieve a further increase in the spinline stress, the extrusion temperature was lowered to 275 °C. Though the spinline stress value was found to adjust itself adequately, it was noticed that the freeze line location was shifted considerably away from the spinneret. This would have an adverse effect on the spinline stability and product uniformity. It is known that the quench air temperature influences this parameter greatly. By reducing the quench air temperature it is possible to move the location of the freeze line closer to the spinneret without any significant changes in the spinline stress. A 50% decrease in the reference quench air temperature was found to give conditions such that the spinline stress as well as the freeze line location were maintained at the original values, as can be seen from Table 5.6.

5.9 CONCLUSIONS

A simple mathematical model is proposed to simulate the melt-spinning of PET filaments. The model uses readily measurable process variables for predicting spinline stress by computer simulation.

Based on available literature data, it is shown that the molecular orientation developed in the filament during the spinning step is uniquely determined by the spinline stress. This behaviour appears to be generally valid for vitrified polymers like polystyrene and PET filaments spun at speeds up to $3000 \, m \, min^{-1}$. Since the mechanical properties and drawability of the as-spun filaments are governed by the orientation level, these product properties are also unique functions of the spinline stress. The combination of the process simulation and stress–orientation relation gives us a procedure for identifying the important spinning process variables that would affect the spinline stress, and hence the mechanical properties and fibreline processability of the as-spun filaments. Such a process sensitivity analysis for PET indicates that the critical process variables are the extrusion temperature, intrinsic viscosity of the polymer, melt extrusion velocity, and the take-up speed. Specific implications of the sensitivity analysis for process trouble-shooting and product quality improvement are highlighted.

The use of the computer simulation approach for process optimization and product development has been demonstrated with reference to commercially relevant case studies. Thus, the technical feasibility of increasing production on a given spinning position can be assessed using simulation. The directional changes in spinning process variables required for developing subdenier fibres and low-pill fibres can also be predicted using this approach. The scope of experimentation is then clearly defined, thereby eliminating the trial-and-error approach and leading to significant savings in time and effort.

REFERENCES

1. Kase, S. and Matsuo, T. (1965) *J. Polym. Sci.*, **A3**, 2541–2554.
2. Kase, S. and Matsuo, T. (1967) *J. Appl. Polym. Sci.*, **11**, 251–287.
3. Hamana, I., Matsui, M. and Kato, S. (1969) *Melliand Textilber.*, **50**, 382–388.
4. Prastaro, A. and Parrini, P. (1975) *Textile Res. J.*, **45**, 118–127.
5. Yasuda, H., Sugiyama, M. and Yanagawa, H. (1979) *Sen-I-Gakkaishi*, **35**, 370–375.
6. Gagon, D.K. and Denn, M.M. (1981) *Polym. Eng. Sci.*, **21**, 844–853.
7. George, H.H. (1982) *Polym. Eng. Sci.*, **22**, 291–299.
8. Ziabicki, A. and Kedzierska, K. (1962) *J. Appl. Polym. Sci.*, **6**, 111–119.
9. Ziabicki, A. and Kedzierska, K. (1962) *J. Appl. Polym. Sci.*, **6**, 361–367.
10. Oda, K., White, J.L. and Clark, E.S. (1978) *Polym. Eng. Sci.*, **18**, 53–59.
11. Ishibashi, T., Aoki, K. and Ishii, T. (1970) *J. Appl. Polym. Sci.*, **14**, 1597–1613.
12. Nadella, H.P., Henson, H.M., Spruiell, J.E. and White, J.L. (1977) *J. Appl. Polym. Sci.*, **21**, 3003–3022.
13. Zieminski, K.F. and Spruiell, J.E. (1988) *J. Appl. Polym. Sci.*, **35**, 2223–2245.
14. Chen, S., Yu, W. and Spruiell, J.E. (1987) *J. Appl. Polym. Sci.*, **34**, 1477–1492.
15. Yasuda, H., Ishihara, H. and Yanagawa, H. (1978) *Sen-I-Gakkaishi*, **34**, 20–27.
16. Dutta, A. and Nadkarni, V.M. (1984) *Textile Res. J.*, **54**, 34–42.
17. Bhuvanesh, Y.C. and Gupta, V.B. (1990) *Indian J. Fiber Textile Res.*, **15**(12), 145–153.
18. Dutta, A. (1987) *Polym. Eng. Sci.*, **27**(14), 1050–1058.
19. Shenoy, A.V. and Nadkarni, V.M. (1984) *Textile Res. J.*, **54**, 778–783.
20. Shenoy, A.V. and Nadkarni, V.M. (1985) *Fiber World*, September, pp. 52–58.
21. Isayev, A.I. (1991) In *Modelling of Polymer Processing* (ed. A.I. Isayev), Hanser Publishers, Munich.
22. Ishihara, H., Hayashi, S. and Ikeuchi, H. (1987) Computer simulation technology of melt spinning in fiber industry. Paper read at the 2nd International Conference on Man-made Fibers, 26–29 November 1987, Beijing, China.
23. Gregory, D.R. (1972) *J. Appl. Polym. Sci.*, **16**, 1479–1489.

Solution-spinning processes

6

V.B. Gupta

6.1 INTRODUCTION

If a polymer can be melted under reasonable conditions, its conversion to a fibre by melt-spinning is preferred over the solution-spinning process, mainly as the former does not involve the use of solvents and the problems associated with their use, namely their removal, recovery, the associated environmental concerns and the low spinning speeds. When melt-spinning cannot be carried out, either because the polymer degrades before melting or the melt is thermally unstable, distinction as to the type of process is made depending upon whether the solvent is removed by evaporation by heating (dry-spinning) or by coagulation in another fluid which is compatible with the spinning solvent, but is itself not a solvent for the polymer (wet-spinning). Historically, the formation of fibres by dry-spinning was the first to evolve as a method for manufacturing polymer-based fibres, as pointed out in Chapter 3. In the present chapter, the solution-spinning processes will be briefly described.

In dry-spinning, solidification of the filament is achieved by solvent evaporation through the application of heat, which is slower than solidification by cooling as in melt-spinning. However, the former is faster than solidification by coagulation in another fluid. These differences are more clearly understood in terms of the rate-controlling processes involved in these methods, namely heat transfer in the case of melt-spinning, heat transfer and one-way mass transfer, in the case of dry-spinning, and heat transfer and two-way mass transfer in wet-spinning.

A consequence of this is that the speeds achieved in the normal dry-spinning process are considerably less than those used for melt-spinning. However, in dry-spinning, considerably higher spinning speeds (500–1500 m min^{-1}) can be achieved than can be attained with wet-spinning (30–300 m min^{-1}). Furthermore, a greater percentage of solids can be tolerated in the spinning solution used in dry-spinning (15–45%) than in that used in wet-spinning (5–30%), since the solution is spun at a relatively high temperature. In dry-spinning, large amounts of heat have to be applied to the spinning solution as well as to the extruded filaments for solvent removal. The amounts of heat so required can affect adversely the properties of the filaments, particularly with regard to colour. This is not the case with wet-spinning which involves lower temperatures and is therefore gentler on the fibre. This advantage of the wet-spinning process has made it the more acceptable process with major manufacturers. The low rates of wet-spinning are taken advantage of by drawing the filaments immediately after spinning and then crimping and cutting them in a continuous operation. This is generally not possible with conventional melt- and dry-spinning techniques. Thus if continuous filaments are desired, the dry-spinning technique offers the advantage of high speed. However, for cut (staple) fibres, the wet-spinning technique offers the advantage of having all the operations (spinning, drawing, crimping, heat-setting and cutting) in one continuous process.

Recently significant developments in the field of solution-spinning have made it possible to use spinning speeds up to 1000 m min^{-1} in wet-spinning [1]. To achieve this, high concentrations of the coagulant are used to aid the phase separation process. Thus both staple fibre and continuous filament can be produced by wet-spinning. Similarly, speeds up to 2000 m min^{-1} can be used with dry-spinning. The production of staple fibre through the dry-spinning route operating at 250–400 m min^{-1} has also become possible in which tows of up to 500 000 dtex are drawn off by special take-off rollers.

The fibres which are produced by dry-spinning include secondary cellulose acetate, cellulose triacetate, acrylic (e.g. Orlon^{TM}), Spandex^{TM}-type polyurethane elastomeric fibres (e.g. Lycra^{TM}), polyvinyl chloride (PVC) and chlorinated PVC. The wet-spinning technique is used to produce viscose rayon, cuprammonium rayon, acrylic (e.g. Courtelle^{TM}, Acrilan^{TM}), Spandex^{TM}-type elastomeric fibre (e.g. Vyrene^{TM}), polyvinyl alcohol and aromatic polyamides.

The wet-spinning process falls into two broad classes. Fully synthetic fibres like acrylics and modacrylics employ a solvent/non-solvent system, while regenerated natural fibres like viscose rayon employ a chemical reaction to dissolve and precipitate the polymer. Recently Courtaulds of Great Britain have introduced a solvent-spinning technique

for industrial production of cellulose-based fibre; this is described in Chapter 17.

The development of wholly aromatic polyamide fibres was significantly assisted by a spinning process which is generally considered to be a combination of the dry- and wet-spinning processes, namely the dry-jet wet-spinning process. This process is described in Chapter 18.

6.2 THE PROCESS VARIABLES FOR SOLUTION-SPINNING

The technologically important process variables for melt-spinning were listed in Chapter 4. Some additional variables and some modifications to their description need to be considered in the case of solution-spinning. The two additional variables are [2]: initial polymer concentration and the concentration dependence of crystallization rate for a given polymer–solvent system. The extension ratio or spin draw ratio, which is defined as V_L/V_0 (where V_L is the velocity at the take-up point and V_0 the velocity at the spinneret exit), is equal to d_0^2/d_L^2 in the case of melt-spinning (d_0 and d_L are the filament diameters at the spinneret exit and at the final take-up point, respectively). In solution spinning, on the other hand,

$$\frac{V_L}{V_0} = \frac{Q_L}{Q_0}\frac{d_0^2}{d_L^2},$$

where Q refers to the volume of polymer solution flowing out in unit time and the subscripts have the same meaning as given earlier. Since the volume of polymer solution decreases with increasing distance from the spinneret, so Q_0 is larger than Q_L and consequently Q_L/Q_0 is smaller than unity. Thus the true extension ratio in solution-spinning is always smaller than it would appear from the filament diameter.

Besides polymer concentration, the type of solvent used plays an important role in solution-spinning. The presence of a solvent reduces the entanglement density and enhances the rate of crystallization.

6.3 DRY-SPINNING

6.3.1 PREPARATION OF THE DOPE

The first step in dry-spinning is the preparation of the spinning solution or dope. For a long time, it was considered that a good dry-spinning solvent should have a boiling point not higher than 80 °C; the current practice uses solvents of higher boiling points. Some typical polymer–solvent combinations are listed in Table 6.1 [3].

The dissolving power of the solvent must be good. Moreover, the solvent must be relatively volatile and not too expensive. All necessary

Table 6.1 Some typical polymer–solvent combinations for dry-spinning

Spun polymer	Solvent	Boiling point (°C)
Cellulose acetate	Acetone	56
Cellulose triacetate	Methylene chloride	40.7
	Ethyl (or methyl) alcohol	78.4 (64.8)
Chlorinated PVC	Acetone	56
PVC	Mixture of acetone and carbon disulphide	39
Polyacrylonitrile	Dimethyl formamide (DMF)	153
Spandex	DMF	153
Polyvinyl alcohol	Water	100

precautions must be taken against flammability, the possibility of explosion and toxicity. The dissolution is achieved in conventional mixers or kneaders at temperatures of 100 °C or higher. Some unavoidable impurities such as water may be present in the dope or some optional additives such as delustring agents or coloured pigments may be added. The dope is filtered thoroughly at moderate temperatures in two or three successive stages with filtering media such as cotton, paper, fabrics, etc. and then deaerated before spinning. The polymer concentrations in the dope, as quoted in the literature, are: cellulose triacetate 20%, cellulose acetate and polyacrylonitrile (PAN) 25%, PVC 30% and chlorinated PVC 45%. Above a certain concentration, the flow properties of the dope are no longer satisfactory and the extruded gel is not sufficiently coherent to allow stretching. Typical dope viscosity ranges from 500 to several thousand poise at 40 °C. The filtered, deaerated dope is then subjected to the spinning process.

6.3.2 THE SPINNING PROCESS

(a) Rheology of the spinning solution

Like typical polymer fluids, spinning solutions are (1) generally pseudoplastic, i.e. their viscosity decreases with increasing shear rate, and (2) they are viscoelastic and are thus able to store elastic energy. As discussed in Chapter 3, the presence of molecular entanglements is believed to be responsible for these effects. The use of static mixers in the pipework assists in ensuring that the dope is uniform and homogeneous. The rheological characteristics of the spinline are governed by the elongational viscosity of the fluid and its dependence on strain rate.

(b) The spinning cell

A typical dry-spinning cell is shown in Fig. 6.1. The primary function of the cell is the removal of the solvent through evaporation. Solidification
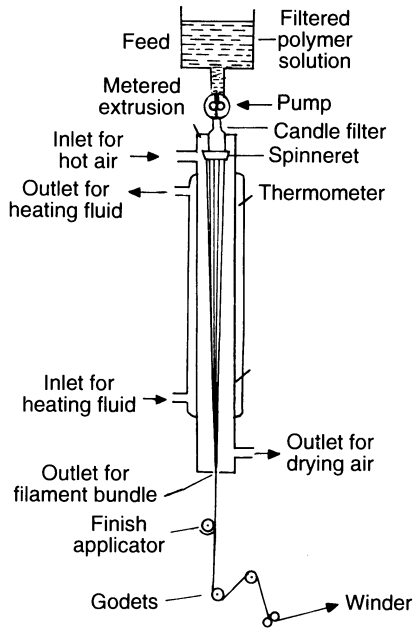
Fig. 6.1 A dry-spinning unit.

is achieved together with cooling of the filament bundle within the spinning cell. The process particulars are considered in this section.

The filtered and deaerated spinning solution is conveyed to the metering pump in the spinning head at a fixed temperature and a pressure usually of 10–20 bars and sometimes up to 80 bars. The temperature of the solution is raised in the spinning head as it passes through a further filtration stage into the spinneret (in the case of polyacrylonitrile solution, for example, the temperature may be raised from 90 to 140 °C [4]). The spinnerets are made of tantalum, nickel or stainless steel with thickness up to 5 mm (in special cases, when pressures are high, the thickness may be up to 15 mm). The distance between the holes is relatively larger and the hole diameter at the capillary end varies within wide limits, 0.02 to 0.03 mm. Bowl- or hat-shaped spinnerets are used for spinning filaments, while ring or bowl spinnerets generally with up to 2800 holes are used for spinning fibres. In the case of ring spinnerets, the drying is accelerated as the gas used to dry the fibres can be introduced both centrally through the inner mount and outside around the spinneret.

The spinning solution, as it exits the spinneret capillary, bulges slightly as the stored energy is released. The greater the relaxation period and the shorter the residence time in the capillary tube, the more the solution bulges. The spinnability of the material is restricted

on the one hand by filament breakages if it is spun at too low a viscosity and, in particular, if it is spun at very high temperatures; on the other hand, filament breakages also occur if the viscosity of the spinning solution and the take-off speed are too high [4].

The solvent evaporates in the hot atmosphere of the spinning tube and polymer concentration and temperature-related diffusion coefficients are the important parameters at this stage. The amount of residual solvent in the fibre material (which, for polyacrylonitrile, is generally retained at a level of 5–25% to aid the subsequent drawing process [4]) depends on the time it is held under evaporation conditions, the take-off speed, the length of the spinning tube, the temperature of the heated jacket and the gas temperature.

The spinning cell is usually 6–10 m long and 25–45 cm in diameter. The tube is kept at the requisite temperature by a jacket heated by a fluid and in-flowing hot gas or air. The drying gas is generally made to flow along the same direction as the filament bundle heated to a temperature above the boiling point of the solvent; in the case of a solution of polyacrylonitrile in dimethyl formamide, the temperature is reported to be 300–350 °C [4]. The gas enters the tube through filters positioned close to the spinneret and is removed at the other end through suction. The flow rate of the gas depends on a number of factors, e.g. throughput rate and solvent content of the spinning solution, the desired residual solvent content, and the physical properties of the solvent, such as evaporation rate and explosive limits. The gas flow rate is stated to be around $1–2\,\mathrm{m\,s}^{-1}$ during the production of polyacrylonitrile yarns [4].

The drying chamber must be leakproof and the density of the solvent in the chamber must not be allowed at any time to go above its explosive limit; for dimethyl formamide the lower explosive limit is stated to be $50–55\,\mathrm{g\,m}^{-3}$ and the upper limit $200–250\,\mathrm{g\,m}^{-3}$ [3]. In order to make sure that the threshold limits are met in the premises, all working areas should have adequate ventilation and air extraction devices. Finally, arrangement for solvent recovery must be such that not more than 10% solvent on the weight of the yarn is lost.

After emerging from the drying chamber an oil-based finish is applied to the yarn before winding. This is mainly to impart cohesion, reduce friction and to reduce static accumulation. The yarns are then wound at $200–1500\,\mathrm{m\,min}^{-1}$.

(c) Fibre cross-section formation [3, 4]

While the use of a round spinneret orifice results in a filament with circular cross-section in melt-spinning, this may not be the case for dry-spun filaments. This is because in dry-spinning the extrudate is a solution of polymer in a solvent and the solvent has not only to diffuse

$$\frac{\text{Evaporation rate}}{\text{Diffusion rate}}$$

~ 1

> 1

$\gg 1$
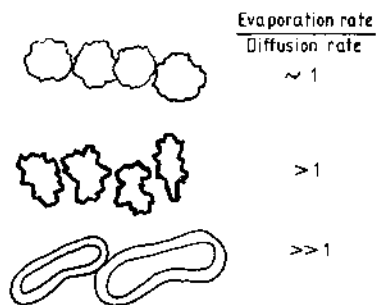
Fig. 6.2 Dependence of filament cross-section on ratio of evaporation to diffusion rate.

out to the outer surface of the filament but also to evaporate in the drying chamber. If the rates of diffusion and evaporation are approximately matched, a circular or near-circular cross-section is obtained. However, if the rate of evaporation is much higher than the rate of diffusion, a surface skin of relatively dry polymer will form; the higher the rate of evaporation in relation to the rate of diffusion, the greater the thickness and hardness of the surface skin. As the remaining solvent diffuses through the skin and evaporates, the volume of the dope inside the tube decreases and therefore the skin will be longitudinally distorted. Thus depending on the ratio of the evaporation rate to diffusion rate, the filament may be flat or peanut-shaped, highly serrated or round (Fig. 6.2).

(d) Spin-stretch during dry-spinning [3]

Consider a cylindrical dope (a longitudinal section of which is shown in Fig. 6.3) of length L cm, diameter D cm and volume V cm^3, the volume concentration of the polymer being C. On solidification, the filament
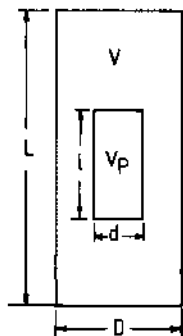
Fig. 6.3 Construction for calculating spin-stretch.

obtained from this cylindrical dope has a length l cm, diameter d cm and volume V_p cm^3. We may write

$$V_p = VC = \frac{\pi D^2 LC}{4}.$$ (6.1)

Now since V_p can also be expressed as

$$V_p = \frac{\pi d^2 l}{4},$$

we get

$$l = \left[\frac{D}{d}\right]^2 LC.$$ (6.2)

Ideally, drying will proceed without distortion of the macromolecular structure. Then the shrinkage of the dope due to the evaporated solvent will be the same along the length and the width, i.e.

$$\frac{l}{L} = \frac{d}{D},$$

which gives

$$l = LC^{1/3}.$$ (6.3)

Under continuous spinning, if L is taken to be the dope length extruded from one spinneret hole in unit time (say 1 min), it can be estimated from the dope supply and the total cross-sectional area of the spinneret orifice. With a pump supply of Q ml min^{-1}, a spinneret of N holes, and with each hole of cross-section x cm^2,

$$L = \frac{Q}{Nx}$$

which, applied to equation (6.3), gives

$$l = \frac{Q(C)^{1/3}}{Nx}.$$ (6.4)

The spin-stretch, corresponding to the distortion of the polymer cylinder when wound at a spinning speed of v cm min^{-1}, is given by the relation

$$\frac{v}{l} = \frac{vNx}{Q(C)^{1/3}}$$ (6.5)

where Q is expressed in ml min^{-1}, x is in cm^2 and v is in cm min^{-1}.

Spin-stretch in dry-spinning cells varies according to polymer spun, the fineness of the individual filaments, the type of spinning device, and the qualities required for the spinning yarn. Its value usually lies in

the range from about 1 to 3 but may be as high as 500 in special cases. The stretch imparted during spinning is not as effective as the stretch imparted during post-stretching the filament, as the molecular orientation induced in the filament is much higher when it is stretched in the solid state than when it is stretched in the dope or gel state.

(e) Finish application and winding

An oil-based finish is applied to the filaments as they issue out of the drying cell. However, it is also possible to apply the finish just at the bottom of the cell itself [4]. The filaments are then drawn off via godet rollers and wound, usually at speeds of 200–500 m min^{-1}. In the production of tow, the filaments emerging from between 10 and 70 spinning cells are combined together to form tows of up to 500 000 dtex, which are wound at speeds of 250–450 m min^{-1} before being coiled in spin cans for further processing.

6.3.3 POST-SPINNING OPERATIONS

After spinning, the filaments are subjected to further treatments which may include drawing, washing, finish treatment, drying, crimping, cutting, heat-setting and packaging. These treatments differ from fibre to fibre and are included in chapters dealing with specific fibre systems.

6.3.4 SPECIALITY FIBRES [4, 5]

Speciality fibres include profiled, hollow, bicomponent and adsorbent fibres. More recently microfibres are emerging as a value-added product with enhanced comfort and aesthetics. Their production is based on slight modification of the spinning solution and/or spinning conditions.

An example of a profiled fibre is a fibre with multilobal cross-section. It may be recalled that even fibres spun from circular holes may be greatly distorted for the reasons described earlier. However, to give the desired profile, the spinnerets are specially designed so that the required shapes can be obtained. In addition, the solutions are of higher concentration and also contain a small quantity of precipitating agent (for example, water in the case of polyacrylonitrile fibre).

For producing hollow fibres by the dry-spinning method, ring spinnerets are used and a counter-current of hot gas is made to flow through the central gap. Solutions of relatively higher viscosity are used.

Bicomponent fibres with well-defined phase boundaries between the two components are produced by combining these components, before spinning by feeding each component to a defined point in the cross-section along the length of the filament with either side-by-side or

sheath core geometry [5]. Side-by-side bicomponent fibres are most commonly used for producing self-crimping. Two polymers differing in chemical structure, comonomer content, molecular weight or some other property are used to produce an oriented fibre in which the two oriented components undergo differential shrinkage. When subjected to some thermal or other relaxing treatment, the product develops helical crimp.

Fibres like polyacrylonitrile with very low moisture sorption can be made more comfortable by making them more absorbent by creating a pore system inside the fibres. The porous core is protected by a sheath of suitable thickness containing a number of tiny channels. To achieve this, a mixture of the solvent and a non-solvent with medium precipitation power is used to dissolve the polymer; the greater the proportion of non-solvent used, the more hydrophilic the fibre.

Fibres and filaments with linear density less than 1 dtex are produced by using polymer of relatively lower molecular weight and preparing a spinning solution whose viscosity is stable prior to spinning, i.e. the viscosity remains stable for several hours. Slow solvent evaporation and high stretch ratios (30–500) allow fibres of 0.6 dtex or still finer fibres to be produced [4].

6.4 WET-SPINNING

6.4.1 SOLUTION PREPARATION AND TRANSPORT

The methods of solution preparation and transport for wet-spinning are similar to those used in dry-spinning. The polymer is mixed and dissolved in a vessel provided with a stirring device. The limits of polymer concentration in the spinning solvents are determined by factors such as polymer solubility and solution spinning pressure limitations. Since the solution is spun at relatively lower temperatures, a lower percentage of solids is used in spinning solutions in wet-spinning; the range is 10–30% in comparison with 15–45% in dry-spinning. The polymer solution has a viscosity of several hundred poises and is degassed to remove any unreacted monomers and air. The degassed solution is filtered to remove any physical impurities and after filtration it is homogenized. The solution is then sent through a metering pump to the spinning machine (Fig. 6.4) with a spinneret generally having 200–600 holes. The temperature is relatively low. The pressures used are also low and spinnerets are thin and made from malleable, precious metals. The hole diameter is 0.005–0.025 cm. Spinnerets with between 2000 and 50 000 holes are sometimes used and the holes can be very close to each other as the liquid coagulation bath, in which the spinneret is submerged, provides sufficient antisticking spacing between the filaments.
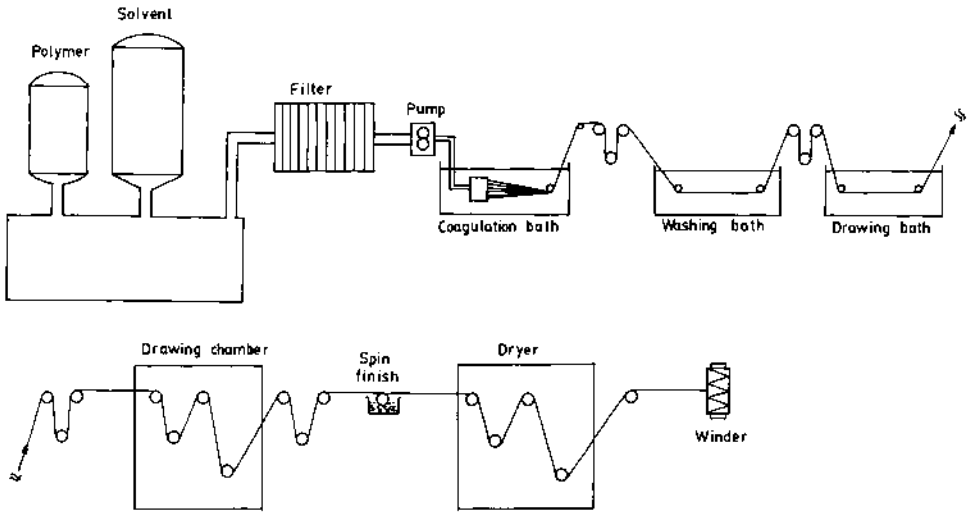
Fig. 6.4 A wet-spinning setup.

In the case of polyacrylonitrile, the fibre-grade polymer is generally produced by either suspension or solution polymerization. The procedure described above is applicable to polymer powders prepared by suspension polymerization. In the case of solution polymerization, the polymer solution is obtained directly by polymerization which, after removing the unreacted monomer and adjusting the viscosity, is fed to the spinlines. The rest of the process is as described above.

6.4.2 COAGULATION

(a) The coagulation process

The emerging filaments are coagulated in a precipitating bath or a series of baths of increasing precipitant concentration; this perhaps represents the most critical element in a solvent-spinning process [6]. This is because during its short residence time in the coagulation bath, the fibre forms and its structure takes shape as a result of complex interactions of numerous factors. These factors include the particular solvents, polymers, temperature, and non-solvents used, as well as variables such as flow, etc. Interaction between these produces the conditions in which counter diffusion of solvent and non-solvent and the phase separation of the polymer take place. It is at this stage that a fluid, viscous solution is transformed into a highly elastic rubber-like solid as a result of gelation. It has been stated that commercial spinning is performed under conditions of moderate bath concentration and at low temperatures.

These conditions are probably close to optimum [7] since solution viscosity, jet stretch and coagulation rate are balanced so as to allow near maximum tension and jet stretch and probably the minimum chance of thread breakage.

(b) Spin-stretch during coagulation

In wet-spinning, the spin bath stretch is generally taken to be the ratio of the take-up velocity (of the first driven godet) to the polymer solution velocity at the exit of the capillary, the latter being computed theoretically [6]. The velocity of filament travel in the spin bath is low because of the large hydraulic drag; this means low spin-stretch.

In the wet-spinning process, material deformation occurs in two or more steps [8]. The filament emerges from the spinneret hole as a fluid and is quickly converted to a gel network by coagulation. The filaments are removed from the bath at a velocity which is much lower than the take-up velocity. Most of the resulting deformation in the spin bath is absorbed by the fluid portion of the filament before it coagulates. Under this condition, the relaxation rates are rapid and therefore deformation of the viscoelastic fluids is not very effective in producing orientation. The drawing is achieved as the partially coagulated filaments move through the subsequent processing steps, namely washing and drying, and the degree of stretch may reach up to 30 times.

In cases where chemical reaction takes place during coagulation, the gelling of the filaments is more rapid in comparison with precipitation by diffusion of non-solvent and the maximum possible spin-stretch is lower.

(c) Fibre cross-section shapes

Taking advantage of the flexibility of the wet-spinning process, a wide variety of cross-sectional shapes can be produced. Using a round capillary, the cross-section will be bean-shaped or circular. The latter is produced either by increasing the coagulation rate and building a thick outer structure that remains round as diffusion proceeds, or by decreasing the coagulation rate and producing a thin outer structure that uniformly coagulates the interior of the fibre.

(d) Further manufacturing operations

The further manufacturing operations differ from fibre to fibre. However, in general, after coagulation the fibres are washed to remove residual solvent and then dried. Then the finish is applied and yarns are converted to give a tow for processing, as in the case of dry-spinning.

In the case of acrylics, several bundles of filaments are combined in a tow – these are washed and stretched wet in either steam, boiling water or in other devices maintaining a high temperature. The tow is dried, oiled and crimped and then subjected to a setting treatment by allowing it to relax to give it the right elongation characteristics. The tow is then cut into appropriate staple lengths and baled.

6.5 DEVELOPMENT OF STRUCTURE AND MORPHOLOGY DURING SOLUTION-SPINNING

In solution-spinning, the solution dramatically changes the whole process of crystallization in relation to crystallization from the melt [9]. At the same degree of supercooling, the crystallization rate increases with increasing concentration of the solution. However, it appears that there is no maximum in the variation of the rate of crystallization from solution with temperature, as in the case of crystallization from the melt. If such a maximum exists, then it is shifted towards higher degrees of supercooling. These facts show why, in solution-spinning processes, it is practically impossible to obtain low crystalline as-spun fibres unless the polymer in question, by its very nature, crystallizes poorly and slowly.

In melt-spinning, the important structural characteristics of as-spun fibres regarding their crystalline texture (degree of crystallinity, crystallite orientation, crystallite size, etc.) are very sensitive to spinning conditions and they affect the behaviour of melt-spun fibres in drawing and in subsequent textile operations. In this way they indirectly control the properties of finished yarns and fibres. This is not true in solution-spinning as the parameters of crystalline texture are generally found to be insensitive to spinning conditions. This is apparently due to the high molecular mobility in fibres containing large amounts of solvent (dry-spinning) or fibres swollen by a mixture of solvent and precipitation agent (wet-spinning). Crystallinity of the spinning line close to the end of the spinning path seems to be more or less close to thermodynamic equilibrium without any great effect of spinning conditions. On the other hand, some other spin-sensitive features appear (not so important in melt-spinning) which control the quality of solution-spun fibres. These include microscopical features (presence of large voids and capillaries, shape of cross-sections, radially differentiated structure) as well as heterogeneity in the submicrometre region, fibrillar structure, etc.

In melt-spinning an important role is played by mechanical and heat-transfer factors, such as stress and velocity fields in the spinning line, and intensity of cooling. In dry- or wet-spinning, the role of these factors is secondary; microscopical and morphological structure, as well as the mechanical properties of fibres, are strongly dependent on the intensity

of mass transfer between the spinning line and the surrounding medium and all kinds of concentration-controlled transitions (phase separation, gelation, etc.).

6.6 SOME SALIENT COMPARATIVE FEATURES OF THE SPINNING PROCESSES

This section deals with some aspects related to an intercomparison of the spinning processes.

1. Quenching of filaments, so that they do not stick together, is easier when the dope is spun into a liquid bath, so many more filaments can be spun from a single spinneret in wet-spinning.
2. The spinnability of a polymer solution is limited, as in melt-spinning, by surface tension instability and cohesive fracture. In dry-spinning the first mechanism is operative and results in dripping in place of continuous spinning. The second mechanism, namely cohesive fracture, appears to be important in wet-spinning.
3. The relative importance of the individual force contributions in dry-spinning is more or less the same as in melt-spinning at corresponding speeds in that the rheological force, F_{rheol}, is an essential contributor to filament dynamics. In wet-spinning, in addition to the contribution of F_{rheo}, the hydraulic drag, which is the equivalent of aerodynamic force F_{aero} in melt-spinning and is referred to as F_{drag}, is also an important component of the measured tension of the spinning line. F_{rheo} is considered to be a constant along the spinning line where the velocity gradient is non-zero, while F_{drag} will be dependent upon the distance from the spinneret exit [10].
4. The properties of as-spun fibres are quite similar for the two solution-spinning processes: a high degree of crystallinity, low crystal orientation, skin-core effect, voids and cracks formed during removal of the residual solvent and reaction by-products from the almost solid filaments, and some degree of deformation of the originally cylindrical fibre form. However, depending on the boiling point of the solvent used in dry-spinning, the crystallization process may proceed at a relatively high mean temperature. In wet-spinning, such high crystallization temperatures are usually unattainable. In wet-spinning, the relatively low temperature of the coagulation bath and the high hydraulic drag cause a much higher degree of orientation compared with dry-spinning.

REFERENCES

1. Tsurumi, T. (1994) In *Advanced Fiber Spinning Technology* (eds K. Kajiwara and J.E. McIntyre), Woodhead Publishing Ltd, Cambridge, UK.

2. Walczak, Z.K. (1977) *Formation of Synthetic Fibers*, Gordon and Breach, New York.
3. Corbiere, J. (1967) In *Man-made Fibers: Science and Technology*, Vol. I (eds H.F. Mark, S.M. Atlas and E. Cernia), Interscience Publishers, New York.
4. Von Falkai, B. (1995) In *Acrylic Fiber Technology and Applications* (ed. James C. Masson), Marcel Dekker Inc., New York.
5. Hicks, E.M., Tippets, E.A., Hewett, J.V. and Brand, R.H. (1967) In *Man-made Fibers: Science and Technology* (eds H.F. Mark, S.M. Atlas and E. Cernia), Interscience Publishers, New York.
6. Capone, G.J. (1995) In *Acrylic Fiber Technology and Applications* (ed. James C. Masson), Marcel Dekker Inc., New York.
7. Han, C.D. and Segal, L. (1990) *J. Appl. Polym. Sci.*, **14**, 2999–3119.
8. Paul, D.R. and McPeters, A.L. (1977) *J. Appl. Polym. Sci.*, **21**, 1699–1713.
9. Ziabicki, A. (1976) *Fundamentals of Fiber Formation*, John Wiley & Sons, New York, pp. 249–350.
10. Frushour, B.G. and Knorr, R.S. (1985) In *Fiber Chemistry* (eds M. Lewin and Eli M. Pearce), Marcel Dekker, New York, pp. 171–370.

Spin finishes for manufactured fibres

7

P. Bajaj

7.1 INTRODUCTION

Manufactured fibres require spin finishes for efficient processability and conversion to textile materials for various applications. Although a spin finish is a layer only a few molecules thick on the surface of the fibre, it is one of the most important variables dictating the performance, quality and uniformity of processing.

The basic requirements in fibre or filament production are yarn transport with necessary directional changes, precise stretching and relaxation to control the mechanical properties, precise twisting, texturing, etc. and correct wind-up to form a commercially acceptable package. The requirements imposed on the spin finish are many and a finish characteristic which is helpful at one particular stage of the process may be detrimental at another. As a result most available finishes represent a compromise between different requirements and there is no ideal finish. Also there is no universal finish which can be used for all types of fibres. Hence, special finishes for specific end uses are being developed.

A number of good comprehensive reviews have been published [1–12] on the basic technology of spin finishes, describing their preparation and properties. However, there is a lack of information on specific compositions and their performance. In this chapter, an attempt has been made to give an overview of this field and the properties of some specific formulations are discussed.

7.2 PROPERTIES OF SPIN FINISHES

The primary functions of a spin finish are to provide surface lubrication to the fibre/filament, antistatic action and good fibre-to-fibre cohesion. In order to perform these functions, a spin finish should have the following desirable properties:

1. It should provide good lubricity to reduce the fibre-to-metal (F/M) friction in order to prevent fibre abrasion and maintain low, uniform tension during processing.
2. It should reduce the static charge build-up during processing.
3. A balanced degree of cohesion is necessary, as too much lubricity may cause fibre slippage resulting in package distortion in winding and other operations.
4. It should have a controlled viscosity range; too low a viscosity causes difficulties in slinging and low yarn frictional values, while too high a viscosity causes excessive add-on coupled with high frictional values.
5. For consistent viscosity, the spin finish must be resistant to bacterial growth; it also should not form insoluble resinous compounds in the presence of oxygen.
6. Scourability (ease of removal): poor scourability would cause dyeing problems and potential soiling spots.
7. It must be corrosion resistant and should not cause damage to rollers, guides or needles.
8. It should be non-allergenic, non-toxic and ecologically acceptable.
9. Spin finishes are generally applied in emulsion, hence they should be easily emulsifiable.

7.3 ROLE OF SPIN FINISHES

Although the spin finish is only a minor, transient part of the total fibre production system, it plays a very important role in the processing, performance and quality of the final product. The spin finish coat is the true interface between the fibre and any other contact surface, for example a guide roll, hot plate, knitting needle, etc. In order to understand the specific role of the spin finish, it is necessary first to consider the basic mechanisms involved in the three primary functions of a spin finish, namely lubrication of the fibre surface, antistatic action and cohesion of filament in a fibre assembly.

7.3.1 LUBRICATION

The general frictional behaviour of liquid lubricated yarns is summarized in Fig. 7.1. It shows how the coefficient of friction is related to a parameter which is a function of processing speed, finish viscosity and
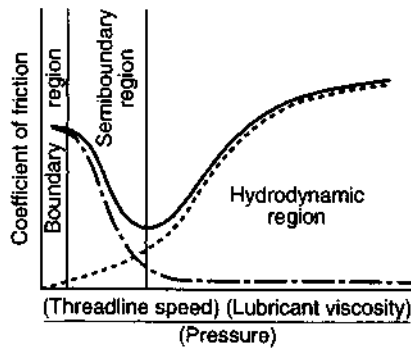
Fig. 7.1 General frictional behaviour of liquid lubricated textile yarns [9].

pressure (force/area of contact). The behaviour is similar to that found in metal lubrication in that there are two distinct regions – the boundary region and the hydrodynamic region – with an intermediate semiboundary region.

The dash-dotted line represents the contribution of the boundary component of friction. At low speeds of yarn sliding contact, and where high contact pressures exist, boundary lubrication results from thin films of pressure-resistant lubricants. In boundary conditions, the sliding surfaces are separated by a lubricant film of molecular dimensions, and solid contacts frequently penetrate the protective film [9].

Hydrodynamic friction, the other extreme represented by the dashed line, results from the shear stresses within a thicker liquid film, at least several molecular layers thick, between the two surfaces.

(a) Boundary lubrication

According to Olsen [13] the important factors which influence boundary lubrication and friction are:

1. chemical nature of the lubricant and the sliding surface;
2. shear strength of the lubricant;
3. physical structure of the substrates; and
4. pressure at the area of contact.

In both the boundary and the semiboundary areas, a phenomenon of stick–slip occurs between the yarn and the guide contact surfaces at low speeds and/or high pressure, large area contacts. As the speed increases the stick–slip disappears. At this point the friction changes from semiboundary to hydrodynamic. The stick–slip phenomenon is, however, more pronounced if the pressure at the area of contact is increased or the lubricant film has low shear strength. Because of their poor film
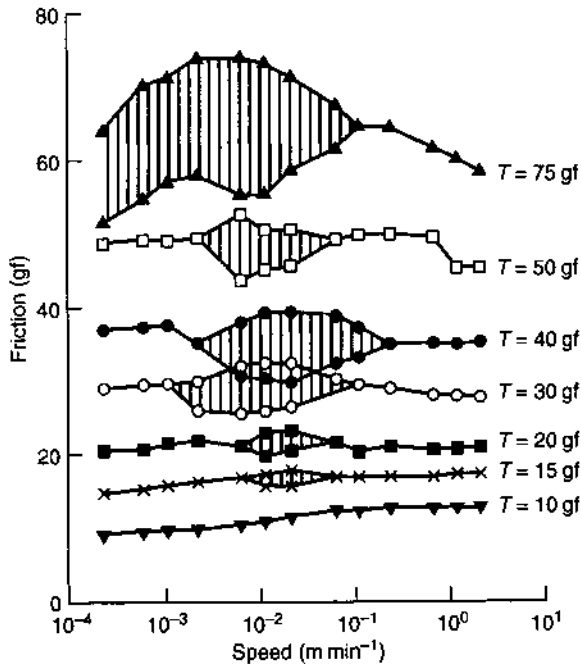
Fig. 7.2 Effect of pretension (*T*) on the stick–slip phenomenon. Test conditions: Chemstrand F-meter, F/F 2.5 turns, 2.5 in 5 pulleys; yarn, bright nylon 66, 200/34 (Du Pont); finish, 1% wof of *n*-butylstearate; temperature, 70 °F; RH, 50% [14].

strength weak lubricants allow the two contacting surfaces to rub together, thereby increasing the friction and the magnitude of the stick–slip. The effect of pretension and speed for bright nylon 66 with a 1% butyl stearate lubricant film is shown in Fig. 7.2. The magnitude of the stick–slip decreases with increasing speed. Interestingly, there is no stick–slip at the lower input tension level of 10 g, while at pretension levels of 15–50 g the stick–slip is continuous and large in magnitude [14]. However, the disappearance of the stick–slip phenomenon at higher speeds indicates the transition from semiboundary to hydrodynamic friction. Thus, stick–slip disappears with the onset of continuous film formation.

In contrast, the abrupt disappearance of stick–slip at lower speeds may be attributed to changes in the elastic deformation of the fibre. The continuous presence of stick–slip even with high input tension of 75 g at low speeds is presumably due to the significant elastic deformation at this load. The measurement of frictional properties at low speed/high pressures is therefore important to the understanding of any fibre-finish processing system even though the process normally operates at hydrodynamic conditions. Several suggestions have been put forward to

explain the stick–slip process. Bowden and Tabor [15] discriminate between a static friction coefficient obtained during the stick period and a kinetic friction coefficient found during motion, while de Jong [16] has presented the relation between stick time and static friction force, based on Lavrentev's bond exchange hypothesis.

(b) Hydrodynamic lubrication

As stated above, most spin finish formulations are designed to maintain the friction in the hydrodynamic region of the hypothetical curve (Fig. 7.1). The important variables are listed below:

- finish (viscosity and concentration of the spin finish);
- fibre (denier per filament, topography, and shape of the fibre);
- manufacturing process (speed, applied tension, contact surface roughness, contact surface area, temperature and relative humidity).

Among these, contact area, viscosity and the amount of spin finish are the major variables influencing the frictional properties of synthetic fibres [17]. Since hydrodynamic friction arises from shear within the liquid film, and it normally requires more force to shear more viscous films, it should be expected that higher viscosity finishes would give a higher coefficient of friction and higher yarn running tensions in a given processing system.

The effect of viscosity and speed on friction has been studied for Nopcostat^{TM} finishes (Fig. 7.3). It can be seen that in the low speed region there is relatively less difference in the coefficient of friction of the three lubricants tested despite the differences in their viscosities. At higher speeds, the friction increases with viscosity. This shows that the friction is independent of viscosity in the boundary region and highly
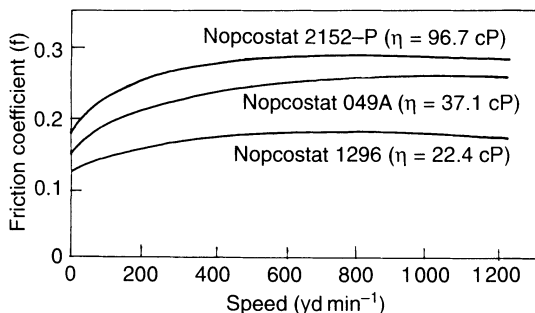
Fig. 7.3 Variation of friction with speed in the high speed region. Test conditions: Rothschild F-meter; yarn, bright nylon 66, 200/34 (Du Pont); finish, 1% wof; chrome pin RMS 60, 0.5 in diameter; contact angle 360°; $T = 10$ g; temperature, 70 °F; RH, 50% [14].
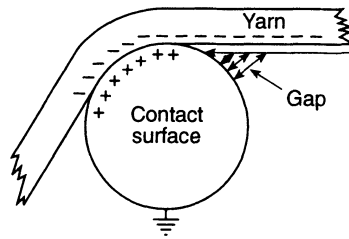
Fig. 7.4 Static electrification [9].

dependent on viscosity in the hydrodynamic region. Since the fibre contacts the metal frequently at low speeds, only the film strength influences the friction; the increase in friction is apparently due to the increased shear strength of the lubricant film with increase in viscosity.

7.3.2 ANTISTATIC ACTION

In a fibre–finish–guide surface system (Fig. 7.4), three factors which influence the static electrification of the finished yarn are charge transfer during surface contact, charge leakage across the gap and charge flow along the surface. It is immaterial whether the actual charge carriers are electrons or ions; the results are expected to be the same.

Major variables affecting static in fibre processing are surface contact area and force, relative humidity, yarn speed, nature of the fibre finish and temperature. The development of a charge on a moving fibre surface is directly associated with frictional contact with other sufaces, and most of the variables influencing lubrication also influence electrostatic charge generation.

It is difficult to control charge generation through finish composition. The spin finish can help only in the dissipation of the charges as soon as they are generated. Hence, judicious selection of an 'antistat' in a spin finish formulation is necessary for the dissipation of charges, depending on the nature of the fibre and its process of manufacture.

Ionic compounds are found to be better antistats than non-ionic compounds. Details of the antistats and their performance will be given later. However, it is worth noting here that with an increasing amount of finish and an increasing concentration of antistat, both hydrodynamic friction and antistatic action increase.

7.3.3 COHESION

The third primary function of a spin finish is to provide cohesion between the filaments of a fibre assembly (tow). This function becomes important in zero twist continuous filament yarns and staple fibre processing.

Cohesion provided by the fluid can be measured by the force to shear the fluid in a plane parallel to the tow. Then the force vector for shearing the liquid film along the fibre axis would be the hydrodynamic friction. Thus, the variables influencing the fibre–fibre cohesive forces are the same as those affecting hydrodynamic friction. An increase in the fibre cohesion with a fluid finish would also increase the hydrodynamic friction. Processing problems related to cohesion can therefore be easily interpreted in terms of hydrodynamic friction.

7.4 SPIN FINISH COMPONENTS

A spin finish invariably contains a large number of chemical components. The major components are lubricant, antistatic agent and emulsifier [2–7]. In addition, spin finishes contain small proportions of antioxidants, antibacterial products, corrosion inhibitors, defoamers, rubber adhesion promotors (for tyre cord), etc. Excellent accounts of recent developments in the chemistry of spin finishes [2–4] and fibre lubricants and surfactants are given by Kleber [6] and Lee [7]. The chemicals used in each category are:

1. *Lubricants*
    (a) Natural lubricants: mineral oils and waxes, vegetable oils and waxes, coconut oil, sperm oil, animal oils and fats.
    (b) Synthetic lubricants: esters (butyl stearate); ethoxylated esters, ethoxylated fatty acids; ethoxylated fatty alcohols, polyethers, synthetic waxes, silicones.
2. *Antistatic agents*
    (a) Anionic: alkyl acid phosphates and their salts (metal and alkanolamine); ethoxylated derivatives of the above materials, phosphated ethoxylates of fatty acids and alcohols, organic sulphates and sulphonates.
    (b) Cationic: quaternary ammonium, pyridinium, imidizolinium; quinolinium compounds such as chlorides, metho- and ethosulphates; alkylamine oxides.
    (c) Amphoteric: ethoxylated fatty acid amides; betaines.
3. *Emulsifiers*
    (a) Anionic: fatty acid soaps (metals, alkanolamine salts), sulphated vegetable oils, alkane sulphonates, alkylsulpho succinate salts, ethoxylated alkyl phosphate salts.
    (b) Cationic: fatty amines, ethoxylated fatty amines, quaternary ammonium and ethoxylated quaternary compounds.
    (c) Non-ionic: polyglycols, polyglycol esters and ethers, glyceryl fatty acid esters, ethoxylated alcohols, fatty acids, fatty amides, alkyl phenols.
    (d) Amphoteric: amino acids and their salts and betaines.

Tests performed by Olsen [13] have shown that cationic products in general can improve the shear strength of polymers. However, the extremely high fibre-to-fibre dynamic friction imparted by cationics leads to the generation of enough heat to destroy the lubricating film, so that the finish is no longer effective. It is therefore advisable to combine the cationics with a low friction finish, to improve the shear strength of the spin finish film. Daefler [18] has found that some copolymeric additives are very effective in reducing wear by improving the shear strength of the polymer. The most effective and suitable lubricants are special phosphate esters and non-ionics which provide only half the friction force of the best known finishes for the conventional cotton spinning process.

However, in addition to low friction, antiwear and antistatic protection are also required, particularly in very high speed processes. For antistatic protection, finishes must be polar, while for low friction finishes non-polar products are suitable. To meet these contradictory requirements, the finish formulation is generally a compromise.

In another study of spin finishes for texturing polyester yarn, the static properties of some of the formulations (Table 7.1) containing 30–40% non-ionic emulsifier show the high performance of quaternary ammonium compounds (formulations C and F) [19], although they must be used at low concentrations to minimize heater plate deposits. On the other hand, neutralized phosphate ester (formulation H) at a concentration 10–15% higher than that used in formulations C and F improves the static protection to a level equivalent to that of the quaternary ammonium compounds. On decomposition neutralized phosphate ester leaves a fine white powder on heater plates and does not interfere with

Table 7.1 Static properties of some spin finish formulations [19]

Finish code	Lubricant	Antistatic agent	Static half-life (s)
A	Butyl stearate	Nonionic	3600
B	Butyl stearate	Neutralized phosphate ester	425
C	Butyl stearate	Quaternary ammonium compound	125
D	High mol. wt ester	Non-ionic	220
E	High mol. wt ester	Neutralized phosphate ester	150
F	High mol. wt ester	Quaternary ammonium compound	30
G	Complex ester	Non-ionic	180
H	Complex ester	Neutralized phosphate ester	50

the yarn processability. The lubricant selected also influences the static charge generation. Butyl stearate generates the highest static charge and the complex ester the lowest.

7.5 SPIN FINISH APPLICATION TECHNIQUES

The main requirement of any finish application system is that it is capable of applying the same level of finish along the length and over the perimeter of all the filaments.

The application techniques described below have been used to achieve this requirement.

7.5.1 DIPPING ROLLER METHOD

A schematic sketch of the dipping roller method, which is the oldest and most widespread method of lubrication, is shown in Fig. 7.5. The roller, which rotates at constant speed, is partially immersed in a trough to which the spin finish solution is supplied from an overhead tank. An overflow arrangement provides for a constant level of filling, with the excess solution flowing back to an intermediate vessel. The spin finish adheres to the roller surface in film form. The film thickness depends on the roller speed and the viscosity and concentration of the spin finish solution. The filament yarns generally touch the kiss roller tangentially or at a very slight wrapping angle. The direction of yarn travel and roller rotation must be the same. If they move in opposite directions, there is more splashing and finish application is also greater. Lubricant application depends upon lubricant viscosity, its wetting properties and the roller speed, which must be determined experimentally [20].
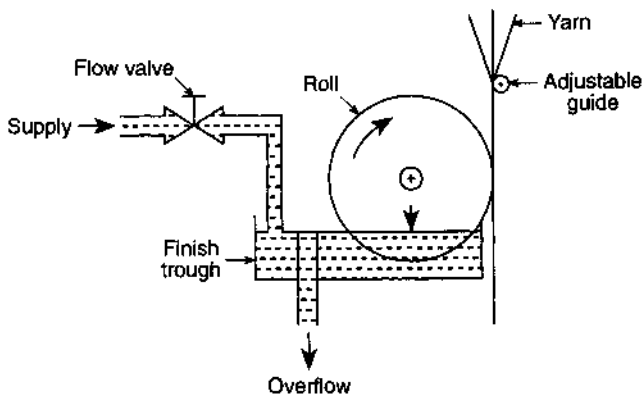
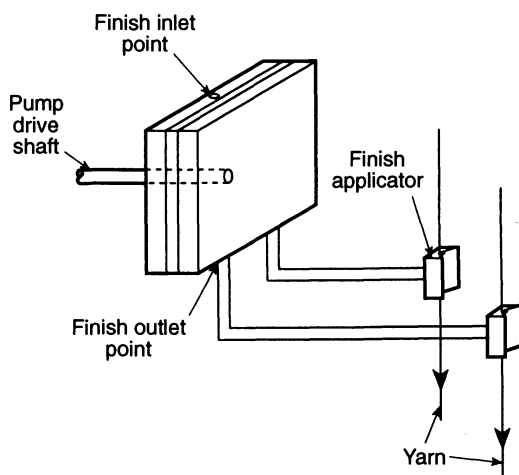

Fig. 7.5 Dipping roller system.

This system is most useful for high filament deniers and other products which require a relatively high amount of spin finish to be applied uniformly, e.g. carpet yarns and staple fibres.

The disadvantage of this system is a certain degree of irregularity (±10%) in application which, however, may not be detrimental in most cases. Because this system is open, it is also more vulnerable to bacterial growth. Excellent accounts of this system, its advantages and disadvantages, and a comparison with the metered finish system are given by Schubert [20], Vaidya [5] and Nevrekar and Palan [12].

7.5.2 METERED FINISH SYSTEM

Since the introduction of high speed spinning, the metered finish system has established itself because of its ability to apply even very small amounts of lubricant exactly and uniformly. Figure 7.6 shows a metered finish application system. In this system, the yarn guide is supplied with the spin finish formulation by means of a gear pump. Most of the lubricating yarn guides are made from sintered aluminium oxide. An expensive closed circuit is used for highly bacteria-sensitive spin finishes. Factors affecting the operation of this system are: (1) variation in rev min^{-1} of the pump drive, (2) viscosity, and (3) differential pressure across the pump.

This system is suitable for high speed spinning processes (both polyester and nylon), for fine counts and for sensitive subsequent processes including friction texturing. No guide is required prior to the applicator and hence there is less drag than in systems with a thread guide, for

Fig. 7.6 Metered finish system.

example using the dipping roller method. The basic rules and guidelines to be followed for successful application of this technique are discussed by Schubert [20]. The shortcoming of this system is reduced flexibility, and major changes are necessary in order to change the number and denier of the filaments.

7.5.3 QUENCH DUCT LUBRICATING SYSTEM

Conventionally, lubricating systems are mounted at the bottom of the quench duct, but there are several advantages in locating the system at a variable height inside the quench duct. Figure 7.7(a) is a schematic representation of the thread path between the spinneret and the take-up bobbin showing all the installations available for treating the filament. The spin finish application system is installed in or just below the lower portion of the cross-flowing air cooling zone. Figure 7.7(b) shows an enlarged section of the oiler pin with filament passing. The arrangement of the oiler pins in the base frame of the air quench duct requires a special design to ensure an easier spin start, so that continuous spinning is not hindered.

If thread guides are arranged immediately below the oiler pins and thread sensing parts are sited at the lower end of the falling tube, the warp space can be turned between the lower end of the quench chamber and the winding machine, resulting in a considerable saving in building
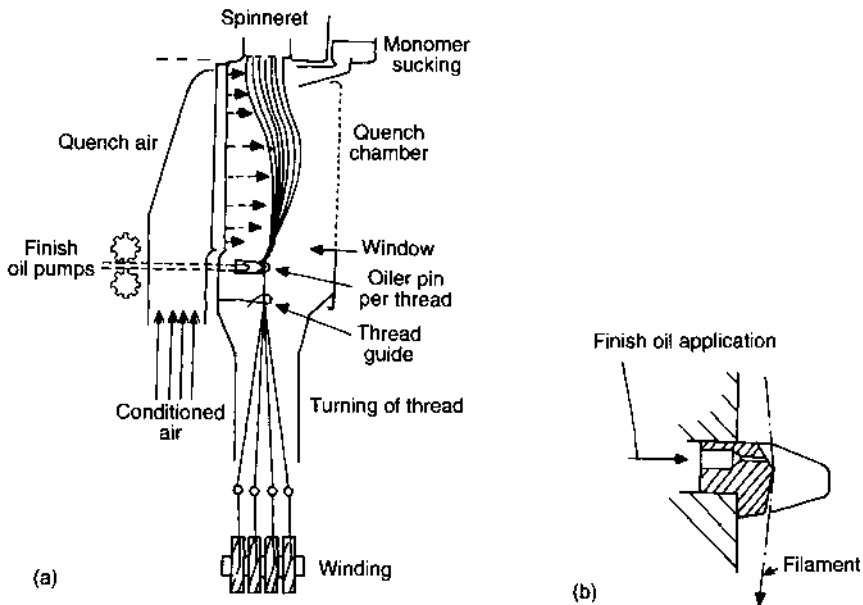

**Fig. 7.7** (a) Quench duct lubrication system; (b) oiler pin [21].

height. Fourne [21] claims the following advantages for the quench duct filament oiling system:

- better filament cooling in a shortened path between the spinneret and the winder;
- godet rollers are eliminated which reduces the cost and leads to easier winding without the risk of lapping on the godet rollers;
- change and/or reduction in thread oscillation and displacement of resonance, and thus better titre uniformity;
- the multifilament, after passing the oiler pin, results in significant reduction in tension, e.g. 166 dtex polyester spun at $3500\,\mathrm{m\,min^{-1}}$ speed, with the former take-up machine oiling system developing a tension of about 70 g which can be reduced to less than 35 g tension with the new quench duct oiler system. With modern air quench chamber techniques, this tension of 35 g can be further reduced to 20 g filament tension which is apparently optimum for a good bobbin shape with high speed winders;
- if the finish oil system is arranged in the base frame of the air quench chamber, more time is available for distribution of the finish to the filament surface. Overall, given the optimal design, the quench duct oiling system is the best technique for high speed spinning.

7.5.4 SPRAY TECHNIQUE

In staple fibre production, the final finish is usually applied after crimping by using a spray technique. The tow is passed between the spray nozzles which spray the finish on the tow at a controlled rate (Fig. 7.8). The amount of finish applied depends on the concentration and the viscosity of the finish, rate of supply of the finish by the dosing pump, tow denier, line speed and the number of nozzles used in the spray. The spray finish combined with crimp makes possible the further processing of the fibres in the textile mills. An excellent account of oversprays with some case studies has been given by Savage [22].
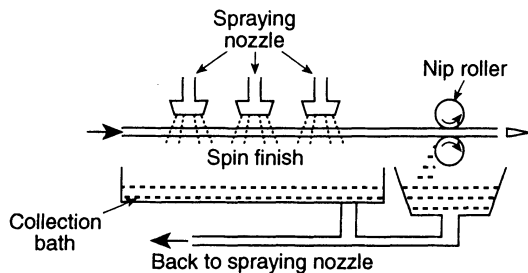
Fig. 7.8 Spraying system.

7.6 SPIN FINISHES FOR STAPLE FIBRE PRODUCTION AND PROCESSING

7.6.1 SPIN FINISH REQUIREMENTS FOR STAPLE FIBRE PRODUCTION

An extensive technology is used in the production of staple fibres, and hence the finish has to meet a number of requirements right from melt-spinning to the final yarn production. Because of this, it is customary to apply different finishes at different stages of staple fibre manufacture, in particular at the following three different stages [12, 23]:

1. *Spin finish:* this is applied during melt-spinning of multifilament yarns (a number of which are later combined to form a tow) just after quenching using the dipping roller technique. The spin finish should give good antistatic and low sliding friction properties to the tow. Also the thread cohesion must be good, so that the tow can be laid into the cans without any ballooning or sticking of the filaments due to static charge accumulation. Since water acts as a cohesive agent, the water-retaining capacity of the spin finish is important.

2. *Drawing finish:* this is usually the same as the spin finish used at stage (1) or only water and is applied before drawing by the immersion bath method to give an even distribution of the finish on individual filaments. The drawing finish is expected to perform the following functions:
   - it should facilitate the drawing process, which requires separation of the individual filaments;
   - it should not allow migration of oligomers to the fibre surface, thus having an oligomer retarding effect;
   - slippage at the drawing rollers and adhesion of the tow to the rollers must be prevented;
   - it should be stable thermally, in order to withstand heat-setting processes.

3. *Staple finish:* the staple finish is applied in the post-drawing operations and it must satisfy the following requirements:
   - it should facilitate the stuffer box crimping and cutting operations. It should prevent overheating as well as any tendency to form deposits;
   - for stretch breaking, fibre-to-fibre transverse adhesion should be avoided. Also antistatic properties should be good. In general, low moisture content avoids adhesion of the finish;
   - in the blow room, the finish should allow optimum opening without making the package too bulky;
   - operation on card requires good web cohesion, no card loading, satisfactory antistatic behaviour and no tendency to form deposits;

- in ring spinning the requirements are that there should be no tendency to wrap formation, low fibre-to-metal friction, and good fibre-to-fibre cohesion.

7.6.2 SELECTION OF STAPLE FIBRE FINISHES

The selection of the proper finish for staple fibres is quite important as static charges and/or improper cohesiveness can lead to problems in fibre processing, e.g. roller lapping.

The spin finishes for staple fibres generally consist of tow cohesion sarcosides, antistatic agents like $POCl_3$-based esters, a large amount of water and ethoxylates of different fatty acids. The drawing finish is usually the same as the spin finish or may be only water. The staple finish (final finish) may contain P_2O_5-based esters, sulphates, sulphonates, ethoxylates and quaternary compounds.

Water serves as a diluent and reduces the viscosity of the oil finish. It also helps to suppress static generation. For this reason, staple fibre finishes invariably contain water.

Compatibility of the spin finishes is an important factor. Mahajan and Nadkarni [24] report an interesting case study in which bales meant for blending with cotton got mixed up with those for viscose. This made it impossible to process polyester/cotton or polyester/viscose blends due to incompatibility of the spin finishes. In another study, difficulties in the processing of polyester/polynosic blends have been reported due to the incompatibility of the two finishes, namely the presence of a cationic finish on the polyester and an anionic finish on the polynosic.

The universal application rates for polyester staple fibres are as follows:

For cotton blend	<1.5 den, 0.1–0.2% owf (on the weight of fibre)
For rayon blend	1.5–2.5 den, 0.3% owf
For wool blend	3 den, 0.2–0.3% owf
For others	5 den, 0.4–1% owf

7.6.3 SPIN FINISH REQUIREMENTS FOR ROTOR AND FRICTION SPINNING

For staple processing, a number of factors – among which are an ever-increasing demand for higher throughput direct feed carding, high speed ring spinning, rotor spinning speeds up to 100 000 rpm, and finer yarn counts – place great and often conflicting demands on the spin finish. Recently, Daefler [18] has discussed the requirements of a spin finish suitable for the high speed spinning of polyester and acrylic fibres. Focusing on rotor and friction spinning processes, Daefler stated

that the key step indicating the limits of the whole process is the fibre drafting step, which involves fibre-to-fibre (F/F) friction and fibre-to-needle friction and high rotor speeds generating heat. Very rapid heat generation destroys the lubricating film and the finish becomes ineffective. High speed opening needles splash or pluck the polymer film from the fibre onto the rotor where it is deposited. Therefore the nature of the spin finish dictates whether or not a fibre will run successfully. It has been demonstrated that a spin finish with low dynamic fibre-to-fibre and fibre-to-metal friction and increased shear strength of the polymer surface, due to the formation of a strong boundary or elastohydrodynamic (EHL) film, appears to be ideal for rotor spinning.

It has been further observed that bright fibre causes more trouble in rotor spinning as compared with semidull (TiO_2) fibre because the F/F and F/M dynamic friction forces are about four times higher with the bright fibre. Similar observations have been made by Sinha [25] based on an analysis of Shick's data [26] for bright and dull nylon 66 fibres. Schick's experimental results, plotted in Fig. 7.9(a), indicate that friction increases on decreasing the fibre surface roughness in the hydrodynamic region. It appears that increased fibre surface roughness disrupts the
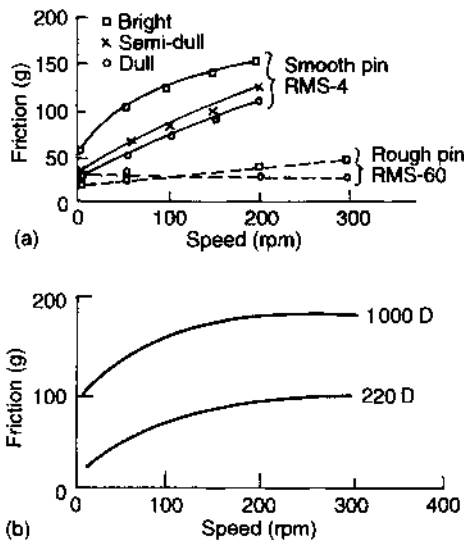
Fig. 7.9 (a) Effect of fibre lustre and pin roughness on friction. Test conditions: Rothschild F-meter; yarn, nylon 66, 200/34 (Du Pont); finish, 1% wof; chrome pin 0.5 in diameter; contact angle, 0–360°; tension, 0.05 g den^{-1}; temperature, 70 °F; RH, 50% [26]. (b) Effect of denier on friction at the fibre/metal interface. Test conditions: Rothschild F-meter; yarn, polyester, bright (Du Pont); finish, 1% wof; chrome pin RMS 60, 0.5 in diameter; contact angle, 0–360°; tension, 0.05 g den^{-1}; temperature, 70 °C; RH, 50% [25].

continuous fluid film between the yarn and the guide, resulting in a shift towards conditions simulating a semiboundary region with consequent lowering of friction. It has also been claimed that TiO_2 affects the surface geometry, i.e. bright fibres have a smooth surface, whereas dull fibres have a rough surface. However, the difference between the friction values of bright and dull nylon yarns in the hydrodynamic region is minimized by using a rough pin (RMS-60) as shown in Fig. 7.9(a). The effect of denier on the friction at fibre/metal interface is shown in Fig. 7.9(b).

It is important to note that spin finishes and components for shear resistance improvement are different from those needed to reduce dynamic friction. Moreover, for very high speed process, much better antistatic protection is required. Therefore, when looking for low friction and antiwear finishes with acceptable static friction (adhesion or cohesion), antistatic protection is expected to be poor, because low friction finishes must be increasingly non-polar products whilst finishes with antistatic protection must be polar. Hence, the finish formulation must be a compromise between the two desired properties.

For acrylic fibres to run with the same speeds as achieved with polyester, using a high speed rotor spinning system, it is necessary to achieve the same surface properties (friction and low wear) as those of PET fibres by a judicious selection of spin finish components. Most wet-spun acrylic fibres are brittle, and possess strong anionic character; it is therefore necessary to formulate a spin finish with low friction and better shear strength properties. In fact, the anionic character of the surface favours cationic products for obtaining durable EHL films, while the brittleness of the fibres, which cannot be influenced by the final finish, can be reduced by adding certain modifiers in the acrylic spinning dope. If these requirements are fulfilled then acrylic fibres can be smoothly run on a rotor spinning system.

A number of formulations based on partial phosphate esters of an alkylated alkyl phenol such as poly(oxyethylene)$_{5-15}$ nonyl phenol or poly(oxyethylene)$_{5-10}$ lauryl alcohol are given in the literature for polyester staple fibres [27]. The chemical composition of a finish which facilitates the stretch breaking of polyester tow into sliver and spinning of sliver into yarn has also been reported [28].

7.7 SPIN FINISHES FOR FILAMENT YARNS

High speed spinning is very often combined with the drawing step, thus forming the modern high speed spin–draw winding system. Final winding speeds for textile polyester filaments of over $6000\,\mathrm{m\,min^{-1}}$ have been achieved. The requirements of a spin finish at high winding speeds are:

- keeping the filament bundle together;
- facilitating the drawing of the filaments;
- avoiding the splicing of the capillaries from the filament bundle on the godets;
- providing good package formation on the winder;
- imparting low friction.

In spin–draw winding, the most important problem seems to be that of cohesion. From the finish point of view specific problems can be expected, if high denier filaments such as those in industrial yarns are considered. For geometric reasons such filaments need a high amount of finish in order to obtain cohesiveness. However, such a high amount of finish on the filament can increase the tar formation on the godets. Furthermore, the drawing of the filaments between the godets requires finishes with high F/M (filament-to-metal) cohesiveness in order to fix the draw point. A high amount of finish for cohesion or sticky finishes and low tar formation on the godets are contradictory requirements. If one uses highly cohesive finishes, cleaning cycles of the godets become so frequent that the high speed of the process is difficult to maintain.

For further processing steps like texturing, warping, knitting, twisting, etc. additional finishes are sprayed on filaments prior to winding. Modern spin finishes for polyester and polyamide filaments have been described by Schulberger [29].

Selivansky, Walsh and Frushour [30] have studied the interactions of spin finishes with partially oriented PET yarns (POY). A low temperature dyeing technique developed as a characterization method revealed thermally activated interactions between the POY polyester and the spin finish containing polyethylene glycol.

This basic study was an outcome of an important observation made by the Monsanto Company of the USA while producing POY yarn as a feedstock for continuous draw texturing. By using this low temperature test, they observed that the dye depth was critically dependent on the specific composition of the finish used in the spinning of the fibre. Further examination of these spin finish compositions showed that the finishes containing a large proportion of anionic surfactants tended to decrease the dye uptake the most. It has now been established that the thermally activated interaction of PEG or its derivatives with POY is responsible for the dye blocking owing to the high degree of order and intermolecular cohesion in the POY. The most efficient dye blocking PEG is therefore the one most compatible with PET based on the solubility parameter (δ for PEG [400 g mol^{-1}] is 10.1 cal$^{1/2}$ cm$^{-3/2}$).

In another study, Herlinger, Koch and Buhler-Neiens [31] have investigated the diffusion effect of spinning lubricants on nylon 6 filament yarns.

7.7.1 SPIN FINISHES FOR TEXTURING

The texturing of POY, and in some cases of flat yarn, is the major process that continues to place rigorous demands on spin finish performance, particularly as speeds have increased to 900–1000 m min^{-1} and even higher, and as the trend to use polyurethane discs, rings and belts for friction texturing has increased. Therefore, the search goes on for spin finish compositions that are satisfactory for all the demands imposed by high temperatures, extensive metal plate and guide contact, and the various types of twist devices. Furthermore, new problems are being imposed owing to the use of finer filaments for texturing, which are more susceptible to damage.

The general requirements of a spin finish for texturing purposes can be summarized as follows [32–34].

1. Optimum build-up of feed bobbin: this is important to allow high drawing speeds. This requires low fibre-to-metal friction together with high filament cohesion to achieve good packaging and to avoid overthrown ends or loops.
2. Yarn properties should not be altered during storage. For this the spin finish components should not penetrate the fibres and alter the fibre structure either by plasticization or by changing the crystallinity.
3. In the drawing zone, important considerations are volatility, thermal degradation, heater plate residue and dripping from the overhead primary heaters.
4. The thermal variability will affect the processing performance as well as the physical properties of the yarn. In order to minimize heat losses, the finish should have low specific heat and the heat of vaporization of the volatile components should also be low.
5. Frictional characteristics: the filaments should have suitable frictional characteristics depending upon the type of twisting unit. For magnetic spindles the filament-to-metal friction should be a minimum, as transmission of torque is done positively. In the case of friction texturing, the spin finish should give the required friction coefficient so that transfer of torque takes place.
6. Draw texturing: in the case of draw texturing, to ensure a reduction in filament breaks, the dynamic filament-to-filament friction should be low. Draw texturing of multilobal yarn necessitates the use of spin finishes with low friction coefficients to improve drawability and to reduce filament breakage. A cohesive component in the spin finish which volatilizes off the yarn as it passes over the heater plate can fulfil the conflicting requirements of high fibre-to-fibre friction for POY package build-up and low friction for draw texturing. The remaining components will exhibit low fibre-to-fibre friction.

7. For polyurethane discs used in friction texturing, the finish components should not soften or swell the disc material.
8. The spin finish should ensure minimum heater deposits, otherwise frequent heater cleaning by stopping the machine will make the process uneconomical.

When hard discs are used in friction texturing, the discs abrade the yarn, producing a white deposit called 'snow'. Spin finish can drastically affect the amount and the type of snow. Snow, however, is not only caused by spin finish but also by (a) the oligomers and monomers content in the feeder yarn, (b) the nature of the disc surface, disc number and disc profile. In a case study on PET texturing, Knowlton, Pierce and Popper [35] found that, on average, the disc snow consists of $60 \pm 10\%$ polymer and $40 \pm 10\%$ feeder yarn finish.

A compromise must be made regarding the frictional properties of the filaments, since higher frictional coefficients lead to more snow generation while lower frictional coefficients lead to twist slippage. If the feeder yarn contains a higher percentage of oligomers and monomers, the spin finish should suppress their migration. Knowlton, Pierce and Popper [35] observed that the higher the finish level, the higher the snow generation, and there is a direct correlation between the two. Hence, very low finish levels, preferably 0.25–0.3%, would minimize snow generation, and the choice of optimum molecular weight components will produce dry snow. The snow should not be sticky and should always fly off the system without making the discs sticky.

(a) Spin finish composition for texturing

In formulating an acceptable spin finish, it is often necessary to make a number of compromises. The combination of proper lubricants, antistatic agents and emulsifiers has to be made in such a manner that the finish provides static protection and frictional properties which maintain minimum tensions through the discs with minimum abrasion of the filaments. A comparison of thermal properties of finish formulations along with their fibre-to-fibre and fibre-to-metal friction data is given in Table 7.2. From these data it is evident that ethoxylated silicone products are the better lubricants as they combine thermal stability with water solubility or self-dispersibility. Amongst the antistatic agents, phosphate esters of fatty alcohols and fatty alcohol ethoxylates meet the antistatic and heat stability requirements but they have a tendency to cause wear on metal surfaces. On the other hand, quaternary compounds meet the antistatic requirements (Table 7.1) but their heat stability had led to their rejection by a number of fibre manufacturers.

Table 7.2 Properties of fibre finishes and false-twist textured yarns with these finishes[a]

Product composition	Viscosity (cP)	Volatility (mg cm^{-2})	Coefficient of friction				Specific resistivity (Ω cm)
			Fibre/metal		Fibre/fibre		
			20°C	220°C	Static	Dynamic	
Lubricants							
Tridecyl stearate	25	11.5	0.31	0.63	0.17	0.13	—
Lauric ester of trimethylol propane	60	2.2	0.44	0.58	0.16	0.12	—
Lauric ester of trimethylol ethane	30	6.8	0.35	0.38	0.16	0.12	—
Ethoxylated silicone	ca. 1000	28.0	0.59	0.61	0.11	0.08	1.3 × 10^9
Ethoxylated silicone	700	35.0	0.57	0.57	0.08	0.06	1.4 × 10^9
Emulsifiers							
Short-chain ethoxylate of a fatty alcohol	30	25.2	0.41	0.68	0.14	0.10	2.8 × 10^9
Medium-chain ethoxylate of a fatty alcohol	55	26.5	0.50	0.60	0.14	0.11	5.1 × 10^8
Long-chain ethoxylate of a fatty alcohol	20–25	30.5	0.54	0.60	0.15	0.10	1.3 × 10^8
Stabilizers							
Alkyl phenol ethoxylate	260	10.7	0.73	>0.75	0.15	0.13	6.0 × 10^8
Polyoxyethylene sorbitol hexalaurate	210	25.1	0.59	0.63	0.13	0.11	5.0 × 10^8
Polyoxyethylene sorbitol hexaoleate	200	13.0	0.63	0.69	0.12	0.08	2.7 × 10^8
Antistatic agent							
Quaternized fatty amine ethoxylate	690	25.7	0.77	>0.8	0.14	0.12	3.8 × 10^6
Polyol ester ethoxylate	275	7.2	0.59	0.69	0.13	0.11	9.3 × 10^7
Potassium alkyl phosphate	35	23.6	0.39	0.51	0.15	0.09	2.6 × 10^7

[a] Data of J. Earnshaw, D. Greaves and D.G. Duncan (Technical Bulletin, ICI Organics Division, Manchester, UK).

Obetz [19] has also reported the thermal properties of a number of spin finish formulations. It may be seen that more thermally stable lubricants such as high molecular weight esters and complex esters capped with alkyl aryl (POE) ethers may be used in combination with *trans*-esters and/or neutralized phosphate esters to give a low, scourable residue.

7.7.2 SPIN FINISHES FOR WEAVING AND KNITTING

Finish requirements for filament yarns used in weaving and knitting are largely met with current technology, except perhaps in the case of water jet loom weaving. However, efforts at fine tuning continue in order to obtain still better lubricants or finish components. Desirable properties of the finish are:

- provision of low F/M dynamic friction;
- compatibility with any kind of size and conditions of weaving;
- low viscosity oils to reduce the friction and tension on high speed warping (draw-warping) and knitting process;
- compatibility with water in water jet looms.

It is worth pointing out that unwinding tension is also related to the kind of finish used. In the case of sheeting fabrics which are heat-set without scouring, lubricant or coning oil should be stable to heat up to temperatures of 190–200 °C.

7.7.3 SPIN FINISHES FOR NYLON AND POLYESTER TYRE CORDS

The main process development in the manufacture of tyre cords has been the continuous high speed spin–draw process. Here temperatures as high as 240 °C are used, hence a low volatility of the spin finish and low deposition on hot rollers are essential. The finish should not show more than 5–10% loss during processing. In addition, the finish must not affect the adhesion to rubber and at the same time should be compatible with the adhesion activators used to treat the yarns.

A number of formulations by various firms have been disclosed in patent literature [2]. In 1966, Du Pont (USA) disclosed the use of glycerol triacetate, glycerol trioleates and coconut oil with emulsifier for use on nylon tyre cords. Monsanto (USA) in 1967 cited the use of polyvinyl alcohol, vegetable, marine and petroleum oils as well as polyalkylene glycols and many kinds of esters, particularly fatty acid esters of mixed triglycerides, for increasing the tensile strength, abrasion resistance, durability and flex life of nylon tyre cord. Drew Chemical Corporation (USA) in 1969 recommended the use of high smoke point trimethylol alkane esters to provide good fibre/metal lubricity and resistance to

oxidation. In 1972, Allied Chemical (USA) was granted a patent using a high melting wax to obtain greater strength in plied yarns used for tyre cord. The wax is prepared by reacting monocarboxylic acid with a polyhydroxy alcohol. Sanya Chemical Ltd (Japan) claimed the use of biphenyl derivative to produce heat-resistant nylon tyre cords with good adhesion to rubber, in place of a lubricant containing oleyl oleate.

In another patent (US Patent 4 086 949), the use of a finish containing diundecyl phthalate, polymethyl vinyl ether and magnesium stearate (90:8:2) gave good adhesion as compared with the conventional coconut-based coating. Firestone Tire Co. (USA) has claimed the use of non-aqueous spin finish formulations for producing high tenacity ($10\,\mathrm{gf\,den^{-1}}$) nylon 6 tyre cord yarn in low humidity (45% RH) environments. The spin finish applied was a solution comprising 85% of a deodorized kerosene and 15% of Textolene 4018$^{\mathrm{TM}}$ (an anionic tyre cord oil manufactured by Sonneborn Chemical Co.).

Koenig [36] has also emphasized the use of thermally stable spin finishes because the calendering and heat-setting of the fabric occurs at temperatures between 180 and 260 °C. He claims the most widely used lubricants for tyre cord are isohexyldecyl stearate and trimethylol-propane trispelargonate due to their favourable viscosity/frictional properties. Moreover, non-uniform spin finish application can cause friction variation among the filaments which would result in non-uniformity of tyre yarn processing [37].

7.8 INFLUENCE OF SPIN FINISH ON DYEING OF YARN/FABRIC

If the spin finish has not been completely removed from the yarn prior to dyeing, it will form an emulsion in the acid or cationic dye bath during dyeing of nylon and acrylic fibres, leading to uneven dyeing. The presence of spin finish also influences the thermal migration of dyes. Thermal migration involves the desorption of the dye from the dyed fibre and its transference to the fibre surface. During heat-setting the dispersed dye therefore migrates from the polyester fibre to its surface, which affects the shade and can result in staining of adjacent material in subsequent thermal treatment such as ironing. It can also cause reduced rubbing, dry cleaning, wet and light fastness.

7.9 ANALYSIS OF SPIN FINISH FORMULATIONS

7.9.1 SOLID CONTENT

The solid content is determined by evaporating the spin finish sample at 100–110 °C in an air oven for about 2 h.

7.9.2 VOLATILITY

To determine the volatility a 5 g sample is exposed in a 5 cm internal diameter weighing dish in a ventilated oven at 200 °C for 2 h. The loss in weight per unit area of exposed surface is related to the volatility of a given spin finish.

7.9.3 SURFACE TENSION

The critical surface tension of the lubricant should be less than that of the fibre in order to achieve uniform wetting and distribution on the fibre surface.

Surface tension can be measured using a Fisher Auto-tensiomat. In this device, a pre-cleaned platinum–iridium ring of known dimensions is suspended from the arm of a balance and immersed in the spin finish sample medium. The sample is held in a jacketed glass vessel which is on a motor-driven platform elevator. For surface tension measurement, the platform elevator is simply lowered at a controlled and constant rate of descent. As the platinum–iridium ring is withdrawn from the sample and breaks the liquid surface, a force proportional to the surface tension is exerted on the balance beam. During the measurement, the transducer provides a force–displacement signal which is proportional to the force or weight measured:

$$F = ma$$

and

$$\text{surface tension, } \gamma = F/2L = ma/2L$$

where m is the mass of the sample (g), a is the acceleration due to gravity and $2L$ is twice the ring circumference (cm).

In this manner, surface tension values of spin finish solutions at various concentrations can be measured. For good wetting properties, non-ionic and special anionic surfactants are preferred in the spin finish formulations for the spinning of POY-PES. Sometimes spin finish solutions of surface tension less than $30 \, \text{mN} \, \text{m}^{-1}$ are recommended, as this will provide a uniform coating of spin finish onto the filaments in a very short contact time of 0.0001 s during finish application at high speed spinning.

Surface tension values of various surfactants in water (0.1% aqueous solution) are given in Table 7.3 [29].

7.9.4 VISCOSITY MEASUREMENT

Viscosity can be measured by a Farranti portable viscometer, or by a Saybott or Angular viscometer. It is also important to know the change in viscosity with concentration at different temperatures.

Table 7.3 Surface tension in water (0.1% aqueous solution) of various surfactants [29]

Agent	Surface tension ($mN\,m^{-1}$)
Non-ionic	30–40
Anionic	28–33
Cationic	33–45
Fluorochemical	20–25
Silicone	25–32

7.9.5 AGEING STABILITY

A finish should have a low iodine number so as to have better ageing stability. This can be determined quantitatively by chemical analysis.

7.9.6 FINISH LEVEL MEASUREMENT ON THE YARN

Several methods [38–40] are available to measure the finish content applied to the fibres, some of which are discussed below.

(a) Soxhlet method

The Soxhlet method has been in use for quite some time. It requires a large sample size (~10 g) of fibre/yarn which is placed in a funnel. Solvent is then added and the funnel agitated for 3–5 min to ensure complete removal of the finish from the yarn. The finish dissolved in the solvent is weighed after removing the solvent through evaporation. Finish add-on is then calculated by dividing the weight of the finish by the weight of the yarn.

The solvent for the extraction of spin finish from the yarn must be chosen carefully to ensure that the finish is completely soluble in the cold solvent, and the solvent must not solubilize fibre oligomers. Solvents recommended for the extraction of spin finish from polyester, nylon and polypropylene are listed in Table 7.4.

Table 7.4 Selection of optimum extraction solvents [11]

Solvent	Polarity	Polyester	Polyamide	Polypropylene
Water	Polar			×
Methanol	Polar	×		×
Isopropanol	Polar	×		
Petroleum ether	Non-polar		×	
1,1,1-Trichloroethane	Non-polar	×	×	×
Dichlorodifluoroethane	Non-polar	×	×	×
Cyclohexane	Non-polar	×	×	×

In the Wool Industry's Research Association (WIRA) rapid extraction apparatus, 2 g of the finished fibre/yarn is weighed out precisely. The textile material is pressed into a tube with a stamp, and then about 10 ml of an easily volatile solvent, for example dichloromethane, is poured into the tube. The solvent penetrates the sample and the extract drops out of the tube into an aluminium vessel which is fixed onto a temperature-controlled heating plate. The weight increase of the aluminium vessel corresponds to the spin finish extracted from the sample. For occasional tests, a Soxhlet extraction followed by gravimetric measurement is recommended. A correction for oligomer content based on UV spectrophotometric measurements may be made. Routine testing is more conveniently carried out photometrically after the spin finish has been stained blue in a thiocyanate/cobalt nitrate mixture in toluene.

(b) Automated solvent method

As reported by Honeycutt [40], the finish level can be determined through rapid automated infrared (IR) analysis. A small amount of the fibre or yarn (1 g) is placed in a container and a known volume of the solvent is added. After agitating the container, finish is extracted from the sample and the solvent/finish solution is then loaded into an IR cell. Infrared absorbance is determined at a constant wavelength. The percent finish can be calculated from a calibration curve (Fig. 7.10).

The operation is simplified with the automated IR analyser. In this system, the yarn sample is placed on an integrated balance for automatic weighing. The instrument automatically fills the cup with solvent, agitates and pumps the solvent/finish to an IR analyser for absorbance detection.

(c) Non-solvent reflectance method

Near-infrared reflectance analysis (NIRA) is another technique used for measuring the finish level on the fibre without the use of solvents.
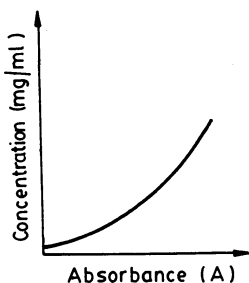
Fig. 7.10 Calibration curve for the infrared (IR) analysis of spin finish of known concentration [40].
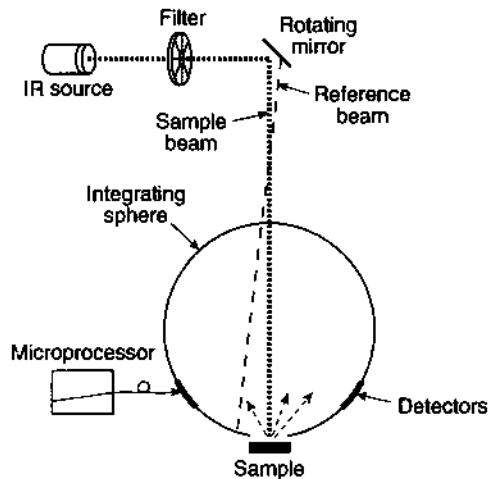
Fig. 7.11 A near-infrared reflectance analyser [40].

When light strikes a yarn/fibre sample, some of the light is absorbed and the rest is reflected. The percentage of light absorbed varies according to the chemical nature of the yarn and the finish. By comparing the intensity of the original light with that of the reflected light it is possible to determine the finish level on the yarn. For this purpose, a series of standard samples of yarns with different levels of finish are scanned by the instrument to find a correlation between the standard sample and the sample under test.

As shown in Fig. 7.11, an IR source is directed onto a sample. Reflected light (carrying information about the sample) is collected by an integrating sphere and measured with a pair of detectors. A microprocessor calculates absorbance, generates absorbance vs. wavelength plots and determines the level of finish on the unknown samples.

(d) Labelling of spin finish with radioactive tracer

When the spin finish is labelled with a radioactive tracer, it is then possible to follow the deposition with the help of a Geiger counter or indirectly from contact photography of the yarn.

(e) X-ray photoelectron spectroscopy

X-ray photoelectron spectroscopy (XPS) can be used to give a picture of the surface deposition of spin finish.

(f) Ultraviolet illumination

Uniformity of the finish applied along the length of top, roving or yarn can also be determined by scanning the sample using UV illumination if the spin finish component/formulation is visible in UV light. Sometimes UV illumination may reveal very long-term irregularity of spin finish deposition or coating. Analog Devices (USA) have developed the portable M803 tester for measuring the spin finish on running yarn.

7.9.7 DISTRIBUTION OF FINISH ON THE SURFACE OF FILAMENT YARN

In high speed spinning, the deposition of spin finish on the rapidly moving yarns occurs during extremely short contact times. The distribution of the finish along the length of the filament yarn influences significantly the frictional properties of the yarn and other specific functions of the finish in subsequent mechanical processing.

Textile Research Institute, Princeton, USA, has developed the following techniques for determining the distribution of finishes along the length of the filament [42, 43].

(a) Surface wettability scanning

This technique has been extremely useful in studying the distribution of surface finishes on continuous filament yarns. The experimental arrangement for wettability scanning by the liquid membrane method is shown in Fig. 7.12 along with a vector analysis of the forces exerted by the liquid meniscus on the solid surface:

$$F = P\gamma_{LV}(\cos\theta_a - \cos\theta_r)$$

where P is the fibre perimeter, γ_{LV} is the membrane liquid surface tension, and θ_a and θ_r are the advancing and receding contact angles, respectively.

A stainless steel ring 5–10 mm in diameter is mounted on a stage that can be moved up or down at a given speed by a rack and pinion arrangement. A filament about 300 mm long is mounted on the recording microbalance with hooks at each end.

The specimen is taken through the ring, and an appropriate weight is mounted on the lower hook. After preparing the mounted specimen, liquid is carefully introduced into the ring so as to form a film or a membrane within its perimeter. The force exerted by the liquid membrane on the filament is then recorded continuously as the ring with the liquid membrane moves up or down the filament. The force recorded by the electrobalance is thus a function of both the advancing and receding wetting forces.
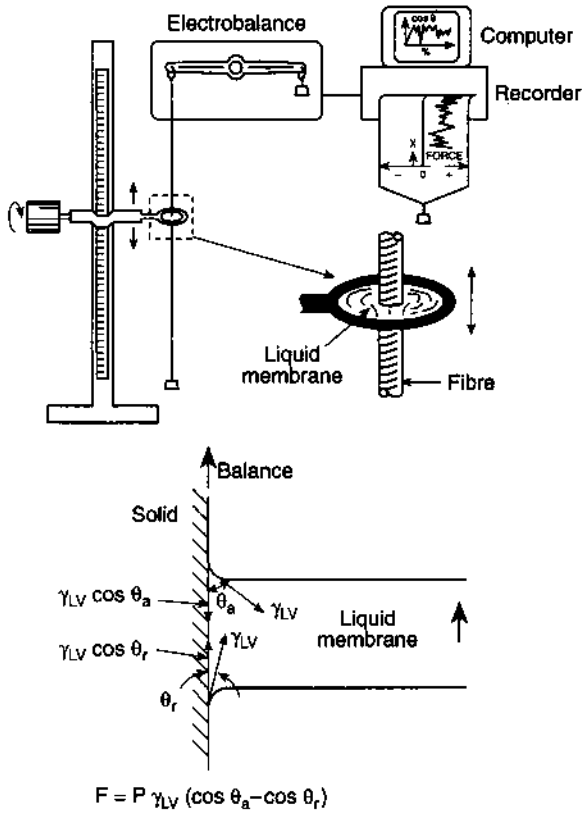
Fig. 7.12 The liquid membrane method of analysing spin finish content [42].

Taking $\cos\theta_r$ as a constant, $\cos\theta_a$ values are calculated and plotted as a function of distance along the filament. Such a plot can be used as a measure of the distribution of the finish along a filament. The data can also be used to determine the surface coverage parameter. Figure 7.13 illustrates the surface coverage and cumulative distribution on a PET sample containing 0.15% spin finish. With such a low percentage of spin finish, the average surface coverage is nearly 75%; saturation coverage is attained with 1% spin finish.

(b) Microfluorimetry [43]

Another method of analysing finish distribution is to preferentially stain the spin finish coated filaments with fluorescent tracers, or the tracer can be included in the finish formulation. Ultraviolet excitation and reflectance scanning are then used to determine the distribution of the tracer, and therefore of the finishing agent, along the length of the filament.
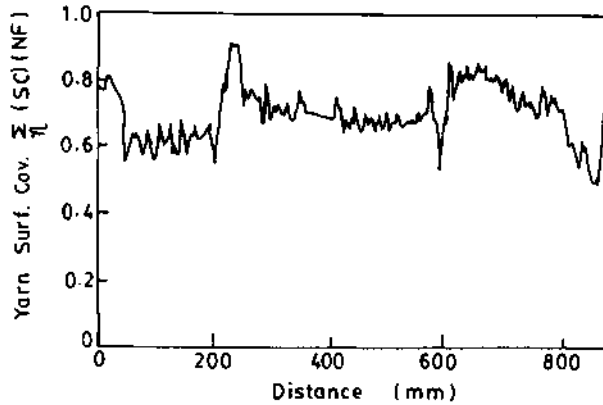
Fig. 7.13 The distribution of spin finish on PET yarn containing 0.15% finish [42].

Only small amounts of fluorescing tracer are required to provide high sensitivity in longitudinal scanning. In addition to giving the longitudinal distribution of the spin finish, this technique provides information about the spreading behaviour of finishes on both single and multifilament yarns.

(c) Capacitance sensor technique

Rossa [41] has suggested a method for on-line measurement of spin finish application and distribution on polyester yarn using a capacitive sensor system. The total dielectric comprises polyester and active agent. Non-uniform distribution of spin finish film appears to be caused mainly by the dynamics of the spinning process.

7.10 PROBLEMS ENCOUNTERED IN FINISH APPLICATION

Some of the problems which may be encountered when using spin finishes are summarized below.

7.10.1 BACTERIAL GROWTH/MICROBIAL CONTAMINATION OF SPIN FINISH EMULSION

Finish emulsions are highly susceptible to bacterial attack. Therefore, a bactericide should be added to control bacteria in the fibre production plant as well as on the yarns. Bacterial attack on the spin finish causes emulsion breakdown and gel formation, which can lead to clogged lines and poor finish uniformity on the filament yarn.

Tris(oxymethyl)hexahydrotriazine and/or sodium salts of pyridenethiol oxide are suggested as preservatives for spin finishes. Various

methods for controlling the microorganisms in spin finish systems have been discussed by Harrill [44]. Schenick [45] has also suggested the use of hydroxymethylamino alcohols, chlorinated azoniaadamantane and dimethyltetrahydrothiadiazine thione (0.1–0.3% of the weight of the spin finish) as bactericides.

7.10.2 DISPOSAL OF SPIN FINISH WASTE

At the completion of processing, fibres are scoured with detergents to remove the spin finish. The resulting waste water may contain 1.0–1.5% oil which must be disposed of. A typical synthetic fibre plant may produce from 5000 to 15 000 gallons per day of this waste.

Attempts to treat spin finish waste in activated sludge systems have met with a serious problem of foaming and low organic removal efficiencies. The COD to BOD (chemical oxygen demand to biological oxygen demand) ratio is quite high, i.e. 3.0–4.0, indicating very poor biodegradability. Hence, spin finish waste should be kept segregated from other plant waste streams and treated by physical and chemical means. Alley [46] has recommended the concentration of spin finish waste by a combination of ultrafiltration or reverse osmosis and evaporation to an oil content that will permit final disposal by incineration. The challenges involved in improving fibre finishes, including their biodegradability, have been discussed by Ross [47].

REFERENCES

1. Schick, M.J. (1975) Friction and lubrication of synthetic fibers, *in* Fiber Science Series Vol. 7, *Surface Characterization of Fibers and Textiles*, Part I (ed. M.J. Schick), Marcel Dekker, New York.
2. Redston, J.P., Bernholz, W.F. and Schlatter, C. (1973) *Textile Res. J.*, 4, 325.
3. McGregor, T.R. (1979) *Textile Res. J.*, 49, 485.
4. Postman, W. (1980) *Textile Res. J.*, 50, 444.
5. Vaidya, A.A. (1982) *Synthetic Fibers*, 11(4), 7.
6. Kleber, R. (1984) *Chemiefasern Textilindustrie*, 34/86, 412(E55).
7. Lee, D.E. (1991) *Int. Fiber J.*, 6(4), 94.
8. Vaidya, A.A., Rao, B.V. and Devnath, K.K. (1985) *Synthetic Fibers*, 14(3), 1.
9. Billica, H.R. (1984) *Fiber Producer*, April, p. 21.
10. Bajaj, P. and Katre, R.A. (1987) *Colourage*, 34, November, p. 16.
11. Crossfield, R.J. (1990) *Int. Fiber J.*, 5, October, p. 4.
12. Nevrekar, N.B. and Palan, H.B. (1990) *Man-made Textile in India*, September, p. 315; *Part II*, March 1991, p. 111.
13. Olsen, J.S. (1969) *Textile Res. J.*, 39(1), 31.
14. Rangaswamy, R.S., Kothari, V.K. and Sengupta, A.K. (1988) *Inst. Eng. J. Textile Eng.*, 69, 42.
15. Bowden, F.P. and Tabor, D. (1964) *The Friction and Lubrication of Solids*, Part I, Oxford University Press, London.

16. de Jong, H.G. (1993) *Textile Res. J.*, **63**(1), 14.
17. Schick, M.J. (1974) *Textile Res. J.*, **44**, 758.
18. Daefler, P. (1987) Spin finish influence on high speed spinning/processing of synthetic fibers. *Proceedings of the 2nd International Conference on Man-made Fibers*, 26–29 November, Beijing, China.
19. Obetz, J.E. (1978) *Fiber Producer*, October, p. 10.
20. Schubert, G. (1980) *Melliand Textilber* (Eng. ed.), **12/80**, 1516.
21. Fourne, F. (1979) *Chemiefasern Textilindustrie*, **29/81**, 838/E113.
22. Savage, P.R. (1978) *America's Textile Rep.*, **7**(8), 50.
23. Riggert, K. (1977) *Chemiefasern Textilindustrie*, **27/79**, 1084.
24. Mahajan, S.D. and Nadkarni, J.Y. (1984) *J. Textile Assoc.*, **45**(6), 205.
25. Sinha, T.B. (1977) *Indian Textile J.*, **88**(12), 121.
26. Schick, M.J. (1980) *Textile Res. J.*, **50**(11), 675; *Idem.* (1974) *ibid.* **44**, 758.
27. Anon. (1978) New finishes, *Res. Discl.* No. 69, Abstr. No. 16907.
28. Anon. (1978) New finishes, *Res. Discl.* No. 173, Abstr. No. 17309.
29. Schulberger, A. (1990) *Indian Textile J.*, November, p. 62.
30. Selivansky, D., Walsh, W.K. and Frushour, B.G. (1990) *Textile Res. TAPPI J.*, **60**, 33.
31. Herlinger, H., Koch, W. and Buhler-Neiens, G. (1987) *Translation of TAPPI*, **5**, 529.
32. Dafler, P. (1978) *Chemiefasern Textilindustrie*, **28/80**, May, p. E80–82.
33. Schulberger, A. (1990) *Man-made Fiber Year Book*, Chemiefasern Textilindustrie, Frankfurt, p. 70.
34. Earnshaw, J., Greaves, D. and Duncan, D.G. (1975) *Fiber Finishes for False Twist Textured Yarn*. Technical Bulletin, ICI Manchester, p. 74.
35. Knowlton, R.C., Pierce, N.C. and Popper, P. (1978) *Fiber Producer*, **6**(8), 18.
36. Koenig, H.S. (1985) *Chemiefasern Textilindustrie*, **35/87**, E89.
37. Perkin, W.G. (1988) *Int. Fiber J.*, **3**, 38.
38. Schutz, R.A. (1976) *Spin Finishes, Properties, Characteristics and Effects on Textile Processing*, Shirley Publication, Manchester, UK, **S24**, p. 15.
39. Bogatzki, B.F., Marth, J. and Falk, I. (1980) *Textiltechnik (Ger)*, **30**, 61.
40. Honeycutt, M. (1990) *Int. Fiber J.*, **5**, 52.
41. Rossa, R. (1992) *Melliand Textilber*, **73**, 692/E315.
42. Kamath, Y.K., Dansizer, C.J., Hornby, S. and Weighmann, H.D. (1991) *J. Appl. Polym. Sci., Appl. Polym. Symp.*, **47**, 281.
43. Kamath, Y.K., Ruetsch, S.B. and Weigmann, H.D. (1993) *Textile Res. J.*, **63**(1), 19.
44. Harrill, T.G. (1990) *Int. Fiber J.*, **5**, 35.
45. Schenick, J.H. (1990) *Int. Fiber J.*, **5**, 51.
46. Alley, F.C. (1990) *Int. Fiber J.*, **5**, 44.
47. Ross, S.E. (1993) *Int. Fiber J.*, **8**, 78.

Drawing of melt-spun fibres

8

A.K. Sengupta

8.1 INTRODUCTION

The drawing or orientation stretching process is a vital post-spinning operation for a melt-spun fibre. An undrawn fibre deforms inelastically under low loads and has a poor stress value. Such a material has very little utility for most textile applications. Through the drawing operation the fibre is orientationally strengthened due to alignment of the molecular chains along the fibre axis and shows enhanced recovery. Drawing also induces changes in the levels of crystallinity and sometimes in the crystalline form. Both semicrystalline fibres with a lamellar morphology in the undrawn state and amorphous fibres with an entangled network of molecular chains are transformed into a fibrillar structure through the process of drawing. An increase in draw ratio increases the orientational order as well as conformational conversions, resulting in a structure which has much higher strength, modulus and dimensional stability compared with its undrawn state.

The extent to which a fibre can be drawn is dependent, amongst other things, on the spinning speeds employed in the extrusion of the fibre. It is well known that an increase in spinning speed increases the orientation of the molecular chains along the fibre axis as a consequence of which the residual draw ratio of the fibre reduces with the increase in spinning speed. Figure 8.1 shows the residual draw ratios for some fibres in relation to their spinning speeds. The drawing methodologies also vary depending on spinning speeds and end use applications.
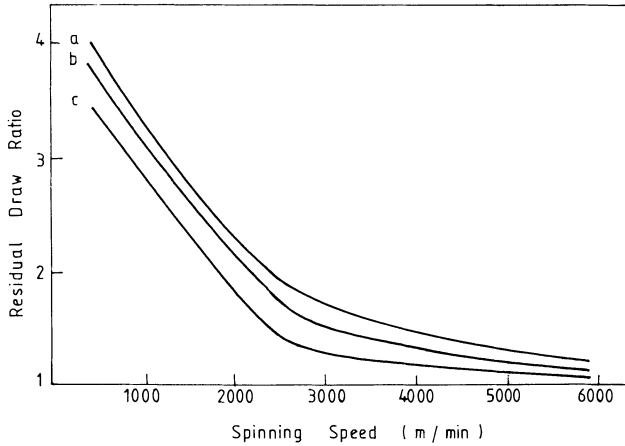
Fig. 8.1 Influence of spinning speed on draw ratio for (a) PET, (b) nylon 66, (c) nylon 6.

Fibres spun above $6000\,\mathrm{m\,min^{-1}}$ (fully oriented yarn or FOY) can be used directly without the need for drawing for some special end uses while for the high speed spun yarns (highly oriented yarn or HOY) spun between 4000 and $6000\,\mathrm{m\,min^{-1}}$, the drawing operation is generally integrated with spinning. Medium speed yarns (partially oriented yarn or POY) produced at spinning speeds between 1500 and $4000\,\mathrm{m\,min^{-1}}$ are either draw-twisted, draw-textured or the drawing operation is integrated with spinning. Yarns produced using low speed spinning (LOY) between 500 and $1500\,\mathrm{m\,min^{-1}}$ are generally draw-twisted.

The conditions under which drawing takes place are of paramount importance to the properties and end uses of the drawn yarn. Small changes in the drawing parameters can often have significant effects on the characteristics of the drawn yarn.

8.2 THE DRAWING UNIT

The undrawn fibre is stretched to several times its original length on a draw twister, a schematic diagram of which is shown in Fig. 8.2. A draw twister has two sections: first, the drawing section where the melt-spun yarn is stretched and, second, the packaging section which is similar to a ring twisting assembly, where a nominal twist of about 8 to 15 turns $\mathrm{m^{-1}}$ is inserted into the yarn during the course of winding. The drawing unit essentially consists of two sets of rollers, the feed and the draw rollers, which have different circumferential speeds, the ratio of which determines the machine draw ratio. The actual draw ratio is somewhat lower than the machine draw ratio as the drawn yarn undergoes some
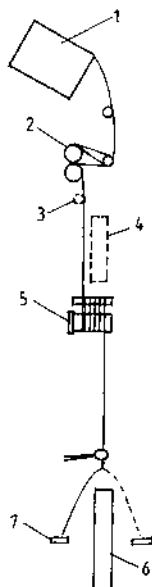
Fig. 8.2 A draw twister unit: (1) undrawn yarn, (2) feed rollers, (3) snubbing pin, (4) heater plate, (5) draw rollers, (6) bobbin of drawn yarn, (7) ring holder.

relaxation between the drawing and the packaging section. Yarns are both hot and cold drawn. Nylon can be drawn at room temperature while polyester needs to be drawn at a temperature above the fibre's second-order transition temperature, generally around 90 °C. In the case of high tenacity, low stretch yarns, heat-stabilizing treatment is given to reduce shrinkage. This is achieved by the provision of a heater plate in the draw zone. Frequently, a snubber pin is introduced in the draw zone around which the yarn is wrapped before its passage to the draw roller. The snubbing pin stabilizes the deformation or the necking point and also acts as a tension barrier so that the full drawing tension is not transmitted to the feed roller nip.

8.3 THE DRAWING BEHAVIOUR OF THERMOPLASTIC POLYMERS

8.3.1 THE NATURE OF THE LOAD–EXTENSION BEHAVIOUR

The undrawn polymer can be extended to several times its original length when a suitable stretching force is applied. This high extension is, however, not elastic and recoverable but irrecoverable and inelastic; the stretched polymer does not return to its original length when the stretching force is removed.
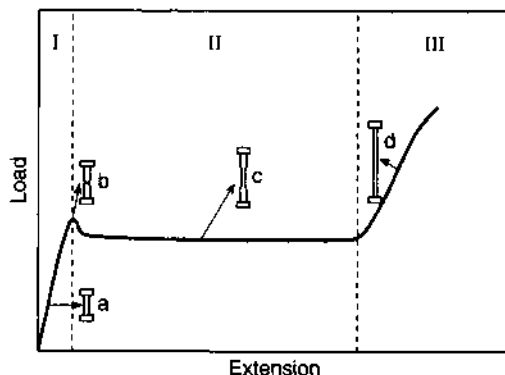
Fig. 8.3 Load–extension behaviour of an undrawn fibre at room temperature.

The load–extension curve of an undrawn fibre at room temperature is shown in Fig. 8.3, which may be divided into three regions. In the first region (region I), the load–extension relationship is approximately linear and the deformation is more or less reversible. The load then reaches a maximum and falls slightly. The extension at which the maximum occurs is called the yield strain and the corresponding stress value is known as the yield stress. Following the yield stress the fibre deforms plastically (region II) under constant load conditions. In this region, in which cold drawing takes place, the sample first yields with the appearance of a neck and thereafter the neck propagates through the sample; the deformation is not recoverable. As the final breaking point is approached (region III), the stress rises sharply with a small increment in strain signifying strain hardening before catastrophic failure occurs. The dimensional changes that occur in a polymer strip in these regions are also schematically illustrated in Fig. 8.3. In region I, up to the yield point, the extension is uniform along the length of the specimen (as in a). At the yield point, a constriction or a neck appears at a particular point (as in b). In region II, the material draws through a neck and the reduced cross-sectional area spreads through the neck (as in c) through the whole length of the specimen. In region III, the whole strip thins down to a still more reduced but uniform cross-sectional area (as in d). Further drawing leads to rupture of the specimen.

8.3.2 THE MECHANISM OF DRAWING THROUGH A NECK

The appearance of a neck is generally associated with non-uniformity in the stress distribution during tensile deformation. When a fibre is drawn, some portion of it will be under higher stress than the remainder, either due to its cross-sectional area being less or due to other causes which

lead to stress concentration. In region I of Fig. 8.3 the stress–strain curve is steep and small differences in stress here will not make the strain level in the weaker portion much different from that in the remainder. At the yield point, however, small differences in stress values will produce large differences in strain and hence the thin portion will start getting thinner. A neck will appear and the material will start drawing through the neck. If the thinning process is not arrested the material will fail and no drawing will be possible. Thus, for drawing through a neck, it is essential that as soon as the neck is formed, the thin portion must strain harden to a constant diameter. According to Vincent [1], neck formation is caused by mechanical instability occasioned by strain softening, and cold drawing or drawing through a neck is accomplished by stabilization of the neck through strain hardening resulting from molecular orientation. Cold drawing is prevented by insufficient strain hardening, which may be caused by high stretching rates, giving adiabatic heating, or by low molecular weight.

A case of drawing instability associated with adiabatic heating condition is illustrated in Fig. 8.4. As hydrogen has a higher thermal conductivity than air, the heat evolved during stretching is dissipated so rapidly that the drawing process is arrested and has to be reinitiated. The more or less isothermal heating conditions in air do not lead to disruption of the drawing process while the loss of heat in hydrogen is so large that the drawing process is repeatedly brought to a halt.

In the case of drawing a low molecular weight polymer there would be a greater proportion of chain slippage and hence less orientation. This would reduce the strain hardening, leading to a failure to stabilize the neck.
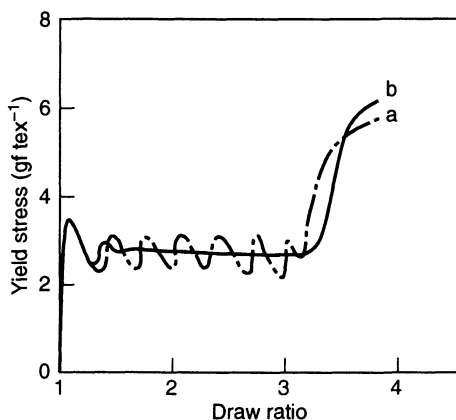
Fig. 8.4 Stress–strain curves of polyester filaments of 50 mm length (a) in hydrogen and (b) in air. Drawing temperature 20 °C, drawing speed 500 mm min^{-1} [2].

8.3.3 THE NECKING BEHAVIOUR OF POLY(ETHYLENE TEREPHTHALATE)

On extension PET necks down to a smaller cross-section at some point. The length then increases as the shoulders of the neck move apart at constant load. Thompson [3] observed that when amorphous PET is deformed above the glass transition temperature two deformation regions may be distinguished. In one region, occurring at high strain rates, necking and high stresses occur. Deformation in this region is accompanied by the formation of a high degree of crystallinity and molecular orientation. This region is referred to as the stress-induced crystallization region. The second deformation region, called the flow deformation region, is characterized by a low deformation stress with little crystallization and molecular orientation. Several researchers have observed that a significant degree of crystallization occurs when the material is deformed through a neck.

A detailed study [4] of the influence of strain rate on the deformation behaviour of amorphous PET showed that when the latter is strained above T_g two deformation regions occur, namely the flow deformation and stress-induced crystallization regions (Fig. 8.5). The percentage crystallinity in the as-deformed PET is very small and is relatively insensitive to the strain rate during flow deformation but tends to increase rapidly with strain rate in the stress-induced crystallization region. Thus, little crystallinity and orientation are produced under the low drawing stress which occurs in the flow deformation region, while higher strain rates produce necking, crystallization and a high degree of orientation in the stress-induced crystallization region. Stress-induced crystallization occurs only when the strain rate is sufficient to generate a critical stress value; the effect of temperature is secondary in that an increase in
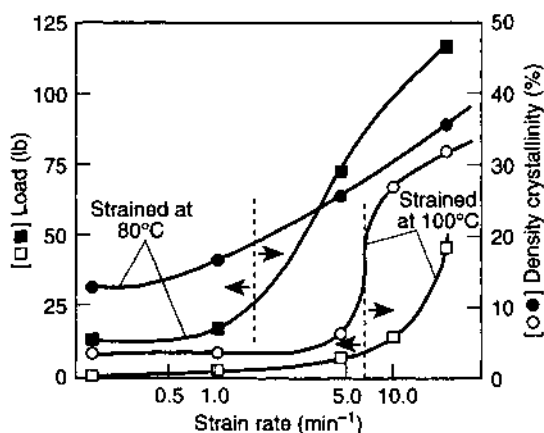
Fig. 8.5 Stress-induced crystallization and flow deformation regions [4].

temperature increases molecular mobility and hence requires a higher strain rate to arrive at the critical stress value needed for stress-induced crystallization to occur, as shown in Fig. 8.5. It has been shown [5] that the degree of orientation of the PET precursor also plays an important role in that while PET LOY shows flow-drawing at 90 °C in water and 120 °C in air at a strain rate of 2–50 min^{-1}, the POY sample has the necessary initial rigidity to sustain the stress and does not show flow-drawing.

The above studies reveal that the drawing of PET proceeds through necking and stress-induced crystallization occurs by drawing through a neck. It has, however, been observed that the sharpness of the neck as described by the neck angle is influenced by the drawing conditions; this in turn determines the structure and properties of the drawn filament. Kobayashi [6] varied the neck angle by varying the drawing conditions, such as preheater temperature, hot pin temperature, draw ratio, feed speed, etc. He observed that an increase in the necking angle is associated with an increase in the threadline tension and the necking draw ratio increases with the increase in necking angle. An increase in the necking angle increases the molecular orientation as shown by birefringence studies. An increase in the necking draw ratio is accompanied with an increase in the crystallinity of the drawn sample as observed from the density values. Kobayashi's results indicate that drawing through a sharp neck angle is more favourable as it induces higher molecular orientation as well as crystallinity. However, such drawing with a sharp neck may lead to an unstable process. Hence the normal industrial practice is to use a temperature sufficiently high for adequate molecular mobility. For amorphous polymers this is conventionally above the glass transition temperature T_g, while for crystalline polymers it is in the range of the crystalline α phase relaxation so that the molecular chains can move through the crystalline regions [7].

8.3.4 NECK DRAWING OF NYLON 6

In contrast to PET, which is amorphous in the as-spun state, nylon 6 is crystalline. It is, however, important to remember that the crystallinity of nylon 6 develops after spinning, possibly on the bobbin, after moisture pick-up. Thus humidity plays an important role in both the drawing and storage behaviour of nylon 6. Like polyester, nylon also draws through a neck.

The behaviour of nylon 6 in cold drawing under industrial drawing conditions was studied by Fujimoto et al. [8]. The speed distribution in the running filament for two different drawing speeds is shown in Fig. 8.6. When drawing is done at a faster speed, the equilibrium point at which the filament speed coincides with the drawing speed shifts
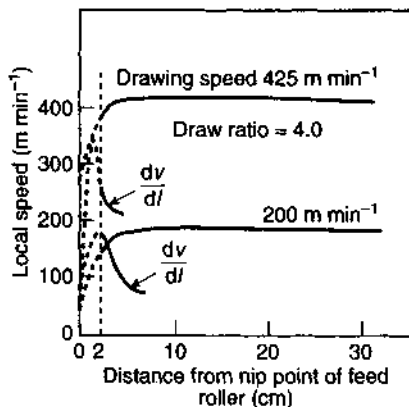
Fig. 8.6 Speed distribution of running filament with different drawing speeds [8].

towards the nip point. The equilibrium point is about 3.5 cm from the nip point at 425 m min^{-1} and at about 5.0 cm from it at 200 m min^{-1}.

Judging from the results in the literature, it appears that the necking angle may be sharper when the drawing speed is faster.

In Fig. 8.7, a schematic illustration of the development of molecular orientation during drawing is presented. It may be observed that while the crystallite orientation gradually rises to a constant value in the vicinity of the draw roller, the amorphous orientation rises sharply up to the necking point and then stress relaxes gradually to a low value on
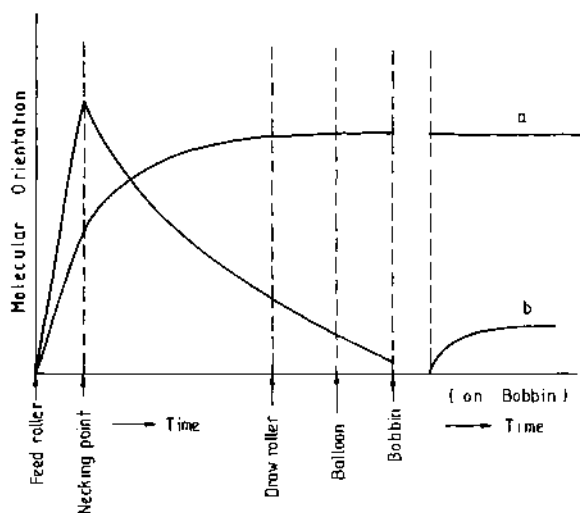
Fig. 8.7 Schematic illustration of molecular orientation during drawing. (a) Crystallite orientation, (b) amorphous orientation [8].
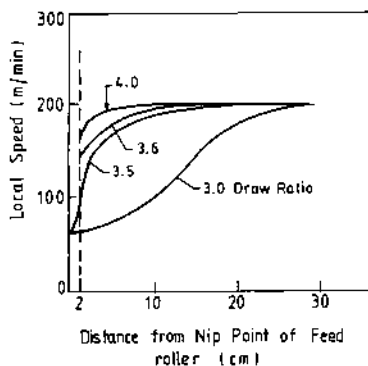
Fig. 8.8 Speed distribution for a running filament drawn at 200 m min^{-1} with different draw ratios [8].

the bobbin. It rises again when stored on the bobbin but the final value is considerably lower than that observed at the necking point.

Figure 8.8 shows the shifting of necking point with draw ratio at a constant drawing speed of 200 m min^{-1}. It can be seen that the necking point travels closer to the feed roller as the draw ratio increases.

8.4 INFLUENCE OF DRAWING ON STRUCTURE AND PROPERTIES OF FIBRES

Orientation stretching is one of the basic methods of increasing the strength of polymeric fibres and films. The properties of nylon 6 yarn as function of draw ratio are presented in Table 8.1 [9].

Similar behaviour has been reported for other fibres. It should, however, be emphasized that orientation stretching of a polymer entails complex processes, a decisive part in the realization of which is played by the rotational isomeric conversion in the macromolecule chains of the structurally heterogeneous regions of the polymer. An increase in draw ratio results not only in an improvement in the orientational order and conformational conversions, but also in an accumulation of irreversible

Table 8.1 Some properties of nylon 6 yarn [9]

Draw ratio	Denier	Tenacity (gf den^{-1})	Breaking elongation (%)	Elastic modulus (kgf mm^{-2})
1:3.2	17.5	4.8	62	14
1:3.5	15.8	5.3	41	23
1:3.9	14.8	5.7	30	34
1:4.2	13.5	6.5	22	39

discontinuities in the molecular chain of the polymer. It is clear that the competition between the various processes ultimately determines the strength of the polymeric material.

8.4.1 DRAWING-INDUCED STRUCTURAL CHANGES

Crystallizable amorphous fibres develop crystallinity during drawing through stress-induced crystallization. A fibre which is initially crystalline or semicrystalline produces orientation of crystallites and of molecules in the non-crystalline portions of the sample. Sometimes there is formation of new crystals or destruction of existing ones, and occasionally a change in crystal habit. Drawing encourages the formation of bundle-like crystals which consist of extended molecules in a parallel array and in the process some unfolding of the folded chains in crystalline regions of the starting sample may occur.

The influence of draw ratio on crystallinity for polypropylene fibre is presented in Fig. 8.9 [10]. It can be seen that crystallinity increases initially with increasing stretch ratio and then tends to peak at around a draw ratio of 2; above this level the crystallinity shows a significant decrease. The amorphous layer thickness, however, continues to rise, though at a reduced rate.

For a cast PET film of low crystallinity it was observed [11] that, after an initial rise, the crystallinity remained constant with further increase in drawing. The initial rise was attributed to stress-induced crystallization. With a highly crystalline PET film, however, the crystallinity was found to decrease initially with draw ratio and then remained constant.

With nylon 6, Urbanczyk [12] reported an initial decrease followed by a rise in crystallinity as the draw ratio was increased. The change in crystallinity was not very high and reached a maximum increase of 20–25% compared with the undrawn fibre. In another study of drawing behaviour of nylon 6 produced with varying spin draw ratio (SDR), it
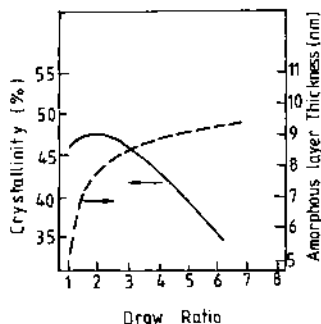
Fig. 8.9 Effect of draw ratio on per cent crystallinity (X-ray) of polypropylene [10].
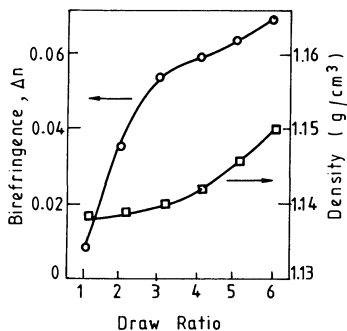
Fig. 8.10 Birefringence and density of nylon 66 as a function of draw ratio [14].

was observed that while there was an increase in crystallinity for feeder yarn with low SDR, there was little change in the total crystalline content of the high SDR samples during drawing at 90 °C [13]. However, the increase in density with draw ratio for all samples was large. The disparity between crystallinity as measured by X-ray and by density was attributed to the conversion of γ phase to α phase; the latter is relatively denser.

For nylon 66 a greater increment of birefringence in the low draw ratio range was observed [14], indicating that more orientation is established in the early stages of drawing (Fig. 8.10). On the other hand, the increase in density occurs mainly at the higher draw ratio range. This suggests that the mechanical stress applied to the fibre during drawing acts initially to align polymer segments along the direction of the force until a certain degree of orientation is established; then it gradually increases the lateral order. Similar behaviour of birefringence and density in relation to draw ratio was reported for nylon 6 [8], as shown in Fig. 8.11. The sharper rise in density value at higher drawing stress for nylon 6 compared with nylon 66 is probably due to conversion of the γ form of crystallites to the denser α form.
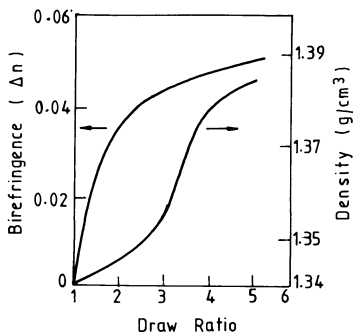
Fig. 8.11 Birefringence and density of nylon 6 as a function of draw ratio [8].
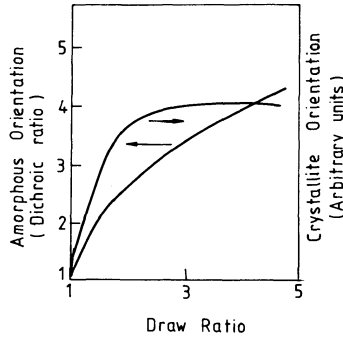
Fig. 8.12 Crystalline and amorphous orientation as a function of draw ratio for nylon 6 [9].

The influence of draw ratio on orientation of nylon 6 was analysed [9] by measuring the orientation of the crystalline phase using X-ray diffraction and that of the amorphous phase by dichroic ratio developed by drawing an undrawn fibre dyed with a dichroic dye. It appears from the results presented in Fig. 8.12 that until the natural draw ratio is reached the orientation of the crystalline phase is dominant, while the orientation of the amorphous phase keeps on improving with draw ratio even after the crystalline orientation reaches an equilibrium value. In the case of PET, it has been reported that after three- to four-fold stretching the crystallites attain complete orientation while the macromolecules in the amorphous regions still have a considerable reserve in orientation [15]. In the case of polypropylene, crystalline orientation reached a constant level at a stretch ratio above 4, while the measured strength continued to increase with a further increase in draw ratio, presumably due to continued improvement in amorphous orientation with stretch [10].

A mechanism to explain the drawing behaviour of fibres between intermediate and high draw ratios has been proposed by Provorsek *et al.* [16]. This mechanism was proposed for nylon 6 fibres, but is also claimed by Provorsek *et al.* to apply to nylon 66 and PET fibres. According to these authors, at draw ratios between intermediate and high the microfibrils are not stretched but rather slip past one another. In this process the microfibrils are sheared with respect to each other and the matter removed from the surfaces of the microfibrils forms an interfibrillar phase whose density is similar to the average density of the microfibril. The observations of densification of fibre with drawing, low moisture uptake by nylon at high draw ratio, lack of agreement between X-ray crystallinity and density crystallinity at high draw ratios, as well as the fact that crystalline orientation reaches a constant value at an early stage of drawing, are all consistent with the mechanism proposed by Provorsek *et al.*

8.4.2 ORIENTATION STRENGTHENING AND LIMITING DRAW RATIO

When a fibre is drawn beyond its natural draw ratio – the natural draw ratio being the draw ratio up to which the fibre undergoes plastic deformation at constant load – a steep rise in the load is observed and ultimately the fibre ruptures. The limiting value of this draw ratio is dependent on the prehistory of the polymer and the drawing conditions, but for a given polymer drawn repeatedly under the same conditions, this limiting draw ratio is reproducible experimentally. The termination of drawing is thus not due to random defects, but is probably associated with certain changes in supermolecular structure which finally leads to local overstresses. Thus, the orientational drawing terminates as a result of two competing processes, namely the strengthening associated with the formation of a more oriented fibrillar structure, and an increase in the structural heterogeneity along the orientation axis as the fibre approaches its limiting draw ratio. According to Slutsker and Utevskii [17], the process of strengthening is to a considerable extent due to longitudinal shear of the fibrillar structure of the polymer, which causes longitudinal shift and splitting of the fibrils and, in some cases, splitting of the crystallites. These rearrangements probably account for decreasing dispersion in molecular length in each amorphous region and result in a more homogeneous distribution of load over the molecules. According to some currently accepted models of semicrystalline fibre morphology, the interfibrillar tie molecules which bind together the microfibrils comprising the fibre make the predominant contribution to the tenacity of the fibre.

The process of rupture of polymers under drawing, according to Slutsker and Utevskii, is associated with increasing dispersion in length of the intercrystalline amorphous regions. In those regions which are considerably below the average size, local overstress will probably appear. The molecules will rupture because the relative deformation of these regions will be much larger than those of the adjacent regions in the cross-section of the sample. The draw ratio in the case of as-spun, amorphous PET fibre has also been interpreted [18] as the extension of a network to a limiting extensibility with the molecular entanglements acting as physical crosslinks. The network forms during fibre spinning and cold drawing then extends the network to its limiting extensibility. On this model, the yield process and the subsequent cold drawing do not involve long-range molecular flow but are associated with molecular rearrangements between points of entanglement.

8.4.3 DRAWING STRESS AND MOLECULAR DISCONTINUITIES

While an increase in draw ratio increases molecular orientation, it also increases the drawing tension (Fig. 8.13). A high drawing tension results
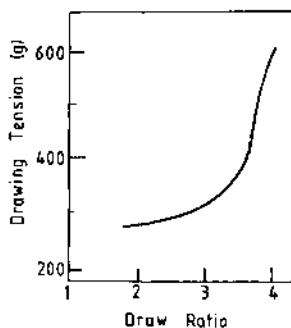
Fig. 8.13 Influence of draw ratio on drawing tension [8].

in chain scission so the maximum permitted draw ratio for a given drawing condition will be limited by the rate at which the molecular discontinuities accumulate. The influence of draw ratio on the total number of end groups formed in nylon 6 during stretching has been studied [19] with the help of IR spectroscopy. The accumulation of the number of end groups during orientation stretching was analysed in the region of stretching vibrations of the C=O groups (1700–1800 cm^{-1}) because in air it is predominantly oxygen-containing end groups that are formed. The growth in concentration of oxygen-containing end groups with the draw ratio at drawing temperature of 20 °C and 170 °C is shown in Fig. 8.14 in terms of concentration of molecular discontinuity. In the first stages of the stretching process the concentration of end groups varies only slightly and the number of discontinuities increases rapidly as stretching continues. The process of orientation stretching terminates when the concentration of end groups reaches a critical magnitude. The critical concentration of end groups for specimens stretched at room temperature is reached sooner and at a lower
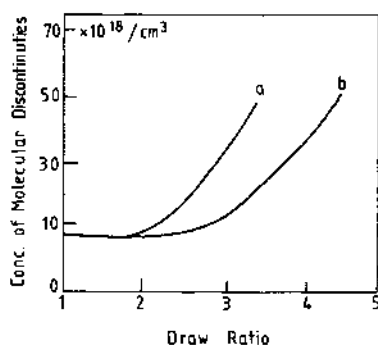
Fig. 8.14 Concentration of molecular discontinuities vs. draw ratio for nylon 6 drawn at (a) 20 °C and (b) 170 °C [19].
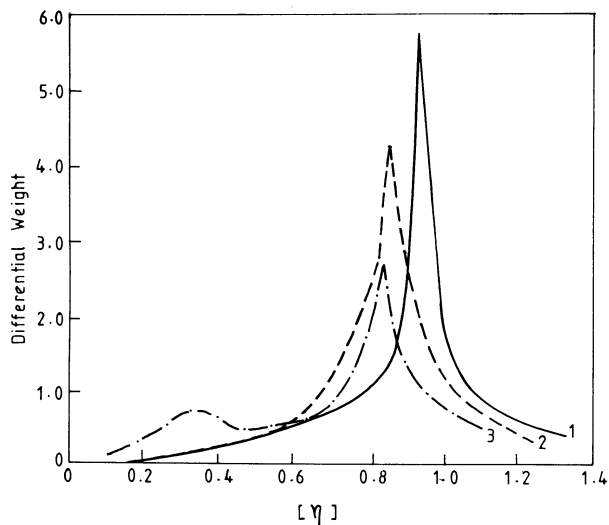
Fig. 8.15 Differential distribution curves for nylon 6: (1) undrawn, (2) drawn to 2.92 DR, (3) drawn to 4.00 DR. $[\eta]$ represents intrinsic velocity in dlg^{-1} [20].

draw ratio than for a polymer orientation-stretched at a temperature nearer the melting point.

The effect of draw ratio on the degree of polymerization of nylon 6 drawn at room temperature has been studied by mapping the molecular weight distribution curves (Fig. 8.15) of samples drawn to different extension [20]. It is noteworthy that as the draw ratio is increased, the peak of the differential distribution curve shifts to a lower molecular weight value. At high draw ratio the distribution curve becomes bimodal, showing a hump at the lower value of viscosity number, signifying a considerable increase in the proportion of low molecular weight fraction of the polymer.

8.5 ORIENTATION STRETCHING FOR HIGH STRENGTH

To obtain very high tensile strength, it is necessary that molecular weight, orientation and crystallinity are all high. Since the drawing tension increases with both crystallinity and draw ratio, hot drawing is used; the higher molecular mobility present in hot drawing facilitates the drawing process by reducing drawing tension and increasing crystallinity.

To obtain high strength PET yarns, two-stage drawing with a draw ratio of around 3 in the first stage at a drawing temperature slightly above T_g, followed by second stage final draw at a much elevated temperature, has been recommended [21] on the basis of a study of the

relaxation of mechanical stresses in fibres drawn to various draw ratios. At draw ratio above 3 the rate of relaxation is sharply retarded and the time spectrum of relaxation times becomes broader. The increase in relaxation time continues with further stretching. With the increase in drawing stress the chains are loaded increasingly non-uniformly. To avoid this, higher temperature and lower stretching rates are necessary as the fibre orientation increases. Similar recommendations have come from other sources. It is suggested that the first drawing should be accomplished at around 90 °C within the limits of the natural draw ratio and further drawing of the necked fibre should be performed at a temperature 80–100 °C above the first zone to the desired maximum possible degree of stretch.

In another study [22] a thick PET monofilament was subjected to two-stage cold drawing with each stage followed by high temperature annealing; a filament with high strength was obtained. It is postulated that condensation and transfer (exchange) reactions occur during annealing. Thus it is suggested that both physical and chemical changes must be taken into account to explain the strength enhancement.

8.6 HIGH SPEED SPINNING AND THE SPIN–DRAW PROCESS

With the advent of high speed spinning, drawing of unoriented filaments is fast becoming outdated. Depending on the spinning speeds employed, yarns with varying precursor orientations are now fully drawn using conventional two-stage spinning and drawing processes or an in-line spinning–drawing sequence known as the spin–draw process. Crystalline, fully oriented yarns are also produced in a single step spinning sequence using high speed spinning. Since these processes have been described in detail in Chapter 4, they will not be considered further here.

In a comparison between PET fibres spun at progressively higher wind-up speeds and fibre drawn from low wind-up speed feedstock, Brody [23] has shown that although winding speed increases birefringence through the process of draw-down, the structure obtained is not the same as that obtained by normal drawing. An increasing wind-up speed results in a broadening of the distribution of the length of the molecules between ordered regions of microfibrils. The tie molecular chains in fibres spun at low wind-up speed and subsequently drawn have lengths which are closer to each other in value. Consequently, for the same modulus and breaking extension values the birefringence is higher for the drawn fibre. Somewhat similar results have also been reported for nylon 6 and nylon 66, where it has been shown that fibres spun with low spinning speeds and then drawn have higher tenacity values than the high speed spun fully oriented yarns.

8.7 DRAWING OF PREORIENTED YARNS AND DRAW-WARPING

While higher orientation and onset of crystallization in the feeder yarn have been reported to be disadvantageous for achieving high strength through conventional drawing, it has been shown [24] that when oriented and partially crystalline PET fibres spun at spinning speeds in the vicinity of $4500 \, \mathrm{m \, min^{-1}}$ are annealed first at temperatures above T_g (120 °C, 150 °C), and then drawn at temperatures closer to their melting point (230 °C, 250 °C) in a continuous operation, much higher draw ratios and tenacities result than could be achieved with low orientation precursor fibres. The high degree of orientational relaxation that precedes crystallization during annealing has an embrittling effect in the lower oriented precursor fibres. This is a consequence of almost complete relaxation of orientation prior to crystallization, resulting in fewer tie chains between the crystals. The fibres spun at higher speeds retain their ductility even after annealing due to improved stress transfer. This is achieved through the increased degree of connections between the crystals formed, since oriented crystallization occurs with only partial relaxation of orientation in the fibres spun at high speeds.

Yarns with varying degrees of preorientation are drawn in the form of a warp sheet where more than a thousand ends are drawn together to form a warp beam. All types of yarns which need drawing can be used and the degree of residual drawing is of secondary importance. The drawing equipment consists of several rollers or godets around which the yarn sheet is wound and which are driven according to the desired degree of drawing. There is also a provision for heat-setting the drawn yarn sheet. Drawing more than a thousand ends together in the form of a warp sheet imparts greater uniformity than could be obtained with single end drawing. Moreover, the flexibility of the draw-warping process allows for a stricter control over the properties of drawn yarn like strength, modulus, elongation, uniformity, denier and shrinkage.

REFERENCES

1. Vincent, P.I. (1960) *Polymer*, **1**(7), 7–19.
2. Ludewig, H. (1964) *Polyester Fibres Chemistry and Technology*, Wiley-Interscience, London, p. 230.
3. Thompson, A.B. (1959) *J. Polym. Sci.*, **35**, 741.
4. Spruiell, J.E., McCord, D.E. and Beuerlein, R.A. (1972) *Trans. Soc. Rheol.*, **16**(3), 535–555.
5. Gupta, V.B., Sett, S.K. and Venkataraman, A. (1990) *Polym. Eng. Sci.*, **30**, 1252.
6. Kobayashi, K. (1970) *Sen-i-Gakkaishi*, **26**, 550–559.
7. Brody, H. and Ward, I.M. (1992) In *Concise Encyclopedia of Polymer Processing and Applications* (ed. P.J. Corish), Pergamon Press, Oxford, pp. 298–299.
8. Fujimoto, F., Yamaguchi, K., Ikide, H., Kishida, H. and Arai, T. (1973) *J. Textile Mach. Soc. Japan*, **19**, 1–6.

9. Sbrolli, W. (1968) In *Man-made Fibres*, Vol. 2 (eds H.F. Mark, S.M. Atlas and E. Cernia), Interscience Publishers, New York, p. 267.
10. Gill, R.A. and Benjamin, C. (1979) Polypropylene Fibres and Textiles, 2nd International Conference, Plastic and Rubber Institute, September, pp. 10.1–10.11.
11. Ito, M., Tanaka, K. and Kanamoto, T. (1987) *J. Polym. Sci., Polym. Phys.*, **25**, 2127–2138.
12. Urbanczyk, G.W. (1962) *J. Polym. Sci.*, **59**, 215–220.
13. Gianchandani, J., Spruiell, J.E. and Clark, E.S. (1982) *J. Appl. Polym. Sci.*, **27**, 3527–3551.
14. Sakuma, Y. and Rebenfeld, L. (1966) *J. Appl. Polym. Sci.*, **10**, 637–652.
15. Novak, I.I., Suchikov, V.A. and Zosin, L.P. (1969) *Vys. Sod.*, **11**(6), 1325–1329.
16. Prevorsek, D.C., Harget, P.G., Sharma, R.K. and Reimschuessel, A.C. (1974) *J. Macromol. Sci., Phys.*, **B9**, 127–155.
17. Slutsker, L.I. and Utevskii, L.E. (1984) *J. Polym. Sci., Polym. Phys. Ed.*, **22**, 805–826.
18. Allison, S.W., Pinnock, P.R. and Ward, I.M. (1966) *Polymer*, **7**, 66.
19. Pakhomov, P.M., Pantev, V.A. and Shablygin, M.V. (1979) *Khim. Volokna*, March–April, pp. 32–34.
20. Sengupta, A.K., Singh, R.K. and Majumdar, A. (1974) *Textile Res. J.*, **44**, 155–163.
21. Gribanov, S.A. and Aizenshtein, E.M. (1981) *Khim. Volokna*, May–June, pp. 18–23.
22. Fakirov, S. and Evstatiev, M. (1990) *Polymer*, **31**, 431.
23. Brody, H. (1983) *J. Macromol. Sci., Phys.*, **B22**(3), 407–423.
24. Yoon, K.J., Desai P. and Abhiraman, A.S. (1986) *J. Polym. Sci., Polym. Phys. Ed.*, **24**, 1665–1674.

Heat-setting of thermoplastic fibres

9

A.K. Sengupta

9.1 INTRODUCTION

Synthetic filaments such as nylon and polyester are extruded as continuous filaments and drawn afterwards to the required level to impart strength and stability. The drawn nylon and polyester filaments are semi-crystalline and oriented and exhibit thermal shrinkage when they are heated to temperatures above the glass transition but still well below the crystalline melting point. The decrease in length arises mainly from the relaxation of molecular chains. The magnitude of shrinkage is dependent upon structural parameters such as orientation and crystallinity of the fibres and upon external variables such as temperature, tension, time, etc. Thus, drawn but unset fibres, although possessing good tenacity and elasticity properties, cannot be used for most textile and technical purposes since they do not possess dimensional stability. Furthermore, twisted or doubled filaments have a strong tendency to curl; this has a deleterious effect on further processing. Apart from this, planar structures like fabrics produced from these unset, continuous filaments or fibres display unfavourable creasing behaviour when in use. Therefore it is necessary to 'set' the drawn or twisted filaments in order to attain resistance against shrinkage, and dimensional changes, curling and creasing. This can be achieved by the action of heat in the absence or presence of swelling agents, with or without tension. In practice, hot water, saturated vapour or dry heat treatments are used.

The favourable effect of the setting process lies in the fact that it relieves the strains in the filaments resulting from the manufacturing

Table 9.1 Physical properties of some synthetic fibres [1]

	Nylon 6	Nylon 66	PET
Density in filament form (g cm^{-3})	1.14	1.14	1.38
Melting point, T_m (°C)	215	264	267
Temperature of maximum crystallization rate (°C)	145.6	150	190
Maximum crystallization rate (s^{-1})	0.14	1.66	0.016
T_g: dry (°C)	59	70	85
T_g: 65% RH (°C)	~10	~25	~80
Optimum setting temperature, dry (°C)	190	225	210

process (e.g. spinning, drawing or twisting). The mechanism of strain relief may be described as follows: the linkages between the molecular chains or the crystallites which were frozen-in under tension and the mechanical stresses can be balanced by the supply of heat, thus giving rise to greater freedom for molecular motion. This gives the bonds an opportunity to 'snap' into the sites of least energy. Subsequent cooling, therefore, generally results in a state of lower strain. Furthermore, the action of heat induces crystallization processes, resulting in a more stable structure with higher cohesive energy. The sequence of events that occurs in the thermosetting processes is: (1) weakening of inter-molecular bonds and increasing the segmental mobility of structural elements at higher temperatures; (2) thermal relaxation; and (3) stabiliza-tion of the structure and re-formation of bonds at new places on cooling the yarn. The rate processes associated with these events depend on the strain history and setting conditions, as well as inherent properties of the polymer. Table 9.1 summarizes some of the important physical properties of nylon 6, nylon 66 and polyethylene terephthalate (PET) fibres [1].

From the data in Table 9.1 it can be seen that the crystallization rate is the highest for nylon 66 and the lowest for PET. However, the level of orientation dramatically influences the crystallization rate for PET and hence the crystallization rate calculated when the polymer is cooling from the melt must be seen in this context.

Smith and Steward [2] studied the rate of crystallization of oriented, amorphous PET at 100, 120 and 150 °C, when the sample was held at constant length to prevent shrinkage. The crystallization process was observed by measuring changes in density and boiling water shrinkage. Smith and Steward found that the rate of crystallization is strongly dependent on the degree of orientation. Nucleation and initial growth of crystallites occur in times of the order of milliseconds at 120 °C in samples of birefringence 0.08, compared with times of several minutes in isotropic samples.

9.2 NATURE OF SET

The term 'setting' is used in practice to describe the stabilization of a structure in a particular form and is concerned with the equilibrium form which a textile material assumes. The term 'degree of setting' indicates to what extent this equilibrium is achieved.

Set is categorized into three types, namely temporary, semipermanent and permanent [3]. The differences lie in the levels of energy required to reverse their reference set states. Thus, when the stability of set is lost in ordinary usage through light, warmth, moderate mechanical action, wetting or changes in humidity, the set is called temporary set. A semipermanent set is stable to ordinary usage but can be reversed by more severe treatment. A permanent set which involves structural changes cannot be totally reversed without destroying the structure. All three types of set can occur together in a fibre. In false twist texturing, for example, both permanent and temporary sets occur simultaneously and the latter is later reversed. Generally, no sharp distinction is made between temporary and semipermanent set. They are combined together and referred to as temporary set.

9.2.1 MECHANISM OF TEMPORARY SET

In principle, any transition in the fibre which is demonstrated by a sharp drop in stiffness may be used as a mechanism for inducing temporary set. Thus polyester may be deformed above 80 °C, which is the T_g of the polymer, and cooled in the deformed condition to impart a temporary set which, however, will be easily reversed, as the intermolecular forces responsible for 'freezing' the strain are only weak van der Waals forces. In nylon, hydrogen bonds can be broken and re-formed in a new site to impose a temporary set. Again, this set can be removed by moisture and slight warmth. A more durable temporary set can be induced in polyacrylonitrile due to relatively stronger polar attractions of the nitrile groups. Acetates have very high T_g and the material can be subjected to heat treatment above T_g to induce a set which is irreversible under normal usage.

9.2.2 MECHANISM OF PERMANENT SET

The more important mechanism of setting is the modification of fibre structure. Because most fibres are partially crystalline, set effects are associated with a change in crystalline morphology. The most important mechanism of permanent setting in crystalline polymers is through partial melting and recrystallization, whereby partial melting of small, imperfect crystals takes place below the melting point to allow the growth of larger more perfect and regular crystalline units. This is

brought about in the deformed configuration of the material so that the internal stresses are released and a more stable structure is formed.

The probable mechanism involved in heat-setting of nylon is revealed from the infrared studies of Parisot and Bouriot [4]. When a drawn nylon fibre is heated, a weakening of interactions between adjacent molecules is induced through intensification of micro-Brownian motion. An increase in the heat treatment temperature causes the cohesive forces to become less and less pronounced. The spacing out of the macro-molecular chains causes some hydrogen interactions to disappear and free NH groups are formed. Due to thermal agitation, the metastable structural arrangement built up during the course of stretching tends to loosen and the molecular chains are allowed to relax. The average orientation of the macromolecular chains is therefore reduced. The crystallinity decreases and the amorphous content increases. On subsequent cooling, the hydrogen interactions are fully reconstituted but the orientation is not restored. The mean degree of orientation compared with that of the untreated fibre is reduced, while the size of the crystalline area is enlarged.

The action of heat is thus to cause a relaxation of the structure, together with a reorganization of the molecular arrangement. At sufficiently high temperature, there is a freedom of motion of the macro-molecules and, hence, increased opportunity for them to rearrange themselves to occupy a minimum of space consistent with their stabilized structure without being subjected to any strain. A return to normal temperature causes no change in their new form or their new arrangement.

Thus, in terms of simple physics, the mechanism of heat-setting is to lead the structure to a position of lower minimum energy from the state prior to heat-setting. When a material achieves a new equilibrium position as a result of heat-setting, the internal structural parameters are changed as a result of setting and it cannot be brought back to the original form unless every individual element is arranged in the same way as before [3]. This is impossible in the case of textile fibres which have multiple energy minima. The change in the internal structure through loosening of molecular chains and rearranging them in an energetically favourable conformation requires a partial melting of crystallites, as demonstrated in the Parisot and Bouriot experiments, followed by recrystallization. It is important to note that the term 'melting point of a fibre' usually means the melting temperature of the relatively large and more perfect crystals. Fibres usually contain crystals of different sizes and perfections. It has been shown by several researchers that, depending upon its previous history, a material will show different melting points. It has also been shown that, as heating proceeds, the smaller crystals melt and form larger ones having higher melting points.

CRYSTAL SIZE OR PERFECTION

FREQUENCY

Melting Point   B   D   F

(A)

FREQUENCY

(C)

(E)

(G)

T₁ T₂ T₃

Temperature (°C)

A) Variation of crystal melting temp. with size or perfection.

B) Frequency diagram of crystal size.

C) Corresponding melting temp. frequency diagram.

D) Crystal size after annealing.

E) Corresponding temperatures

F) Crystal size after second heat treatment.

G) Corresponding temperatures.

Fig. 9.1 Change in crystal size and dispersion with heat treatment temperature [3].

Hearle [3] has represented the variations of melting points with crystal size and perfection together with a hypothetical frequency distribution of crystal sizes that represents a real fibre. Hearle related the mechanism of heat-setting to the melting of crystals and changes in crystallization pattern. When a fibre is heated to a temperature T_1, small or imperfect crystals will melt and larger crystals will grow. This is a typical process of annealing and is shown schematically in Fig. 9.1. If the annealing process is carried out with the fibre in a deformed state, the deformed configuration will be stabilized through recrystallization (Fig. 9.2) and a new distribution of crystal sizes will result. Subsequent treatments at higher temperatures, say at T_2 and above T_2, will allow further changes in the distribution pattern and new sets to be achieved.

(a)   (b)   (c)
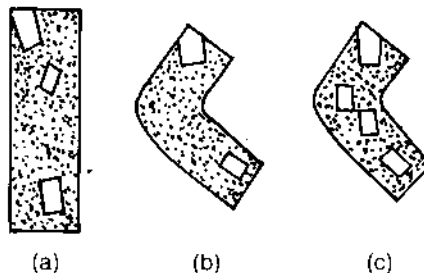
Fig. 9.2 Set through crystallization (the rectangles represent crystallites in an amorphous matrix). (a) Schematic model of fibre structure, (b) deformation without recrystallization, (c) deformation stabilized by recrystallization [3].

9.3 HEAT-SETTING BEHAVIOUR OF POLYAMIDE AND POLYESTER FIBRES

9.3.1 CHANGES IN STRUCTURE AND PROPERTIES ON HEAT-SETTING

When synthetic fibres, yarns or fabrics are set, many important physical properties are affected. The stress–strain characteristics are influenced to a significant degree. Tenacity, elongation, modulus, form recovery and work recovery, shrinkage, swelling properties, dyeing behaviour and lustre are all affected significantly by the setting treatment. Commercial polyamide and polyester fibres are generally similar in their heat-setting behaviour and it is, therefore, useful to consider the setting behaviour of these fibres together.

Dismore and Statton [5] studied the effect of heat-setting temperature on the structure and properties of nylon 66. Some of their results are discussed below.

Figure 9.3 shows the effect of a high temperature annealing treatment on the tensile strength of a nylon 66 fibre in a slack unrestrained condition. A drastic reduction in strength on high temperature annealing is evident. Per cent shrinkage and elongation to break data are presented in Figs 9.4 and 9.5, respectively. It is observed that the shrinkage increases slowly at first with increase in annealing temperature up to 220 °C and then increases rapidly as the temperature is raised further. The per cent elongation of the annealed fibres initially shows an increase with increase in annealing temperature up to 220 °C and then drops sharply when the temperature of heat treatment is raised further. When the shrinkage and elongation behaviour are taken together one unmistakable fact become clear, namely that shrinkage is not merely a disorienting process. If this was so, per cent elongation would increase
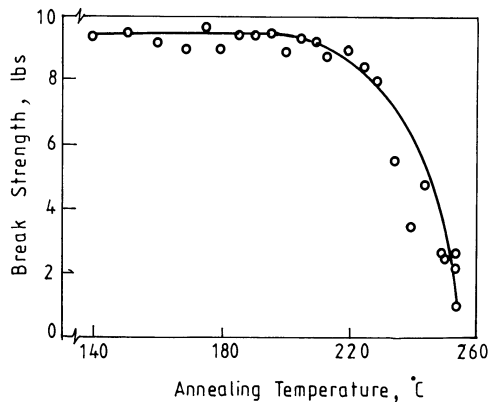
Fig. 9.3 Change of breaking strength with annealing temperature [5].
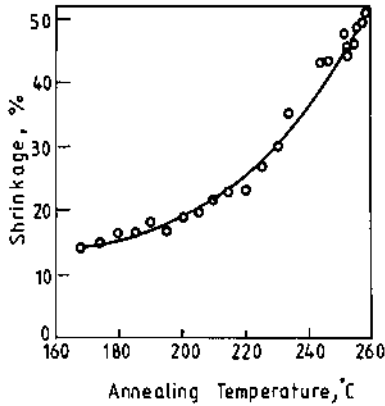
Fig. 9.4 Shrinkage during slack-annealing [5].

continuously with the increase in shrinkage. The sharp decline in elongation when the rate of shrinkage is a maximum shows that shrinkage is a two-stage process. With the increase in annealing temperature shrinkage causes disorientation of the molecular chains which later fold to give a chain-folded stable structure. Dismore and Statton [5] have proposed structural models of drawn and annealed yarns which are presented in Figs 9.6(a) and (b), respectively. During annealing, the intermolecular bonds with the highest energy will dissociate or melt, allowing short lengths of molecules to rearrange and form more stable bonds. The local order or crystallinity will increase because local melting will allow recrystallization to occur through chain folding, using folds which are
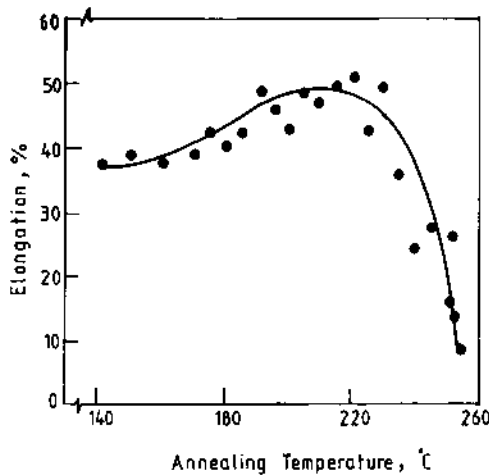
Fig. 9.5 Dependence of elongation to break on annealing temperature [5].

(b) Model of annealed yarn

(a) Model of drawn yarn
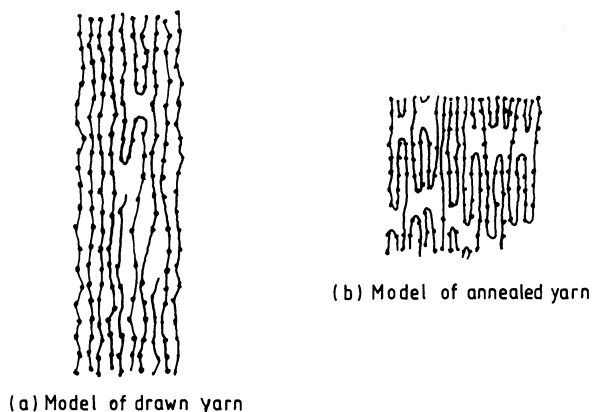
Fig. 9.6 Structural models of (a) drawn and (b) annealed yarn [5].

already present in the oriented structure as nuclei. Annealing would thus result in an increase in the number of folded chain segments. The large shrinkage that accompanies annealing at high temperature in the free state of the fibre is accommodated in the structure through an increase in the number of chain folds, which in turn increases the dimensions of the crystalline region. Structural studies following annealing show a close agreement with the model proposed. There is an increase in both density and X-ray crystallinity with increase in annealing temperature. The crystallite orientation remains largely unaffected but the sonic modulus decreases with increase in annealing temperature, showing a greater molecular disorientation, mostly amorphous disorientation, with an increase in annealing temperature.

Dumbleton [6], working on PET fibres, observed that the tenacity of PET fibres decreases sharply after high temperature annealing treatment in a relaxed condition, as in the case of nylon 66. However, nylon 66 is stable up to a higher temperature than PET. It is also observed that shrinkage is not recoverable in the form of elongation on stretching the sample after the high temperature annealing treatment; therefore, as in the case of nylon 66, shrinkage is also not simply a disorientation process in PET. Dumbleton further observed that the results on drawn and annealed PET suggest that drawn PET consists of highly extended molecules, essentially parallel to one another with few folds present, but on heating more extensive chain folding occurs.

Evidence for chain folding in PET at elevated temperature was also reported by Koenig and Hannon [7]. Infrared (IR), small angle X-ray scattering and broadline nuclear magnetic resonance techniques all showed that annealing treatments at elevated temperature definitely cause an increase in chain folding (which is characterized in IR by

a specific absorption peak assigned to the regularly folded chain segments).

Wilson [8] observed that shrinkage in PET is a two-stage process involving a rapid initial stage in which shrinkage is associated with disorientation in the amorphous zones, followed by a crystalline stage during which chain folding, observed in the IR spectrum, occurs. Chain folding occurs after shrinkage; there is therefore no unique relationship between chain folding and fibre length change.

9.3.2 EFFECT OF TENSION ON PROPERTIES

The structure and properties of heat-set fibres under variable stress have been studied widely. It is generally observed that while free annealing reduces molecular orientation and tenacity, it increases diameter and denier of the fibre. With tension annealing, there is generally an increase in tenacity but no significant change in diameter or denier. The crystallinity also increases. While crystallinity, crystallite orientation, birefringence and amorphous orientation relate to the mechanical properties to some degree, knowledge of these alone is inadequate to explain the differences between mechanical properties and dye uptake of free and tension annealed samples. To understand these differences a clearer concept of the order–disorder situation is necessary, the important features of which are number and size of crystallites, crystallite distribution within a non-crystalline matrix and distribution of orientation within the non-crystalline region. According to Valk, Jellinek and Schroder [9], all the above factors influence the segmental mobility within the non-crystalline matrix and show good correlation with mechanical properties. They have explained this concept using two models (Fig. 9.7) which illustrate the change in crystallite dispersion within PET fibres. The changes in glass transition temperature and tenacity with respect to heat-setting temperature and tension (Figs 9.8 and 9.9) are explained with reference to the two models. In going from model (a) to model (b) above a 'critical' setting temperature, although there is a total increase
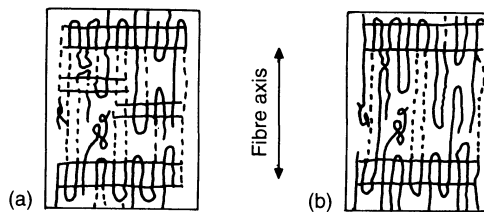
Fig. 9.7 Change in crystal dispersion within PET fibres annealed at (a) low temperature/high tension, (b) high temperature/low tension [9].
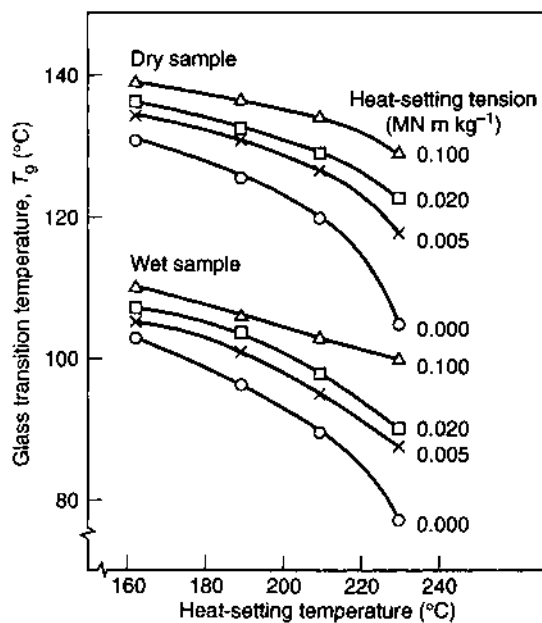
Fig. 9.8 Glass temperature of heat-set PET in the dry and wet state [9].
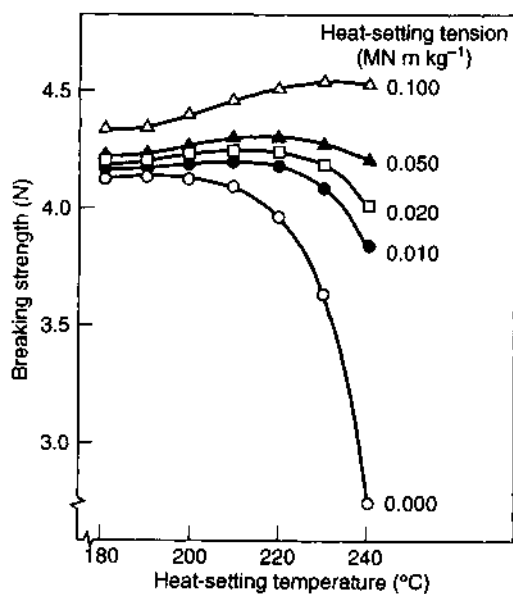
Fig. 9.9 Tenacity of PET in relation to heat-setting temperature [9].

in crystallinity, the number of crystallites dispersed within the non-crystalline matrix decreases and a larger non-crystalline volume is created with respect to each crystal. Due to reduced crosslink density (physical crosslinking by crystals) the chain molecules have greater mobility, with a consequent reduction in T_g. There are also fewer tie molecular chains bridging intercrystalline domains, which accounts for a drop in tenacity.

Model (a), which is broadly representative of a sample heat-set at low temperature or under tension, shows a higher physical crosslinking by crystals as the number of crystals per unit volume is greater. The segmental mobility is reduced, which enhances the T_g. The number of tie molecular chains bridging the intercrystalline regions is greater, which accounts for better stress transfer and higher tenacity. The models are also useful in explaining dye uptake behaviour.

Detailed studies [10] on the elastic, viscoelastic and stress–strain behaviour of PET yarns heat-set under two conditions, namely when free to shrink and when held taut at constant length, emphasized the need to take into account the morphological differences between the two sets of samples to explain their properties. These studies showed that while a two-phase series model was satisfactory to explain the behaviour of free annealed samples, it was totally inadequate for the taut annealed samples. It was postulated that while in the free annealed sample the coupling between the crystalline and amorphous regions is likely to be predominantly of the series type, a significant degree of parallel coupling is expected to exist in the taut annealed sample. An analysis of the experimental data [11] showed that the nature of coupling can affect such important physical properties as the modulus, thermal shrinkage, recovery from tensile deformation and rate of dye uptake.

9.3.3 THERMAL HEALING

One interesting aspect of heat-setting which has received only limited attention is the aspect of thermal healing or sealing of fissures, surface cracks, etc. caused by the stressing operations. It has been reported that the strength distribution of individual filaments in a multifilament nylon 66 drawn yarn is bimodal in nature. This bimodality disappeared after heat treatment. In the case of drawn unannealed yarn, the bimodality is explained through the postulate that flaws within the fibres cause one type of failure while surface defects produce another type. The thermal treatment of fibres changes the distribution pattern by altering the distribution of internal flaws or more probably by healing surface defects. It has been pointed out [12] that during thermal treatment chemical healing, arising from solid state reaction, may play a more

dominant role than physical healing which involves diffusion of macro-molecules.

9.3.4 SETTING UNDER DRY AND WET HEAT

Warwicker studied the structural changes in nylon 6, nylon 66, and poly-ester yarns when subjected to dry and wet heat [13]. His results show that for both nylon 6 and 66, steam-setting under relaxed condition gives rise to a higher increase in density than found in dry-set yarns. This may be because nylon in steam, under relaxed conditions, is able to develop the folded structure discussed earlier with the growth of larger amorphous regions. Under dry conditions, the chains are not so mobile and the folded structure is not markedly developed. It was observed by Warwicker that while density and birefringence both increase with dry and steam heat treatments, there is a decrease in moisture regain with an increase in dry heat-setting temperature while there is little change in the moisture regain values of the steam-set samples. The increase in birefringence with the increase in setting temperature is found to be due to an increase in X-ray orientation factor. For polyester also density increased for both dry and steam heating with an increase in treatment temperature.

Warwicker's results show that the effectiveness of setting is consider-ably enhanced with wet heat for nylon, as observed from the density changes [13]. In the presence of moisture there is a considerable depres-sion in melting point of the nylons, which would result in a higher degree of set due to greater mobility of the molecular chains. With polyester, no appreciable difference in the densities between dry and wet heat-set samples is noticeable.

9.4 HEAT-SETTING OF CELLULOSE TRIACETATE FIBRES

Cellulose triacetate fibres are thermoplastic and their ability to be heat-set is an extremely valuable textile property. It is well known that crystallinity in triacetate occurs considerably below the melting point (about 300 °C).

Hindeleh and Johnson [14] studied the heat-setting behaviour of cellu-lose triacetate at constant length in a nitrogen atmosphere in the temperature range 20–300 °C. They observed that while both crystallinity and crystallite orientation improved sharply from 172 °C onwards, the tenacity dropped equally sharply from the onset of crystallization onwards. Thus, crystallinity and tenacity appear to be inversely related in heat-set triacetate fibres.

In his work on the heat-setting of Arnel 60[TM] and Arnel[TM], Sprague [15] observed that while in the former heat-setting improves tenacity and

modulus, exactly opposite results are obtained with the latter. According to Sprague, during heat-setting both crystallization and relaxation of chains take place simultaneously. The rates at which these two events occur, however, differ for the two fibres. Arnel 60, having greater orientation and considerably improved tautness distribution – a term Sprague employs for the distribution of free chain segment lengths lying between points of intermolecular attraction – is in a better position to crystallize rapidly before molecular relaxation occurs to a significant degree, whereas in Arnel, during heat-setting the distribution of free chain segment lengths between points of intermolecular attraction broadens, resulting in poorer tensile properties following heat-setting.

9.5 SETTABILITY AND THE MEASUREMENT OF THE DEGREE OF SET

The purpose of heat-setting is to relax molecular chains to attain a stress-free configuration in which the new reference state attained after setting the molecular chains is in a lower level of energy than before setting. The success of the setting operation lies in the degree and permanence of set which need to be measured; the two methods for measuring these are the critical dissolution time (CDT) method and recovery from bending strains.

9.5.1 CRITICAL DISSOLUTION TIME

The CDT method estimates the time needed to dissolve a filament in a solvent of known concentration at a given temperature. In practice, the filament is held in loop form secured on a hook and weighted with a small weight. The looped filament is then submerged in the solvent contained in a glass tube. When the filament dissolves, the weight falls to the bottom of the tube. The time elapsing between immersing the filament loop with the weight in the solvent and the weight falling to the bottom of the tube is recorded by a stopwatch. This is the critical dissolution time.

As the dissolution takes place selectively in amorphous or poorly ordered regions of the fibre, it is assumed that the rate of diffusion of solvent molecules into the fibre matrix would depend upon the amount of non-crystalline material present and, hence, on the crystallinity. Galil [16] observed that critical dissolution time can be well correlated with crystallinity as well as with dye diffusion behaviour. He reported a correlation coefficient of 0.98 between density and log CDT for polyester fibres. As heat treatment results in an increase in crystallinity a more crystalline fibre will take more time to dissolve than a less crystalline fibre.

It has already been suggested that in a heat-setting operation the mechanism of permanent set is stabilization through crystallization. The values of critical dissolution time can, therefore, be used to compare the effectiveness of the heat-setting operation between different samples. Even small differences in structure caused by variations in heat-setting conditions can be picked up using this technique.

9.5.2 RECOVERY FROM BENDING STRAINS

One of the most important methods for the assessment of set is the recovery from bending strains. This is an extremely important require- ment for apparel fabrics where crease and wrinkle recovery are of utmost importance.

Prevorsek, Butler and Lamb [17] measured settability and permanence of set against bending deformation for nylon and polyester fibres. For measurement of degree of set, they wound fibres under constant tension onto a rod of suitable diameter (the diameter of the rod was changed to vary the strain) for a predetermined number of turns. After heat-setting for 10 min, the rod was allowed to cool. The fibre was then released so that it was free to recover. Measurements were then made of L_2 and N_2 (described below) after 10 min or at various stages during recovery of the helix.

The set, S, was estimated using the formula

$$S = (N_2/N_1)[1 - (L_2)^2]^{1/2} \times 100$$

where L_1 is the initial axial length of the helix, L_2 is the length of the recovered helix, N_1 is the initial number of helical turns and N_2 is number of turns after recovery.

The recovery as a function of time measured over a period of about 2000 min was used to ascertain the permanence of set.

Prevorsek, Butler and Lamb observed that in terms of both degree and permanence of set, polyester demonstrates better settability than nylon. Whereas the set in PET is more or less permanent with time, nylon has a tendency to gradually lose its set over the time span of the experiment. In the case of nylon, the loss increases with the increasing recovery temperature. For nylon 6 set at 170 °C and having a degree of set of 85% when recovered at 23 °C, this value reduces to about 80% at 50 °C and 35% at 100 °C. For a similarly heat-set polyester, the degree of set remains unchanged over this range of temperatures.

The studies of Prevorsek and co-workers also indicate that set by crys- tallization from a non-crystalline or low crystalline state induces a higher degree of set than is obtained through partial melting and recrystalliza- tion. Thus, the level of crystallinity developed during the heat-setting operation is the major requirement for imparting a durable set.

REFERENCES

1. Smith, R.L., Pieters, R. and Morrison, M.E. (1972) *Trans. Soc. Rheol.*, **16**(3), 558–576.
2. Smith, F.S. and Steward, R.D. (1974) *Polymer*, **15**(5), 283.
3. Hearle, J.W.S. (1966) Skinner's Record, Aug–Sept, and Hearle J.W.S. (1971) in *The Setting of Fibres and Fabrics* (eds J.W.S. Hearle and L.W.C. Miles), Merrow Publishing Co., Watford, UK, chs 1, 5.
4. Parisot, A. and Bouriot, P. (1966) In *Bulk, Stretch and Texture*, Proceedings of the Annual Conference of the Textile Institute, Textile Institute, Manchester.
5. Dismore, P.F. and Statton, W.O. (1966) *J. Polym. Sci.*, **C13**, 133.
6. Dumbleton, J.H. (1969) *J. Polym. Sci.*, **A2**, 7, 667.
7. Koenig, J.L. and Hannon, M. (1970) *J. Appl. Phys.*, **41**(11), 4290–4295.
8. Wilson, M.P.W. (1974) *Polymer*, **15**(5), 277–282.
9. Valk, V., Jellinek, G. and Schroder, U. (1980) *Textile Res. J.*, **50**, 46–54.
10. Gupta, V.B. and Kumar, S. (1979) *J. Polym. Sci., Polym. Phys. Edn.*, **17**, 1307; *Idem* (1981) *J. Appl. Polym. Sci.*, **26**, 1865, 1877, 1885, 1897.
11. Gupta, V.B. (1995) *J. Textile Inst.*, **86**, 299.
12. Fakirov, S. (1990) Solid state reactions in linear polycondensates, in *Solid State Behaviour of Linear Polyesters and Polyamides* (ed. J.M. Schultz and S. Fakirov), Prentice Hall, Englewood Cliffs, NJ, pp. 1–74.
13. Warwicker, J.O. (1970) *J. Soc. Dyers and Col.*, **86**, 303–310; *Idem* (1971) *Br. Polym. J.*, **3**, 68–73; *Idem* (1972) *J. Soc. Dyers and Col.*, **88**, 142.
14. Hindeleh, A.P. and Johnson, D.J. (1971) *Polymer*, **11**, 666–680.
15. Sprague, J. (1960) *Textile Res. J.*, **30**, 697.
16. Galil, F. (1973) *Textile Res. J.*, **43**, 615.
17. Prevorsek, D.C., Butler, R.H. and Lamb, G.E. (1975) *Textile Res. J.*, **45**(7), 535–540.

Characterization of polymers and fibres

10

A.K. Gupta

10.1 INTRODUCTION

Characterization of manufactured fibres is an integral part of the fibre production process, as every manufacturing unit has to ensure that its products are as per the specifications. Though fibre characterization has significant areas of commonality with polymer characterization, the emphasis is often different, necessitating adaptation of the techniques to meet specific needs and sometimes the use of special techniques. However, fibre characterization has received relatively less attention than polymer characterization [1–3].

Characterization of the products at various stages of manufacture of fibres in the industry is essential for achieving the desired quality of the final products. In the case of most textile fibres characterization is required at the following stages.

1. Characterization at the molecular level, which involves measurement of molecular weight and molecular weight distribution and sometimes also the characterization of chemical structure.
2. Characterization of thermal properties, namely the measurement of temperatures of glass transition, melting, crystallization and decomposition.
3. Characterization of physical structure and morphology, specially the parameters which directly govern the properties of fibres. This includes the measurement of crystallinity, crystal size, crystal size distribution, average molecular and amorphous orientation and morphological studies through microscopy.

This chapter deals with the various techniques used in such characterization of fibres and their parent polymers.

10.2 CHARACTERIZATION AT THE MOLECULAR LEVEL

10.2.1 MOLECULAR WEIGHT AVERAGES [4–7]

Polymers are aggregates of large molecules comprising well-defined repeat units. The number of times the repeat unit occurs in a molecule is called its DP (degree of polymerization), and DP multiplied by M_0 (molecular weight of the repeat unit) is equal to the molecular weight of the polymer. An idea of the enormity of the molecules of fibres is obtained from the following example. A molecule of nylon 6 of molecular weight 22 500 has nearly 200 repeat units (molecular weight being 113 for the repeat unit of nylon 6 of chemical structure $-NH-(CH_2)_5-CO-$). Such a molecule would be about 1720 Å long, assuming the approximate length of the repeat unit as 8.6 Å. The conventional techniques for measurement of molecular weight of other materials are not entirely suitable for measuring such high molecular weights. The techniques used for polymers will be described here.

An important feature of polymers is that all their molecules are not of identical molecular weight. The molecular weight distribution, which influences the properties of the final product, must be characterized and controlled through appropriate variation of process parameters. Moreover, owing to the existence of a molecular weight distribution (MWD) in any polymer sample, the measured molecular weight is an average value. The different kinds of averages of molecular weight are defined below.

(a) Number average molecular weight

Number average molecular weight (usually denoted as $\bar{M}_n$) is defined as the total weight of all the molecules in a given sample divided by the total number of molecules

$$\bar{M}_n = \frac{\sum_i N_i M_i}{\sum_i N_i}$$

where N_i and M_i are respectively the number and molecular weight of the ith species of the molecules.

(b) Weight average molecular weight

Weight average molecular weight (usually denoted as $\bar{M}_w$) is defined as the total of the number of molecules multiplied by the square of

molecular weight of all the species divided by the total weight of all the species of the molecules present in the given sample:

$$\bar{M}_w = \frac{\sum_i N_i M_i^2}{\sum_i N_i M_i}.$$

(c) z Average molecular weight

This is a higher power average as defined by the following expression, and is useful in the interpretation of certain properties such as melt flow of polymers:

$$\bar{M}_z = \frac{\sum_i N_i M_i^3}{\sum_i N_i M_i^2}.$$

(d) Polydispersity

As their mathematical expressions show, the weight average molecular weight is always greater than the number average molecular weight in a polydisperse sample, while in the case of a monodisperse sample (i.e. one in which all molecules are of identical weight) both these averages have equal values. Thus the ratio $\bar{M}_w/\bar{M}_n$, which is equal to unity for monodisperse samples, has a value greater than unity in most practical cases. The value of this ratio is often described as a measure of polydispersity in the sample.

Since the final product's properties are dependent on both molecular weight and molecular weight distribution (MWD), the characterization at molecular level requires the measurement of molecular weight by more than one technique so as to obtain both these parameters.

Typical values of polydispersity of polymers prepared by different routes, listed in Table 10.1, show a wide range in many cases, suggesting the need for their appropriate control.

10.2.2 DETERMINATION OF MOLECULAR WEIGHT

The methods for molecular weight determination may be grouped in two classes:

Table 10.1 Typical values of polydispersity of polymers

Polymer type	$\bar{M}_w/\bar{M}_n$
Polymers prepared by addition polymerization	1.5–2.0
Polymers prepared by condensation polymerization	2.0
High conversion vinyl polymers	2.0–5.0
Branched polymers	20–50

1. primary or absolute methods, which determine molecular weight from first principles. These include end group analysis, osmometry, light scattering, etc.
2. secondary methods, which require calibration with known molecular weight standards, such as the methods based on viscometry and gel permeation chromatography. The secondary methods offer the advantage of experimental convenience.

(a) End group analysis [8, 9]

The number average molecular weight $\bar{M}_n$ of certain linear polymers can be found by estimating the number of end groups by chemical analysis. The end groups are often acidic or basic in type, as exemplified by the carboxylic groups of PET or the amino groups of conventional polyamides.

Measurement of amino end groups in conventional polyamides

The amino end groups in nylon are determined by dissolving 1 g of polymer in 25 ml methanol/phenol mixture (70% w/w phenol) by refluxing for 30 min. The contents are cooled and titrated against 0.02 N HCl using thymol blue as an indicator. A blank is also run.

$$\text{Amino end groups} = \frac{(A - B) \times \text{normality of HCl} \times 1000}{\text{weight of the sample}}$$

$$= NH_2 \text{ milliequivalent per kg}$$

where A is the volume in ml of 0.02 N HCl for the sample and B is the volume in ml of 0.02 N HCl for the blank.

Measurement of carboxyl end groups in nylon

The carboxyl end groups in nylon are determined by dissolving 1 g of sample in 25 ml benzyl alcohol by refluxing it for 30 min. The contents are then titrated with 0.02 N alcoholic KOH using phenolphthalein as an indicator. A blank is also run.

$$\text{COOH end groups} = \frac{(A - B) \times \text{normality of KOH} \times 1000}{\text{weight of the sample}}$$

$$= COOH \text{ milliequivalent per kg}$$

where A is the volume in ml of 0.02 N KOH for the sample and B is the volume in ml of 0.02 N KOH for the blank.

Measurement of carboxyl end groups in PET

Determination of carboxyl end groups in PET is important not only for calculating number average molecular weight (together with hydroxyl end groups), but also for the elucidation of damage to the polyester by hydrolysis, heat and light. In this method 4 g of PET chips are taken in a 250 ml round bottomed flask. Then 55 ml of a 2:3 phenol:chloroform mixture is added and the contents are refluxed for 2 h to dissolve the polymer. This is followed by cooling and titrating against 0.1 N KOH solution in benzyl alcohol using 0.5 ml tetrabromophenol as an indicator to blue end point. A blank experiment is also carried out.

$$\text{COOH groups} = \frac{(A - B) \times \text{normality of KOH} \times 1000}{\text{weight of sample}}$$

$$= \text{COOH milliequivalent per kg}$$

where A is the volume in ml of 0.1 N KOH for the sample and B is the volume in ml of 0.1 N KOH for the blank.

The molecular weight $\bar{M}_n$ can be calculated from the end group analysis using the following relationship:

$$\bar{M}_n = \frac{(\text{weight of polymer}) \times (\text{number of end groups per molecule})}{\text{total number of end groups determined}}.$$

(10.1)

The end group analysis method has a limitation that its sensitivity decreases with increasing molecular weight of the polymer, which restricts its use to molecular weights up to 20 000.

(b) Osmometry

Osmotic pressure is a colligative property that depends on the number of molecules, hence the molecular weight determined by this technique is the number average molecular weight. Two commonly used osmometers are those based on membrane or vapour phase osmometry.

Membrane osmometry

In this technique the solution is separated from pure solvent by means of a semipermeable membrane which only permits the passage of the solvent molecules. The solvent diffuses through the membrane so as to equalize the chemical potential on both sides. This diffusion causes an increase of pressure on the solution side, until an equilibrium is reached when the excess pressure on the solution side becomes equal to the osmotic pressure (Π). The osmotic pressure depends on the concentration
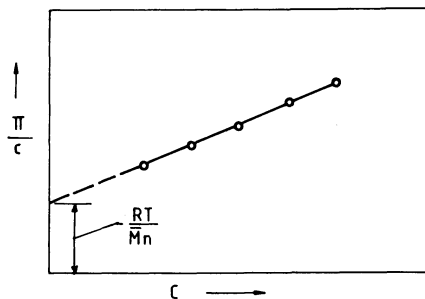
Fig. 10.1 Plot of π/c against c.

of the initial solution, in addition to the characteristics of the solute and solvent.

As a function of concentration c the specific osmotic pressure (Π/c) varies according to the van't Hoff equation

$$\frac{\pi}{c} = \frac{RT}{\bar{M}_n} + A_2 c \qquad (10.2)$$

where R and T are the gas constant and temperature respectively and A_2 is the second virial coefficient representing the solute–solvent interaction.

The experiment for determining the molecular weight of polymers involves the measurement of osmotic pressure at several concentrations, and then plotting the data as (Π/c) against c (see Fig. 10.1). The concentration of starting solution for this experiment is generally about 0.1–0.2%, which is diluted up to about one fourth of its value. The straight line passing through the data points may be extrapolated to give the intercept at zero concentration as $RT/\bar{M}_n$, from which $\bar{M}_n$ can be calculated. Furthermore, by equation (10.2) the slope of the experimental straight line must be equal to A_2. Thus the intercept and slope of the straight line passing through the experimental data enable us to determine the number average molecular weight and solute–solvent interaction.

Osmotic equilibrium takes several hours to reach, hence modern membrane osmometers are so designed that the pressure difference between the two sides of the membrane is produced by an electro-mechanical device which is just sufficient to prevent diffusion through the membrane.

The membrane is tightly held between two discs which have continuous spiral-shaped grooves to hold solvent and solution on the two sides of the membrane. These groove-like compartments are extended into the capillaries to measure the heights of liquid columns. The solution compartment is extended through a flexible tube so that the level can be lowered or raised to bring it to the level consistent with the osmotic pressure. An air bubble is inserted in the capillary connected to the solvent

compartment and its position is maintained at constant height by raising the level of the liquid in the solution side. In modern equipment an automatic electro-mechanical device is provided for this purpose. Thus an equilibrium is achieved in less than half an hour, and the pressure difference (i.e. hydrostatic pressure of the liquid column) is equal to the osmotic pressure corresponding to the initial concentration of the solution.

Another modern piece of equipment, which adds to operational convenience, is the Knauer membrane osmometer. This has a steel measuring cell divided into two halves by a semipermeable membrane. The lower half is filled with solvent and sealed while the upper half is filled with solution by injecting with a syringe. Diffusion of solvent through the membrane into the solution results in a negative pressure on the solvent side. A steel membrane constituting the lower part of the solvent chamber deflects under the action of the negative pressure, and this is detected as a change in capacitance of the electronic circuit calibrated in terms of osmotic pressure.

The semipermeable membranes used are generally regenerated cellulosics which are conditioned in the solvents prior to use. Conditioning sometimes involves successive immersions in a series of intermediate solutions of decreasing concentrations ending with 100% pure solvent.

Vapour phase osmometry

This technique is based on the lowering of vapour pressure, and is particularly suitable for low molecular weights. Here the transport of solvent to solution proceeds through vapour phase and involves the measurement of small temperature changes caused by condensation of solvent from the vapour on a dilute polymer solution.

The equipment consists of two matched thermistors enclosed in a thermostatted chamber. The chamber is initially saturated with solvent vapour at the given temperature. A small amount of solvent is placed on one thermistor and the solution is injected onto the other thermistor using a syringe. The difference in vapour pressure causes the solvent vapours to condense onto the solution with a resultant rise in temperature of the solvent due to the evolution of the latent heat of vaporization. The measured temperature difference is directly proportional to the difference of vapour pressure of the solution (p) and solvent (p_0), and the instrument is calibrated to read directly in terms of the vapour pressures. The polymer molecular weight $\bar{M}_n$ is then determined using the following equation:

$$\ln (p/p_0) = -\frac{V}{\bar{M}_n} c \qquad (10.3)$$

where V is the molar volume of the solvent and c is the concentration.

(c) Light scattering [1]

When a light beam passes through a solution, part of its intensity is lost due to scattering caused by optical discontinuities at solute–solvent boundaries. The scattering is quite considerable in polymer solutions, and depends on concentration as well as the shape and size of the molecules. This allows light scattering measurements to be used to determine the molecular weight and dimensions of polymers. For the case of a polydisperse sample, the light scattering method gives the weight average molecular weight.

In this method a monochromatic beam of light is made to pass through the sample solution kept in a glass-walled cell. The cell is surrounded by a thermostatted liquid whose refractive index matches that of the glass of the cell so as to avoid intensity loss due to scattering at the cell wall. From the intensity of the incident and transmitted light beam, a quantity called 'turbidity' can be calculated, which is a measure of the total loss of intensity due to scattering in all directions. The turbidity, τ, is defined as

$$\tau = \frac{1}{l}\ln\left(I_0/I\right) \tag{10.4}$$

where I and I_0 are transmitted and incident intensities and l is the length of the scattering medium traversed.

Another quantity which measures the light scattering from a given solution is the 'Rayleigh ratio', which is a measure of scattering at a given angle. The Rayleigh ratio, R_θ, at an angle θ from the direction of incident beam, is defined as

$$R_\theta = \frac{I_\theta r^2}{I_0} \tag{10.5}$$

where I_θ and I_0 are scattered intensity at angle θ and incident intensity, respectively, and r is the distance of the observer from the scattering volume.

For polymer solutions the following expressions have been derived from the basic theory of Rayleigh scattering.

$$\frac{Hc}{\tau} = \frac{Kc}{R_\theta} = \frac{1}{\bar{M}_w P(\theta)} + 2A_2 c \tag{10.6}$$

where

$$H = \frac{32\pi^3 n^2 (dn/dc)^2}{3N_0\lambda^4} \tag{10.7}$$

$$K = \frac{2\pi^2 n^2 (dn/dc)^2}{N_0\lambda^4} \tag{10.8}$$

and

$$\bar{R}_\theta \doteq R_\theta \text{ (solution)} - R_\theta \text{ (solvent)}. \tag{10.9}$$

Here (dn/dc) is the specific refractive index increment of the solution, n and c are refractive index and concentration, N_0 is Avogadro's number, λ is the wavelength of light, A_2 is the second virial coefficient related to solute–solvent interaction, and $P(\theta)$ is the particle scattering factor which is non-negligible (i.e. non-unity) when the scattering particles are larger than $\lambda/20$ in dimensions. A widely used expression relating $P(\theta)$ to the molecular dimensions (mean square radius of gyration $\langle s^2 \rangle$) is as follows:

$$\frac{1}{P(\theta)} = 1 + \frac{16\pi^2 n^2}{3\lambda^2} \langle s^2 \rangle \sin^2 (\theta/2). \tag{10.10}$$

It may be noted that at $\theta = 0$, $[P(\theta)]^{-1}$ becomes unity, hence the effect of molecular dimensions will not be discernible from the measurement of turbidity (i.e. for the measurement at $\theta = 0$). Hence the complete expression relating molecular weight and molecular dimensions, obtained by combining equations (10.6) and (10.10), may be written only for the case of Rayleigh ratio (R_θ) and not in terms of turbidity (τ). The final expression is therefore:

$$\frac{Kc}{\bar{R}_\theta} = \frac{1}{\bar{M}_w} + \frac{1}{\bar{M}_w} \left(\frac{16\pi^2 n^2}{3\lambda^2} \right) \sin^2 (\theta/2)\langle s^2 \rangle + A_2 c. \tag{10.11}$$

Thus from the light scattering measurements at several concentrations and over a range of fixed angles at each concentration, the three quantities $\bar{M}_w$, $\langle s^2 \rangle$ and A_2 can be determined with the help of equation (10.11) by making the sets of plots described below. A plot of $Kc/\bar{R}_\theta$ against c at constant θ (Fig. 10.2) results in a straight line, which when extrapolated to $c = 0$ gives the value of Kc/R_θ at the respective value of θ. The other set of plots is that of $Kc/\bar{R}_\theta$ against $\sin^2 \theta/2$ at constant c (Fig. 10.3), which
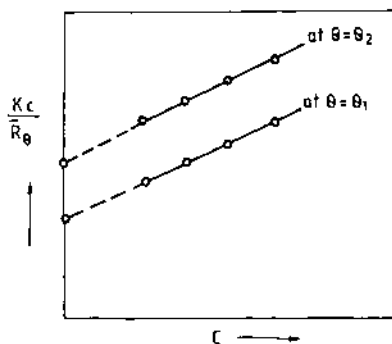
Fig. 10.2 Typical $Kc/\bar{R}_\theta$ vs. c plot.
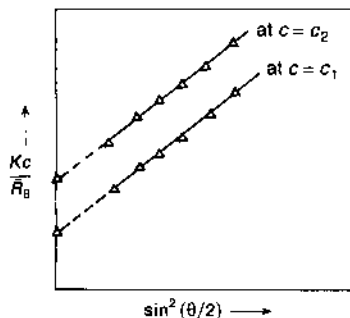
Fig. 10.3 Typical $Kc/\bar{R}_\theta$ vs. $\sin^2(\theta/2)$ plot.

is linear and gives, on extrapolation to $\sin^2 \theta/2 = 0$, the values of $(Kc/\bar{R}_\theta)_{\theta=0}$ at the respective concentration. Further plots are made using these extrapolated values, i.e. $(Kc/\bar{R}_\theta)_{c=0}$ against $\sin^2 \theta/2$ (Fig. 10.4) or $(Kc/\bar{R}_\theta)_{\theta=0}$ against c (Fig. 10.5), both of which are also linear and can be suitably extrapolated to yield the value of $(Kc/\bar{R}_\theta)_{\theta=0,c=0}$ which is equal to $1/\bar{M}_w$ according to equation (10.11). This allows the determination of the weight average molecular weight.

Furthermore, the mean square radius of gyration $\langle s^2 \rangle$ and second virial coefficient A_2 can be determined from the slopes of plots of $(Kc/\bar{R}_\theta)_{c=0}$ against $\sin^2 \theta/2$ and $(Kc/\bar{R}_\theta)_{\theta=0}$ against c, respectively, according to equation (10.11).
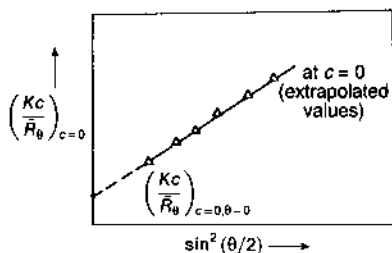
Fig. 10.4 Typical plot of the data obtained after the extrapolation shown in Fig. 10.2.
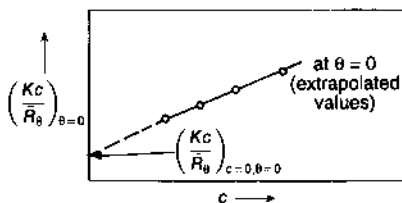
Fig. 10.5 Typical plot of the data obtained after the extrapolation shown in Fig. 10.3.
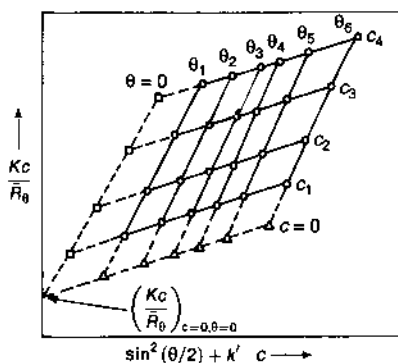
Fig. 10.6 Typical Zimm plot.

Conventionally, the whole assembly of the light scattering data are presented on a single plot combining all the above-mentioned sets of plots. This single plot is called the Zimm plot; a typical Zimm plot is shown in Fig. 10.6. Here k' is an arbitrary constant which is conveniently chosen as 100 or 1000, so as to achieve good separation of data points at different concentrations on the same ($\sin^2 \theta/2$) axis; or in other words to accommodate both the variables $\sin^2 \theta/2$ and c on the same axis without any overlap.

Light scattering photometer

A typical light scattering photometer is shown schematically in Fig. 10.7. It has a source of light (S), usually a mercury vapour lamp with a suitable filter (F) (the wavelength used is 546 nm), or an He–Ne laser of wavelength 633 nm. The light beam passes through a collimating lens (L) and a polarizer (P) and finally reaches the sample cell (S.C). The intensity of this incident beam is measured through the scattering from a liquid of known Rayleigh ratio, as the direct exposure of this incident light may damage the detector (which is usually a photomultiplier or a
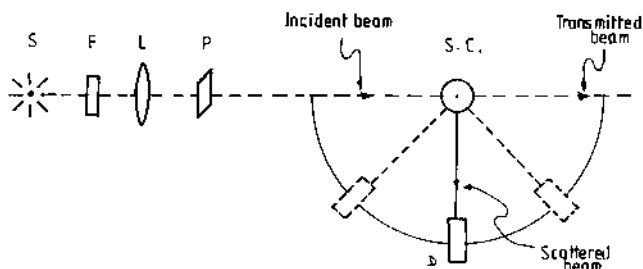
Fig. 10.7 The light scattering photometer.

photon counter). The detector (D) is mounted on a rotating table revolving about the axis, passing through the centre of the sample cell.

Two types of sample cells are generally used: one has a circular cross-section, which enables measurements at any angle, while the other one typically has a hexagonal cross-section, which is normally designed to make measurements at fixed angles of 45°, 90° and 135°. This latter type of sample cell uses the ratio of scattering at 135° and 45° through appropriate correction terms to account for the large particle size effect, in place of $P(\theta)$ described in equation (10.6) above.

(d) Viscometry

Polymer solutions show very high viscosity which varies not only with concentration but also with molecular weight. This property of polymers has been used as a method of determining the molecular weight of polymers.

A parameter called 'intrinsic viscosity' (also called 'limiting viscosity number' in modern nomenclature), denoted with brackets as $[\eta]$, is strongly dependent on the molecular dimensions of the solute particles. Since molecular dimensions depend on molecular weight, suitable calibration curves have been developed which lead to a well-known relation called the Mark–Houwink equation:

$$[\eta] = K\bar{M}^a \qquad (10.12)$$

where K and a are constants and $\bar{M}$ is the molecular weight of the polymer. $\bar{M}$ may represent $\bar{M}_n$ or $\bar{M}_w$, depending on the molecular weight average used in the calibration curve.

The intrinsic viscosity $[\eta]$ is defined as follows:

$$[\eta] = \lim_{c \to 0} \left(\frac{\eta - \eta_0}{\eta_0 c} \right) = \lim_{c \to 0} \left(\frac{\eta_{sp}}{c} \right) \qquad (10.13)$$

where η and η_0 are the viscosities of the solution and the solvent, respectively, and c is the concentration. The last expression on the right-hand side is simply to define the symbol η_{sp} (specific viscosity) in subsequent discussion. The intrinsic viscosity is therefore determined by plotting η_{sp}/c against c and extrapolating the plot to zero concentration, as shown in Fig. 10.8.

The experiment for determination of intrinsic viscosity involves the measurement of solution viscosity at about four concentrations and the viscosity of the solvent under identical conditions. In the capillary viscometer the time of flow is measured in the same capillary for all experiments and the specific viscosity is calculated as $(t - t_0)/t_0$, where t and t_0 are the times of flow for the solution and the solvent, respectively; the constant of proportionality between η and t will be identical in
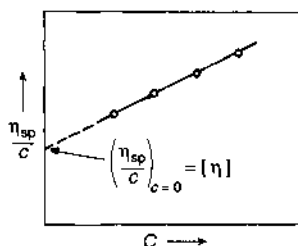
Fig. 10.8 Typical plot of data for determining intrinsic viscosity.

all cases and will thus mutually cancel out in the numerator and the denominator.

Thus, after determining the intrinsic viscosity of a given polymer sample in any solvent at a fixed temperature, the molecular weight can be calculated through equation (10.12) using appropriate values of the constants K and a. The values of these constants are found in the *Polymer Handbook* (eds J. Bandrup and E.H. Immergut, Wiley, New York, 1975) for a wide variety of polymer–solvent systems at various temperatures. For any new system, for which the K and a values are not known, the general practice is to take the values reported for the system with the closest resemblance.

Furthermore, the K and a values reported in the literature are based on calibrations using molecular weights determined by some other technique, hence the values of K and a reported in the *Polymer Handbook* clearly state whether they were based on $\bar{M}_n$ or $\bar{M}_w$ (i.e. osmometry or light scattering values). Thus, the molecular weight calculated by equation (10.12) would be a 'number average' or 'weight average' value depending on the technique used for the determination of K and a.

Another type of molecular weight average, called the 'viscosity average' molecular weight $\bar{M}_v$, which is required in theoretical development of various solution properties of polymers, can be calculated from the value of exponent a using the following expression:

$$\bar{M}_v = \left[\frac{\sum_i N_i M_i^{(1+a)}}{\sum_i N_i M_i} \right]^{1/a} \tag{10.14}$$

where N_i and M_i are number and molecular weights of the ith species.

(e) Gel permeation chromatography

Gel permeation chromatography (GPC) is quite useful for routine estimate of molecular weight, owing to its convenience and the possibility of simultaneous evaluation of various averages of molecular weight, thus providing information about the molecular weight distribution.
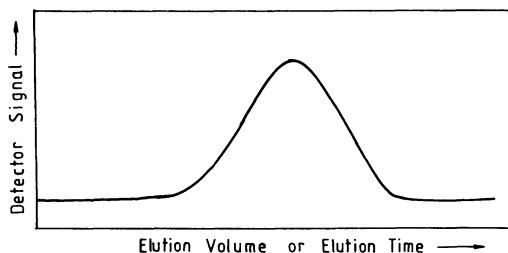
Fig. 10.9 Typical GPC curve for a polydisperse polymer sample.

The GPC technique is based on the separation of solute molecules according to their sizes by passing the polymer solution through a column packed with microporous gel particles. A known small volume of polymer solution is injected into an already stabilized current of the solvent through the column, and then the out-flowing liquid from the column is analysed for the concentration of the solute as a function of time. Separation of molecules occurs by their preferential penetration into the pores of the gel filled in the column, depending on their sizes. Small molecules penetrate more easily than the larger ones, while the very large ones may either partially penetrate or not penetrate at all. Thus, during the passage of the solution through the column the largest molecules will take the shortest time while the smallest ones will take the longest time to elute from the column. The eluting liquid passing through a detector is measured for its solute concentration through its refractive index or optical density. The detector signal, which is proportional to the solute concentration, thus gives a trace as a function of time or elution volume, as shown in Fig. 10.9 for a polydisperse polymer sample.

Molecular weight averages from a GPC curve

The set of columns used in a GPC experiment can be calibrated with narrow molecular weight distribution polymer samples of known molecular weight to provide the elution volume as a function of molecular weight. Standard monodisperse polystyrene samples in a wide range of molecular weights are commercially available for this purpose. Any set of columns to be used for an experiment has to be freshly calibrated. This is done by injecting the solutions of four or five different standard samples and recording the GPC curves, which eventually show sharp peaks corresponding to each individual sample at their respective elution volumes. The plot of molecular weight against elution volume is generally linear, as shown in Fig. 10.10. The calibration curve deviates from linearity if the range of molecular weights used is very wide.
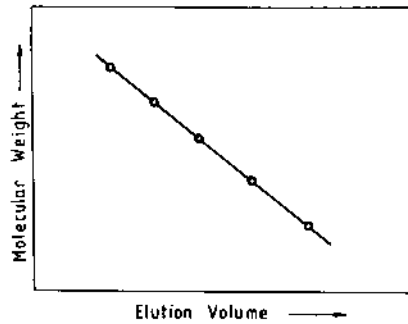
Fig. 10.10 Typical GPC calibration curve.

With the use of the calibration curve, the GPC curve experimentally recorded as 'detector signal vs. elution volume' can be converted into 'detector signal vs. molecular weight' by converting each point of the abscissa of Fig. 10.9 (i.e. elution volume) into the corresponding value of molecular weight determined from Fig. 10.10. After doing this, the next step is the calculation of various molecular weight averages, which is described below.

The GPC curve, with elution volume axis converted to molecular weight, is subdivided into narrow strips, as shown in Fig. 10.11. Each strip corresponds to one species of molecules, which may be denoted by the subscript i, where $i = 1, 2, 3, \ldots$. The height of a strip, h_i, is proportional to the solute weight of that species, such that $h_i = N_i M_i$, where N_i and M_i are respectively the number of molecules and molecular weight of the ith species. In this way, the data for all the n strips can be tabulated as shown in the first three columns of Table 10.2. Note that in the relationship $h_i = N_i M_i$ the constant of proportionality is ignored, simply because this gets cancelled in the numerator and denominator of the expressions of the molecular weight averages. From the data thus collected in the first three columns, the other relevant quantities like
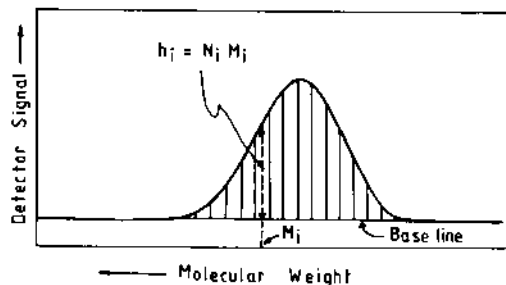
Fig. 10.11 Subdivision of the GPC curve into narrow strips for calculation purposes.

Table 10.2 Quantities calculated from the GPC curve

1 Strip no. i	2 M_i	3 $h_i = N_i M_i$	4 $h_i M_i = N_i M_i^2$	5 $h_i / M_i = N_i$
1				
2				
$\vdots$				
n				
Total	$\sum_i M_i$	$\sum_i N_i M_i$	$\sum_i N_i M_i^2$	$\sum_i N_i$

$N_i M_i^2$, N_i, etc. may be calculated as shown in the last two columns of Table 10.2. The summations of each column provide the quantities given at the bottom of the column, which are the same as required for the calculation of various molecular weight averages from the expressions stated earlier, e.g. number average molecular weight is obtained by dividing the quantity at the bottom of column 3 by that of column 5; and weight average molecular weight is determined by dividing the summation quantity of column 4 by that of column 3.

Molecular weight distribution

The knowledge of $\bar{M}_w$ and $\bar{M}_n$ enables the description of polydispersity of any given sample, through the value of the ratio $\bar{M}_w / \bar{M}_n$. Thus, with the use of GPC, it is possible not only to evaluate molecular weight of the sample, but also the polydispersity or the molecular weight distribution (MWD).

The GPC data can be summed to give the integral or cumulative weight distribution curve, which is normalized to give the total weight of the sample as unity. The differential of this curve gives the differential weight distribution of the given polymer sample, which enables the estimation of the weight fraction eluted up to any given elution volume or time (or with molecular weight less than any specified value M).

GPC equipment

The main components of GPC equipment, shown schematically in Fig. 10.12, are:

1. solvent delivery system to maintain a constant linear velocity of flow through the column;
2. column containing microporous gel particles of an appropriate range of pore sizes (columns filled with Styragel^{TM}, a crosslinked polystyrene, are commonly used);
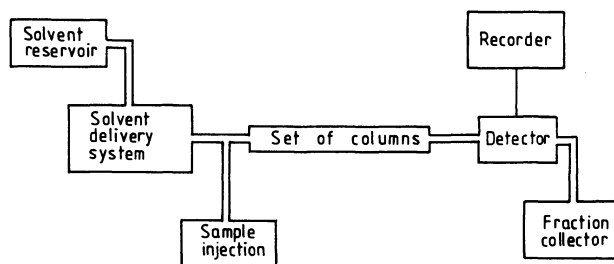
Fig. 10.12 Schematic representation of a GPC system.

3. injection system for injecting small volumes of sample solution without disturbing the solvent flow;
4. detector system to monitor the output from the column on a continuous basis;
5. recorder to give a continuous tracing of detector signal as a function of time (which is proportional to elution volume in the case of linear velocity of flow).

Some modern GPC equipment incorporates an automatic data handling facility to convert the recorded data into molecular weight averages.

10.3 CHARACTERIZATION OF PHYSICAL STRUCTURE

Characterization of the structure in the bulk state is essential for the structure–property correlation of polymers and fibres. The packing of long polymer chains in a three-dimensional structure is largely governed by their molecular characteristics (like flexibility, linearity and structural regularity) and intermolecular interactions and external constraints (like temperature, stress, etc.). In general, polymers and fibres have a two-phase structure comprising an ordered (also called crystalline) and a disordered (also called amorphous) phase. Owing to the long molecules and restrictions on their free mobility, it is impossible for polymers to form a 100% crystalline structure. However, a 100% amorphous structure is formed in those polymers which cannot crystallize owing to the complete irregularity in the chemical structure along the molecular chain (for example, atactic polymers).

Most fibre-forming polymers are semicrystalline and their structure (or properties) can be varied through manipulation of the process variables at the manufacturing stage. The structural parameters which are commonly used for correlation with properties are:

1. crystallinity, or the fraction of crystalline structure (often expressed as a percentage by multiplying the fractional crystallinity by 100);

2. crystallite size, or the average value of the crystallite thickness in the specified direction. At identical value of crystallinity, the structure may differ in terms of mean crystallite size;
3. orientation of the molecules in the structure. This is relevant to fibres and films and greatly influences their properties. The molecules in amorphous regions as well as the crystallites have a high degree of orientation in the direction of fibre axis; the former is called 'amorphous orientation' while the latter is called 'crystalline orientation'.

Five techniques that are widely used for characterizing the physical structure of fibres are (1) density measurement, (2) optical birefringence, (3) X-ray diffraction, (4) small angle X-ray scattering and (5) infrared spectroscopy.

10.3.1 DENSITY MEASUREMENT

Owing to regular packing of the molecules, the crystalline phase has a higher density than the amorphous phase. Thus the total density of a given polymer or fibre will depend on the crystallinity of the sample. An accurate measurement of density may thus be used for estimating crystallinity.

The specific volume (i.e. the volume per unit mass) of a semicrystalline polymer may be expressed by the simple additivity rule

$$V = XV_c + (1 - X)V_a, \tag{10.15}$$

where X is the mass fraction of the crystalline phase and V_c and V_a are specific volumes of crystalline and amorphous phases, respectively. If specific volume is replaced by density ρ, i.e. $V = 1/\rho$, then the above equation yields

$$\frac{1}{\rho} = X\frac{1}{\rho_c} + (1 - X)\frac{1}{\rho_a} \tag{10.16}$$

where the subscripts a and c refer to the amorphous and crystalline phases, respectively. This equation may be simplified to yield

$$X = \left[\frac{\rho - \rho_a}{\rho_c - \rho_a}\right]\frac{\rho}{\rho_c}. \tag{10.17}$$

Thus the fractional crystallinity (or the per cent crystallinity $100X$) can be determined by measuring the density of the given sample and using the literature values of ρ_a and ρ_c (i.e. densities of perfectly amorphous and perfectly crystalline sample) for the given polymer.

The value of ρ_a is estimated by preparing a completely amorphous sample by suitable quenching and measuring its density, while ρ_c is calculated theoretically from the structure and geometry of the crystalline unit cell (because of the impossibility of forming a 100% crystalline

Table 10.3 Densities of crystalline and amorphous phases of some fibre-forming polymers

Polymer	ρ_c (g cm^{-3})	ρ_a (g cm^{-3})
Poly(ethylene terephthalate)	1.515	1.335
Nylon 6	1.210	1.090
Polypropylene	0.936	0.850

structure in polymers). The literature values of ρ_a and ρ_c for some common fibre-forming polymers are given in Table 10.3.

With the advent of the density gradient column, the measurement of density of fibres has become quite convenient. The technique is used for routine testing in industrial laboratories.

The density gradient column is a 1 m long glass tube held vertically in an enclosure containing thermostatted liquid. The column is filled with a mixture of two partially miscible liquids in proportions varying gradually up the column, thus showing a gradual variation of density from bottom to top.

The column is prepared by mixing the two liquids through a two-flask device shown in Fig. 10.13. Initially both flasks A and B are filled to the same level with the chosen low and high density liquids, respectively. Then the liquid from flask B is gradually allowed to flow into the column; the flow is directed down the column wall to avoid turbulence. This is followed by the flow of liquid from flask A to B to equalize the
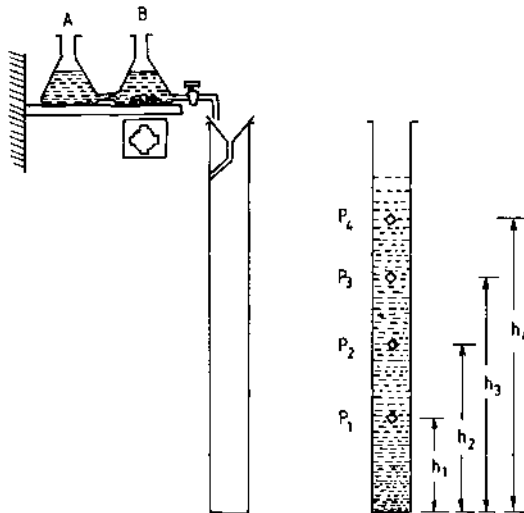
Fig. 10.13 Preparation of a density gradient column.

Table 10.4 Appriximate densities at room temperature of some liquids used in density gradient columns

Liquid	Density $(g\,cm^{-3})$
n-Heptane	0.7
Isopropanol	0.8
Diethylene glycol	1.1
Carbon tetrachloride	1.6
Pentachloroethane	1.7
Ethylene dibromide	2.2
Tetrabromoethane	3.0

level in the two flasks. The magnetic stirrer provided in flask B does the mixing which readjusts the density of liquid in flask B to a lower value. In this way, the liquid flowing to the column from the flask B gradually decreases in density and thus a gradient of density is produced in the column. The column is left for a few hours to stabilize and then it is ready for measurements. A list of the liquids used in a density gradient column of varying ranges of densities is given in Table 10.4. The density gradient column is calibrated for its density as a function of height with the help of standard floats of known densities. The standard floats are immersed into the column and simultaneously the given sample of unknown density is also immersed. After several hours the positions of the floats and the unknown sample stabilize at the points where their densities match with the density of the liquid column. The heights of the floats are then measured with the help of a telescope sliding on a graduated vertical scale. Thus a calibration curve (Fig. 10.14) is prepared as the plot of height against density of the standard floats.

From this calibration curve the density of the unknown sample ρ can be determined by finding the point corresponding to its height in the column h (shown as a square in the figure) and reading off its
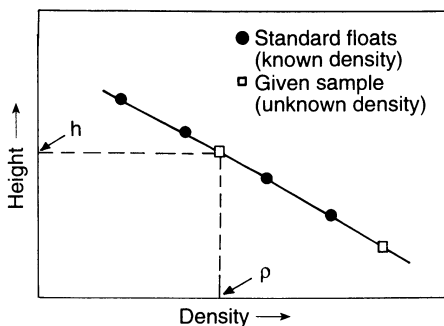
Fig. 10.14 Calibration curve for a density gradient column.

corresponding density on the abscissa of the calibration curve (as indicated by a dashed line in the figure).

10.3.2 OPTICAL BIREFRINGENCE [10]

Birefringence is defined as the difference between values of refractive index measured in two orthogonal directions. In the case of fibres, the molecules have a preferred orientation in the direction of the fibre axis, hence the refractive indices measured with the plane of polarization parallel (i.e. $n_{\parallel}$) and perpendicular (i.e. $n_{\perp}$) to the fibre axis will have different values; the difference Δn is called the birefringence.

$$\Delta n = n_{\parallel} - n_{\perp}. \tag{10.18}$$

The magnitude of the birefringence depends on the degree of orientation and on the characteristics of the chemical bonds present in the molecules (i.e. their bond polarizability, etc.).

Birefringence can be measured using a setup like that shown schematically in Fig. 10.15. Plane polarized light travelling in the x-direction is incident on the specimen kept with its prominent axis (the fibre axis in the case of fibres) parallel to the vertical axis (z-axis). The plane of polarization is such that the electric vector vibrates in the yz plane at an angle of 45° to the vertical (or z-axis).

If the amplitude of the electric vector is A, then its components in the y and z directions will be $A/\sqrt{2}$. These two components travel at different velocities. If n_{xy} is the refractive index for light with its plane of polarization in the xy plane and n_{xz} is the refractive index for light with its plane of polarization in the xz plane, then the path difference between the two components after traversing the specimen of thickness Δx will be $\Delta x(n_{xz} - n_{xy})$, which is called the relative retardation.

For fibres, which are oriented along the fibre axis, the refractive index in the other two perpendicular directions will be identical, hence $n_{xz} - n_{xy} = n_{\parallel} - n_{\perp} = \Delta n$, the birefringence. Thus the determination of birefringence is based on the measurement of relative retardation, namely $\Delta x \Delta n$.

The phase difference between the two components is $(2\pi/\lambda)$ (path difference) $= (2\pi/\lambda)(\Delta x \Delta n)$, where λ is the wavelength of the light. The amplitudes of the two components will be $A/\sqrt{2}$ and

Source   Polarizer   Specimen   Compensator   Analyser   Observer
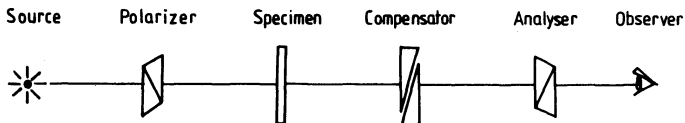
Fig. 10.15 Setup for measuring birefringence.

$(A/\sqrt{2})\cos(2\pi\Delta x\Delta n/\lambda)$. When the analyser is set at 90° to the polarizer, the amplitudes of the two components after passing through the analyser will reduce to $(A/\sqrt{2})\cos 45°$ and $(A/\sqrt{2})[\cos(2\pi\Delta x\Delta n/\lambda)]\cos 135°$, respectively, giving a resultant of $A[1 - \cos(2\pi\Delta x\Delta n/\lambda)]/2$ on recombination.

Hence the birefringence may be determined by measuring the intensities of the incident and transmitted light or by the compensator method described below.

A compensator is a birefringent device that can be adjusted to compensate for relative retardation imposed by the specimen. One such compensator, the Babinet compensator, consists of two birefringent quartz wedges cut with their optical axes perpendicular to one another. Thus for light travelling in the x-direction with its plane of polarization in the xz plane, the optical pathlength is greater near the top than at the bottom of the assembly. On the other hand, the light with xy as its plane of polarization has an optical pathlength larger near the bottom than at the top. Hence, the relative retardation varies along the length of the compensator and consequently fringes are seen.

Thus, by measuring the displacement required for one of the wedges to shift the fringes by one fringe spacing, the compensator can be calibrated for relative retardation. In this way, from the measured relative retardation produced by a specimen of thickness Δx, the birefringence Δn is calibrated from the following relationship:

$$\text{relative retardation} = \Delta x \Delta n.$$

(a) Orientation from birefringence

If the fibre is assumed to be made up of transversely isotropic units whose axes of symmetry are inclined at an angle ϕ to the fibre axis, the average molecular orientation in the fibre is represented by a quantity called the Hermans orientation function f defined as

$$f = (1/2)(3\overline{\cos^2\phi} - 1) \tag{10.19}$$

where the bar over $\cos^2\phi$ denotes its average value. The orientation function f equals unity for the case of perfect orientation as $\cos^2\phi = 1$ in this case and f equals zero for completely random orientation as $\cos^2\phi = 1/3$ in this case.

The orientation function and the birefringence are related as follows:

$$\Delta n = (\Delta n_{\max}/2)(3\overline{\cos^2\phi} - 1) \tag{10.20}$$

where $\Delta n_{\max}$ is the maximum theoretical birefringence, which is the value of birefringence for the case of perfect orientation of the fibre. In other words, the orientation function, which is directly proportional to

the birefringence, is obtained by dividing the sample's birefringence by its maximum theoretical birefringence.

It may be noted that the optical birefringence depends on the orientation of the chemical bonds in the chain. Hence the orientation of the molecular chains in both amorphous and crystalline phases will contribute to the value of the orientation function determined from the optical birefringence. Such an orientation function is thus called the 'overall orientation function', as distinct from the 'crystalline orientation function' determined by X-ray diffraction.

10.3.3 X-RAY DIFFRACTION [11–13]

X-ray diffraction may be used to estimate crystallinity, crystallite size and degree of orientation of crystallites, in addition to its traditional application for the determination of crystallographic structure.

X-rays, which have wavelengths comparable to interatomic distances, are quite appropriate for measuring the crystalline structure of polymers. A crystalline structure is a three-dimensional regular packing of atoms. A large number of sets of parallel planes can be considered to pass through any regular three-dimensional array of atoms. Some of these are more sensitive than others to the reflection of an X-ray beam, depending on the total electron density of the atoms in the set of planes. Thus the incident X-ray beam reflected through such sets of planes may interfere constructively to produce enhanced intensity, which produces a diffraction point on a photographic plate or a maximum in the diffraction pattern recorded through a detector. The condition for such constructive interference, or the occurrence of a diffraction maximum, is described by Bragg's equation:

$$2d \sin \theta = n\lambda \qquad (10.21)$$

where d is the interplanar spacing, θ is the Bragg angle (or half the angle between incident and diffracted beam directions), λ is the wavelength of the X-rays and n is the order of diffraction (usually $n = 1$ for the most intense diffraction maxima).

Fibres have high degree of crystallite orientation, hence their diffraction patterns are recorded using two types of samples:

1. powder samples, where the fibres are cut into small pieces (almost like a powder) and mixed randomly to form a compressed pellet. Thus the crystallites are randomly oriented and one obtains the diffraction maxima in the form of uniform intensity circles (Fig. 10.16(a));
2. fibre samples, where the fibres are held mutually parallel and straightened along their fibre axis in a bunch. Owing to the preferred
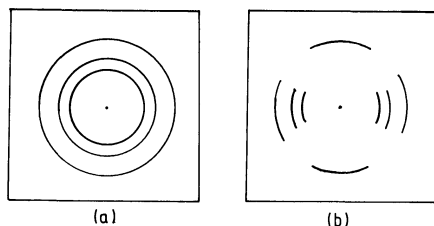
Fig. 10.16 X-ray diffraction patterns from (a) powder sample (unoriented) and (b) fibre sample (oriented).

orientation of crystallites, the diffraction maxima appear as arcs with arc length depending on the degree of orientation (Fig. 10.16(b)). The greater the degree of orientation, the smaller is the arc length.

In the case of the 'powder pattern', since the intensity is uniform over the entire circle (Fig. 10.16(a)), it is useful to record the diffraction pattern directly as a radial scan for the purpose of calculation of crystallinity and crystallite size. A radial scan is preferable, as it takes much less time than the recording of the diffraction pattern on a photographic plate. In the case of the 'fibre pattern' (Fig. 10.16(b)), a radial scan is not taken simply because it would not be identical along all the radial directions. Thus for the determination of degree of orientation the fibre pattern recorded on a photographic plate is used for further calculation, as will be described.

The most common arrangement of the X-ray diffractometer is shown in Fig. 10.17. The powder sample is mounted on the sample holder such that its surface is sufficiently flat. An X-ray beam, which is slightly divergent even after collimation, impinges on the sample which is rotated slowly. At any given position of the sample with respect to the incident beam, the intensity of the reflected beam reaching the photon counter is measured and recorded on an $X–Y$ recorder whose X axis is coupled with the photon counter while the Y axis is coupled with the rotation of the sample. Thus the plot of intensity (I) against diffraction angle (2θ) is obtained.
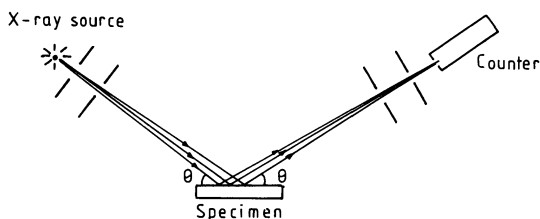
Fig. 10.17 X-ray diffractometer setup.
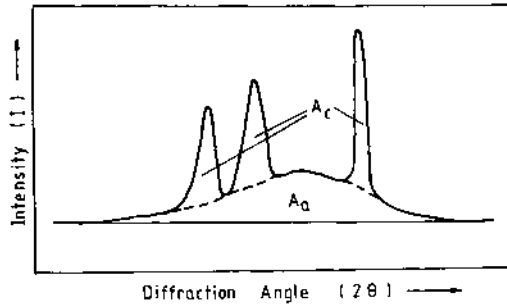
Fig. 10.18 Typical X-ray diffraction scattered intensity plot for a semicrystalline polymer.

(a) Calculation of crystallinity

In the case of semicrystalline polymers the diffraction pattern has not only the sharp diffraction maxima but also a diffuse scattering due to the amorphous phase spread over a wide range of diffraction angles. A typical diffraction pattern (the radial scan) for a semicrystalline polymer is shown in Fig. 10.18. This has three intense diffraction maxima due to the crystalline phase superposed on the diffuse scattering (i.e. below the dotted line curve) due to the amorphous phase.

Estimation of crystallinity is based on the separation of the intensities due to the amorphous and crystalline phases on the diffraction pattern. The three most common ways of achieving this separation are:

1. by recording the diffraction pattern of a completely amorphous sample, and then subtracting the area of this pattern from the area of the total diffraction pattern to obtain the area due to crystalline diffraction;
2. by judicious extrapolation of the amorphous diffraction pattern intensity and then doing similar subtraction to obtain the area due to crystalline diffraction. This method (2) is often preferred to avoid the extra experimentation involved in method (1) and the difficulties of making a perfectly amorphous sample;
3. by using a computer aided curve resolving technique in which the diffraction profile is assumed to be the sum of crystalline peaks corresponding to the principal planes and an amorphous peak and linear background. After deconvolution, the peak areas can be measured and crystallinity estimated.

Thus, after the separation the total area of the diffraction pattern is divided into two parts: the crystalline (A_c) and amorphous (A_a) components. In Fig. 10.18, the area between the baseline and the dotted line curve is the amorphous component A_a, while the area between the

dotted line curve and the diffraction curve is the crystalline component A_c. The per cent crystallinity X_c (%) of the sample is thus determined from the ratio of crystalline area to the total area through the following expression:

$$X_c \ (\%) = \frac{A_c}{A_a + A_c} \times 100 \ (\%). \tag{10.22}$$

(b) Determination of crystal size

For small crystals the line-broadening effect in the X-ray diffraction pattern is significant. For example, when a crystal is oriented close to but not exactly at the Bragg position, the diffracted intensity would be zero only for large perfect crystals which provide the possibility of complete destructive interference of all scattered waves due to the large number of scattering sites they contain. On the other hand, if the crystal is small, complete cancellation of the intensity of all the scattered waves is not possible, and a residual intensity remains even when the crystal setting departs from the Bragg position. Thus the small crystal size results in line-broadening in X-ray diffraction. The line-broadening is related to crystal size by Scherrer's equation:

$$t = \frac{K\lambda}{B \cos \theta} \tag{10.23}$$

where t is the crystal thickness (in the same units as λ) in the direction perpendicular to the lattice planes corresponding to the diffraction line in question. B is the half-width (in radians) of the diffraction line, θ is the Bragg angle, λ is the wavelength of the X-rays and the constant K has a value close to 0.9.

Thus the crystallite size corresponding to each diffraction maximum can be determined from the measurement of the half-width of the diffraction peak.

(c) Determination of crystalline orientation

As already stated, orientation of crystallites results in the formation of arcs in the X-ray diffraction pattern recorded on a flat photographic plate. The degree of orientation may be related to the angle subtended by the arc.

A more complete appraisal of the orientation can be made by measuring the intensity of the arc at selected intervals, as shown in Fig. 10.19. The intensity can be plotted against the azimuthal position (i.e. as a function of azimuthal angle ψ), as in Fig. 10.19(b). The degree of orientation of the crystallites will determine the shape of the azimuthal scan.
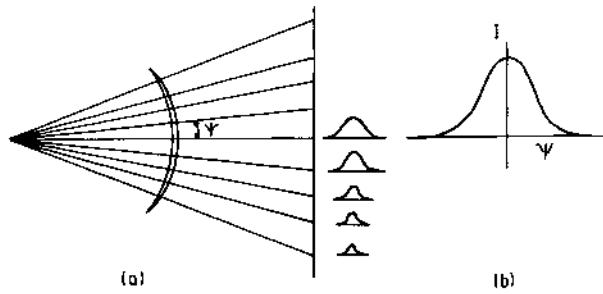
Fig. 10.19 (a) Intensity profiles at various azimuthal angles. (b) Azimuthal intensity profile.

Hermans orientation function for crystalline orientation, f_c, is defined as

$$f_c = 1 - (3/2)\overline{\sin^2 \phi} \tag{10.24}$$

where ϕ is the angle between the c-axis of the unit cell and the fibre axis. The average value of $\sin^2 \phi$ is given by the expression

$$\overline{\sin^2 \phi} = \frac{\int_0^{\pi/2} I(\phi) \sin^3 \phi \, d\phi}{\int_0^{\pi/2} I(\phi) \sin \phi \, d\phi}. \tag{10.25}$$

For meridional planes, the angle ϕ has the same significance as the azimuthal angle ψ. However, this will not be true for off-meridional planes. As stated earlier, for perfect orientation $f_c = 1$ and for perfectly random orientation $\sin^2 \phi = 2/3$, hence $f_c = 0$.

10.3.4 SMALL ANGLE X-RAY SCATTERING

As stated in the previous section the X-ray scattering intensity at any angle is governed by Bragg's equation (equation (10.21)), which predicts that the dimension of regularity of the order d (or repeat distance in the order–disorder structure, or the interplanar distance in the crystalline structure) varies inversely with the angle of scattering 2θ. Thus a structure which has an order corresponding to large repeat distances will produce scattering intensity maxima at low values of θ. Such large repeat distances correspond to the so-called long period, i.e. the average vertical distance between two crystallites in the fibril (which is also equal to the average value of the size of a crystallite) and an amorphous zone (see Fig. 10.20).
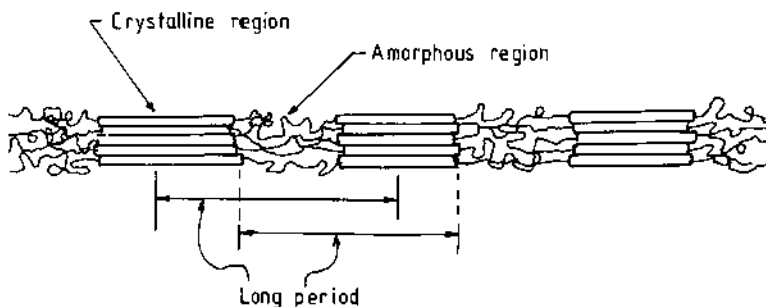
Fig. 10.20 The long period of a semicrystalline polymer.

The long periods of semicrystalline polymers or fibres are of the order of 100 Å or more. Regularity of similar magnitude occurs in solution-grown single crystals. A simple calculation of the value of θ corresponding to this high value of $d = 100$ Å for X-rays of wavelength $\lambda = 1.54$ Å and for the first order of diffraction, i.e. $n = 1$, from the Bragg equation (equation (10.21)), yields a 2θ value of around $1°$ or less. Such low values of θ are not within the measurable limits of the conventional X-ray diffraction equipment used in the wide angle X-ray scattering (WAXS) or the X-ray diffraction technique described in Section 10.3.3. Small angle X-ray scattering (SAXS) is thus a versatile technique for measuring the regularity of large dimensions in the structure of fibres.

(a) The SAXS equipment

The SAXS technique requires precise measurement of intensity at small angles, quite close to the direct beam. Hence the equipment has to be designed so as to avoid the excessive exposure due to the direct beam intensity. Also, to increase the angular range of the diffracted beam, the distance between the sample and the detector (or the photographic film) has to be quite large. For such a large pathlength of the scattered beam, it is essential to evacuate the path so as to avoid the loss of intensity due to scattering from air. Thus the SAXS camera has to be larger than the WAXS equipment and requires evacuation.

Modern SAXS instruments provide plots of intensity against 2θ. Alternatively, photographs can be obtained or two-dimensional iso-intensity contours can be plotted.

10.3.5 INFRARED SPECTROSCOPY [1, 14–21]

Infrared (IR) spectroscopy provides detailed information on polymer structure through the characteristic vibrational energies of the various

groups present in the molecule. The vibrational frequencies are sensitive to the molecular environment, chain conformation and morphology of the polymers. In IR spectroscopy the vibrational energies are detected by scanning the transmitted intensity continuously through the frequency range. The energies of molecular vibrations correspond to the electromagnetic radiation wavelength range 2.5–25 μm, or in terms of wavenumber 4000–400 cm^{-1}. The frequency and wavenumber are related as follows: frequency in wavenumber $(cm^{-1}) = 10^4/$wavelength in μm. Sometimes the boundary ranges are also of interest, namely the near-infrared (NIR) from 0.7 to 2.5 μm (14 000 to 4000 cm^{-1}) and the far-infrared (FIR) from 50 to 800 μm (200 to 12 cm^{-1}).

(a) Group frequency approach [1]

Interpretations of IR spectra are mostly based on an empirical approach, using the concept of group frequencies, i.e. vibrational frequencies of particular chemical groups in the molecules (e.g. C=O, CH_3, CH_2, CH, OH, etc.) behave largely independently of the rest of the molecule. Thus it is possible to assign particular absorption bands to vibrations in the groups by reference to standard correlation tables. However, when the coupling between neighbouring groups is significant, the absorption bands shift on the frequency scale. These spectral shifts provide valuable information on the molecular environment of the particular groups, as for example the effect of changing molecular conformations, variation in intermolecular interactions, etc. Such effects are more prominent on bending modes than on stretching modes, since the force constants are greater for bond stretching than for bending.

(b) Quantitative analysis [1]

The decrease in intensity of the light passing through an absorbing medium may be expressed by the Beer–Lambert law

$$A = \log{(I_0/I)} = \varepsilon cl, \tag{10.26}$$

where A is the absorbance, I_0 is the incident intensity and I is the intensity of transmitted light after passing through a length l of the medium, c is concentration of the absorbing species and ε is the absorptivity or extinction coefficient of the medium. The transmittance $T (= I/I_0)$ is measured as a function of wavelength (or wavenumber) while recording the IR spectra. Thus the concentration of an absorbing species can be determined by application of the Beer–Lambert law if the extinction coefficient of the species at the particular wavelength is known.

(c) Experimental techniques

IR spectrometers [1]

Conventional IR spectrometers are double beam spectrometers where the source emits radiation over the whole IR region. Suitable monochromators are used to select the desired wavelength for sample illumination. Detectors used include thermopiles or bolometers. Any absorption of radiation by the sample results in a difference in intensity between the two beams. The sample absorption can, by suitable electronic means, be used to display the percentage transmission as a function of wavelength or wavenumber.

Fourier transform infrared (FTIR) spectrometers [1, 14]

This technique is based on interferometry. The basic construction of an interferometer instrument is illustrated in Fig. 10.21(a). The light from the source passes through a Michelson interferometer. The essential
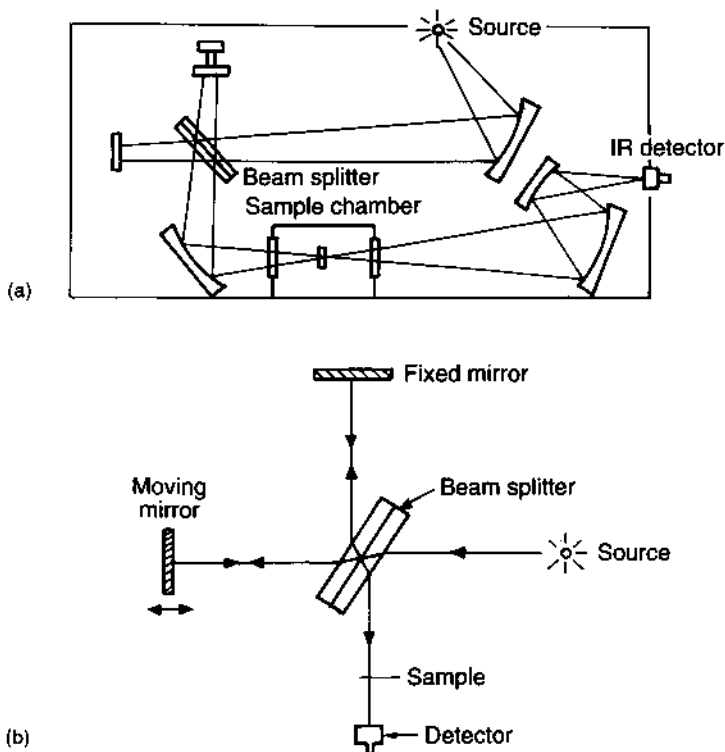
Fig. 10.21 Interferometer instrument used for FTIR.

$$I(x)$$
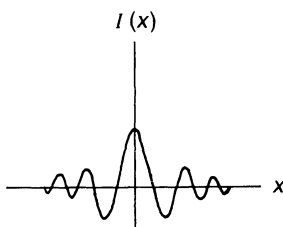
Fig. 10.22 Intensity vs. path difference in a typical FTIR interferogram.

components of this interferometer (Fig. 10.21(b)) are the two mirrors (one fixed and the other movable) and the beam splitter, which is set at an angle of 45° to the path of the collimated beam. The beam is partially transmitted and partially reflected at the beam splitter. These two beams are incident normal to the two mirrors and after reflection recombine at the beam splitter where they produce interference effects. The beam is then passed through the sample and on to the detector. If the mirrors are located equidistant from the beam splitter or at an optical path difference of integral number of wavelengths, the reflected beams are in phase and thus produce constructive interference. Conversely, when the optical path difference is an odd multiple of half wavelengths, destructive interference will occur. Thus, when the movable mirror is moved axially, relative phase difference occurs resulting in an oscillatory pattern or interferogram, which is a representation of the spectral distribution of the absorption signal reaching the detector.

A typical IR interferogram is shown in Fig. 10.22. If the movable mirror is moved at a constant velocity, the output signal is modulated dependent on the velocity of the mirror and the spectral distribution of the absorption signal. The true absorption spectrum is derived from the interferogram by Fourier transform analysis.

The transformation is carried out on a range of intensity values at different pathlengths to give the spectral intensity at the given frequency. The signal must be sampled at precise path differences. This is achieved by using an He–Ne laser whose beam traverses the same optical path (not shown in Fig. 10.21(a)) and the interference produced by the laser is used to trigger the sampling of the IR signal. The Fourier transformation is usually carried out by means of a built-in dedicated microprocessor, enabling the absorption spectrum to be produced in a relatively short time.

The resolution of the spectrum depends on the movement of the mirror in the different frequency ranges. Rapid scan speeds ($3\,\mathrm{mm\,s^{-1}}$) are used for the middle IR region (MIR) (4000–$400\,\mathrm{cm^{-1}}$), whereas lower scanning speeds ($0.005\,\mathrm{mm\,s^{-1}}$) are required for the FIR region. Interferometers used in the MIR range also differ from those used for FIR
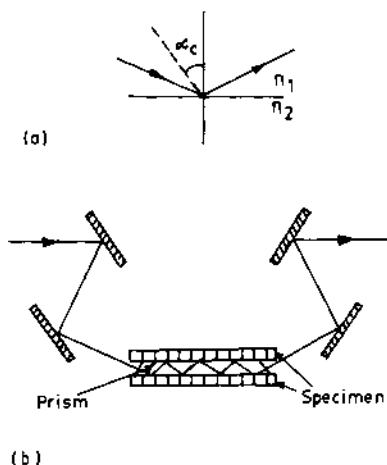
Fig. 10.23 (a) Total internal reflection of light incident at an angle greater than the critical angle. (b) Optical arrangement for multiple reflections in the ATR technique.

spectroscopy in using a different source (Nernst filament), using semiconductor dielectrics supported on potassium bromide as the beam splitter, and employing a different detector system (pyroelectric device).

Attenuated total reflectance (ATR) [1, 15]

When light is incident on a surface at an angle of incidence which exceeds the critical angle, then the light is reflected from the surface rather than being refracted through it (Fig. 10.23). At the interface, the electric field component of the electromagnetic radiation penetrates to some small extent into the surface layers of the less dense material. The depth of penetration depends on the wavelength of the light, increasing with increasing wavelength, and on the relative values of the refractive indices; typically it is of the order of several micrometres. Thus, light of wavelength corresponding to the absorption spectrum will be absorbed in proportion to the depth of penetration. This implies that there will be greater absorption of light of longer wavelength.

Infrared dichroism [1]

Infrared spectroscopy employing polarized light provides structural information, particularly on chain orientation. This involves the measurement of IR dichroism, expressed by the dichroic ratio $R = A_{\parallel}/A_{\perp}$, where $A_{\parallel}$ and $A_{\perp}$ are the absorbances respectively parallel and perpendicular to the reference axis in the sample. When the plane of polarization of the incident radiation is in the direction of the vibrating group

dipole the absorbance will be a maximum, while it will be zero in the perpendicular direction. Thus, depending on the degree of orientation, the absorbance will differ when the plane of polarization of the incident radiation is parallel or perpendicular to the direction of orientation. Hence the dichroic ratio will be a measure of the orientation.

For IR dichroism measurement, the polarizer is located in the beam before it passes through the monochromator. By rotation of the polarizer, it is possible to record the absorbance with plane of polarization successively parallel and perpendicular to the reference axis.

(d) Sample preparation

In the solid state, samples in the form of thin films (film thickness typically 0.001–0.05 mm) are preferred, owing to high IR absorption of materials. Solvent cast films are generally used. Alternatively, the IR absorbing species may be dispersed in an IR-transparent medium, such as potassium bromide (KBr). The standard sample preparation technique involves making KBr discs, with finely ground polymer samples dispersed in the discs at concentrations of less than 1%; they are prepared by compressing in a pellet-making press. Fibres and yarns may also be used; sample preparation techniques using these have been described in various references [15, 16].

(e) Applications [1, 14–21]

Infrared spectroscopy can be usefully applied to the study of polymers in various ways, e.g. identification of polymers and additives, studies of coupling effects, conformational studies, stereochemical studies, studies relating to crystalline forms, crystallinity of polymers and fibres, orientation in polymers and fibres, and end group analysis.

Identification of polymers and additives

This involves extraction or separation in order to avoid interference of overlapping spectral lines. This is done by solvent extraction of additives or dissolution and reprecipitation of the polymer. An alternative approach is to use a spectral subtraction technique in which the total spectrum of the polymer is subtracted from the observed spectrum, leaving the spectrum of the additives. Subtraction is best carried out using a computer.

Identification of an unknown polymer involves detection of characteristic absorption bands of the various chemical groups. Reference is made to the group frequency tables. The concept of group frequencies, which is applied here, depends on the existence of only a small degree of

coupling between vibrations, so that the shifts of the spectral lines due to coupling effects may be neglected.

Coupling effects

Interactions between vibrating groups lead to shifts in the absorption frequencies. The interactions between intramolecularly adjacent groups are more marked than the interchain interactions. As a result, coupling effects are greater for deformational modes (bending) than for stretching vibrations, and they are also reduced when the vibrating atoms have different masses. The coupling may affect both peak intensity and peak position.

Conformational studies

Conformational isomerism gives rise to pronounced coupling effects. The presence of *trans* and gauche conformations influences the vibration frequency of the $C-X$ bond such that it is split into a doublet. Since there is a distribution of different conformations along a polymer chain, this can result in a very complex spectrum. For example, in PET the situation has been shown to be very complex with a number of bands assigned to *trans* and *cis* conformations of the glycol residue [16]. However, the bands at $973\,\mathrm{cm}^{-1}$ and $889\,\mathrm{cm}^{-1}$ have been assigned as the most important vibrations associated with the *trans* and gauche conformations, respectively, of the glycol residue in the PET chain. Quantitative measurement of these conformers can be made by taking the band at $795\,\mathrm{cm}^{-1}$ (assigned to the benzene ring vibration) as an internal standard [17]. Using the ATR technique, the *trans* and gauche contents in PET have also been determined from the total absorbance, $A_0 = (A_\parallel + 2A_\perp)/3$, of the *trans* band at $1342\,\mathrm{cm}^{-1}$ and the gauche band at $1370\,\mathrm{cm}^{-1}$, taking the total absorbance band at $1410\,\mathrm{cm}^{-1}$ as reference [15].

Stereochemical studies

Infrared spectra may be used to determine the stereochemical structure of polymers. For example, the IR spectra of isotactic, syndiotactic and atactic polypropylene show considerable differences [1] as the intensities of a number of bands in polypropylene relate to the proportion of the material in the helical conformation, i.e. will closely correlate with tacticity. However, there are difficulties involved in making correct assignments for the bands observed in crystalline, stereoregular non-crystalline and atactic samples [1]. Nuclear magnetic resonance (NMR) spectroscopy provides another route for stereochemical studies.

Crystalline forms

The different crystalline forms of several polyamides have been examined by IR spectroscopy. The bands at $1198\,cm^{-1}$ and $1181\,cm^{-1}$ have been employed for measuring α and γ crystalline content in nylon 66. In nylon 6, α-crystalline-sensitive bands occur at 1028, 960, 950, 930 and $830\,cm^{-1}$ while γ-crystalline-related bands occur at 1120, 990 and $970\,cm^{-1}$ [18].

Crystallinity of polymers and fibres [20]

The absorbance subtraction technique has proved to be useful for estimating crystallinity because the absorption of the amorphous phase can be subtracted from the spectrum of a semicrystalline polymer to yield a difference spectrum which is primarily characteristic of the crystalline component. In the difference spectrum, the absorption bands associated with the crystalline phase can be clearly isolated [19]. In nylon 66, the bands at $936\,cm^{-1}$ and $1140\,cm^{-1}$ have been used to measure the crystalline and amorphous contents, respectively. In nylon 6 there is a crystalline band at $1260\,cm^{-1}$ and an amorphous band at $979\,cm^{-1}$ [18]. The bands relating to specific crystalline forms of nylon 66 and nylon 6 have been listed above. In the case of PET yarns, it has been reported that the crystalline band near $848\,cm^{-1}$ is very reliable for measuring crystallinity [20].

Orientation in polymers and fibres

The IR dichroic ratio R is correlated with the orientation of the vibrating groups. For example, for a stretched sample of polyamide, the measured value of $R = 0.67$ for the N–H stretching vibration is consistent with the N–H bond lying perpendicular to the chain direction. The degree of chain orientation may be determined from the changes in IR dichroism with an increase in draw ratio.

One of the most important and useful applications of IR spectroscopy to the study of fibres is the possibility of using the IR data in combination with X-ray data to estimate amorphous orientation. This arises because (a) the *trans* conformation is present in both crystalline and amorphous regions and the gauche conformation only in the amorphous region, and (b) the gauche component is disoriented [17].

The Hermans amorphous orientation factor for PET obtained using the technique described above comes out to be lower than the values obtained from sonic modulus measurements, but quite close to values obtained from birefringence measurements. However, estimates from birefringence require a knowledge of intrinsic birefringence values,

which are quite controversial. Thus IR spectra provide a good method for characterizing amorphous orientation.

End group analysis

The laborious chemical methods to determine end groups described earlier have been largely displaced by IR spectrometric techniques. For example, in PET this method is based upon the measurement of intensity of hydroxyl and carboxyl stretching vibrations, respectively, at $3542 \, cm^{-1}$ and $3256 \, cm^{-1}$ [21].

Methyl groups in polyethylene have been estimated by appropriately adjusted subtraction of the spectrum of high density polyethylene from the spectrum of low density polyethylene; the band at $1378 \, cm^{-1}$ yields an isolated CH_3 band which allows the quantitative evaluation of the CH_3 end groups [19].

10.4 THERMAL CHARACTERIZATION

Thermoanalytical techniques are used for characterization of glass transition and melting temperatures, thermal stability and other properties as a function of temperature of polymers and fibres [22]. The principal techniques used for this purpose are: (1) DTA (differential thermal analysis) and DSC (differential scanning calorimetry), (2) TG (thermogravimetry), (3) TMA (thermomechanical analysis), and (4) DMA or DMTA (dynamic mechanical thermal analysis).

The DTA and DSC techniques give the same information, hence only one of them is used; normally DSC is preferred owing to its advantages over DTA. This technique measures the glass transition temperature, melting and crystallization temperatures, heat of melting and various parameters related to the crystalline structure, and finally the temperatures of decomposition reactions.

Thermogravimetry measures the weight loss as a function of temperature and thus provides information about the thermal stability of the sample.

Thermomechanical analysis measures changes in certain mechanical properties (normally the probe penetration) as a function of temperature and enables one to measure the positions of the melting and glass transitions.

Dynamic mechanical analysis or DMTA is based on the measurement of dynamic mechanical properties as a function of temperature, from which the positions of principal secondary transitions in the given sample are located from the loss peaks.

The basic principle of all these thermal analysis techniques is the measurement of some property as a function of temperature using a programmed heating (or cooling) rate.

10.4.1 DIFFERENTIAL THERMAL ANALYSIS AND DIFFERENTIAL
SCANNING CALORIMETRY

In DTA the given sample and a reference material (which does not
undergo any transition in the temperature range of interest) are kept in
separate crucibles in the same furnace which is heated at a programmed
heating rate. Two thermocouples attached to the crucibles measure the
temperature difference between them (ΔT), which is recorded as a func-
tion of the overall temperature of the furnace. This recording is called the
DTA trace, and will be described briefly.

In DSC the sample arrangement is the same as in DTA and both
crucibles are heated at the programmed heating rate of the furnace.
There is an extra heater provided just below the crucible carrying
the sample, which operates on instructions received from the device
measuring the temperature difference (ΔT) between the sample and
the reference, to maintain the ΔT as zero. Thus the DSC trace records
the extra heat (ΔH) supplied per unit time to the sample crucible as a
function of the overall temperature of the furnace.

Thus, both DTA and DSC traces are identical, since the quantity ΔH in
DSC is directly proportional to the temperature difference ΔT in DTA.
A typical DTA or DSC trace is shown in Fig. 10.24.

In this trace the baseline remains unchanged so long as there is no
thermal transition in the sample. Second-order transitions, such as the
glass transition of polymers, cause a shift in the baseline, as indicated
by T_g in Fig. 10.24. First-order transitions, namely crystallization and
melting, appear as peaks in the exothermic and endothermic directions,
respectively, and their respective peak temperatures are marked as
T_c and T_m. After melting the material may undergo decomposition
reactions at higher temperatures which give broad peaks; these may
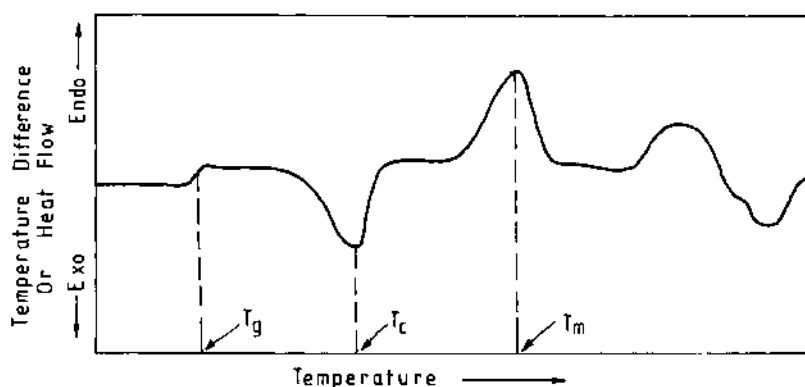
Fig. 10.24 Typical DTA or DSC trace.

be generally exothermic but are sometimes more complex in shape. Thus the DSC (or DTA) trace enables the determination of T_g, T_m and T_c and the approximate positions of the thermal decomposition temperatures.

The crystallization peak is sometimes not observed because the sample may be in its maximum crystalline state and so no further crystallization occurs during the DSC run. On the other hand, good crystallization peaks may be recorded during the cooling cycle (at an appropriately chosen cooling rate), starting from the melt state.

The areas of the crystallization or melting peaks are proportional to the heat involved in the process, and the areas can be accurately calibrated in terms of heat by using known standard samples. From the heat of melting of a given experimental sample (ΔH_{exp}), one may calculate the degree of crystallinity X_c using the value of heat of fusion for an ideal crystalline material (ΔH_f), i.e.

$$X_c = \frac{\Delta H_{exp}}{\Delta H_f}. \tag{10.27}$$

10.4.2 THERMOGRAVIMETRY

This technique employs a thermal balance, enclosed in a controlled programmed temperature enclosure, which measures the weight of the sample very precisely as a function of temperature. The TG trace depicts the residual weight or weight loss as a function of temperature (Fig. 10.25). An additional trace representing the derivative of the weight (or weight loss) as a function of temperature, called the differential thermogravimetric (DTG) trace (Fig. 10.25), is also provided in some modern
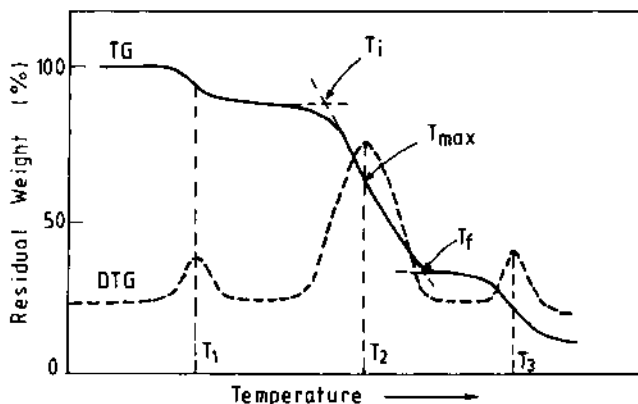
Fig. 10.25 Typical TG and DTG traces.

equipment. The advantage of the DTG trace is that it aids detection of the steps of decomposition which involve very small weight loss.

The typical TG trace shown in Fig. 10.25 represents three steps of decomposition: the first at T_1 represents a smaller weight loss than the second at T_2, while the third at T_3 is still a small weight loss step. It may be noted that the final weight is different from zero, consistent with the char yield of the sample. Each of these steps is represented by peaks in the DTG curves shown by a dotted line.

The principal parameters representing any step of decomposition are shown in Fig. 10.25 for the middle step of decomposition. These parameters are T_i (the initial decomposition temperature), T_f (the final decomposition temperature) and T_{max} (the temperature corresponding to the maximum rate of weight loss). Similar parameters can be defined for each individual step of decomposition, and the steps of decomposition can be identified from the associated amount of weight loss and the temperature range of the respective reaction.

10.4.3 THERMOMECHANICAL ANALYSIS

In this technique the polymer sample in the form of film or thin sheet is placed on a hard platform and a probe carrying constant weight is placed over it. The whole assembly is enclosed in a chamber heated at a programmed rate of heating. As the temperature increases the sample undergoes changes in its properties, which in turn affect the displacement or penetration of the probe. The probe displacement is measured precisely and recorded on a chart as a function of temperature. The TMA trace has the shape shown in Fig. 10.26. At the glass transition, the material transforms to a flexible state, thus facilitating the displacement
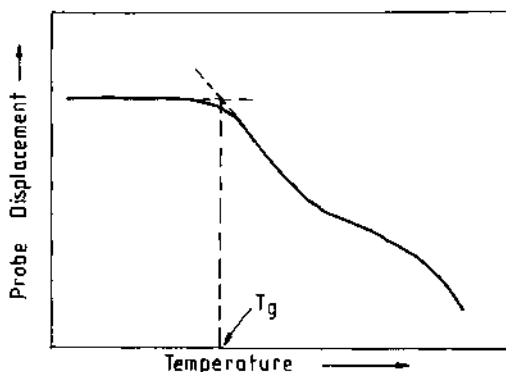
Fig. 10.26 Typical TMA trace.

of the probe. Thus the T_g can be located, as shown in Fig. 10.26, from the TMA trace.

10.4.4 DYNAMIC MECHANICAL ANALYSIS OR DYNAMIC MECHANICAL THERMAL ANALYSIS

These are the two different names for the same technique. In this method dynamic mechanical properties, namely the storage and loss modulus of the given sample, are measured at fixed frequencies as a function of temperature. Whenever a transition occurs in the sample, the storage modulus (E') undergoes a change from a constant value to another value, while the loss modulus (E'') or loss tangent (tan $\delta = E''/E'$) passes through a maximum (or shows a peak), as shown in Fig. 10.27. A polymer may undergo several transitions which give rise to loss peaks at the respective transition temperatures. The most prominent is the primary viscoelastic transition occurring at the T_g. In addition there are transitions at lower temperatures corresponding to various secondary transitions. Thus an estimate of the value of T_g can be obtained from the loss peak temperature of the most prominent transition. This loss peak temperature varies with frequency, thus the T_g value so determined will be an apparent value. A more accurate value of T_g can be calculated from this by applying the WLF equation or a simplified
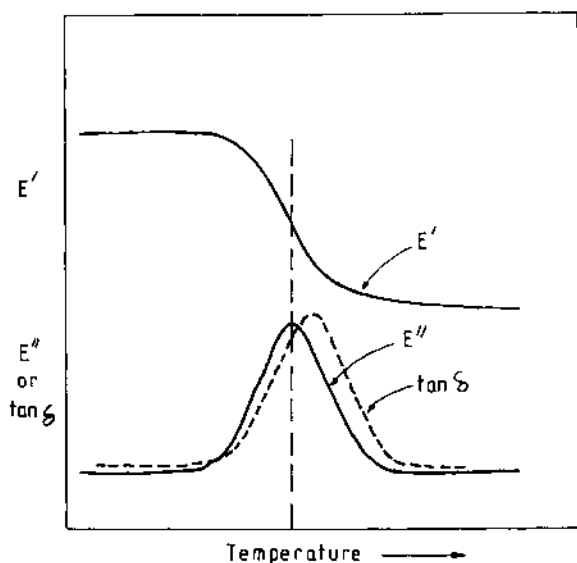
Fig. 10.27 Variation of dynamic mechanical properties (storage modulus E' and loss modulus E'') as a function of temperature.

expression derived from it [23], which is as follows:

$$T_g = b + \frac{(T_1 + T_2)}{2} - \frac{(T_2 - T_1)}{2}$$

$$\times \left[1 + \left\{ \frac{4ab}{(T_2 - T_1) \log (f_2/f_1)} \right\}^{1/2} \right] \tag{10.28}$$

where a and b are the constants of the WLF equation and T_1 and T_2 are the relaxation temperatures at frequencies f_1 and f_2, respectively.

10.5 MICROSCOPIC CHARACTERIZATION

Microscopic observations enable the characterization of fibres in various ways, depending on the magnification ranges and radiation used. The microscopic techniques are of two types: light and electron microscopy.

10.5.1 LIGHT MICROSCOPY [24]

(a) Conventional light microscopy

Conventional light microscopy uses visible light as the radiation and both magnification and resolving power are quite low in this type of microscope. Light microscopes are used to examine the texture of fibres, their cross-sectional shapes, diameter and large-scale surface irregularities, etc. in the reflected light mode. In the transmitted light mode, light microscopy can be used on films or on very thin sections of fibres.

(b) Polarized light microscopy

A further modification of light microscopy is 'polarized light microscopy', where the plane of polarization of the incident light is rotated after transmission. This rotation is caused by the presence of crystalline materials. Thus polarized light microscopy enables the detection of crystalline units, particularly the large units called spherulites whose structure is studied with the sample held between crossed polarizers. Thus characteristics such as spherulite growth rate and the crystalline melting temperature can be determined by polarized light microscopy using a suitable hot-stage.

(c) Phase contrast microscopy

This technique allows observation of structural features involving differences in refractive index rather than absorption or transmission or rotation of plane of polarization of light, as in other light microscope techniques. A pattern is formed depending on the phase differences

in the neighbouring beams travelling through the media of different refractive index. The pattern provides information about the structure of the sample.

10.5.2 ELECTRON MICROSCOPY [25]

In electron microscopy, electron beams are used as the radiation. The wavelength depends on the energy of the electrons, which depends on the voltage applied for their acceleration. The resolution, which depends on the wavelength of the radiation used, is as low as a few angstrom units in the most efficient electron microscopes.

Electron microscopy can be performed in both reflection and transmission modes. In the reflection mode the beam is scanned over the specified area of the sample and the image is formed; thus the technique is generally known as scanning electron microscopy (or SEM). In the case of transmission electron microscopy (TEM), modern versions of the equipment also have scanning arrangements and are called scanning transmission electron microscopes (STEM). Furthermore, instead of just simple microscopy, these electron microscopes provide the possibility of studying various phenomena such as electron diffraction, emission of secondary electrons, the cathodoluminescence effect, etc.

(a) Electron microscope

An electron microscope works on the same principle as a light microscope. The beam of electrons emerging from a hot metallic cathode is accelerated by applying a high voltage and collimated to a fine beam through electromagnetic lenses. The collimated beam is converged by another set of electromagnetic lenses called the 'objective' and directed onto the specimen. The beam after transmission (or reflection) converges at the focal point to form the image, which is subsequently magnified through another set of electromagnetic lenses. The final image is then formed on a fluorescent screen or can be recorded photographically.

In the scanning electron microscope, the fine collimated beam of electrons is deflected through a suitable scanning coil device, so that it falls on different areas of the specimen surface at different moments of time. The circuit for detection of the reflected beam is synchronized with the initial scanning coils to detect the reflected beam from each area of the specimen surface at the respective moment of time. Thus the scanning detector measures the intensity of reflected beam from different areas of the specimen surface at different instants of time, and finally it forms an image on the fluorescent screen which appears in a continuous and stable form owing to the very small time involved in scanning the whole area (less than the time of persistence of vision).

Light Microscope   TEM   SEM
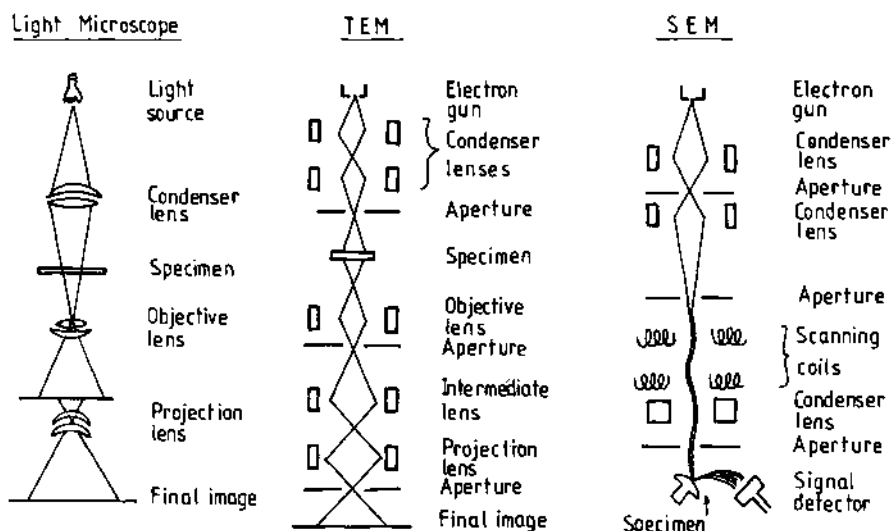
Fig. 10.28 Comparison of the light microscope with TEM and SEM.

A schematic representation of SEM and TEM compared with a typical light microscope is given in Fig. 10.28.

(b) Sample preparation for electron microscopy

Samples for TEM

The samples for TEM have to be very thin to allow sufficient transmission of the electrons. Thin sections cut on a microtome or thin films grown on substrates are used for this. Replica films are also useful in the study of surface texture and observation of polymeric single crystals.

Staining of the samples is an important technique in TEM studies of polymers containing conjugated or unsaturated chemical structures, as is the case with many elastomers and copolymers. On staining these systems with OsO_4 (osmium tetraoxide) oxidation takes place and the metallic osmium deposits in the regions of unsaturation, which makes them opaque to the electron beam. Thus the stained regions appear black in the TEM, which provides a useful picture of the morphology of such systems.

Samples for SEM

In SEM scanning is done on the surface of the specimen in the reflection mode, hence the surface has to be natural without any markings of the knife or microtome blade. Such surfaces are obtained by breaking the

sample with an applied deformation force (impact or tensile fracture surfaces) or by simple manual flexing at cryogenic temperature. This low temperature is needed because it avoids plastic deformation and also because breaking of polymers may often be difficult at ambient or temperatures higher than T_g. The sample is suitably cut into a small piece without disturbing (or touching) the main fracture surface. This small piece is mounted on the sample holder of the SEM.

The second step in sample preparation for SEM is coating the sample with metal. This is essential in order to avoid the accumulation of electrons or the generation of static charge owing to the poor conductivity of polymers. The metallic film deposited on the surface is so thin that it does not disturb the surface topography, while it provides the means for discharge of the accumulated static charge. The metal coating is done by vacuum deposition of metals like silver, gold or platinum.

Etching is another important process used in sample preparation, particularly in multicomponent systems. By the use of selective dissolution using appropriate solvents, some components can be etched out of the sample surface, thus enabling good detection of the morphology of dispersion.

(c) Application of electron microscopy

Electron microscopy has a practical resolution limit of about $100\,\text{Å}$, and hence allows structural features of very small dimensions to be detected by this technique. Typical applications of electron microscopy to fibres are in the study of (1) surface texture of fibres, (2) cross-section of very fine filaments, (3) structure and morphology of fibrils, (4) structure of single crystals, (5) voids in the fibres, (6) macroscopic features of two-phase morphology, (7) morphology of dispersion of blends and in multicomponent fibres, (8) measurement of particle size of additives, (9) interface morphology and adhesion and differential contraction of the phases in multicomponent fibres, and (10) mechanism of fracture and deformation.

REFERENCES

1. Campbell, D. and White, J.R. (1989) *Polymer Characterization: Physical Techniques*, Chapman & Hall, London.
2. Spells, S.J. (ed.) (1994) *Characterisation of Solid Polymers: New Techniques and Developments*, Chapman & Hall, London.
3. Schroder, E., Müller, G. and Arndt, K.F. (1988) *Polymer Characterization*, Hanser Publishers, Munich.
4. Billingham, N.C. (1977) *Molar Mass Measurements in Polymer Science*, Wiley, New York.
5. Collins, E.A., Bares, J. and Billmeyer, F.W. (1973) *Experiments in Polymer Science*, Wiley, New York.

6. Billmeyer, F.W. (1984) *Textbook of Polymer Science*, Wiley-Interscience, New York.
7. Bark, L.S. and Allen, N.S. (eds) (1982) *Analysis of Polymer Systems*, Applied Science, London.
8. Vaidya, A.A. (1988) *Production of Synthetic Fibers*, Prentice Hall of India, New Delhi, p. 316.
9. Besnoin, J.M. and Choi, K.Y. (1989) *J. Mater. Sci. Rev. Macromol. Chem. Phys.*, **C29**(1), 55–81.
10. Read, B.E., Duncan, J.C. and Meyer, D.E. (1984) *Polymer Testing*, **4**, 143.
11. Alexander, L.E. (1969) *X-ray Diffraction Methods in Polymer Science*, Wiley, New York.
12. Kakudo, K. and Kasai, N. (1972) *X-ray Diffraction by Polymers*, Elsevier, Amsterdam.
13. Cullity, B.D. (1967) *Elements of X-ray Diffraction*, Addison-Wesley, Reading, MA.
14. Ferraro, J.R. and Krishnan, K. (eds) (1990) *Practical Fourier Transform Infra-red Spectroscopy*, Academic Press, San Diego.
15. Jain, A.K. and Gupta, V.B. (1990) *J. Appl. Polym. Sci.*, **41**, 2931–2939.
16. Yazdanian, M., Ward, I.M. and Brody, H. (1985) *Polymer*, **26**, 1779–1790.
17. Padibjo, S.R. and Ward, I.M. (1983) *Polymer*, **24**, 1103–1112.
18. Reimschuessel, H. (1985) Polyamide fibers, in *Fiber Chemistry* (eds M. Lewin and Eli M. Pearce), Marcel Dekker, New York, pp. 73–169.
19. Siesler, H.W. (1980) *J. Mol. Struct.*, **59**, 15–37.
20. Heuvel, H.M. and Huisman, R. (1985) *J. Appl. Polym. Sci.*, **30**, 3069–3093.
21. McIntyre, J.E. (1985) Polyester fibers, in *Fiber Chemistry* (eds M. Lewin and Eli M. Pearce), Marcel Dekker, New York, pp. 1–71.
22. Turi, E.A. (1982) *Thermal Analysis of Polymers*, Academic Press, New York.
23. Gupta, A.K. (1980) *Makromol. Chemie. Rapid Comm.*, **1**, 201.
24. Sawyer, L.C. and Grubb, D.T. (1987) *Applied Polymer Microscopy*, Chapman & Hall, London.
25. Thomas, G. and Goringe, M.J. (1979) *Transmission Electron Microscopy of Materials*, Wiley-Interscience, New York.

Testing of manufactured fibres

11

V.K. Kothari

11.1 INTRODUCTION

Testing of manufactured fibres, filaments and their yarns is important from the points of view of quality control, process control, product development and process optimization. Fineness, crimp, shrinkage, tensile and evenness are some of the properties tested depending on the material and end use requirements. The exact norms for these properties are not normally available but, depending on the product and end use requirements of the customer, each plant establishes certain norms for each important property. Besides satisfying these norms, the fibres and yarns should have consistent properties. The principles and methods of evaluating these properties are discussed in this chapter.

11.2 FINENESS

Fibre and yarn fineness is normally measured in terms of mass per unit length and is referred to as its linear density. This method of fineness measurement is adopted in view of difficulties associated with diameter measurement, the non-circular cross-section of many fibres, variability in the tested materials and the time required for testing.

The linear density is measured either by direct weighing of a known length of fibre or by vibroscope procedures. The preferred method for measuring linear density is the direct weighing method. The linear density is determined from the mass of a specified length of the sample and is expressed in denier or tex units.

11.2.1 DIRECT WEIGHING METHOD

The specimen is first conditioned free from tension and a suitable length of yarn, preferably in multiples of 10 m for tex and 9 m for denier measurement, is received by a wrap reel without alteration of twist under a constant yarn tension of 0.45 ± 0.09 cN tex^{-1} (or 0.05 ± 0.01 cN den^{-1}), so that the mass of the specimen is at least 5 g. Testing of at least six test specimens is recommended. Each specimen is put in a ventilated drying oven maintained at 105 ± 3 °C and fed with air from a standard atmosphere. Drying is continued till the difference between any two successive weighings made at intervals of 20 min does not exceed 0.1%. The oven dry mass of each test specimen is recorded correct to 1 mg. Linear density for each specimen is then calculated using either of the following two expressions:

$$\text{tex} = (100 + R) \times \frac{10M}{L}$$
$$\text{denier} = (100 + R) \times \frac{90M}{L}$$

where R is the percentage commercial moisture regain of the fibre being tested, M is the oven dry mass (g) and L is the length of the specimen (m).

Percentage commercial regain values (R) of some of the man-made fibres corresponding to standard atmospheric conditions of 20 °C temperature and 65% RH are given in Table 11.1.

11.2.2 VIBROSCOPE METHOD

This method, based on the use of the vibroscope, is particularly suitable for measuring linear density of single fibres below 1 tex. It involves the use of the principle of the vibrating string. The fundamental resonant frequency of transverse vibration of a fibre is measured under known

Table 11.1 Percentage commercial regain values (R) of some manufactured fibres under standard atmospheric conditions (20 °C and 65% RH)

Material	R (%)
Polyester	0.4
Polyamide	4.5
Rayon	11.0
Acrylic	1.5
Spandex^{TM}	1.3
Olefins	0
Glass	0
Metallic	0

conditions of length and tension and from the conditions at resonance, the linear density is obtained as follows:

$$\text{Linear density, dtex} = \frac{t}{4L^2 f^2} \times 10 \times 10^5$$

$$\text{Linear density, denier} = \frac{t}{4L^2 f^2} \times 9 \times 10^5$$

where t is the fibre tension (dyn), L is the effective fibre length (cm) and f is the fundamental resonant frequency (Hz).

Crimp in the fibre, if present, must be removed by the use of sufficiently heavy tensioning weight as the presence of crimp leads to deceptively high linear density values. Vibroscopes are therefore designed with either a variable frequency range to allow the measurement of the fundamental frequency of vibration of a fixed short length of fibre, or a variable length to obtain resonance at a given frequency of vibration. In both cases the measurements are made under the required tensioning load.

In the case of staple fibres, the average linear density of single fibre is calculated on the basis of measurement of mass of a bundle of fibres of known length and the number of single fibres in the bundle [1]. A sample bundle of fibres containing a sufficient number of fibres weighing between 0.5 and 0.75 g, when cut to the specific length, is first selected. After arranging the fibres in parallel alignment, the bundle of fibres is placed in a cutting device or on a flat cutting surface. The bundle is then pretensioned to remove the crimp in fibres, if present, before cutting it using a template, a die or a cutting device. Average linear density is then found by weighing the bundle and counting the number of fibres in the bundle and then using the following relationships:

$$\text{Average linear density, dtex} = \frac{10\,000\,W}{L \times N}$$

$$\text{Average linear density, denier} = \frac{9000\,W}{L \times N}$$

where W is the mass of the bundle (mg), N is the number of fibres in the bundle, and L is the length of the fibres (mm).

11.3 FIBRE CRIMP

Fibre crimp refers to waviness of a fibre and crimp frequency and is characterized by percentage crimp value. Crimp frequency in manufactured staple fibres refers to the number of crimps or waves per unit length of extended or straightened fibre. Percentage crimp is the difference between two points on the fibre as it lies in an unstretched

condition and the same two points when the fibre is straightened under specific tension, expressed as a percentage of the unstretched length.

A simple method of measuring crimp frequency in staple fibres [2] is to place the fibre on an oil-coated glass plate or on a short pile or plush surface. The wave peaks are then counted using a magnifying glass. Crimp is characterized by a change in the directional rotation of a line tangent to the fibre as the point of the tangent progresses along the fibre. Two changes in rotation constitute one unit of crimp. ASTM standard D3937-90 provides a standard reference chart for crimp counting. After the number of waves/crimps have been counted, the fibre is straightened carefully without deformation and its uncrimped length is measured. Crimp frequency is then calculated as the number of crimps per unit of extended length.

For measuring percentage crimp, two points on a fibre are marked and the distance between them in the crimped state of the fibre is measured. The fibre is then clamped in two jaws at the marked points and one jaw is moved just enough to remove the crimp without stretching it. The distance between the jaws gives the uncrimped length of the fibre. A tensile tester could be used for the above purpose. Percentage crimp is then calculated from the measured values of crimped and uncrimped lengths. An instrument like the Vibrotex from Lenzing can characterize the crimp in staple fibres automatically. The clamps for holding the fibres are operated by electromagnetic forces and the moving clamp is driven by a DC motor. The crimp of the fibre is first partially removed without stretching the fibre. Subsequently, fibre recovers its crimp during the return movement of the clamp. The resulting stress–strain diagram of the crimp is indicated by the recorder. Up to four correlated figures of tension and lengths of fibre during recovery of crimp are used to calculate the characteristic values of crimp properties.

11.4 TENSILE PROPERTIES

Tensile properties of textile materials are measured using machines designed to impart, or transmit, force/extension to the material and measure the response of the material to the applied action. Tensile testing machines for textile materials are classified according to their operating principle as follows [3].

Type   *Principle of operation*
CRE   Constant rate of extension
CRT   Constant rate of traverse
       (pendulum type)
CRL   Constant rate of loading
       (inclined plane type)

Most fibre and filament yarn testers employ constant rate of extension (CRE) as the straining principle because there are difficulties in extension measurement on constant rate of loading (CRL) testers due to creep and the accuracy achieved using constant rate of traverse (CRT) testers is much lower than that achieved with other types of tester. The load–elongation characteristic curves (LE characteristic curves) obtained on CRE testers provide important information about the relationship between force and elongation during the time up to the fibre/yarn rupture and can be used to determine a number of important tensile test parameters.

11.4.1 TERMS AND DEFINITIONS

Figure 11.1 shows a typical load–elongation curve for a fibre. The following parameters are determined with reference to this curve:

- *Breaking load (or force)* – the peak load (or force) that is reached during a tensile test (units: N, cN, mN).
- *Breaking elongation* – the elongation in the specimen up to breaking load. The elongation produced due to pretensional load is ignored (units: m, cm, mm).
- *Breaking extension* – the elongation at breaking load expressed as a percentage of the original length (unit: %).
- *Pretensional load* – the force acting on the test sample before the beginning of a tensile test. It primarily helps in determining an accurate
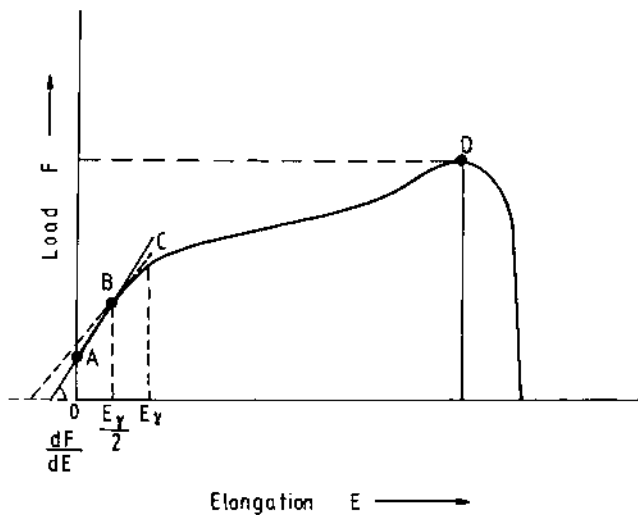
Fig. 11.1 Typical load (force)–elongation curve.

value of elongation and is prescribed by most standard testing methods as $0.5\,\text{cN}\,\text{tex}^{-1}$.

- *Tenacity* – the breaking load per unit linear density of the unstrained specimen (units: $N\,\text{tex}^{-1}$, $\text{cN}\,\text{tex}^{-1}$, $\text{cN}\,\text{dtex}^{-1}$).
- *Initial modulus* – the slope of the stress–strain curve at pretensional load. It can be calculated as

$$IM = \frac{dF}{dE} \times \frac{GL}{\text{tex}}$$

where *IM* is initial modulus, dF/dE is the slope of the load–elongation curve at pretensional load, GL is the gauge length at pretensional load, and tex is the linear density (units: $N\,\text{tex}^{-1}$, $\text{cN}\,\text{tex}^{-1}$, $\text{cN}\,\text{dtex}^{-1}$).
- *Modulus of elasticity or Young's modulus* – the slope of the stress–strain curve in the elastic region between the origin and the yield point. It is calculated from the slope of the load–elongation curve at the midpoint of the elongation in the elastic region (units: $N\,\text{tex}^{-1}$, $\text{cN}\,\text{tex}^{-1}$, $\text{cN}\,\text{dtex}^{-1}$).
- *Work of rupture* – the work done from the point of pretensional load to the point of breaking load. The energy required to bring a specimen to the breaking load can be obtained from the area under the load–elongation curve. Work of rupture is dependent on the linear density and length of the specimen (units: $N\,\text{m}$, $\text{cN}\,\text{cm}$).
- *Toughness or specific work of rupture* – the energy per unit mass required to rupture the specimen. It is the integral of the nominal stress–strain curve and is calculated by dividing the work of rupture by the mass of specimen under test:

$$\text{Toughness} = \frac{\text{work of rupture (N m)}}{\text{mass of specimen (mg)}}$$

(units: $N\,\text{tex}^{-1}$, $\text{cN}\,\text{tex}^{-1}$, $N\,\text{dtex}^{-1}$).

11.4.2 CRE TENSILE TESTERS

Recording of load (force) on most CRE testers is based on the principle that metal wire changes its resistance when subjected to a tensile or compressional force. The wire used must have a linear resistance–strain relationship and be stable with respect to temperature and relative humidity. The strain gauge measuring grid is generally manufactured from copper–nickel alloy which has a low and controllable temperature coefficient and the resistance change is virtually proportional to applied strain. The actual form of the grid is accurately produced by photo-etching techniques. Thermoplastic film is used to encapsulate the grid, which helps to protect the gauge from mechanical and environmental
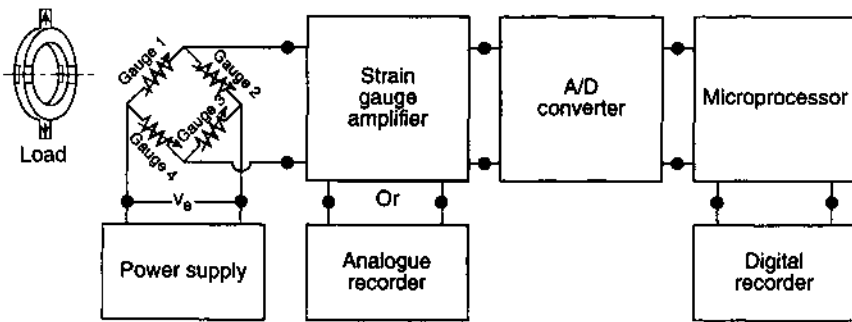
Fig. 11.2 Load measuring system based on the strain gauge principle.

damage and also acts as a medium to transmit the strain from the object to the gauge material.

If ΔR is change in resistance of a strain gauge from the unstressed value of resistance R and ΔL is change in its length from original unstressed length L, then

$$\frac{\Delta R}{R} = K\frac{\Delta L}{L}$$

where K is a constant known as the gauge factor. The change in resistance of the strain gauge can therefore be utilized to measure strain ($\Delta L/L$) accurately when connected to an appropriate measuring and indicating circuit. The strain gauge(s) is cemented to a suitable load-sensitive element like a metal bar, a ring or a tube. Under the action of a tensile load, the curvature of the ring shown in Fig. 11.2 is changed such that the inner gauges undergo tension while the outer gauges experience compressive forces. The changes in their dimensions are proportional to the applied load. Thus by measuring the changes in resistances of the strain gauges cemented as shown, the magnitude of the load applied on the ring can be obtained. In order to get an accurate estimate of the load, the gauges are connected in the form of a full bridge as shown in Fig. 11.2. Before applying the load, the bridge is balanced so that the voltage output is zero. When a load is applied, the deformation of the ring causes the values of resistances to change such that the output voltage is proportional to the applied load. The output voltage is then suitably amplified, converted into a digital signal and fed to a microprocessor and can be recorded; alternatively the amplified voltage signal can be used to drive the pen motor of a strip chart recorder. The system of load measurement based on changes in resistances of strain gauges has proved to be extremely sensitive to loads and load changes, and operates with only a negligible amount of inertia.

(a) Setting of tensile testers

In order to obtain maximum precision in determining tensile behaviour, the factors which must be considered [4–6] are: (1) gauge length, (2) crosshead speed, (3) full scale load, and (4) chart speed.

Gauge length

Gauge length is an independent variable and is generally kept between 10 and 500 mm. The greater the length, the less influence the constant dimension clamp errors have on the results obtained. However, the distribution of flaws along the length introduces greater probability of the sample length containing a large flaw as the gauge length increases. Hence tenacity usually decreases as the gauge length is increased. This immediately suggests the necessity of standardizing on a fixed gauge length for testing. The gauge length specified by most standard test methods for filament yarns is 500 mm. For staple fibres, gauge length will depend on fibre length. However, it is recommended that the gauge length should not be less than 10 mm.

Crosshead speed

The crosshead speed is a dependent variable selected to give the desired rate of extension, depending on the gauge length. ASTM standards D2101-90 and D3822-90 recommend certain rates of elongation, depending on the breaking extension of the specimen (Table 11.2).

These rates may have to be adjusted, depending on the average breaking extension of the specimen, if the time to break is to be kept as 20 ± 3 s. Unfortunately, these criteria do not include consideration of the actual rates of deformation experienced by a filament both in subsequent processing and in its end use performance.

Full scale load

ASTM standard D76-93 recommends a choice of full scale load such that maximum load on the specimen falls between 10 and 90% of full scale for

Table 11.2 Recommended rates of elongation for different breaking elongation of the specimen (ASTM D3822-95a)

Breaking extension of specimen (%)	Rate of elongation (% initial specimen length min^{-1})
Under 8	10
8–100	60
Over 100	240

CRE type testing machines. However, it is better if full scale load is so adjusted that breaking load is recorded at a point between 50 and 85% of the value selected. For example, for a yarn with a breaking load in the range 600–800 cN, the full scale load should be 1000 cN. In this manner, maximum resolution of the load scale is achieved and smaller differences can be more easily detected.

Chart speed

The selection of proper chart speed is extremely important if modulus values are desired. The recommended practice is to select a chart speed which results in the initial straight line portion of the load–elongation curve forming as close to a 45° angle as possible with the baseline of the chart. If the slope is greater, small errors in determining the slope of the line cause wide variations in the load level used to calculate the modulus, while a lesser slope increases chart consumption.

(b) High speed testing

All known standard methods of test for tensile testing prescribe a testing time of 20 ± 3 s up to achieving the breaking load. However, these standard methods were set out at a time when tensile testing instruments were not able to test much more quickly. With the modern microprocessor-controlled tensile testers, it is possible to increase the clamp speed up to 5000 mm min^{-1} and reduce the test time considerably. In order to reduce the overall test duration and utilize the capabilities of modern tensile testers, it is important also to reduce the standard test time. A strain rate of 1000% of the gauge length min^{-1} could be used for high speed testing.

11.5 EVENNESS TESTING

Irregularity or non-uniformity in a variety of properties exists in textile yarns. Variation in linear density of a yarn is usually understood to mean yarn unevenness. Variations in fineness of textile fibres and yarns are inevitable because they arise from the fundamental nature of the fibres, their manufacturing methods and the arrangement of fibres in the yarn in the case of staple fibre yarns. Granulate heterogeneity, spinning process irregularity, faults in subsequent yarn cooling and winding operations, together with machine defects and drafting faults quickly lead to mass variations which can extend over long lengths of material. Such variations in unstretched or partly stretched yarns often cause difficulties in the subsequent processes, for instance in secondary stretching or drawing, and in texturing or dyeing of material. In addition,

irregularity in linear density can arise due to knots or splices, neps, slubs, etc. introduced during the production process. These irregularities reduce the quality of the yarn and a comprehensive evenness testing is a must for a quality control programme.

A number of methods are available for determining yarn evenness but the basic method consists of cutting and weighing many specimens of yarn of a fixed length. However, this method is tedious, lacks precision and is of limited use.

Capacitive methods of determining yarn evenness are the most popular and widely used methods. The yarn is passed through a parallel plate air capacitor/condenser continuously and changes in capacity are monitored electronically. A change in the mass of the dielectric (non-conducting material) in the condenser changes its capacitance, the change being proportional to the weight of material present. If the material is drawn through the condenser continuously, the changes in capacitance will follow the variation in the weight per unit length of the strand, the unit length being the length of the capacitor. Many evenness testers based on the above principle are available but Uster Evenness Testers are the most widely used for evenness testing. Many models of these testers, including the Uster Tester 3C and the Uster Tester I/IIC, are currently in use and their fully configured installation can provide the following data:

1. diagram showing the variations in weight per unit length along the length;
2. mean quadratic irregularity (CV (%)) of these variations;
3. a representation of variation in mass per unit length as a function of wavelength (known as a spectrogram) for detecting period irregularity;
4. variance length curve.

When the Uster Tester is working in 'normal test' mode the irregularity, as illustrated on the diagram and expressed by the CV(%) or U(%), is based on a measuring zone of length 17 mm in the case of filament yarns. Therefore, in this mode it is possible to detect mass variation of comparatively short extent. When measuring the evenness of man-made filament yarns, there are some cases where medium- and long-term variations are of particular interest. In order to focus on such variations, short-term variations can be suppressed by using the 'half inert' and 'inert' test modes. In the case of the Uster Tester IIC, the 'L-test' mode allows selection of any L-factor between 0.1 and 10 on a knob provided. The equivalent cut length L can be calculated from the formula:

$$L = (L\text{-factor}) \times \frac{V}{100}$$

where V is the speed of the test material chosen from 4, 8, 25, 50, 100, 200 and 400 m min^{-1}. Thus with the Uster Tester IIC, any number of points
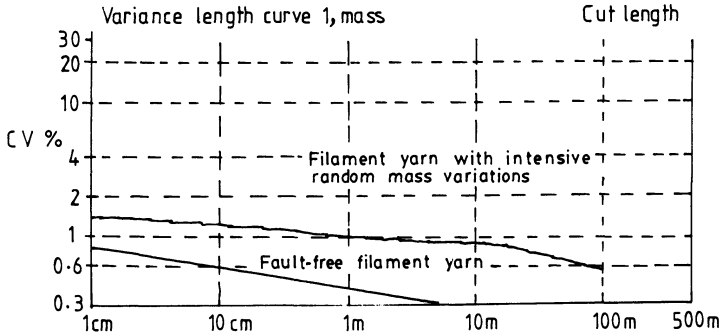
Fig. 11.3 Variance–length curve [8].

on the variance–length curve up to 40 m can be determined. The variance–length curve is a graphical representation of the coefficient of variation value CV for various cut lengths. The L-factor has a fixed value of 5.6 in the case of the Uster Tester IC in the 'inert' mode of operation. The CV(%) corresponding to the cut lengths of 0.1, 1, 3, 10, 50 and 100 m are printed out in the single/overall results protocol for the Uster Tester 3C. Figure 11.3 shows a variance–length curve obtained using this tester. This curve indicates that the filament yarn tested has intensive random mass variations compared with the fault-free filament yarn.

The Uster Tester IIC prints out a figure at the end of each measurement which is referred to as the average value factor AF. This factor is proportional to the mean count of the tested sample length. Accordingly, the value AF = 100 corresponds to the count at the beginning of the first sample of a series of measurements.

If, for instance, the count of the second sample is 5% lower than the value at the beginning of the first sample, then, at the end of the second measurement, the figure 95 will be printed out. Relative count determinations of this type are only possible with the same material and with reference to the same processing stage.

The 'cut length', over which the count is determined, corresponds to the value of 'material speed' × 'evaluating time'. With a material speed of, for instance, 400 m min^{-1}, and an evaluating time of 2.5 min, the cut length would be 400 × 2.5 = 1000 m.

11.5.1 DIAGRAMS

The variation of mass per unit length in the 'normal', 'inert' or 'half inert' modes of operation can be recorded on a chart which is known as a diagram. These diagrams are extremely useful in indicating the nature of variability present in the material. They can also be used to locate the missing filament in a section of the yarn and in locating short thick
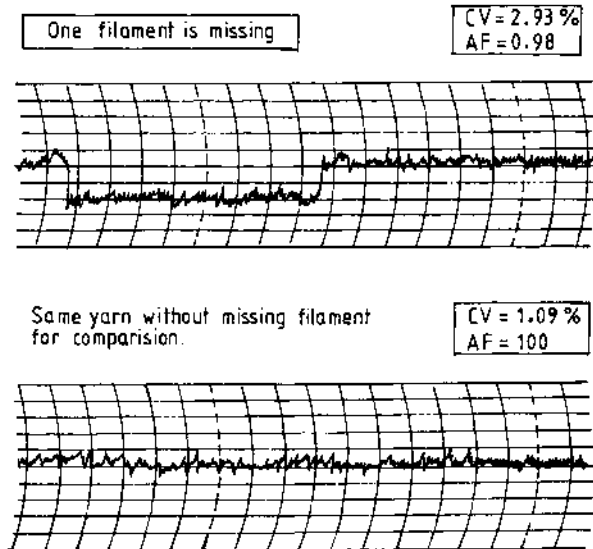
Fig. 11.4 Diagram indicating a missing filament over a length in yarn [7].

places in filament yarns. Uster Testers GGP-C, IC and IIC allow a maximum sensitivity of ±12.5%, while a sensitivity of ±6.25% is possible with the Uster Tester 3C.

Changes in the number of filaments in the yarn will be shown in the diagram. One missing filament from a 78 dtex/20 filament yarn represents a 1/20 (5%) change in overall count, which can be easily identified in the measuring range of ±12.5% as shown in Fig. 11.4. In fact in this measuring range an extra or missing filament can be identified if it represents more than 1% change in overall yarn count.

Diagrams are also useful in locating three types of short thick places in filament yarns which are referred to as 'spin graining', 'textile graining' and 'broken filaments' [7].

Spin graining

Spin graining can occur when the melt includes certain additives which were either present before polymerization or were added in the melt during the preparation processes. Possible additives would refer to:

- foreign matter, which was already present in the chips;
- unsuitable drying of the chips (decomposition products and products arising from burning due to local overheating);
- unsuitable heating of the melt (parts of the melt remain too long on the heater surfaces);

- inclusion of fragments of quartz sand which is used for filtration purposes;
- inclusion of metal fragments which are produced by metal rubbing at some positions in the manufacturing process; and
- titanium dioxide which is added to the melt to reduce lustre and which has not been powdered enough or which forms small aggregates in the melt.

The length of the spin graining in the undrawn state can be a few millimetres and in the drawn state a few millimetres to a few centimetres. The count of the filament in the region of the spin graining reaches approximately two to three times the normal count. The additives referred to above are normally only to be found in one filament.

Textile graining

Textile graining occurs in drawn yarns in the form of thick places whose size lies between that of the undrawn and the drawn yarn and whose length varies between one and a number of centimetres.

The reason for textile graining is a non-homogeneous condition of the undrawn yarns. If at a hard position in the drawing field a softer position follows, the zone of the softer place will be drawn more than that of the harder place. With textile graining, all filaments will be thicker at the position concerned.

Broken filaments

A broken filament can lead to a short thick place as well. This will happen when the broken filament is pushed up. In this case the filament appears as a nep-like thick place.

An example of 'textile graining' in a filament yarn is shown in Fig. 11.5. The corresponding diagram shows needle-shaped peaks. In this particular example a 295 dtex nylon 6 with 34 filaments was tested with
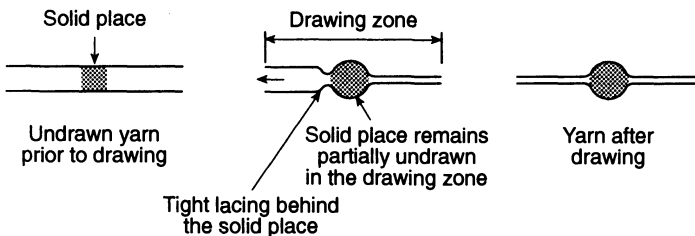
Fig. 11.5 Diagram indicating presence of 'textile graining' in a filament yarn [7].

a sensitivity range of $\pm 12.5\%$ at $400\,\text{m}\,\text{min}^{-1}$. The diagram speed is $10\,\text{cm}\,\text{min}^{-1}$. The positive spikes are caused by the formation of globules of titanium dioxide while the negative spikes are due to the overshoot of the recorder pen.

11.5.2 SPECTROGRAM

A spectrogram is an irregularity spectrum obtained by plotting the amplitude of irregularity against wavelengths. The wavelength spectrum is theoretically a continuous curve. Technically, it is not possible, without considerable costs, to investigate each separate frequency (or wavelength). Generally a number of filters are used to represent a number of frequency ranges. Figure 11.6 shows a diagram and a spectrum of a multifilament yarn of nylon 66 produced on Uster Tester IIC. The spectrogram clearly indicates that there are three major periodic faults in the yarn with wavelengths 45 cm, 4.5 m and 20–40 m. Investigation of the manufacturing process [7] revealed that

- periodic variation of 4.5 m wavelength is a result of the spinning package running eccentrically;
- periodic faults with 45 cm wavelength have resulted from an eccentric running drafting roller at the draw-twisting machine;
- higher wavelength variations have been caused due to irregular vibrations in the material brought about by the currents of cooling air passing through the spinning tube.

The Uster Tester 3C allows the spectrograms from a number of packages to be printed out simultaneously, as shown in Fig. 11.7(b),
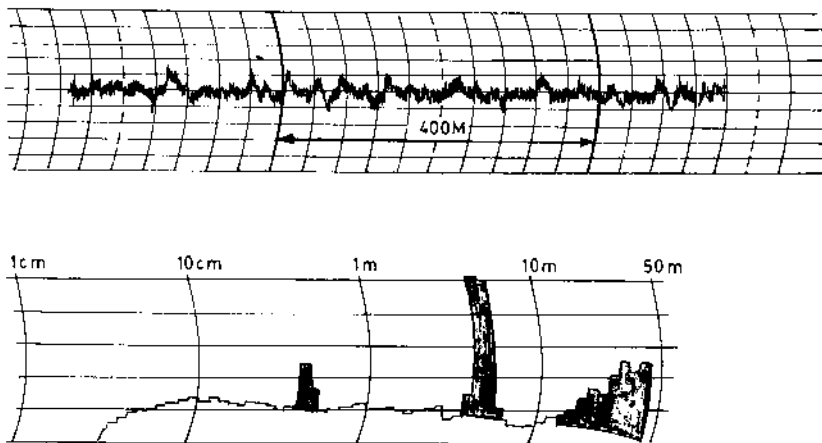
Fig. 11.6 A diagram and a spectrogram of the same yarn (adapted from reference [7].

(a)

(b) Spectrograms of 12 packages

(c) Detailed spectrogram of an individual package.
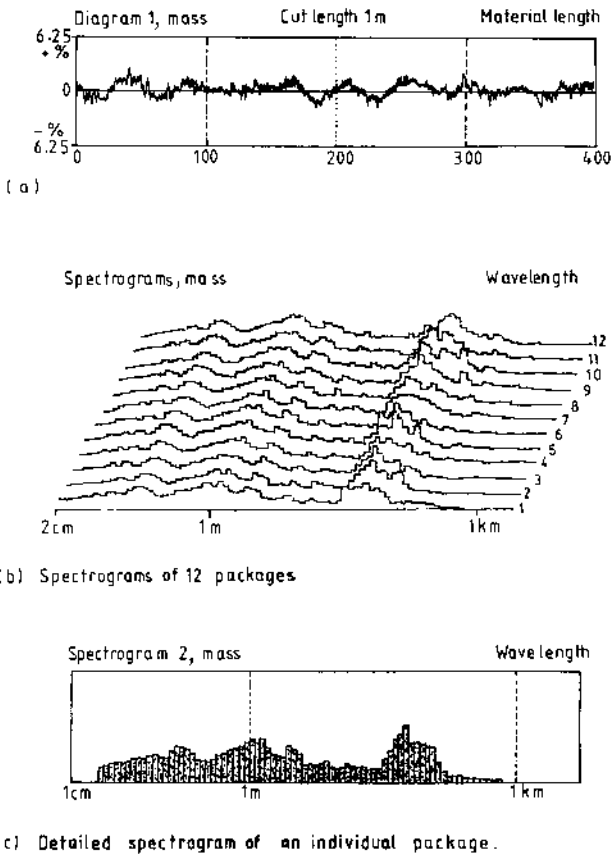
Fig. 11.7 Evenness analysis using the Uster Tester 3C [8].

in addition to the separate spectrograms [8]. This simultaneous representation of spectrograms allows us to identify periodic faults in the whole sample as against faults present in individual packages. With filament yarns, this tester covers a wavelength range of 2 cm to 2560 m for spectrogram analysis and assessed periodic mass variations which occurs at least 25 times as being statistically significant; these are shaded. Periodic variations occurring 6–25 times are regarded as being not statistically significant and are not shaded. Periodic mass variations occurring less than six times are not drawn out. If a periodic fault appears in the non-shaded range, then it is advisable to repeat the measurement with a longer evaluation time in order to assess the periodic faults shown in this range more accurately.

11.6 FRICTIONAL PROPERTIES

Friction refers to the resistance to the relative motion of one body sliding, rolling or flowing over another body with which it is in contact. The friction when this relative motion starts from rest is known as static friction, while the friction in the course of the relative motion is known as kinetic friction. Static friction is always greater than kinetic friction. Frictional properties of staple fibres affect the processing behaviour of these fibres and the properties of the resultant yarns. Yarns encounter many friction surfaces before they are processed into fabrics and their frictional properties can affect their processing behaviour significantly. For example, it may become very difficult to produce a weft-knitted fabric from a yarn with a high coefficient of friction. Torque transmission and filament migration during false-twist friction texturing is dependent on the frictional properties of filament yarns. Similarly air-jet texturing behaviour of filament yarns is also critically dependent on interfilament friction.

A number of methods for measuring frictional characteristics of fibres and yarns have been described in the literature [9, 10]. In the case of fibres, resistance to the movement of a block on a fibre pad can be measured to calculate the fibre friction:

$$F = \mu N$$

where F is the force needed to move the block, N is the normal load on the friction surface, and μ is the coefficient of friction.

In the case of yarns, friction measuring methods generally involve measurement of tensions in the yarns before and after their contact with a metal pin/pulley (Fig. 11.8(a)). In a number of instruments these
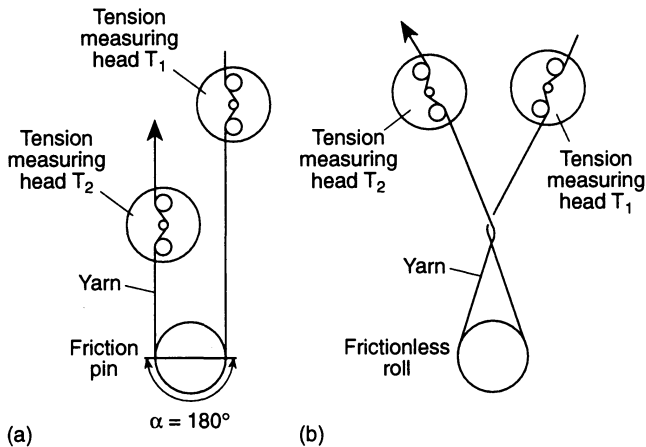
Fig. 11.8 Friction measurement: (a) yarn-to-metal; (b) yarn-to-yarn.

tension values are used to rotate a lever so that the coefficient of friction can be indicated directly on a scale based on Amonton's law:

$$\frac{T_2}{T_1} = e^{\mu\theta}$$

where T_2 is the output tension, T_1 is the input tension, θ is the angle of wrap of yarn over friction pin/pulley, and μ is the coefficient of friction.

In some cases, it is recommended that either the difference between T_2 and T_1, i.e. $(T_2 - T_1)$, or their ratio (T_2/T_1), is used as a measure of yarn friction as Amonton's law is not exactly applicable to textile yarns. In the case of yarn-to-yarn friction, the tension in the yarn before and after wrapping around itself for one or two turns can be used (Fig. 11.8(b)). A number of instruments including the Rothschild's F-Meter, CSI's CS-151 Tester, Zweigle μ-Meter (G-530), Shirley Yarn Friction Tester and Lawson-Hemphill's Yarn Friction Meter are available to determine fibre-to-metal and fibre-to-fibre friction.

The above methods can be used to measure both static and kinetic friction.

A number of factors such as polymer type, the amount of lubricant applied, lubricant viscosity, fibre denier and twist level affect the fibre-to-fibre, fibre/yarn-to-metal and yarn-to-yarn friction. In addition to these, test conditions affect the friction values [10, 11]. In order to get consistent readings, yarn speed, input tension, diameter of the friction pin, guide surface roughness, temperature and relative humidity must be standardized.

11.7 SHRINKAGE BEHAVIOUR

Fibre or yarn shrinkage refers to the decrease in length of a specimen when it is placed without any constraints in a hot environment, e.g. boiling water, a dry oven or a steam chamber, for a specific length of time. The shrinkage is calculated as a percentage change of the original specimen length:

$$\text{Shrinkage (\%)} = \frac{L_0 - L}{L_0} \times 100$$

where L_0 is the initial specimen length and L is the specimen length after shrinkage. In some cases, there is an increase in length rather than a decrease. This is referred to as a negative shrinkage or stretch [12].

The amount of fibre shrinkage and the development of the shrinkage force either due to hot/boiling water or dry heat will affect the processing behaviour of these yarns and will bring about dimensional changes in the fabrics made from these yarns. Differences in shrinkage behaviour of either warp or weft threads may lead to a cockled appearance in the
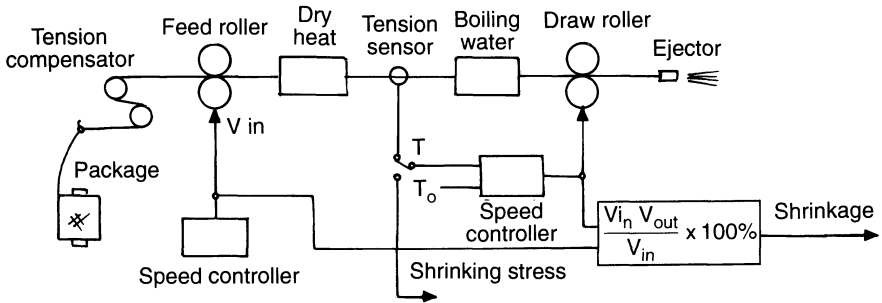
Fig. 11.9 Toray Yarn Thermal Analysing System FTA-500.

fabric after the hot-wet treatments in the course of finishing. In the normal flat polyester yarn, shrinkage may vary between 5 and 8%; however, with proper heat-setting, residual shrinkage can be reduced to a level less than 1%. In a quality control programme, there must be a means of assessing and controlling shrinkage behaviour of the yarn. Assessment can be done by measuring the shrinkage in either a discontinuous/continuous test or through the measurement of shrinkage force generally in a continuous test.

Discontinuous tests can be carried out on a single fibre, a bundle of fibres, a yarn or a skein of yarn. The length of a conditioned specimen is measured under a specific load which is sufficient to straighten but not stretch the specimen. The specimen is then immersed in hot/boiling water or exposed to dry heat/other shrinkage media for a fixed length of time. The specimen is then reconditioned and the length measured again; the change in length is estimated as a percentage of the length before immersion or exposure.

The Toray Yarn Thermal Analysing System shown in Fig. 11.9 can measure four parameters, namely (1) boiling water shrinkage, (2) boiling water shrinkage force, (3) dry heat shrinkage, and (4) dry heat shrinkage force, on a running yarn. For shrinkage measurement, the yarn is pretensioned before being fed in the measuring zone at constant speed. The yarn is then heated in either the dry heat furnace or the boiling water bath. It develops a shrinkage force which is measured by a tension sensor. The speed of the output rollers is adjusted to keep the testing tension constant. Measurement of the draw roller and feed roller speeds allows the calculation of percentage shrinkage, which can be constantly recorded.

For the measurement of shrinkage force, the speed of the output roller is also kept constant at a predetermined value and the tension, which represents the shrinkage force, is measured.

The Dynamic Shrinkage Tester (CTT-DST) from Lawson–Hemphill Inc. utilizes its ability to maintain constant tension in running yarns at

speeds between 20 and $240 \, \text{m min}^{-1}$, and at temperatures up to 250 °C for determining shrinkage and shrinkage variations in synthetic filaments or yarns.

Other instruments for measuring the shrinkage force in the case of drawn yarns and the drawing force in the case of POY or undrawn yarns based on a similar principle are the Dynafil from Textechno and the DEFT (Dynamic Elongation Force Tester) and CCT (Continuous Crimp-force Tester) from Rothschild.

An instrument like the Dynafil measures the contraction force on running yarn with predetermined length changes or without length alterations, at room temperature or with yarn heated in the test zone using the basic setup shown in Fig. 11.10. In addition to measuring shrinkage force, the instrument can also be used to measure the drawing force in the case of POY yarns and the crimping force in the case of textured yarns. The unit employs a tubular heater of length 70 cm with adjustable temperature from room temperature to 280 °C. Adjustment of length can be carried out by change godets between −50% and 400%, depending on the requirements of the test.
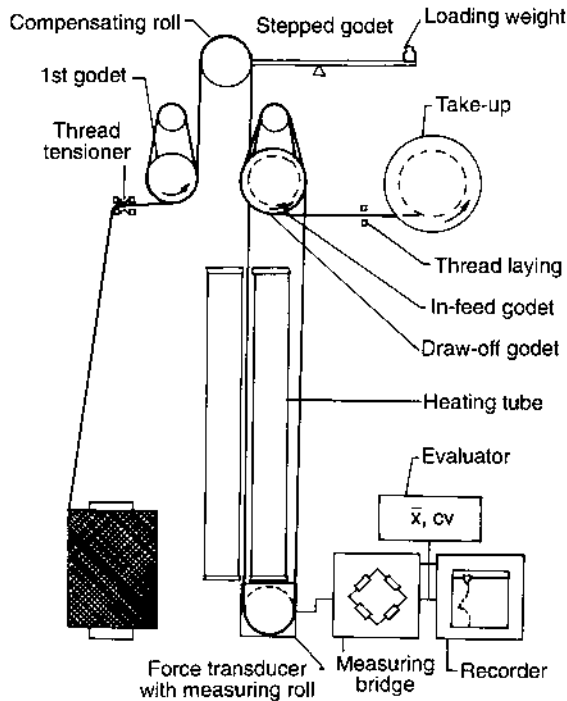
Fig. 11.10 Dynamic thermal stress tester Dynafil.

Drawing force testing on partially oriented yarn (POY) is carried out by hot drawing of the thread accompanied by tensile force measurement in the drawing zone. Draw ratios similar to those in downstream processing of these yarns are kept on the instrument. Faults in the spinning process like changes in polymer properties, spinning temperature, quench air conditions or take-up speed – which in turn cause problems in downstream processing or defects in the end product – are reflected in a deviating level or changed variation limits of the drawing force. Stein [13] has compared various methods for testing POY yarns to find the effect of variations in air blast velocity in the spinning tower, the spinneret temperature and the polymer viscosity on POY properties. It has been shown that the drawing force test on running thread using the Dynafil tester is the most effective in detecting changes in POY properties due to changes in process variables.

While testing shrinkage force on textured yarns, tension in the thread is measured as it runs through the heater with an overfeed of either 0 or 5%. These values are closely correlated to the conditions of yarn production, i.e. texturing and also spinning conditions. Stein and Wallas [14] have described the use of the Dynafil for measuring the shrinkage force on a running thread.

Crimp force testing is a special case of shrinkage force testing on textured yarns. A relatively low heating tube temperature is used, causing optimal crimp development without much shrinkage, and provides a measure of crimp contraction for textured yarns.

11.8 ENTANGLEMENT TESTING

Filament yarns are air entangled during spinning (also high speed spinning), drawing, texturing (false-twist and BCF texturing), winding and draw-warping to improve the further processability of these yarns without true twisting or sizing. In most cases a temporary cohesion is imparted to the yarn through entanglement of filaments, normally at length intervals, and this cohesion is expected to be removed by the applied tension in the final fabric form.

Entangled yarns consist of sections of intimate interlacing of the filaments alternating with sections where the filaments run almost parallel (open sections). Entangled yarns are characterized by their opening length, i.e. the distance between two entangled points. Besides the average opening length, other important parameters of an entangled yarn are the number of entanglements per unit length of the yarn and the stability and distribution of entanglements.

There are various methods available to determine the entanglement characteristics in filament yarns:

- manual needle method, in which a needle is inserted into the pre-tensioned yarn and moved from one entangled point to the next;
- automatic needle method, in which a needle is inserted into the yarn and the yarn moved along its axis until the needle registers an entangled point (Rothschild's Entanglement Tester);
- electrostatic method, i.e. separation of the filaments by electrostatic charges, accompanied by optical monitoring of the running yarn (Obestat, Enka Technica System);
- automatic thickness measurement, i.e. registration of entangled spots (points) on the running yarn by measurement of yarn thickness (Itemat, Reutlingen Interlacement Counter).

Each of the above mentioned techniques/principles is discussed below.

11.8.1 MANUAL NEEDLE METHOD

To determine the opening length, the yarn is fixed at two ends with the required tension. The yarn is split in the middle by a needle which is pushed in by hand. The needle is pulled forward in the yarn in the direction of filaments till it encounters an entangled point. The distance covered by the needle is then measured. The experiment is carried out repeatedly and an average distance between entangled points is obtained; this is taken to be the opening length.

11.8.2 AUTOMATIC NEEDLE METHOD

The Rothschild/Celanese NPT (Needle Pull Tester R-2040/2050) is a device which automatically measures the opening length, records it and gives the value after a fixed number of tests.

The yarn to be tested is pretensioned by two hysteresis brakes in such a way that the yarn tension at the NPT input is $0.2\,\mathrm{gf\,den}^{-1}$. After running through a preset yarn length, the yarn is jammed by two yarn guides and spread by two grooves, whereupon it is pierced by a needle. The yarn then advances automatically at an adjustable speed, while the yarn tension measuring head of the electronic tensiometer checks the yarn tension. After a preset trip level tension has been reached, the yarn stops and the needle is withdrawn from the yarn. The yarn length up to this critical point is then measured by an electronic counter relay and stored in a memory. A series of such measurements is carried out automatically and the test results are printed after the completion of a preset number of tests.

11.8.3 ELECTROSTATIC METHOD

The Obestat apparatus for the examination of entangled yarns is based on the electrostatic principle. The yarn specimen is led at constant speed

through a hollow electrode which is connected with a controllable high voltage DC source of about 50 kV. Moist air is also led into the electrode to wrap the yarn and thereby increase its electric surface conductivity. This ensures that sufficient electric potential is conveyed to the yarn and is uniformly distributed, regardless of the type of yarn material and finish. Having passed the electrode and entered the free space between the electrode and an insulated yarn guide, the filaments spread out under the influence of the repulsive action of like charges. The structure of the entangled yarn is thus made visible.

To achieve uniform spreading of the filaments, a certain amount of tension (about $0.05\,\mathrm{cN\,tex^{-1}}$) is maintained in the yarn by advancing the yarn through a feeding mechanism with predetermined forwarding speed and arranging for suction to maintain the required tension level.

The tangle distance of the entangled yarn is determined by optical scanning of the yarn in its spread condition by means of a light barrier. The difference in the shadows of the open sections of the yarn and the entangled knots is registered in the photodetector and transformed into impulses which are tuned up and counted electronically. Simultaneous metering of the scanned yarn length by monitoring the forwarding rollers in relation to the entanglement or knot impulses allow continuous determination of the tangle distances which are displayed digitally, transferred into printing or punched tape and also registered. A small computer processes the data and at the end of the test gives the mean value of the tangle distance as well as its standard deviation.

11.8.4 AUTOMATIC THICKNESS MEASUREMENT

Instruments have been developed to measure continuously the yarn diameter. A change in diameter is encountered as an entangled knot passes through the sensor. For the purpose of measurement two principles could be used.

(a) Optical method to find the diameter of the yarn

The Toray yarn profile tester works on this principle. The sample is unwound from the package. Tension is set by a tension compensator. The yarn is fed to a testing block at a constant speed after being taken up by the feed rollers. Afterwards, it is removed by the draw roller and passes out through the ejector. The tension sensor at the testing block measures tension and maintains it at the preset value by automatically adjusting the draw roller speed.

The yarn is illuminated by the lamp in the testing block. The image of its shadow is transmitted to the image sensor through a lens. The yarn external diameter is then measured from the size of the image.

(b) Mechanical method to find the diameter of the yarn

When a yarn passes between a fixed plate and a spring-loaded plate, the spring pressure displaces the filaments and arranges them in parallel tape configuration while interlaced sections resist the flattening and are registered as a thick place; the increase in thickness is proportional to the degree of interlacement. The movement of the pin is transferred to a highly sensitive meter whose signals are fed to two switches set to different threshold values. Depending upon the size of thick place in the yarn, the signal passes the first or both thresholds, activating the counter which registers the number and size of the signals, thus determining the degree of interlacement. Two commercial instruments based on this principle are the Itemat Interlacing and Tight Spot Tester and the Reutlingen Interlacement Counter.

REFERENCES

1. ASTM Standard D1577-79 (1990) Standard test methods for linear density of textile fibers, *Annual Book of ASTM Standards*, Vol. 7.01, ASTM, Philadelphia.
2. ASTM Standard D3937-90 (1990) Standard test method for crimp frequency of man-made staple fibers, *Annual Book of ASTM Standards*, Vol. 7.02, ASTM, Philadelphia.
3. ASTM Standard D76-90 (1990) Standard specification for tensile testing machines for textiles, *Annual Book of ASTM Standards*, Vol. 7.01, ASTM, Philadelphia.
4. Singleton, R.W. (1967) Fiber testing, in *Man-made Fibers: Science and Technology*, Vol. 3 (eds H.F. Mark, S.M. Atlas and E. Cernia), John Wiley & Sons, New York.
5. Furter, R. (1985) *Manual of Textile Technology: Strength and Elongation Testing of Single and Ply Yarns*, The Textile Institute, Manchester.
6. *Uster News Bulletin* (1984) No. 32, October.
7. Zellweger Uster AG. *Fault Lexicon for Man-made Continuous Filament Yarns*, Zellweger Uster AG Publication.
8. *Uster News Bulletin* (1988) No. 35, October.
9. Morton, W.E. and Hearle, J.W.S. (1975) *Physical Properties of Textile Fibres*, William Heinemann Ltd, London and the Textile Institute, Manchester.
10. Schick, M.J. (ed.) (1975) *Surface Characteristics of Fibres and Textiles*, Part I, Marcel Dekker, New York.
11. Smith, D.E., Burns, N.D. and Wray, G.W. (1974) *J. Textile Inst.*, **65**, 337.
12. ASTM Standard D2102-90 (1990) Standard test method for shrinkage of textile fibers, *Annual Book of ASTM Standards*, Vol. 7.01, ASTM, Philadelphia.
13. Stein, W. (1981) *Int. Textile Bull., Spinning*, No. 3, pp. 259–276.
14. Stein, W. and Wallas, K. (1976) *Melliand Textilber.*, **57**, 97–103.

Poly(ethylene terephthalate) fibres **12**

V.B. Gupta, A.K. Mukherjee and S.S. Cameotra

12.1 INTRODUCTION

Poly(ethylene terephthalate), or PET, is the most outstanding member of the family of polyester fibres. Polyester is defined by the International Standards Organisation (ISO) as 'a polymer comprising synthetic linear macromolecules having in the chain at least 85% (by mass) of an ester of a diol and terephthalic acid' [1]. A comprehensive compendium on PET dealing with historical, technical, research and commercial aspects has been recently published [1].

In the early 1940s, the use of terephthalic acid for the development of polyester fibres was implemented at almost the same time in Germany by Schlack at a branch of Agfa Wolfen and in the UK by Whinfield and Dickson in the laboratories of the Calico Printers' Association. The initial efforts in making polyester are shown by the following scheme [2a]:
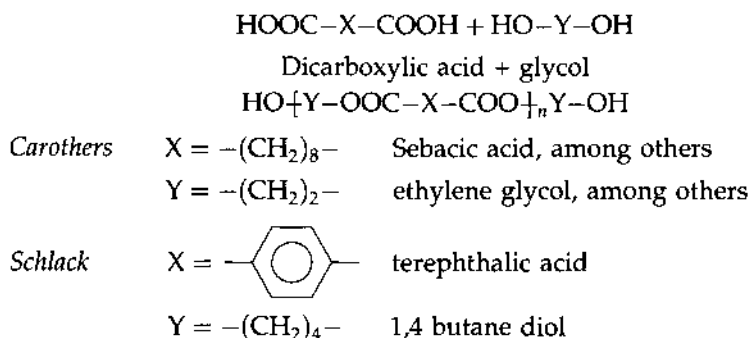
$$HOOC-X-COOH + HO-Y-OH$$

Dicarboxylic acid + glycol

$$HO\{Y-OOC-X-COO\}_n Y-OH$$

Carothers $X = -(CH_2)_8-$ Sebacic acid, among others

$Y = -(CH_2)_2-$ ethylene glycol, among others

Schlack $X = -\langle O \rangle-$ terephthalic acid

$Y = -(CH_2)_4-$ 1,4 butane diol

Whinfield and Dickson $X = -\langle\bigcirc\rangle-$ terephthalic acid

$Y = -(CH_2)_2-$ ethylene glycol
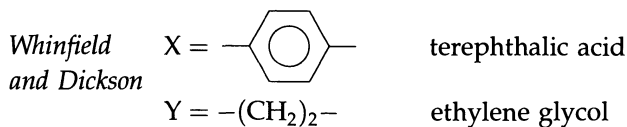
The combination chosen by Whinfield and Dickson was the most favourable from the point of view of economy and application to textile usage. Technological development of this process was carried out from 1947 in the USA by Du Pont and in the UK by ICI after both companies had acquired the patent rights from the Calico Printers Association Ltd in Manchester, UK; Du Pont for the USA and ICI for the rest of the world. Du Pont began PET production in North Carolina in the USA in 1953 and ICI initiated production in the UK in 1954.

The present scenario and the future trends for polyester fibres have been considered by McIntyre [3] and are seen to be dominated by acute pressure on the price margins of this commodity fibre. As a result of this, the producers are interested in cheaper intermediates, large-scale production lines, elimination or integration of stages and automation of manufacture. However, so much has already been achieved in this direction that further progress is increasingly difficult, but it may be necessary to stay competitive. Against this backdrop the growth in production of standard commodity fibres, according to McIntyre, is likely to be located largely in developing countries and in China, while producers in the more developed countries will look for products with a higher return to improve their profitability. There is keen interest in the developed countries in speciality fibres and fabrics, as fine and ultra fine counts, spun aesthetics in continuous filament yarns, profiled and hollow fibres, bicomponent and matrix–fibril structures and suedes. Industrial fibres have withstood recession better than conventional apparel and domestic products and the geotextile market is an important one. The pattern for fibre production in all industrialized nations is changing rapidly, moving towards lower volume but much higher value-added products.

This chapter will deal with the production of PET polymer and the production and processing of PET filament and staple fibre. Their structure and mechanical properties and their important applications will also be very briefly considered.

12.2 POLYMER PRODUCTION

Poly(ethylene terephthalate) is a step growth (condensation) polymer and is produced industrially by one of the following two routes:

1. DMT route: raw materials are dimethyl terephthalate (DMT) and monoethylene glycol (MEG);

2. PTA route: raw materials are terephthalic acid (TPA) and monoethylene glycol (MEG). [In this chapter the process based on the use of TPA will be designated as the PTA (purified terephthalic acid) process.]

12.2.1 RAW MATERIALS

In the early stages of PET production technology, polymer-grade TPA was not available and so the indirect method of synthesizing via DMT was developed. By the early 1960s processes for TPA were commercialized, and since then the direct process of PET manufacture using TPA has been increasingly used.

The principal raw materials are produced industrially as follows: TPA by bromine-controlled oxidation of *para* xylene [4–6], DMT by esterification of crude TPA with methanol [7–9], and MEG by direct catalytic oxidation of ethylene followed by hydrolysis of ethylene oxide formed [10, 11].

The criteria of purity [2b, 2c, 3b] are stringent, as given in Table 12.1.

Table 12.1 Criteria of purity for DMT, MEG and TPA [2b, 2c, 3b]

Parameter	Required value
DMT	
Melting point	141 °C
Boiling point	280 °C
Acid number	0.2
Saponification number	578
Residue on ignition	0.08
Ester interchange value	96% in 2 h
Halogen content	Trace
Iron content	0.0005%
Nitrogen content	0.00005%
MEG	
Boiling point	195–198 °C
Density	1.110–1.112 g cm^{-3} at 20 °C
Refractive index	1.4330–1.4340 at 20 °C
Water content	0.1%
Ester interchange value	90
Halogen content	Trace at most
TPA	
p-Carboxybenzaldehyde	$\leq$25 ppm
p-Toluic acid	$\leq$150 ppm
Total metal	$\leq$9 ppm
Water	$\leq$0.2 ppm
Ash	$\leq$15 ppm
Colour in 2 N KOH	10 (Hazen unit)
Particle size range	50–600 µm

12.2.2 PRODUCTION PROCESSES

A high molecular weight PET is an essential prerequisite for fibre formation. To obtain high molecular weight PET, it is imperative that the two monomers are present during reaction in equimolar (1:1) proportion. Otherwise the resultant product will be of low molecular weight.

To ensure this stoichiometry ratio of 1:1, an intermediate reaction is conducted between the two monomers (DMT and MEG or TPA and MEG) to produce a new intermediate, diglycol terephthalate (DGT). In DGT, the acid:glycol ratio is chemically fixed at 1:2. This is the first stage in PET production and is based on the patent of Whinfield and Dickson [12].

(a) The two routes

The process involved in the reaction between DMT and MEG (shown below) is referred to as ester interchange (EI) or transesterification (TE).

$$H_3C-OOC-\langle\bigcirc\rangle-COO-CH_3 + 2HO-(CH_2)_2-OH$$

<div align="center">DMT   MEG</div>

$$HO-(CH_2)_2-OOC-\langle\bigcirc\rangle-COO-(CH_2)_2-OH + 2CH_3OH$$

<div align="center">DGT   Methanol</div>
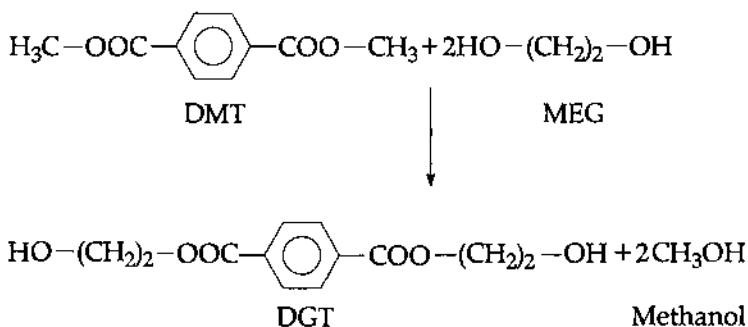
On the other hand, direct esterification (DE) occurs if TPA and MEG are used, as shown below.

$$HOOC-\langle\bigcirc\rangle-COOH + 2HO-(CH_2)_2-OH$$

<div align="center">TPA   MEG</div>

$$HO-(CH_2)_2-OOC-\langle\bigcirc\rangle-COO-(CH_2)_2-OH + 2H_2O$$

<div align="center">DGT</div>
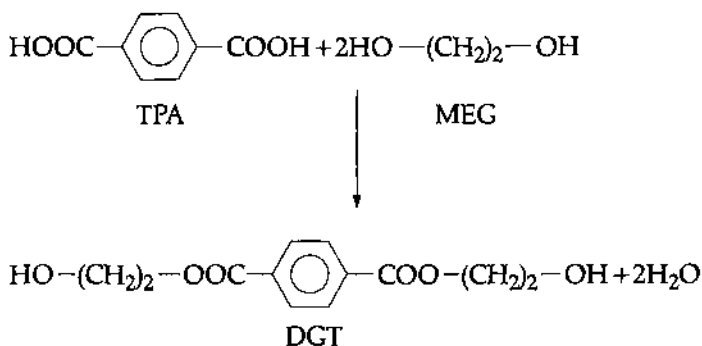
Once DGT is formed, the second stage of polycondensation is similar for both routes, as shown below.

$$n\text{HO}-(\text{CH}_2)_2-\text{OOC}-\langle\bigcirc\rangle-\text{COO}-(\text{CH}_2)_2-\text{OH}$$

DGT

$$\text{HO}\left[\text{CO}-\langle\bigcirc\rangle-\text{COO}\,(\text{CH}_2)_2-\text{O}\right]_{n-1}\text{H}+(n-1)\text{HO}-(\text{CH}_2)_2-\text{OH}$$

PET   MEG
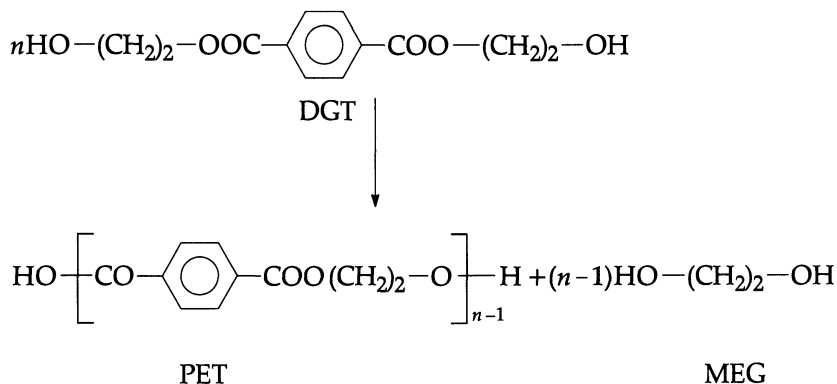
The intermediate DGT formation leads to a number of advantages compared with a direct mixture of monomers subjected to polycondensation. These advantages are:

1. the polycondensation process is applied to a uniform, chemically pure, monomeric starting material;
2. wider choice of catalysts;
3. fewer side reactions;
4. higher speed of reaction;
5. good colour of the polyester;
6. better thermal stability of the melt; and
7. better drawability, etc.

(b) Batch and continuous processes

Irrespective of the route followed, i.e. the DMT or the PTA route, the production of PET fibre-forming polymer can be achieved by either the batch or the continuous process. However, the continuous process is favoured because it offers the following advantages [13].

- The fibre produced is uniform, day in and day out, provided the plant is operated at the normal level of throughput.
- The fibre being produced from a polymer melt that is superior on account of its thermal history, is of better quality.
- The fibre, being free from oxidative degradation, is whiter than the batch process polyester fibres, despite the fact that it has not been given optical brightening treatment, which creates only a temporary illusion of whiteness.
- The fibre is stronger, other things remaining the same.
- The fibre is less liable to 'merge' change, given uniform quality of raw materials and normal levels of throughput.

Though the continuous process offers a number of advantages, it has low flexibility and high power failure sensitivity.

In general, the existing commercial plants can be classified [13] into the following three categories:

1. Batch process (batch polymerization and screw melter spinning, as shown in Fig. 12.1(a)). The polymer produced by the batch process shows considerable fluctuation in quality from batch to batch and the PET chips are therefore blended before spinning. To eliminate chip agglomeration and melt hydrolytic degradation, chips are crystallized and dried before being remelted in screw melter and then fed to spinning machines.
2. Semicontinuous process (continuous polymerization and screw melter spinning, as shown in Fig. 12.1(b)). In this process also the chips are blended before melt-spinning.
3. Continuous process (continuous polymerization and direct spinning, as shown in Fig. 12.1(c)). In this process, the polymer from the last polycondensation vessel is pumped directly to spinning machines for melt-spinning into fibres and therefore eliminates the PET chips manufacture, handling, drying and remelting steps.

A comparison of the three processes is made in Table 12.2.

Two new trends are worth highlighting [13]. The first is the development of transfer line injection (Fig. 12.1(d)), and the second is the use of artificial intelligence as expert systems. In transfer line injection, instead of adding additives such as titanium dioxide delustrant, colour pigments, UV stabilizers and fillers upstream in the monomer line, they are directly injected downstream, as shown in Fig. 12.1(d). This reduces the time for product changes from 2–4 h to less than 20 min. The expert system is a computer line which makes process changes automatically.

(c) Process via the DMT route

In the DMT route, the first step is transesterification followed by polycondensation (PC). A flow diagram of PET manufactured by this route is shown in Fig. 12.2 [14]. The following four aspects relating to this process will be considered first: (1) catalysts used, (2) side reactions, (3) degradation, and (4) thermal stabilizers. This will be followed by a description of the process.

Catalysts used

Transesterification involving DMT and MEG is a slow process and requires a catalyst to augment the process. The catalyst can be (1) a
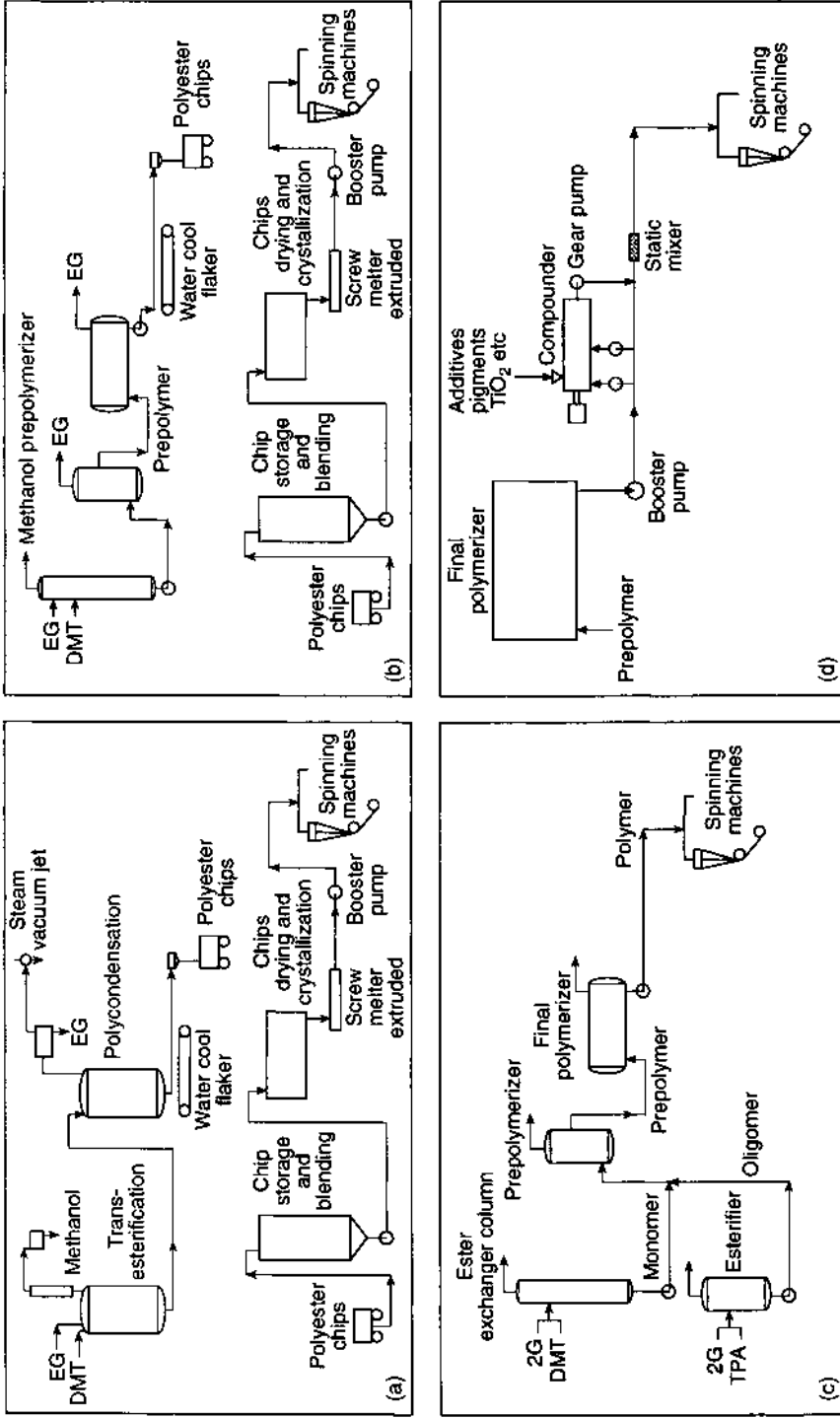
Fig. 12.1 Various production routes: (a) batch polymerization and screw melter spinning (batch process); (b) continuous polymerization and screw melter spinning (semicontinuous process); (c) continuous polymerization direct spinning (continuous process); and (d) transfer line injection on-line compounding [13].

Table 12.2 Manufacturing processes: a comparison [13]

Parameter	Processes		
	Batch	Semicontinuous	Continuous
Operation/Process			
Design	Simple	Complex	Complex
Investment			
>75 t day^{-1}	High	Medium	Low
<50 t day^{-1}	Low	High	Medium
Building space	Large	Large	Small
Equipment utilization	Low	Medium	High
Yield	Low	Medium	High
Labour cost	High	Medium	Low
Energy requirements	High	Medium	Low
Operation	Complex	Complex	Simple
Operating cost	High	Medium	Low
Quality feedback	Slow	Slow	Fast
Power failure sensitivity	Low	Medium	High
Flexibility	High	Medium	Low
Quality/Uniformity			
Degradation	High	Medium	Low
Thermal heating	Non-uniform	Uniform	Uniform
Colour	Fair	Good	Better
DEG	High	Medium	Low
COOH	High	Medium	Low
Filter pack life	Short	Medium	Long
Molecular weight uniformity	Fair	Good	Better
Product quality/uniformity	Fair	Good	Better

metal, (2) a metal oxide, or (3) a metal salt. Usually a metal oxide or a metal salt of a weak or volatile acid is used. Acetates of various metals are most commonly employed in industry; the catalytic reactivity of these acetates follows the order [3d]:

$$Zn > Pb > Mn > Co > Mg > Ca > Sn > Na > Sb$$

as shown in Fig. 12.3 [15] for some catalyst systems.

Usually, the more powerful catalyst also enhances the most undesirable (ether-forming) side reaction, as indicated by the following order:

$$Zn, Co > Mn, Pb, Ca.$$

To achieve a balance between these two opposing effects, usually a combination of a high activity catalyst with a low activity one is used in the industry. A catalyst amount of 0.02–2% is common. It must
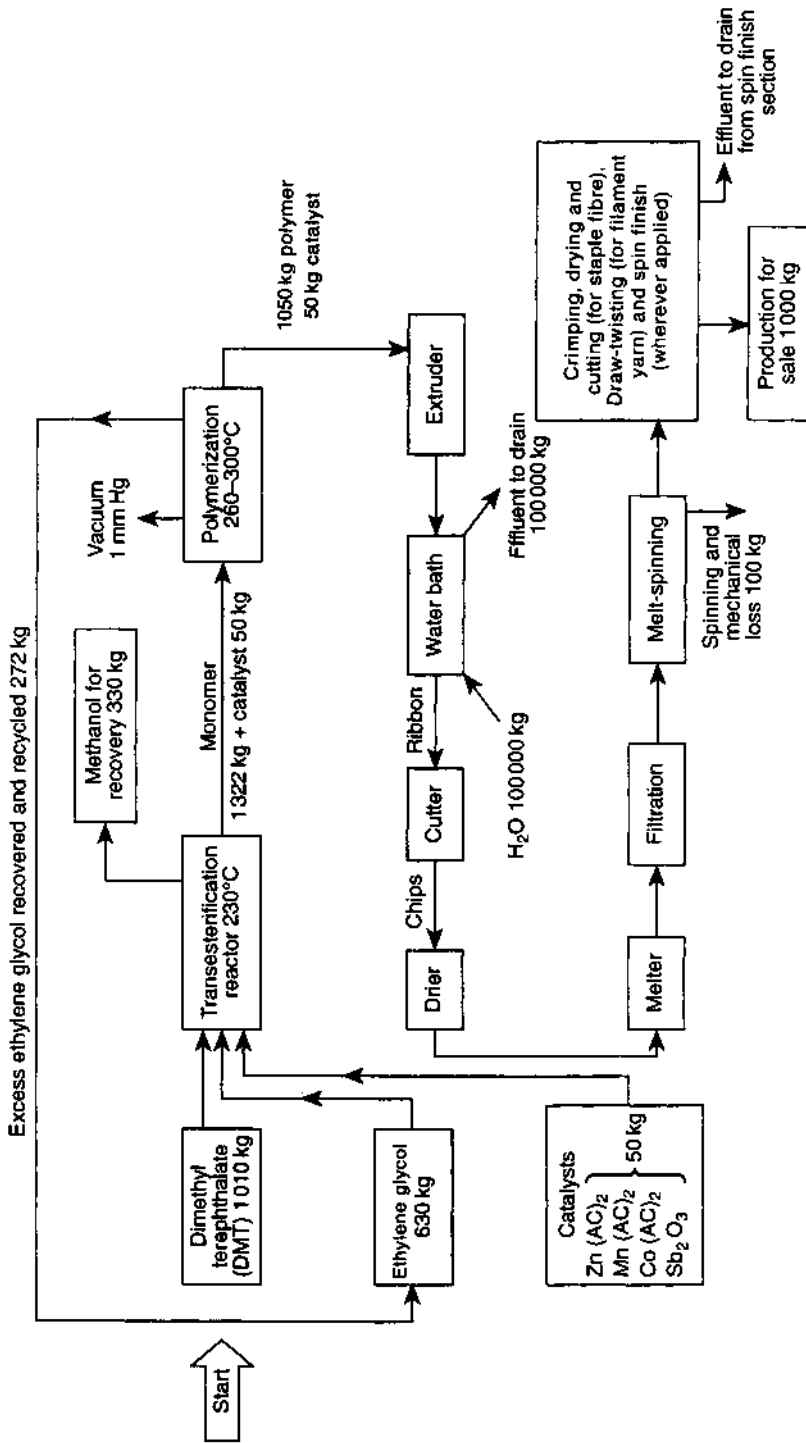
Fig. 12.2 Flow diagram for the manufacture of polyester fibre by the DMT route [14].
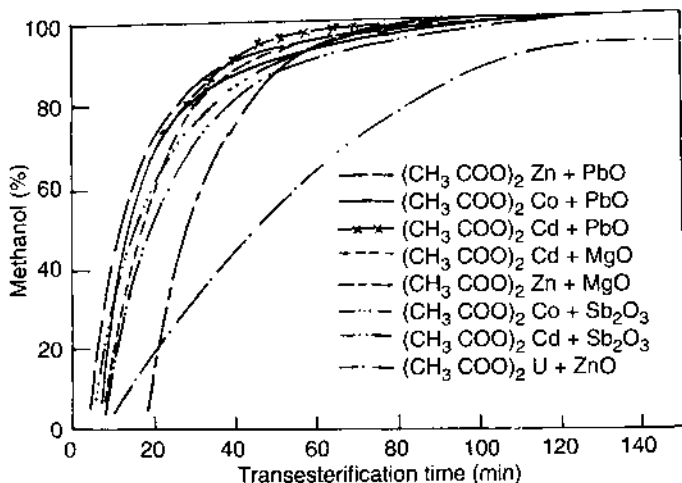
Fig. 12.3 Course of methanol cleavage during ester interchange at 200 °C as a function of different combinations of catalysts [2, 15].

be remembered that all catalysts used in the TE step enhance PET degradation in the PC stage. For this reason it has become customary to use catalyst deactivators in the PC stage.

Antimony-based catalysts are unique as they do not catalyse the EI step but become active in the PC step. The most commonly used antimony-based catalysts include antimony trioxide and antimony triacetate.

Side reactions

Several side reactions may occur during the EI step. They also occur in the DE step in the PTA route. Of these the following two are the most important and difficult to avoid completely.

1. Ether group formation between two PET molecules:
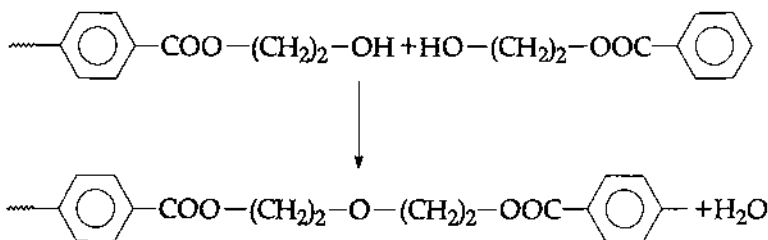
This reaction may deactivate the catalyst.
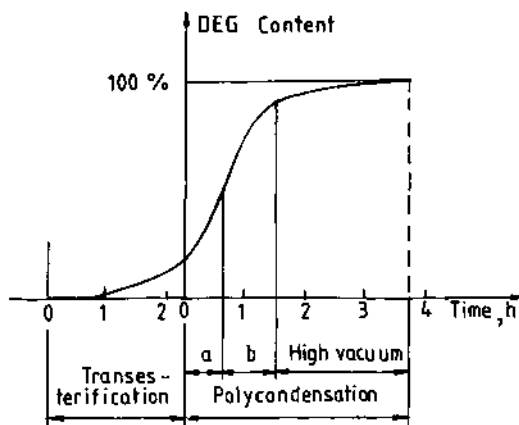
Fig. 12.4 DEG formation rate in different stages of PET synthesis: a, preheating; b, low vacuum [16].

2. Reaction between two ethylene glycol molecules:

$$HO-(CH_2)_2-OH + HO-(CH_2)_2-OH$$

$$\downarrow$$

$$HO-(CH_2)_2-O-(CH_2)_2-OH + H_2O$$

Diethylene glycol (DEG)
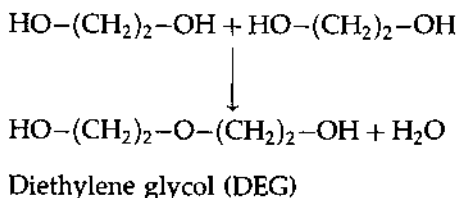
The catalyst system chosen for polymerization affects the molecular structure of PET and has a considerable influence on the crystallization behaviour of PET. Diethylene glycol is formed at each stage of PET synthesis [16]. From Fig. 12.4, it is seen that DEG (~70%) is formed during the preheating and low vacuum stage of polycondensation. Only about 20% is formed during transesterification and about 5–10% is formed in the final stage of polycondensation. DEG often confers an irregular structure to the fibre.

Some of the DEG gets removed with recovered glycol (PC stage) while some remains in the polymer. Each mol % DEG depresses the PET melting point by about 2.5 °C.

DEG increases the dye affinity of PET fibres. It is difficult to maintain a constant level of DEG and hence with a varying amount of DEG, dye affinity will also change. Presence of DEG in the product makes it soft and the pills break away more easily with an increasing amount of DEG. Various oligomers up to a degree of polymerization (DP) of about 4 are

also formed [17]; a trimer is shown below:

$$HO \left[OC - \bigcirc - COO - (CH_2)_2 - O \right]_3 H$$

Trimer   m.p. 325– 327°C
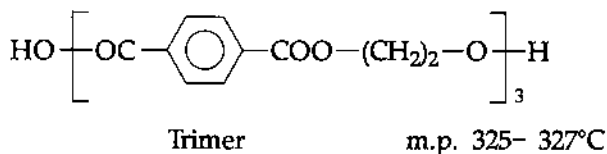
Some cyclic oligomers (about 1.5%) are also formed [18, 19], as shown below:

$$\left[\begin{array}{c} -COO - (CH_2)_2 - O - CO \\ \bigcirc \quad\quad \bigcirc \\ OC - O - (CH_2)_2 - OOC \end{array} \right]_{n\,=\,2-4}$$

$$\begin{array}{c} COO - (CH_2)_2 - O - (CH_2)_2 - OOC \\ \bigcirc \quad\quad\quad \bigcirc \\ COO \underline{\quad\quad} (CH_2)_2 \underline{\quad\quad} OOC \end{array}$$
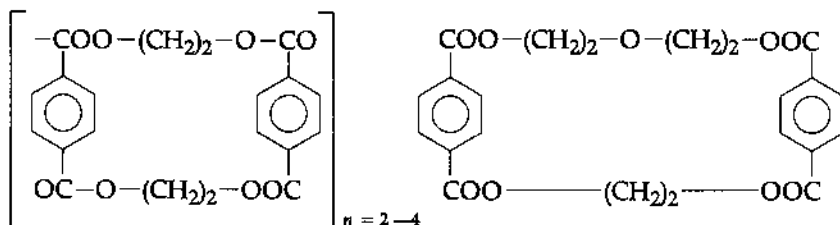
Degradation

The PET melt is thermally unstable and undergoes degradation at high polymerization temperatures, particularly above 150 °C, especially during the PC stage. Once degradation starts, the degraded products can undergo further reactions and it is not possible to predict the course of such reactions. The degradation may initiate at chain ends [20], or it may originate by scission of a PET chain [21–23]. Frequently, discoloration of PET occurs during degradation and it has been postulated that acetaldehyde formation has a role to play in it [24].

Some degradation reactions are shown below [24].

1. Chain end reactions:

$$\sim\sim\bigcirc - COOCH_2CH_2OH \longrightarrow \sim\sim\bigcirc - COOH + CH_3CHO$$

$$\sim\sim\bigcirc - COOCH_2CH_2OH \longrightarrow \sim\sim\bigcirc - \overset{O}{\overset{\|}{C}} - O - \overset{O}{\overset{\|}{C}} - \bigcirc\sim\sim$$

$$+ HO(CH_2)_2 - O - (CH_2)_2 - OH$$
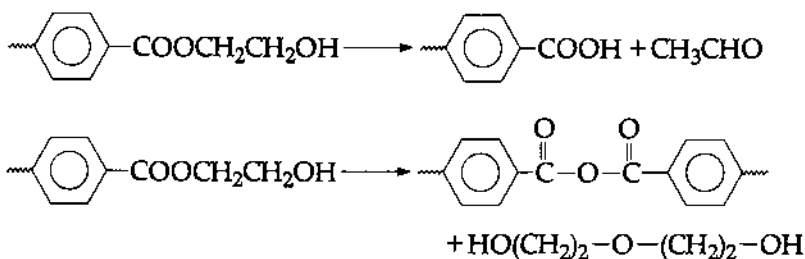
2. Chain scission:
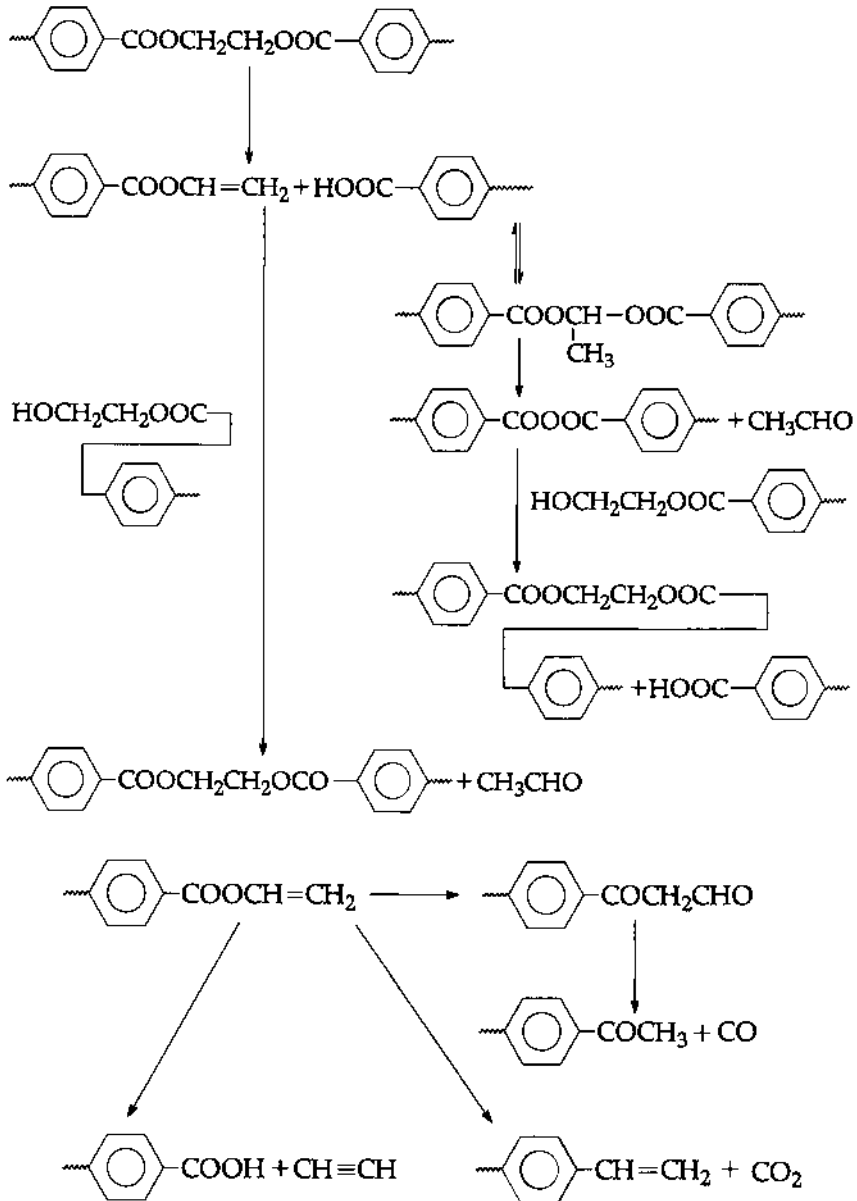
In general, the final product is affected by the degradation in the following ways:

- the molecular weight is lowered and becomes unpredictable;
- there is yellow coloration; and

- there is an increase in carboxyl end groups with a resultant decrease in the thermal stability of PET.

Thermal stabilizers

To minimize thermal degradation of the PET melt, thermal stabilizers are added. Generally, compounds of phosphorus or phosphoric acid are added prior to the PC stage. They deactivate the catalysts used during the EI step [25–29]. Commercially, triphenyl phosphite (TPP), trimethyl phosphate (TMP), tetraethyl ammonium hydroxide (TEAOH) and trisnonyl phenyl phosphite (TNPP) are commonly used.

However, some of the antimony-based catalysts used during the PC stage are reduced to metallic antimony (Sb) by such stabilizers. This occurs more for P^{3+} than P^{5+} stabilizers. Formation of antimony metal imparts a grey-green tinge to PET. It is claimed that TNPP does not affect antimony triacetate.

To produce a completely white PET, the use of germanium oxide (GeO_2) as a catalyst is recommended in the PC stage instead of antimony trioxide [3c].

The process

Dissolution of DMT in MEG   The EI process is preceded by dissolving the solid DMT in hot MEG. This can be achieved in either of the following two ways.

1. Dissolution of DMT in MEG:

$$\text{MEG}$$
$$\downarrow \text{Heat (150°C)}$$
$$\text{Hot MEG}$$
$$\downarrow \text{Add DMT}$$
$$\text{DMT solution in hot MEG}$$
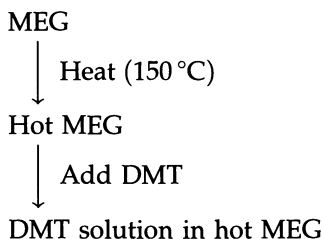
2. Melting of DMT followed by mixing with hot MEG:

$$\begin{array}{ccc} \text{DMT} & & \text{MEG} \\ \downarrow \text{Heat (150°C)} & & \downarrow \text{Heat (150°C)} \\ \text{DMT melt} & & \text{Hot MEG} \end{array}$$

$$\downarrow \text{Mix}$$
$$\text{DMT solution in hot MEG}$$
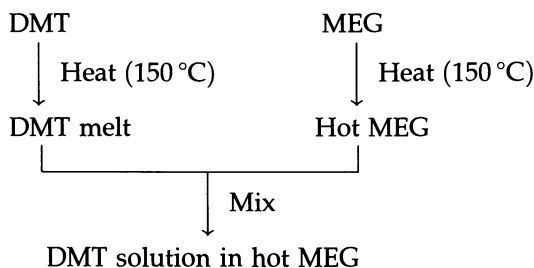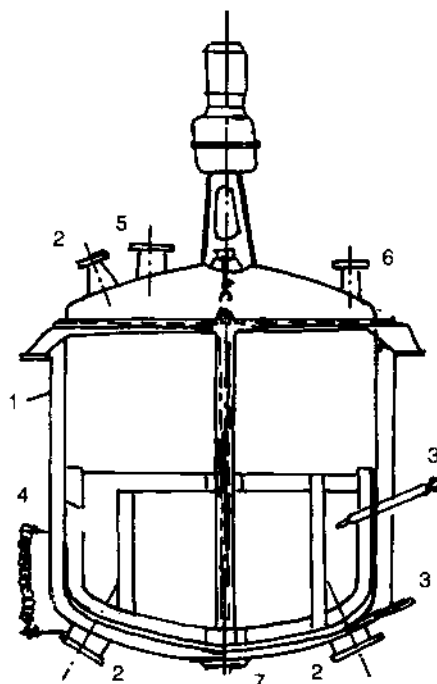
Fig. 12.5 Kettle for dissolving dimethyl terephthalate in glycol [2]. Key: 1 = Dinyl heating jacket; 2 = electric Dinyl heating brackets; 3 = thermometer; 4 = level indicator for Dinyl liquid; 5 = DMT inlet; 6 = glycol inlet; 7 = discharge for solution.

The kettle (Fig. 12.5) in which solid DMT is dissolved in glycol is made of non-rusting material with an iron double casing for 'Dowtherm^{TM}' vapour or 'Dinyl' heating [2d]. Dowtherm, which is a mixture of biphenyl and biphenyl oxide, is a product of Dow Chemical Co., USA. The lower part of the kettle is cone-shaped or rounded and has welded supports for the heating tubes. The cover is usually fitted with supports for the filter, a nitrogen connection, air vents, ports with reflux cooler, an observation window and a stirrer. The outlet ports are positioned at the lowest part of the kettle.

After pouring glycol into the dissolving kettle, titanium dioxide (particle size 0.5–1.5 µm) in the form of 30% suspension, and in the proportion of 0.3–0.6% based on DMT, is added together with DMT with stirring. A small current of nitrogen gas is passed through the kettle to provide an inert atmosphere. Temperature in the range 150–160 °C is most favourable for dissolution and a charge of about 1000 kg (1 t) requires 3–6 h for complete dissolution.

Melting and mixing The melting and subsequent mixing process offers several advantages over the dissolution process [2e]. They are: (1) the
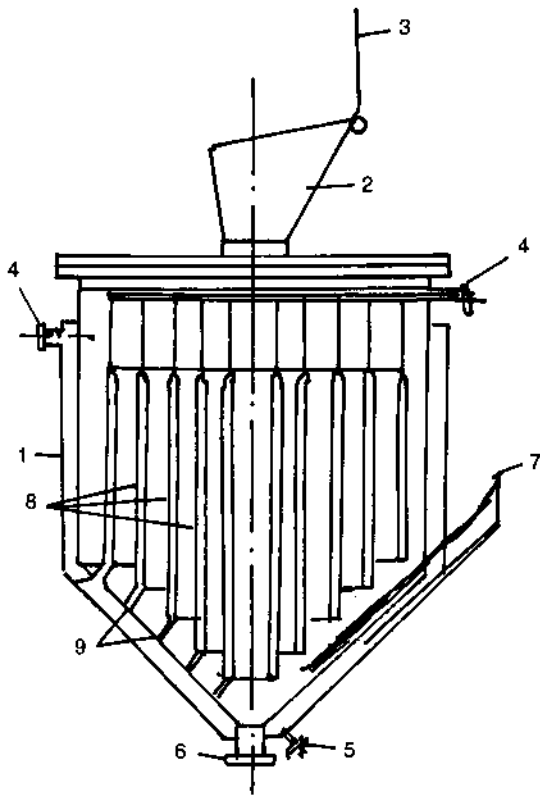
Fig. 12.6 Kettle for melting dimethyl terephthalate [2]. Key: 1 = steam-heated jacket; 2 = DMT filling funnel; 3 = lid above filling funnel; 4 = steam inlet valve; 5 = outlet for condensed water from heating jacket; 6 = DMT melt outlet; 7 = thermometer; 8 = heating element; 9 = outlet for condensed water from heating element.

solution is produced more rapidly, (2) the premelting of DMT imparts better stability to the melt, (3) side reactions are fewer, and (4) dwell time in the kettle is reduced.

The process can have several variations. In one of them, the melting kettle (Fig. 12.6) has a double casing, and may be round, square, or any other shape. It is heated by high pressure steam, biphenyl or by direct fire. The cover has brackets for light, an observation window and a filling port. The melting area may be increased by special arrangement, e.g. several perpendicular heating elements sloping upwards may be fitted. Pressing accelerates the melting and is done by means of a ram that presses the DMT against the heated grating.

Before filling, the kettle is heated to the required temperature and DMT is then introduced. The DMT is melted at 170–180 °C on the
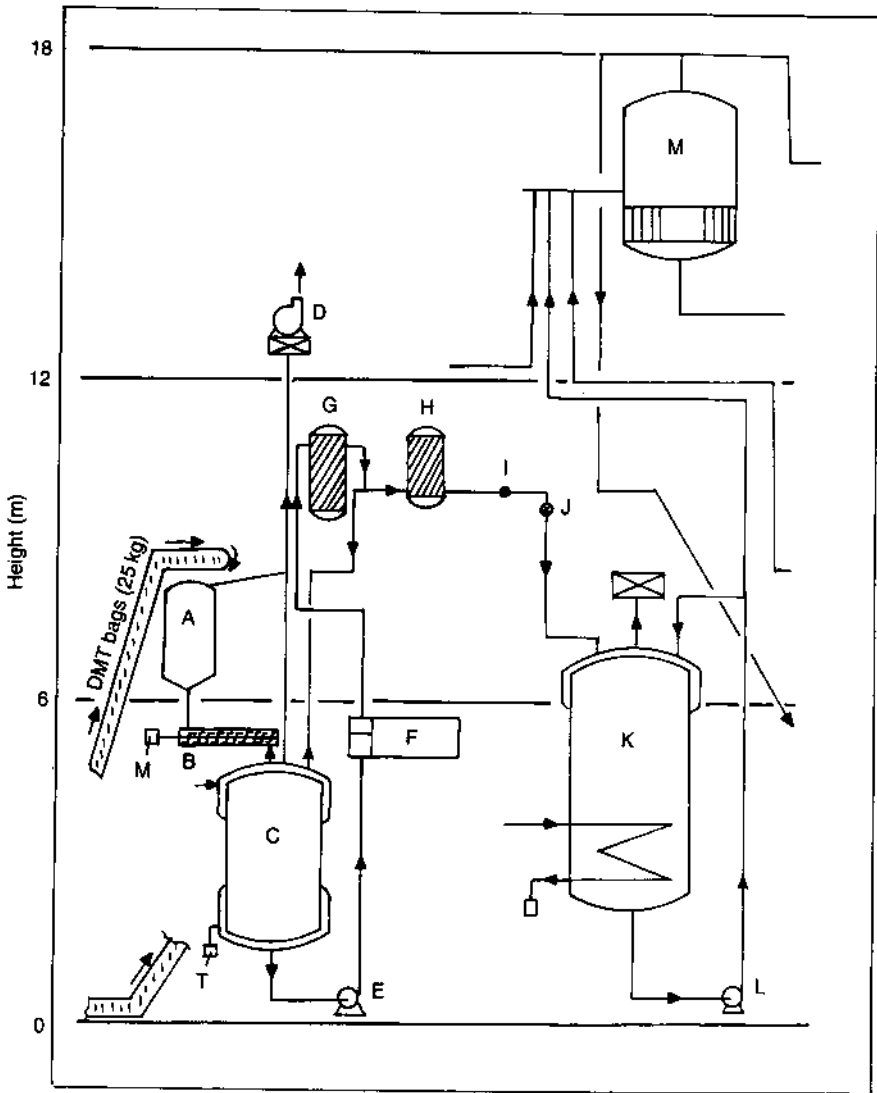
Fig. 12.7 An alternative system for dimethyl terephthalate [2]. Key: A = container; B = screw conveyor; C = DMT melter; D = blower; E = pump; F = distributor; G = filter-pack; H = filter pack II; I, J = valves; K = reservoir; L = pump; M = transesterification vessel. Condensed water from the heating jacket of the melter C can be taken out through the outlet T.

heated element and passes into the ester interchange vessel containing MEG at 150 °C. The melting capacity is normally $1\,t\,h^{-1}$.

In another variation (Fig. 12.7), DMT bags are carried by an endless conveyor belt and emptied into a container (A), from where DMT is

conveyed by a screw conveyor (B) into the DMT melter (C) maintained at 150 °C. As the DMT melts, air escapes through a vent at the top. The escape is facilitated by a blower (D) operating at the top of the insulated pipe, thus causing suction. However, some DMT sublimes and escapes from the melter. This is usually cooled and collected in filter dust bags. Alternatively, the DMT dust is wetted and washed down by water spray, collected, dried and reused.

The DMT melt is continuously drawn from the melter (C) by a heavy duty pump (E). The melt is forced through filter-pack (G) via a distributor (F). Usually the use of a coarse sand filtration device efficiently removes any unmelted DMT, which is fed back to the melter (C). The melt subsequently passes through a second filter-pack (H) into the reservoir (K) via valves (I and J). The reservoir is maintained at a temperature of 150 °C and keeps the DMT in the molten condition. As and when required, DMT melt from the reservoir (K) is drawn by the pump (L) and fed into the first cascade transesterification vessel (M).

Ester interchange (EI) or transesterification (TE) The transesterification vessel [29] shown in Fig. 12.8 is one in a series of cascade (prepoly) reactors (usually four). It is made of stainless steel, the bottom is rounded or
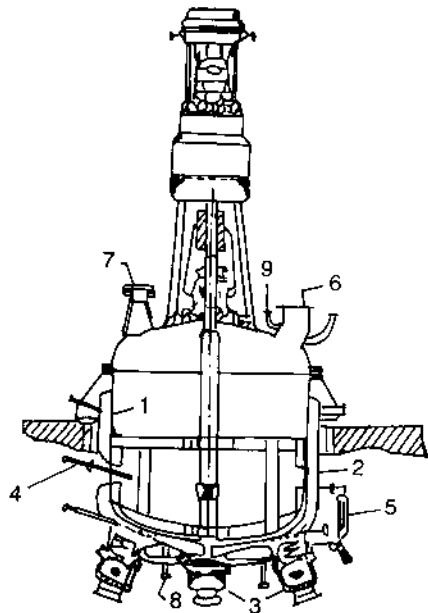
Fig. 12.8 Transesterification vessel [2]. Key: 1 = vessel; 2 = Dinyl heating jacket; 3 = electrical heating; 4 = thermometer; 5 = Dinyl level indicator; 6 = cooler port; 7 = observation window; 8 = cooling coil; 9 = vacuum connection.

cone-shaped and of ample diameter so that methanol can be readily distilled off. Heating brackets are welded into the heating tubes running obliquely from bottom to top (not shown in the figure). The lid of the vessel contains a port for molten DMT feed, a steam outlet and a connection for the column, as well as ports for delustring agent, catalysts, nitrogen, glycol, and the safety device. Brackets for lighting and an observation window are also provided. The thermometer tube is welded into the inner casing so that it is completely submerged in the melt. The outlet port is located at the lowest part of the base. An agitator, made of high grade steel, rotates at 40 rev min^{-1}. The column, made of stainless steel or aluminium, serves as a separator for the methanol–glycol mixture.

With smaller batches the reaction is carried out below the boiling point of MEG (197 °C) and without a reflux column. However, DMT may sublime and clog the condensers and outlet pipes, and the reaction time is longer.

In the continuous process the reaction is usually performed at the boiling point of MEG. The reflux column returns the MEG to the reaction mixture. This method is suitable for large-scale production. The sublimed DMT is continuously rinsed back by condensing MEG to the reaction mixture. As the reaction temperature is high, a shorter reaction time is necessary. Completion of the reaction is indicated by a steadily reducing flow of methanol. However, it is not necessary to await the end of this reaction. With a high degree of conversion, the melt can be sent directly for the polycondensation process. The melt normally acquires a temperature of 200–235 °C at the end of the process. The time required is between 3 and 6 h. The DGT formed continuously flows into the polycondensation cascade reactor.

Polycondensation Several factors determine the polymer grade produced during polycondensation; the most important are the reaction temperature, vacuum, agitation, the type of vessel, and the chemical nature and concentration (should be more than 0.02%) of the catalyst used. The following points are noteworthy.

1. With the increase in temperature, the rate of polycondensation increases rapidly and the polymerization time to attain the same melt viscosity is considerably reduced. However, there is more degradation at higher temperatures, especially above 280 °C.
2. The polycondensation process is predominantly diffusion controlled. Therefore, an increase in residence time in the reactor of PET melt does not increase its viscosity appreciably. On the other hand, the possibility of degradation increases at long residence time.

3. Another consequence of the process being diffusion controlled is that an increase in the rate of agitation causes more intense mixing of the melt, resulting in increased viscosity.

4. Again, due to diffusion control of the process, increase in vacuum leads to more efficient and quicker removal of MEG vapour (unreacted and split during polycondensation), resulting in attainment of the desired melt viscosity at shorter residence time at the same temperature. However, too rapid a removal of MEG may lead to the escape of DMT vapour, which might be present due to the non-completion of the TE process. This may clog pipe systems, causing considerable problems in running the plant. It is, therefore, desirable to apply the vacuum in stages (usually three) so that TE is complete in the initial stages of PC and the process can run smoothly.

5. Increase in carboxyl end group content may deactivate the catalyst, thus slowing down polycondensation.

For the batch process, the polycondensation vessel may be constructed in the same manner as the ester interchange vessel. The melt from the ester interchange process is filtered through a cylindrical mild steel gauze or ceramic material by a nitrogen pressure of 1–2 atm. It is then passed through a valve into the preheated polycondensation vessel. The charging melt consists of DGT, its oligomers and glycol. The agitator is started at a speed of 40–60 rev min^{-1} and vacuum (up to 1 Torr) applied while raising the temperature to 280 °C. The increase in viscosity is followed by the requirement of more power to drive the agitator at the same speed. When the desired viscosity is reached the melt is rapidly forced by means of a booster pump or nitrogen pressure through spinnerets and the extruded filaments are cooled by passage through a cold water bath. This is followed by cutting and drying.

In the continuous process, the process proceeds as shown in Fig. 12.9. From the last of the cascade prepoly (TE or EI) reactors, low viscosity melt (consisting mainly of DGT) is fed into the first disc ring reactor (DRR) of the cascade PC train (A$_1$). In this reactor, delustrant, thermal stabilizer and PC catalyst (if not added earlier) are incorporated with the low viscosity incoming melt. The temperature is raised progressively as the melt passes from the reactor and enters the finishing reactor (A$_2$). Inside A$_1$ and A$_2$ a series of discs fitted at fixed intervals on a slowly revolving (less than 10 rev min^{-1}) shaft act as the agitator. The temperature rises as the melt moves from the low (inlet), via medium (middle), to the high (outlet) temperature zone. The reactor operates under vacuum; usually 2 mm Hg is sufficient to obtain a fibre-grade product (molecular weight $\bar{M}_n \sim 20\,000$). The vacuum system consists of a duct (B) which directs the vapours leaving the DRR to a series of strippers. The vapour in the first stripper (C) meets a spray of previously condensed MEG
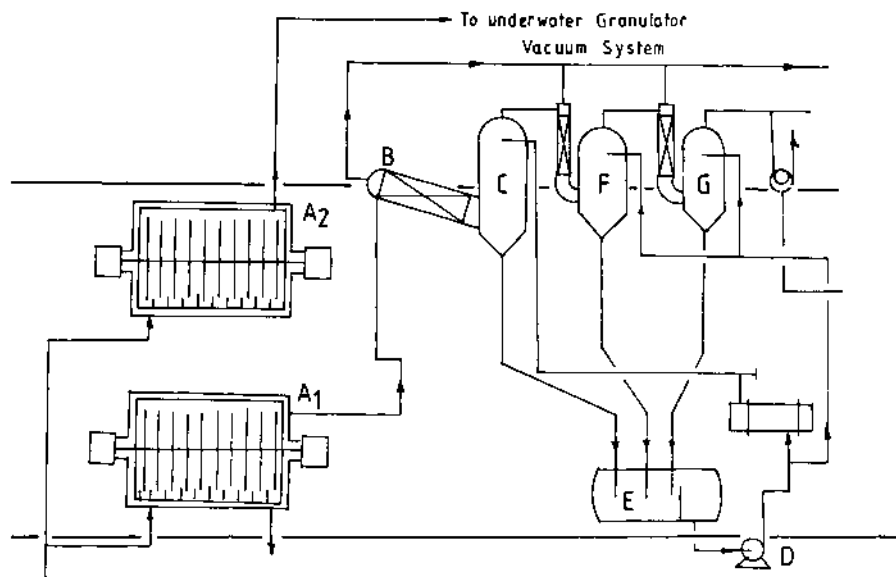
Fig. 12.9 Continuous polycondensation process. A_1 and A_2 = reactors; B = duct; C = stripper; D = pump; E = reservoir; F and G = strippers.

which is pumped out by the pump (D) from the reservoir (E). The condensed MEG flows into E. Any residual vapour is condensed in further strippers (F and G) the liquid MEG is collected in E. From time to time MEG is drawn out of the system by D and recycled in the process. A more detailed description of DRR can be seen in reference [30].

The polymer melt is continuously discharged from the DRR using either a discharge screw or a gear pump which leads the melt to the spinning manifold.

(d) Process via the PTA route

This newer method has certain advantages over the DMT route; some of these are:

1. cost of TPA is usually less than DMT;
2. during DGT formation, the by-product methanol is not formed;
3. the DE step is self-catalysed;
4. product quality is superior;
5. the reaction product in the DE step has a higher molecular weight than that obtained in the EI step.

The following two aspects relating to this process will be considered first: (1) catalysts used, and (2) side reactions. This will be followed by a

description of the process and the modifications required to produce fibres with special properties.

Catalysts used

TPA itself accelerates the DE step. However, if necessary, stronger acids or esters of titanic acid can be used as additional catalysts. Due to the absence of a metal catalyst in this route, the degradation reactions catalysed by a metal catalyst in the EI step cannot occur in the PC stage. However, some degradation of PET occurs during the PC stage because the thermal decomposition temperature of PET is close to the temperature used in the PC stage.

Side reactions

The side reactions occurring in the DE step are similar to those that occur in the EI step. However, ether (DEG) formation is greater. The tendency for greater ether formation can be suppressed by the addition of a small amount of NaOH or an organic quaternary hydroxide. Use of higher temperature (280–290 °C) is also helpful. In general, PET produced via the PTA route has lower average molecular weight, lower melting point and higher dye uptake than PET obtained through the DMT route. These properties are generally attributed to the higher DEG content in the PET obtained by the PTA process.

The process

The sequence of PET manufacture by the PTA route is shown with the help of a flow diagram [14] in Fig. 12.10. The DE process can be carried out in a similar vessel to that used in the EI step.

The solubility of TPA is low in MEG. It requires a temperature of 240–260 °C at a pressure of 400 kPa to prepare the mix in the proportion of TPA:MEG=1:1 to 1:1.3. The process proceeds smoothly and water, which is produced as a by-product, is allowed to distill off from the system. Hence no reflux system attachment is necessary as required for methanol reflux in the EI system.

When the process is complete, a thermal stabilizer is added to the low viscosity melt, before transferring the melt to the PC vessel.

The PC stage is common to both the DMT and PTA processes. If necessary, a second dose of catalyst is added here. The attainment of the final molecular weight of the polymer is diffusion controlled rather than being chemically controlled. Hence progressive reduction of pressure leads to a high molecular weight polymer.
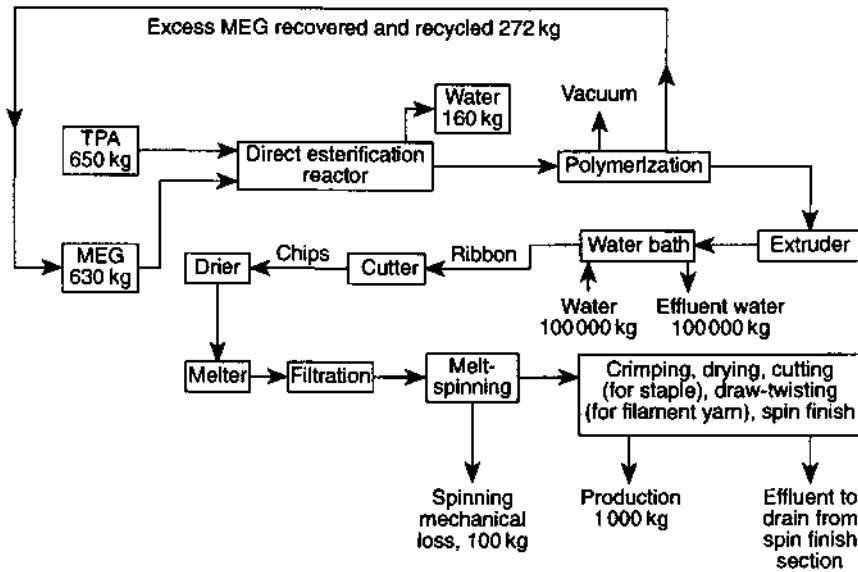
Fig. 12.10 Flow diagram showing sequence of PET manufacture by the PTA route [14].

Additives for fibres with special properties

Modification is sometimes carried out during polymerization in order to obtain fibres with special properties. This is achieved by the addition of specific ingredients during polymerization. Some of them are listed here [31,32]; a more detailed account of these additives appears in Chapter 14.

• Bright fibres used in PET/cotton blends and in sewing threads are produced by incorporating a suitable optical whitener and a very low amount (not exceeding 1%) of titanium dioxide in PET melt.
• Mass-coloured PET can be manufactured by incorporating the desired colouring agent in the titanium dioxide slurry, followed by the addition of a suitable dose into the PET melt during the PC stage. The particle size of the colourant should not exceed 1 μm to ensure homogeneity.
• Cationic dyeable PET is manufactured by using an ionic comonomer such as a monosodium salt of 5-sulfoisophthalic acid dimethyl ester (DMS salt) in small amounts during polymerization.
• A simple technique to increase the dyeability of PET fibre is to incorporate an aliphatic glycol salt during polymerization. Such fibres can be dyed at boil without any carrier.

- Incorporation of a suitable antibacterial agent in the PET melt can impart bacterial resistance to PET fibres.
- Suitable natural oils have been blended with PET to produce polymer having a fragrance such as jasmine or lavender.
- Various flame retarding agents (e.g. phosphorus-based compounds) can be blended or by suitable choice copolymerized with PET-forming monomers, producing flame retardant PET.

High molecular weight PET

PET tyre cord is an important material in its own right. However, because of the very high molecular weight and thermal stabilization requirement it cannot be produced by the technique used for normal-grade PET. In the technique described earlier, during the PC stage with increase in residence time there is an increase in the number of terminal carboxyl groups in the polymer. As a consequence it is difficult to obtain a polymer having carboxyl end group content less than 20×10^{-6} $m\,eq\,g^{-1}$ polymer and an intrinsic viscosity of more than $0.9\,dl\,g^{-1}$.

To obtain a high molecular weight and low carboxyl content either or both of the following methods can be adopted.

Use of chain extenders These additives react with the terminal carboxyl end group in PET during the PC stage with the elimination of water or phenol. The rate of diffusion of water or phenol is faster than that of MEG. Hence, these by-products can escape quickly from the reaction mixture and the diffusion controlled PC takes place at an enhanced rate. Thus polymerization time is greatly reduced, fewer carboxyl groups remain and high molecular weight product results. Chain extenders used at a level of 0.5–2% include benzene boronic anhydride, diphenyl carbonate, diphenyl oxalate, diphenyl terephthalate, diphenyl malonate and tetraphenyl orthocarbonate. The various by-products formed due to reaction of the chain extenders with entities in the PET melt include 1-hydroxyethyl acetate, ethylene oxide, cyclic ethylene oxalate and others. Usually such by-products do not affect the application properties of tyre cords.

Solid-phase polymerization Production of PET by solid-phase polycondensation is practised commercially and is becoming important for the production of PET for industrial fibres. To carry out this process, a preliminary melt polycondensation is carried out until the product has an intrinsic viscosity (IV) of $0.1–0.4\,dl\,g^{-1}$. Then this polymer is cast in solid form and broken into minute pieces or melt-extruded and then granulated. The particulate or granular polymer is first crystallized by heating with forced agitation to prevent sintering, then heated in flowing

nitrogen or under reduced pressure at a temperature above 200 °C (220–260 °C) under nitrogen until the desired molecular weight is attained. One of the major problems is the adhering of PET particles to the reactor surface. Addition of 0.2–0.5% of powdered glass has been found to be beneficial in preventing the sticking problem. Use of other inorganic salts such as sodium sulphate, sodium chloride and calcium carbonate has been recommended to avoid agglomeration of PET granules. Solid-phase processes are also operated with a feed polymer of IV of 0.55–0.65 $dl\,g^{-1}$ in chip form in order to raise the molecular weight to still higher values for industrial yarn production [3e].

In a reported study [33], PET chips (2 mm × 3 mm × 4 mm) of IV 0.68 $dl\,g^{-1}$ with melting point (T_m) of 259 °C, produced by the usual esterification–polycondensation route, were subjected to solid state polycondensation in a small rotary vacuum reactor at a pressure of 0.05–0.1 mm Hg at a temperature of 225–245 °C and batch times of 5–20 h. It was found that at the lower temperatures, the reaction rate is chemically determined; at high temperatures, on the other hand, it becomes progressively more physically determined by the rate of diffusion of glycol out of the particles. Consequently, the rate is then affected by particle size; large particles such as standard polymer chip polymerize slowly. As a consequence the size of the particles or granules influences the carboxyl group content and molecular weight. Thus a reduction of particle size from 7 mm to less than 2 mm leads to an increase in molecular weight from 26 000 to 39 000 $g\,mol^{-1}$ and a reduction of carboxyl end group content from 46.3×10^{-3} to 30.0×10^{-3} g eq by post-polymerization.

Polymer with IV of 1.1 $dl\,g^{-1}$ and T_m of 265 °C could be obtained by this method and the filaments prepared from them gave a tenacity value of 9.0 $g\,den^{-1}$ and elongation to break of 8%, thus providing good quality industrial yarn.

Even higher intrinsic viscosities (molecular weights) can be achieved and these PET grades are used for making bottles. The method has the additional advantage that acetaldehyde, formed by secondary reactions, evaporates. The granulate thus becomes suitable for beverage bottles. A number of plants of 100 t per day capacity have been set up to produce such grades of PET.

Polycondensation units are available with the following three separate stages. The first step is PC polymerization, carried out with molten PET typically at 270–280 °C under a vacuum of 10 mm Hg. The second step is known as melt-polymerization and is carried out at high vacuum (0.55 mm Hg) at 280–290 °C to ensure removal of ethylene glycol vapour. The third step is a solid state polycondensation and is carried out either under vacuum or under inert dry nitrogen atmosphere at 227 °C.

12.3 FIBRE PRODUCTION

The fundamentals of fluid flow and the spinning process, including some aspects of PET spinning, have been described in Chapters 3 and 4. In the present section, the production of PET filament yarns and staple fibre will be considered in some detail.

12.3.1 PRINCIPAL STAGES IN FIBRE PRODUCTION

The principal stages in a typical fibre production sequence are summarized in Fig. 12.11 [3f]. PET fibre produced by the continuous polymerization and direct spinning technique distinguishes itself from the batch process PET fibre in that in the former the polymerization process is controlled to produce a uniform feedstock which is directly fed to the manifold, while in the batch process the additional processes of casting, cutting, blending, drying and melting are necessary.

12.3.2 BLENDING, DRYING AND MELTING [3g]

Batch-wise production results in differences in molecular weight, molecular weight distribution, melting point, colour and DEG content, etc. The differences may be from batch to batch or even within the same batch. Hence blending is practised to obtain uniform, homogeneous product and for this, large-scale blending facilities are required. Such blending is of greater relevance in filament yarn production than in staple yarn production since in the latter, fibre blending as practised during the yarn production achieves the same objective.

To prevent hydrolysis of ester groups, the blended PET chips are dried before being subjected to melting. Drying is usually carried out in large driers at around 170 °C by passing dry hot air through a bed of polymer granules. The moisture content in the dried polymer should be no more than 0.005% by weight.

To avoid fusion of polymer chips during drying, the granules are precrystallized at 100–120 °C in batch-wise dryers. Since dried polymer picks up water very rapidly, it is fed directly to the hopper of the extruder under dry nitrogen without further exposure to air.

The melting is generally achieved in a screw extruder. The extruders are single or twin screw vented types, which feed manifolds leading to spinning heads that contain individual gear pumps. A brief description of the extruders has already been given in Chapter 4.

12.3.3 PRODUCTION OF FILAMENT YARNS

The chemistry and technology of the production of PET polymers have already been dealt with earlier in this chapter. The main principles of
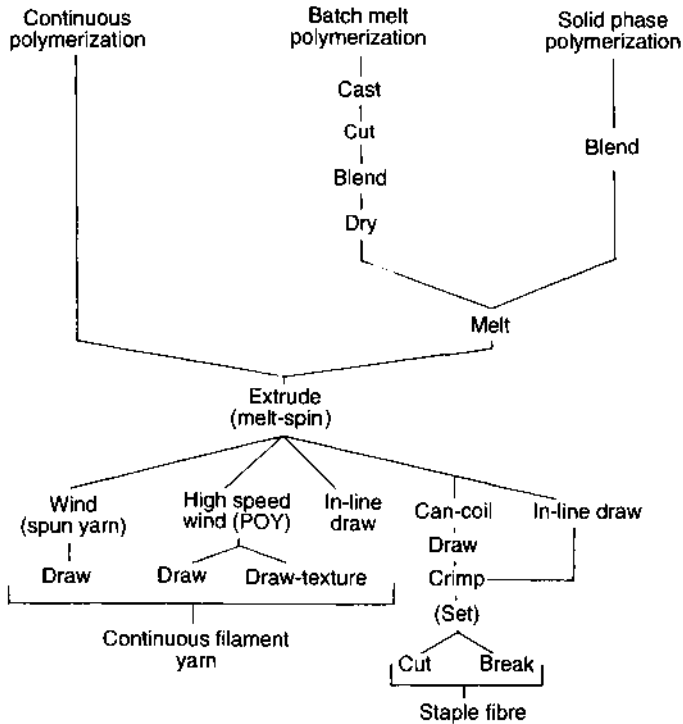
Fig. 12.11 Principal stages in the production of PET yarns and fibres [3f].

spinning and a description of the spinning line have already been given in Chapter 4. In this section some important aspects of the technology of production of PET filament and staple fibre and their structure, properties and applications will be briefly considered.

(a) Spinning of filament yarn [34]

PET melt-spinning processes can be considered to fall broadly into two distinct classes [3h]: (1) in which relatively low wind-up speeds are used to produce a spun yarn possessing little or no orientation, and (2) in which relatively high wind-up speeds are used to produce a partly oriented spun yarn.

A further division may be made into (a) processes in which spinning and drawing are separate, and (b) integrated spin–draw processes.

The above classification or any other classification based on spinning speed is not sharp and clearly defined. A more elaborate classification based on the level of molecular orientation developed in the as-spun fibre has been suggested [34] and differs from the one given in Chapter 4, Sections 4.1 and 4.4.2. Table 12.3 illustrates the broad range of PET

Table 12.3 Broad range of PET fibre processes and products [34]

	Staple and tow	Industrial filament	Textile filament: flat and textured		
			Medium speed (POY)	High speed (HOY)	Very high speed (FOY)
Process					
Spinning	Low speed (LOY)	Low speed (LOY)	Medium speed (POY)	High speed (HOY)	Very high speed (FOY)
Drawing/crimping	Large draw frames and crimpers	Draw-twist or integrated with spinning	(a) Draw-twist or integrated with spinning for flat (b) Draw-texture	(a) Integrated with spinning (b) Draw-texture	Direct use or texture
End uses	100% and blends	High denier	Apparel – top weights		
	Apparel – top weight	Tyres	Apparel – bottom weight		
	Apparel – bottom weights	Conveyor belts	Outerwear		
	Underwear	Seat belts	Sportswear		
	Carpet	Hose	Upholstery		
	Upholstery	Ropes	Curtains/drapes		
	Non-wovens	Cords	Sheets		
	Sleeping bags	Coated fabrics	Sewing thread		
	Pillows	Dryer belts	Underwear		
	Mattresses	V-belts	Sleepwear/loungewear		
	Curtains/drapes	Low denier	Linings		
	Sheets	Sewing thread	Narrow wovens		
	Filters	Sailcloth			
	Towels	Coated fabrics			
	Sewing thread				

fibre products and processes and considers the products in four categories of spinning speeds, namely:

1. low spinning speed in the range 500–1500 m min^{-1}: the product is called low-oriented yarn (LOY);
2. medium speed in the range 1500–4000 m min^{-1}: the product is called partially oriented yarn (POY);
3. high speed in the range 4000–6000 m min^{-1}: the product is called highly oriented yarn (HOY);
4. very high speed in the range above 6000 m min^{-1}: the product is called fully oriented yarn (FOY).

These four categories of fibre products and processes will now be briefly considered.

LOY spinning processes

The as-spun PET fibre obtained at spinning speeds in the 500–1500 m min^{-1} range is virtually amorphous, has very little strength, is highly deformable and typically must be drawn to four to five times its original length to obtain a useful fibre. Typical stress–strain curves obtained for fibres spun at various speeds are given later when mechanical properties are considered (Section 12.4.2).

A starting fibre which is amorphous and has low orientation (like the LOY) can be drawn to high draw ratios which give it the high strength needed for industrial applications. The practical approach is to spin a fairly high molecular weight PET at very low speeds and sometimes with a retarded quench to obtain minimum spin orientation and then subject it to a draw ratio in the 5–7 range. The drawn filament can develop high birefringence of 0.21 or even more.

LOY products are also used for textile applications and the production of tow and staple are described later in this chapter. Here only adequate strength is usually desired and other factors such as dimensional stability and dyeability are important. These requirements are met by giving the fibres a slightly higher spin orientation and a draw ratio of up to 4.

Traditionally, a major end use of LOY was as a textured yarn. The LOY was first drawn and then false-twist textured to create a bulky, textured filament yarn. This has now been overtaken by draw-texturing of POY, which combines drawing and texturing and can operate at faster speeds.

POY spinning processes

POY became a commercial reality in the early 1970s mainly because of the availability of commercial winders with higher speed range

(3000 m min^{-1} or higher) around that time and also because of the introduction of simultaneous draw-texturing in 1970.

The tensions generated in the yarn are now higher and though the as-spun fibre is almost completely amorphous, the level of orientation developed gives it substantially higher strength and lower extensibility than LOY.

POY overcomes both the shortcomings of LOY, namely the difficulty in stringing-up on the texturing machine and the shelf-life problem of the low speed spun yarn.

Because of its increased orientation, the crystallizability of POY is many orders of magnitude higher than that of LOY. Consequently it allows for crystallization to occur in draw-texturing at a significantly lower temperature. For example, for POY with a birefringence of 0.038, the crystallization temperature is reduced by 30 °C compared with LOY. The DTA thermograms shown in Fig. 12.12 clearly illustrate this [35]. Thus the partial crystallization that occurs when POY contacts the heater plates greatly reduces the sticking that normally occurs above T_g. In addition, the high level of spin orientation and reduced crystallization temperature result in very rapid crystallization in the draw-texturing process which leads to increased bulk and a very stable 'robust' texturing process.
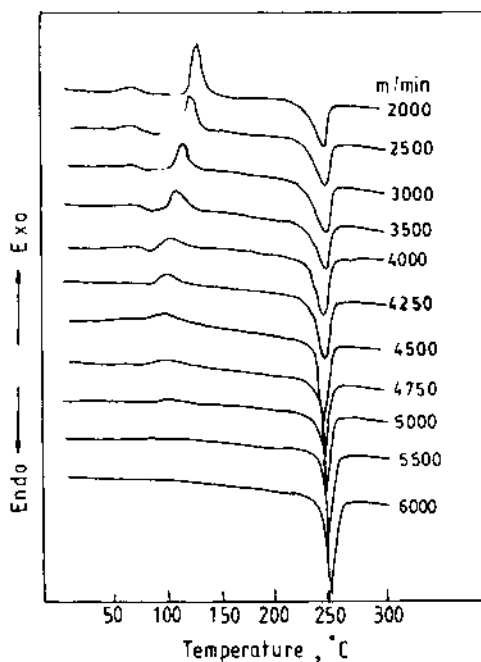
Fig. 12.12 DTA traces of PET yarns wound at the velocities indicated [35].

In general, POY spinning is currently carried out at relatively high speed (3000 m min^{-1}) without godets, as shown in Chapter 4, Fig. 4.2(a). This offers advantages in the areas of capital costs and ease of string-up, but has the major disadvantage of lack of wind-up tension control. Industrial units with godets (Fig. 4.2(b)) overcome this disadvantage.

HOY spinning processes

The high threadline tension in this speed range arises from air drag (associated with the large volume of air pumped downwards by the filaments) and inertial (associated with the acceleration of the threadline to the final spinning velocity) contributions. It causes very rapid filament attenuation and extensive molecular orientation. The threadline tension is the key process parameter controlling threadline crystallization kinetics. However, the oriented, crystalline PET yarn does not have the characteristics of a fully oriented spun and drawn yarn. This aspect has already been considered in Chapter 4.

FOY spinning processes

A considerable amount of work on ultra high speed spinning of PET yarn at speeds in the range 6000–8000 m min^{-1} has shown that neck-like deformation occurs at high temperatures and the fibre has a strong skin–core structure. As a consequence the mechanical properties are quite close to but not equal to those of fully drawn yarns. Efforts to produce the latter continue to be made, particularly in Japan.

The other aspects of production, e.g. spinning parameters, quench chamber design, etc. have already been described in Chapter 4. The extrusion temperatures for normal molecular weight are in the range 280–290 °C. However, products of low molecular weight may be spun at temperatures down to 265 °C and those of very high molecular weight at 300 °C or above.

(b) Drawing of filament yarn [3i]

The spun yarn of low orientation is subjected to a stretching or drawing process to convert it into commercially useful yarn of high orientation. Total draw ratios lie between 3 and 6. The higher draw ratios are for high tenacity yarns and often involve a two-stage drawing process, wherein the second stage is carried out at a somewhat higher temperature than the first (which is usually carried out at 90–100 °C) and applies a draw of up to 1.5.

The process of drawing introduces some crystallinity but insufficient to stabilize the yarn against thermal shrinkage. Further setting during the draw process itself through passage over a hot plate at 140–220 °C or by using a heated draw roller at a similar temperature is usual in filament yarn production.

Early production of continuous filament yarns was based upon use of draw twisters operating at up to 1200 m min^{-1}. Draw winders based on side-winding can operate at up to 6000 m min^{-1} and they introduce no twist. Further details on drawing appear in Chapter 8.

(c) Texturing of filament yarns

Simultaneous draw-texturing of POY using friction-twisting devices based on aggregates of intermeshing discs and operating at speeds up to 1000 m min^{-1} is often adopted to produce false-twist textured yarns. Other texturing methods can also be used to produce textured yarns from POY supply.

12.3.4 PRODUCTION OF STAPLE FIBRE

The process to be described here is based on continuous polymerization and direct spinning using two grades of PET; the first with degree of polymerization of 92 with intrinsic viscosity of 0.60 dl g^{-1} and $\bar{M}_n$ of 18 724, and the second with degree of polymerization of 95.2 with intrinsic viscosity of 0.62 dl g^{-1} and $\bar{M}_n$ of 19 454.

(a) Melt-spinning and take-up

The polymer fluid is conveyed from the last polycondensation vessel (finisher reactor) to a spinning unit at a pressure of 40–50 kg cm^{-2} via double jacketed tubes (heated by circulation of Dowtherm) and delivered through a distributor to two different spinning/take-up lines. Each line consists of three to four manifolds and each manifold has six spin blocks (Fig. 12.13), representing six spinning positions. Each spinning position is equipped with individual spin pump. Each spin block is equipped with a filtration assembly which is located above a rectangular spinneret having 1000–2000 circular holes (for cotton-type PET fibres). The capillary diameter is 0.20–0.30 mm and height 0.40–0.60 mm (Fig. 12.14). Sometimes to improve handle, lustre or dyeability, non-circular orifices are used.

The filament bundle is cooled in the quench chamber where it solidifies in the crossed air stream. The air flow must be uniform and without any whirling motion. The fibre diameter attenuation occurs in the first 1.5 m from the spinneret exit. The spin orientation in the filament

(a)

From Finisher reactor

(b)
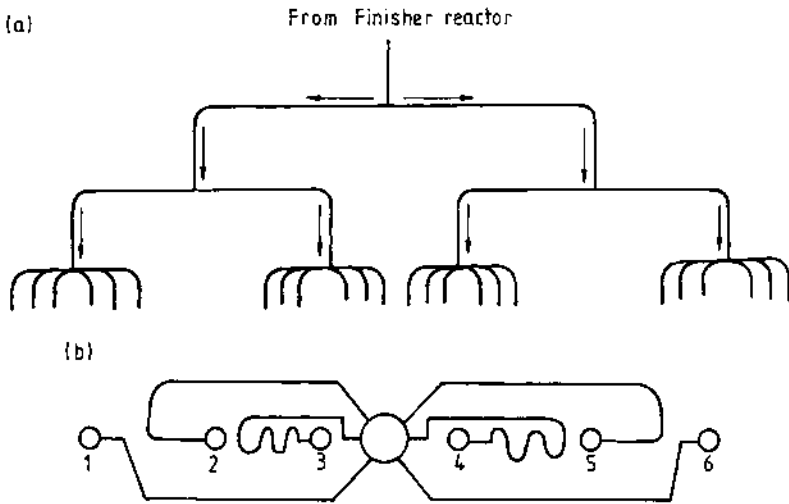
Fig. 12.13 Schematic sketch of (a) manifold with 24 spinneret lines, and (b) six-way distributor.

depends upon the difference between the godet and extrusion speeds, velocity of quench air and humidity and temperature of quench air. The filaments then pass through the spinning chimney onto the godet rollers. On the way, spin finish is applied (Fig. 12.15) to reduce the coefficient of friction and static charge generation and also to bind the filaments together. The filament ribbons from all the spinning positions pass individually over godet rollers. The ribbons from all positions of one spinning/take-up line are joined in one cable which is fed through guides and reels to a can after passing through mesh rolls.
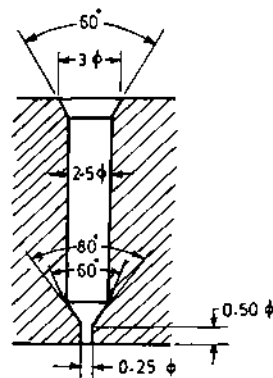
Fig. 12.14 A section of a typical spinneret channel.
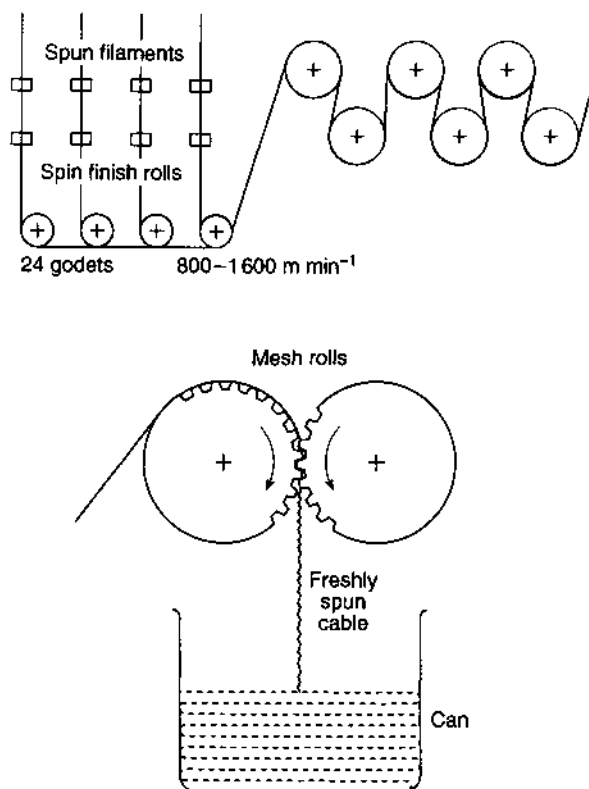
Fig. 12.15 An intermediate stage in PET staple fibre production.

The spinning and take-up parameters are summarized below:

Intrinsic viscosity of polymer	$0.61-0.62$ $dl\,g^{-1}$
Spinning temperature	$285-290\,°C$
Number of holes in the spinneret	$1000-2000$
Hole diameter	$0.2\,mm$
Output per spinneret	$600-1000$ $g\,min^{-1}$
Quench air temperature	$20-22\,°C$
Quench air humidity	70%
Take-up speed	$800-1500$ $m\,min^{-1}$
Spun denier per filament	$4.0-12.0$
Moisture pick up from take-up	$18-20\%$
Weight of filament per can	$350-1000\,kg$

To produce uniform filaments, the spinning fluid must be homogeneous, the throughput must be constant, spinning temperature should be optimum, dirty and choked spinneret holes must be avoided, the

quench air flow rate must not fluctuate and the take-up/godet speed must be constant.

(b) Conditioning and creeling of cans

The cans containing the cable are kept in the conditioning room so that polyester undrawn filaments attain moisture equilibrium. Although the undrawn filaments tend to take a long time to reach equilibrium, in practice after a few hours they are very close to equilibrium. Dry cans create problems during the drawing process and may also lead to formation of undrawn portions. It is generally known that a higher moisture content reduces the work of drawing and therefore facilitates the drawing process. With diminishing moisture content, the work needed to stretch the fibre increases. The cans are arranged to make a creel of about 40 cans, depending on denier and production. Usually a total drawn tow denier of 1.0–1.5 million is employed in the fibre line. The can-type of creel consists of a frame and guides and a lifting and lowering device.

(c) Post-spinning operations

Drawing

The yarn is spun at relatively low speed and has very poor orientation. Consequently it is not suitable for textile applications. Uniaxial drawing of the filament along the fibre axis to about three to four times its original length brings the molecules close to one another and this can introduce some crystallinity and convert it into a commercially useful product. As a result of drawing, the filament denier is reduced while its modulus and tenacity are increased. However, its elongation to break and dyeing affinity decrease. When polyester is spun it is dull-looking, but on drawing brilliant lustre/whiteness is achieved.

Although polyester yarns can be oriented by drawing at room temperature, the stress required to initiate drawing at this temperature is high and the process is found to be unstable. To obtain a uniform product, it is necessary to draw at a temperature close to or above the glass transition temperature of the spun yarn. For an as-spun PET fibre with $\bar{M}_n$ of about 20 000, the glass transition temperature is around 60–80 °C and drawing is usually done around this temperature.

The actual drawing process is influenced by the preorientation present in the undrawn filaments, the filament regularity and the required draw ratio.

The process of drawing involves passing the tow of spun yarns around driven rollers with successively higher surface speeds to produce the
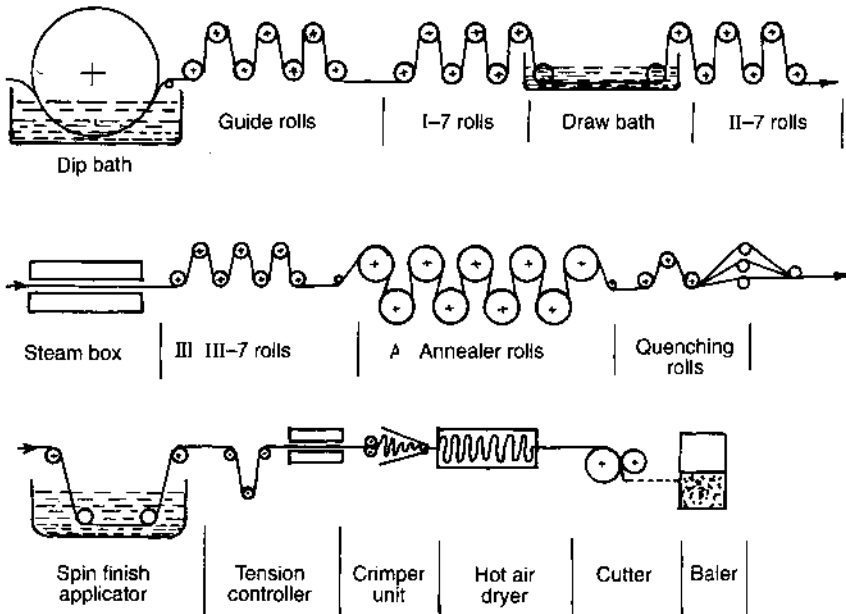
Fig. 12.16 Typical fibre line for staple fibre production.

degree of stretch (draw ratio) required. For tows, contact with a single feed roller or snubbing pin is inadequate both for heat transfer and for tension build-up. More than one roller – commonly three, five or seven – is used at each stage of the drawing process (there may be two to three such stages) and the drawing is located in a zone of good heat transfer such as a hot water bath or steam chest.

Drawing at temperatures close to the glass transition temperature takes place inhomogeneously by the formation of a neck in the filament and the propagation of this neck at almost constant force.

The sequence of operations in a typical fibre line is shown in Fig. 12.16. For each can-type creel, 30–40 cans are arranged and the tow is guided through a dipping bath by feed rolls at constant tension. The dipping bath applies moisture and spin finish to the tow uniformly. The normal oil concentration in this bath is usually kept at 0.3–0.4%. The tow is then guided in uniform and specific widths by seven tow guide rolls, each 15 cm in diameter and 55–65 cm wide. The roller speeds can be independently adjusted to suit the required tow tension in the first seven-roller frame (I-7). The excess finish solution applied in the dipping bath is squeezed out at this stage.

The main drawing zone comprises the first and second seven-roller frames shown in Fig. 12.16 (I-7 and II-7). The process conditions are so

selected that the actual necking point is located in the draw bath between the first and second seven-roller frames. The rollers are 25 cm in diameter and 55–65 cm wide. The tow is drawn three to four times and the roller speeds therefore depend on the draw ratio and the fibre line speed. For example, for a line speed of 180 m min^{-1}, the speed of the first seven rollers would be about 45 m min^{-1} and of the second seven rollers 180 m min^{-1}.

Heat-setting

The tow is stabilized by passing it through a steam box in which the tension is maintained with the help of the third seven-roller frame, as shown in Fig. 12.16. The roller diameter is 25–26 cm and width 55–65 cm. Second stage drawing now occurs under the effect of heat in the stabilizing box by maintaining the desired surface speed of the rollers in the third seven-roller frame with reference to the second seven-roller frame.

The drawn and stabilized tow is then guided through the nine-roller device called the annealer roller unit (Fig. 12.16) and it stabilizes the tow further to a specified shrinkage. The running tow is guided so that it makes contact with each annealer roller in such a manner that the looping angle is the highest possible; this ensures that the drying and setting of the tow are most efficient. Depending on the physical property requirements, a slight overfeed of about 2% may be given at this stage. Depending on the dyeability requirements, the steam pressure in the first five rollers is generally of the order of 9 kgf cm^{-2} and in the last four rollers around 10 kgf cm^{-2}.

The tow then passes through the next seven-roller frame (Fig. 12.16), which quenches the tow to the desired temperature before it goes into the spin finish applicator. Quenching freezes the orientation and a fibre of required tenacity and elongation to break is obtained. This seven-roller frame also provides the necessary tension to the nine-roller annealing device.

Subsequent post-spinning operations

The post-spinning operations after drawing and heat-setting are spin finish application, crimping, drying, cutting and baling, as shown in Fig. 12.16.

The application of spin finish to the fibre ensures that the fibre will perform satisfactorily during textile processing. The amount of spin finish has to be just right as lower or higher amounts than the optimum can create problems during textile processing. Generally less spin finish

is applied to fine denier fibre compared with the finish applied to coarse denier fibre.

The tow then passes through dancing rollers to the crimper units. The dancing rollers keep the tow tension at a constant level and control the delivery speed.

Before introducing crimps with the help of a crimper, the tow is first made pliable by passing it through a steam box which is superheated at a pressure of around $6.0\,kgf\,cm^{-2}$.

The heated tow now enters the stuffer box through pressing rollers under high pressure and thus crimps are introduced. The crimp frequency (number of crimps per cm) is dependent on the pressure in the stuffer box. Pressure in the stuffer box must be lower than the pressure between rolls, otherwise crimping will not take place. The crimper rollers are 20 cm in diameter and 12–16 cm wide, depending upon the tow denier to be run in the fibre line.

The tow that comes out of the crimper unit is still wet and is therefore passed through a hot air dryer which is maintained at temperatures of between 80 and 120 °C, and the tow is laid on a conveyor belt in the transverse direction, as indicated in Fig. 12.16. Besides drying the tow, the dryer also gives final stabilization by setting the crimps and the fibre shrinkage. The tow entering the dryer has 4–6% shrinkage which reduces to around 1% after it comes out of the dryer. The crimp stability, which is very poor before the tow enters the dryer, is considerably improved (to more than 65%) as a result of setting in the hot air dryer.

The crimped and stabilized tow is next passed through tension-adjusting rollers before cutting so that the crimps are removed but not overstretched. The cutter then cuts the tow to the desired staple length. The quality and sharpness of the cutting blades are very important requirements, for if cutting is not accurate due to blunt blades or slippage through contact points of the disc, overlength fibres (i.e. with nominal staple length + 1 cm) will be produced, which is not desirable for the textile processing applications.

Finally the cut staple is sucked into the baling press chamber where the fibres are packed in a bale of required dimension under specified pressures. The bales have a mass of about 250 kg.

(d) Fibre line parameters and typical fibre properties

The fibre line parameters are listed below:

Tow denier	1.0–1.2 million
Line speed	170–240 m min^{-1}
Total draw ratio	3.5–4.5

Table 12.4 Typical fibre properties

Property	Denier			
	1.2	1.4	2.1	3.0
Denier	1.20 ± 0.03	1.40 ± 0.03	2.10 ± 0.03	3.00 ± 0.03
Tenacity (gf den^{-1})	6.5–7.0	6.3–6.8	5.5–6.0	5.0–5.5
Elongation (%)	18–25	20–28	25–35	35–45
Arcs (cm^{-1})	5.0–6.5	4.5–5.5	4.0–4.5	4.0–4.5
Boil shrinkage	<1%	<0.5%	<1%	<1%
Over-long fibres (%)	<0.05	<0.05	<0.05	<0.05
Melting point (°C)	256	256	256	256
Degree of whiteness	82	82	82	82
% finish pick-up	0.14	0.15	0.18	0.20

Second stage draw ratio	1.1–1.2
Spin finish dip bath temperature	40–50 °C
Drawing temperature	60–75 °C
Annealer rolls steam pressure	10–15 kgf cm^{-2}
Quench rolls temperature	30–40 °C
Crimps	5–6.5 cm^{-1}
Dryer temperature	100–130 °C
Drying time	8–10 min
Staple cutter speed	200–300 m min^{-1}
Staples normally cut	38, 44, 52 and 61 mm

Typical fibre properties are given in Table 12.4.

(e) Some problems in the plant and their causes

Some of the more common problems which are encountered in the plant during the production of PET staple fibre are listed here, together with their possible causes.

1. High drips
   (a) Insufficient cooling of filaments
   (b) Dirty spinnerets
   (c) Ineffective filtration
   (d) Low viscosity
   (e) Low quench air velocity
   (f) Thinner filaments due to channelling in pack.
2. Spun denier variation
   (a) Speed fluctuation in take-up
   (b) Differential speed variation between godet and feed roller, feed roller and reel

(c) Improper sand size

(d) breakage of sand with time

(e) Variation in throughput from position to position.

3. High number of wraps

   (a) Poor pack life

   (b) Quench air velocity too low in some positions

   (c) Differential speed in take-up not correct

   (d) Dents in reels, feed rolls or godets

   (e) Reel alignment disturbed

   (f) Additional moistening guide cutting filament

   (g) Improper moisture pick-up in take-up

   (h) Reel grip either too loose or too tight.

4. Tenacity (lower side)

   (a) Draw point position in the stretching bath should be inside the bath or at extreme bottom of the seventh roller of the first seven rolls (I-7).

   (b) Low second stage draw

   (c) Too high draw ratio

   (d) Poor surface condition of the second seven rolls (II-7)

   (e) Viscosity variation

   (f) Greater preorientation or greater spun denier variation

   (g) Temperature of stretching bath high

   (h) Blunt knives

   (i) Damaged knives due to plasticized material

   (j) Reels of cutter surfaces rough-catching filaments before cutting

   (k) Rough guides and bars in creel room and cutter area.

5. Over-length

   (a) Low draw ratio

   (b) Malfunctioning of annealer temperature controller

   (c) Coarse spun denier

   (d) Low viscosity.

6. Tip fusion

   (a) Blunt knives

   (b) Tow still hot while being cut

   (c) Too high tow denier.

7. Dyeability problem (dark shade)

   (a) Coarse final denier

   (b) Variation in spun denier on coarser side

   (c) Low draw ratio

   (d) Annealer surface temperature low.

8. Wrapping problem

   (a) High draw roll temperature

   (b) Low spun denier cable

   (c) Surface of rollers damaged.

12.4 STRUCTURE AND MECHANICAL PROPERTIES OF FIBRES

The structure of the fibre has the predominant effect on its properties and therefore there is considerable interest in characterizing the structure so that the properties can be suitably engineered. Fibre structure develops at different stages of the production sequence and some information on how crystallinity and molecular orientation develop during spinning and post-spinning of PET fibres has already been presented in earlier chapters. Here some more information on these structural aspects is provided. The mechanical properties of different types of PET fibre are also briefly considered.

12.4.1 FIBRE STRUCTURE

Melt-spinning of PET at low speeds results in a fibre which is essentially amorphous and unoriented. As the spinning speed increases, the uniaxial stress field in the spinline progressively increases and its orienting influence overcomes to an increasing extent the disorienting influence of thermal relaxation process. Also the temperature at which crystal formation can commence is considerably enhanced at higher spinning speeds; however, it is not raised to a high enough level to prevent molecular relaxation. This has been a cause of disappointment to the fibre producers who would very much like to achieve the highest possible orientation in a one-step process.

The spinline crystallization of PET at high speeds involves significantly large undercooling; the melt temperature may decrease from 280 °C to 180 °C in 0.005 s. The nucleation rate is consequently very high and the concentration of nuclei is very dense. The critical size of the nucleus for crystallization to proceed is considerably reduced and approaches the unit cell dimensions of PET [36]. This occurs because in an oriented melt the entropy change on crystallization is small. At a given supercooling the free entropy change is correspondingly increased. This has been termed 'nucleative collapse' [36] because a large number of small nuclei come together to form a crystallite. This type of crystallization is distinctly different compared with the usual nucleation and growth process that dominates the crystallization of a melt in the stress-free state or at low stresses.

There is yet another type of crystallization that has received considerable attention, particularly in the case of ultra high molecular weight, high density polyethylene. This type of crystallization gives highly crystalline, extended chain morphology, as shown in Fig. 2.8(b) in Chapter 2. The structural model for such a fibre is derived from entanglement concepts. Since the fibre is made by first spinning from a gel and then drawing, the entanglement density is low and the length of the molecular chain between entanglements is very high. Such fibres have

very high modulus and strength. Spinning of filament from high molecular weight PET has also been attempted and high modulus, high strength PET fibres have been produced.

The stabilization of PET fibres and fabrics through heat-setting is an important industrial practice. On heat-setting, crystallization can occur either by melting of smaller, imperfect crystals at the crystallization temperature followed by recrystallization into a new form, or by solid state transformation in which molecules in the amorphous regions, which are not in exact register, can, with the aid of thermal energy, gain enough mobility to reduce their free energy by forming small crystallites. It is believed that both these mechanisms are operative, although at very high temperatures of heat-setting, crystal perfection is the predominant mechanism of reorganization of structure in which no large-scale melting occurs but crystal defects migrate out of the crystal.

It is worth pointing out that the crystallization behaviour of PET can also be affected by other factors such as the catalyst system used for polymerization. An interesting study [37] on PET makes a number of noteworthy observations. For example, it was found that for polymers of similar molecular weight, soluble polymerization catalyst systems exhibited lower rates of crystallization than those using an insoluble catalyst. Also a titanium-based catalyst exhibited the lowest crystallization rates for PET of equivalent molecular weight. Furthermore, the catalyst system could exhibit a greater influence than molecular weight in controlling the rate of crystallization of PET. This may be partly due to the secondary molecular structures (through side reactions) introduced by the use of different polycondensation catalysts. Another possible explanation is that residual catalysts may act as a nucleating agent and thus enhance the nucleation rates.

12.4.2 STRESS–STRAIN BEHAVIOUR

(a) Filaments spun at different speeds

The stress–strain curves of PET (intrinsic viscosity $0.66 \, dl \, g^{-1}$) filaments are plotted in Fig. 12.17(a) for various spinning speeds [38]. The mechanical properties of the filaments spun at high speeds are quite different from those of conventionally drawn filaments. The natural draw ratio characteristic of low-oriented yarns disappears as the spinning speed increases.

(b) Staple fibre and filament yarns

The stress–strain curves of PET staple fibre and filament for a variety of textile and industrial uses are shown in Fig. 12.17(b) [39]. The breaking
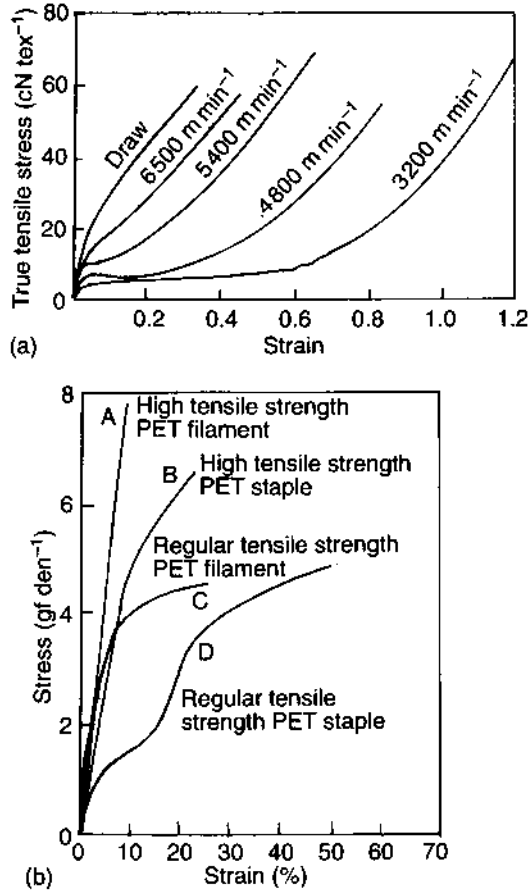
Fig. 12.17 Typical stress–strain curves for (a) PET filaments [38] and (b) PET staple and filament [29].

elongation ranges between 10 and 50% while tenacity values lie between 4 and 8 gf den^{-1}.

The tensile properties of some PET fibres are summarized in Table 12.5 [3j].

12.5 APPLICATION AREAS

12.5.1 APPAREL AND HOUSEHOLD SECTORS

In the general apparel area, polyester (PET) has gained considerably [3k] in significant segments of the market at the expense of polyamides, mainly because of the better easy-care characteristics and wrinkle

Table 12.5 Tensile properties of some PET fibres [3j]

Type of product	Limiting viscosity number	Tenacity (cN tex^{-1})	Extensibility (%)
Low pill staple fibre	0.38–0.48	26	40
Regular cotton-type staple fibre	0.55–0.65	35	45
High tenacity staple fibre	0.70–0.75	65	24
Regular filament yarn	0.55–0.65	50	15
Industrial filament yarn	0.75–1.00	85	7
Carpet fibre	0.60	34	50

resistance of polyester. One of the largest markets for polyester fibres at present lies in cotton blends. If certain handle and performance requirements can be met, there is the possibility that 100% polyester staple fibre may become competitive in this market. The high modulus and resilience of PET allows its use as a filling fibre for quilts, pillows and sleeping bags which can be laundered.

A remarkable development reported from Japan is the production of woven and knitted fabrics using PET multifilament yarn of 220 denier with 2200 filaments and 110 denier with 1100 filaments, featuring the characteristic microfibre and having ultrasoft handle and heavy weight [40]. The manufacture of microfibre is described in Chapter 14.

Various innovative achievements through modification of technique or product have made it possible to confer the comfort and coolth of cotton, the soft warmth of wool and the glamour and rustle of silk to this synthetic fibre. Some of these speciality fibres are described in Chapter 14.

Cotton-like effects can be given to fine polyester staple of 1 denier or less with microporous surface. This improves moisture absorption. Micro-crimped polyester filaments with irregular cross-section have improved comfort and aesthetics. Wool-like effects can be imparted by dyeing cationic-dyeable polyesters to deep shades. Anti-pilling effects can be introduced by using fibres of lower tenacity and higher elongation. Polyester textured yarns have wool-like characteristics since they have better thermal insulation and more moisture retention. The hollow polyester fibres have good thermal insulation. To give silk-like effects, blends of differentially shrinkable polyester filament yarns with thick and thin sections can be prepared. Polyester fibres with trilobal and pentalobal cross-sections are used to increase lustre for carpet application. A conductive fibre containing a white metal compound has antistatic properties. This can be combined with a differentially shrinkable bicomponent speciality polyester yarn. These will not attract dust.

12.5.2 BIOMEDICAL APPLICATIONS

PET fibres make one of the strongest and longest-lasting sutures. In surgical sutures, properties of particular importance are tensile strength, strength retention in the body's environment, and knot strength. Furthermore, fibres must be biologically compatible with the surrounding body tissue. PET fibres meet these requirements much better than others.

For surgical implants, e.g. replacement for diseased or malfunctioning blood vessels, knitted or woven PET porous tube with a smooth, lightly napped surface is the material of choice. Tensile strength, long-term durability, biocompatibility and a controlled degree of porosity are the requirements of the woven or knitted tubing used in arterial replacements. Polyester fibres have also been used in tendon implants.

12.5.3 INDUSTRIAL APPLICATIONS

Polyester has more flat-spotting resistance than nylon and is an important reinforcing fibre for car tyres. Due to their high modulus and strength, polyester fibres are useful for conveyor belt and rubber hose reinforcement.

In soil engineering (geotextiles), polyesters find considerable use as fibrous structures, mainly non-woven, for drainage and reinforcement. They are mainly used for earth stabilization in the construction of roads, embankments and dams.

12.5.4 FUTURE TRENDS

PET, because of its many advantages, is expected to dominate the apparel and household market; the largest market will continue to lie in cotton blends. However, the commodity fibre production is likely to pass on progressively to the Third World countries while the advanced countries will concentrate on speciality and industrial fibres.

REFERENCES

1. Brunschweiler, D. and Hearle, J.W.S. (eds) (1993) *Polyester: 50 Years of Achievement*, The Textile Institute, Manchester.
2. Ludewig, H. (1964) *Polyester Fibres: Chemistry and Technology*, Wiley-Interscience, London: (a) p. 4, 5; (b) p. 76; (c) p. 48; (d) p. 93; (e) p. 94; (f) p. 95; (g) p. 104.
3. McIntyre, J.E. (1985) In *Polyester Fibres in Fibre Chemistry* (eds M. Lewin and E.M. Pearce), Marcel Dekker, New York: (a) p. 57; (b) p. 5; (c) p. 13; (d) p. 11; (e) p. 17; (f) p. 19; (g) p. 20; (h) p. 21; (i) p. 23; (j) p. 35; (k) p. 56.
4. Imperial Chemical Industries Ltd, British Patent 804 612 (1958).

5. MidCentury Corp., British Patent 807 091 (1959).
6. Standard Oil Co., British Patent 994 769 (1965).
7. Eastman Kodak Co., British Patent 1 017 373 (1966).
8. Nakaoka, K., Mizama, Y., Matsuhisa, S. and Wakamatsu, S. (1973) *Ind. Eng. Chem. Proc. Res. Dev.*, **12**, 150.
9. Anon. (1980) *Chemiefasern Textilindustrie*, **30/82**, 487 and E53.
10. Halcon International Inc., British Patent 1 272 820 (1972).
11. Union Carbide Corp., Belgian Patent 815 841 (1974).
12. Whinfield, J.R. and Dickson I.T., British Patent 578 079 (1941).
13. Ho, C.H. (1988) *Man-made Fibre Year Book*, Chemiefasern Textilindustrie, Frankfurt.
14. Central Board for the Prevention and Control of Water Pollution (1980) *Comprehensive Industry Document-Man-made Fibre Industry*, Central Board for the Prevention and Control of Water Pollution, New Delhi, p. 11.
15. Mihail, R., Istratoire, R. and Lupu, A.L. (1958) *Studii Si Cerc. de Chimie*, **1**, 161.
16. Renwen, H., Feng, Y., Tinzheng, H. and Shiming, G. (1983) *Macromol. Chem.*, **129**, 159.
17. Zahn, H. and Krzikalla, R. (1957) *Makromol. Chem.*, **23**, 31.
18. Ross, S.D., Coburn, E.R., Leach, W.A. and Robinson, W.B. (1954) *J. Polym. Sci.*, **13**, 406.
19. Goodman, I. and Nesbist, B.F. (1960) *J. Polym. Sci.*, **48**, 423; *Idem* (1960) *Polymer*, **1**, 384.
20. Marshall, J. and Todd, A. (1953) *Trans. Faraday Soc.*, **49**, 67.
21. Pohl, H.A. (1951) *J. Am. Chem. Soc.*, **23**, 5560.
22. Ritchie, P.D., Allan, R.J.P., Forman, R.L., Jones, E. and Jenger, H.V.R. (1955) *J. Chem. Soc.*, 2717; (1956) 3563; (1957) 524, 2107, 2556.
23. Goodings, E.P. (1961) *Chem. Ind. (London), Monogr.*, **13**, 211.
24. Zimmermann, H. (1962) *Faserforsch n. Textiltech.*, **11,13**, 481.
25. British Patent 588 833/34 (1944).
26. Zimmermann, H. (1962) *Fascherforsch u. Texiltech.*, **11,13**, 481.
27. Terechowa, G.M. and Petuchow, B.W. (1960) *Chemisafern. Textilindustrie* **4**, 8.
28. Schnock, G. (1960) Thesis, Humbold-Universitat, Berlin.
29. Chang, S., Fa Shen, M. and Hsi Chang, N. (1983) *J. Polym. Sci., Polym. Chem. Ed.*, **20**, 2063.
30. Kilpatrick, L.L. (to Du Pont), US Patent 3 248 180 (26 April 1966).
31. J.K. Synthetics Ltd (1990) *Jaykay Customer Digest*, May, J.K. Synthetics Ltd, Kota, India.
32. Jain, S.L. and Gautam-Purkar, S. (1990) *Man-made Textiles in India*, **33**, 247.
33. Guanbao, H., Wu Rongrui, Dashen, Z. and Li Yanli (1987) *Study on High Viscosity Polyester for Technical Yarn*. Paper presented at the 2nd International Conference on Man-made Fibers, 26–29 November 1987, Beijing, China.
34. Davis, G.W., Everage, A.E. and Talbot, J. R. (1984) *Fibre Producer*, February, p. 22.
35. Heuvel, H.W. and Huisman, R. (1985) In *High Speed Fiber Spinning* (eds A. Ziabicki and H. Kawai), Wiley-Interscience, New York, p. 235.
36. George, H.H. (1985) Spinline crystallization in poly(ethylene terephthalate), in *High-speed Fibre Spinning: Science and Engineering Aspects* (eds A. Ziabicki and H. Kawai), John WIley, New York, pp. 271–291.
37. Jabarin, S.A. (1987) *J. Appl. Polym. Sci.*, **34**, 85.

38. Perez, G. (1985) Some effects of the rheological properties of poly(ethylene terephthalate) on spinning line profile and structure developed in high speed spinning, in *High Speed Fibre Spinning* (eds A. Ziabicki and H. Kawai), John Wiley & Sons, New York, p. 354.
39. Brown, A.E. and Reinhart, K.A. (1971) *Science*, **173**, 287–293.
40. *Japanese Textile News* (1987) June, pp. 42–82.

Nylon 6 and nylon 66 fibres

13

B.L. Deopura and A.K. Mukherjee

13.1 INTRODUCTION

Nylon 66 and nylon 6 are two important members of a group of polymers known as polyamides. The structural units of a polyamide are joined together by an amide, $-NH-CO-$, group. A polyamide manufactured from aliphatic monomer(s) is commonly designated as nylon. However, the US Federal Trade Commission has defined nylon as a manufactured fibre in which the fibre-forming substance is a long-chain synthetic polyamide in which less than 85% of the amide linkages are attached directly to two aromatic rings, while a polyamide in which at least 85% of the amide links are joined to two aromatic groups is known as an aramid. Aramid fibres are mainly used for industrial applications and are described in Chapter 18.

   The pioneering work of Wallace Carothers of the Du Pont Company in the USA led to the discovery of nylon 66 in the 1930s. This polymer was melt-spun to give to the world the first synthetic fibre. The fibre was introduced commercially by Du Pont in 1939 [1] using a patent of W.H. Carothers granted in 1938 [2]. The success of nylon 66 led to the vigorous growth of the synthetic fibre industry. Subsequently Paul Schlack in Germany discovered nylon 6, which was produced through another route, in 1939. Both these fibres now occupy an important place amongst the commodity fibres and have had a far-reaching impact on the international fibre front. This chapter will deal with the production of nylon 6 and nylon 66 polymers, their conversion to fibre, the structure and properties of the fibres, and their applications.

13.2 NYLON 6 POLYMER PRODUCTION

A polyamide that is derived from a diacid and a diamine is categorized as AABB type (e.g. nylon 66). On the other hand, a polyamide synthesized from an amino acid or a lactam is termed as AB type (i.e. nylon 6). Straight chain aliphatic nylons are identified either as nylon XY or nylon Z, where X, Y and Z represent the number of carbon atoms present in the respective structural units in the monomer. In an AABB type, the number X refers to the number of carbon atoms in the diamine and Y to that in the diacid. In the case of AB type, Z represents the number of carbon atoms in the monomer. Examples are given below.

Example 1
Raw materials: $H_2N-(CH_2)_6-NH_2$ + $HOOC-(CH_2)_8-COOH$
Name: Hexamethylene diamine (HMDA)   Sebacic acid (SA)
Type: AA   BB
Polymer repeat unit: $\dashv NH-(CH_2)_6-NH-CO-(CH_2)_8-CO\vdash$
Name: Nylon 610
Type: AABB
$$X = 6, Y = 10$$

Example 2
Monomer: $OC-(CH_2)_5-NH$
Name: Caprolactam
Type: AB
Polymer repeat unit: $\dashv OC-(CH_2)_5-NH\vdash$
Name: Nylon 6
Type: AB
$$Z = 6$$

13.2.1 RAW MATERIALS

(a) Caprolactam specification

Caprolactam can be synthesized via a number of methods. All procedures use raw materials like phenol, benzene, toluene or cyclohexane. The crude caprolactam must be carefully purified to have the following specifications [3].

Property	Value
Freezing point (dry basis) (°C)	69.0 (minimum)
Percentage transmission at 410 nm (65 wt % aqueous solution)	92.0 (minimum)
Permanganate number	7 (maximum)
Moisture (%)	0.10 (maximum)
Iron (as Fe) (ppm)	0.5 (maximum)

Volatile bases (as NH_3) (ppm)	5 (maximum)
Ignition residue (ppm)	10 (maximum)
Water insoluble	Passes test
Cyclohexanone oxime (ppm)	10 (maximum)
Free alkalinity ($meq\,kg^{-1}$)	0.04 (maximum)

The basic impurities are measured as fixed basic compounds by direct titration of an aqueous solution and as volatile substances distilled in the vapour stream from a solution in 1 N NaOH solution in which case the distilled vapours must not consume more than 0.015 ml HCl (0.1 N) per 1 g caprolactam.

The reducing agents are estimated from the degree of decolorization of an aqueous solution (1 g/100 ml), to which 1 ml of 0.01 N potassium permanganate solution has been added. The decolorization is then calibrated by a standard solution containing 0.25 g cobalt nitrate and 0.001 g potassium dichromate in 100 ml water; the time elapsing from the start of the test to the point where an equal colour intensity is reached in solution must exceed 200–300 s. Detailed analytical methods are available in the literature, e.g. references [4–6].

13.2.2 TYPES OF CATALYST

Caprolactam (CL) does not polymerize in a completely dry condition [5–7]. It requires a catalyst which converts a small amount of CL to aminocaproic acid (ACA). This is followed by polymerization. The catalyst can be an acid, a base, or simply water. The conditions required and the effect of each type of catalyst system are given in Table 13.1.

Table 13.1 Some characteristics of catalyst systems for polymerization of caprolactam

	Catalyst systems		
Parameter	Acid	Base	Water
Type	Strong like hydrochloric acid or their salts	Carbonate, hydride, alcoholate, and hydroxide of alkali and alkaline earth metals	–
Rate	Fast	Very fast	Slow
Special condition	Anhydrous	Anhydrous	–
Yield	Low	High	High
Use	Not used commercially	Shows promise	Commercially used

Table 13.2 Effect of various parameters on caprolactam polymerization

Increase in parameter	Molecular weight	Time of polymerization	End groups	Relevant figure number
Water concentration	Decreases	Decreases	Increase	13.1 & 13.2
Temperature	Decreases	Decreases	Decrease	13.3 & 13.4
Stabilizer content	Decreases	–	–	–
Time of polymerization	Increases	–	Decrease	–

The base-catalysed system has the advantage of high production rate, high molecular weight and narrow molecular weight distribution. However, the control of the reaction is difficult and a high degree of sophistication is necessary in using the technology. Generally, the water-catalysed system is used in industry.

13.2.3 PARAMETERS IN THE WATER-CATALYSED SYSTEM

The effect of various parameters on the polymerization of caprolactam catalysed by water is summarized in Table 13.2 [8–10]. In industrial practice the polymerization is controlled by (1) temperature in the range of 225–280 °C, and (2) amount of water present in the dissolved phase (5–10%). Figures 13.1–13.4 show the effects of changes in these parameters. Water solubility in caprolactam at constant temperature is proportional to water vapour pressure as demanded by Henry's law. Increase in operating temperature, therefore, decreases the amount of water in the dissolved phase (molten polymer).

13.2.4 CONTROL OF MOLECULAR WEIGHT

The molecular weight (MW) of nylon 6 is related to the degree of polymerization (DP) by the following relationship:

$$MW = 113 \times DP. \tag{13.1}$$

The principal factors which control molecular weight are: (1) temperature, (2) amount of water, (3) time of polymerization and (4) stabilizer content (up to 1%). The stabilizer can be either acidic (e.g. acetic acid, benzoic acid) or basic (e.g. benzylamine). An acidic stabilizer leaves the carboxyl end group in the polymer free, thus making it reactive to basic dyes. On the other hand, use of a basic stabilizer yields an acid-dyeable nylon. In the case of tyre cord production, a thermal stabilizer has also to be incorporated. The following relationship [11, 12] provides a useful
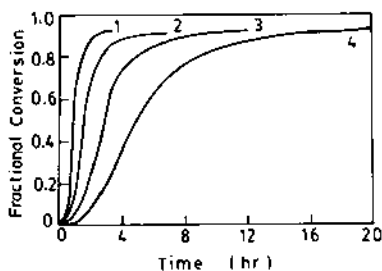
Fig. 13.1 Effect of initial water concentration (W_0) on rate and extent of conversion at 265 °C [10]. W_0 values are: 1, 0.08; 2, 0.04; 3, 0.02; and 4, 0.01.

means to industry to control the DP of nylon 6:

$$DP = \frac{p + r + q}{(1 + r)(1 - p)}$$

where

$$p = 1 - \frac{[COOH] + [NH_2]}{[COOH]_0 + [NH_2]_0}$$

$$r = \frac{[NH_2]_0}{[COOH]_0}$$

and

$$q = \frac{[COOH]_0'}{[COOH]_0}.$$

Here $[COOH]_0$ and $[COOH]$ represent the carboxyl group concentration at the start of polymerization and after time, t, respectively; $[NH_2]_0$ and $[NH_2]$ represent the amino group concentrations at the initial (start) and final (end) stage, respectively; and $[COOH]_0'$ represents the initial concentration of carboxyl group of a monofunctional acid acting as a stabilizer (e.g. acetic acid).
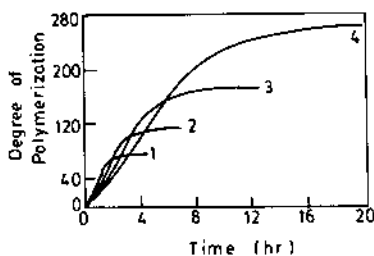
Fig. 13.2 Effect of initial water concentration (W_0) on rate and degree of polymerization [10]. W_0 values are: 1, 0.08; 2, 0.04; 3, 0.02; and 4, 0.01.
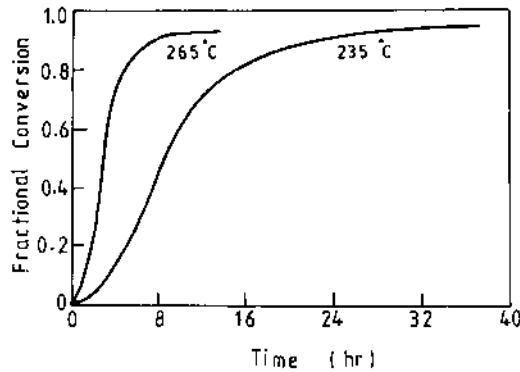
Fig. 13.3 Effect of temperature on rate and extent of conversion ($W_0 = 0.02$) [10].

(a) Mechanism

Caprolactam polymerization is preceded by a hydrolysis step,

$$OC-(CH_2)_5-NH + H_2O \rightarrow HOOC-(CH_2)_5-NH_2$$

$$CL + water \rightarrow ACA \text{ (aminocaproic acid)}$$
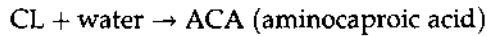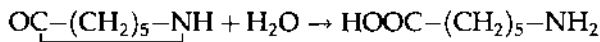
ACA, thus produced, adds to further monomer units, initiating polymerization. This is known as step addition,

$$ACA + CL$$

$$HOOC-(CH_2)_5-NH_2 + nOC-(CH_2)_5-NH$$

$$\Updownarrow$$

$$HOOC-(CH_2)_5-[NH-(CH_2)_5-CO]_n NH_2$$

$$PCL$$
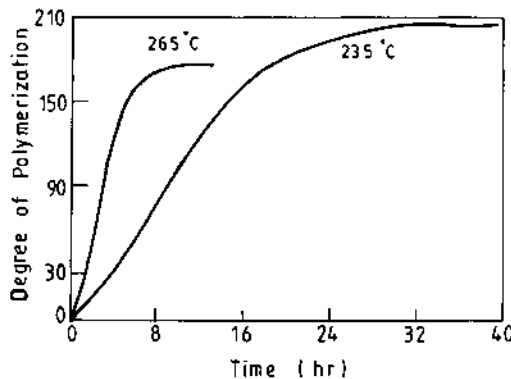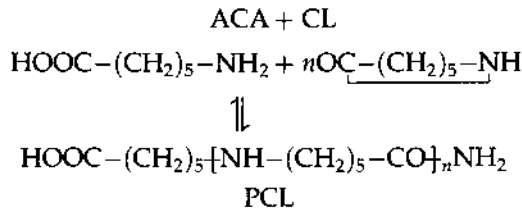
Fig. 13.4 Effect of temperature on rate and degree of polymerization ($W_0 = 0.02$) [10].

After polymerization has proceeded for some time, the process reaches equilibrium. In industrial practice, under optimum conditions, the reaction forms an equilibrium with 90% in favour of polycaprolactam (PCL).

$$CL \underset{10\%}{\overset{PCL}{\rightleftharpoons}} \underset{90\%}{PCL}$$
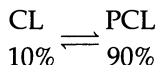
Once the equilibrium is reached, which usually takes about 4–6 h in a VK tube (described later), a step growth (condensation) polymerization occurs involving the PCL molecules formed. This reaction leads to an increase in molecular weight.

$$HOOC-(CH_2)_5\{NH-(CH_2)_5-CO\}_x NH_2$$
$$+$$
$$H_2N\{(CH_2)_5-CO-NH\}_y(CH_2)_5-COOH$$

$$\downarrow$$

$$HOOC-(CH_2)_5\{NH-(CH_2)_5-CO\}_{x+y}NH_2 + H_2O$$

$$(PCL)_x + (PCL)_y \rightarrow (PCL)_{x+y}$$
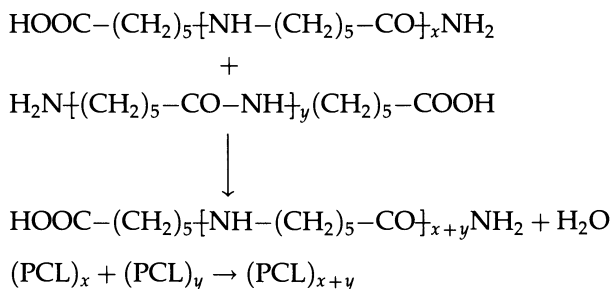
(b) Side reactions

During CL polymerization, the most important side reaction is the formation of cyclic oligomers, as illustrated by the following example:

$$\begin{array}{ccc}
 & (CH_2)_5 & \\
 \diagup & & \diagdown \\
OC & & NH \\
| & & | \\
HN & & CO \\
 \diagdown & & \diagup \\
 & (CH_2)_5 & \\
\end{array}$$

Dimer
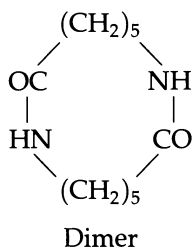
Formation up to tetramer has been reported [13–16]. The solubility of the oligomers is greater than that of the nylon polymer and, therefore, the former can be removed by extraction with boiling methanol. This provides a basis for the quantitative evaluation of oligomers [17].

13.2.5 PRODUCTION PROCESS

Caprolactam polymerization can be conducted through three processing routes, namely batch, continuous and integrated.

(a) Batch process

This process is conducted in a conventional polymerization kettle. It offers the advantage of being able to produce different grades in the same vessel and is therefore suitable for the manufacture of speciality grades. However, the production time is greater and the operation is more costly than the other routes. Also the quality may vary from batch to batch.

During any operation involving the polymer produced, such as melt-spinning, the water partition coefficient will change, causing polymerization of the residual caprolactam. This is termed post-polymerization [18] and the role of water content in the melt has been confirmed experimentally [11]. It is, therefore, absolutely necessary that residual caprolactam is brought down to a minimum (less than 1%) in nylon 6 before melt-spinning can be undertaken. Similarly, the residual water content must be very low (0.01–0.04%) [8] in the polymer to avoid problems during melt-spinning.

The batch process has been described in detail in the literature [19, 20].

(b) Continuous process

A flow diagram for nylon 6 production is presented in Fig. 13.5 [21], while a schematic diagram of a VK (from the German *Vereinfacht Kontinuierlich*, meaning simplified continuous) tube is shown in Fig. 13.6 [22]. This is a continuous process, which is well established all over the world.

The VK tube is 8–10 m high and its diameter depends upon the required production capacity. The tube is made by assembling several independent sections. Each section has its own heating system (Dowtherm vapour or electricity) and control. Inclined baffles are placed in the tube which force the reactants to take a downward zigzag course. The angle of inclination and design of these baffles are crucial in determining the course of the reaction. Bubble caps are occasionally provided in the baffle plates to facilitate escape of volatiles. The topmost zone serves as the feed zone and acts as a reflux system. Several inlet and outlet pipes are provided for feed and outgoing vapours. At the bottom of the tube a high capacity extruder is placed which continuously pumps out molten nylon 6 from the VK tube in the form of a strand, which after being cooled to a temperature just above T_g (about 50 °C) is guided to a cutter.

There is also a feed pipe for nitrogen at the top. Nitrogen sweeps away any air from the system and acts as a blanket preventing thermo-oxidative degradation. Above the surface of the reaction mix, the outlet is fitted to a rectification column (dephlagmator). Excess water leaving the
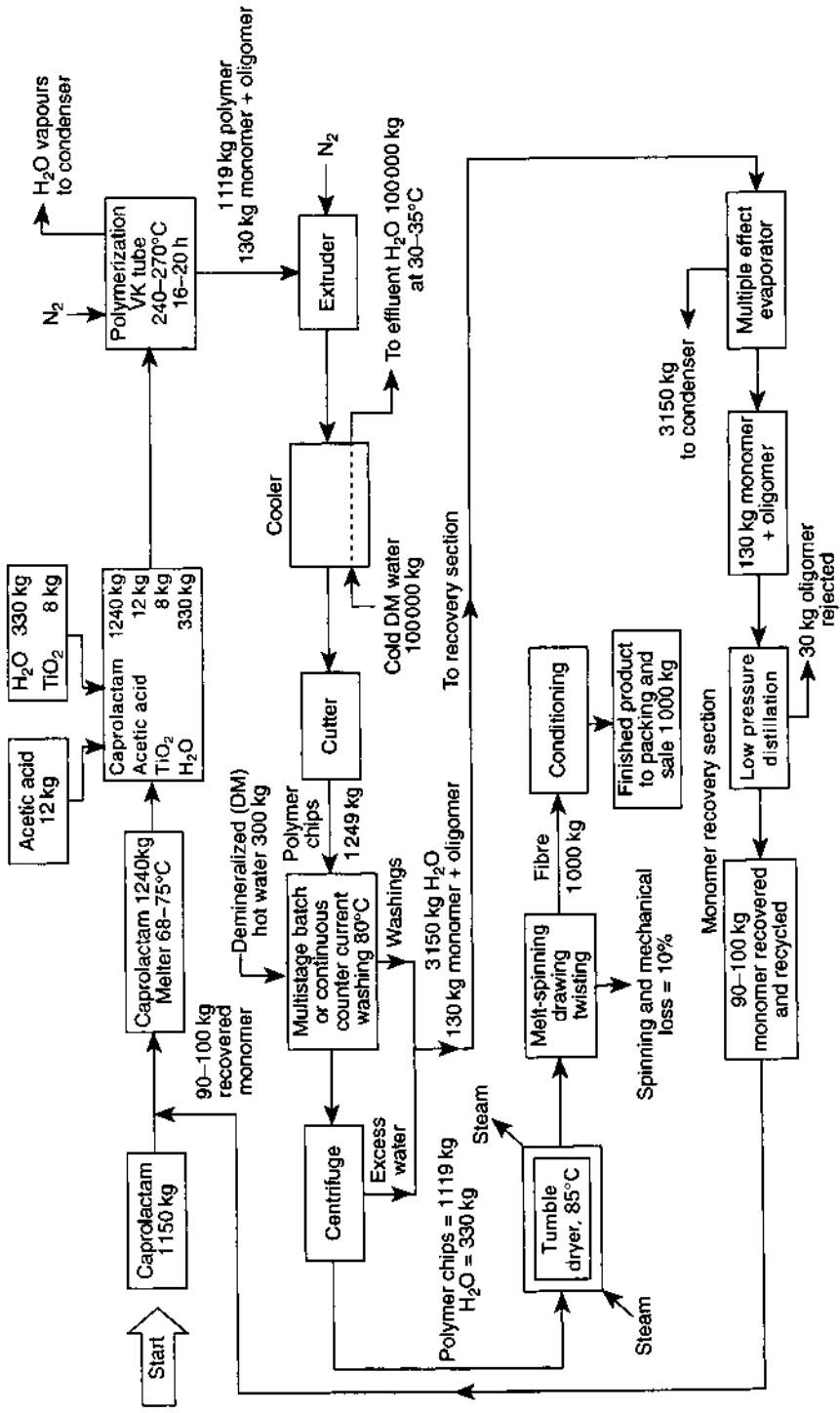
Fig. 13.5 A flow diagram for nylon 6 production [21].
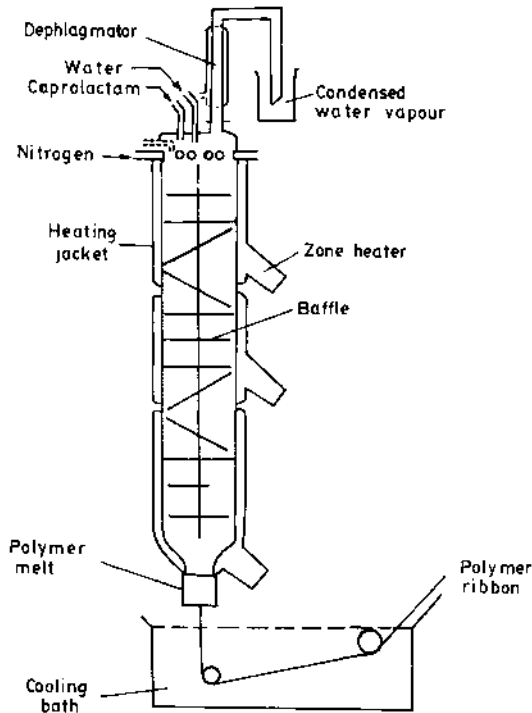
Fig. 13.6 A VK tube [22].

system is condensed; its volume provides a measure of the course of the reaction. At this stage caprolactam, if any, flows back to the reactor.

The plant operates on a continuous basis. The feed consists of molten CL with the requisite amount of water (catalyst), and viscosity stabilizer (acid or base). Optional ingredients may include one or more of the following:

- a delustrant (e.g. titanium dioxide) to produce dull or semi-dull grade;
- an antistatic agent to reduce development of static electricity by friction during spinning and use;
- a light stabilizer to combat degradation of nylon 6 by ultraviolet radiation during use;
- a heat stabilizer to protect it from thermal degradation during use at elevated temperature (this is frequently added in tyre cord production);
- pigment (e.g. carbon black), which produces a mass-coloured polymer.

As the feed enters the topmost zone, the molten mixture appears to boil due to water bubbles escaping the liquid phase. The course of the polymerization is decided by the temperature in this zone. The material

moves downwards and the step addition process is complete within 6 h. The remaining time (total residence time 12–24 h) spent by the material in the reactor is primarily to increase the DP.

After polymerization is complete, the highly viscous melt passes through the extruder, from which it comes out in the form of strands which are cooled and cut into chips.

Modifications

Caprolactam polymerization is a two-stage process, as discussed earlier. A high water concentration is optimal in the first stage of conversion of caprolactam to aminocaproic acid, followed by step addition polymerization. Subsequently, polycondensation involving two polyamide molecules leads to an increase in the degree of polymerization and eliminates water as a by-product. At this second stage, therefore, water concentration is maintained at a low optimum level to hasten the process and in fact removal of water is helpful at this stage. With appropriate reaction conditions, the time of polymerization can be reduced by almost a half at a given temperature in this two-stage process. The course of polymerization during this process is shown schematically in Fig. 13.7 [23]. The use of two tubes in series offers significant advantages compared with a single VK tube. The first tube acts as a prepolymerization unit and the product is transferred to the second VK tube for the completion of
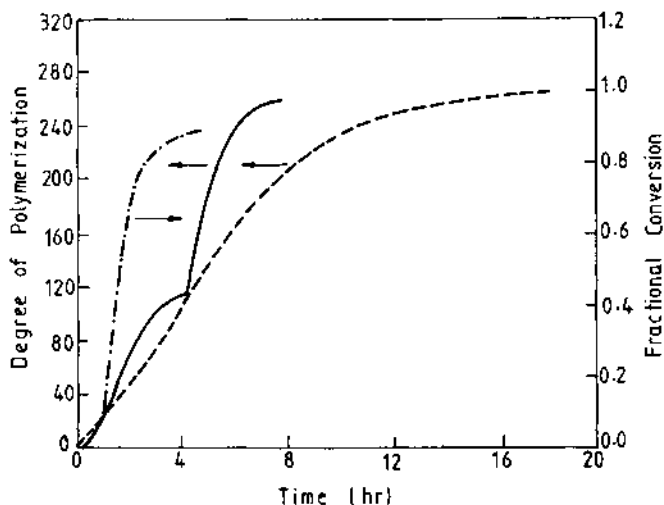
Fig. 13.7 Course of polymerization for a two-stage process. Solid line: two-stage process (initial water concentration $W_0 = 0.04$ mol/mol CL; free water removed at conversion equilibrium). Dotted line: conversion at $W_0 = 0.04$. Broken line: one-stage process, $W_0 = 0.1$ [23].
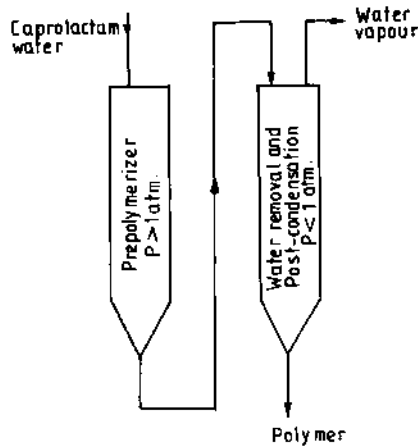
Fig. 13.8 Continuous two-stage polymerization process [25].

polymerization. Such systems result in greater capacity of plant, better control on the reactions, reduced polymerization time and improved product quality [24]. A schematic diagram of such a system is presented in Fig. 13.8 [25].

Increasingly, in designing new reactors, the advantages of multistage reactors is being realized. Suitable modifications as well as other specific requirements including optimum heat and mass transfer and flow patterns are being incorporated. Usually these multistage reactors are tubular flow reactors. However, as efficient heat transfer is a crucial factor in reducing the time of polymerization and improving product quality [26], a cascade of stirred tank reactors or a combination of cascade (first stage) and a tubular flow reactor (second stage) is ideal. It has also been reported that continuous flow stirred tank reactors (CSTR) yield polymers with narrow molecular weight distribution (MWD), while tubular reactors produce polymers with extremely narrow molecular weight distribution [27].

An altogether different method to reduce the polymerization time is to add a small amount (2–10%) of amino caproic acid to the caprolactam before feeding it into the VK tube. The ring-opening step is thus eliminated and the total residence time in the VK tube is reduced [25].

Washing

The nylon 6 polymer chips contain 90% PCL, 8–9% CL and up to 3% oligomers. The chips are subjected to a counter-current water wash at 95 °C (Fig. 13.9) to remove CL. This is necessary as it prevents post-polymerization during melt-spinning. The following process variables are important

Washing of PCL
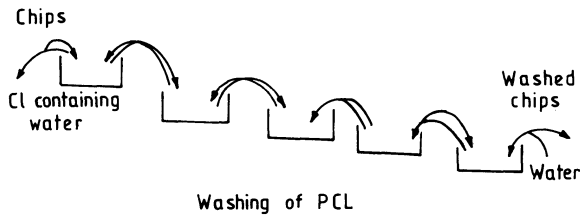
Fig. 13.9 Washing sequence of polycaprolactam chips.

at this stage: (1) water:polymer ratio, (2) water temperature, (3) specific surface area of the chips, and (4) the efficiency of the process.

The residual monomer content in the polymer decreases as follows:

After first wash:	5%
After second wash:	2–5%
After third wash:	1–1.5%
After final wash:	0.5%

The wash water, rich in CL, is sent for monomer recovery treatment.

Drying

The wet nylon 6 chips are then sent to a rotary drum dryer rotating at 1–$5\,rev\,min^{-1}$ and operating at 100–$120\,°C$, either under vacuum (10^{-1} Torr) or in a nitrogen atmosphere. The drying takes place for 20–50 h, yielding chips having residual moisture content of 0.02–0.04%. The chips (size 3 mm × 3 mm) are stored under nitrogen.

(c) Integrated continuous process

This is a modified form of the conventional VK tube method. The modification is aimed at removing the monomer and oligomers from the melt by application of vacuum so that the melt can be directly used for melt-spinning. This eliminates the subsequent washing, drying, and remelting of the chips. Alternatively, chips can also be produced by this method.

In this process, the melt from the VK tube in an incomplete state of polymerization is spread over a large surface in a thin film evaporator operating under vacuum, as shown schematically in Fig. 13.10 [28]. The heat transfer is now better and this helps to remove the residual monomer quickly. However, the molecular weight increases somewhat due to disturbance of the equilibrium. The melt is then led either through an extruder to a cutter to yield chips or is directly fed into the melt-spinning unit.

The efficiency of the integrated continuous process (ICP) depends on the amount of vacuum, residence time, design of equipment, and the
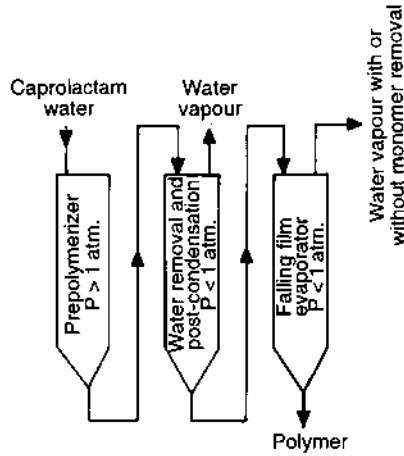
Fig. 13.10 The integrated continuous process [28].

process design, especially of the part concerned with condensation and transfer of cyclic oligomers. The following advantages accrue.

- Polymer melt can be directly melt-spun or converted to chips.
- No extraction and drying steps are necessary.
- Monomer recovered by vacuum can be directly recycled to the monomer feed section.

However, the method has the following shortcomings.

- It is less effective in removing the water-soluble constituents of the equilibrium polymer.
- Higher amounts of oligomers are retained.
- The water-soluble materials retained in the polymer are in the range 2.8–3.8% compared to 1% in the conventional process.

The steps involved in the VK tube and the integrated continuous process (ICP) methods are summarized below schematically:
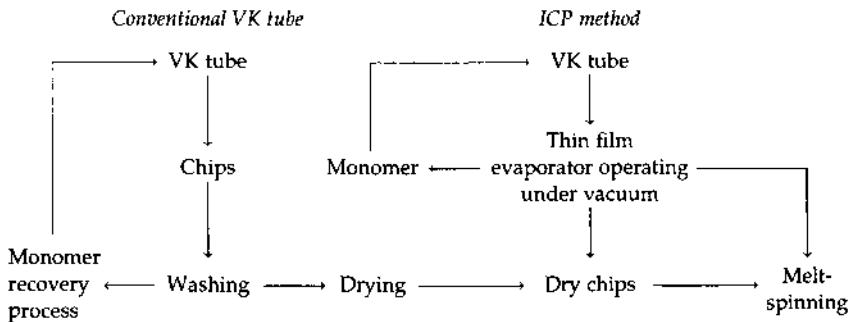
13.3 NYLON 66 POLYMER PRODUCTION

13.3.1 RAW MATERIALS

The raw materials for nylon 66 synthesis are hexamethylene diamine (HMD) and adipic acid (AA). AA is usually synthesized from cyclohexane and less commonly from 1,3-butadiene or tetrahydrofuran [29, 30]. HMD is also made from 1,3-butadiene, but can be synthesized from adipic acid or tetrahydrofuran as well [31–33].

(a) Specifications

Both the raw materials should be pure. The general specifications for them are given below.

Adipic acid

Criterion	Description/value
State	White crystal
Molecular weight	146
Acid number	768
Melting point (°C)	152
Boiling point at 760 mm Hg (°C)	216
Ash (%)	12 maximum
Colour, APHA, 20 g in 100 ml methanol	10 maximum
Iron (ppm)	2 maximum
Water (%)	0.20 maximum

The amount of steam-volatile acids, especially monobasic aliphatic acids, in adipic acid should be low as they act as chain terminators during polycondensation. Also ash and iron content should be low as they give rise to a coloured polymer [34].

Hexamethylene diamine

Criterion	Description/value
State	Colourless crystal
Molecular weight	116
Melting point (°C)	40
Boiling point (°C)	204–205

Steam-volatile bases should be absent as they may act as chain terminators or disturb the stoichiometric ratio of acid and diamine [34].

13.3.2 PRODUCTION PROCESS

It is necessary to maintain a molar ratio of $1:1$ of adipic acid : HMD to ensure the high molecular weight of the product. This is achieved by reacting the two components in methanol solution at an elevated temperature, leading to the formation of adipic acid–HMD salt (AH salt or nylon 66 salt) which precipitates out from the methanol solution.

The reaction that occurs is:

$$H_2N-(CH_2)_6-NH_2 + HOOC-(CH_2)_4-COOH$$
$$\text{HMD} \qquad\qquad\qquad \text{AA}$$

$$\downarrow$$

$$H_3N^+ ---(CH_2)_6 --- N^+H_3$$
$$\vdots \qquad\qquad\qquad \vdots$$
$$^-OOC-(CH_2)_4-COO^-$$
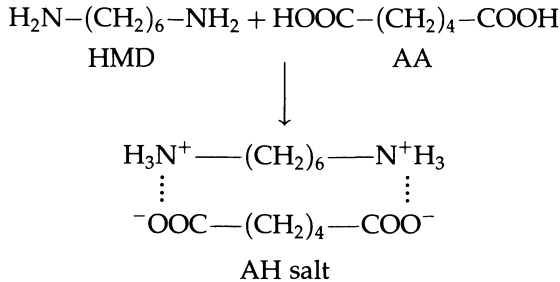
AH salt

The AH salt so obtained is dissolved in distilled water, producing a 60% solution. This solution is then subjected to polycondensation above 250 °C, producing polyhexamethylene adipamide.

$$H_3N^+-(CH_2)_6-N^+H_3$$
$$\diagup \qquad\qquad \diagdown$$
$$^-OOC-(CH_2)_4-COO^-$$

$$\downarrow$$

$$H\text{+}HN-(CH_2)_6-NH-OC-(CH_2)_4-CO\text{+}_nOH + H_2O$$

Nylon 66
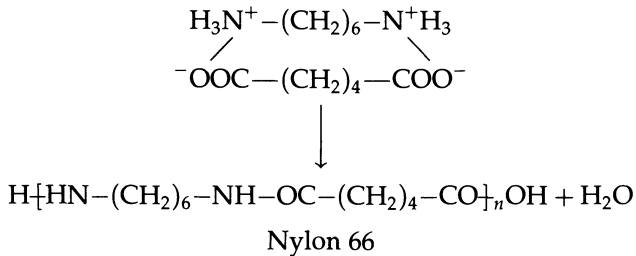
It should be mentioned here that during the PC stage, 13.5% of the weight of the monomer used is lost in the form of water. It is interesting to recall that in caprolactam polymerization, only 2% by weight of CL is lost in the recovery of equilibrium monomer and oligomers. Therefore, taking into account a 6% loss during fibre-forming operations after polymerization, one should use an additional amount of monomer (19% in the case of nylon 66 and 6% for nylon 6) for the production of the same amount of the polymer [35].

The production process for nylon 66 was first commercialized as a batch process because it was necessary to manufacture the intermediate AH salt. However, due to variation in product quality and other production considerations, continuous polymerization is favoured nowadays.
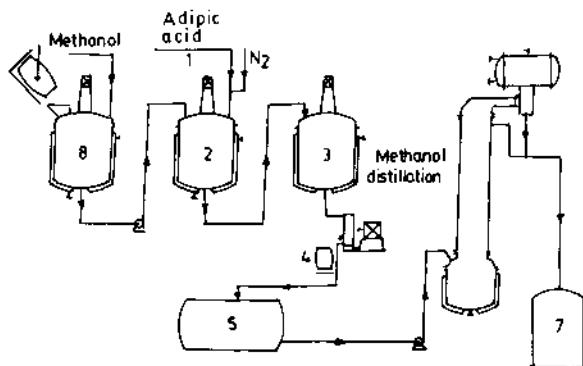
Fig. 13.11 The process used to produce AH salt [36]. For description, see text.

(a) Batch process

The batch process is carried out in two stages. In the first stage AH salt (nylon 66 salt) is prepared; in the second stage AH salt is subjected to polycondensation, producing nylon 66.

AH salt

The process for the preparation of AH salt is shown schematically in Fig. 13.11 [36]. Hemamethylene diamine (HMD) is dissolved in methanol in vessel 8 and transferred as 60–70% solution to vessel 2. Adipic acid (AA) is fed as 20% solution in methanol through an opening at 1 to vessel 2 under nitrogen atmosphere. The mixture thus produced in equimolar proportion is transferred to the reaction vessel 3. The exothermic reaction of AH salt formation is controlled by the evaporation of methanol. The slurry is centrifuged at 4 and the crude mass is collected in storage vessel 5. The excess methanol is removed by distillation and collected for reuse in vessel 7. The precipitated AH salt is dissolved in water and stored as 60% solution.

Polycondensation (PC)

Polycondensation is carried out in a stainless steel autoclave of appropriate capacity as shown in Fig. 13.12 [37]. The autoclave is heated by using Dowtherm or steam (at 65 atm.) passing through either an internal coil or an external jacket. The autoclave is purged with pure nitrogen to ensure complete oxygen removal from the system so that thermo-oxidative degradation of the polymer cannot take place. The autoclave is capable of operating at both high and low pressure.
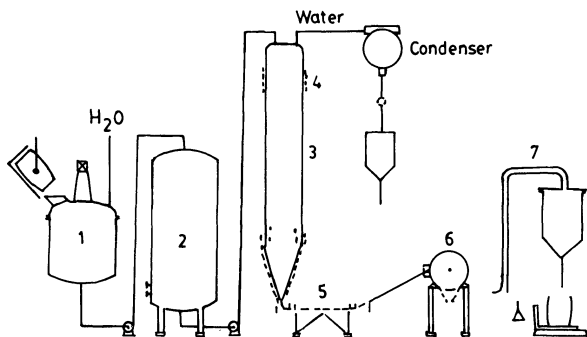
Fig. 13.12 The polycondensation process [37]. For description, see text.

AH salt, as 60% aqueous solution, together with a small amount (usually not exceeding 0.5%) of a monofunctional agent (such as acetic acid) acting as molecular weight stabilizer, is pumped from vessel 1 into the autoclave 2 heated to 260–280 °C. In the initial stage, there is evaporation of water (which is used as solvent), which along with some amount of reaction water vapour raises the pressure to 15 atm. At this stage the pressure in vessel 3 is gradually reduced to atmospheric level and then to high vacuum (up to 10^{-5} Torr), maintaining the heating. The reaction water is removed from the top by the application of vacuum at 4 and condensed. As a result, the DP increases and the viscosity of the melt rises. After the desired DP has been achieved, the melt is extruded by nitrogen pressure through a die in the form of a ribbon which is cooled by cold water at 5 and finally cut into chips at 6, which are stored after drying at 7.

(b) Continuous polymerization

There are a large number of patents relating to continuous polymerization; only two representative methods will be described here.

A flow sheet is shown in Fig. 13.13 for the continuous polymerization of nylon 66 salt solution [38]. Nylon 66 salt solution from the two mixing tanks is conveyed to the evaporator by a pump positioned in the feed line. The mass is continuously moved inside the thin film evaporator by pump P1. The solution is heated to 105–115 °C by using steam or Dowtherm flowing through the heat exchanger H1. Steam escapes through the outlet O1, leaving 60–70% nylon 66 salt in solution. The solution is continuously transferred to the reactor operating at 225–260 °C and 240–260 psig (psig stands for per square inch gauge pressure; the absolute pressure is equal to the psig reading + 14.7 psi). This reactor is a thin film evaporator and is designed in such a way that the mass moves via a turbulent path, thus ensuring a high surface-to-volume
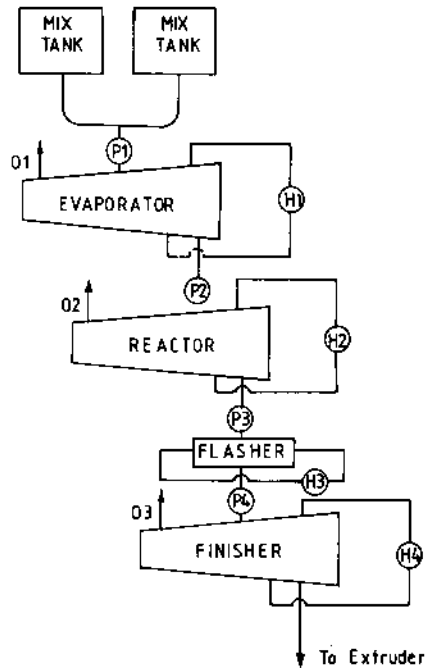
Fig. 13.13 Flow diagram for the continuous polymerization of nylon 66 salt solution [38]. For description, see text.

ratio. Polycondensation proceeds and water is removed by the outlet O2. The low molecular weight product is conveyed to the pressure reduction unit or flasher. Here the pressure drops quickly to atmospheric level, causing flash evaporation of water and increase in the degree of polymerization of the product. The mass is conveyed to the finisher where the polymerization is completed. The mass is then led to the extruder as indicated.

In another variation [39] of the method (Fig. 13.14), aqueous AH salt solution is prepolymerized in the reactor R heated by hot vapours passing through a jacket. The mass is conveyed via a pump into the flasher. The flasher consists of three sections of tubes having increasing diameter connected in series as shown in Fig. 13.14. Thus the forward moving mass polymerizes under gradually reducing pressure. The tubular reactor is jacketed and the heating fluid enters at the indicated point. The reaction mass then moves through the steam separator for water vapour removal into the finisher, which comprises a cylindrical vessel and an inner vessel (thus forming an annular space), a screw pumping device and a pump for discharging the molten polymer. Further details of the design appear elsewhere [40].
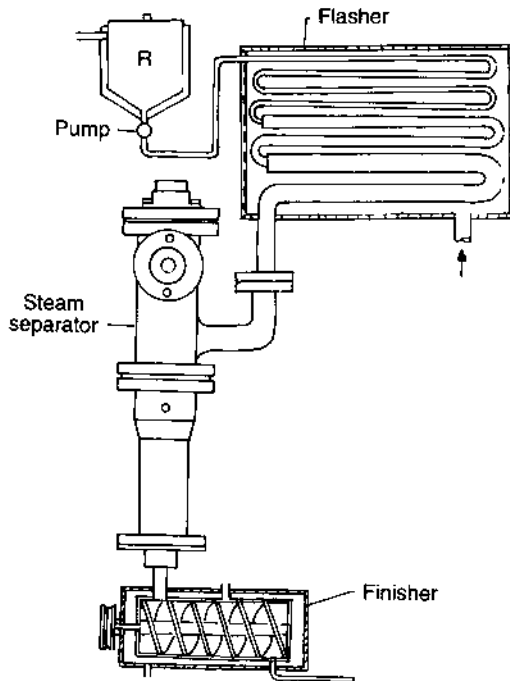
Fig. 13.14 A set-up for continuous polymerization of nylon 66 salt solution [39].

(c) Polymerization using dry nylon 66 salt

There are several disadvantages in using nylon 66 salt solution for poly-condensation. These are: (1) 50–60% (by weight) of the solution needs to be evaporated during polymerization; (2) a large amount of energy is consumed for water removal; (3) some unconverted HMD remains in the nylon 66 salt solution and is carried forward during water removal; and (4) as the molten material remains static for a considerable period during the PC stage for water removal, the advantages of a continuous process are partially lost.

These problems can be substantially overcome by polymerizing solid nylon 66 salt in dry form. Particle size is a crucial determinant in this and should be small for successful polymerization. In one such process [41] the dry AH salt is preheated to 150 °C and then rapidly heated to 240 °C so that melting takes place without much polycondensation. The melt is conveyed into a vertical conduit and polymerization occurs at high pressure and temperature. Water vapour leaves the reactor and the HMD vapour carried along with it is condensed and returned to the reactor. Nylon 66 is continuously withdrawn from the second reactor.

(d) Direct polymerization

As the name implies, direct polymerization is carried out without the formation of an intermediate AH salt [42]. Molten adipic acid and diamine are drawn from separate melters in approximately equimolar proportion in a low temperature polymerizer with slight excess of adipic acid. The temperature is accurately maintained so that a melt is produced which remains water-soluble and the major fraction does not polymerize. The mass is transferred to a regulator where accurate adjustment of the desired molar ratio is done. The mass is then transferred to a polymerizer operating at high temperature for polycondensation. Reaction water is continuously removed and nylon 66 is withdrawn from the reactor after the product has reached the desired molecular weight.

13.4 DEGRADATION REACTIONS

Nylon 66 and nylon 6 undergo various types of degradative reactions, generally of the following types – thermal, thermo-oxidative, mechanochemical and hydrolytic [43]. However, depolymerization of polyamides, especially nylon 6, which takes place smoothly at 300 °C, when heated in nitrogen, is generally not considered as a degradation process.

Thermal degradation of nylon 6 or nylon 66 appears to proceed via a free-radical mechanism involving the amide bond [44, 45]. Products of degradation include volatiles such as carbon dioxide, ammonia and water as well as a cross-linked solid.

Thermo-oxidative degradation takes place at a much lower temperature (at 190 °C for nylon 6) and also proceeds via a free-radical mechanism. Molecular weight decreases and subsequently gelation takes place with continued oxidation. Volatiles such as carbon dioxide, formaldehyde and methanol are formed [46–48]. Even slight thermo-oxidative degradation causes yellowing of polyamides which is unacceptable in the product. On account of its industrial importance, this area has been the subject of several studies [49–51].

The amide bond in polyamides is easily susceptible to hydrolysis. Immersion of nylon 6 in water at 25 °C results in deterioration of physical properties [52]. In this case, primary bond rupture is usually preceded by breaking of intermolecular hydrogen bonds. All polyamides undergo mechano-chemical degradation, particularly during spinning and subsequent processes [43]. As polyamides are prone to degradation in demanding applications such as in tyre cords, addition of thermal and thermo-oxidative stabilizers becomes a necessity.

13.4.1 DEPOLYMERIZATION

Nylon 66 and nylon 6 can be smoothly depolymerized to their constituents. For example, nylon 6 yields caprolactam when heated in a nitrogen atmosphere at 300 °C. Depolymerization can be more easily carried out in the presence of acids such as orthophosphoric acid [53], boric acid [54], and basic catalysts [55–58]. Acid-catalysed depolymerization is usually carried out at atmospheric pressure, whereas base-catalysed (e.g. sodium hydroxide) depolymerization is best conducted under reduced pressure [58].

Depolymerization is practised in industry for the recovery of monomers from polyamide waste.

13.4.2 POST-POLYMERIZATION

As pointed out earlier, a caprolactam–polycaprolactam equilibrium sets up during the manufacture of nylon 6. Usually, under the industrially used conditions, about 10% caprolactam and oligomers are present. The following relationship expresses the polymer–caprolactam equilibrium:

$$K_3 = \frac{[CL][S_n]}{[S_{n+1}]}$$

where K_3, the equilibrium constant, depends on the degree of polymerization of polycaprolactam formed and water : caprolactam ratio, [CL] is the concentration of caprolactam, $[S_n]$ the concentration of the monomer and $[S_{n+1}]$ the concentration of $(n + 1)$th mer.

13.5 ADDITIVES

Modification of nylon 66 and nylon 6 is carried out to improve specific properties. Some of the important additives which are used industrially to produce modified nylons are briefly described below.

Mass-coloration of nylons may be carried out by the addition of suitable colouring materials during polycondensation. Such mass-coloured products have several advantages, including excellent light and wash-fast fabric properties and no barriness (a problem arising from non-uniform dyeing where a fabric shows bars of different shades). The chemical processing step is also largely eliminated and the rate of production is high. Some of the important characteristics required in a colouring agent are: (1) it should not influence the course of the polymerization, (2) it should not degrade at the spinning temperature, and (3) it must possess good compatibility with the polymer melt so that phase separation does not occur. Both dyes and pigments (organic and inorganic) are in use. Of the various inorganic pigments, carbon black and titanium dioxide are most widely used, whereas organic pigments

belong to the anthraquinone, dioxazine, bisazoindanthrone, phthalo-cyanine, peryle and quinacridone classes. Due to the tendency of agglomeration, difficulty in pigment dispersion and consequent non-uniformity of colour in the fibre, it is preferable to use polymer-soluble dyes. Such dyes should also possess good thermal stability and non-volatility under polymerization conditions [59]. Mass-coloration may also be carried out to a limited extent in the chip stage, or by mixing master batch containing dye or pigment in the polymer chips during melt-spinning [60]. This is described in more detail in Section 13.6.5.

The use of other additives and procedures for making nylons with enhanced hydrophilicity (which also results in improved antistatic properties), flame retardant characteristics, deep acid-dyeable and differentially dyeable have been covered in Chapter 14.

Tyre cords are subjected to high use temperatures in a running tyre and therefore a thermal stabilizer must be incorporated, preferably during polymerization. It may be added here that for the manufacture of tyre cord, the polymer should be of higher molecular weight than that of normal textile-grade polymer. This is mainly for achieving appropriate mechanical properties in the tyre cord. For this, in the case of nylon 6 for example, polymerization is continued for a longer period in the presence of a lower amount of chain regulator so that a polymer of high molecular weight is obtained. Various copper salts at the level of 45–60 ppm copper are frequently used as thermal stabilizers for nylon 6 and nylon 66 [61, 62]. It is customary to use various other organic or inorganic materials which act as synergistic co-stabilizers with copper salts. Alkali metal iodides and bromides are most noteworthy in this regard. Frequently, the tyre yarn has not only to meet high temperatures during use but also bear high load (frequently due to overloading of the vehicle beyond what is recommended by the tyre rating). Under such conditions use of 9,9-dialkyldihydroacrid compounds at a concentration of 0.4–1.0 wt % on monomer before or during polymerization is recommended [63].

13.6 FIBRE PRODUCTION

Both nylon 6 and nylon 66 polymers are converted to fibres through the melt-spinning route in which the molten polymer, obtained either directly from the polymerization reactor system or by melting of polyamide chips, is extruded through a die or spinneret.

13.6.1 MELT-SPINNING

Generally polymer chips in the whole line (i.e. silo/hopper to extruder) are kept under nitrogen atmosphere to avoid oxidative degradation. The

chips are dried before being transferred to the silos, so that moisture content is less than 0.02%. The melt is extruded at a fixed temperature and at a constant throughput rate.

The molten polymer is fed by means of an accurately controlled metering pump to either a disc or a rectangular spinneret via the filter-pack containing layers of special sand and stainless steel screens or sintered stainless steel plates. The filtration step improves melt homogeneity and does not allow foreign particles, gel particles, or precipitated additives to enter the spinneret. It is important that the flow against pressures as high as 60–70 MPa must be controlled against any fluctuations that usually give rise to inadequate final products [64].

The spinning temperature is in the range of 260–290 °C. The filaments emerging from the spinneret, generally with circular orifices, are cooled in quench ducts by a cross-current of air, wetted with a finish, and wound on bobbins at take-up speeds varying from 100 to 6000 m min^{-1}.

The spin finish is applied in the 0.2–1.00% range. In addition to the specific functions of the individual components of the finish, as described in Chapter 7, a principal function of the finish is to saturate the filaments with equilibrium water concentration for the relative humidity prevailing during the subsequent fibre-processing operations.

In nylon spinning, spinline stress can be controlled to a large extent with relative humidity of the quench air, thereby affecting the glass transition and freeze line position [65]. The value of relative humidity used in practice ranges between 30 and 60% and is typically 55%. The temperature of the quench air is kept in the range of 18–20 °C. A large variation of relative humidity of the quench air could result in non-uniformity or significant structural changes, as nylon 6 is very sensitive to moisture regain.

13.6.2 DEVELOPMENT OF STRUCTURE ALONG THE SPINNING LINE

Unlike PET fibres, which formed the subject matter of the previous chapter, nylon 66 and nylon 6 crystallize relatively more rapidly, primarily because of more flexible molecular chains. Also they can crystallize at relatively lower wind-up speeds, even in that part of the spinline where stress is low. There are two more features about these fibres that are distinctly different from those of PET. First, a variety of crystalline phases, some more stable than the others, can occur in these fibres as a function of spinning speed. For example, nylon 6 fibres obtained by melt-spinning at different speeds contain mixtures of α, γ and pseudo-hexagonal forms [65] in different proportions, though only two of these, namely α and γ forms, are generally identified [66] and considered to be important. However, there is an absence of distinctly different crystalline forms in nylon 66 filaments melt-spun at low speeds, but at higher

speeds, as discussed later, the γ form predominates. Second, the moisture content of the ambient environment has a very strong influence on fibre crystallizability. Studies made by Heuvel and Huisman [66] on nylon 6 fibres have shown, for example, that like PET, freshly spun, fully dry nylon 6 yarns do not develop crystallinity up to $3000\,\mathrm{m\,min^{-1}}$ wind-up speeds but crystallize at higher speeds. However, a large difference exists between PET yarn and nylon 6 yarn in a normal moisture-containing environment. This difference arises from the high moisture sensitivity of nylon 6. Thus under normal conditions in the winding room, PET fibres are predominantly amorphous up to $3000\,\mathrm{m\,min^{-1}}$, while nylon 6 yarns develop crystallinity at much lower speeds. It has been suggested [66] that while nylon 6 is above its glass transition temperature under normal conditions in the winding room, PET is well below its T_g. It follows that the structure present in conditioned nylon 6 yarn spun at lower speeds is due mainly to crystallization after moisture pick-up, while the crystals in the yarns wound at speeds higher than $3000\,\mathrm{m\,min^{-1}}$ are already present, having been generated during the spinning process. Similar behaviour is shown by nylon 66 fibres as far as their crystallizability is concerned.

The two structure-forming mechanisms for nylon 6 as-spun fibre are believed to involve the slow growth of α crystals at low temperatures under the conditions of the winding room, while during cooling of the spinline the orientation-induced nuclei grow preferentially into γ crystals [66]. From Fig. 13.15 it follows that γ crystals are favoured by an increase in winding speed; apparently the orientation-induced crystallization favours the formation of the γ phase [66].

The effect of winding speed on the birefringence of dry-wound and conditioned nylon 6 yarns (Fig. 13.16) also suggests that the sign change in birefringence of dry-wound fibres corresponds to the transition of structure-formation mechanism [66]. It also confirms that at high
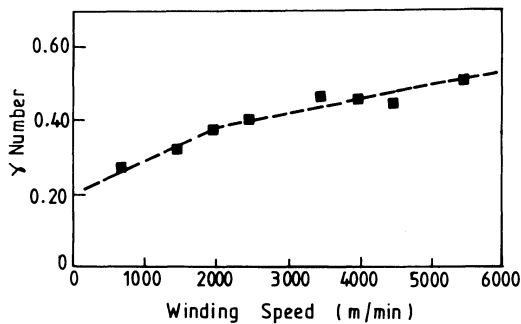
Fig. 13.15 Dependence of γ-phase content in as-spun nylon 6 fibre on winding speed [66].
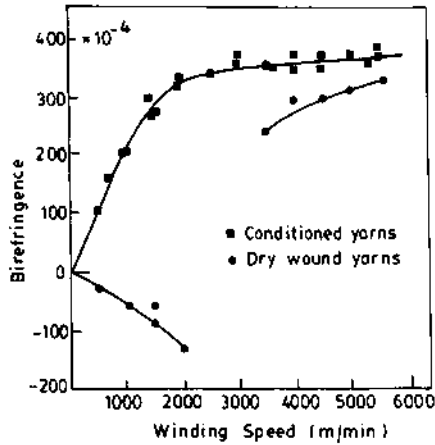
Fig. 13.16 The effect of winding speed on the birefringence of dry-wound and conditioned nylon 6 yarns [66].

winding speeds, the crystallization process is nearly complete before moisture pick-up. The large change in birefringence during conditioning of yarns wound at low speeds points to appreciable structural changes in these yarns during wetting. A detailed study [67] of deformation during the melt-spinning of fibre-grade nylon 66 and nylon 6 at take-up speeds of 4200–5500 m min^{-1} has shown that neck-like deformation occurs at speeds above 4200 m min^{-1} immediately above the solidification point (freeze line), which was found to be around 70–80 cm from the spinneret exit. The solidification was attributed by the authors to fast stress-induced crystallization, which takes place at the end of the neck. The neck-like deformation takes place over a length of 6–7 cm at a take-up speed of 5500 m min^{-1} and 10–12 cm at a take-up speed of 4500 m min^{-1}. Thus it is very different from the neck formation during cold drawing of solid filaments which occurs over much shorter distances (of the order of the filament diameter). For both polyamides, the authors observed the pure γ crystalline form at these spinning speeds.

At the same take-up speeds, nylon 6 and nylon 66 were found to have similar crystallization temperatures but different crystallization rates; nylon 66 crystallizes faster than nylon 6. However, the effect of take-up speed on orientation was found to be greater for nylon 6. The molecular processes taking place during high speed spinning have been explained by Haberkorn et al. [67] in terms of the melt behaving as a network in which entanglements play the role of temporary crosslinks. At small distances from the spinneret, the temperature is high and the disorienting thermal relaxation proceeds much faster than the tensile strain rate; thus the chains become randomly coiled. Farther down the spinline, the temperature reduces and the elastic strain contributions become important;

Take-up Velocity (km/min)
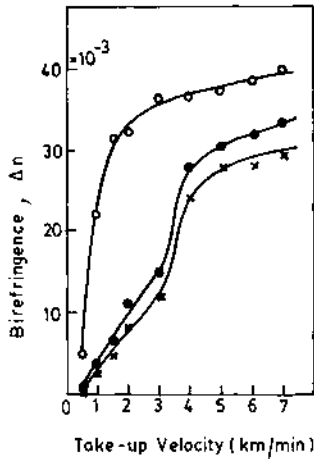
Fig. 13.17 The effect of elapsed time on the birefringence of nylon 6 fibres produced at different winding speeds: ×, birefringence immediately after spinning; ●, birefringence 3 min after spinning; and ○, birefringence after prolonged conditioning [65, 68].

consequently the chains begin to elongate causing the network to deform. The self-reinforcement of the filaments becomes significant as temperature is reduced farther along the spinline. As a consequence, the mobility of the chains is reduced rapidly to a point where the molecules can no longer respond to the applied deformational force by a disentanglement process via chain reptation. The immobilization of the entanglements gives rise to a rubber network and the formation of a neck can be described as a rubber elastic deformation which in turn promotes orientation (stress)-induced crystallization.

Shimizu et al. [65, 68] showed that there is a significant change in the birefringence of the as-spun nylon 6 fibres with the time elapsed just after winding the fibres on the bobbin (Fig. 13.17). The difference in birefringence observed for fibres spun at the same spinning speed kept for a long time and those kept for a short time seems to correspond to the change of crystallinity after spinning. The birefringence increase is maximum at a wind-up speed of $2000\,\text{m}\,\text{min}^{-1}$. The increase in birefringence can be used as a measure of the structural instability of nylon 6 fibres [65].

As a result of the unstable structure of nylon 6 and nylon 66 fibres spun at low speeds, the structure and physical properties of as-spun fibres show strong dependence on time and can have important consequences on the stability of the package. The time dependence of axial contraction of as-spun nylon 66 filaments conditioned at room temperature is shown for filaments produced at take-up velocities of
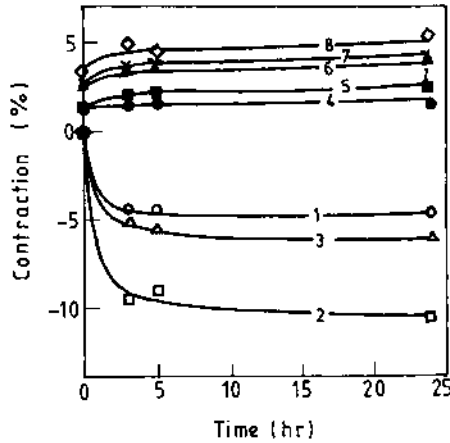
Fig. 13.18 The time dependence of axial contraction of nylon 66 filaments conditioned at room temperature [65,69]. The numbers 1 to 8 indicate the take-up velocity in km min^{-1}.

1–8 km min^{-1} [65,69] in Fig. 13.18, while the axial contraction after 24 h conditioning is shown as a function of take-up velocity in Fig. 13.19 [65,69]. Contraction was calculated from the change in fibre length using samples with initial length equal to the circumference of the take-up bobbin and kept at room temperature. Fibres spun in the range of 1000–3000 m min^{-1} exhibit spontaneous elongation with the passage of time, and those spun above 4000 m min^{-1} contract immediately after removal from the bobbin. In general, polyamide fibres elongate during the time of conditioning because of the effect of air humidity. Maximum
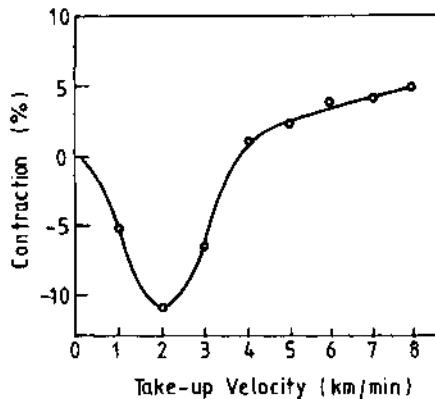
Fig. 13.19 The axial contraction after 24 h conditioning of nylon 66 yarn as a function of take-up velocity [65,69].

elongation occurs at a take-up speed of about $2000 \, \text{m min}^{-1}$ and contraction starts at $4000 \, \text{m min}^{-1}$, a result similar to that for nylon 6 [65].

It would appear from the above discussion that when producing polyamide yarns, moisture conditions are of crucial importance. The process parameters have to be balanced in such a way that the yarn package on the winder is in a suitable equilibrium between post-shrinkage and lengthening [70]. Thus from the time they leave the spinneret until they reach the winder the filaments must not only be cooled and solidified, but also treated in such a way as to facilitate stable package formation. Uneven moisture distribution in the as-spun fibre, besides creating problems in stable package formation, can also give rise to undrawn sections in the stretched fibre. It has been suggested [71] that the mean moisture content may be fixed at 4.7% at temperature of $21 \pm 1 \, °C$ and relative humidity of $62 \pm 5\%$; this is approximately the equilibrium moisture content under these conditions. All bobbins with fresh spun yarns should be conditioned for some period in the ambient medium of the draw-twisting room. The air conditioning for polyamide fibre plants needs special care and has been discussed in the literature [72, 73].

13.6.3 INTEGRATED SPIN–DRAW PROCESS

The integrated spin–draw (SD) process was briefly described in Section 4.7 in Chapter 4 and a typical unit for the production of nylon 66 tyre yarn was shown in Fig. 4.16. In this process the yarn is first spun at relatively low speeds and then drawn in two stages on heated rollers. Finally the filaments are allowed to relax before passing through an air or steam jet intermingler just before winding. The usual production speeds are around $3500 \, \text{m min}^{-1}$ but machines with a speed of $6000 \, \text{m min}^{-1}$ are also available [74].

This process eliminates draw-twisting and fully drawn yarn like the two-stage conventional yarn is manufactured in a single step. The package size in this process is 9 kg or more compared with a package size of 3 kg for the two-step conventional process due to inherent limitations in the ring-winding systems. This process is free from high stress during twisting and variation in winding tension and orientation associated with the ring-winding system. The yarn has much better dimensional stability and the properties of yarn produced using this process are claimed to be superior to those of yarn produced by the conventional process.

The SD technique may also be used for the production of bulked continuous filament (BCF) yarn. Since this process is described for polypropylene in some detail in Chapter 16, it will not be discussed here.

13.6.4 PRODUCTS MADE AT DIFFERENT SPINNING SPEEDS

In general, an appropriate combination of spinning speed and post-spinning operation dictates the end use application of nylon 6 or nylon 66 filaments. As in the case of PET, nylon 6 and nylon 66 multi-filament yarns may be produced in the form of low-oriented yarn (LOY), partially oriented yarn (POY), highly oriented yarn (HOY) and fully oriented yarn (FOY). These products, spun at different speeds, will now be briefly described.

(a) Low-oriented yarn (LOY)

LOY is spun at spinning speeds in the range of 100–1500 m min^{-1}. The continuous filament is subjected either to (1) draw-twisting for use as sports wear, fish net twine, rope, etc., or (2) draw-texturing for making socks, for example. Alternatively, the continuous filament bundle (tow) may be drawn, crimped and cut mainly for use in carpets or for blending with wool fibre. The old spinning systems also run at these slow speeds for manufacturing apparel-grade yarn in which case the as-spun yarn is subsequently given a further draw of around two times. Correct moisture content during spinning, during spin finish application and at take-up are quite critical for the spinning of nylon [75].

Textile-grade filaments are typically in the denier range of 30–120 comprising between 10 and 24 filaments. Fishnet yarns are produced in filament denier range of 210–240 comprising around 24 filaments. In the case of industrial-grade filaments, high viscosity chips (relative viscosity 3.1–3.2 as opposed to 2.5 for normal chips) are used; the number average molecular weight of the polymer ($\bar{M}_n$) is in the range 25 000–30 000 g mol^{-1}, as compared with 18 000–20 000 g mol^{-1} for textile-grade polymer. The denier of the drawn multifilament yarn is between 500 and 2000 with denier per filament being between 6 and 10. To produce high denier filaments, the mass throughput rate has to be relatively high and for uniform melting and homogeneous mixing, maximum dwell time in the extruder is favoured. An appropriate extruder screw must be used to give high production capacity, generally in the range 200–300 kg h^{-1}. A slightly higher screw diameter is used for this purpose with the length-to-diameter (L/D) ratio being 24–28. The barrel temperature is kept at ~265 °C for nylon 6 and 285–290 °C for nylon 66. The other conditions of melt-spinning of industrial grade nylon 6 and nylon 66 are similar. Production of nylon staple fibre includes spinning in the speed range of 1000–1300 m min^{-1} with tow deniers in the range of 100 000 to 200 000. Tows are subsequently drawn, heat-set and cut for baling. The shelf-life of as-spun LOY is only a few days when kept under room temperature conditions.

(b) Partially oriented yarn (POY)

As stated in Chapter 12, PET POY is generally produced at wind-up speeds of between 2800 and 3500 m min^{-1}, though the use of wind-up speeds of 4000 m min^{-1} has been reported in the literature [76,77]. For polyamide POY production, wind-up speeds of 3500–5500 m min^{-1} [76] and 4500–5000 m min^{-1} [77] have been reported. The use of relatively higher speeds in polyamide POY production was discussed in Chapter 4. The polyamide POY spun at these speeds is characterized by orientation-induced crystallization, as already discussed earlier in this chapter, and it provides higher strength and lower elongation to break compared with LOY samples. The significant crystalline content also makes the poly-amide POY thermally more stable, unlike polyester POY which has a boiling water shrinkage of 50–60% because it is predominantly amor-phous; thus the former can be used directly in plain form.

As opposed to polyester, the majority of polyamide yarn is sold as flat material. As such the polyamide market has been less influenced by POY and draw-texturing developments [78]. This has led to the belief that the benefit of the high speed spinning in the case of polyamide yarns can be much higher if fully drawn yarn is obtained at high wind-up speeds [79], say at 6000 m min^{-1} or above.

(c) Highly oriented yarn (HOY) and fully oriented yarn (FOY)

Spinning speeds above 4000 m min^{-1} greatly increase the rate of stress-induced crystallization. Useful fibres from nylon 6 and nylon 66 can be prepared directly without drawing by spinning at 6000–7000 m min^{-1} as the tenacity, elongation and shrinkage values of the fibres are acceptable for a number of applications.

The high air resistance of the filaments at very high speeds causes the filament winding tension to increase so much that often proper bobbin build-up becomes extremely difficult. Therefore, in all high speed spinning processes without godets, means have been sought to close the filament bundle as far up the conveying duct as possible and thus reduce the air friction. The integrated spin–draw process described in section 13.6.3 also leads to a fully drawn yarn (FDY).

13.6.5 SPINNING OF MASS-COLOURED NYLON 6

As described in Section 13.5, mass-coloured nylon can be produced using different methods. The two processes described here, namely dyeing chips with water-soluble dyes and dyeing using water-insoluble pigments, usually by the master batch techniques, proceed during the spinning process.

(a) Chip dyeing process for nylon 6

Raw nylon 6 chips are washed free of extractables before dyeing. The chips may be dried to about 4% moisture. The rate of diffusion of dyes in the dried chips is low; however, it gives accurate shades and matching of the shade from batch to batch. If wet, undried chips are to be used to avoid double-drying; the moisture in the chips must be considered during the calculation of percentage shade.

To maintain uniformity between different batches, a single dye should normally be used as it gives minimum tonal and shade variations on the final yarn. If two dyes are used, they may have different thermal stabilities and catalytic interactions. The mixture of dyes is likely to show shade and tonal variations on the yarn.

After washing, the chips are removed from the dyeing unit before the next batch and the unit cleaned for change of colour. Dilute alkali wash of the entire plant is helpful. The shades may be programmed from light to dark hues for minimum cleaning. The wet dyed chips can be stored for a short time before drying.

The chips are dried in a tumble dryer and conveyed to the silo above the extruder. The melt dwell time in the extruder and spinning head should be as small as possible. All the organic dyes have limited thermal stability and higher dwell time of the melt means an increase in the thermal degradation of the dye in the melt, and in turn, a drop in the depth of shade and/or change in tone. The shade is reproducible as long as time and temperature conditions are maintained on a given machine. It is necessary to have a schedule of pack change. None of the spinning positions should be stopped so that the dwell time of the melt is not increased. Furthermore, dye decomposes in the inlet pipe of the spin head and soon chokes the new pack. Thus spinning of coloured chips needs special supervision for pack filter changes.

(b) Master batch process

It is possible to use dyed chips as a master batch and mix them with undyed chips during drying. The dilution ratio could be around 1 : 5 or less. In place of white chips, chips dyed with another different colour can also be blended.

13.7 POST-SPINNING OPERATIONS

13.7.1 DRAWING

Nylons are produced as apparel- and industrial-grade filaments. The drawing conditions of these two grades are quite different and while

Table 13.3 Some typical characteristics of fully drawn nylon 6 yarns made by two different routes [80]

Route	dtex/no. of filaments	CV (%)	Yarn uniformity (Uster %)	Elongation at break (%)	Tenacity (cN dtex^{-1})	Boiling water shrinkage (%)
Conventional two-stage drawing	44/13	0.9	1.0	35	4.4	12
Non-godet high speed process	44/13	0.6	0.5	50	4.0	9

some aspects related to this have already been discussed in Chapter 8, some specific points are highlighted here. Apparel-grade as-spun nylon is conventionally drawn at drawing speeds of 400–600 m min^{-1} in a single-stage draw-twisting machine to a draw ratio of 3.2–4.0 at room temperature. In the case of as-spun industrial-grade nylon 6 produced at spinning speeds of ~100 m min^{-1}, the drawing is usually carried out in two steps. In the first stage, in which a snubbing pin is generally provided, the filaments are drawn to a draw ratio of around 3 at 30–50 °C. Alternatively, the first-stage drawing to the natural draw ratio of 2.5–3 at 100–125 °C produces superior feed material for second-stage drawing. These filaments are then subjected to a second-stage drawing in sequence with a further draw of ~1.5 at 170–190 °C. Environmental humidity is kept at around 50%.

A comparison of the conventional two-stage (spun and drawn) nylon 6 yarn with a directly spun yarn produced at a wind-up speed of 5200 m min^{-1} is made in terms of some typical characteristic parameters in Table 13.3 [80].

13.7.2 TEXTURING

To obtain yarn characteristics such as greater apparent volume and stretch, partially oriented nylon 6 yarns may be textured for some limited applications, mostly by false-twist texturing of fine yarns at speeds of 1000–1200 m min^{-1}, which are higher than the speeds used for texturing PET yarns, namely 600–700 m min^{-1} [77]. The feed yarn should have low crystallinity and high orientation for achieving optimum properties including crimp rigidity. This is met by having a high percentage of γ form in nylon 6 yarn and is obtained by spinning with take-up speeds of approximately 4200 m min^{-1}. For conventional speeds of 1000 m min^{-1}, the filaments may be drawn simultaneously or sequentially during texturing. In the texturing process filaments are heated to about 185 °C. This is followed by twisting to introduce 30–40 turns per cm, using spindle or friction devices. The yarn is then cooled and

untwisted. For higher bulk and low stretch the yarn is subjected to a second heater step or treated with steam or hot water in an autoclave. Self-crimping yarns, in which texture is developed or released by after-treatments, have also been developed.

13.7.3 HEAT-SETTING

The properties of nylon 6 yarns are especially sensitive to their thermal history and almost as sensitive to their 'hydro-history'. Thus the yarns and fabrics can be heat-set over a wide temperature range through a suitable combination of temperature and humidity. Certain construc-tions of carpets require a high degree of twist to develop aesthetic qual-ities; current industry practice divides heat-setting technologies into three basic groups [81]. In the autoclave batch process, yarn twist is set by heating in high pressure steam (as high as 30–35 psig) in an autoclave. The Superba process is a continuous version of the autoclave process in which the yarn is coiled into layers onto a conveyor of perforated stain-less steel. The belt passes into steam chambers (about 98 °C) where the tensionless yarn is first relaxed and pre-bulked at atmospheric pressure, and then heat-set in saturated steam at 5 atm. pressure and 150 °C tem-perature. In contrast to the autoclave and Superba processes, the Suessen process is a dry heat-setting process in which heat-setting temperatures up to 220 °C are used [81].

13.8 GLASS TRANSITION TEMPERATURE AND FIBRE STRUCTURE

Nylon 6 and nylon 66 exhibit polymorphism, as stated earlier. The struc-tural parameters are of importance for optimizing fibre processes as well as for predicting and assessing performances of fibre production in par-ticular applications. Since T_g plays an important role in this, it will also be briefly considered in this section.

(a) Glass transition temperature (T_g)

The T_g of nylon 6 is reported to be around 50 °C and is known to be sensitive to moisture regain in the manner shown in Fig. 13.20 [82]. The nature of interaction of water molecules with nylons is such that in the initial stages of moisture absorption in dry nylon, the water molecule forms bonds between two carbonyl groups. In the regain range of about 2–3.5%, the water molecules get attached between carbonyl and amide groups with negligible thermal effects and little change in T_g. Further addition of water is in the form of indirectly attached water molecule or loosely bound water. The moisture regain range between 2.0 and 3.5% is
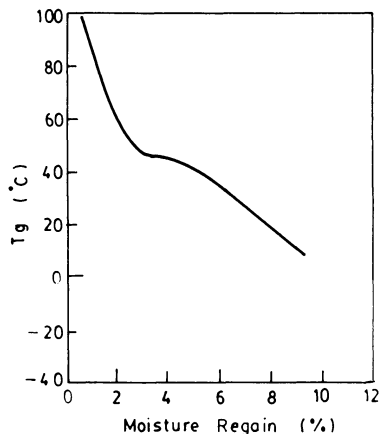
Fig. 13.20 The variation of the T_g of nylon 6 with moisture regain [82].

specially suitable during production of fibre, where a minimum change of T_g is observed. The T_g of nylon 66 shows a similar dependence on moisture content.

(b) Structure of nylon 6

Nylon 6 fibres are semicrystalline products in which the crystalline, ordered state exhibits polymorphism, while the state of the disordered regions varies considerably, depending on the processing conditions.

The crystal structure of nylon is highly dependent on the manner of hydrogen bonding between $-CO-$ and $-NH-$ moieties. The most favoured arrangement is a sheet-like structure formed by adjacent chains. The crystal is built as a result of stacking of these hydrogen-bonded sheets. In nylon 6, the hydrogen-bonded sheets of α form are characterized by antiparallel alignment of the extended chain segments. The stacking of these sheets is marked by an alternating up and down displacement of about 0.37 nm parallel to the chain direction.

Stable polymorphic modifications are possible in nylon 6 due to directionality, which in polyamides is caused by steric polarity resulting from the invariable sequence of the CONH groups [64]. As shown in Fig. 13.21, steric polarity is absent in nylon 66 but is present in nylon 6. One of these modifications is the γ form of nylon 6. This structure is formed and is stable up to around 170 °C. The adjacent chains are aligned parallel to one another. However, the chains are no longer fully extended but have a slight twist due to rotation by about 60° about the $-CH_2NHCO-$ unit.

As stated earlier, the as-spun nylon 6 fibres contain a mixture of α, γ and pseudohexagonal crystal forms. The perfection of the crystal lattice
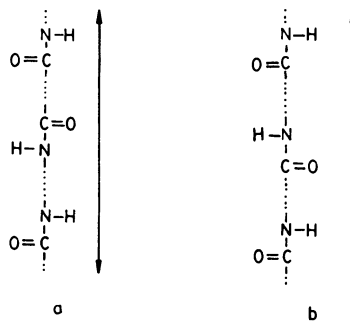
Fig. 13.21 Steric polarity in polyamides: (a) nylon 66, (b) nylon 6 [64].

and the dimensions of the unit cell are significantly affected by processing conditions during fibre formation. For example, rapid quenching of nylon 6 from the molten state results in a pseudohexagonal structure, described as a bundle-like arrangement of chain segments of both parallel and antiparallel directionality. Upon drawing at low temperatures, the ratio of the concentrations of the two forms, namely α and γ forms, changes. Increasing the draw temperature results in an increased conversion to α form; in combination with increasing draw ratio, the amount of γ form becomes negligible.

(c) Structure of nylon 66

The stable structure of both nylon 6 and 66 is the α form and as such comprises stacks of sheets of planar hydrogen-bonded extended chain segments. These sheets are characterized in nylon 66 by a parallel alignment of the adjacent extended molecules. The stacking of the hydrogen-bonded sheets entails a perpendicular sheet-to-sheet distance of 0.36 nm and a displacement of each successive sheet of about 0.5 nm in the chain direction. Due to lack of directionality of nylon 66 molecules (Fig. 13.21), any lattice disorder may correct itself readily.

The antiparallel alignment of extended chain segments within the lattice planes characterizes the α form, whereas parallel directionality within the lattice planes identifies what is generally referred to as the γ form. Both crystallographic period and chain packing of the γ form are different from those of the α form.

13.9 MECHANICAL BEHAVIOUR

Figures 13.22 and 13.23 show the effects of take-up speed on the initial Young's modulus, elongation at break, tenacity, and the yield stress of as-spun nylon 6 fibres [65]. Elongation at break decreases monotonically
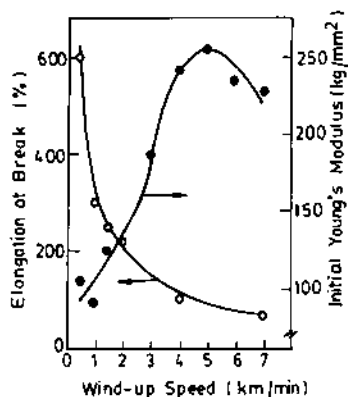
Fig. 13.22 Initial Young's modulus and elongation at break of as-spun nylon 6 filaments as a function of take-up speed [68].

to 80%. Tenacity, Young's modulus and yield stress increase with take-up speed but reach maxima at a take-up speed of about $5000\,\text{m}\,\text{min}^{-1}$. Reduction of the mechanical characteristics at speeds higher than $5000\,\text{m}\,\text{min}^{-1}$ has been attributed to radial variation of molecular orientation in the fibre cross-section [65, 68].

The stress–strain curves for as-spun nylon 66 filaments spun at various take-up speeds are shown in Fig. 13.24 [65]. A yield point is clearly observed for fibres spun at $1000\,\text{m}\,\text{min}^{-1}$, and their properties are very similar to those of typical undrawn fibres. A yield point also appears for fibre spun at $2000\,\text{m}\,\text{min}^{-1}$. Above $4000\,\text{m}\,\text{min}^{-1}$, these characteristic
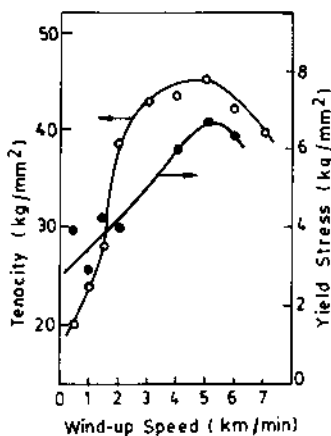
Fig. 13.23 Tenacity and yield stress of as-spun nylon 6 filaments as a function of take-up speed [68].
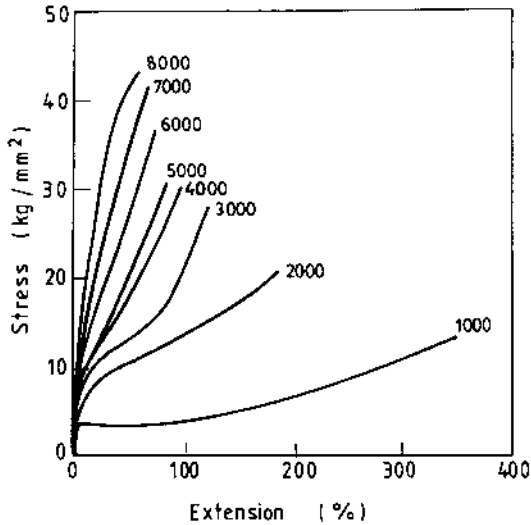
Fig. 13.24 Stress–strain curves of as-spun nylon 66 filaments spun at speeds indicated in m min^{-1} [65].

points disappear from the stress–strain curves, and the tensile properties are similar to those of drawn fibres [65].

Some typical properties of normal and high tenacity nylon 6 and nylon 66 fibres are given in Table 13.4 [64]. The initial modulus of nylon is rather low and is associated with the flexibility of the hydrocarbon section of the chain and with the possibility of breaking hydrogen bonds. The mechanical properties of these fibres may be associated

Table 13.4 Mechanical properties of nylon fibres [64]

	Nylon 6	Nylon 66
Tenacity (N tex^{-1})		
Normal	0.4–0.6	0.4–0.6
High tenacity	0.6–0.9	0.6–0.9
Breaking extension (%)		
Normal	20–40	20–30
High tenacity	15–20	15–20
Initial modulus (N tex^{-1})		
Normal	1.5–3.5	2.0–3.5
High tenacity	4.0–5.0	4.5
Work of rupture (mN tex^{-1})		
Normal	70–80	60–70
High tenacity	60–70	50–60

predominantly with their disordered regions and the manner in which these regions are organized in relation to the ordered, crystalline phases.

13.10 APPLICATIONS

Nylon 6 and nylon 66 fibres find a number of uses in both the apparel wear and industrial sectors. Light-weight and sheer garments have been produced from nylon fibres for a long time where their low modulus and high strength and abrasion resistance characteristics are of particular importance. Preset fabrics made from monofilaments of 7–15 denier are used as ladies' stockings; they show excellent shape retention due to the high elasticity of nylon filaments. It is interesting to note that nylon fibres show a low initial modulus which increases with increasing extension, a typically rubbery behaviour unlike that shown by fibres like PET. This makes nylon a unique material for stockings [83]. Setting in steam allows dimensional stability, permanent pleating and reduction of liveliness. Ironing may not be required for such fabrics. Men's socks are mostly made from nylon. Fabrics made from fine filaments are extensively used for ladies' sarees. Furs from nylon are also popular for the same reasons and are used extensively due to their long life.

In the technical and industrial fields, nylon fabrics are widely used for conveyor belts, V-belts, safety belts in cars, hoses, typewriter ribbons and light-weight canvas for luggage. They are also used for making parachutes. Nylon cords are used for reinforcement of rubber in tyres. Nylon ropes and cordage have strength and durability and resistance to water. Fishing nets are mostly made from nylon twine and, in addition to the properties listed earlier, they have high wet strength. Sail cloth made from nylon allows deformation due to wind and recovery on reduction of wind speeds, thus allowing maximum advantage from wind velocity. Thick monofilaments of nylon are used for making brushes, including toothbrushes.

The chemical resistance of nylon has been utilized in applications like filter fabrics. Nylon fabrics are used for fruit crushing and can be easily sterilized.

Bulk continuous filament nylon is used for making carpets. Nylon is amongst the best carpet fibres because of its stability, durability, and price advantage. These carpets are specifically useful where heavy traffic is present. Nylon staple is mostly used for this purpose. Nylon staple is also blended with wool to improve the durability of wool.

REFERENCES

1. Snider, O.E. and Richardson, R.J. (1969) In *Encyclopedia of Polymer Science and Technology*, Vol. 10 (eds H.F. Mark, N.G. Gaylord and N.M. Bikales), Interscience, New York, p. 348.

2. Carothers, W.H. U.S. Patent 2 130 523 (1938).
3. Caprolactam, Product Data Sheet, Allied Chemical Corpn., Morristown, New Jersey, June, 1980; Caprolactam, Standard Test Methods Bulletin, Allied Chemical Corpn., Morristown, New Jersey, June 1980; and Caprolactam, Technical Bulletin KL-42001, Bayer AG, Leverkusen, Germany, 1975.
4. Bonfield, J.H. and Northcott, J. (1969) *Encylopedia of Industrial Chemical Analysis*, Vol. 8 (ed. L.S. Ettre), Wiley-Interscience, New York, p. 114.
5. Carothers, W.H. and Berebet, J. (1930) *J. Am. Chem. Soc.*, **52**, 5289.
6. Hermans, P.H. (1955) *J. Appl. Chem.*, **5**, 493.
7. Wiloth, F. (1955) *Makromol. Chem.*, **15**, 106.
8. Reimschuessel, H.K. (1957) *J. Polym. Sci.*, **41**, 457.
9. Sbrolli, W. (1968) *Man-made Fibers: Science and Technology*, Vol. 2 (eds H.F. Mark, S.M. Atlas and E. Cernia), Wiley-Interscience, New York, p. 232.
10. Reimschuessel, H.K. (1985) *Handbook of Fiber Science and Technology – Fiber Chemistry*, Vol. IV (eds M. Lewin and E.M. Pearce), Marcel Dekker, New York, pp. 146, 147.
11. Fukumoto, O. (1956) *J. Polym. Sci.*, **22**, 263.
12. Ref. 10, p. 76.
13. Rothe, M. (1958) *J. Polym. Sci.*, **30**, 227.
14. Hermans, P.H. (1953) *Rec. Trav. Chim.*, **72**, 798.
15. Rothe, I. and Rothe, M. (1955) *Chem. Ber.*, **88**, 284.
16. Heikens, D. (1956) *Rec. Trav. Chim.*, **75**, 1199.
17. Van Velden, P.F., Van der Want, G.M., Heikens, D., Kruissink, C.A., Hermans, P.H. and Staverman, A.J. (1955) *Rec. Trav. Chim.*, **74**, 1376.
18. Ref. 9, p. 248.
19. Ref. 9, p. 240.
20. Vaidya, A.A. (1988) *Production of Synthetic Fibres*, Prentice-Hall, New Delhi, p. 57.
21. Central Board for the Prevention and Control of Water Pollution (1980) *Comprehensive Industry Document – Man-made Fibre Industry*, Central Board for the Prevention and Control of Water Pollution, New Delhi, p. 1.
22. Ref. 9, p. 243.
23. Ref. 10, p. 149.
24. Mukherjee, A.K. (1991) *Indian J. Fibre Textile Res.*, **16**, 84.
25. Ref. 20, p. 62.
26. Keinstrever, C. and Agarwal, S. (1986) *Int. J. Heat Mass Transfer*, **29**, 979.
27. Tarmy, B.L. (1988) Reactor technology, in *Encyclopedia of Polymer Science and Engineering*, Vol. 14 (eds H.F. Mark, N.M. Bikales, C.G. Overberger and G. Menges), Wiley-Interscience, New York, p. 197.
28. Allied Chem. Corp., US Patent 816 286 (1969).
29. Cannepin, A. (1938) *J. Polym. Sci.*, **8**, 35.
30. Magat, E.E. (1951) *J. Am. Chem. Soc.*, **73**, 1031.
31. Hatch, L.F. (1963) *Hydrocarbon Process Pet. Refiner*, **42**, 160.
32. Reynolds, R.J.W. (1953) In *Fibers from Synthetic Polymers* (ed. R. Hill), Elsevier, Amsterdam, p. 123.
33. Floyd, D.E. (1958) *Polyamide Resins*, Reinhold, New York, p. 32.
34. Putschur, R.E. (1982) *Encyclopedia of Chemical Technology*, 3rd edn, Vol. 18 (eds H.F. Mark, D.F Othmer, C.G. Overberger and G.T. Seaborg), Wiley-Interscience, New York, p. 353.
35. Ref. 1, p. 353.

36. Hopff, H. (1968) *Man-made Fibers: Science and Technology*, Vol. 2 (eds H.F. Mark, S.M. Atlas and E. Cernia), Interscience, New York, p. 189.
37. Ref. 36, p. 190.
38. Soverign, G.W. (Monsanto Co.), US Patent 3 218 297 (1965).
39. Li, W.H. (to Du Pont), US Patent 3 113 843 (1963).
40. Coygeshak, A.C. US Patent 3 244 485 (1966).
41. Wiloth, F. (to Veresnighe Glantstoff: Fabrican), US Patent 3 130 180 (1969).
42. Stump, W.L. (to Du Pont), US Patent 2 840 547 (1958).
43. Bhattacharya, T.K. (1978) Ph.D. thesis entitled *Studies on false twist texturisation of nylon 6*, Indian Institute of Technology, Delhi.
44. Kamerbeck, B., Kroes, G.H. and Grolle, W. (1961) *Soc. Chem. Ind. (Lond.)*, **13**, 357.
45. Achhammer, B.G., Reignhart, F.W. and Kline, G.M. (1951) *J. Appl. Chem.*, **1**, 301.
46. Levantovskaya, I.I., Korderskaya, B.M., Meoman, M.B. and Draylan, G.V. (1964) *Vysokomol. Soedin*, **6**, 569.
47. Sbrolli, W., Capaccioli, I. and Bertolli, E. (1960) *Chim. Ind.*, **42**, 1325.
48. Sbrolli, W., Capaccioli, I. and Bertolli, E. (1960) *Chim. Ind.*, **42**, 357.
49. Rochas, P. and Martin, J.C. (1959) *Bull. Inst. Textile France*, **83**, 41.
50. Steiger, P.H. (1957) *Textile Res. J.*, **27**, 459.
51. East, G.C., Lupton, C.J. and Truter, E.V. (1975) *Textile Res. J.*, **45**, 863.
52. Neiman, M.B. *Aging and Stabilization of Polymers*, Consultants Bureau, New York, 1965.
53. Petru, K. (1969) *Plast. Hmoty Kano*, **6**, 165.
54. Mikula, F. and Petru, K. (1967) *Chem. Prum.*, **17**, 132.
55. Ishimoto, M. Japanese Patent 7131, 541.
56. Munenchik, K. Japanese Patent 7131, 871.
57. Inoue, R. and Sumato, M. (1955) *Chem. High Polym. (Japan)*, **12**, 131.
58. Mukherjee, A.K. and Goel, D.K. (1978) *J. Appl. Polym. Sci.*, **22**, 361.
59. Rao, B.V. (1991) Paper presented at Seminar on Mass Dyeing, Sandoz India Ltd., New Delhi.
60. Manabe, T. (1991). Paper presented at Seminar on Mass Dyeing, Sandoz India Ltd., New Delhi.
61. Hinens, D. (1956) *J. Polym. Sci.*, **22**, 65.
62. Smoluk, G.R. (1983) *Mod. Plast.*, **61**, 43.
63. Schule, E.C. (to Allied Chemical Corpn.), US Patent 3 003 995 (10 October 1961).
64. Reimschuessel, H. (1985) In *Fiber Chemistry* (eds M. Lewin and Eli M. Pearce), Marcel Dekker Inc., New York, pp. 73–169.
65. Shimizu, J., Okui, N. and Kikutani, T. (1985) In *High Speed Fibre Spinning* (eds A. Ziabicki and H. Kawai), Wiley-Interscience, New York, pp. 429–483.
66. Heuvel, H.W. and Huisman, R. (1985) In *High Speed Fiber Spinning* (eds A. Ziabicki and H. Kawai), Wiley-Interscience, New York, pp. 295–331.
67. Haberkorn, H., Hahn, K., Breuer, H., Dorrer, H.-D. and Matthies, P. (1993) *J. Appl. Polym. Sci.*, **47**, 1551.
68. Shimizu, J., Okui, N., Kikutani, T., Ono, A. and Takaku, A. (1981) *Sen-i-Gakkaishi*, **37**, T-143.
69. Shimizu, J. (1982) *Sen-i-Gakkaishi*, **38**, 499.
70. Vaidya, A.A. (1988) *Production of Synthetic Fibres*, Prentice-Hall of India, New Delhi, p. 100.

71. Aver'Yanov, A.A., Arkhipova, L.M., Yu, B. and Meshkova, D.V. (1979) *Fil'bert, Khim. Volonka*, No. 6, November–December, pp. 6–7.
72. Nielsen, E.K. (1984) *Fiber Producer*, February, p. 42.
73. Fourne, F. (1989) *Man-Made Fiber Year Book*, Chemiefasern Textilindustrie, Frankfurt, pp. 66–71.
74. Saunders, J.H. (1988) Polyamide fibres, in *Encyclopedia of Polymer Science and Engineering* (eds H.F. Mark, N.M. Bikales, C.G. Overberger and G. Menges), Wiley-Interscience, New York, pp. 410–445.
75. Deopura, B.L. and Bhaumik, K.N. (1987) *Synthetic Fibres*, **16**, 23.
76. Specker, H. (1986) *Chemiefasern Textilindustrie*, **39/91**, 1061–1065.
77. Lückert, H., Stibal, W. and Kemp, U. (1993) *Man-Made Fiber Year Book*, Chemiefasern & Textilindustrie, Frankfurt.
78. Hughes, A.J., McIntyre, J.E., Clayton, G., Wright, P., Poynton, D.J., Atkinson, J., Morgan, P.E., Rose, L., Stevenson, P.A., Mohajer, A.A. and Ferguson, W.J. (1976) *Textile Progress*, **8**, 1–177.
79. Hoffmeister, R. and Landenberger, P. (1976) *Fiber Producer*, **4**(4), 5.
80. Taken from a paper on *New developments in polyamide high speed spinning*, presented by Dipl. Ing. J. Pantelic of Lurgi, Frankfurt, on 7 October 1983 at a Symposium on Man-Made Fibres held at IIT, New Delhi.
81. Dennis, L.A. and Buchanan, D.R. (1987) *Textile Res. J.*, **37**, 625–639.
82. Kettle, G.J. (1977) *Polymer*, **18**, 742.
83. Ward, I.M., Cansfield, D. and Carr, P. (1993) in *Polyester: 50 Years of Achievement* (eds D. Brunschweiler and J.W.S. Hearle), The Textile Institute, Manchester, UK, pp. 192–195.

Speciality polyamide and polyester yarns: an industrial approach to their production and rheology

14

T. Manabe

14.1 INTRODUCTION

The widely used conventional commodity yarns of polyamide (nylon 6 and nylon 66) and polyester (polyethylene terephthalate) are usually melt-spun from the standard polymer and the filaments have a round cross-section. The so-called 'speciality yarns' are also melt-spun either from a chemically modified polymer or through a process involving physical modification or special equipment. The wide spectrum of such yarns includes such diverse products as deep-dyeable nylons, cationic-dyeable polyesters, antistatic fibres, flame resistant fibres, hollow fibres, microporous fibres, fibres of different cross-sections and fine, ultra fine and micro fibres. The modified products offer a number of advantages and also lead to value addition to the product; this makes their production attractive. Their industrial production may involve some special considerations and these will be highlighted in this chapter.

The successful commercialization of new types of yarns requires the technological ability to produce acceptable products on the one hand, and an environment with favourable market conditions on the other.

The technological requirements include commercial availability of special new materials at reasonable cost, special equipment to produce the speciality products and process know-how to produce them. Suitable market conditions include the availability of customers who not only appreciate the products but also are willing to pay the higher prices for them. Such an environment exists in the more advanced countries although in developing countries also production units are coming out with such products for various applications. This chapter describes some recently commercialized speciality nylon and polyester yarns and includes a brief description of raw materials, manufacturing processes and applications. Some rheological principles which are of industrial relevance, particularly during the production of speciality yarns, will also be discussed.

14.2 PRODUCTION OF MODIFIED POLYMERS FOR MAKING YARNS WITH DIFFERENT DYEABILITY CHARACTERISTICS

14.2.1 MODIFIED NYLON POLYMER

(a) Introduction

When ε-caprolactam is polymerized with water as the initiator and without any acidic or amine stabilizer, the resultant nylon 6 polymer has an equal number of amino ($-NH_2$) and carboxyl ($-COOH$) end groups. For textile-grade, regular dyeing nylon 6 yarn, the quantity of amino and carboxyl end groups is about $60 \, eq \, t^{-1}$. The amino end groups in nylon 6 have a predominant effect on dye pick-up when dyed with acid dyes, as is clear from the data presented in Table 14.1.

The amino end groups are the functional sites in nylon for the adsorption of anionic dyes in acidic solution; the polymer and acid dyes are

Table 14.1 Dependence of acid dye pick-up on amino end group content in nylon 6

$-NH_2$ end group content in nylon 6 $(eq \, t^{-1})$	Dyeability with acid dyes
10–15	Light
35–45	Regular
80–90	Deep
95–100	Ultra deep
115–130	Super ultra deep

ionically coupled in the dye bath as follows:

$$H_2O \rightarrow H^+ + OH^-$$

$$\text{Nylon polymer}-NH_2 + H^+ \rightleftarrows \text{Nylon polymer}-NH_3^+$$

$$\text{Acid dye}-SO_3Na \rightleftarrows \text{Acid dye}-SO_3^- + Na^+$$

$$\text{Nylon polymer}-NH_3^+ + \text{Acid dye}-SO_3^- \rightarrow$$

$$\text{Nylon polymer}-NH_3^+O_3S^- - \text{Acid dye}$$
(dyed nylon polymer with acid dye).
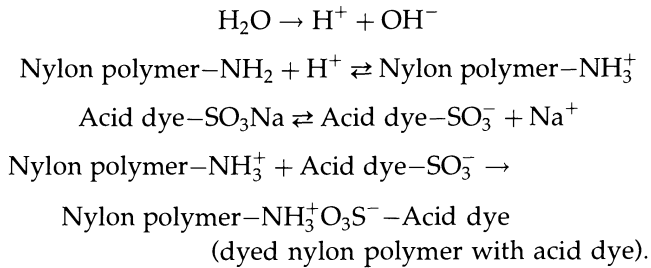
By introducing the anionic sulphonate group ($-SO_3^-$), nylon polymer becomes cationic dyeable, as is clear from the following dyeing scheme:

$$\text{Nylon polymer}-SO_3Na \rightleftarrows \text{Nylon polymer}-SO_3^- + Na^+$$

$$\text{Cationic dye}-N^+Cl^- \rightleftarrows \text{Cationic dye}-N^+ + Cl^-$$

$$\text{Nylon polymer}-SO_3^- + \text{Cationic dye}-N^+ \rightarrow$$

$$\text{Nylon polymer}-SO_3^-N^+ - \text{Cationic dye}$$
(dyed nylon polymer with cationic dye).
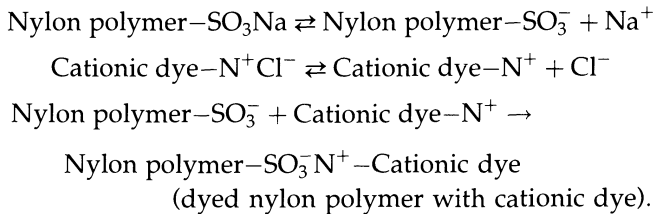
The sulphonate group content of nylon yarns with the cationic dyes should be in the range of 40–70 eq t^{-1}; the higher the sulphonate group content, the deeper the shade.

(b) Production of modified nylon for making light-shade dyeable yarns when dyed with acid dyes

As shown in Table 14.1, in order to produce light-shade dyeable nylon yarns using acid dyes, the amino end group content should be reduced to the level of 10–15 eq t^{-1} from the 62 eq t^{-1} present in textile-grade nylon 6 yarns without a carboxylic acid stabilizer.

The reduction of an amino end group is achieved by adding an appropriate stabilizer. The amino end group of nylon polymer reacts with the carboxyl group ($-COOH$) of the stabilizer as follows:

$$\text{Nylon polymer}-NH_2 + \text{Stabilizer}-COOH \rightarrow$$

$$\text{Nylon polymer}-NHCO-\text{Stabilizer} + H_2O.$$
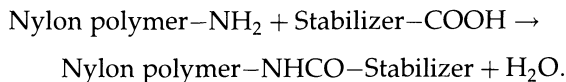
The rate of polymerization is slow and the resultant degree of polymerization is normally low for nylon 6 polymer dyeable to a light shade with acid dyes. This is because the additives required for dyeability alteration are bound to reduce the number of amino or carboxyl end groups, which are themselves essential for the amide-forming nylon 6 polycondensation.

In order to minimize the effect of acidic additive with carboxyl group on polymerization rate in the light-shade dyeable nylon polymer, a dicarboxyl acid such as sebacic acid is normally used instead of a mono-carboxylic acid such as acetic acid. The reaction between nylon polymer and dicarboxylic stabilizer is as follows:

HOOC−Nylon polymer−NH$_2$ + HOOC−Stabilizer−COOH →

HOOC−Nylon polymer−NHCO−Stabilizer−COOH + H$_2$O.
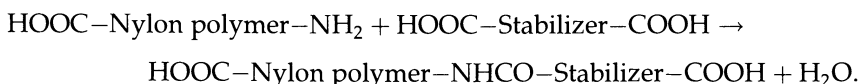
In other words, the amino end group is converted into the carboxyl end group. Thus the use of dicarboxylic acid stabilizer not only decreases the number of reactive amino end groups, but also increases the number of carboxyl end groups. The following steps are involved in the production of light shade dyeable nylon 6 polymer when dyed with an acid dye.

Step 1

The first step involves selection of polymer of the right molecular weight and with an appropriate number of amino end groups.

The number average molecular weight, $\bar{M}_n$, of nylon 6 is related to the number average degree of polymerization, (DP)$_n$, as follows:

$$\bar{M}_n = 113.16(DP)_n \tag{14.1}$$

where 113.16 is the molecular weight of caprolactam.

In industry, the relative viscosity (RV) of the polymer is generally taken as a measure of its molecular weight; the following empirical relationship (T. Manabe and R. Kumar, unpublished) is generally used:

$$(DP)_n = 95.70(RV - 1). \tag{14.2}$$

If the relative viscosity of nylon 6 solution (1 g/100 ml) in 96 wt % sulphuric acid at 25 °C is 2.48, then from equation (14.1) (DP)$_n$ comes out to be equal to 141.636 and this gives $\bar{M}_n = 16027.53$, which is the selected molecular weight of nylon 6 polymer. The −NH$_2$ content for light shade acid dyeable nylon 6, as stated earlier, may be taken as 15 eq t^{-1}.

Step 2

The second step involves taking a decision regarding the additive for polymerization, in particular its chemical nature and concentration. As already stated, it is advisable to use sebacic acid, HOOC(CH$_2$)$_8$COOH with a molecular weight of 202.25 g mol^{-1} as the stabilizer. To estimate the concentration of the additive for polymerization, it may be recalled that one sebacic acid molecule converts one amino end group of the

polymer into one carboxyl group as per the following scheme:

(Polymer without additive)

HOOC —————— NH$_2$
HOOC ——⋮—— NH$_2$ +   HOOC —————— COOH   (Sebacic acid)

↓

HOOC —————— COOH
HOOC ——⋮—— NH$_2$
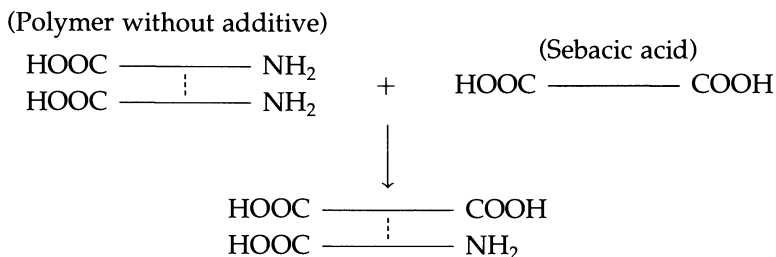
Now the total number of −NH$_2$ end groups in the unstabilized polymer is 62.39 eq t^{-1}. As a result of the reaction of amino end group with sebacic acid, 47.39 eq t^{-1} of carboxyl end groups are formed. This leaves 15.00 eq t^{-1} of unreacted amino end groups.

If the equilibrium polymer concentration at the end of polymerization is 90 wt %, the sebacic acid concentration may now be calculated as follows. The number of sebacic acid-converted polymer molecules in equivalent per ton of polymer is $10^6/(113.16 \times 141.636) - 15 = 62.39 - 15 = 47.39$. The sebacic acid concentration is thus $47.39 \times 202.25 \times 10^{-6} \times 100 \times 0.90$, i.e. 0.8626 wt % of caprolactam.

Step 3

The third step involves the selection of the polymerization conditions, in particular the polymerization end temperature and the free water content, so that the required molecular weight is obtained. Based on experience and literature, the polymerization end temperature is selected to be 260 °C (533 K).

As in the case of chemical reactions of small molecules, condensation polymerization also has an equilibrium, particularly at higher conversions. The equilibrium constant, K, is given by

$$K = \frac{[-\text{NHCO}-][\text{H}_2\text{O}]}{[-\text{NH}_2][-\text{COOH}]} \tag{14.3}$$

where [−NHCO−], [H$_2$O], [−NH$_2$] and [−COOH] are the measured concentrations of the species in the reaction mass at equilibrium.

From previous data, the known concentrations are:

$$[-\text{NHCO}-] = (10^6/113.16) \times 0.90 = 7953.34 \, \text{eq t}^{-1}$$

$$[-\text{NH}_2] = 15.0 \times 0.90 = 13.50 \, \text{eq t}^{-1} \text{ and}$$

$$[-\text{COOH}] = \left[\left(\frac{10^6}{113.16 \times 141.636} \times 2\right) - 15.0\right] \times 0.90 = 98.81 \, \text{eq t}^{-1}.$$

The temperature dependence of the equilibrium constant, K, may be represented as

$$K = \exp\left[(\Delta S - \Delta H/T)/R\right] \qquad (14.4)$$

where the temperature is in Kelvin.

Tai, Arai and Tagawa [1,2] reported that

$$\Delta S = 0.9437 \, \text{cal mol}^{-1} \, \text{K}^{-1}$$

$$\Delta H = -5946 \, \text{cal mol}^{-1}.$$

Taking $R = 1.987 \, \text{cal mol}^{-1} \, \text{K}^{-1}$, K can now be calculated using equation (14.4). At 260 °C, K comes out to be 441.1.

Finally, the free water content, $[H_2O]$, can be estimated from equation (14.3) and comes out to be $73.98 \, \text{eq} \, \text{t}^{-1}$ or $0.1333 \, \text{wt} \, \%$ based on charged caprolactam. If the free water content is higher than this, the amino end group content will become greater than $15 \, \text{eq} \, \text{t}^{-1}$ and the relative viscosity will become lower than 2.48.

Step 4

The fourth step involves establishing the polymerization conditions to achieve the desired free water content. For continuous polymerization in a VK tube of the closed type, the free water content would be the difference between the amount of water charged into caprolactam (in $\text{eq} \, \text{t}^{-1}$) at the beginning of polymerization, $[H_2O]_0$, and the amount of water used during polymerization, remembering that the reaction between an amino end group and a carboxylic stabilizer produces one water molecule. This consideration leads to the following relationship:

$$[H_2O]_0 = [H_2O] + [-NH_2] \qquad (14.5)$$

where $[H_2O]$ represents the equilibrium free water content. Thus $[H_2O]_0 = 73.98 + 13.50 = 87.48 \, \text{eq} \, \text{t}^{-1}$ or, in wt %,

$$(87.48 \times 18.02 \times 10^{-6} \times 10^2) = 0.1576.$$

Thus a very small amount of water is required at the beginning of polymerization in the closed VK tube reactor compared with the open VK tube and batch polymerization.

In the case of continuous polymerization using a VK tube of the open type, 90–96% of the water goes out of the tube before or after reacting with caprolactam. The free water content at the end of polymerization is consequently dependent on several factors including the amount of water charged, the temperature profile of the VK tube along its length and the polymerization rate.

In batch polymerization, it is possible to control the free water content in polymer–oligomer–monomer mixture liquid phase by controlling the

gas phase pressure, which therefore needs to be estimated. Tai, Arai and Tagawa [2] have suggested the following relationship to determine X_W, the mole fraction of free water in the liquid phase, vs. P_W, the partial pressure of water in the vapour phase:

$$\log_{10}(X_W/P_W) = (3570/T) - 11.41 \tag{14.6}$$

and

$$\log_{10} P_L = -(4100/T) + 9.6 \tag{14.7}$$

where P_W and P_L are respectively the vapour pressures (in mm Hg) of water and caprolactam in the gas phase in the polymerization reactor, and T is the absolute temperature in Kelvin.

The gas phase pressure in the polymerization reactor, P_T, resulting from the water (P_W) and the caprolactam (P_L), is given by

$$P_T = P_W + P_L. \tag{14.8}$$

The mole fraction of free water in the liquid phase, X_W, is estimated from the following relationship:

$$X_W = \frac{[H_2O]}{[-NHCO-] + [CL] + [H_2O]} \tag{14.9}$$

where [CL] is the concentration of the monomer and oligomers based on the caprolactam unit. The value of X_W comes out to be 0.008302.

Using equation (14.6), P_W is then estimated to be 427.8 mm Hg. From equation (14.7), P_L is estimated to be 80.8 mm Hg. Finally, from equation (14.8), P_T comes out to be 508.6 mm Hg, which means that vacuum has to be applied in the polymerization reactor at the closing stages. Alternatively, the gas phase of the reactor should be swept with dry nitrogen gas to reduce the free water content in the liquid phase.

(c) Production of nylon for making ultra-deep dyeable yarns when dyed with acid dyes

An increase in amino end group content, as shown in Table 14.1, results in nylon yarns which can be dyed to deep shades with acid dyes. This is generally achieved by replacing the carboxyl end groups of nylon polymer with amino groups present in a diamine stabilizer as per the following scheme:

H_2N-Nylon polymer$-COOH + H_2N-$Stabilizer$-NH_2 \rightarrow$

$\qquad\qquad H_2N-$Nylon polymer$-CONH-$Stabilizer$-NH_2 + H_2O$.
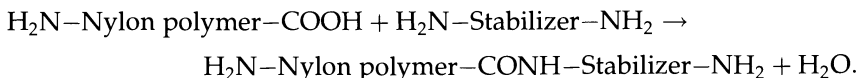
Characteristics of deep dyeable polymer

The industrial practice for the production of ultra- or super ultra-deep dyeable textile-grade nylon 6 yarn is to use polymer of relative viscosity

(RV) 2.480 with a number average degree of polymerization $(DP)_n$ of 141.636, $-NH_2$ end group content of $110 \, eq \, t^{-1}$ and $-COOH$ content of $14.79 \, eq \, t^{-1}$.

Polymerization conditions

The stabilizer used is generally hexamethylene diamine (HMDA), $H_2N-(CH_2)_6-NH_2$, of molecular weight $116.21 \, g \, mol^{-1}$; $0.4979 \, wt \, \%$ of it is charged in molten caprolactam and the polymerization completes at a temperature of $260 \, °C$ (533 K).

The equilibrium constant K, free water content $[H_2O]$, initial water added in the closed polymerization reactor $[H_2O]_0$, mole fraction X_W of free water in the polymer, and the pressures P_W, P_L and P_T are estimated from the equations given earlier and come out to be, respectively,

$$K = 441.1$$

$$[H_2O] = 73.06 \, eq \, t^{-1}$$

$$[H_2O]_0 = 0.1556 \, wt \, \%$$

$$X_W = 0.0082$$

$$P_W = 422.5 \, mm \, Hg$$

$$P_L = 80.8 \, mm \, Hg$$

$$P_T = 503.3 \, mm \, Hg.$$

Sometimes instead of using diamine as the stabilizer, a linear polyamine such as diethylene triamine, $H_2N \, CH_2-CH_2-NH_2-CH_2-CH_2-NH_2$, is used as the amine stabilizer. Theoretically one diethylene triamine molecule converts one carboxyl end group of nylon polymer into one primary amino end group ($-NH_2$) and one secondary amine group ($-NH-$). Although this stabilizer results in an extra secondary amine group in comparison with the diamine described earlier, the secondary amine group is not as effective for acid dye dyeability as the primary amino end group.

(d) Production of anionically modified nylon yarns for dyeing with cationic dyes

To produce cationic-dyeable fibres, the nylon polymer is modified by introducing anionic sulphonate ($-SO_3^-$) groups in the nylon molecules. This can be achieved by using a stabilizer during polymerization which has one or two carboxyl groups (which can react with the amino end groups of nylon polymer) and one or two sulphonate groups (which make the polymer anionic). An example of such a stabilizer is disodium

3,5-disulphobenzoic acid $(NaO_3S)_2C_6H_3-COOH$, i.e. Na_2DSBA; it converts one amino end group into two sulphonate groups as follows:

$$HOOC-Nylon\ polymer-NH_2 + HOOC-C_6H_3(SO_3Na)_2 \rightarrow$$

$$HOOC-Nylon\ polymer-NHCO-C_6H_3(SO_3Na)_2 + H_2O.$$
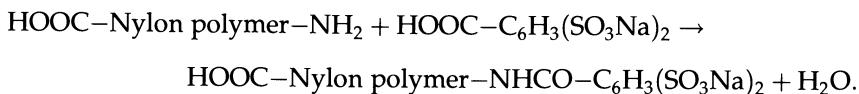
Other alkali metal salts, e.g. lithium salt, can also be used. In addition, 5-sodium sulphoisophthalic acid is also used for introducing sulphonate groups in the polymer chains of nylon 6, rather than at the polymer chain ends with Na_2DSBA.

The desired characteristics of cationic-dyeable nylon 6 polymer and the appropriate conditions of polymerization when using Na_2DSBA as the stabilizer are as follows.

Polymer characteristics

Assuming that there is no effect of the sulphonate groups on solution viscosity, a polymer with a relative viscosity (RV) of 2.480 is used, as in the earlier two cases; the number average degree of polymerization $(DP)_n$ of the polymer is thus 141.636. The functional groups in the polymer are $-SO_3Na$ (72.60 eq t^{-1}), $-COOH$ (62.39 eq t^{-1}) and $-NH_2$ (26.09 eq t^{-1}).

Polymerization conditions

The polymerization conditions can be established using the empirical equations given earlier and are briefly considered below.

Disodium 3,5-disulphobenzoic acid (Na_2DSBA), which has a molecular weight of 326.20 g mol^{-1}, may be used as the stabilizer to the extent of 1.0657 wt %.

The equilibrium constant K at the reaction temperature of 260 °C (533 K) comes out to be 441.1, assuming that there is no effect of the sulphonate group on K. The free water content $[H_2O]$ comes out to be 73.13 eq t^{-1}, while the initial water content which is charged into the closed polymerization reactor, $[H_2O]_0$, should be 0.1741 wt %.

The other polymerization parameters for this case come out to be $X_W = 0.008208$ and P_W, P_L and $P_T = 423.0$, 80.8 and 503.8 mm Hg, respectively.

(e) Comparison of the polymer and polymerization conditions for different types of dyeable nylon

Table 14.2 summarizes the principal polymer characteristics and polymerization conditions for producing nylon 6 polyamide which can be

Table 14.2 Polymerization parameters for producing light-, ultra deep-, and cationic-dyeable nylon 6 polymer of relative viscosity 2.480

Parameter	Type of polymer		
	Light-dyeable	Ultra deep-dyeable	Cationic-dyeable
$-NH_2$ (eg t^{-1})	15.0	110.0	26.1
$-COOH$ (eg t^{-1})	109.8	14.8	62.4
$-SO_3Na$ (eg t^{-1})	0	0	72.6
Stabilizer type	Sebacic acid	HMDA	Na_2DSBA
Stabilizer quantity (wt %)	0.863	0.498	1.066
Temperature (°C)	260	260	260
(H_2O) (wt %)	0.133	0.132	0.132
$(H_2O)_0$ (wt %)	0.158	0.156	0.174
P_L (mm Hg)	81	81	81
P_W (mm Hg)	428	422	423
P_T (mm Hg)	509	503	504

used for making light shade, ultra-deep and cationic-dyeable nylon 6 yarns, respectively. These calculations show that except for the type and amount of stabilizer, light, ultra-deep and cationic dyeable nylon polymers can be produced under very similar polymerization temperature and total vapour pressure.

(f) Differentially dyeable nylons

Differential dyeing, using the modified nylons described in the previous sections, is possible using the following routes.

Combination of yarns made from nylons with different amino end group contents

As an illustration, a fabric which consists of normal dyeable (amino end groups 40 eq t^{-1}) and super ultra-deep dyeable (amino end groups 130 eq t^{-1}) yarns may be subjected to the following treatments.

1. Dyeing in a dye bath used for normal nylon yarn fabric dyeing. The dye picked up by the two sets of yarn will be different and the light and deep shaded yarns will form a differently dyed fabric.
2. Dyeing under slow dyeing conditions, e.g. high dye bath pH of 8–10, use of certain levelling agents or low dyestuff concentration in the dye bath. The yarns which have fewer amino end groups will not be dyed at all and only the high amino end group yarn will be dyed with the acid dye used. Thus a differentially dyed fabric with two colours will be obtained in a sequential acid dye dyeing.

3. Dyeing using a combination of an acid dye (say yellow) and a disperse dye (say blue). The acid dye will make only the deep acid-dyeable yarn yellow while the disperse dye will render both the yarns blue. The resultant colour of the light acid-dyeable yarn will be blue while the deep acid-dyeable yarn will be rendered green, thus resulting in a fabric with two colours.

Combination of acid-dyeable and cationic-dyeable yarns

Two-colour differential dyeing can be achieved with a mixture of selected acid and cationic dyes in the same dye bath to dye a fabric containing yarn dyeable with deep acid dyes as well as cationic-dyeable nylon yarn. Alternatively, for the same fabric, a mixture of cationic and disperse dyes may be used.

14.2.2 MODIFIED POLYESTER POLYMER

Polyester polymer lacks any ionic groups such as sulphonate group ($-SO_3^-$) or amine group ($-NH_2 + H^+ \rightarrow -NH_3^+$), and therefore it cannot be dyed with ionic dyes such as cationic dyes or acid dyes. This has led to the widespread use of disperse dyes for the dyeing of normal polyester yarn and fabric. Alternatively, ionic groups may be introduced into the polymer chain of the normal polyester, when it becomes dyeable by cationic dye or acid dye as per the following schemes.

Scheme I Cationic dye – dyeable by introducing an anionic group ($-SO_3^-$).

$$\text{Polyester polymer} - SO_3Na \rightleftarrows \text{Polyester polymer} - SO_3^- + Na^+$$

$$\text{Cationic dye} - N^+Cl^- \rightleftarrows \text{Cationic dye} - N^+ + Cl^-$$

$$\text{Polyester polymer} - SO_3^- + \text{Cationic dye} - N^+ \rightarrow$$

$$\text{Polyester polymer} - SO_3^- - N^+ - \text{Cationic dye}$$
$$\text{(Polyester polymer dyed by cationic dye).}$$
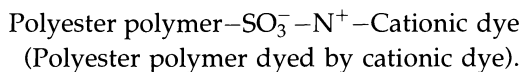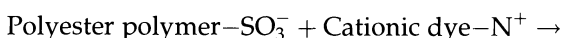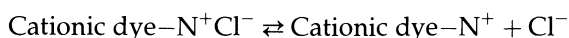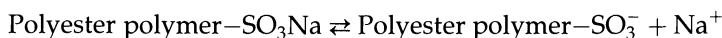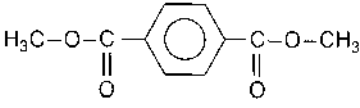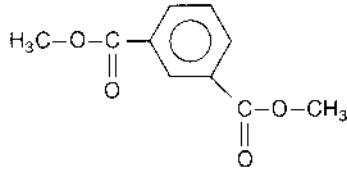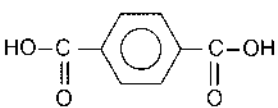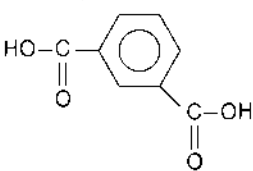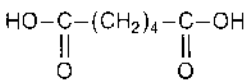
Scheme II   Acid dye – dyeable by introducing cationic group.
In this case an amine substituted diol may be used and the reaction scheme is similar to scheme I.

(a) Production of modified polyester for making deep dyeable yarns when dyed with disperse dyes

Normal polyester yarn, or more specifically poly(ethylene terephthalate) (PET) yarn, has a rigid backbone; this, combined with significant

Table 14.3 Suitable copolymer components for producing PET copolymers

Raw material used for normal polyester	Corresponding copolymer component

DMT

H_3C-O-C ⬡ $C-O-CH_3$
‖ ‖
O O

Dimethyl isophthalate

H_3C-O-C ⬡
‖
O
$C-O-CH_3$
‖
O

TPA

$HO-C$ ⬡ $C-OH$
‖ ‖
O O

Isophthalic acid

$HO-C$ ⬡
‖
O
$C-OH$
‖
O

Adipic acid
$HO-C-(CH_2)_4-C-OH$
‖ ‖
O O

Ethylene glycol
$HOCH_2CH_2OH$

Diethylene glycol
$HOCH_2CH_2OCH_2CH_2OH$

Butylene glycol
$HOCH_2CH_2CH_2CH_2OH$

crystallinity, makes it difficult to dye. One way of reducing crystallinity is to copolymerize the polymer using appropriate comonomer components which behave like DMT or ethylene glycol in the ester interchange reaction, or TPA or ethylene glycol in the esterification reaction. Some of these are shown in Table 14.3. Fibres made from these copolymers dye relatively more easily mainly because of their lower crystallinity.

(b) Production of modified polyester for making yarns which are dyeable with cationic dyes

The general approach used for producing cationic-dyeable PET polymer is to use a third component containing an anionic sulphonate group ($-SO_3$) during polymerization. For the DMT process, 5-sodium

sulphodimethyl isophthalate (NaSDMIP)

$$H_3COOC \diagdown \bigotimes \diagup COOCH_3$$

$$SO_3Na$$
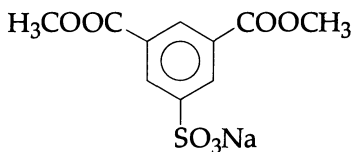
of molecular weight 296.23 is the usual choice. This is available commercially at a reasonable cost.

For the TPA process 5-sodium sulphodihydroxyethyl isophthalate

$$HOCH_2CH_2OOC \diagdown \bigotimes \diagup COOCH_2CH_2OH$$

$$SO_3Na$$
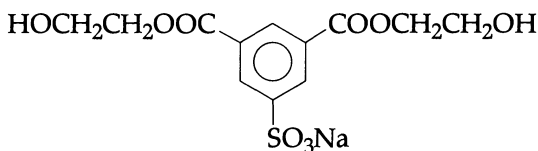
of molecular weight 356.28 is generally used, although NaSDMIP can also be used.

The TPA process presents greater difficulties compared with the DMT process for the following reasons.

1. The added anionic compounds may themselves tend to form anionic homopolymers; to prevent their formation, a small quantity of 5-sodium sulphohydroxyethyl, methyl isophthalate

$$[HOCH_2CH_2OCOC_6H_3(SO_3Na)COOCH_3]$$
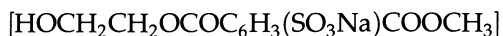
   is added at the beginning of the polycondensation reaction to slow down such homopolymer formation.
2. Due to the acidity of TPA, diethylene glycol formation in the cationic dyeable PET is excessive.
3. Due to the acidity of TPA, TiO_2 agglomerates may form to a significant extent.

The use of NaSDMIP in the DMT process is quite simple and straightforward. However, due to the acidic nature of the sulphonate additive, diethylene glycol and carboxylic end group formation are promoted. To reduce this, about 7 mol% of sodium acetate is added to the charge of NaSDMIP [3]. The sulphonate additive is added to the extent of 1.50 mol% with respect to DMT or TPA to the ester interchange or esterification reactor. This means that the sulphonate content in the polymer is

$$\frac{10^6}{192.17} \times \frac{1.5}{100} = 78 \, eq \, t^{-1}$$

which corresponds to the deep dyeing category in nylon 6 (Table 14.1). The sequence of charging of raw materials and additives is as follows:

ethylene glycol (EG) charge, DMT charge, EG solution of sodium acetate charge, EG solution of NaSDMIP charge, EG solution of ester interchange catalyst charge.

(c) Production of modified polyester for making yarns which are dyeable with acid dyes

Partly due to the non-availability of cationic modifiers on a commercial scale, polyester that has been cationically modified so that it can be dyed using acid dyes has not been produced on a commercial scale as yet; examples of such polyester yarns using amine-substituted diols

$$HO-CH_2-CH_2-O-C \underset{\underset{\underset{\underset{N(CH_3)_2}{|}}{C}}{\overset{\overset{N}{\diagup}}{\underset{N}{\diagdown}}} C-O-CH_2-CH_2-OH$$

and

$$HO-CH_2-\underset{\underset{CH_3}{|}}{\overset{\overset{N(CH_3)_2}{|}}{\underset{CH_2}{\overset{|}{C}}}}-CH_2-OH$$
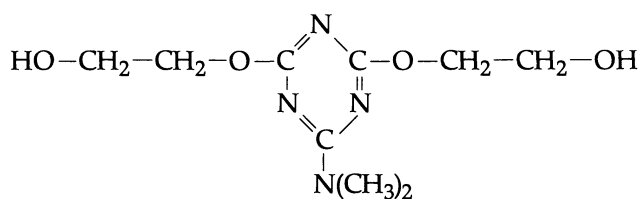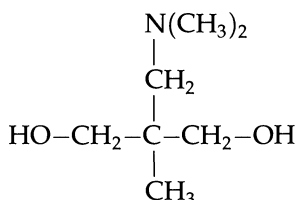
appear in references [4] and [5], respectively.

(d) Differential dyeing of polyester yarns with cationic dyes and disperse dye

When a fabric made from normal polyester and cationic-dyeable polyester is dyed with a cationic dye, it will be expected that only the cationic-dyeable polyester will be dyed while the normal polyester will not pick up any dye. In practice, however, the carboxyl end groups, which are present to the extent of $30\text{--}40\,\mathrm{eq}\,\mathrm{t}^{-1}$ in the normal PET yarn, will attract the cationic dyes in the dye bath.

If the dye bath contains both cationic dye and disperse dye, the normal polyester yarn in the polyester fabric is dyed only with the disperse dye, while the cationic-dyeable yarn in the fabric is dyed both with the disperse dye and the cationic dye. In this case, therefore, the cationic-dyeable yarn in the fabric gets two colours.

14.3 ANTISTATIC NYLON AND POLYESTER YARNS

In general, synthetic fibres are poor conductors of electricity and create problems related to electrostatic charge development. The general principles governing the electrical behaviour of fibres will be discussed in Chapter 18; in this chapter the approaches used to make nylon and polyester fibres antistatic will be briefly considered.

14.3.1 ANTISTATIC NYLON YARNS

The following three procedures are generally adopted to confer antistatic properties to nylon yarns.

1. Chemical modification of nylon polymers to make them more hydrophilic is achieved by introducing polyether or polyacrylamide units during polymerization; the chemical bonding ensures wash fastness. The resulting yarns absorb more moisture which makes them antistatic.
2. Physical blending of nylon polymer using hydrophilic polymers such as polyether is carried out during the melt-spinning of nylon 6 polymer; the physical blending is not done during polymerization as the additive is likely to be extracted during subsequent processing and drying. The wash fastness of the fibre made from blended polymer is not very good.
3. Electrical conducting materials such as carbon, metal or metal oxide powders are added to the melt during melt-spinning.

The above three processes and their application to nylon 6 polymer will now be briefly discussed.

(a) Chemical modification of nylon 6 polymer during polymerization

The two hydrophilic polymers which are used for chemical modification of nylon 6 polymer are poly(ethylene glycol) and poly(acrylamide).

Chemical modification with poly(ethylene glycol)

In order to make poly(ethylene glycol) react with nylon 6 polymer, the additive selected must have amino or carboxyl end groups so that they can attach themselves to the end groups of nylon 6 and form a block copolymer. Such a polymeric additive is polyethylene glycol diamino propyl ether,

$$H_2N-CH_2CH_2CH_2-O-(-CH_2CH_2-O-)_n-CH_2CH_2CH_2-NH_2.$$

For $n = 22.3$, the molecular weight is $1114\,\text{g}\,\text{mol}^{-1}$. Sanyo Chemical Industries, Japan, manufacture and market such an additive under the

trade name Ionet YB-100^{TM}, 2 wt % of which is sufficient to confer antistatic properties to nylon 6.

The ethylene glycol diamine acts as a normal diamine stabilizer in polyamide formation. For 2 wt % of Ionet YB-100, the stabilized carboxyl end groups will be $(10^6 \times 0.02)/1114 = 17.95\,eq\,t^{-1}$, which is much smaller than the initial end group content of $62.40\,eq\,t^{-1}$ (as shown earlier); its effect on polymerization will therefore not be unduly large. However, if 8 wt % of Ionet YB-100 is added into the nylon 6 polymer, the additive can stabilize up to $71.81\,eq\,t^{-1}$ of carboxyl groups, which is greater than the number of groups actually present in the polymer of relative viscosity 2.48; as a consequence the polymer viscosity will be considerably lower than 2.48. To overcome this problem, a part of the amino end groups of poly(ethylene diamino propyl ether) must be converted into carboxyl groups. Reaction with a dicarboxylic acid like sebacic acid (molecular weight $202.25\,g\,mol^{-1}$) achieves this.

The amount of Ionet YB-100 to be charged into the reactor during polymerization of caprolactam can be estimated and comes out to be 3.57 wt % based on the caprolactam charged under the usual polymerization conditions. The resulting polymer of relative viscosity 2.48 will, in addition to being antistatic, also be deep acid-dye dyeable with $98.0\,eq\,t^{-1}$ amino end group and $26.8\,eq\,t^{-1}$ carboxyl end group.

Chemical modification with poly(acrylamide)

The amide unit, (−NHCO−), in a polymer attracts moisture, as is evident from the data for the three nylon polymers [6] presented in Table 14.4.

The amide content in poly(dimethyl acrylamide) (PDMAA)

$$\sim\!\!CH_2\underset{\underset{O=CN(CH_3)_2}{|}}{CH}\!\!\sim$$
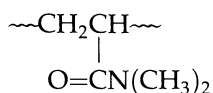
is $10\,101\,eq\,t^{-1}$ and the grafting of PDMMA onto nylon 6 will enhance the moisture absorption of the latter. PDMAA of molecular weight

Table 14.4 Dependence of equilibrium moisture content on amide unit content for three nylons

Parameter	Type of nylon polymer		
	Nylon 4	Nylon 6	Nylon 12
−NHCO unit content ($eq\,t^{-1}$)	11 765	8850	5076
Equilibrium moisture content at 65% RH (wt %)	9.1	4.3	1.3

50 000–100 000, produced by Alcolac Inc., Baltimore, USA, for example, may be added, say to the extent of 10% by weight, to the caprolactam during polymerization, when a copolymer of nylon 6 and poly(dimethyl acrylamide) is produced by the following amine–amide interchange reaction [6]:

$$PDMAA-CH_2-CH\sim + H_2N-Nylon\ 6-COOH \rightarrow$$
$$|$$
$$O=C-N(CH_3)_2$$
$$PDMAA-CH_2-CH- + HN(CH_3)_2$$
$$|$$
$$O=C-NH-Nylon\ 6-COOH.$$
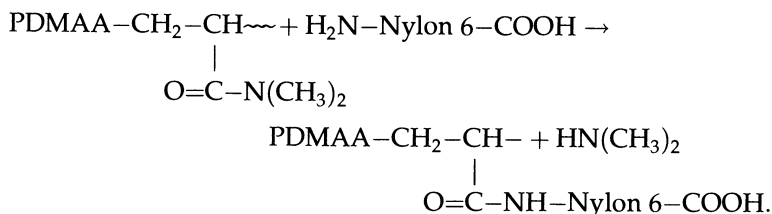
(b) Physical blending of polyethers with nylon 6 during spinning

Polyethers like polyalkylene glycol or polyalkylene oxide of molecular weight 5000 to 30 000, when blended with nylon 6, enhance their moisture uptake and thus confer antistatic characteristics to the fibre. However, since these are waxy and sticky materials, they are melted and charged into nylon polymer melt coming out of the extruder with the help of a metering pump and then mixed thoroughly in a static mixer before entering the metering pump in the spinning block. Due to their high molecular weight, these additives tend to remain within the filament during washing. However, in the absence of chemical bonding, they eventually come out after repeated washings. A number of products are commercially available.

(c) Adding electrical conducting materials to nylon 6

The conducting materials, which are generally used in the powder form, are: carbon black; silver, copper, nickel and other metal and alloy powders; and zinc oxide, titanium dioxide and other metal oxide powders.

In order to make the fibres antistatic, the electro-conductive particles in the polymer matrix must be close enough. For this, 10–30 wt % of the additive is generally required, depending on the type of additive and its particle size and size distribution. If the polymer and the conducting particles are dry-mixed and then melt-spun, the tenacity of the resulting filament is very low. For this reason, the conjugated bicomponent filament spinning technology is used to produce such filaments in order to increase the tenacity. Since the appearance of the conductive powder containing polymer is generally very different from that of the base polymer, the conductive element is often buried partially or totally inside the filament (Fig. 14.1).
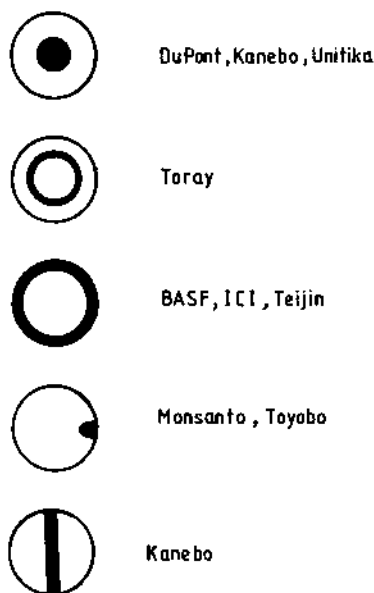
Fig. 14.1 Melt-spun conjugated bicomponent filaments (the electro-conductive element appears as the dark portion) [7].

The following steps are involved in the production of electro-conductive nylon 6 filaments [7].

First, fully dull melt of base polymer (nylon 6) with 5 wt % of titanium dioxide and melt viscosity of 600 poise at 280 °C is prepared. The second step involves the preparation of 30 wt % carbon black powder containing nylon 6 polymer of melt viscosity 1000 poise at 290 °C. Third, conjugated filaments are spun from the above base polymer and electro-conductive polymer using the arrangement shown in Fig. 14.2. The electrical resistance characteristics of the filaments are shown in Fig. 14.3 as a function of the weight percentage of conducting material used during step two described above. The fourth step involves the hot drawing of conjugated filament yarns at 180 °C; the high temperature of drawing ensures that minimum voids form around the electro-conductive particles.

The resultant conjugated filament yarn of light grey colour has an electrical resistivity of $10^2 \, \Omega \, cm$ at 10–20 wt % of conducting polymer element, a tenacity of 3–4 gf den^{-1} and a breaking elongation of 35–45%. It is interesting to add that if 25 wt % of conducting polymer is uniformly mixed with 75 wt % of the base polymer and then melt-spun and drawn, the resultant yarn has an electrical resistivity of $2 \times 10^5 \, \Omega \, cm$, tenacity of 0.6 gf den^{-1} and breaking elongation of 50%.

Nylon polymer

Carbon black containing
conductive nylon polymer

Nylon polymer
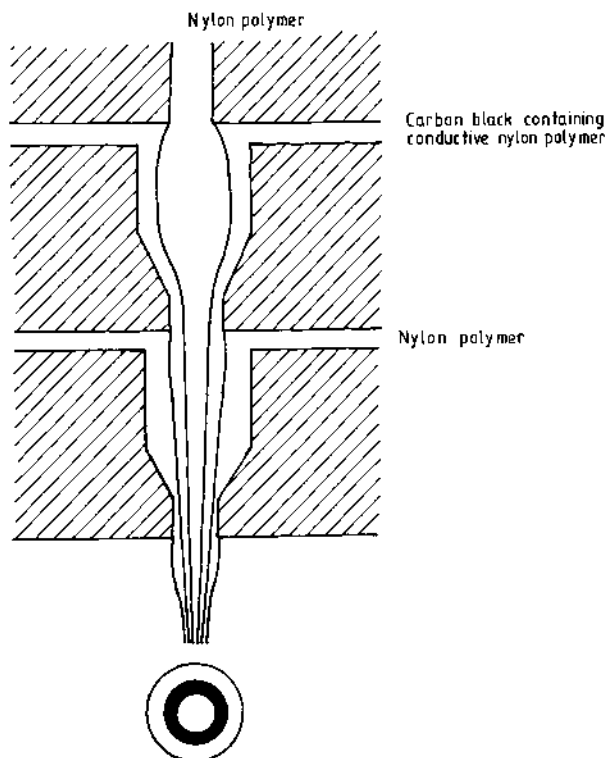
Fig. 14.2 A spinneret for conjugated bicomponent spinning (top) and cross-section of the resultant electro-conducting filament [7].

The conjugated bicomponent filament technology is commercially used to prepare filaments in which the conducting element is located in different geometries, as shown in Fig. 14.1 [7].

14.3.2 ANTISTATIC POLYESTER YARNS [8,9]

The low electrical conductivity of polyester yarns leads to accumulation of surface charges and problems of electrostatic discharge under conditions of relatively low humidity. The techniques for modifying polyester fibres to reduce development of electrostatic charge are similar to those described earlier for modifying nylon fibres. Useful antistatic effects can be obtained by copolymerizing polyether segments with the polymer to form a block polyetherester. In particular, staple fibres containing polymer end groups derived from the monoethyl ether of polyethylene glycol, $CH_3CH_2O(CH_2CH_2O)_nH$, together with chain branches derived
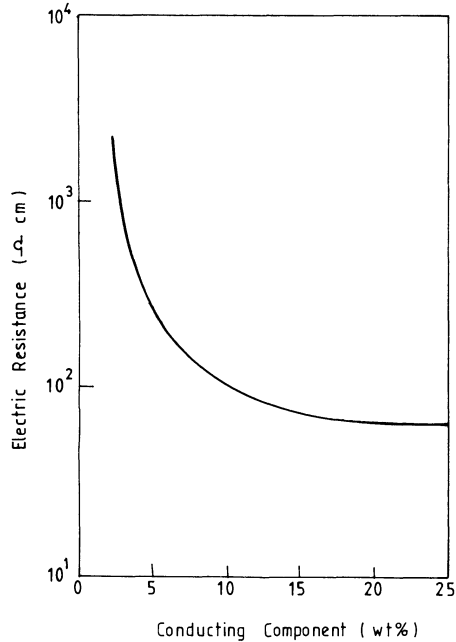
Fig. 14.3 Electrical resistance of conjugated filament as a function of the weight percentage of conducting material.

from pentaerythritol, have better antistatic properties than unmodified polyester. Formation of sheath–core bicomponent fibres with a hydrophilic or conductive polymer as the sheath or as the core is also practised; ICI (UK) produce a polyester staple fibre with conductive carbon particles embedded in its surface to a depth and at a concentration sufficient to reduce the resistivity of the fibre very substantially. This product is made using the sheath–core bicomponent technology to provide a tow of filaments whose sheaths are lower melting than their cores. When the filaments are contacted with carbon particles and heated to a temperature high enough to soften the sheath, the particles sink into and become embedded in the surface. The fibres made by cutting this tow are black, but when incorporated at 0.5–1.0 wt % into staple blends for domestic use, they provide a high level of protection against electrostatic charge with little effect on colour. They are incorporated at 2–3% into blends for industrial use for still greater protection. Dispersion of a hydrophilic or conductive polymer in the polyester matrix is also a possible method to produce antistatic polyester. Metallization or graphitization of the surface of the fibre is another method to achieve the same objective.

14.4 FLAME RETARDANT YARNS

Polyester and polyamide fibres have been widely used to produce apparel ware and other household products such as curtains that pass legislative tests controlling flammability regulations. Their inherent resistance to combustion, as measured by the limiting oxygen index test (which uses top ignition and downward propagation), is not much greater than that of cotton, as the data in Table 14.5 show [10]. The polyester and polyamide fibres can be made flame retardant via the following three routes:

1. by introduction of phosphorus-containing compounds in the fibre either through physical mixing with the polymer or through chemical reaction with the polymer;
2. by introduction of halogen-containing compounds in the fibre either through physical mixing with the polymer or through chemical reaction with the polymer;
3. by using aromatic raw materials for producing wholly aromatic polyester or polyamide polymer with very rigid chains. This category of fibres is intrinsically and truly flame retardant. This method has been particularly successful with polyamides.

14.4.1 FLAME RETARDANT POLYESTER

(a) Use of phosphorus-containing compounds

For effective flame retardance, 5–10% by weight of phosphorus-containing compound is added either during esterification or polycondensation of polyester or dry mixed with the granules and complete mixing is achieved during melt-spinning. When phosphorus-containing fabric burns, the burning portions of the fabric drip down as molten lumps and continue to burn on the floor; the flame intensity is consequently reduced and the burning retarded.

Table 14.5 Comparative limiting oxygen index (LOI) values for some fibres

Fibre	LOI
Polypropylene	0.18
Acrylic	0.18
Cotton	0.18
Polyester	0.21
Nylon 6 and nylon 66	0.22
Wool	0.24
Aramid (Nomex™)	0.28

(b) Use of halogen-containing compounds

The effective amount of halogen-containing organic compounds is around 10–15% by weight and this is physically or chemically combined with polyester. The compound tris(2,3-dibromopropyl) phosphate, $(CH_2Br.CHBr.CH_2O)_3PO$, containing both phosphorus and halogen, was once widely used as a flame retardant for polyester but was abandoned when it was realized that it could be carcinogenic.

The following compound is commercially available as a flame retardant additive:

2,2 bis[3,5-dibromo 4-(2-hydroxy ethoxy) phenyl] propane

$$HOCH_2CH_2O-\overset{\overset{Br}{|}}{\underset{\underset{Br}{|}}{\bigcirc}}-\overset{\overset{CH_3}{|}}{\underset{\underset{CH_3}{|}}{C}}-\overset{\overset{Br}{|}}{\underset{\underset{Br}{|}}{\bigcirc}}-OCH_2CH_2OH$$
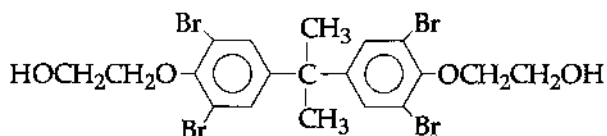
This compound of molecular weight $632\,g\,mol^{-1}$ is manufactured by Takenoto Oil & Fat Co. Ltd in Japan and marketed under the trade name Delion PFR-501^{TM}. The similarity of this compound with diglycol terephthalate (DGT), $HOCH_2CH_2OCOC_6H_4COOCH_2CH_2OH$, is noteworthy and therefore, if added at the beginning of polycondensation, it behaves just like a monomer of polyester. Unlike the physically blended flame retardant, this compound forms a copolymer and does not exude out. This compound should not be added after the polycondensation reaction for the following reason. If 10 wt % of this additive is added to the spinning melt, which comprises 90% by weight of normal polymer of molecular weight 19 262, say, then there is a possibility that during the spinning hold up time of 10–20 min, the polymer may react with the additive and molecular weight redistribution may occur without changing the total number of molecules. Then the resultant number average degree of polymerization will be

$$\left[\left(\frac{90}{19\,262}\times 100\right)+\frac{10}{632}\right]\bigg/\left[\frac{90}{19\,262}+\frac{10}{632}\right]=23.6$$

which is only about one-quarter of the initial number average degree of polymerization of 100.

14.4.2 WHOLLY AROMATIC POLYESTER AND POLYAMIDE FIBRES

These fibres are described in Chapter 18 and only one illustration of the ultimate flame resistant fabric will be given here. Teijin Ltd of Japan have introduced a new fabric, aptly called Xfire^{TM}. It is a combination of the *meta*-aramid fibre Teijin Conex^{TM}, which is believed to be [10–12] a

block copolymer of poly(*m*-phenylene isophthalamide) and poly(3,4-diphenylether isophthalamide)
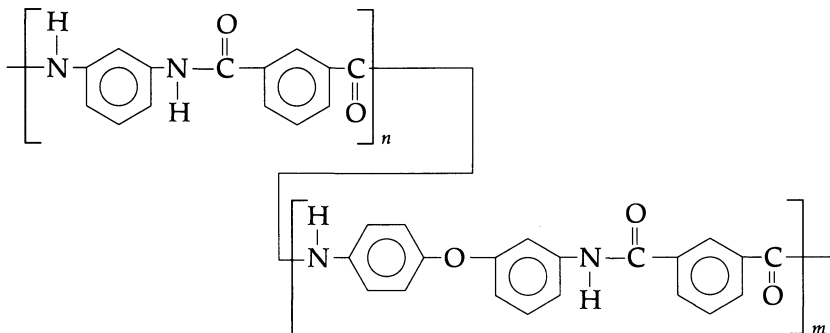
and the *para*-aramid fibre Technora™ manufactured by Teijin Ltd. Yarns made from a combination of these two fibres have a strength of $5\,gf\,den^{-1}$ and a breaking elongation of 39%. Xfire fabric resists temperatures of up to 1200 °C and even a flash of 5000 °C will not burn through the cloth [13].

14.5 POLYESTER YARNS WITH MICROGROOVES, MICROVOIDS AND MICROCRATERS

The introduction of microgrooves, microvoids and microcraters is of particular significance in polyester yarns, and yarns containing such discontinuities have been commercialized in Japan since around 1985 [14, 15]. There are two main reasons for their introduction; the first is related to an increase in the transport of penetrants like dyes, moisture, perspiration, etc., and the second to aesthetics like enhancement of depth of colour, improved handle, silk-like effect, etc.

The procedures used to produce fibres containing grooves, voids or craters are generally based on blending an inorganic, organic or polymer additive of roughly 1 μm size or smaller into the base polymer, then to spin and draw to form fibres and finally to dissolve out the additive from the surface of fibres. For polyester fibres, the solvent application is done on woven or knitted fabrics, normally with aqueous solution of sodium hydroxide at around 80–100 °C; this results in weight reduction to give light fabrics.

14.5.1 FIBRES WITH MICROGROOVES

Toray [16] of Japan produce a multi-microgroove polyester filament yarn as follows. Polyethylene glycol (0.82 wt % of yarn), $H(CH_2CH_2O)_nH$, and dodecyl benzene sulphonate sodium salt (0.13 wt %), $C_{12}H_{25}C_6H_4SO_3Na$,

are charged into the extruder in pellet form together with polyester chips; the spun yarn is drawn on a draw twister using the same conditions as in the case of the standard polyester yarn to produce a 24 filament, 50 denier bright polyester yarn. Using hot sodium hydroxide solution, weight reduction of 13 wt% is allowed as microgrooves are created on the filament surface. The origin of the microgrooves can be explained as follows. If the additive has a melting point similar to or lower than that of polyester, it will be stretched along with the surrounding polyester polymer both during spinning and drawing. In normal multifilament textile-grade polyester yarn production, the total draw ratio, which may be taken as the product of the draft applied during spinning and the draw ratio achieved during drawing, is around 150–300. Assuming that a spherical globule of molten additive is stretched during spinning and drawing into a cylinder in the drawn yarn, then the length-to-diameter ratio of the cylinder will be (total draw ratio)$^{3/2}$, i.e. around 2000–5000. Thus very fine and long grooves form on the surface of the filament and very fine and long capillaries are created in the filament after alkali weight reduction with hot sodium hydroxide solution.

14.5.2 FIBRES WITH MICROVOIDS

A typical fibre with microvoids is shown schematically in Fig. 14.4. A good example of a multi-microvoid polyester fibre is Teijin's Wellkey^{TM} [17]. The voids are spherical in size and not stretched out as microgrooves
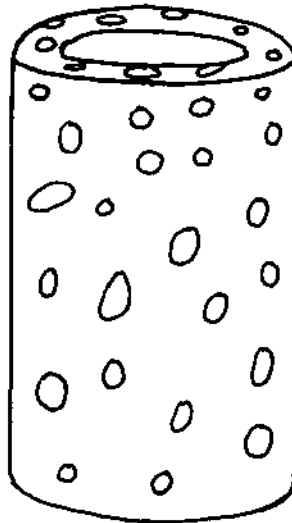
Fig. 14.4 Schematic sketch of a hollow fibre with microvoids.

as in the previous case. It is likely that the additive, which is mixed with polyester before spinning, is or includes an inorganic material of melting point higher than 300 °C such as a salt or oxide of alkali earth metals [18].

14.5.3 FIBRES WITH MICROCRATERS

To produce polyester yarns with microcraters, inorganic particles, e.g. colloidal silica, aluminium oxide, calcium carbonate or barium carbonate, of size of about or less than 0.1 μm without agglomerates, are uniformly dispersed in molten polyester polymer and later removed when the drawn yarn comes in contact with hot sodium hydroxide solution. Kuraray of Japan produce and market a multi-macrocrater polyester yarn [15, 19] which is covered with microcraters of diameter 0.1 to 1.0 μm, their number exceeding one billion per square centimetre of filament surface. The very high surface area provides not only a deeper colour shade but an improvement in lustre and handle of the fibres.

14.6 SUPER MICROFILAMENT YARNS BY CONJUGATED BICOMPONENT YARN SPINNING

The normal melt-spinning route has been used to produce partially oriented nylon and polyester yarns of around 0.7 denier per filament (dpf), from which drawn yarn of around 0.5 dpf can be made. Reduction of linear density per filament below 0.5 dpf is accompanied by frequent filament breaks at the spinneret surface because the spinning line at the orifice is too thin or because the melt throughput rate per orifice is too low. In the former case cohesive fracture occurs, whereas in the latter case droplets form due to the surface tension of the polymer melt.

The production of super microfilaments of around 0.1 dpf or less is through a different route which has been developed in Japan, and involves the initial production of conjugated bicomponent filaments of >1 dpf and then splitting each filament into 10 or more filaments [20–25]. The three companies which are in the forefront in this area, use the following approaches.

1. The islands-in-the-sea fibres are manufactured by Toray, Japan (Fig. 14.5). As shown in the figure, about 16 or more microfilaments from one type of polymer (islands) are embedded within a large round matrix (sea) of another type of polymer. The microfilaments can be nylon or polyester in a sea of polystyrene, for example, which can be dissolved easily in an ordinary organic solvent (e.g. tetrahydrofuran or toluene).

2. The radial petal-like conjugated fibre without central hole is manufactured by Kanebo, Japan (Fig. 14.6). The figure shows a typical, radially
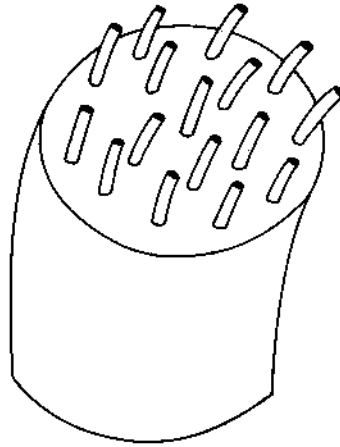
Fig. 14.5 Islands-in-the-sea type Toray conjugated bicomponent filament for producing super microfilaments.

conjugated fibre being split into eight triangular segments (polyester) and a radial segment (nylon 6). The splitting is achieved either through mechanical force impact generated by highly pressurized water or by thermal action. Alternatively the radial segment may be dissolved out; in the case of polyester, hot aqueous solution of sodium hydroxide is a good solvent.

3. The radial petal-like conjugated fibre with central hole is manufactured by Teijin, Japan (Fig. 14.7). The petals may be alternately nylon 6 and polyester and are split, as described in case (2); in most
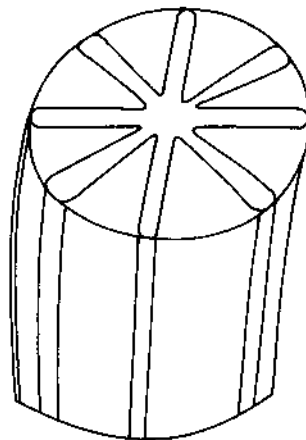
Fig. 14.6 The radial petal-like conjugated fibre without central hole for producing super microfilaments [20, 21].
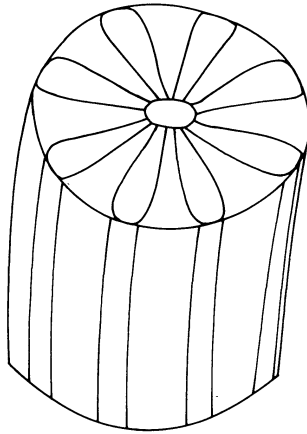
Fig. 14.7 The radial petal-like conjugated filament with central hole.

cases, the splitting is done after the knitting or weaving process [25], since it is very difficult to handle the super-fine filament yarn at the drawing, texturing, knitting and weaving stages.

The super microfilaments have extremely low flexural rigidity and the fabrics made from them are very light and soft. Besides being used as suedes, air-permeable and water-repellent fabrics are also produced from them as the dense array of thin fibres can support water droplets as in a lotus leaf.

14.7 FIBRES WITH NON-CIRCULAR CROSS-SECTION AND HOLLOW FIBRES

The external geometry of the polyester and polyamide filaments depends essentially on the design of the spinneret holes through which the initial extrusion takes place. Normally circular holes give rise to circular cross-section since solidification occurs by heat transfer and the surface tension forces assist in uniform shrinkage in the radial direction. On the other hand, in the fibres spun from solution, coagulation and evaporation processes, which involve mass transfer, result in a non-circular cross-section even when circular holes are used (this is discussed in Chapter 6). It has been observed that the non-circular cross-sections result in greater lustre and covering power and improved handle, and therefore filaments with non-circular cross-sections are being used extensively to achieve these special effects. For this non-circular spinneret orifice shapes are required, which are fabricated by electron beam milling and electro-discharge machinery [26], and will be described in

this section. The modified filament cross-sections result either from coalescence or fusing of melt streams below the spinneret or directly from extrusion through profiled capillaries. Although either method may be used for the manufacture of hollow fibres, the former seems to be mainly practised for this type of fibre. The reshaping of the cross-section along the spinline primarily depends on the time of solidification; the longer this time period, the greater the degree of reshaping. In this context, the factors which increase the potential of reshaping the filament cross-section in the spinline, other factors being constant, can be summarized as:

1. lowering of melt viscosity;
2. lowering of throughput rate;
3. increase of spinning speed, perhaps because of decrease in solidification time;
4. increase of spinning temperature;
5. the more the contour of spinneret orifice departs from circularity.

14.7.1 SPINNERET DESIGN

In designing spinneret orifices for various cross-sectional shapes of filament, the average polymer melt speed per orifice (the extrusion velocity) has first to be fixed. In practice, for textile-grade polyester and polyamide melts, the polymer melt flow speed is taken to be in the range 4–70 m min^{-1}. With decreasing orifice diameter, other conditions remaining constant, the minimum speed must increase to avoid the possibility of filament breakage because of surface tension effects. For example, for polyester microfilament spinning, the orifice is only 0.2 mm in diameter and the minimum speed has to be kept around 7 m min^{-1}.

Before considering the design of orifices other than circular, it may be noted that in general the dimensions of the spinneret orifices for producing round filaments are in the range: diameter 0.18–0.45 mm, length 0.4–0.8 mm; thus giving a length-to-diameter ratio of 2 to 3. For producing other cross-sectional shapes, some information on the dimensions of the capillary and related data are given below.

(a) Trilobal cross-section

A typical spinneret orifice for producing a trilobal cross-section is shown in Fig. 14.8 and the resulting trilobal filament cross-section in Fig. 14.9. The dimension of the spinneret orifice (Fig. 14.8) would normally be within the range: leg length 0.20–0.45 mm, leg width 0.06–0.14 mm, leg length-to-leg width ratio 2–4, capillary length 0.3–0.8 mm.
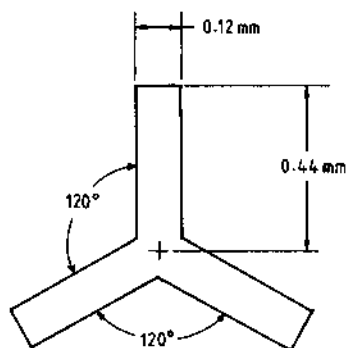
Fig. 14.8 Cross-section of a typical spinneret orifice for producing a filament with trilobal cross-section.
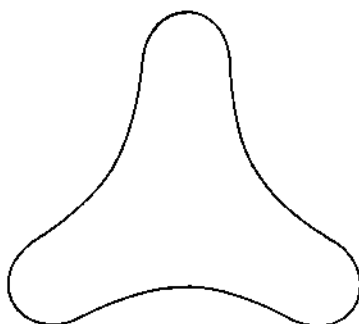
Fig. 14.9 Trilobal filament cross-section resulting from the spinneret shown in Fig. 14.8.

(b) Rectangular cross-section

The spinneret orifice for producing a filament with rectangular cross-section is shown in Fig. 14.10 and the resultant filament cross-section in Fig. 14.11. The length-to-width ratio for the filament cross-section is 3.90 while for the spinneret orifice, this ratio is 13.75; the former is thus 0.284
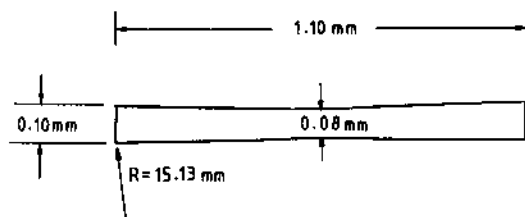
Fig. 14.10 Cross-section of a typical spinneret orifice for producing a filament with rectangular cross-section.
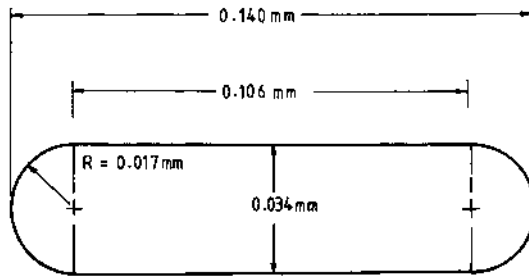
Fig. 14.11 Rectangular filament cross-section resulting from the spinneret shown in Fig. 14.10.

times the latter. This ratio is important in designing a rectangular orifice for the desired filament cross-section.

(c) Hexalobal cross-section

The spinneret orifice design for hexagonal cross-section is shown in Fig. 14.12 and the resulting filament with hexalobal or hexagonal cross-section is shown in Fig. 14.13 for a specific polymer temperature and polymer throughput rate per orifice. It may be noted that if the hexagonal legs were all radiating from the central axis of symmetry, the angle between the legs would be 60°, which is too small for good spinning and
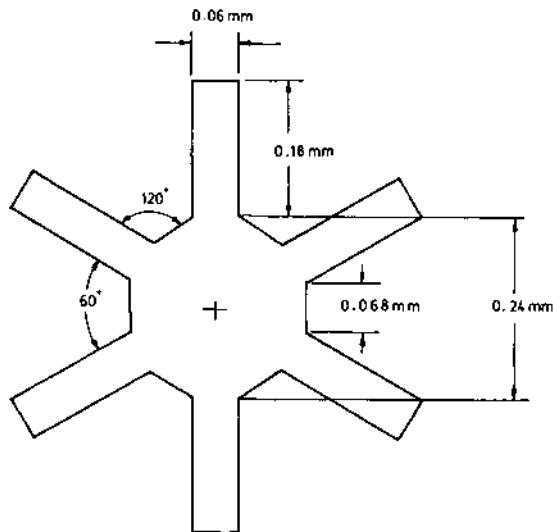
Fig. 14.12 Cross-section of a typical spinneret orifice for producing a filament with hexagonal cross-section.
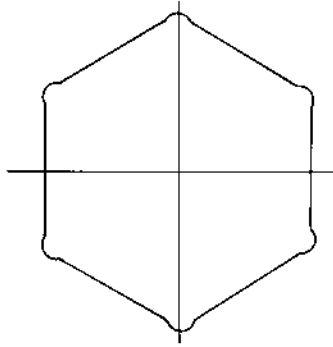
Fig. 14.13 Hexalobal filament cross-section resulting from the spinneret shown in Fig. 14.12.

considerably increases the chances of filament breakage. The spinneret is so designed that the effective angle is doubled (Fig. 14.12) and this results in an improvement in the spinning performance. It is difficult to produce filaments with lobes greater than six for this reason although octalobal filaments are produced.

(d) Round hollow cross-section

The cross-section of a typical hollow filament spinneret orifice is shown in Fig. 14.14 and the cross-section of the hollow filament obtained from it is shown in Fig. 14.15. To characterize the hollow spinneret and filament orifice, we may define the orifice hollow ratio as (diameter of the inner
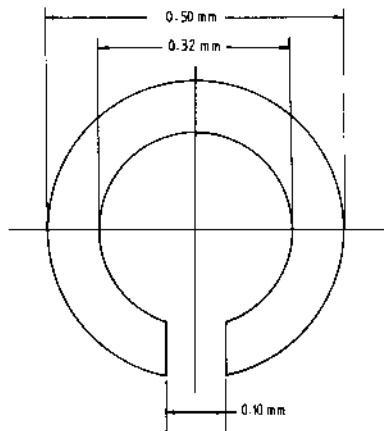
Fig. 14.14 Cross-section of a typical spinneret orifice for producing a hollow circular filament.
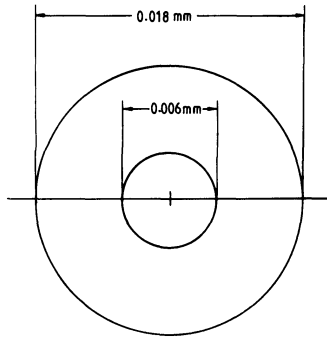
Fig. 14.15 Circular hollow filament cross-section resulting from the spinneret shown in Fig. 14.14.

circle/diameter of the outer circle)^2. It is noteworthy that while the spinneret orifice hollow ratio is 0.41, it is 0.11 for the filament cross-section.

Dieswell or melt bulge is of particular significance in hollow fibre production. This is because with a normal melt bulge of around 0.05 mm in one direction, the gap between two adjacent orifices in the spinneret must be greater than 0.1 mm if merger or fusion of two melt streams is to be avoided.

In designing the spinneret for producing hollow filaments, the 0.10 mm wide bridge, which closes the annular gap (Fig. 14.14), supports the central plate and must be strong enough or wide enough to be able to withstand the polymer melt pressure on the central plate during melt-spinning. The width of the bridge, on the other hand, must be narrow enough for the melt stream to merge as it moves along the spinline. The maximum polymer melt pressure which the bridge can sustain may be estimated as follows.

With reference to Fig. 14.14, we may consider that a rectangular beam of width $b = 0.10$ mm, thickness $t = 0.60$ mm and length $l = 0.09$ mm is supporting the central circular plate of diameter D (0.32 mm) at a fixed point. The maximum extensional stress (σ_{max}) due to bending moment

$$M = Wl \qquad\qquad (14.10)$$

where W is total weight applied on the beam, is given by

$$\sigma_{max} = \frac{t}{2} \times \frac{M}{I} \qquad\qquad (14.11)$$

where I is the moment of inertia for rectangular cross-section, and is given by

$$I = \frac{1}{12}bt^3. \qquad\qquad (14.12)$$

The applied weight, W, is given by

$$W = \frac{\pi D^2}{4} \cdot P \tag{14.13}$$

where P is the polymer melt pressure applied on the central plate.
   From equations (14.10) to (14.13), we obtain

$$P = \frac{2bt^2 \sigma_{max}}{3\pi l D^2}. \tag{14.14}$$

The limiting value of σ_{max} is $63\,\mathrm{kgf\,mm}^{-2}$, which is the breaking stress for stainless steel 316. The limiting value of P from equation (14.14) is

$$P = 5220\,\mathrm{kgf\,cm}^{-2}.$$

The bridge length of $0.09\,\mathrm{mm}$ being very small, we may also take into consideration the possibility of breaking of the bridge by shear. If S is the breaking shear strength of the stainless steel,

$$S = \frac{W}{bt}. \tag{14.15}$$

This gives $P = 4btS/(\pi D^2)$, which leads to a value of P of $3510\,\mathrm{kgf\,cm}^{-2}$. Since the effect of temperature up to $300\,°\mathrm{C}$ on stainless steel strength will be very small, it may be stated that the polymer melt pressure should not exceed $3000\,\mathrm{kgf\,cm}^{-2}$. It may thus be concluded that in the melt-spinning of hollow filaments, a bridge in the spinneret orifice of $0.1\,\mathrm{mm}$ width and $0.6\,\mathrm{mm}$ thickness is strong enough to support a $0.32\,\mathrm{mm}$ circular plate upon which about $1000\,\mathrm{kgf\,cm}^{-2}$ pressure can be applied with a safety factor of 3.5.

(e) Twin trilobal cross-section by conjugate spinning

Toray of Japan are producing a silk-like polyester yarn with the cross-section shown in Fig. 14.16 [27]. Such filaments can be produced by conjugated bicomponent spinning of trilobal cross-section yarn. The three tips of trilobal cross-section may consist of easily soluble polymer which is dissolved out with a solvent, leaving the special twin trilobal cross-section as shown in Fig. 14.16.

14.7.2 LUSTRE OF TRILOBAL YARNS

The trilobal cross-section was the first departure from round cross-section and was introduced commercially by Du Pont in the USA; the primary aim was to obtain lustrous yarns and fabrics. Werny [28] measured the intensity of light reflected from trilobal yarn parallel wound on card, the incident light, the trilobal filament and the reflected light being
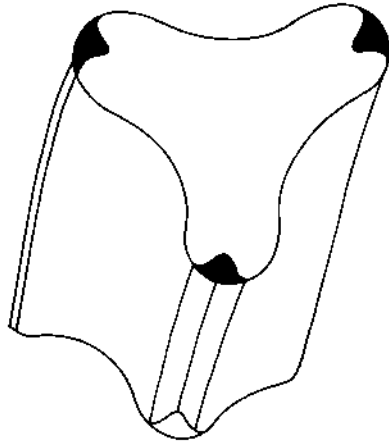
Fig. 14.16 Cross-section of conjugated trilobal filament (the dark portions are dissolved out) (T. Manabe, unpublished).

on the same plane. In 1990 T. Manabe (unpublished) analysed Werny's data in terms of the following parameters defined on the basis of the construction given in Fig. 14.17.

r_1 radius of trilobal tip (cm)
R_1 radius of inscribed circle (cm)
R_2 radius of circumscribed circle (cm)
MR modification ratio, R_2/R_1
TR tip ratio, r_1/R_2.

Yarn lustre may be represented by I_{max} (trilobal)/I_{max} (round), where I_{max} (trilobal) and I_{max} (round) are the maximum intensities of reflected light from trilobal and round filament yarns respectively.
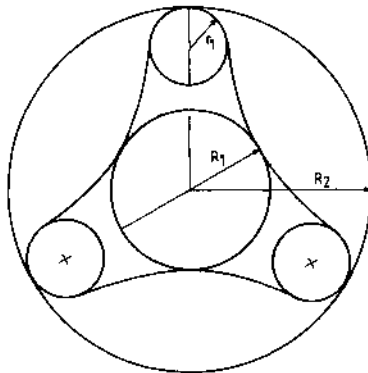
Fig. 14.17 Construction for defining parameters representing lustre of a trilobal filament (for details, see text).

Table 14.6 Calculated yarn lustre for some fibres

Filament cross-section	MR (R_2/R_1)	TR (r_1/R_2)	Relative yarn lustre
Trilobal	1.50	0.44	1.384
Trilobal	1.55	0.36	1.302
Trilobal	1.78	0.31	1.225
Trilobal	1.90	0.20	1.105
Equilateral triangle	2.00	0.00	0.902
Trilobal	3.50	0.14	0.843
Round	1.00	1.00	1.000

Manabe's analysis of Werny's data showed that the following equation represented the experimental data for a number of fibres quite well:

$$\frac{I_{max}\ (\text{trilobal})}{I_{max}\ (\text{round})} = 1.158 - 0.128\ (\text{MR}) + 0.950\ (\text{TR}) \qquad (14.16)$$

for MR between 1.5 and 5 and TR between 0.10 and 0.45. The predictions of this equation for seven filaments – five of them trilobal with different MR and TR values, one triangular and one round – are summarized in Table 14.6.

A number of important conclusions can be drawn from the data in this table, some of which are listed below.

1. Reflected light intensity is stronger at lower MR and higher TR, as is also indicated by equation (14.16).
2. The filament with triangular cross-section with zero TR has low lustre. It must be remembered that lustre has been measured in terms of the reflected light input only.
3. Filaments with appropriately designed trilobal cross-section are more lustrous than round filaments.
4. For a trilobal spinneret hole, in general, the higher the MR, the lower the TR.

14.8 MELT RHEOLOGY DURING SPINNING OF SPECIALITY YARN

The general principles of melt rheology were considered in Chapter 3 and with specific reference to melt-spinning in Chapter 4. The need to have uniform pressure distribution at different positions and within the same spinneret was emphasized as it minimizes the denier and property variations in spun filaments. The pressure above the spinneret plate has to be optimum; too low a pressure makes it impossible to maintain constant pressure at each spinneret orifice, while too high a pressure can result in high shear rates and melt fracture of the extrudate besides

leading to leakage of the melt from the joints of the spin pack and the spinning head. In industrial melt-spinning, the pressure is kept within $40\text{--}80\,\mathrm{kgf\,cm^{-2}}$ gauge.

For speciality yarns, use of appropriate pressure above the spinneret plate is of utmost importance, as would be clear from the following discussion.

In Chapter 4, it was shown that the average extrusion velocity, V_0, is given by the expression

$$V_0 = \frac{4W}{n\rho_0\pi d_0^2},$$

where W is the mass output rate, n the number of orifices in the spinneret, ρ_0 the density of the melt and d_0 the diameter of the spinneret channel. In Chapter 3, it was shown that Poiseuille's equation for a Newtonian fluid can be written as

$$P = \frac{8\eta QL}{\pi R^4} = \frac{8\eta WL}{\pi \rho_0 R^4}$$

For melt-spinning of a microfilament yarn, which will give a final denier (after drawing) per filament of, say, 0.5, the throughput rate W will be relatively low and, with normal spinneret orifice, the plate pressure will be low. The extrusion velocity may therefore become so low that surface tension effects may lead to the formation of spherical drops and filament breakage. This problem can be overcome by using spinnerets with narrow orifices; as a result the extrusion velocity becomes much higher and spinning without breaks becomes possible. A second illustration is of hollow filaments, in which case the thin spinneret channel necessitates the use of high pressures leading to dieswell at the spinneret exit. This reduces the degree of hollowness. However, melt bulge is a requirement for closing the gap of C-type flow so that it is rendered into an O-type filament. Thus, these contradictory requirements need a fine balancing and an understanding of the complex rheological parameters helps in achieving this balance. The approach taken in this section is empirical in nature and is aimed at solving industrial problems.

14.8.1 SHEAR VISCOSITY OF NYLON 6 POLYMER MELT

The data on the molecular weight and temperature dependence of the zero shear rate viscosity, η_0, in poise, of nylon 6 polymer which has no extractable monomer or oligomers [29], may be represented by the following empirical equation (from T. Manabe, unpublished):

$$\eta_0 = \bar{M}_n^{3.4} \exp\left[\frac{7212}{T + 273} - 39.1153\right] \tag{14.17}$$

where $\bar{M}_n$ is the number average molecular weight of nylon 6 in g mol^{-1} and T the melt temperature in °C.

In practice, however, nylon 6 contains extractables to the extent of 1 wt %, which can reduce the melt viscosity considerably. Moreover, an additional 1 wt % of extractables may form during melt-spinning. Thus the utility of equation (14.17) is rather limited.

The effect of extractables on the Newtonian melt viscosity of nylon 6 has been studied by Mukouyama and Takegawa [30] and their data can be represented by the following relationship (T. Manabe, unpublished):

$$\ln \eta_0 = (3.532 \ln \bar{M}_n - 23.8122)(1 - 0.01 W_e) + \frac{8031}{T + 273} - 18.5154 \quad (14.18)$$

where W_e is the amount of extractables in weight per cent in the polymer.

At $W_e = 0$, equation (14.18) reduces to

$$\eta_0 = \bar{M}_n^{3.532} \exp \left[\frac{8031}{T + 273} - 42.3276 \right]. \quad (14.19)$$

Based on Laum's data [29], equations (14.18) and (14.19) can be written as:

$$\ln \eta_0 = (3.50 \ln \bar{M}_n - 23.8122)(1 - 0.01 W_e) + \frac{7212}{T + 273} - 16.3200 \quad (14.18a)$$

$$\eta_0 = \bar{M}_n^{3.5} \exp \left[\frac{7212}{T + 273} - 40.1322 \right]. \quad (14.19a)$$

Equations (14.17) and (14.19a) give close results.

14.8.2 RELATIONSHIP BETWEEN SOLUTION VISCOSITY AND MOLECULAR WEIGHT FOR NYLON 6

For a relative viscosity, RV of nylon 6 polymer in 96 wt % concentrated sulphuric acid solution at 25 °C at a polymer concentration of 1 g dl^{-1} and an intrinsic viscosity, IV, in dl g^{-1}, the following empirical relationships are found to hold [T. Manabe and R. Kumar, unpublished; 31]:

$$\bar{M}_n = 113.16 \times 95.70(RV - 1) \quad (14.20)$$

and

$$IV = 5.52 \times 10^{-4} \bar{M}_n^{0.79}. \quad (14.21)$$

Equations (14.20) and (14.21) become identical at the Huggins constant 0.24.

14.8.3 SHEAR VISCOSITY OF POLYESTER POLYMER MELT

A number of workers have proposed empirical relationships for the Newtonian melt viscosity η_0 of PET in poise, most prominent among

them being Gregory [32] and Manaresi [33]. Gregory's equation

$$\eta_0 = [IV]^{5.145} \exp\left[\frac{6802.1}{T+273} - 2.3241\right] \qquad (14.22)$$

provides a good starting point. A possible improvement of this equation involves the inclusion of an additional term which accounts for the effect of diethylene glycol (DEG) on the viscosity. This has led to the following modified equation [34]:

$$\eta_0 = [IV]^{5.145} \exp\left[\frac{8286}{T+273} - 4.64 - 0.16(DEG)\right] \qquad (14.23)$$

where (DEG) is the DEG content in weight percentage.

The zero shear rate viscosity η_0 and intrinsic viscosity (IV) of cationic-dyeable PET are affected by the sodium sulphoisophthalate content. For measurements made in 100% orthochlorophenol at 25 °C, the following equations represent the data for cationic-dyeable PET (T. Manabe, unpublished):

$$\eta_0 = [IV]^{5.056} \exp\left[\frac{7361}{T+273} + 0.64(CD) - 0.159(DEG) - 3.2485\right] \quad (14.24)$$

and

$$IV = 7.044 \times 10^{-4} \bar{M}_n^{0.683} \exp[-0.127(CD) + 0.031(DEG)] \qquad (14.25)$$

where (CD) represents the extent of sodium sulphoisophthalate in the polymer in mol %. From improved versions of the above two equations, the following relationship between η_0 and $\bar{M}_n$ is obtained:

$$\eta_0 = \bar{M}_n^{3.453} \exp\left[\frac{7361}{T+273} - 39.9458\right]. \qquad (14.26)$$

It may be noted that the Newtonian melt viscosity vs. molecular weight–temperature relation is similar in nylon 6 (equation (14.19a)) and PET (equation (14.26)). As an illustration, it is interesting to note that for a PET and a cationic-dyeable PET with CD of 1.5 mol %, both of number average molecular weight $\bar{M}_n = 20\,000\,\text{g mol}^{-1}$, and with DEG contents of 0.65 and 2.5 wt %, respectively, the above equations show that their melt viscosities, η_0, at 285 °C are both 1707 poise, whereas their intrinsic viscosities, IV, are 0.62 and 0.54 dl g^{-1}, respectively. This emphasizes that during fibre production by melt-spinning, characterization in terms of melt viscosity is essential.

14.8.4 INTRINSIC VISCOSITY–MOLECULAR WEIGHT RELATIONSHIPS FOR POLYESTER

A number of relationships between molecular weight and intrinsic viscosity of PET have been proposed, two of which are described below.

1. Using orthochlorophenol as the solvent at 25 °C, Ravens and Ward [35] proposed that

$$IV = 1.7 \times 10^{-4} \bar{M}_n^{0.83}.$$ (14.27)

2. Using phenol/tetrachloroethane in 60:40 by weight ratio as the solvent at 25 °C, Hergenrother and Nelson [36] proposed that

$$IV = 3.72 \times 10^{-4} \bar{M}_n^{0.73}.$$ (14.28)

Various other relationships have been established using different solvent systems and differing temperatures; even slight differences in the constants can give considerable differences in the estimates of $\bar{M}_n$ when applied to the same polymer sample.

14.8.5 MODIFIED FLUID RESPONSE AT HIGH SHEAR RATES

As stated in Chapter 3, polymeric fluids are shear-thinning and up to shear rates that are not too high, they show a shear rate dependence which is represented by curve (1) in Fig. 14.18.

This behaviour lies between that shown by an ideal Newtonian fluid (line 2) and an ideal Rabinowitsch or power law fluid (curve 3). The actual behaviour can thus be considered to be Newtonian at low shear
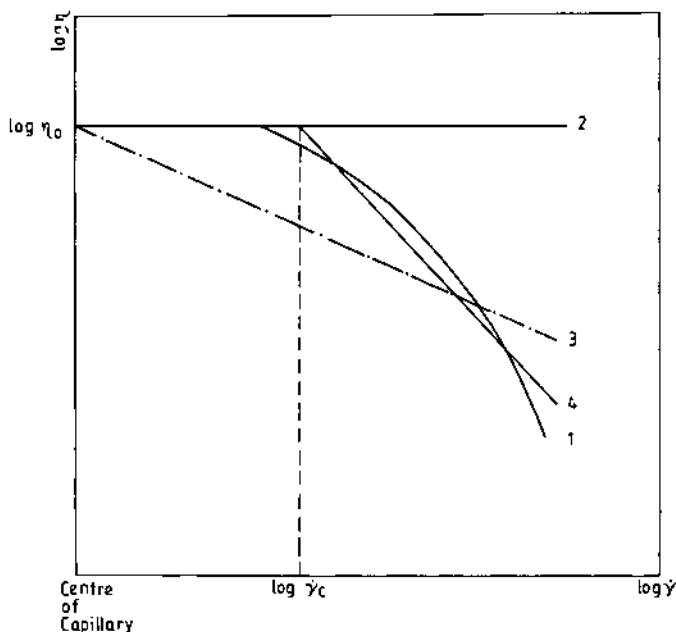
Fig. 14.18 The shear viscosity (η) dependence on shear rate (γ) for different fluid types (for details, see text).
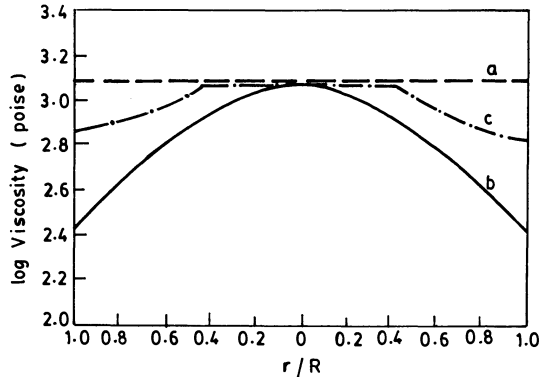
Fig. 14.19 Viscosity distribution along the capillary radius assuming fluid response to be ideal Newtonian (a), ideal Rabinowitsch (b), and modified fluid (c) [34].

rates, followed by non-Newtonian like that of a Rabinowitsch fluid at high shear rates and represented by an idealized modified fluid (T. Manabe, unpublished), as shown by curve (4). In the modified fluid, the transition occurs at a shear rate $\dot{\gamma}_c$. Since the shear rate is zero at the centre of the capillary and maximum at the capillary wall, the viscosity across the capillary during extrusion is not constant; the response of the fluid near the core would be Newtonian due to the low shear rates prevailing in that region, while towards the capillary walls, the flow pattern would be non-Newtonian. The viscosity distributions across the capillary radius, assuming ideal Newtonian (a), ideal Rabinowitsch (b) and modified fluid (c) responses are shown in Fig. 14.19 for PET melt at 285 °C [34]; for estimating response (b), the flow index n has been assumed to be 0.635.

For the traditional Rabinowitsch fluid, it is assumed that $\dot{\gamma}_c = 1\,\mathrm{s}^{-1}$ [37]. Since the deviation occurs at much higher shear rates, the modified fluid model is more appropriate. Figure 14.19 represents the viscosity response for the modified fluid, which represents more realistically the behaviour of actual polymer melts. The response of the fluid near the core of the spinneret orifice is Newtonian due to the low shear rates prevailing in that region, while towards the capillary walls, the flow pattern is non-Newtonian. Thus for a power-law fluid, the decrease of shear viscosity with an increase in shear rates at higher shear rates may be derived through the approach given in Chapter 3; e.g. equation (3.13) may be rewritten as

$$\eta = \eta'(\dot{\gamma}/\dot{\gamma}')^{n-1} \qquad (14.29)$$

where η' is the viscosity at some arbitrary shear rate $\dot{\gamma}'$.

Assuming that this refers to the Newtonian region, we may write

$$\eta = \eta_0 (\dot{\gamma}_r / \dot{\gamma}_0)^{n-1} \tag{14.30}$$

for a non-Newtonian, Rabinowitsch fluid, where $\dot{\gamma}_r$ and $\dot{\gamma}_0$ are the shear rates at radius r from the centre of the capillary and at the centre of the capillary, respectively. The volumetric throughput dependence on pressure, which is given by $Q = \pi P R^4 / 8 \eta L$ for a Newtonian fluid, becomes

$$Q = \frac{n}{3n+1} [\pi R^3 \dot{\gamma}_0][PR/2L\eta_0\dot{\gamma}_0]^{1/n} \tag{14.31}$$

for a Rabinowitsch fluid [37].

The calculation of Q through a capillary for the modified combination fluid is achieved by assuming the inner zone of the capillary to be Newtonian and the outer zone being of the Rabinowitsch type; for this we get (T. Manabe, unpublished):

$$Q = \frac{n}{3n+1} \left[\frac{\pi R^3 \tau_c}{\eta_0} \right] \left[\frac{PR}{2L\tau_c} \right]^{1/n} \left[1 + \frac{1-n}{4n} \left(\frac{PR}{2L\tau_c} \right)^{-(3n+1)/n} \right]. \tag{14.32}$$

In industrial melt-spinning

$$\frac{PR}{2L\tau_c} \gg 1 \quad \text{and} \quad \left(\frac{1-n}{4n} \right) \left(\frac{PR}{2L\tau_c} \right)^{-(3n+1)/n} \ll 1. \tag{14.33}$$

These approximations, when applied to equation (14.32), give

$$Q = \frac{n}{3n+1} \left[\frac{\pi R^3 \tau_c}{\eta_0} \right] \left[\frac{PR}{2L\tau_c} \right]^{1/n}. \tag{14.34}$$

This may be re-written as

$$\tau_c = \left[\frac{n}{3n+1} \times \frac{\pi R^3}{\eta_0 Q} \right]^{n/(1-n)} \left[\frac{PR}{2L} \right]^{1/(1-n)}. \tag{14.35}$$

Thus n may be determined from a plot of $\log P$ vs. $\log Q$ and τ_c from equation (14.35).

14.8.6 FLOW THROUGH RECTANGULAR SLIT

The throughput vs. pressure relationship for Newtonian fluids through a rectangular opening for cross-sectional area ab (a being the longer side and b the shorter side of the rectangle), when the opening is a long parallel slit, i.e. $b/a \ll 1$, is [37]:

$$Q = \frac{ab^3 P}{12L\eta_0}. \tag{14.36}$$

For a modified combination fluid, Q can be shown to be [T. Manabe, unpublished]

$$Q = \frac{n}{2(2n+1)} \left[\frac{ab^2 \tau_c}{\eta_0} \right] \left[\frac{bP}{2L\tau_c} \right]^{1/n} \left[1 + \frac{1-n}{3n} \left(\frac{bP}{2L\tau_c} \right)^{-(2n+1)/n} \right]. \qquad (14.37)$$

For industrial melt-spinning

$$\frac{bP}{2L\tau_c} \gg 1 \quad \text{and} \quad \frac{1-n}{3n} \left(\frac{bP}{2L\tau_c} \right)^{-(2n+1)/n} \ll 1. \qquad (14.38)$$

Then equation (14.37) reduces to

$$Q = \frac{n}{2(2n+1)} \left[\frac{ab^2 \tau_c}{\eta_0} \right] \left[\frac{bP}{2L\tau_c} \right]^{1/n} \qquad (14.39)$$

which for $n = 1$ is reduced to equation (14.36).

14.8.7 THE ENTRANCE EFFECT AND ITS CONSEQUENCES

At the capillary entrance, the pressure decreases at a much higher rate [37] than in the region away from the polymer melt inlet, as shown in Fig. 14.20. As discussed in Chapter 3, this will have a significant effect on throughput rate in spinneret orifices that have low L/D ratio (1–3). The effective length of the capillary should therefore be increased to $L_e = L + 2NR$ [37], when Q vs. P relationships are evaluated for round
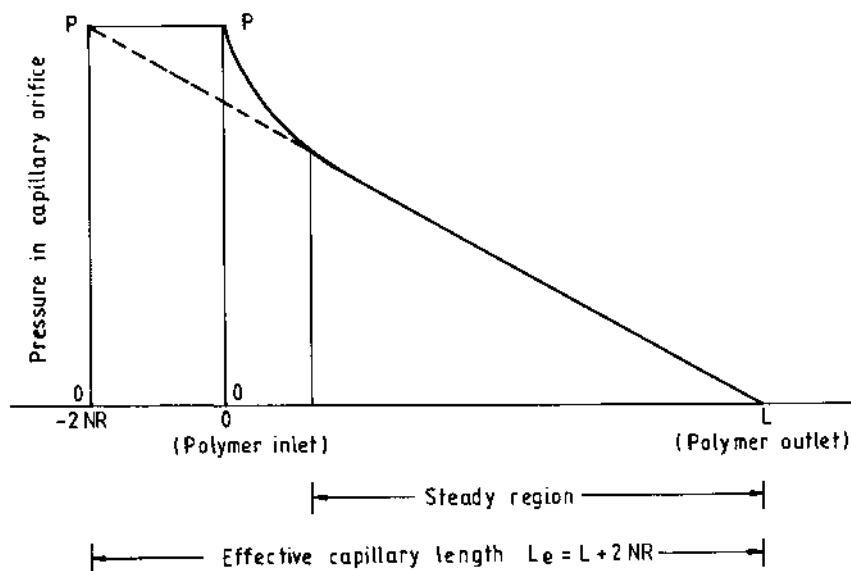
Fig. 14.20 Pressure drop along the capillary length [37].

Table 14.7 Non-Newtonian melt flow constants, n, τ_c and N for nylon 6 and PET

Constants	Polymer	
	Nylon 6	PET
n	0.397	0.636
τ_c (dyn cm^{-2})	3.4×10^6	0.965×10^6
N	0.48	0.48

capillaries of radius R; for rectangular openings the capillary length should be increased to $L + Nb$, where b is the shorter side of the rectangle. N is a shear-rate-dependent constant.

For a circular hole, equation (14.32) then becomes

$$Q = \frac{n}{3n+1} \left[\frac{\pi R^3 \tau_c}{\eta_0} \right] \left[\frac{PR}{2(L+2NR)\tau_c} \right]^{1/n}$$

$$\times \left[1 + \frac{1-n}{4n} \left(\frac{PR}{2(L+2NR)\tau_c} \right) \right]^{-(3n+1)/n} \tag{14.40}$$

and equation (14.35) may be rewritten as

$$\tau_c = \left[\frac{n}{3n+1} \times \frac{\pi R^3}{\eta_0 Q} \right]^{n/(1-n)} \left[\frac{PR}{2(L+2NR)} \right]^{1/(1-n)}. \tag{14.41}$$

The pressure, P, thus may be rewritten from equation (14.34) after making a correction for L as

$$P = \frac{2(L+2NR)\tau_c}{R} \left[\frac{3n+1}{n} \times \frac{\eta_0 Q}{\pi R^3 \tau_c} \right]^n. \tag{14.42}$$

N is calculated from equation (14.40) by neglecting the term in the third bracket, as it is much smaller than the other terms. This gives

$$N = \frac{P}{4\tau_c} \left[\frac{n}{3n+1} \times \frac{\pi R^3 \tau_c}{\eta_0 Q} \right]^n - \frac{L}{2R}. \tag{14.43}$$

The non-Newtonian melt flow constants n, τ_c and N were determined for nylon 6 and PET in commercial spinning of circular cross-section yarns; they are listed in Table 14.7.

14.8.8 SOME CASE STUDIES

(a) Case study 1

The objective is to produce a 50 denier/100 filament drawn circular cross-section polyester microfilament yarn from 75 denier/100 filament POY

using a 100 orifice spinneret of orifice diameter 0.18 mm and capillary length 0.50 mm, spun at 3200 m min^{-1} and drawn to a draw ratio 1.50.

It is first necessary to ascertain whether the yarn is spinnable and, if so, to find the pressure required to be maintained.

We proceed as follows. First we estimate the zero shear rate viscosity, η_0, using equation (14.24) and the known characteristics of the PET polymer, namely its IV = 0.610 dl g^{-1}, DEG content = 0.60 wt % and cationic-dyeable component = 0. This gives $\eta_0 = 1554$ poise at 285 °C, which is the spinning temperature. Second, we calculate the volumetric throughput rate as follows. The length of filament being spun per second is 3200/60 m. The denier per drawn (draw ratio = 1.5) filament is 50/100 = 0.5 and hence its spun denier is 0.75, i.e. 9000 m of the spun filament weighs 0.75 g. Remembering that the yarn picks up spin finish and moisture during spin finish application, the polymer weight fraction in the POY may be taken as 0.985 and thus the weight of polymer melt coming out of each orifice per second is

$$W = \frac{0.75 \times 0.985}{9000} \times \frac{3200}{60} \, \text{g s}^{-1}.$$

The volumetric throughput per second (Q) is the weight divided by the density, i.e. 1.161 g cm^{-3}. This gives

$$Q = 3.7707 \times 10^{-3} \, \text{cm}^3 \, \text{s}^{-1} \text{ per orifice.}$$

We next calculate the extrusion velocity as follows. The volume of polymer flowing out per minute per orifice is $3.7707 \times 10^{-3} \times 60 \, \text{cm}^3$. This volume divided by the cross-sectional area ($\pi \times 0.009 \times 0.009 \, \text{cm}^2$) gives the length in cm coming out every minute from the spinneret orifice and comes out to be 889 cm min^{-1} or 8.89 m min^{-1}, which is higher than the minimum speed of 7 m min^{-1} for microfilament yarn spinning. Thus under the conditions stated above, the multifilament yarn is spinnable.

The spinneret plate pressure P can be calculated using equation (14.42) by substituting the following values (including the values in Table 14.7 for PET):

Capillary radius, $R = 0.009$ cm
Length of capillary, $L = 0.05$ cm
Power-law exponent, $n = 0.636$
Critical shear stress, $\tau_c = 0.965 \times 10^6$ dyn cm^{-2}
Constant $N = 0.48$

and comes out to be

$$P = 62.7 \, \text{kgf cm}^{-2} \text{ gauge.}$$

Since the plate pressure is within the normal pressure range of 40–80 kgf cm^{-2}, smooth spinning is possible with no slow orifices due to low pressure and no polymer leakage from the spin pack.

(b) Case study 2

A 50 denier/36 filament bright cationically dyeable trilobal polyester yarn is to be spun via the POY route using the trilobal spinneret shown in Fig. 14.8. The task is to ascertain whether the yarn is spinnable.

In an attempt to answer this question, we first estimate the zero shear rate viscosity, η_0, using equation (14.24) and the known characteristics of the CD PET polymer, namely its IV = 0.51 dl g^{-1}, DEG content = 2 wt %, and cationic-dyeable component = 1.8 mol %. This gives $\eta_0 = 1592$ poise at 285 °C, which is the spinning temperature.

Second, we calculate the volumetric throughput rate as follows. The length of filament being spun per second is 3200/60 m. The denier per drawn (draw ratio = 1.6) filament is 50/36 and hence its spun denier is $50/36 \times 1.6$, which is thus the weight in grams of 9000 m of the filament. The polymer weight fraction in the POY is 0.985 and thus the weight of polymer melt coming out of each orifice per second is

$$W = \frac{50}{36} \times \frac{1.6 \times 0.985}{9000} \times \frac{3200}{60}\ \mathrm{g\,s^{-1}}.$$

The volumetric throughput per second (Q) is the weight divided by the density, i.e. 1.161 g cm^{-3}. This gives

$$Q = 1.1172 \times 10^{-2}\ \mathrm{cm^3\,s^{-1}}\ \text{per orifice.}$$

The cross-sectional area of the trilobal orifice in Fig. 14.8 is 1.5216×10^{-3} cm^2. Therefore, the average polymer melt flow speed at the exit of the orifice is 4.4 m min^{-1}, which is higher than the minimum speed of 4 m min^{-1} for the normal textile denier yarn. This would ensure that the number of filament breaks would not be too high and therefore the yarn is spinnable.

REFERENCES

1. Tai, K., Arai, Y. and Tagawa, T. (1980) *J. Appl. Polym. Sci.*, **25**, 77.
2. Tai, K., Arai, Y. and Tagawa, T. (1982) *J. Appl. Polym. Sci.*, **27**, 731.
3. Matsui, H., Igarashi, N. and Ohsaki, F. (to Teijin), Japanese Patent Tokukai Sho 48-66650 (1973).
4. Inoue, T. (to Toyobo), Japanese Patent Tokuko Sho 58-1133 (1983).
5. Funakata, F. (to Toyobo), Japanese Patent Tokuko Sho 49-40880 (1974).
6. Lofquist, R.A., Saunders, P.R., Tam, T.Y. and Twilley, I.C. (1985) *Textile Res. J.*, **55**, 325.
7. Yamamoto, M. and Nagayasu, N. (1988) *J. Textile Machinery Soc. Japan*, **41**, 109.

8. McIntyre, J.E. (1985) Polyester fibres, in *Handbook of Fibre Science and Technology*, Vol. IV: Fiber Chemistry (eds M. Lewin and Eli M. Pearce), Marcel Dekker Inc., New York, pp. 1–71.
9. McIntyre, J.E. (1974) *Rep. Prog. Appl. Chem.*, **59**, 99.
10. Takeda, T. (1986) *Japanese Textile News*, **385**, 20.
11. *Japanese Textile News*, **391**, (1987) 57.
12. *Japanese Textile News*, **412**, (1989) 67.
13. Teijin Ltd., *Textile Horizons*, June 1989, p. 37.
14. Sujuki, T. and Wada, O. (1985) *Sen-i-Gakkaishi*, **41**, 401.
15. Hirano, Y. (1984) *J. Textile Machinery Soc. Japan*, **37**, 131.
16. Sano, K. *et al.* (to Toray), Japanese Patent Tokuko Sho 47-11280 (1972).
17. *Japanese Textile News* (1986) **385**, 39.
18. Japanese patent (to Teijin), Tokuko Sho 48-27608 (1973).
19. Japanese patent (to Kuraray), Tokukai Sho 55-107512 (1980).
20. Matsui, M. (1988) *J. Textile Machinery Soc., Japan*, **41**, 122.
21. *Japanese Textile News* (1987) **387**, 50.
22. *Japanese Textile News* (1987) **387**, 52.
23. Okamoto, M. (1994) Spinning of ultra-fine fibers, in *Advanced Fiber Spinning Technology* (eds K. Kajiwara and J.E. McIntyre), Woodhead Publishing Ltd, Cambridge, UK, p. 187.
24. Kubo, E. and Watanabe, M. (1994) Spinning for non-wovens, in *Advanced Fiber Spinning Technology* (eds K. Kajiwara and J.E. McIntyre), Woodhead Publishing Ltd, Cambridge, UK, p. 105.
25. Matsui, M. (1994) The spinning of highly aesthetic fibres, in *Advanced Fiber Spinning Technology* (eds K. Kajiwara and J.E. McIntyre), Woodhead Publishing Ltd, Cambridge, UK, p. 115.
26. Reimschuessel, H. (1985) Polyamide fibres, in *Handbook of Fiber Science and Technology*, Vol. IV: Fiber Chemistry (eds M. Lewin and Eli M. Pearce), Marcel Dekker Inc., New York, p. 156.
27. *Japanese Textile News* (1988) **400**, 12.
28. Werny, F. (1985) *Textile Res. J.*, **55**, 686.
29. Laum, H.M. (1979) *Rheol. Acta*, **18**, 478.
30. Mukouyama, E. and Takegawa, A. (1956) *Kobunshi Kagaku*, **13**, 323.
31. Müller, H., Neurary, D. and Horbach, A. (1981) *Makromol. Chem.*, **182**, 177.
32. Gregory, D.R. (1972) *J. Appl. Polym. Sci.*, **16**, 1479.
33. Manaresi, P., Giachetti, E. and Fornasari, E. De (1968) *J. Polym. Sci., Part C*, **16**, 3133.
34. Varma, R.K., Bhuvanesh, Y.C., Gupta, V.B., Manabe, T. and Jalan, R. (1991) *Indian J. Fibre Textile Res.*, **16**, 39.
35. Ravens, D.A.S. and Ward, I.M. (1961) *Trans. Faraday Soc.*, **57**, 150.
36. Hergenrother, W.L. and Nelson, C.J. (1974) *J. Polym. Sci., Polym. Chem. Ed.*, **12**, 2905.
37. McKelvey, J.M. (1962) *Polymer Processing*, John Wiley & Sons, Inc., New York, pp. 32–91.

Acrylic fibres

15

P. Bajaj

15.1 INTRODUCTION

Next to polyester and polyamides, acrylic fibres occupy an eminent position in the family of synthetic fibres. The importance of acrylic fibres has been shown by their phenomenal growth and their popularity throughout the world. Acrylic fibres have replaced wool in many major applications, particularly in hand knitting and hosiery garments. The majority of knitting yarns are usually bulky yarns which go into the manufacture of pullovers, sweaters, socks, etc. Blankets and carpet are other applications where acrylic fibre competes with wool because of its high elasticity, colour brilliancy, voluminosity, ease of washing, resistance to pilling and good light and colour fastness. Because of these properties, and also due to the ease with which modifications can be made during synthesis, spinning and finishing, acrylic fibres have experienced a tremendous growth since their introduction by Du Pont, USA, in 1950.

Acrylic fibres are made using acrylonitrile as one of the major monomers. Among the vinyl monomers, acrylonitrile is the only monomer used for the production of a commodity synthetic fibre. Other vinyl monomers lack cohesive forces between the molecular chains of their polymers and therefore cannot compete with acrylonitrile. The term 'acrylic fibre' refers to a fibre containing at least 85% acrylonitrile monomer, while in modacrylics the percentage of acrylonitrile must be less than 85% but greater than 35%.

15.2 POLYMER MANUFACTURE

Acrylic fibre manufacture requires a polymer with specific composition, controlled molecular weight, and some dye sites. Thus, the polymerization process is an important step in the overall fibre manufacturing process. All acrylic fibres are made from acrylonitrile (90–94%) combined with at least one or two comonomers.

15.2.1 COMONOMERS USED IN ACRYLIC FIBRE MANUFACTURE

The most commonly used comonomers fall into two main categories, neutral comonomers and ionic comonomers.

(a) Neutral comonomers

Neutral monomers such as methyl acrylate (MA), methylmethacrylate (MMA) or vinyl acetate (VA), which enhance the solubility of the polymer in spinning solvents, modify the fibre morphology and improve the rate of diffusion of dyes into the fibre. The amount of neutral comonomer in commercial acrylic fibres varies in the range 3.5–5.5 mol % or 6–10 wt %. All dry-spun acrylic fibres use MA, as VA is expected to reduce the stability of the spinning dope at high temperatures in the spinning tower.

Methyl acrylate (MA)	$H_2C{=}CH{-}COOCH_3$
Methyl methacrylate (MMA)	$H_2C{=}C{-}COOCH_3$
	$\quad\quad\quad\quad\ \ \mid$
	$\quad\quad\quad\quad CH_3$
Vinyl acetate (VA)	$H_2C{=}CHOOC{-}CH_3$
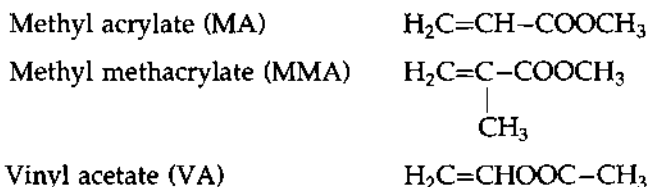
(b) Ionic comonomers

Ionic monomers such as sodium-p-styrene sulphonate, sodium methallyl sulphonate or sodium 2-methyl-2-acrylamido-propane sulphonate are added as comonomers to provide supplemental dye sites and impart differential water sensitivity between the elements in bicomponent fibres [1]. The total number of sulphonate and sulphate sites for dyeing of acrylic fibres with cationic dyes should be around 30–50 meq kg^{-1}.

	$\quad\quad\quad\quad\quad CH_3$
	$\quad\quad\quad\quad\quad\ \ \mid$
Sodium methallyl sulphonate (SMS)	$CH_2{=}C{-}CH_2SO_3Na$
Sodium allyl sulphonate (SAS)	$CH_2{=}CHCH_2SO_3Na$
Sodium styrene sulphonate (SSS)	$CH_2{=}CH{-}C_6H_5{-}SO_3Na$

Sodium 2-methyl-2 acrylamido
propane sulphonate (SAMPS)

$$H_2C=CHCONH-\underset{\underset{CH_3}{|}}{\overset{\overset{CH_3}{|}}{C}}-CH_2SO_3Na$$
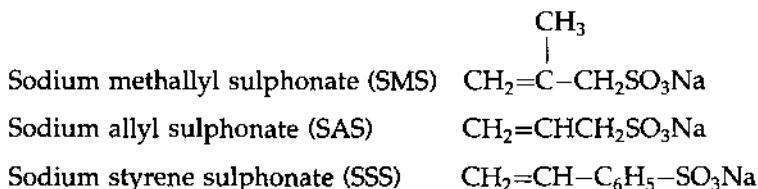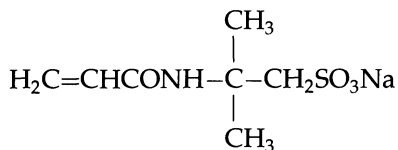
Carboxylic acids such as itaconic, acrylic and methacrylic have also been employed as cationic dye receptors as they partially ionize at dyeing pH. Halogen-containing monomers such as vinyl chloride, vinyl bromide and vinylidene chloride impart flame resistance.

15.2.2 POLYMERIZATION METHODS

Three general methods of polymerization are used commercially, namely the solution, suspension and emulsion methods. Of these, the solution and the suspension methods are most frequently employed for the production of acrylic fibres. A summary of the commercial processes reported by the major acrylic fibre manufacturers [2] is given in Table 15.1.

(a) Solution polymerization

Homogeneous solution polymerization in dimethylformamide (DMF), dimethylacetamide (DMAc), dimethyl sulphoxide (DMSO), and zinc chloride or sodium thiocyanate has the advantage of direct production of spinning dope. However, the problem of achieving high molecular weight products in organic solvents has been overcome by incorporating an aliphatic hydrocarbon into the solvent, by initially performing an emulsion polymerization, and by adding further solvent and completing the reaction as a solution polymerization. Low temperature polymerization has also enabled monomers with highly reactive functional groups to be polymerized successfully. The time required for the polymerization in DMF and DMSO is generally 10–18 h and 2.5–4 h, respectively. However, in aqueous solution of NaSCN (51%) the time required for polymerization usually does not exceed 1.5 h. Thermally active initiators, such as 2,2-azobis-isobutyronitrile (AIBN), ammonium persulphate or benzoyl peroxide, can be used in solution polymerization, but these initiators are slow acting at the temperatures required for producing fibre-grade polymer. A typical half-life of this type of initiator is in the range of 10–20 h at 50–60 °C. Therefore, these initiators are used mainly in batch or semibatch processes, where the reaction is carried out over an extended period. A more active initiator, which also yields sulphonate end groups, is obtained by combining cumyl hydroperoxide and sodium ethylsulphite.

Table 15.1 Commercial processes used by the major acrylic fibre manufacturers [2]

Fibre producers	Trade name	Major comonomer	Spinning method and solvent used	
1. Using aqueous dispersion (suspension) polymerization				
Asahi (Japan)	Cashmilon	MA	Wet	HNO$_3$
Bayer (Germany)	Dralon	MA	Wet	DMAc (Lingen)
			Dry	DMF (Dormagen)
Cydsa (Mexico)	Crysel	VA	Wet	DMF
Courtaulds (UK)	Courtelle	MA	Wet	NaSCN
Cytec (USA)	Creslan	VA	Wet	NaSCN
Daqing (China)	–	MA	Wet	NaSCN
Enichem Fiber (Italy)	–	VA	Wet	DMAc
Hoechst (Germany)	Dolan	MA	Wet	DMF
Hanil (South Korea)	–	MA	Wet	HNO$_3$
Japan Exlan	Exlan	MA	Wet	NaSCN
Kanagafuchi (Japan)	Kanecaron	VCl	Wet	Acetone
Mitsubishi Rayon	Vonnel	VA	Wet	DMAc
Rayon	Finel	MA	Dry	DMF
Monsanto (USA)	Acrilan	VA	Wet	DMAc
Montefibre (Italy)	Leacril	VA	Wet	DMAc
Indian Petrochemicals (IPCL),	Indacryl	MA	Wet	HNO$_3$
India	Supacryl	MA	Dry	DMF
J.K. Synthetics (India)	Jkrylic	VA	Wet	DMAc
Indian Acrylics	Indlon	MA	Dry	DMF
Consolidated Fibers (India)	Concrylon	MA	Wet	NaSCN
2. Using solution polymerization				
Toho Rayon (Japan)	Beslon	MA	Wet	ZnCl$_2$
Toray (Japan)	Toraylon	MA	Wet	DMSO
Pasupati Acrylon (India)	Acrylon	MA	Wet	DMF
Bulana Burgas (Bulgaria)	–	MA	Wet	DMF
Formosa Plastic (Taiwan)	–	MA	Wet	DMF
Mapan (Russia)	–	MA	Wet	DMF

Many of the solvents used for acrylonitrile polymerization are very active in chain transfer reactions. Dimethyl acetamide and DMF both have very high chain transfer constants when compared with acrylonitrile itself (Table 15.2). DMSO and aqueous zinc chloride, in contrast, have relatively low transfer constants; hence the latter solvents are desirable for polymerization reactions. However, several acrylic fibre manufacturers use DMF as a solvent for solution polymerization. A line diagram of the solution polymerization process is shown in Fig. 15.1 [3].

Methyl acrylate (MA) and vinyl acetate (VA) are the two comonomers generally used. Of these, MA is the least active in chain transfer while VA is as active in chain transfer as DMF and DMAc.

In Courtauld's UK patent no. 940 020 of 1963, the use of organic diluents such as acetone, methyl ethyl ketone and aromatic hydrocarbons of low

Table 15.2 Constants for chain transfer in acrylonitrile polymerization[a]

Solvent	Temperature (°C)	$C_s \times 10^{4\,b}$
Acetone	50	1.70
	60	1.13
γ-Butyrolactone	50	0.66
		0.74
N,N-Dimethyl acetamide	50	4.95
		5.05
N,N-Dimethyl formamide	50	1.00
		2.70
		2.83
	60	2.41
		4.49
		5.00
Zinc chloride	50	0.01

Monomer	Temperature (°C)	$C_m \times 10^{4\,b}$
Acrylonitrile	50	0.05
		0.27
	60	0.36
Vinyl acetate	50	4.55
	60	2.60
		2.80
Methyl acrylate	60	0.04
		0.33

[a] Source: Berger, K.C. and Brandrup, G. (1989) In *Polymer Handbook*, 3rd edn, Wiley, New York, Section II, pp. 94–133.
[b] C_s, C_m = chain transfer constant for solvent and monomer, respectively.

chain transfer activity was suggested in conjunction with DMF as the polymerization medium. Details of the polymerization charge are given below:

DMF	70.5 parts
Acetone	20 parts
Acrylonitrile	24 parts
Methyl acrylate	1.6 parts
AIBN	0.5 parts

The mixture is heated to 60 °C for 20 h. The polymer solution obtained has 20 parts of polymer with intrinsic viscosity (IV) of 1.6 dl g^{-1}. When a similar charge without acetone is heated under identical conditions, the polymer solution obtained has only 15.4 parts of polymer with IV of 1.3 dl g^{-1}. This example illustrates how the chain transfer activity of the solvents in solution polymerization influences the rate as well as the degree of polymerization. Tsai and Lin [4] have also reported the use
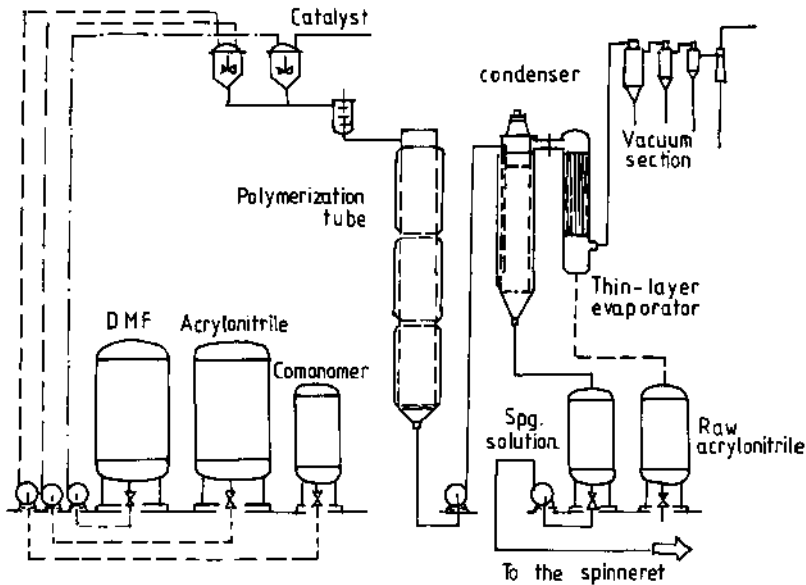
Fig. 15.1 Flow diagram of solution polymerization of acrylonitrile in DMF [3].

of dimethyl sulphoxide and acetone for copolymerization of AN with 2-ethyl hexyl acrylate and itaconic acid at 60 °C using AIBN as the initiator.

In another study [5], the effects of sodium thiocyanate concentration, polymerization temperature and initiator concentration have been described. The polymerization of AN (88% by weight), 12% methyl acrylate and itaconic acid (1.3% on the basis of the monomers) was carried out at temperatures between 70 and 90 °C in 45–55% aqueous NaSCN in the presence of AIBN. It was found that with an increase in the concentration of the aqueous NaSCN solution from 45 to 55% the intrinsic viscosity of the polymer increased. The increase in effective viscosity is related to the decrease in the mobility of the copolymer macroradicals, consequently reducing their collision with one another. This leads to a rise in the molecular weight of the copolymer. Solution polymerization is advantageous as the polymer solution can be converted directly to a spinnable dope by removing unreacted monomer. However, there are some limitations.

• Because of the high chain mobility in solution polymerization, chain termination is quite rapid.
• Incorporation of non-volatile monomers, for example sulphonated monomers, can also be a problem because of their insolubility in organic solvents. Such monomers must be solubilized by converting them to a soluble form, such as amine salts, prior to polymerization.

- Non-volatile monomers are also difficult to recover from the reaction medium since the usual distillation techniques are unsuitable.
- Comonomers such as vinyl acetate and vinyl chloride cannot be incorporated as the reaction rates are low, and polymer colour is inferior.
- The choice of the solvent for polymerization is also limited. If the fibre is to be dry-spun, then the choice is limited to DMF as other organic solvents have very high boiling points.

(b) Aqueous dispersion (suspension) polymerization

The method of polymerization most widely used by the acrylic fibre manufacturers (Table 15.1) is the aqueous suspension method, in which persulphates, perchlorates or hydrogen peroxide are used as radical initiators.

The most common redox system consists of ammonium or potassium persulphate (oxidizer), sodium bisulphite (reducing agent), and ferric or ferrous iron as a catalyst. This system gives the added benefit of supplying the dye sites for the fibre. This redox system works at pH between 2 and 4 where the bisulphite ion predominates. Two main reactions account for radical production:

Reaction I Oxidation of ferrous iron by persulphate

$$S_2O_8^{2-} + Fe^{2+} \rightarrow S\dot{O}_4^1 + SO_4^{2-} + Fe^{3+}.$$

Reaction II Reduction of ferric iron by SO_2 in the bisulphite form

$$HSO_3^{1-} + Fe^{3+} \rightarrow HS\dot{O}_3 + Fe^{2+}.$$
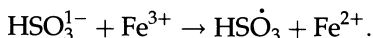
The sulphate radical, thus produced in reaction I, may react further with bisulphite ions to produce more bisulphite radicals:

Reaction III

$$S\dot{O}_4^1 + HSO_3^{1-} \rightarrow SO_4^{2-} + HS\dot{O}_3.$$
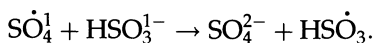
The iron, usually added as ferrous sulphate, is only required in a small quantity (less than 3 ppm) to raise the rate of radical formation.

The dominant initiation reactions in the polymerization of acrylonitrile with persulphate/bisulphite (ammonium or potassium persulphate/sodium metabisulphite) redox system in water are therefore likely to be:

Reaction IV

$$\underset{\overset{\|}{O}}{\overset{O}{\|}}\quad HO-\overset{O}{\underset{\overset{\|}{O}}{\overset{\|}{S}}}{}^{\bullet} + H_2C{=}\underset{CN}{\overset{|}{C}}H \rightarrow HO-\overset{O}{\underset{\overset{\|}{O}}{\overset{\|}{S}}}-CH_2-\underset{CN}{\overset{\bullet}{\overset{|}{C}}H}$$

Reaction V

$$-O-\overset{\overset{\displaystyle O}{\|}}{\underset{\underset{\displaystyle O}{\|}}{S}}-\overset{\bullet}{O} + H_2C=\underset{\underset{\displaystyle CN}{|}}{CH} \rightarrow -O-\overset{\overset{\displaystyle O}{\|}}{\underset{\underset{\displaystyle O}{\|}}{S}}-O-CH_2-\underset{\underset{\displaystyle CN}{|}}{\overset{\bullet}{C}H}$$

Reaction VI

$$H\overset{\bullet}{O} + H_2C=\underset{\underset{\displaystyle CN}{|}}{CH} \rightarrow HO-CH_2-\underset{\underset{\displaystyle CN}{|}}{\overset{\bullet}{C}H}$$
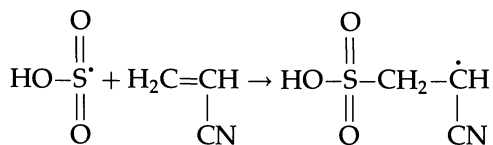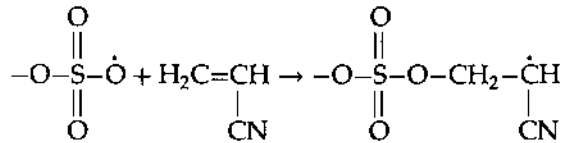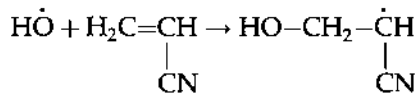
These reactions (IV–VI) would give rise to polyacrylonitrile chains with sulphonate, sulphate and hydroxyl end groups, respectively.

The propagation step is very fast, with a rate constant (R_p) in the range of $30\,000\,l\,mol^{-1}\,s^{-1}$ for dispersion polymerization and $3000\,l\,mol^{-1}\,s^{-1}$ for solution polymerization [6].

The initiation and primary radical growth steps occur in the aqueous phase. Polymer radicals in the aqueous phase may follow either of two routes as shown in Fig. 15.2. Chain growth is limited in the aqueous phase, however, because the monomer concentration is normally very low and the polymer is insoluble in water. If many polymer particles are present, as is the case in commercial continuous polymerizations, the aqueous radicals are likely to be captured on the particle surface by a sorption mechanism. The particle surface then becomes swollen with monomer. The polymerization continues in the swollen layer and the sorption becomes irreversible as the chain end grows into the particle.
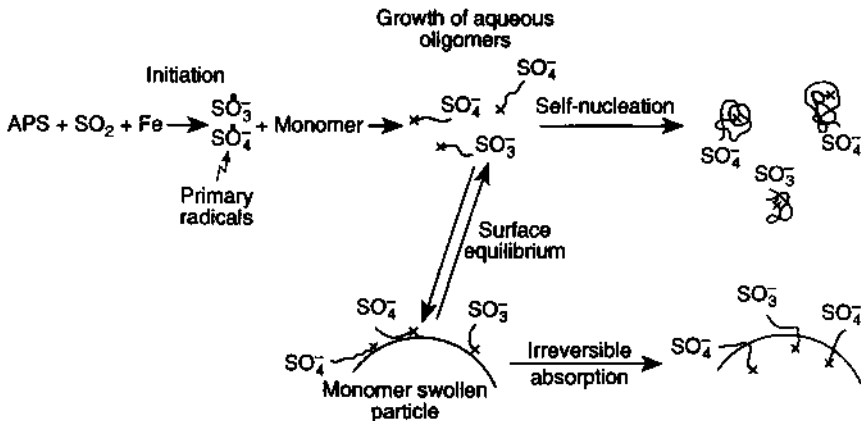
Fig. 15.2 Schematic depiction of particle nucleation and radical absorption during the aqueous dispersion polymerization of acrylonitrile. APS = ammonium persulphate [2].

Termination reactions may occur by the following mechanisms in acrylonitrile polymerization:

Reaction VII   By radical recombination

$$\dot{P}_a + \dot{P}_b \rightarrow P_a - P_b.$$
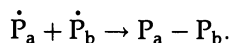
Reaction VIII   By chain transfer through reagents

$$\dot{P}_a + X-Y \rightarrow P_a-Y + \dot{X}.$$
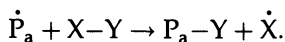
where Y is usually H. Thus

$$HSO_3^- + \dot{P}_n \rightarrow S\dot{O}_3^- + P_nH.$$
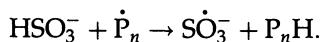
In most commercial processes, chain transfer agents are used to control the molecular weight and also to provide supplemental dye sites. Bisulphite ion, in addition to the reducing agent, is used as a chain transfer agent (reaction VIII). Molar ratios of bisulphite to persulphate of greater than one are generally used in commercial aqueous suspension polymerization.

Ebdon, Huckerby and Hunter [7] have examined the polyacrylonitrile prepared by aqueous free radical slurry polymerization using the potassium persulphate/sodium bisulphite redox initiator at 40 °C by Fourier transform IR (FTIR) and high field ^{13}C and ^{1}H NMR spectroscopy. They have shown the presence of sulphonate and non-sulphur-containing end groups derived principally from initiation by bisulphite radicals and transfer to the bisulphite ion (reactions IV–VI). Some sulphate end groups are also present, although in much smaller amounts than the sulphonate end groups. The ratio of bisulphite to persulphate in the polymerization bath has a considerable effect on the dye sites of the polymer.

(c) Commercial process – continuous aqueous dispersion process

A monomer mixture composed of acrylonitrile and up to 6–10 wt % neutral comonomer, such as methyl acrylate or vinyl acetate, and 0.1–1 wt % sodium methallyl sulphonate or other anionic comonomer is fed continuously. Polymerization is initiated by feeding aqueous solutions of potassium persulphate, sulphur dioxide (reducing agent), ferrous iron (promoter), and sodium bicarbonate (buffering agent). The water/monomer feed ratio could vary from 3 to 5 in such a manner that the dwell time in the reactor is between 40 and 120 min (Fig. 15.3). The product stream, an aqueous slurry of polymer particles, is mixed with ethylene diamine tetra-acetic acid (EDTA.4Na) or oxalic acid as a chain stopper by forming the iron chelate. The resulting slurry is filtered. The polymer cake is washed to remove the salts and impurities, then dried in
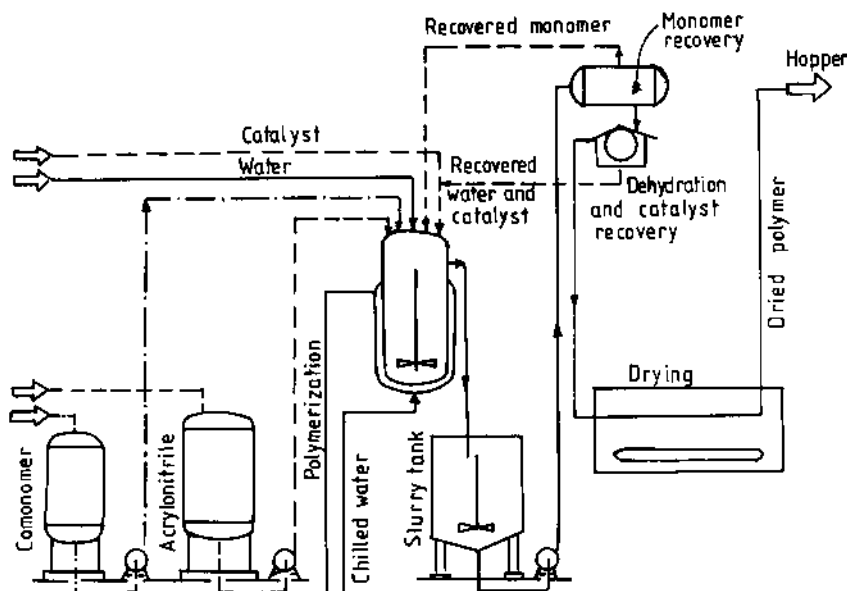
Fig. 15.3 Flow diagram for aqueous suspension polymerization of acrylonitrile.

granulate form and milled. The particle size of the powder should not exceed 200 μm. The wash waters are distilled to recover the unreacted monomers for recycling. Polymerization in water offers the advantage of a high reaction rate, thereby allowing smaller reactors to be used at high productivity levels. Furthermore it is possible to prepare polymer dopes of the high concentration required in dry-spinning. On the other hand, there is a disadvantage of having to set up a fairly complex and costly plant for washing, drying, milling and dissolving the polymer in a solvent. This last operation in particular calls for special attention, since polyacrylonitrile powders tend to form swollen lumps which are difficult to dissolve. Sometimes drying of the polymer could result in dust explosions; adequate precautions must therefore be taken.

15.3 INFLUENCE OF POLYMERIZATION CONDITIONS ON PROPERTIES OF ACRYLIC POLYMER

The molecular weight and the dye sites vary, depending on the following parameters: (1) water/monomer ratio; (2) SO_2/persulphate ratio; (3) reactor temperature; (4) dwell time; (5) pH of the reactor slurry; (6) amount of Fe^{2+} with respect to monomer weight; (7) addition of chainstopper agent; and (8) spinning rate of the agitator. Typical fibre-forming acrylic polymers have $\bar{M}_n$ in the range 45 000–60 000, or say 1000 repeat units, and the $\bar{M}_w$ is in the range 90 000—140 000, with a polydispersity

Table 15.3 Data on number of strong acid groups (SAG eq mol^{-1}) and $\bar{M}_n$ of the polymer prepared under various polymerization conditions[a] [8]

Polymerization conditions				Polymer characteristics			
Water/monomer (wt ratio)	Dwell time (min)	SO$_2$/KPS (mol ratio)	Temperature (°C)	VAc (%)	SAG (×10^5 Eq g^{-1})	$\bar{M}_n$ × 10^{-4}	SAG (eq mol^{-1})
4.0	60	10	50	7.02	3.63	2.51	0.91
2.5	70	10	50	7.13	4.42	2.07	0.91
3.0	60	10	50	7.60	3.88	2.11	0.82
3.0	60	10	60	7.19	4.35	2.18	0.95
3.0	60	4.3	50	7.30	3.87	1.95	0.75
2.0	82	10	50	7.06	3.97	2.60	1.03
2.0	82	10	60	7.04	4.08	2.10	0.86
1.75	89	10	50	7.17	3.82	2.60	0.99
1.75	89	10	60	7.12	4.05	2.02	0.82
1.75	89	4.3	50	6.51	3.91	2.29	0.90

[a]Molar ratio of SO$_2$ to NaHCO$_3$ = 1.3, pH of the polymerization solution = 3, Fe^{2+} = 4 ppm/wt of monomer, $\bar{M}_n$ by osmometry.

index between 1.5 and 3.0. The fibre dyeability is also critically dependent on the molecular weight distribution of the polymer. Since most acrylic fibres derive their dyeability from sulphonate and sulphate initiator fragments at the polymer chain ends, the dye site content of the fibre is therefore inversely related to the $\bar{M}_n$ of the polymer and is very sensitive to the fraction of low molecular weight polymer.

Ito, Okada and Kamada [8] determined the number average molecular weight ($\bar{M}_n$) and strong acid end groups (SAG) of fractionated polymers of AN-vinyl acetate copolymers which were prepared by continuous polymerization in aqueous medium with the persulphate–bisulphite redox system. Average number of SAG per polymer chain was found to be close to unity under the given polymerization conditions (Table 15.3) and the proportion of sulphoxy end groups to SAG was estimated to be around 0.5–0.6. Based on these results, the authors consider the termination reaction to be primarily through disproportionation and transfer to the bisulphite ion.

15.3.1 MOLECULAR DEFECTS GENERATED DURING RADICAL POLYMERIZATION

Two mechanisms specific to branching of PAN have been proposed. Ulbricht [9], in a study of acrylonitrile polymerization in magnesium perchlorate, suggested that branching may occur by a reaction in which a growing radical chain abstracts a hydrogen atom from an α-carbon atom, thereby satisfying a side chain by monomer addition. It was shown that branching occurs when the ratio of polymer to monomer content is greater than one; that is, one branching occurs for every 2000 growth steps.

Peebles and co-workers [10,11], however, reported that branching occurs during polymerization through the nitrile group. They observed the presence of an unusual structure in PAN due to a side chain reaction during polymerization branching that results in a defect in the structure of PAN. It can also occur as a result of radical transfer by disproportionation or other chain transfer reactions. Any reaction that leaves a terminal double bond can lead to long-chain branching if the double bond subsequently reacts with the growing polymer radical. Branching through $C\equiv N$ gives an imine-type radical, which can either continue to grow or combine with a monomer molecule, resulting in a stable enaminonitrile structure or an imine structure. Ketonitrile structure may also occur if polymerization conditions favour hydrolysis of the nitrile group (Fig. 15.4).

It has been reported [12] that enamine formation is high when the content of acrylonitrile is low in the polymerization medium. However, the type and concentration of initiator do not have any effect on the
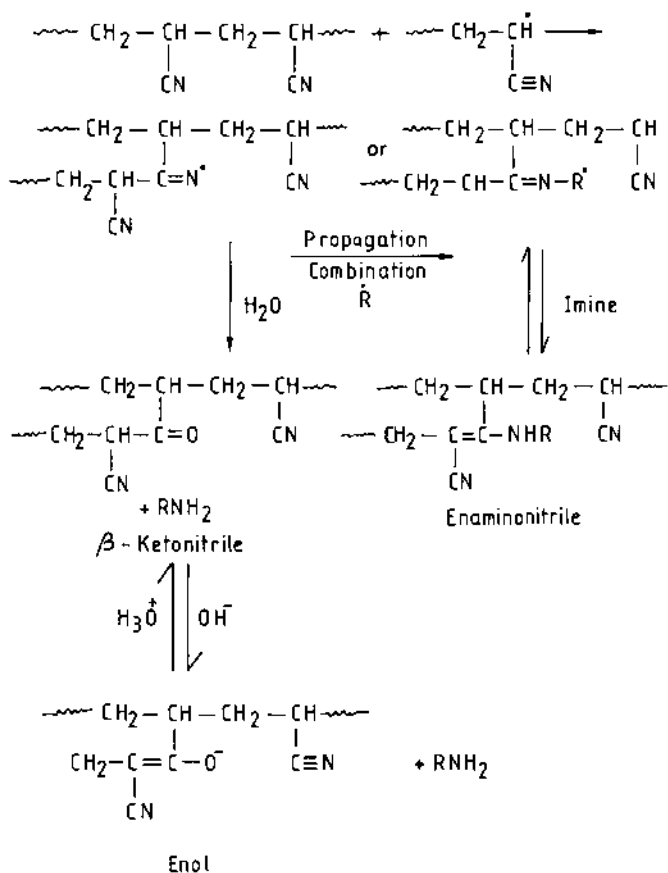
Fig. 15.4 Structural defects generated in polyacrylonitrile through branching [12].

number of defects at low conversion range up to 15%. The concentration of the enaminonitrile group in the polymer remains almost constant during polymerization. Evidence of the presence of β-ketonitrile defects in polyacrylonitrile has also been investigated [13].

There are two more studies on the influence of polymerization conditions on the generation of molecular defects in polyacrylonitrile by thermal analysis [14, 15]. It is well known that polyacrylonitrile undergoes an exothermic reaction due to nitrile oligomerization when heated in an inert atmosphere. A wide variation has been found in the peak temperature, T_{pk}, of the exothermic peak due to nitrile oligomerization: solution polymer (250–275 °C), bulk polymer (260 °C), redox polymer (265–305 °C) and anionic polymer (295–310 °C). These differences in T_{pk} are explained on the basis of certain functional groups in the molecule which initiate the exothermic reaction, e.g. (1) a solvent fragment in the
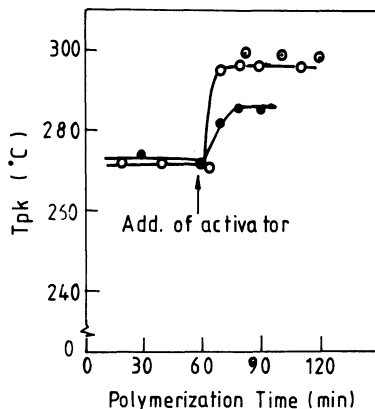
Fig. 15.5 Addition effect of activator on T_{pk} and post-heating effect. Post-heating temperature: • = 50 °C; o, ● = 75 °C [14].

solution polymerization, (2) enaminonitrile for the bulk polymer, and (3) stable and inactive β-ketonitrile for the redox polymer produced in an aqueous medium or under suitable hydrolysis conditions. High T_{pk} of aqueous redox slurry polymer has been explained in terms of the effective inhibition of branch formation due to strong and rapid chain transfer reaction to the activator. It is assumed that on the addition of activator transfer reactions, namely hydrogen abstraction and activator capture, prevail over side chain and main chain branching. Consequently, branching is effectively restrained.

The effect of activator on T_{pk} and post-heating effect is shown in Fig. 15.5 [14]. An apparent rise in T_{pk} following the addition of activator appears to be due to the new forms of the aqueous redox component of low molecular weight giving rise to higher T_{pk}. The effect of temperature (50 and 75 °C) can also be interpreted in relation to this mechanism, i.e. the increase of the latter component in the mixture at higher tempera-ture. In fact, from the observation of the polymerization process, a change to a milky water phase after the addition of the activator was noticed and a newly formed redox component was confirmed. There-fore, one may say that the sample is composed of a physical mixture of two kinds of polymers formed by different mechanisms. Both compo-nents, i.e. primary (initially of flake form) and secondary (newly formed fine particles) forms, can be separated mechanically by decanta-tion as they differ in their sedimentation rates. Differential scanning calorimetry (DSC) studies showed that the mixture produced only one peak in every case, while after the separation, each component showed its own peak. In spite of the physical mixture, two peaks are not observed, perhaps due to intramolecular reaction in addition to

intermolecular cohesion factors in the solid amorphous phase, and the possibility of ion–dipolar bond formation as a result of strong ionization of a redox sample.

On the basis of these studies, it can be concluded that optimization of the polymerization conditions is necessary to obtain the desired molecular weight, dye sites, and to produce a polymer with a smooth performance in the spinning line.

Another study [16] supports the idea that the molecular weight distribution (MWD) is related to the particle size distribution of acrylonitrile polymer produced by suspension polymerization using the persulphate–bisulphite redox system. In this study the particle size distribution was varied by adding varying amounts of an activator which also acted as a coagulant (electrolyte) to the reaction mixture. The results show that the MWD of the polymer narrows with a decrease in the degree of coagulation of the PAN suspension by reducing the activator content, and the MWD of the polymer broadens with an increase in the probability of recombination termination reaction.

15.4 CHARACTERIZATION OF ACRYLONITRILE POLYMERS

The glass transition temperature of PAN and other fibre-forming acrylonitrile copolymers is not typical of glassy amorphous polymers, probably because of their unique structure. Two glass transitions have been observed, one occurring at about 80–100 °C and the other at about 140–160 °C. Andrews and Kimmel [17] have proposed the concept of a heterobonded solid state structure to explain these transitions. According to them the transition at the lower temperature is the result of chain mobility caused by weakening of the van der Waals forces, while the transition at the higher temperature has been attributed to intermolecular dipole–dipole dissociation of the nitrile groups in more localized sections of the chain. On the other hand, Okajima, Ikeda and Takeuchi [18] ascribed the lower transition to the molecular motion in the amorphous phase, and the higher transition to the molecular motion in the crystalline region.

Dielectric studies on PAN and acrylonitrile copolymers in the frequency range 0.1–1.00 kHz showed a tan δ peak at between 110 and 140 °C for PAN, while in copolymers the peak temperature and peak heights depend sensitively on the composition of copolymers [19,20]. The relevant data from DSC scans in the T_g region are shown in Fig. 15.6 for a series of AN/VA copolymers. The T_g appears to be relatively insensitive to vinyl acetate (VA) at low levels of incorporation, i.e. less than 10% by weight. However, at higher levels of VA, the T_g does begin to decrease. A heat capacity change is also observed upon passing through the T_g region in copolymers. The increase in heat capacity for
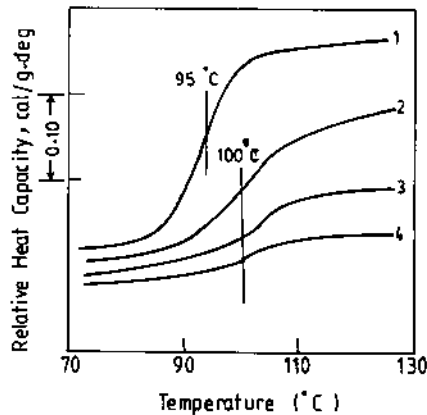
Fig. 15.6 Differential scanning calorimetric traces of glass transition temperature for acrylonitrile/vinyl acetate copolymers: 1, 21.7% VA; 2, 11% VA; 3, 4% VA; and 4, PAN [1].

the PAN homopolymer is approximately 0.03 cal g^{-1}, whereas in most of the glassy polymers the value is 0.06–0.07 cal g^{-1}. The lower value for PAN is due to its internal structure, which is highly constrained through lateral bonding. It is assumed that the most highly bonded chain segments are not able to participate in the T_g region and only the less ordered regions contribute to the increase in heat capacity. Introduction of vinyl acetate, however, loosens the structure and increases the number of chain segments participating in the T_g region.

The effect of water on the glass transition of acrylonitrile polymers is quite pronounced. The T_g of a copolymer having 7% VA decreases from 100 to 64 °C in the wet state (Fig. 15.7).
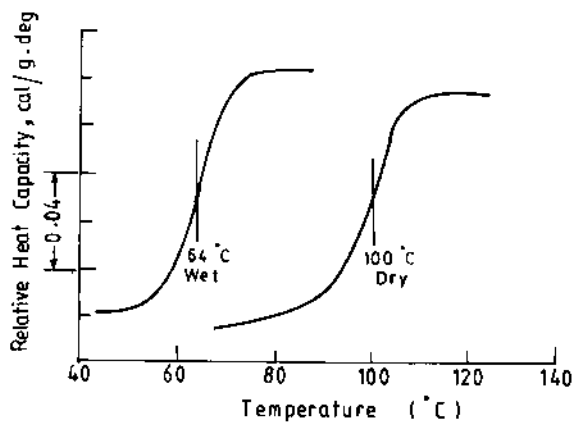
Fig. 15.7 Influence of water on the glass transition temperature of an acrylonitrile/vinyl acetate copolymer containing 7% VA [1].

The melting point, T_m, of dry polyacrylonitrile has been estimated to be close to 320 °C. The polymer degrades or undergoes a cyclization reaction before reaching its melting point. However, at higher heating rates in excess of 80 °C min^{-1}, the melting endotherm of PAN occurs at around 340 °C (Fig. 15.8).
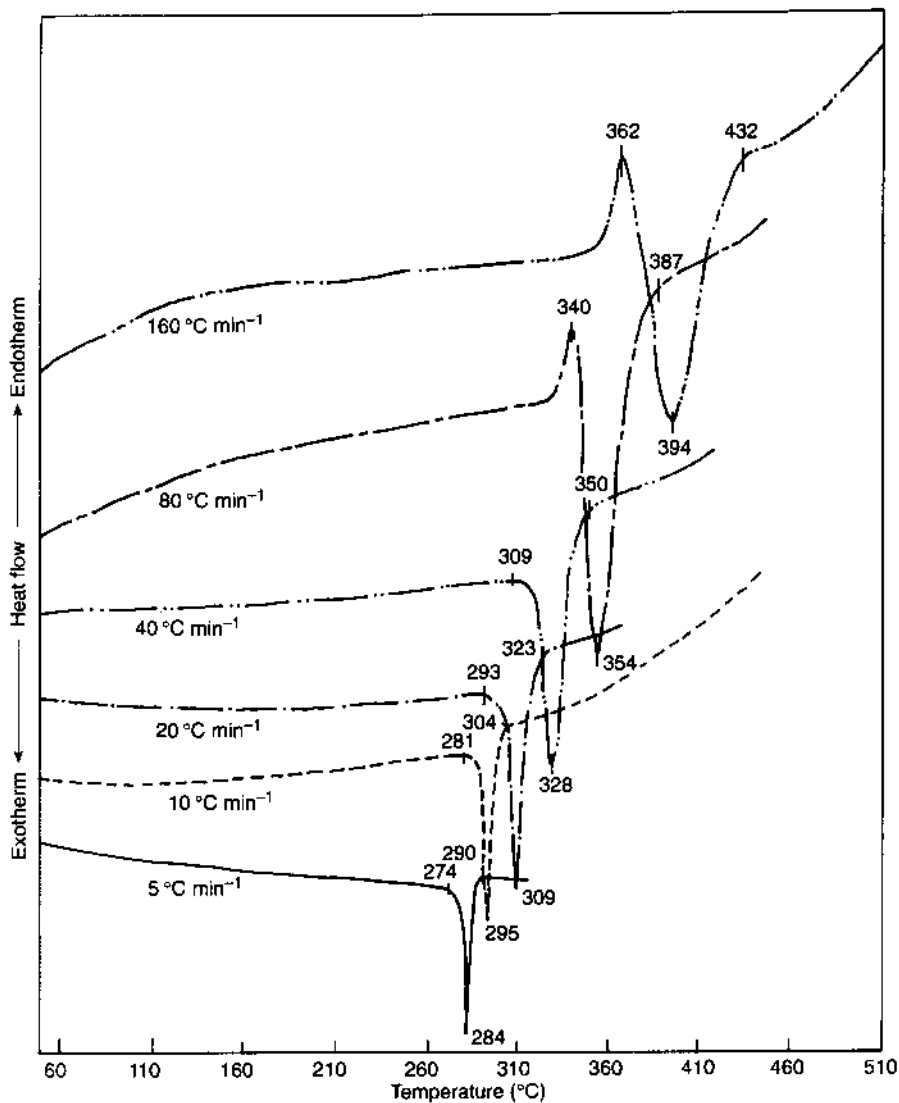
Fig. 15.8 Differential scanning calorimetric traces of PAN under different heating rates in nitrogen atmosphere.
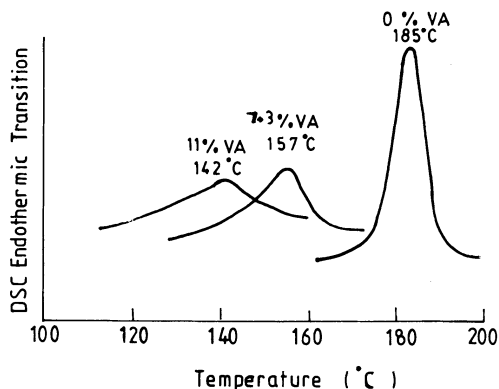
Fig. 15.9 Melting endotherms of acrylonitrile/vinyl acetate copolymer. The polymers were mixed with water (one part polymer: two part water) and sealed in a special high pressure DSC capsule [21].

In a novel thermal analytical technique [21, 22], water was used to depress the melting point and effectively avoid the thermal degradation of acrylonitrile polymers prior to the onset of melting endotherm. In this technique, the acrylic polymer is mixed with water and sealed in a special stainless steel capsule that fits in the sample holder of a Perkin–Elmer DSC II. The capsule must be capable of withstanding the vapour pressure of water up to 200 °C. It was observed that the T_m of PAN decreased from 320 to 185 °C when the percentage of water (based on polymer) was increased from zero to 35% or higher. An amount of water greater than 35% forms an inert phase which does not suppress the melting point any further. The results also show that with increasing comonomer content, the melting point reduces significantly (Fig. 15.9).

Samples of PAN synthesized by different methods have densities in the range 1.17–1.18 $g cm^{-3}$ at 25 °C. Because of its diffuse X-ray diffraction pattern and very small volume change on melting, PAN has been considered to be a crystalline polymer with a low degree of crystallinity. A good deal of controversy exists in the literature as regards the crystal structure and molecular chain conformations of PAN. A number of authors [23–25] favour a model based on two-dimensional order. The lateral order of PAN is generally attributed to the dipolar intramolecular repulsions. But a number of researchers have shown through X-ray and electron diffraction that PAN crystallizes and has a three-dimensional order [20, 26]. Thomsen, Zachmann and Korte [27] have, however, concluded from NMR studies that a single-phase model rather than a two-phase model is more adequate to describe the structure of PAN. Imai *et al.* [28] have shown that PAN can be atactic, isotactic or syndiotactic, depending on its method of preparation. According to Minagawa *et al.*,

radically initiated polymer has nearly an atactic configuration while polymerization of AN induced by γ-ray irradiation in a urea canal complex has predominantly isotactic configuration [29]. Configurational sequence lengths and tacticity in PAN and AN copolymers have been calculated by ^{13}C NMR [30]. The spectra reveal that PAN prepared in water medium using the persulphate–bisulphite redox initiator has a greater percentage of isotactic units (33.4%) than PAN prepared in water–acetone (2:1 v/v) medium (28.3%). Henrichsen and Orth [31] reported that syndiotactic PAN crystallizes in planar zigzag conformation, while Colvin and Storr [32] established the conformation of crystalline PAN as a helix with four monomer units per crystallographic repeat. Hobson and Windle [33] have shown that commercial polyacrylonitrile is predominantly an atactic polymer with a concentration of syndiotactic diads of 0.46–0.48 and crystallinity of about 30%. An explanation that accounts for this apparent paradox is proposed in terms of the formation of crystals from mixed tacticity chains, in which isotactic sequences of an even number of monomer units cocrystallize with planar zigzag syndiotactic units. Thus tacticity greatly affects the intensity ratio of the two principal reflections. Joh [34] succeeded in resolving the principal reflection in X-ray powder diffraction scans (Fig. 15.10).

Minagawa *et al.* [35] have studied the dissolution behaviour of highly isotactic PAN in DMF in comparison with that of an atactic sample. Sharp diffraction characteristics with a reduced half-width value of isotactic PAN have also been reported by Turska and Grobelny [36].
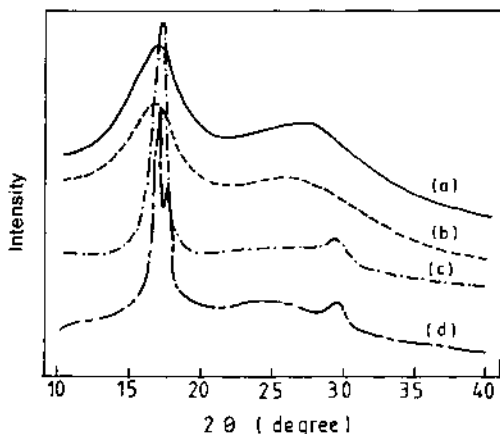
Fig. 15.10 The X-ray diffraction scans for: (a) amorphous polyacrylonitrile as-polymerized; (b) this polymer heat-treated at 180 °C for 3 min in an air oven; (c) hexagonal crystalline form obtained from conventional PAN; (d) an orthorhombic form obtained from the single crystal lamella mats of conventional PAN grown from 0.2% propylene carbonate solution at 90 °C [34].

Furthermore, careful observation has revealed that the diffraction angle of the main peak at 17° (2θ) varies slightly according to the difference in the isotacticity of PAN. Infrared characteristic absorption bands (1250 and 1230 cm^{-1}) of PAN also showed similar results.

Interesting X-ray studies on PAN plasticized with propylene carbonate also indicated the presence of crystallites [37]. It has been postulated that the solvent may be incorporated in the crystalline lattice by dipolar interactions between the carbonyl group of the propylene carbonate and the nitrile groups of the PAN. Further work has demonstrated that compression-moulded gel films can be remelted and drawn uniaxially or biaxially to give oriented films, using the phenomenon of flow-induced chain extension and crystallization [38].

15.5 SPINNING PROCESSES

The spinning process most commonly used for the production of acrylic fibres is solution-spinning through both routes, namely wet- and dry-spinning. Acrylic and modacrylic fibres cannot be melt-spun because they degrade when heated near their melting point. However, some work has been conducted on the melt-spinning of acrylic polymers by decreasing the T_m with the help of some plasticizers or a solvent. As stated earlier, the melting point of acrylic polymers can also be depressed by the addition of water, though under pressure. Apparently, when the polymer–water mixture contains enough water to hydrate some of the nitrile groups, the melt can be extruded, provided one gets a stable phase of molten polymer.

15.5.1 WET-SPINNING

In this process, the spinning dope is extruded through a multiple-hole spinneret into a coagulation bath containing a non-solvent. The jets of dope quickly become coagulated into solid filaments that are continuously removed from the spin bath and subsequently washed free of solvent in hot water and then subjected to drawing, drying, crimping and annealing. The linear speed of the fibre is very low in comparison with the speeds achieved in melt-spinning. So, in order to achieve high productivity multiple spinnerets, each having many thousands of holes, are used and the filaments from several spinnerets are often combined to form a single fibre tow.

The process of wet-spinning involves dope preparation, extrusion of the dope, fibre coagulation and tow processing; these operations, together with some basic rheological principles involved, will be briefly described.

(a) Dope preparation

Dimethyl formamide is one of the commonly used commercial spinning solvents. Other good solvents are dimethyl acetamide (DMAc) and dimethylsulphoxide (DMSO). Acrylic polymer can also be dissolved in concentrated aqueous solutions of some inorganic solvents and salts, for example zinc chloride, sodium thiocyanate and nitric acid. Typical solvents and polymer concentrations for making a dope are listed below:

Solvent	*Polymer concentration (wt %)*
Organic (dry-spun)	25–32
Organic (wet-spun)	20–28
NaSCN (45–55% in water)	10–15
$ZnCl_2$ (55–65% in water)	8–12
HNO_3 (65–75% in water)	8–12
Ethylene carbonate	15–18

Solubility and solution properties are largely dependent on the polymer composition and its molecular weight. A typical spinning dope viscosity would be around 500 poise.

In the case of solution polymerization, the same solvent is used for polymerization and spinning, but in heterogeneous aqueous polymerization, the polymer is usually recovered by filtration in the form of a wet polymer cake. If the spinning dope solvent is an aqueous salt solution, then the wet polymer can be dissolved directly without drying or after drying the polymer.

Preparation of the dope is a very delicate operation, as lumps of acrylic polymer tend to form. These swell externally in the solvent, say dimethyl acetamide, and prevent the dissolution of the polymer within. It is therefore recommended that a finely divided polymer should be added to the solvent at 0–5 °C. The cool mixture is stirred vigorously to form a uniform suspension. When heated to 90–100 °C, the suspension changes to a clear solution and an almost colourless viscous liquid is produced for spinning.

When nitric acid is used as a solvent, the temperature of the dope should not be allowed to increase beyond −5 °C, to avoid polymer decomposition. PAN homopolymer is rarely used for fibre spinning and virtually all commercial acrylic fibres are spun from acrylonitrile polymers containing 5–10% comonomer; AN copolymers are much more soluble in comparison with PAN and make the preparation and storage of the spinning dopes much easier. The resulting fibre is also more extensible and less prone to fibrillation.

A large number of organic additives have been recommended by Gupta and Sharma [39] to inhibit the discoloration of acrylic polymers. A mixture of oxalic acid and maleic anhydride (2% based on the polymer

weight) in the dope has been found to be an effective stabilizer for inhibition of discoloration.

Another important factor which influences the dope viscosity is the gelation rate of the dope. PAN dopes tend to gel upon standing, but this gelation is reversible. When the gelled dope is heated above a specific temperature, the gel melts and the dope reverts back to a viscous solution. The rate at which the liquid dope would gel at room temperature and the melting point of gel are influenced by the polymer composition and its concentration in the dope. Dope made from PAN homopolymer gels very quickly but the addition of comonomers tends to decrease the gelation rate and make the dope easier to handle.

With all other spinning variables held constant, increasing dope solids improve the homogeneity of the fibre structure by reducing the formation of large voids, without any change in the cross-sectional shape of the fibre.

Prasad [40] has reported the effect of lithium chloride (up to 5%) on the dope viscosity and fibre properties of the wet-spun acrylic fibres produced from acrylonitrile, vinyl acetate/sodium methallyl sulphonate terpolymer. It was established that the dope viscosity decreases with an increase in the lithium chloride concentration. It is therefore possible to prepare acrylic dopes with higher solids content (25–32%) and to spin them into filaments without impairing the fibre properties, through the addition of lithium chloride. Furthermore, acrylic dope containing LiCl even at high solids content can be stored at lower temperature for long periods without gelling.

Like other polymer solutions, PAN spinning dope is viscoelastic and, as discussed in Chapter 3, the fine jet or stream of dope would show an expansion when extruded from the spinneret. This expansion is directly proportional to the flow speed of the spinning dope and inversely proportional to the size of the orifice. In industrial production of acrylic fibres, as the spinning speed and spinneret are fixed, the expansion phenomenon would be inversely proportional to the temperature of the dope to be extruded. By increasing the number of holes in the spinneret to say 90 000 and decreasing the distance between the holes under the same spinning conditions, the possibility of sticky fibre formation becomes greater. In order to overcome this problem it is necessary to raise the temperature of the spinning dope; this would reduce fluid elasticity and minimize the expansion effect as well as prevent sticky fibre formation.

(b) Fibre extrusion

In wet-spinning (Fig. 6.4 in Chapter 6) the degassed and filtered dope containing 10–25% polymer is extruded through spinnerets with 10 000–60 000 holes, the hole size ranging from 0.05 to 0.38 mm. Spinnerets with

90 000–130 000 holes are also used. The dope is extruded through a spin-neret capillary into a liquid bath containing coagulant. It is necessary to note that the polymer is not soluble in the coagulant, but the coagulant is miscible with the spinning dope solvent. Fibre formation occurs rapidly as the polymer in the fluid filament coagulates, and is drawn out of the bath for subsequent tow processing. Several spinnerets can be located in a single coagulation bath and the filaments from each spinneret are combined to form a single large tow on the first take-up roll. The linear speeds in the coagulation bath are quite low (3–20 m min^{-1}), but this has the advantage of allowing the subsequent processes (washing, stretch-ing, finishing, drying, cutting, baling or tow packaging) to be effected continuously. The final speed is generally 35–70 m min^{-1}, but in most modern plants it is over 100 m min^{-1} [41].

The fibre denier per filament (weight in g per 9000 m) is calculated by mass balance and is given by the following equation [41]:

$$\text{den/filament} = \frac{9672 \times dc_f Q}{SV} \tag{15.1}$$

where d is the spinning dope density in g l^{-1}, c_f is the polymer concen-tration in the dope expressed as a weight fraction, Q is the volumetric flow rate per spinneret hole in l s^{-1}, S is the overall stretch ratio includ-ing any relaxation, and V is the first roll speed expressed as the linear speed in m s^{-1} at the exit of the coagulation bath.

(c) Optimization of spinning parameters

The factors which affect the spinnability and the mechanism of fibre breakage in the wet-spinning process are coagulation bath composition, coagulation temperature, extrusion rate and take-up velocity. Coagula-tion bath composition and concentration are important because they determine the rate of coagulation, skin formation, free velocity and maxi-mum jet stretch, and tensile stress. Temperature is important primarily because it affects the structural viscosity of the spinning solution; thus the main effect of coagulation bath temperature is upon tensile stress and jet stretch rather than upon coagulation rate. Jet stretch is actually a measure of the filament residence time in the bath; the larger the jet stretch, the shorter will be the filament residence time. Under optimum conditions of temperature and bath concentration, the jet stretch may be considered as an independent variable.

Han and Segal [42] have studied in depth the problem of spinnability using a dope based on aqueous polymer solution consisting of approxi-mately 10% polyacrylonitrile of molecular weight around 100 000 g mol^{-1} and 40% NaSCN. The coagulating bath ranged in concentration from 0% through 25% NaSCN in water at a temperature of 20 °C. Experiments

were performed at temperatures of 0, 20 and 40 °C. The jet stretch $(V_1/\langle V \rangle)$, i.e. the ratio of the speed at which the fibre leaves the spin bath (V_1) to the theoretical speed of the dope within the spinneret capillary $(\langle V \rangle)$, was varied till the thread broke down.

In the wet-spinning of the fibres, the total measured take-up force, F_{tot}, is usually a sum of several forces, the primary components of which are the rheological force, F_{rheo}, and the drag force, F_{drag}. F_{rheo} is the force required for the deformation of a thread, and it is related to the axial stress component, σ_{xx}, and to the elongational viscosity, η_E, through the following equation:

$$F_{rheo}/A(x) = \sigma_{xx}(X) = \eta_E \, dV(x)/dx \qquad (15.2)$$

where $dV(x)/dx$ is the axial velocity gradient and $A(x)$ is the cross-sectional area of the thread line.

Thus F_{rheo} is applicable only in the region where the value of axial velocity gradient is non-zero. Moreover, F_{rheo} is considered to be a constant through the length of the fibre, where the latter condition holds but F_{drag} is considered to be dependent upon the distance x from the spinneret exit [42]. Physically, F_{rheo} may be considered as an internal force while F_{drag} is an external force. Other less important external forces in the wet-spinning line are due to the accelerating mass of the filament, and surface tension forces (which are significant only in the dry- or melt-spinning process); these are grouped together with F_{drag} in the following force balance equation:

$$F_{tot}(x) = F_{rheo} + F_{coag}(x) \qquad (15.3)$$

where F_{coag} is the sum of all the external force components.

At a fixed distance from the spinneret, F_{tot} is found to increase with jet stretch (Fig. 15.11). Furthermore, at constant jet stretch, F_{tot} will also increase as the distance from the spinneret is increased. Extrapolation to $x = 0$ gives F_{rheo}. It has also been shown that F_{rheo} increases as temperature decreases from 40 to 0 °C, but it decreases as the coagulation bath concentration increases in the range 10–20% NaSCN.

It is desirable to measure the elongational viscosity for different spinneret hole sizes at the condition of 'minimum hardening'. It may be noted that the values of elongational viscosity at the spinneret exit (i.e. $x = 0$) correspond to the point where hardening effects are minimized, hence the elongational viscosities at this position should be the lowest in magnitude. In a separate study, Ziabicki [43] reported that under constant tensile force the increase in elongational viscosity is a necessary condition for spinnability, so an increase in the axial velocity due to stretching should increase the elongational viscosity.
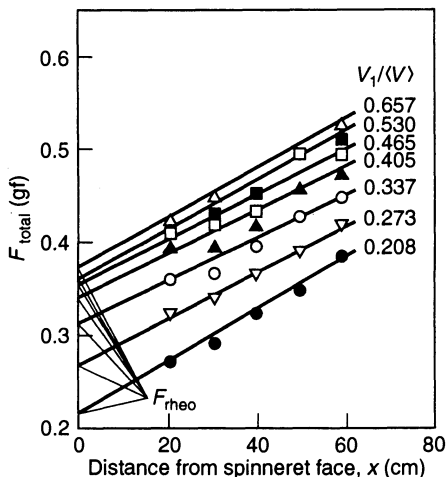
Fig. 15.11 F_{tot} vs. distance from spinneret exit. Bath concentration 10% NaSCN, bath temperature 20 °C, V_1 16.62 cm s^{-1} [42].

(d) Mechanism of fibre breakage during spinning

Commercial spinning is performed under conditions of moderate bath concentration and at low temperature so as to allow near maximum tensions and jet stretch, leading to minimum thread breakage. At extremely low bath concentration, coagulation is very rapid so maximum tension attainable and the maximum jet stretch are both limited. This limitation is due to the breakage of filament skin since at a very low bath concentration the rapid hardening or coagulation causes skin formation which inhibits further coagulation of the fluid core. The resultant breakage therefore may be due to the 'slippage' between the solid skin and the fluid core. This mechanism of breakage may be more dependent on maximum take-up velocity V_{max} than on tensile stress. At higher bath concentration, slower skin formation allows more uniform hardening or coagulation of the entire fibre. Breakage of 'slowly hardened' filament occurs if the critical tensile stress is exceeded and the hardened portion may then separate completely from the fluid at or in the spinneret over the entire cross-section of the filament. This mechanism is slightly different from that suggested by Paul [44], according to whom the skin of the filament ruptures due to an excessive tensile stress. The fluid core can deform easily, while the sheath, which solidifies earlier, can rupture due to stresses. In fact, all the three proposed mechanisms appear to be contributing to fibre rupture phenomena in wet-spinning. From this one may conclude that there is an optimum coagulation rate which is a function of bath temperature and concentration and controls the fluid and skin strength of the partially hardened fibre. Temperature may play
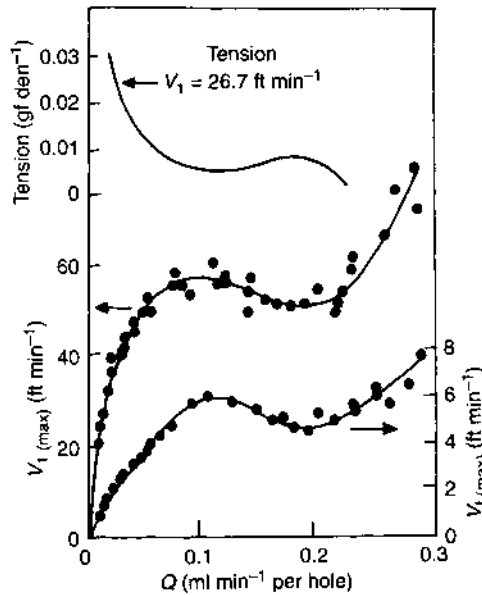
Fig. 15.12 Dependence of maximum first roll take-up speed, $V_{1(max)}$, and free velocity, V_f, on the flow rate per hole, Q. Spin bath 55% dimethyl acetamide and dope concentration 25% polymer [44].

a dual role, as its effect on dope viscosity appears to be more significant than on the coagulation rate.

The dependence of $V_1(max)$, V_f (the free jet velocity) and the spinning line tension on the volumetric flow rate are shown in Fig. 15.12 [44]. Initially both the velocities increase with the flow rate, but then a maximum appears in each curve, followed by a minimum. The maximum in the curve corresponds to the onset of dope instability leading to its fracture. Thus, to maintain a stable spinning line, V_f must be kept below the critical value at which dope instability/fracture is observed. As the coagulation bath conditions change, $V_1(max)$ and V_f values also change. The maximum in V_f occurs at low flow rates as the bath temperature decreases and $V_1(max)$ also decrease accordingly. Therefore, one way to increase the spinnability with minimum filament breakage is to increase the coagulation bath temperature. Zuguang and Anding [45] have also suggested an increase in spinning bath temperature (from 7 to 12 °C) in the NaSCN system to speed up tow formation. This reduces sticky fibre formation and the growth of defects. For increasing the production capacity without sacrificing the fibre properties, they have recommended the use of a circular composite spinneret instead of a rectangular one, increasing the number of holes from 60 000 to 90 000, and adoption of a round bottomed twin overflow coagulation bath instead of a single overflow bath.

(e) Influence of coagulation variables on protofibre structure

One of the fundamental processes governing the formation of wet-spun acrylic fibres is diffusion. The fibre structure is controlled by the diffusion of the solvent from the polymer solution as the solution exits the spinneret capillary and by the counter-diffusion of the non-solvent into the polymer solution. The relative rates of solvent to non-solvent diffusion set the driving force for phase separation and affect the rate of phase separation. Thus, the coagulation variables are dope composition, coagulation bath composition, coagulant temperature and the jet stretch which influence the structure and properties of protofibres. The structure of the gel or protofibres has been extensively studied [39, 40, 46] since it has a major influence on the tensile properties and abrasion resistance of the final finished fibres [47].

Knudsen [48] studied AN/vinyl acetate copolymer of $\bar{M}_w$, about 250 000 containing 94% AN by weight using 40–70% dimethyl acetamide in water as the coagulant. Some of the major findings from such studies are as follows.

1. *Effect of dope composition.* By varying the dope composition, i.e. by raising the dope solids above 20%, homogeneity of the fibre structure improves by reducing the incidence of large voids. An increase in fibre bulk density has also been observed, which reflects the reduction in volume accompanied by the reduction in the number of voids.

2. *Effect of spin bath composition.* Extensive research work can be cited in which various spin bath compositions are employed for making acrylic fibres. In general, spin bath compositions are either (a) aqueous solutions of the solvents employed for the spinning dopes, or (b) non-aqueous organic liquids having high affinities for the solvent employed. In the dimethyl acetamide–water coagulation systems, it appears that slower coagulation is better. This can easily be obtained by raising the concentration of dimethyl acetamide (from 40 to 70%) within the coagulating bath. Although a significant reduction in void frequency has been noticed the density of the fibre and the internal surface or cross-sectional shape are not changed significantly (Table 15.4).

3. *Effect of spin bath temperature.* With the spin bath concentration maintained constant at 55% dimethyl acetamide, a progressive improvement in the fibre density with decreasing spin bath temperature was observed (Table 15.4). Simultaneously with an increase in fibre structure density, an increase in the internal surface and a reduction in the number of large voids was observed.

The mechanism by which reduced bath temperature gives improved fibre structure is probably related to the coagulation rate. At low temperatures, coagulation is retarded and more time is

Table 15.4 Effect of spin bath composition on protofibre structure at 55 °C bath temperature [48]

Coagulant	Coagulation temperature (°C)	Protofibre density (g cm^{-3})	Protofibre surface area (m^2 g^{-1})	Average number of voids per fibre cross-section
40% DMAc + 60% water	55	0.44	100	8
55% DMAc + 45% water	55	0.45	100	4
70% DMAc + 30% water	55	0.47	130	1
55% DMAc + 45% water	70	0.38	65	10
55% DMAc + 45% water	55	0.45	100	4
55% DMAc + 45% water	30	0.50	150	2
55% DMAc + 45% water	10	0.58	210	0
55% DMAc + 45% water	0	0.67	220	0

available for internal adjustment of osmotic stresses, resulting in a denser fibre. In addition, slower coagulation results in less skin formation and this, in turn, probably leads to fewer large voids.

The cross-sections of freeze-dried gel fibres observed under an optical microscope are shown in Fig. 15.13. There is a trend towards a less circular cross-section as the bath temperature decreases. Thus,
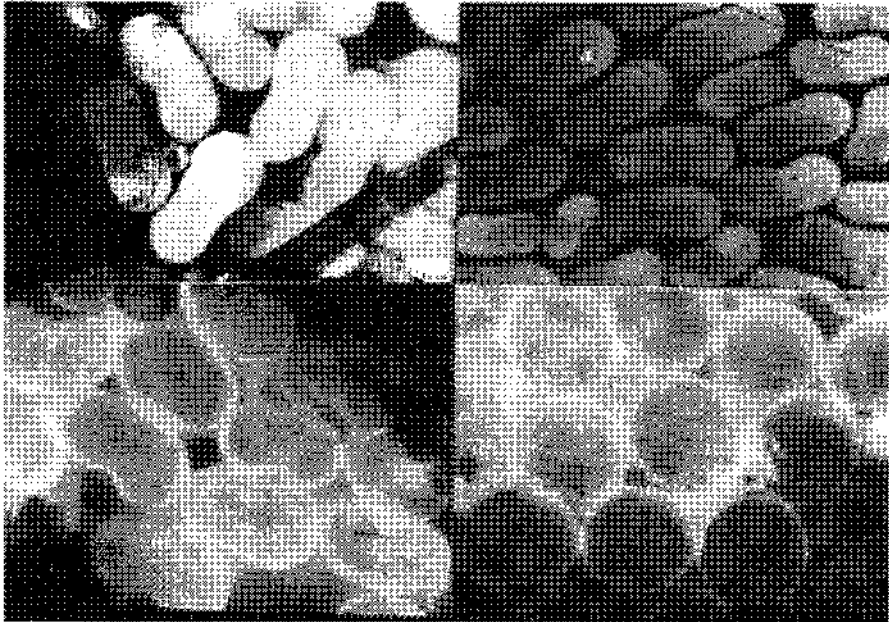
Fig. 15.13 Cross-sections of protofibres viewed under an optical microscope.
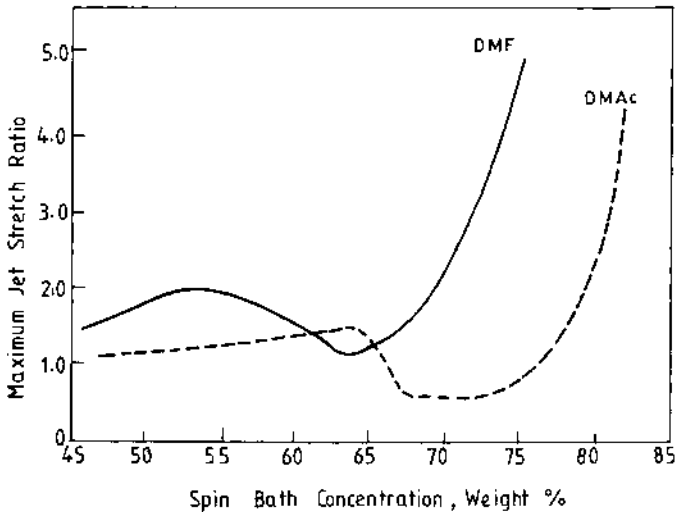
Fig. 15.14 Comparison of DMF and DMAc solvents at the maximum jet stretch ratios [41].

the fibre coagulated at 10 °C attains a dumbell-shaped cross-section. Knudsen has reported that coagulation takes place by counter-diffusion of solvent and non-solvent, in approximately equal volumes, across the fibre surface. As coagulation temperatures are lowered, the outward diffusion of solvent predominates, resulting in non-circular shape, higher fibre density and low pore size.

4. *Effect of jet stretch*. The maximum jet stretch is the highest ratio of jet stretch $(V_1/\langle V \rangle)$ that is attainable without filament breakage in the coagulation bath. From Fig. 15.14, it may be seen that with both the solvents (DMF and DMAc) and water as a non-solvent, the jet stretch goes through a minimum when the spin bath molar ratio of water to solvent is around 2:1 for both DMF and DMAc. As the solvent level is increased further, there is excess solvent relative to water. The radial structure differences within the fibre are less with a thinner skin, and the maximum jet stretch ratio therefore increases dramatically. Paul and McPeters [49] have demonstrated the relation between the jet stretch and the degree of swelling for the fibres coagulated in DMAc–water coagulant at 30 and 50 °C as a function of spin bath concentration. The shape of the curves is the same as that for jet stretch (Fig. 15.15) and a minimum occurs at 70–80 wt % solvent. As the degree of swell decreases, the ability to draw the fibre also decreases and limits the jet stretch. Low jet stretch conditions produce small void structures, giving a lustrous appearance. It is believed that an increase in void number is related to rupturing of the fibre surface during coagulation as the stress imposed by stretching is increased.
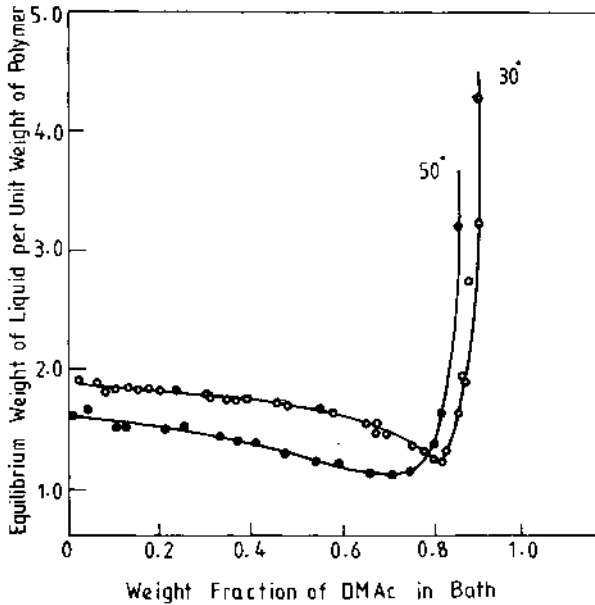
Fig. 15.15 Indirectly measured degree of swelling for fibre coagulated in a bath of DMAc–water at 30 and 50 °C as a function of spin bath concentration [41].

From the structure of protofibres, it has been demonstrated that high initial fibre density and more homogeneous internal structure permit the development of higher strength at lower stretch, higher elongation at a given strength level, high maximum strength and modulus at high stretch ratios, and improved fatigue and abrasion behaviour.

15.5.2 DRY-SPINNING

A brief description of the dry-spinning process was given in Chapter 6. During dry-spinning, the PAN dope at about 120–125 °C is extruded through a spinneret with a varying number of holes, generally 1500–2500, which is placed at the head of a vertical column or tower about 5–6 m high (Fig. 6.1 in Chapter 6) in which preheated inert gas at 300–400 °C is circulated [50, 51]. The filaments are continuously removed from the bottom of the tower, washed free of solvent, and then processed like wet-spun fibres. The vapours of the solvent removed by the inert gas are recovered by condensing. The cooled gases are again heated before being recycled within the spinning column. The solvent is recovered later by distillation. Orlon™ (Du Pont) and Dralon™ (Bayer) are manufactured by the dry-spinning process.

The spinning tower may be divided into two parts, the upper and the lower cells. Hot primary inert gas at about 350–400 °C flows down the

upper cell, stripping off the solvent as filament formation takes place. The vapours of the solvent are removed as they leave the bottom of the upper cell and go for solvent recovery. The secondary inert gas in such towers enters the lower cell from its bottom and the counter-current of this secondary gas helps in cooling down the filament bundle. The secondary gas also returns and goes for solvent recovery. The cooled gases are again heated before being recycled within the spinning column. The spinning cell is jacketed and heated by Dowtherm or any other heating medium to a temperature of 180–270 °C.

The filaments which leave the cell or column still contain 10–20% solvent. They are drawn at a predetermined speed and deposited in cans. The spinning speeds of 300–400 m min^{-1} are used for a finer denier of 3–1.5 den. The tows from many cans are joined together into a bigger tow of a predetermined size (500 000 to 1 million den) and are fed into the stretching line at a much lower speed (30–70 m min^{-1}).

The important variables of dry-spinning are solids content in the dope, dope temperature, temperature and flow of carrier gas, oxygen level in the spinning cell and take-up speed.

Highly concentrated dopes (30–32% solids) are required in dry-spinning in order to evaporate the solvents rapidly. Particular attention must be given to avoid possible turbulence in the gas flow in the spinning cell/column to avoid formation of fused filaments. Another factor that must be carefully checked is the hygrometric state, as well as the oxygen content of the spinning gas fed into the column to remove the solvent. This is necessary to prevent discoloration of the fibres and for safety reasons to avoid fires. The residual solvent content and the high temperature in the spinning column (above 200 °C) inhibit molecular orientation. Overall, the degree of orientation occurring during spinning increases with the viscosity of the spinning solution and the spinning speed, and also to some extent with the spinning draft.

In the production of tow, the finish is applied as the filaments leave the spinning column. The filaments are then passed round a guide roller and combined to form a single tow. Each spinning unit comprises between 10 and 70 spinning columns. Tows of up to 500 000 dtex are drawn off by special take-off rollers at speeds of 250–450 m min^{-1} and coiled in spin cans.

In dry-spinning, the fibres obtained have more regular and compact structure with dog-bone shaped cross-section. Dry-spinning is preferred for spinning of fine denier fibres, i.e. 1.5, 3.0 and 5.0 den.

Considering the techno-economics of both the processes, the dry-spinning process comes out to be more expensive, as adequate systems for gas circulation, heating and solvent recovery are required for an acceptable production rate.

A comparison of fibre properties spun by wet- and dry-spinning using DMF solution shows that the dry-spun fibres have higher bulkiness, better capacity for recovery from deformation and an excellent handle, while wet-spun fibres have a softer handle and are fleecy, especially in fine denier (1.2–3 den). However, dye pick-up in dry-spun fibres is low compared with that in wet-spun acrylic fibres.

For high denier fibre (>8–10 den), the wet-spinning process is recommended because the dry-spinning of such high denier fibres imposes technological problems with respect to the evaporation of the solvent, etc. New developments in the production of dry-spun acrylic fibres are concerned with the process economics, e.g. an increase in the production speed of the after-treatment to avoid the disruption or discontinuity between the spinning and the after-treatment processes, reduction of wage costs and pollution, minimization of solvent losses and stabilization of the quality of the product.

15.5.3 DRY-JET WET-SPINNING

It was shown earlier (Fig. 15.13) that in as-spun or protofibres produced by the wet-spinning process, pear or finger-shaped voids are present. Such voids usually collapse on drying of as-spun fibres, but their remains impair properties of the fibres such as transparency and cause easy fibrillation. A relatively new process of spinning by extruding the dope stream from a dry jet, followed by coagulation through conventional wet-spinning, overcomes some such shortcomings (Fig. 15.16). An air gap of 3–5 mm between the spinning jet and the coagulation bath results in a process of fibre formation that combines the advantages of dry-spinning with those of wet-spinning. Some of these advantages are:

- high speed fibre formation is possible, as the threadline stresses are not transmitted back into the spinneret;
- a high concentration of dope can be used;
- the high degree of jet stretch that usually characterizes the dry-spinning method is present, but the method still retains the capability of controlling the structure of as-spun fibres through adjustment of coagulation bath parameters;
- it is possible to produce filaments of linear density below 1.0 dtex.

An in-depth study of void formation in acrylic fibres has been made by Baojun, Jian and Zhenlong [52] by comparing the structure and morphology of as-spun fibres produced by wet- and dry-jet wet-spinning. The influence of different spinning parameters like jet stretch, height of air gap, concentration of the dope, spinning bath temperature, speed of winding, etc. on the fibres produced by both dry-jet and
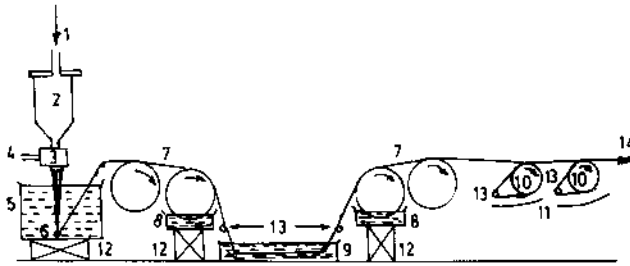
Fig. 15.16 Dry-jet wet-spinning unit: 1 = nitrogen inlet; 2 = dope reservoir; 3 = spinning block; 4 = drive to the gear pumps; 5 = coagulation bath; 6 = thread guide; 7 = advancing reels; 8 = washing baths; 9 = stretch bath; 10 = chrome rollers; 11 = radiant heaters; 12 = adjustable stands; 13 = idler roller; 14 = to the wind-up [51].

immersion-jet (wet-spinning) has been studied through the measurement of the diffusion coefficient of the acrylic fibres. Baojun and co-workers analysed the problem in terms of the diffusion coefficients for DMF coming out of and water going into the fibre.

If D_n is the diffusion coefficient of the non-solvent, and D_s is the diffusion coefficient of the solvent, the ratio D_s/D_n represents the degree of mildness of coagulation. The milder the coagulation, the smaller and fewer will be the voids formed, and vice versa. The reciprocal of this ratio will reflect the power of coagulation.

The diffusion coefficient ratios for dry-jet wet-spinning and conventional wet-spinning are compared in Fig. 15.17. A clear difference can
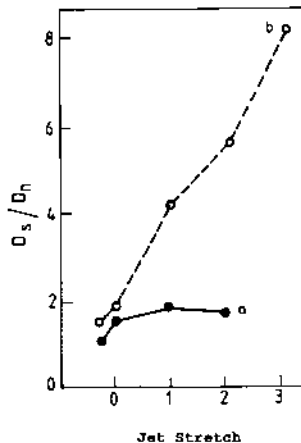
Fig. 15.17 Interdependence of jet stretch and diffusion coefficient ratio: (a) wet-spinning; (b) dry-jet wet-spinning [52].

be observed. At zero stretch, the D_s/D_n values for the two cases are quite close to each other. As the fibres are stretched during wet-spinning, there is little increase in D_s/D_n value for wet-spinning, whereas a sharp and rapid increase is seen in the case of dry-jet wet-spinning from 1.3 to 8 at a jet stretch of 3.

The rate of diffusion of water into the fibre spun by the dry-jet method due to the formation of thin, dense, hydrophobic cuticle decreases sharply. Therefore, irrespective of the change in coagulating conditions, no large voids are formed as confirmed from SEM and TEM studies of the protofibres, resulting in a fibre of high transparency.

Dry-jet wet-spinning allows relaxation in the air gap of the orientation produced in the spinneret, so that the spun fibre is less oriented and more uniform than that from the immersed jet. This permits orientation by subsequent drawing and results in fibres with higher tenacity.

15.5.4 GEL-SPINNING

Another approach to optimize the microvoids in the acrylic fibres is through the 'gel-spinning' method. It is claimed that homogeneous, macrovoid-free fibres can be produced by gel-spinning, apparently by establishing a true gel state prior to phase separation.

Gel-spinning involves the use of high molecular weight polymer solutions which are fluid at the extrusion temperature but which set into a gel when cooled down to ambient temperature. A typical scheme of the gel process cycle is spinning, gelation, extraction, washing and multistage drawing. Maslowski and Urbanska [53] have listed the various gel-spinning processes developed by different companies (Table 15.5) and the mechanical properties of the PAN fibres produced by these processes. It has been disclosed in a number of patents that the most suitable molecular weight of PAN for gel spinning is $\bar{M}_w > 5 \times 10^5$. The concentration of the spinning solution should be in the range 2–15%, depending on the solvent, molecular weight and gel-spinning technology used.

The spinnerets have relatively large orifices with diameters ranging from 0.2 mm to 2.0 mm. The ratio of the spinneret channel length to the diameter, L/D, should be at least 15. Such a geometry of the spinneret minimizes the disturbances associated with viscoelastic properties of the spinning solution.

The spinneret draw ratio should not be more than 10:1. The linear velocity on the first godet is several metres per minute, but the final winding speed at the take-up is high because of the high draw ratios used. The fibre is stretched in several stages, both in the form of a gel and xerogel. The total draw ratio can be as high as 30.

Table 15.5 Mechanical properties of PAN fibres obtained by various gel processes [53]

Company	$\bar{M}_w$ or limiting viscosity [n]	Solvent[a] for polymer	Polymer conc. (%)	Cooling bath	Gelation temperature	Draw conditions	Total draw ratio	Tenacity (cN tex^{-1})	Initial modulus (cN tex^{-1})
Allied	1.63×10^6	DMSO	6	DMSO:water (50:50)	Room temperature	4.07× 135–150 °C 2.11× 146–160 °C	8.6	70	2200
Stamicarbon Toyobo	1.3×10^6 1.4×10^6	DMF + ZnCl$_2$ DMF	5 7	CH$_2$Cl$_2$ Alcohol/dry ice	Room temperature −40 °C	Dry, 180 °C 135 °C and 150 °C on hot plate	28 >12	153 Very high	1860 Very high
Japan Exlan	1.35×10^6	5% NaSCN	5	15% NaSCN	5 °C	2 × water 20 °C 2 × water 85 °C 2.5 × boiling water 1.8 × ethylene glycol 130 °C 1.6 × ethylene glycol 160 °C	28.8	164	2700
Japan Exlan	2.28×10^6	50% NaSCN	5	15% NaSCN	5 °C	2 × water 20 °C 2 × water 85 °C 2.5 × boiling water 1.8 × ethylene glycol 130 °C 1.6 × ethylene glycol 160 °C	28.8	222	–
Toray	[n] = 3.2–5.5	DMSO	5–20	55–60% DMSO	1–20 °C	Hot water, preheated dry 190–240 °C	12–15	100–130	1600–2000
Kuraray	1.65×10^6	50% NaSCN aq.	2.9	15% NaSCN aq. +5% CH$_3$OH	10 °C	2.5 × NaSCN 20 °C 9 × 200 °C	22.5	196	2490

[a] Water was used as solvent for extraction.

(a) Preparation of dope for gel-spinning

Dissolution of PAN with ultra high molecular weight is difficult due to poor penetration of the solvent into the polymer particles because of strong swelling on the surface. It is therefore necessary to provide prolonged and intensive stirring at relatively high temperatures (160–180 °C) to obtain a homogeneous solution. The gel is then disintegrated with a mechanical stirrer into gel-like particles of about 1 mm in size containing occluded solvent. These particles can be lyophilized to obtain xerogel in the form of coarse-grained powder. Gel-like particles containing more than 90% solvent can be used for spinning of PAN fibre.

Stamicarbon Company's process involves the addition of bivalent metal (Zn, Ca) chlorides or bromides, preferably $ZnCl_2$ (0.01–0.2 mol/mol of acrylonitrile), to the spinning solution to prevent phase separation during gelation of the fibres. These additives also increase the susceptibility of the xerogel fibres to drawing and orientation.

From the data given in Table 15.5 for the PAN fibres obtained by gel processes, it may be seen that PAN fibres produced by Japan Exlan from a polymer of $\bar{M}_w = 2.8 \times 10^6$ in 50% NaSCN aqueous solution with a total draw ratio of 28.8 possess maximum tenacity of $222\,cN\,tex^{-1}$. Highly oriented PAN fibres prepared by gel-spinning are not dyeable owing to their compact structure.

15.5.5 MELT-SPINNING

Acrylic fibres could not be produced initially by the melt-spinning technique because they degrade well below their melting point. However, by the addition of water or plasticizers, it is now possible to decrease the melting point and adopt this principle for melt-spinning of acrylonitrile polymer [54–58]. Frushour [21,22] has reported the depression of melting point of polyacrylonitrile (PAN) from 320 to 185 °C using DSC. Similarly, the addition of polyethylene glycol reduces the T_m of the acrylic polymer, thus avoiding the degradation reaction and making it melt-spinnable. A single phase 'plasticized melt' of PAN in water can be produced by heating with 30% by weight of water in a closed system. Min et al. [59] also showed the lowering of the T_m of PAN by the addition of water under autogeneous pressure.

Asahi Chemical Co. Ltd [55] reported the melt-spinning of acrylic polymer containing water and a water-soluble polymer (PEG) to obtain acrylic fibres of tenacity $0.38\,GPa$ ($4.3\,gf\,den^{-1}$). In another patent, the melt-spinning of acrylic polymer at 230 °C has been disclosed to give heat resistant fibres of tenacity $0.25\,GPa$ ($2.9\,gf\,den^{-1}$). Mitsubishi Rayon Co. Ltd [56] has disclosed in its patent the process for melt-spinning of acrylic fibres of tenacity $0.42\,GPa$ ($4.8\,gf\,den^{-1}$).

Grove, Desai and Abhiraman [57] investigated the structure and mechanical properties of melt-spun water-plasticized PAN fibres. The morphology of these fibres is reported to be similar to that of wet- and dry-spun acrylic fibres; however, surface defects and internal voids are more in the melt-spun water-plasticized fibres than in the wet- or dry-spun ones.

Atureliya and Bashir [38] in a recent paper reported the melt-spinning of polyacrylonitrile. PAN was mixed with propylene carbonate (PC) in an equal weight ratio at a temperature above 130 °C. PAN does not dissolve in PC at room temperature; it only dissolves at temperatures above 130 °C. Atureliya and Bashir spun this mixture into fibres at 190 °C. From X-ray studies they observed a crystallographic transition from a hexagonal to an orthorhombic structure in going from the dry polymer powder to the unoriented propylenecarbonate-plasticized filament.

15.6 TOW PROCESSING

Acrylic fibres emerging from the dry-spinning column or spin bath are processed to remove residual solvent and then subjected to drawing and relaxation treatments that are needed to develop desirable tensile properties, abrasion resistance, dyeability and dimensional stability.

Tow processing of dry-spun fibres depends largely on the level of residual solvent. If the solvent level is low, then the bundle of fibres can be immediately drawn between heated rolls since no washing is required. When higher residual solvent, say 10–20%, is left in the dry-spun fibres because of higher throughput rates, then direct introduction into an aqueous tow washing bath is not feasible because the residence time in the bath (at 200–400 m min^{-1}) may not be sufficient to remove the solvent. In such cases tows from several columns are combined into a rope, which is then piddled into a can, and then multiple ropes are creeled together for tow processing. Figure 15.18 illustrates the various steps involved in tow processing.

15.6.1 STRETCHING

Stretching of acrylic fibres is generally carried out in water at 100 °C (~25 °C above T_g). The fibres can be easily drawn to a very high draw ratio. Boiling water causes a marked shrinkage of the individual fibril, with a concomitant increase in diameter. Furthermore, stretching in boiling water not only orients the fibrils in the direction of the fibre axis, but also stretches the individual fibrils even at relatively low orientation ratio. At a near maximum stretch ratio of 5.0, for wet-spun samples, the fibril presumably approaches the size it was prior to shrinking in boiling water.
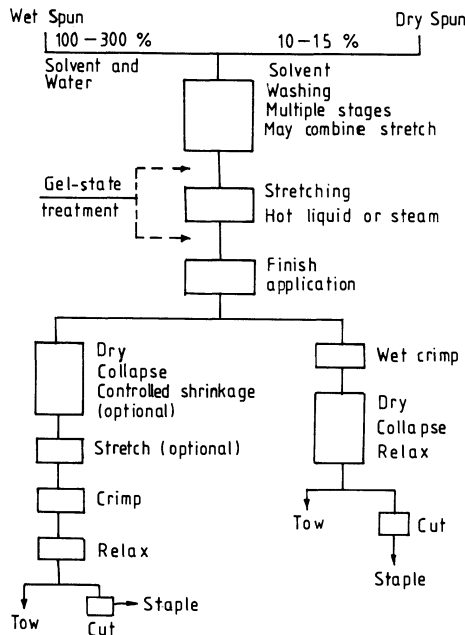
Fig. 15.18 Tow processing of acrylic fibres [1].

Dry-spun acrylic fibres also show a marked change in the structure during stretching. Samples having 10% residual solvent when leaving the spinning tower have no measurable surface area before orientation. But at a very low draw ratio, a marked increase in surface area is observed. The calculated fibril radius decreases with increasing draw ratio as observed in wet-spun samples [60].

Bell and Dumbleton [61] have proposed a structural model combining the concept of Rosenbaum [62] and Knudsen [48]. They visualized the system as being more like a network of springs involving deformation with orientation of the network as a whole. According to Bell and Dumbleton, primary deformation involving slip of fibrils relative to one another takes place during stretching in water at 100 °C. This gives rise to an 'effective viscosity' at high draw ratio. It is interesting to note that properties associated with fibril length remain unchanged after hot wet-stretching; however, a new network is presumably formed with junctions at the fibril ends. It has been observed that some relaxation of the molecules to a less extended configuration takes place during the slip process, as indicated by the stress–strain curves (Fig. 15.19).

An increase in the degree of stretch causes the load (stress)–extension curves to become steeper [63]. The slope of the curves is less marked when the degree of stretching is low, particularly in fibres spun from
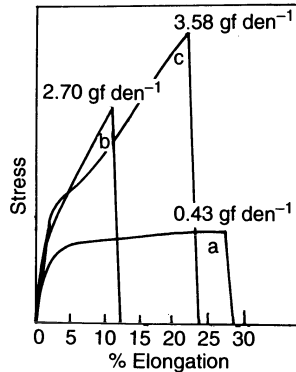
Fig. 15.19 Typical stress–strain curves: (a) after coagulation; (b) after hot, wet stretching; and (c) after drying at 100 °C. Coagulation bath 55% DMAc and temperature 70 °C [61].

low molecular weight polymers, owing to the increased mobility of the macromolecules.

An interesting SEM study [64] of fibre surfaces shows smoothing of the surface with an increase in draw ratio leading to a more intimate or greater area of contact when one fibre slides on another fibre, thus leading to a higher coefficient of friction. Furthermore, it has been shown that steam stretching, instead of dry heat, leads to quick heat transfer because of the latent heat of steam.

15.6.2 DRYING

After washing and finish application, the tow still contains water and therefore has to be dried. Fibres of different shrinkage levels can be produced by different procedures, e.g. the fibres are dried and collapsed with no shrinkage permitted, or controlled shrinkage is allowed by over-feeding the drying rolls, or the fibres are dried and collapsed on a belt without restraint so that shrinkage may occur.

Depending on the dryer design, the tow can be dried by radiation, by contact heat or by a gaseous medium. Drying by contact heat involves running the tow over several large heated drums or calenders. The speed at which these drums revolve can be regulated to control the degree of shrinkage.

Another type of drying unit is the rotating drum covered with a screen or sieve. Air extracted from inside is heated and blown over the fibres. Alternate sides of the material pass across half or more of each drum, depending on their arrangement. One half of the drier is covered. Normally up to 20–26 screen drums are combined to form a large drier with separate regulation of the heat and speed in each zone. Acrylic

tow is generally dried at 120–170 °C with throughput speeds of 100–150 m min^{-1}. Since the tow contains water from the preceding washing process or finish application, the drying process also initiates the setting process. The degree of setting depends primarily on the drying conditions, i.e. temperature, time and humidity. As a high degree of setting makes crimping more difficult, the drying temperature should not be too high.

The presence of moisture in the drying medium affects the shrinkage behaviour of PAN and P(AN-MA) copolymer fibre [65]; tows passed through a drying medium containing 0.05–0.13 kg water per kg drying medium shrink markedly in the temperature range 70–80 °C. Also the effect of water vapour in the hot gas on the compactness of the internal structure of the filament is more marked in the case of P(AN-MA) co-polymer than in the case of PAN homopolymer.

The effects of drying temperature (80–140 °C) and of different degrees of tension on shrinkage behaviour of PAN fibres have also been studied [66]. The increase of stress during drying reduces the shrinkage velocity and total shrinkage, and increases the tensile strength and the Young's modulus of the fibre.

15.6.3 CRIMPING

Crimping is an important post-spinning operation in acrylic fibre production as it increases the fibre-to-fibre cohesion and improves the spinnability of the acrylic fibres. Crimping of the fibre must be done above the glass transition temperature (T_g) of the fibre. However, as stated earlier, the T_g values for dry and wet acrylic fibres before setting are quite different. Accordingly, the heating temperatures for dry- and wet-crimping are generally kept at 78–80 °C and 65–70 °C, respectively. Crimping introduced by mechanical means is unstable and can be easily removed under the action of tension, wetness and temperature in the post-treatment of the fibre. It has been shown that in the wet-crimping process the tow retains about 20–30% water which brings down the T_g and causes loss in crimp during handling in after-treatment, especially in second-stage finishing. The crimp of the fibre leaving the crimper is nearly the same for both dry- and wet-crimped fibres, but in the post-crimping process, the wet-crimped sample showed a significant loss of crimp compared with the dry-crimped sample. An improved dry-crimping technology has been developed by the Shanghai Petro-Chemical Complex, China, by which crimp stability has been significantly enhanced by heat-setting under saturated steam [45]. In this process the two treatments in water bath at 90–95 °C given to the tow in wet-crimping have been eliminated and replaced by a controlled programme of steam setting, i.e. temperature control with a double cycle. As a result,

the fluctuation in setting temperature is reduced and the stability of the full setting cycle increases. The dry-crimped fibres have high thermal stability and crimp stability. Even the dyeing rate and dye uptake of dry- and wet-crimped fibre are different. The dye uptake of dry-crimped fibres at temperatures below 92 °C is lower than that of the wet-crimped fibre. This is due to the more stable structure of dry-crimped fibre.

Furthermore, it has been shown that dry-crimped fibres have a higher degree of crimp, a lower percentage of over-length fibres, and low specific resistance and coefficient of friction. Dry-crimped fibres also show improvement in fibre-to-fibre cohesion and draftability, leading to good spinning performance.

15.6.4 ANNEALING

The setting of tow during drying is not sufficient to relieve all the internal stresses caused by drawing. The filaments only achieve thermodynamic equilibrium state after tensionless heat-setting. Stoyanov [67] has investigated the influence of heat treatment in the presence of steam at 100 °C and drying on shrinkage, tenacity and elongation of acrylic fibre. The shrinkage of the fibres after each heat treatment and residual shrinkage after boiling the fibre in water for 15 min were measured. It has been observed that thermosetting in steam produced greater shrinkage than drying at 125 °C. This has been attributed to the increased segmental mobility in the presence of water molecules. At a high temperature, and in the presence of steam, the supermolecular structure becomes more mobile, resulting in significant axial shrinkage. It has also been reported that elimination of tension in heat treatment increases the elongation and compactness of the fibres after drying.

The effects of heat treatment on dyeability, T_g, and mechanical properties have been reported by Sarmadi, Noel and Birch [68]. Orlon 42 tow was subjected to a series of heat treatments: dry heating at 110 and 150 °C and saturated steam at 110 °C for a period of 5 min under tension or free annealing. Heat treatment with moisture at 110 °C, both slack and under tension (0.22 N tex^{-1} or 0.025 gf den^{-1}), produced the highest values of T_g (108–109 °C), while the treatment at 110 °C (moist, slack) gave the highest dye uptake. Both the free volume and pore mechanisms appear to be operative in the dyeing of these fibres. Shrinkage measurements on the fibres treated with and without tension showed that the length increase induced by heating under tension was not completely stable; only 63% of the length increase was retained after 15 min in boiling water.

The effect of annealing temperature and pre-tension on the thermal shrinkage and shrinkage stress of acrylic fibres through thermo-mechanical analysis has been reported [69]. Figure 15.20(a) shows the effect of
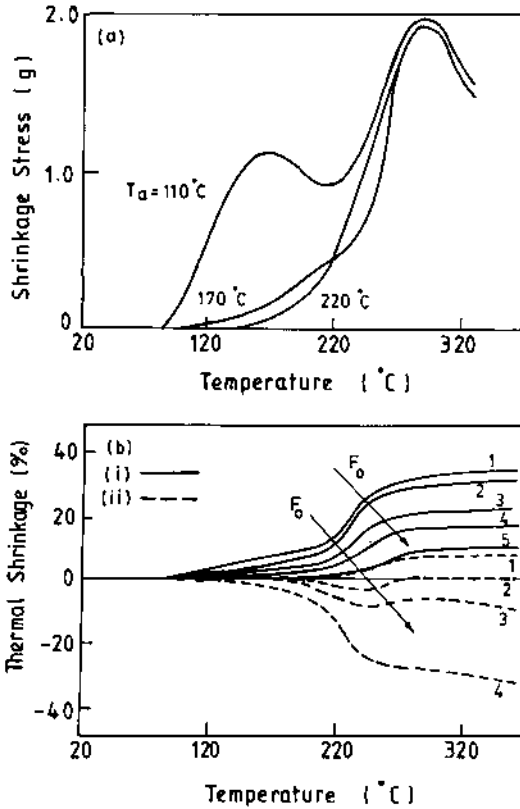
Fig. 15.20 (a) Effect of annealing temperature on the thermal shrinkage stress of PAN (93% AN) fibre. (b) Thermal shrinkage curves of PAN fibre at various pre-applied tensions. Solid line: $F_0 = (1)$ 5 mgf, (2) 50 mgf, (3) 300 mgf, (4) 500 mgf, (5) 800 mgf. Dashed line: $F_0 = (1)$ 1010 mgf, (2) 1200 mgf, (3) 1450 mgf, (4) 1950 mgf [69].

annealing temperature on the thermal shrinkage of acrylic fibre (93% AN content). As the annealing temperature increases from 110 to 200 °C, the shrinkage initiation temperature increases. The shrinkage stress in the samples annealed at 110 °C first increases and then drops. In fact, two peaks can be seen in the shrinkage stress curve obtained from acrylic fibres annealed at 110 °C, but on annealing at higher temperatures the first peak of the shrinkage stress disappears. This implies that the shrinkage stress largely originates from the thermally frozen stress during the formation of the fibre. From the thermal shrinkage curves of acrylic fibre obtained under different pretensions (Fig. 15.20(b)), it is clear that the amount of shrinkage at the same temperature decreases as the pretension increases. If the pretension is very large, elongation takes place instead of shrinkage. It is also observed that under different pretensions

the actual tension is nearly the same after the annealing temperature 170 °C. From apparent shrinkage and shrinkage stress one can easily calculate the thermal shrinkage modulus and the relaxation modulus.

15.6.5 BULKING

High bulk acrylic yarn is produced by mixing the high shrinkage fibres with low shrinkage/non-shrinkable acrylic fibres and then spinning it into a yarn. When the yarn is subjected to steaming or hot air treatment, high shrinkage fibres shrink and force the non-shrinkable fibres to buckle, increasing the voluminosity of the yarn. For bulking, acrylic yarns are generally subjected to steaming for 20 min.

Naik [70] has made an interesting study on the thermal behaviour of shrinkable acrylic fibres of different fineness (2.0 dtex to 10 dtex). Yarns made of coarser fibres were found to result in more voluminous yarns when treated in hot air as compared with steaming treatment. The best crimp contraction for finer fibres was achieved by hot air treatment at 160 °C for 30 s, while for medium and coarser yarns appropriate conditions were 100 °C for 10 s.

15.7 MECHANICAL PROPERTIES OF ACRYLIC FIBRES

Acrylic fibre has a lower breaking elongation and considerably lower work of rupture than nylon and polyester fibres. Hence, acrylics do not compete with these fibres in applications where high load-bearing properties are required. However, it has higher tenacity and work of rupture compared with wool fibre.

The mechanical properties of acrylic fibres are significantly affected by temperature. The load-elongation curves obtained at room temperature show a clear yield point which disappears at around 115 °C in dry and at around 70 °C in wet measurements. When measurements are made in water at 95 °C, a reduction of the modulus by a factor of 50 and of tenacity by two-thirds and a four-fold increase in elongation are observed. The low modulus of acrylics under boiling water conditions results in a tendency for the fibres to lose bulk, shape, and resiliency upon dyeing and other high temperature treatments. The poor hot–wet strength of acrylic fibres may be attributed to the plasticization of laterally bonded molecules of acrylic fibre.

15.8 SPECIALITY FIBRES

Additives are used in the spinning dope to impart special properties to the resulting fibres. A spinning dope containing 0.7% carbon black, antimony/tin oxide or titanium oxide, ammonium or metal salts or copper ions produces conductive fibres. Other spinning dope additives include

fibroin with $\bar{M}_n$ 200 000, polyvinyl acetate with $\bar{M}_w$ 120 000, and poly-caproamide with $\bar{M}_w$ 19 000. Toyobo Co. has reported the use of milk casein as a spinning dope additive to develop Chinon™ silk-like fibres.

Addition of glycerol or tetraethylene glycol in the spinning dope of an AN–methyl acrylate–sodium methallyl sulphonate terpolymer produces acrylic fibres with 10% water retentivity.

15.8.1 WATER-ABSORBENT ACRYLIC FIBRES

For certain applications, acrylic fibres of porous structure with high water retention and warmth and good insulating and dyeing properties are required [71,72]. Bayer Co. in Germany successfully introduced the high water-absorbent acrylic fibre Dunova™ in 1976. Later, similar products were developed by Japanese companies. Researchers at China Textile University have developed water-absorbent fibres with a total water content of 20–35% of the fibre weight. The principle is to add another copolymer, which is soluble in dimethyl sulphoxide but insoluble in polyacrylonitrile molecule, and yet keep the polymer as a macromolecule in the dope. Due to its shrinkage during coagulation, many small pores with connecting passages are formed. These promote capillary action, which absorbs water quickly; this effect remains unchanged during drying and dyeing processes. This type of high water-absorbent acrylic fibre retains the physical and mechanical properties of normal acrylic fibres.

In a Japanese patent [73], acrylic fibres with 54% water retention have been reported. These fibres were obtained by wet-spinning a mixture of regular polyacrylonitrile and acrylonitrile–styrene copolymer. To obtain a porous acrylic fibre, the polyacrylonitrile and the added copolymer must be incompatible. The criterion of incompatibility is the difference in solubility parameter of the blend components. The composition of the copolymer, the sequence distribution of segments in the copolymer and the spinning bath temperature all influence the void structure. Since there are a large number of small holes in the fibre, and its relative density is about 25% less than that of normal acrylic fibre, light and warm wearing comfort is experienced. Hydrophilic microporous acrylic fibres (Acrysorb™) have also been developed by conjugate spinning of polyacrylonitrile with cellulose acetate blend [74]. This new fibre has 25–35% water retention capacity.

15.8.2 ANTISTATIC AND CONDUCTIVE ACRYLIC FIBRES

Acrylic fibre is made of non-ionizing hydrophobic polymer with a high specific resistance of $10^{13}\,\Omega\,cm^{-1}$ which can easily accumulate an electrostatic charge. This can cause dust adherence and also a spark discharge.

A number of formulations have been listed [75–77] for the production of antistatic acrylic fibres. Acrylic fibres can be made conductive by spinning from mixtures containing electroconductive fillers such as carbon black, antimony oxide, tin oxide, titanium dioxide, ammonium or metal salts, or copper ions. Polymeric additives in the fibre-spinning dope include polyester/polyester block copolymers, diacrylic ester of poly(ethylene glycol) and sulphur-containing polyethers. Addition of nylon 6 (5% by weight) to AN–methylacrylate–sodium methallyl-sulphonate and 5–10% poly(ethylene adipate) to AN–methyl styrene–vinyl acetate copolymer gave antistatic fibres.

Electrically conducting acrylic fibres based on treatment with zinc oxide have been reported by Kanebo. Another approach is provided by Exlan, in which a polymer containing 86% acrylonitrile, 11% vinyl acetate and 3% dimethyl-aminoethyl methacrylate is spun into fibres and then treated in a solution containing copper sulphate and $(NH_2OH)_2H_2SO_4$. The resulting fibres are reduced in a solution containing $Zn(HSO_2CH_2O)_2$ to gives fibres rich in copper ions with a specific resistance of only $33\,\Omega\,cm^{-1}$ compared with $10^{10}\,\Omega\,cm^{-1}$ without this treatment.

It has also been demonstrated that partial saponification of acrylic fibre fabrics with 2% NaOH improves the dissipation of static charge significantly [78].

15.8.3 ION-EXCHANGE FIBRES

Fibres possessing ion-exchange properties have been spun from a copolymer comprising acrylonitrile and the quaternary salt of 1,2-dimethyl-5-vinyl pyridine methyl sulphate or 2-methyl-5-vinyl pyridine, and also from poly(acrylonitrile-methyl vinyl pyridine) copolymers. Attempts have been made to produce ion-exchange fibres from mixtures of polyacrylonitrile and poly(ethylene imine).

Through partial saponification with NaOH and reaction with hydrazine, it is possible to obtain an ion-exchanger that can bind metal ions both ionically and in complexes. The capacity and selectivity of the exchange fibres can be influenced by the reaction conditions, concentration, time and temperature.

The large surface area of the fibres controls their ion-exchange property. Simanova *et al.* [79] have reported the use of ion-exchange fibres for the selective exchange of rare metals such as ruthenium, osmium and titanium and for waste water treatment through the absorption of cadium or zinc.

In another study, a fibre exchanger has been used as a second down-stream ion-exchange unit for the removal of zinc ions from industrial effluent.

15.8.4 FLAME RESISTANT ACRYLIC FIBRES

Acrylic fibres have an oxygen index (OI) of 18%, which is the lowest among all textile fibres. Attempts have been made to impart flame retardancy to acrylic fibres through incorporation of halogen or phosphorus-containing vinyl comonomers. Self-extinguishing modacrylic fibres have been produced from a terpolymer containing AN (35–85%), vinylidene chloride (5–30%) and $Me(Et)P(O)CH_2CH_2OOCCH=CH_2$ (5–30%). Main examples are Teklan^{TM} (Courtaulds) and Monsanto SEF^{TM}. The latter is used in the USA for tents, awnings and upholstery. In another study, AN copolymers containing 2–9 mol % haloalkyl acrylate and/or methacrylate have been used for producing hygroscopic and flame retardant acrylic fibres. By far the cheapest of the fire blocking fibres, and the most persistent under flame, are oxidized acrylic fibres like Panox^{TM}. A blend of Panox^{TM}, Kermel^{TM} (polyamide–imide) and wool represents a very useful combination for producing comfortable fibre to wear. R.K. Textiles is one of the world's largest manufacturers of oxidized polyacrylonitrile fibres, which are used in advanced carbon/carbon brake aircraft systems and fire resistant barrier fabrics.

15.8.5 ANTIMICROBIAL ACRYLIC FIBRES

A range of acrylic fibres has been produced through chemical modification to fix bacteriostats. Included in this group are fibres described as having antimicrobial or antibacterial activity, or as being bactericidal. Many patents claim fibres which incorporate phenol derivatives such as 3-methyl-4-isopropylphenol and 2,4,4'-trichlorohydroxydiphenyl ether.

A new high performance acrylic fibre, Courtek M^{TM}, developed by Courtaulds, UK, can prevent the build-up of hazardous bacteria in cloth furnishings and medical equipment. The fibre contains a combination of antimicrobial compounds based on metallic salts. These compounds are bound into the fibre matrix, which means that their effect is not minimized by wear and washing [78].

15.8.6 ACRYLICS IN FILTRATION

Due to their excellent resistance towards acids, acrylonitrile homopolymer fibres are recommended for wet filtration under acidic conditions. Acrylic woven fabrics have, therefore, been used in the chemical, galvanic, petroleum and mining industries. The advantages of such filter media include resistance to rotting under constant moist conditions, easy removal of filter cake, and scouring/cleaning only required at long time intervals. Furthermore, the low swelling capacity ensures that fabrics made of this fibre retain their air permeability in a moist atmosphere. In the form of filter hose and filter bags, acrylic woven fabrics are

used for dry filtration, e.g. in the separation of fly ash in coal-fired power stations, primary and secondary smelters, and dust filtration of glass works and chemical plants. Non-woven fabrics produced from blends of antibacterial acrylic fibre and polypropylene can be used as air filters. Such fabrics have been noted for their high air permeability, low bulk and high efficiency. Hollow fibres have also been recommended for reverse osmosis, gas separation, ion-exchange, ultrafiltration and dialysis. Courtaulds has developed a porous acrylic fibre, Courtek D^{TM}, which can be used as a carrier for the controlled release of pharmaceuticals, bactericides, fungicides, pesticides, horticultural nutrients, and acid and alkali absorbents.

15.8.7 ACRYLIC FIBRES AS A SUBSTITUTE FOR ASBESTOS

Attempts have been made to develop a synthetic fibre that could replace carcinogenic asbestos in fibre-reinforced cement products, e.g. in flat roof sheets and facing slabs, corrugated sheets, and discharge and vent pipes. Polyacrylonitrile appears to be a good candidate for replacing asbestos because of its good chemical resistance in alkaline media. Hoechst AG has developed Dolanit^{TM} fibres (types 10, 12 and 15) by varying certain process parameters in spinning and after-treatment. Fibre-reinforced cement sheets containing 2% (by weight) Dolanit 10 and 4% (by weight) cellulose were tested for flammability and in all the tests the material met the requirements for Building Material Class A$_2$ of DIN Standard 4102, Part 1, and may be classified as a non-flammable building material that develops no toxic gases. Montefibre has also produced a high modulus polyacrylonitrile fibre, RICEM^{TM}, which can be used as a reinforcing medium for cement matrices, as an alternative to asbestos, or in eliminating cracks in mortar or concrete in the curing stage. Flat sheets made with 2% RICEM and 3.5% pulp fibres showed the same bending strength as sheets produced with 15% asbestos.

15.8.8 ACRYLIC AS A PRECURSOR FOR CARBON FIBRES

Among the various precursors for carbon fibre, PAN has a wide acceptability owing to high carbon yield and flexibility for tailoring to a desired product. The weight loss at 1000 °C in helium is quite low for PAN fibres compared with that for various other precursors of carbon fibres.

To produce good quality carbon fibres, special acrylic fibres (SAF) are required. SAF-forming polymers should possess a high molecular weight of approximately 10^5, a molecular weight distribution in the range 2–3, and minimum molecular defects at the polymerization stage [80–82]. The precursor fibre should also have fine denier (10–12 µm diameter), high strength and modulus, broader exothermic peak during

heating due to nitrile group oligomerization and low threshold temperature, and high carbon yield (>50%).

Amongst the various comonomers used for the production of acrylic precursor, itaconic acid (0.5–2 wt %) seems to be superior. It has been established that its carboxylic groups come in the vicinity of nitrile group and initiate the exothermic cyclization reaction at a lower temperature. The propagation step in the thermal cyclization is also slowed down in comparison with that in the PAN homopolymer.

The heat evolved in PAN is quite high during the propagation reaction; this might be detrimental to the properties of carbon fibre if not dissipated efficiently. Hence, acrylonitrile copolymers with a low percentage of acidic comonomer are better candidates for producing precursors for carbon fibres.

Mikolajczyk and Krucinska [83] have reported the effect of the intrinsic viscosity of acrylonitrile–methyl methacrylate copolymer on the mechanical properties of PAN carbon fibre precursor.

In addition to the modifications made during the polymerization stage, extensive work has been carried out in the area of spinning of acrylic fibres for producing high strength precursors for carbon fibres [58].

Japan Exlan, in a patent, disclosed the method for the production of high strength (2.20 GPa or 25.1 gf den^{-1}) acrylic fibres by spinning a 5% polymer solution in 50% aqueous NaSCN and stretching the fibre in different media to a total draw ratio of 14.4.

The processing and properties of acrylic precursor fibres have been documented in exhaustive reviews [81, 84, 85].

REFERENCES

1. Frushour, B.G. and Knorr, R.S. (1985) Acrylic fibres, in *Fibre Chemistry Handbook of Fibre Science and Technology*, Vol. IV (eds M. Lewin and Eli M. Pearce), Marcel Dekker, New York, pp. 171–370.
2. Matzke, R.R. Jr (1995) The acrylic fiber industry today, in *Acrylic Fiber Technology and Applications* (ed. J.C. Masson), Marcel Dekker, New York, pp. 11–35.
3. Vaidya, A.A. (1988) *Production of Synthetic Fibers*, Prentice Hall of India Ltd, New Delhi, pp. 63–72.
4. Tsai, J.S. and Lin, C.H. (1990) *J. Mater. Sci. Lett.*, **9**, 869.
5. Volkova, N.V., Smetanina, I.E., Bolshakova, M.G., Martynenko, V.I., Emelyanov, D.N. and Barsukov, I.A. (1985) *Khim. Volokna*, **6**, 15.
6. Wade, B. and Knorr, R. (1995) Polymerization, in *Acrylic Fiber Technology and Applications* (ed. J.C. Masson), Marcel Dekker, New York, pp. 37–67.
7. Ebdon, J.R., Huckerby, T.N. and Hunter, T.C. (1994) *Polymer*, **35**, Part 1, 250; Part 2, 4659.
8. Ito, S., Okada, C. and Kamada, K. (1986) *J. Appl. Polym. Sci.*, **32**, 4001.
9. Ulbricht, J. (1962) *Z. Phys. Chem.*, **5**, 346.

10. Peebles, L.H. Jr (1958) *J. Am. Chem. Soc.*, **80**, 5603.

11. Peebles, L.H. Jr, Thompson, R.B. Jr, Kirby, J.R. and Gibson, G.E. (1972) *J. Appl. Polym. Sci.*, **16**, 3341.

12. Patron, L. and Bastianelli, U. (1974) *Appl. Polym. Symp.*, **25**, 105.

13. Avrey, G., Chadda, S.K. and Pollar, R.C. (1982) *J. Polym. Sci., Polym. Chem. Ed.*, **20**, 2249.

14. Minagawa, M. and Iwamatsu, T. (1980) *J. Polym. Sci., Polym. Chem. Ed.*, **18**, 481.

15. Grassie, N. and McGuchan, R. (1971) *Eur. Polym. J.*, **7**, 1091.

16. Ovsyannikova, S.A., Bedar, N.M. and Nekrasov, I.K. (1973) *Khim. Volokna*, **3**, 75.

17. Andrews, R.D. and Kimmel, R.M. (1965) *J. Polym. Sci.*, **B13**, 167.

18. Okajima, O., Ikeda, M. and Takeuchi, A. (1967) *J. Polym. Sci.*, **A1**(6), 1925.

19. Ishida, Y., Matsuo, M., Ueno, Y. and Takayanagi, M. (1964) *Kolloid Z.*, **179**, 67.

20. Gupta, A.K. and Chand, N. (1980) *J. Polym. Sci., Polym. Phys. Ed.*, **18**, 1125.

21. Frushour, B.G. (1981) *Polym. Bull.*, **4**, 305.

22. Frushour, B.G. (1984) *Polym. Bull.*, **11**, 375.

23. Bohn, C.R., Schaefgen, J.R. and Statton, W.O. (1961) *J. Polym. Sci.*, **55**, 531.

24. Lindenmeyer, P.H. and Hosemann, R. (1963) *J. Appl. Phys.*, **34**, 42.

25. Hayakawa, R., Nishi, T., Arisawa, K. and Wada, Y. (1967) *J. Polym. Sci., Part A2*, **5**, 165.

26. Hinrichsen, G. (1972) *J. Polym. Sci., Part C*, **38**, 303; *Idem* (1973) *ibid.*, **17**, 3305.

27. Thomsen, T., Zachmann, H.G. and Korte, S. (1992) *Macromolecules*, **25**, 6934.

28. Imai, Y., Minami, S., Yoshihara, T., Joh, Y. and Saito, H. (1970) *J. Polym. Sci., Polym. Lett.*, **B8**, 281.

29. Minagawa, M., Miyano, K., Takahashi, M. and Yoshii, F. (1988) *Macromolecules*, **21**, 2387.

30. Bajaj, P., Padmanaban, M. and Gandhi, R.P. (1985) *Polymer*, **26**, 391.

31. Henrichsen, G. and Orth, H. (1971) *J. Polym. Sci., Polym. Lett.*, **B9**, 529.

32. Colvin, G.B. and Storr, P. (1974) *Eur. Polym. J.*, **10**(4), 337.

33. Hobson, R.J. and Windle, A.H. (1993) *Macromolecules*, **26**, 6903.

34. Joh, Y. (1979) *J. Polym. Sci., Polym. Chem. Ed.*, **17**, 4051.

35. Minagawa, M., Miyano, K., Morita, T. and Yoshii, F. (1989) *Macromolecules*, **22**, 2054.

36. Turska, E. and Grobelny, J. (1983) *Eur. Polym. J.*, **19**, 895.

37. Bashir, Z. (1992) *Polymer*, **33**, 4304.

38. Atureliya, S.K. and Bashir, Z. (1993) *Polymer*, **34**, 5516.

39. Gupta, D.C. and Sharma, R.C. (1990) *J. Appl. Polym. Sci.*, **39**, 1821.

40. Prasad, G. (1985) *Man-made Textiles in India*, **28**, Feb/Mar, p. 57.

41. Capone, G.J. (1995) Wet spinning technology, in *Acrylic Fiber Technology and Applications* (ed. J.C. Masson), Marcel Dekker, New York, p. 69.

42. Han, C.D. and Segal, L. (1970) *J. Appl. Polym. Sci.*, **14**, 2973, 2999.

43. Ziabicki, A. (1976) *Fundamentals of Fiber Formation*, John Wiley & Sons, New York, p. 306.

44. Paul, D.R. (1968) *J. Appl. Polym. Sci.*, **2**, 2273.

45. Zuguang, Ji and Anding, W. (1987) Proceedings of the 2nd International Conference on Man-made Fibres, 26–29 November, Beijing, China.

46. Bajaj, P., Kumari, Surya, Vaidya, A.A. and Gupta, D.C. (1989) *Textile Res. J.*, **51**, 601.
47. Catoire, B., Bouriot, P., Hagege Sotton, M. and Menual, J. (1989) *Textile Asia*, Feb, p. 73.
48. Knudsen, J.P. (1963) *Textile Res. J.*, **33**, 13.
49. Paul, D.R. and McPeters, A.L. (1977) *J. Appl. Polym. Sci.*, **21**, 1699.
50. Von Falkai, B. (1995) Dry spinning technology, in *Acrylic Fiber Technology and Applications* (ed. J.C. Masson), Marcel Dekker, New York, p. 105.
51. East, G.C., McIntyre, J.E. and Patel, G.C. (1984) *J. Textile Inst.*, No. 2, p. 196.
52. Baojun, Q., Jian, Q. and Zhenlong, Z. (1989) *Textile Asia*, **20**, 4, 48.
53. Maslowski, E. and Urbanska, A. (1989) *Fibre World*, May, p. 6.
54. American Cyanamid Co., US Patent 4 301 107 (October 1979).
55. Japanese Patent Kokai 60 094 615 (to Asahi Chemical Industry Co. Ltd) (1985); *Chem. Abstr.*, **103**(12) 89 014 (1985).
56. Japanese Patent Kokai 62 149 918 (to Mitsubishi Rayon Co. Ltd) (1987), *Chem. Abstr.*, **108**(8), 57 798 (1988).
57. Grove, D.A., Desai, P. and Abhiraman, A.A. (1988) *Carbon*, **26**, 403.
58. Sen, K., Bahrami, S.H. and Bajaj, P. (1996) *J. Macromol. Sci., Rev. Macromol. Chem. Phys.*, **C36**(1), 1–76.
59. Min, B.G., Son, T.W., Kim, B.C., Lee, C.J. and Jo, W.H. (1994) *J. Appl. Polym. Sci.*, **54**, 457.
60. Craig, J.P., Knudsen, J.P. and Holland, V.F. (1962) *Textile Res. J.*, **32**, 435.
61. Bell, J.P. and Dumbleton, J.H. (1971) *Textile Res. J.*, **41**, 196.
62. Rosenbaum, S. (1965) *J. Appl. Polym. Sci.*, **9**, 2071, 2085.
63. Stoyanov, A.A. and Natov, M.A. (1979) *Khim. Volokna*, **6**, 19.
64. Gupta, B.S., El-Mogahzy, Y.E. and Selivansky, D. (1989) *J. Appl. Polym. Sci.*, **38**, 899.
65. Takeda, H. and Nukushina, Y. (1964) *Textile Res. J.*, **34**, 173.
66. Todorova, I., Andreevski, B., Rizovska, V., Karkinska, M., Denkovski, G. and Petrov, G. (1991) *Melliand Textilber.*, **72**, 407/E163.
67. Stoyanov, A.K. (1979) *Appl. Polym. Sci.*, **23**, 3123.
68. Sarmadi, A.M., Noel, C.J. and Birch, J.B. (1990) *Ind. Eng. Chem. Res.*, **29**(8), 1640.
69. Qian, B., Sun, Z., Wu, C. and Tian, H. (1987) *J. Polym. Eng.*, **7**(2), 88.
70. Naik, A. (1987) *Melliand Textilber.*, **68**, E306.
71. Bajaj, P. and Paliwal, D.K. (1991) *Indian J. Fibre Textile Res.*, **16**, Mar, p. 89.
72. Qin, J. (1992) *J. Appl. Polym. Sci.*, **44**, 1095.
73. Hiroyoshi, T., Shigerv, F. and Mitsuo, S. (to Toray Industries) Japanese Patent Kokai 79 101 920 (1979).
74. Bajaj, P. (1995) *Melliand Textilber.*, **76**, E52.
75. Brown, D.M. and Pailthrope, M.T. (1986) *Rev. Prog. Color*, **16**, 8.
76. Bajaj, P. and Kumari, S. (1987) *J. Macromol. Sci., Rev. Macromol. Chem. Phys.*, **C27**(2), 181.
77. Nogaj, A. (1986) *Chemifasern Textilindustrie*, **36/88**, E101.
78. Sen, K., Bajaj, P. and Ramesh Babu, J.S. (1995) *Melliand Textilber.*, **72**, E52.
79. Simanova, S.A., Kolmakova, A.I., Konovalov, L.V., Kukushkin, Yu. N. and Lysenko, A.A. (1984) *Zh. Prikl. Khim. (Leningrad)*, **57**(11), 2265.
80. Donnet, J.B. and Bansal, R.C. (1990) *Carbon Fibers*, Marcel Dekker, New York.
81. Gupta, A.K., Paliwal, D.K. and Bajaj, P. (1991) *J. Macromol. Sci., Rev. Macromol. Chem. Phys.*, **C31**, 1.

82. Peebles, L.H. (1995) *Carbon Fibers, Formation, Structure and Properties*, CRC Press Inc., Boca Raton, FL, pp. 7–24.
83. Mikolajczyk, T. and Krucinska, I. (1989) *Textile Res. J.*, **59**, 536, 665.
84. Jain, M.K., Balasubramanian, M., Desai, P. and Abhiraman, A.S. (1987) *J. Mater. Sci.*, **22**, 301.
85. Fitzer, E. (1987) *Carbon*, **25**, 163.

Polypropylene fibres 16

Kushal Sen

16.1 INTRODUCTION

Polypropylene is the first stereoregular polymer to have achieved industrial importance. The fibres from polypropylene were introduced to the textile arena in the 1970s and have become an important member of the rapidly growing family of synthetic fibres. Today polypropylene enjoys fourth spot behind the 'big three' fibre classes, i.e. polyester, nylon and acrylic. However, as opposed to other commodity fibres, its use as apparel and household textiles has been rather limited; the bulk of the fibre produced is used for industrial applications. Nevertheless, the textile and household uses are growing.

Initial attempts to polymerize propylene resulted in a polymer which was not crystallizable and demonstrated a low degree of polymerization and a low melting point; in short the essential requirements of a fibre-forming polymer were missing in this polymer. The work of Ziegler and Natta in the mid 1950s led to the preparation of a crystalline polypropylene. The key to their success lay in the discovery of a coordination catalyst system, now known as the Ziegler–Natta catalyst. The polypropylene thus produced had all, or most, of the pendant methyl groups in a regular position with respect to the polymer backbone – in other words, the polymer was stereoregular. It not only represented a turning point in polymer chemistry but also opened vistas of new technology of vinyl polymerization. The stereospecific polymer, with all the methyl groups on one side, was called isotactic polypropylene. It was crystallizable (melting point 160–174 °C), and could be conveniently converted into

fibres capable of retaining molecular orientation at normal usage temperatures.

The technology has come a long way since then. Isotactic polypropylene, as originally produced, had a broad molecular weight distribution, contained non-crystallizable resin, and the resultant yield was poor. Subsequent developments in the polymerization processes and catalyst system have increased the polymer yield ten-fold, narrowed the molecular weight distribution, and reduced the non-crystallizable resin, resulting in a polymer which is suitable for fibre formation [1].

It must be pointed out that polypropylene, as such, is very susceptible to oxidative and radiation-induced degradation even at room temperature. Consequently, it is essential that degradation is avoided during storage, processing and usage. The success story of polypropylene has, therefore, much to do with the development of antioxidants and thermal and ultraviolet (UV) stabilizers. Another major problem these fibres faced, and because of which their use in apparel sector is restricted even today, is the lack of dyeability; they do not have dye sites as other commercially useful fibres have. Mass-coloration using suitable pigments has led to the introduction of a wide range of coloured fibres in the market and has given a boost to the polypropylene fibre production. In addition, the production of fine denier fibres has also increased its acceptance in the apparel sector. Complete hygroscopicity, which hitherto was considered a bane, has been turned into an advantage because of its wicking properties. In fact, polypropylene is among the strongest performers in hygiene-related applications.

In this chapter, the preparation of the polymer and its conversion to fibre and filament is described. The structure, properties and applications of the fibre are also briefly discussed.

16.2 POLYMERIZATION

Propylene, the monomer for polypropylene, is a liquefiable hydrocarbon gas boiling at $-47\,°C$. Table 16.1 gives data on typical yield of propylene from various feedstocks [2, 3]. It may be inferred from this table that

Table 16.1 Typical yield of propylene from various feedstocks [2, 3]

Feedstock	Propylene yield (% of feedstock)
Liquefied petroleum gas (LPG)	15–25
Iso-butane	80–85
Naphtha	15–20
Crude oil	6–12

Table 16.2 Typical product specifications for propylene [3, 4]

		Commercial-grade	Polymer-grade
Propylene	% mol (minimum)	93.0	99.5
Hydrogen	ppm mol (maximum)	300	300
Methane	ppm mol (maximum)	300	300
Ethylene	ppm mol (maximum)	300	300
Ethane	ppm mol (maximum)	1000	1000
Propane	% mol	Balance	Balance
Methyl acetylene	ppm mol (maximum)	10	10
Propane	ppm mol (maximum)	30	30
Butadiene	ppm mol (maximum)	10	10
Sulphur	ppm mol (maximum)	5	5
Water	ppm mol (maximum)	5	5

isobutane is of considerable interest as feedstock. Polymer-grade propylene, as against commercial-grade, should be at least 99.5% pure. It is necessary to separate most of the propane from propylene, which is a difficult process because the relative volatility between propylene and propane is very low. Super-fractionation is needed for separation. Specifications for a polymer-grade propylene are listed in Table 16.2 [3,4]. In addition, the feedstock may have CO_2, CO, and carbonyl sulphide which may adversely affect the catalyst activity and implant scavengers must be utilized to remove these.

16.2.1 STEREOSPECIFIC POLYMERIZATION

Propylene, as a consequence of its chemical structure, can be polymerized to give several different spatial arrangements.

$$n\text{CH}_2{=}\overset{\overset{\displaystyle \text{CH}_3}{|}}{\text{CH}} \longrightarrow \overset{\overset{\displaystyle \text{CH}_3}{|}}{\{\text{CH}_2{-}\text{CH}\}_n}$$
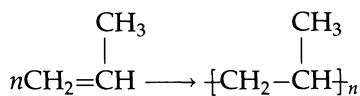
The following three possibilities exist.

1. Atactic or stereo-random: here the methyl groups are, sterically speaking, randomly distributed. This is non-crystallizable and is of no importance as a plastics or a textile product.

$$\text{\textasciitilde}\overset{\overset{\displaystyle \text{CH}_3}{|}}{\text{CH}}{-}\text{CH}_2{-}\overset{\overset{}{|}}{\text{CH}}{-}\text{CH}_2{-}\overset{\overset{}{|}}{\text{CH}}{-}\text{CH}_2{-}\overset{\overset{\displaystyle \text{CH}_3}{|}}{\text{CH}}{-}\text{CH}_2{-}\overset{\overset{}{|}}{\text{CH}}\text{\textasciitilde}$$
$$\qquad\qquad \underset{\text{CH}_3}{|}\quad \underset{\text{CH}_3}{|}\qquad\qquad \underset{\text{CH}_3}{|}$$
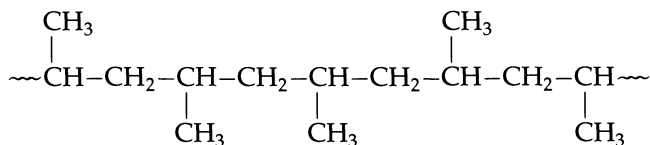
2. Syndiotactic: here methyl groups alternate in sterically regular fashion along the chain. Only imperfect syndiotactic polypropylene

has been made to date and it has little practical significance.

$$CH_3 \qquad\qquad CH_3 \qquad\qquad CH_3$$
$$|\qquad\qquad\quad |\qquad\qquad\quad |$$
$$\sim\!\!\!\sim CH-CH_2-CH-CH_2-CH-CH_2-CH-CH_2-CH\!\sim\!\!\!\sim$$
$$|\qquad\qquad\quad |$$
$$CH_3 \qquad\qquad CH_3$$
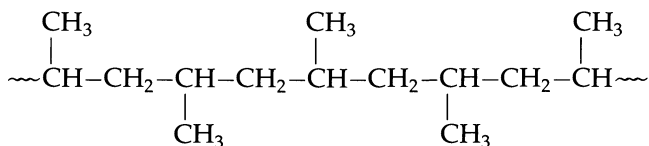
3. Isotactic: building blocks, in this case, are so arranged that the methyl group is found to be in the same relative position in space. Commercially, this is the most important stereospecific configuration.

$$CH_3 \qquad CH_3 \qquad CH_3 \qquad CH_3 \qquad CH_3$$
$$|\qquad\quad |\qquad\quad |\qquad\quad |\qquad\quad |$$
$$\sim\!\!\!\sim CH-CH_2-CH-CH_2-CH-CH_2-CH-CH_2-CH\!\sim\!\!\!\sim$$
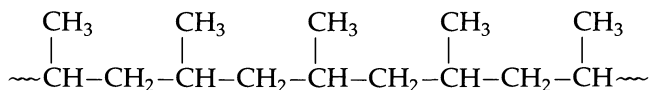
Preparation of stereospecific polypropylene has been possible by the use of stereospecific catalysts, which are the backbone of polymer preparation.

16.2.2 THE CATALYST SYSTEMS

In the early days, typical yields were 500–1000 kg of polymer per kg of catalyst. More recently, however, due to improved efficiency and selectivity of catalyst systems, the yield of polymer has increased by more than ten-fold and at the same time the amount of atactic polymer generated has been reduced. Newer catalysts, called 'high mileage' catalysts, are very efficient. It is claimed that 1 kg of titanium may produce 8000–250 000 kg of polymer. These developments have resulted in less catalyst residue in the polymer so that catalyst washing (de-ashing) is eliminated or significantly reduced. The catalysts generate less amorphous polymer, reactor fouling is eliminated and more often the solvent and monomer can be recycled directly back to polymerization without separation and purification.

Manufacturers, nevertheless, are very selective about their catalyst composition and catalyst preparation processes. A wide variety of Ziegler–Natta catalysts have been reported in patent literature. These are also called anionic coordinated catalysts, based on the polymerization mechanisms which, although not yet proved, have generally been accepted [3, 5].

These catalysts consist of a halide of a transition metal of the fourth group of the Periodic Table (e.g. titanium and vanadium), and an organometallic compound of a metal belonging to one of the three first groups of the Periodic Table (e.g. lithium, beryllium and aluminium). Some examples of popular combinations are:

Metal halide	Organometallic compound
Crystalline $TiCl_3$	AlR_3, AlR_2X, BeR_2
$TiCl_4$	AlR_3, AlR_2X, LiR
$VdCl_3$	AlR_3, AlR_2X, LiR

where R is an alkyl group and X a halide. The transition metal chloride is often used in its highest valence state and reduced, *in situ*, to a lower state. However, preformed crystalline $TiCl_3$ is a superior catalyst. The stereospecificity and overall efficiency determine the commercial value of a catalyst system. Both these, in fact, depend on the nature of each component. For instance, δ-$TiCl_3$ is more active than α-$TiCl_3$, and for a given $TiCl_3$, $Be(C_2H_5)_2$ is more active than $Al(C_2H_5)_3$, which in turn is more active than $Al(C_2H_5)_2X$.

The efficiency of the Ziegler–Natta catalyst systems can be increased by mechanical and chemical means. Dry milling and prolonged heating are advantageous. Secondary and tertiary amines and various Lewis acids have been known as typical activators. It may not be out of place here to mention that oxygen, water, or carbon dioxide, carbon monoxide, carbonyl sulphide, as impurities, inhibit polymerization. Alcohol treatments are frequently used to destroy the catalyst to stop the polymerization.

Several hypotheses have been put forward to explain the mechanism of catalysis. It is generally believed that a catalyst complex is first formed by the alkylation of the transition metal halide with organometallic compound. This may be represented as:

$$\overset{\delta+ \quad \delta-}{Cat-R}$$

where R is the alkyl group bound to transition metal, and the partial negative charge resides on carbon atom. The monomer units are inserted one by one as shown below:

$$\overset{\delta+ \quad \delta-}{Cat-R} + CH_2{=}\underset{\underset{CH_3}{|}}{CH} \longrightarrow \overset{\delta+ \quad \delta-}{Cat-CH_2}{-}\underset{\underset{CH_3}{|}}{CHR}$$
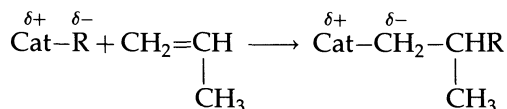
Before entering into the chain, the propylene double bond coordinates with the transition metal of the catalyst complex, and so polymer formation takes place. The molecular weight of the polymer depends on the Al:Ti ratio, temperature and time. The molecular weight varies inversely with temperature and increases asymptotically with the time of polymerization. Chain termination may occur due to chain transfer with monomer, spontaneous rupture of polymer chains, or exchange of alkyl groups. Mechanical blocking of the catalyst surface, as the polymerization progresses, may hinder the catalytic activity. This is generally considered to be the reason for the relatively broad molecular weight

distribution. In fact, the shape and particle size distribution of catalysts has been shown to govern the shape and particle size distribution of the polymer. It is possible to get spherical, granular or irregular flaky polymer particles by suitable selection of catalyst. Uniform spherical particles can obviate the need for expensive pelletization.

16.2.3 INDUSTRIAL POLYMERIZATION PROCESSES

Details of industrial processes for the manufacture of polypropylene are closely guarded secrets. Generally four major steps are involved, namely catalyst preparation, polymerization, polymer purification and polymer finishing. Although catalysts are commercially available, the industries prefer in-house catalyst preparation to reduce cost and to maintain secrecy. As mentioned earlier, the particle size and size distribution of the catalysts must be controlled for reproducibility. In industry, polymerization is carried out either in suspension in a hydrocarbon diluent or in a gas phase reactor.

(a) Continuous suspension polymerization

Most polypropylene production is carried out in hydrocarbon diluents, such as hexane or n-heptane. Isotactic polypropylene is insoluble in n-heptane or hexane up to their boiling points while atactic polymer is soluble. Table 16.3 gives specifications of hexane as demanded by the polymer industry [5]. Suspension polymerization is a convenient process because the viscosity of the medium remains low even at high polymer yield, enhancing the ease of stirring and homogenization.

Figure 16.1 is a schematic representation of the suspension polymerization process for polypropylene. The catalyst is slurried in highly purified heptane (or hexane) and fed along with propylene and diluent (n-heptane/hexane) into the polymerization vessel. Operating temperatures range between 50 and 80 °C while pressures range between 2 and 4 atm. It must be remembered that higher temperatures reduce the amount of isotactic polymer. Crystalline polypropylene forms continuously and precipitates as a solid on the catalyst surface until the slurry becomes very thick (about 40% solids). The reactor slurry flows to a flash

Table 16.3 Specification for hexane [5]

Property	Limits
Density at 15 °C (g cm^{-3})	0.660–0.685
Total sulphur (wt ppm)	5 (maximum)
Aromatics (wt %)	0.05 (maximum)
Oxidizable matter (wt ppm) (as methanol)	5 (maximum)
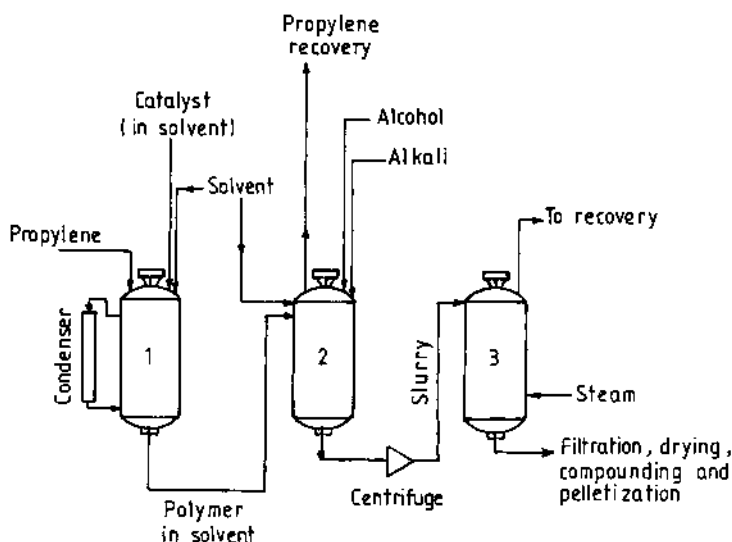
Fig. 16.1 The slurry process: 1 = polymerization; 2 = termination and propylene recovery; 3 = stripping.

tank where unreacted propylene is vaporized for recirculation. Polymer slurry is centrifuged to remove the diluent along with the dissolved atactic polymer. It must be emphasized that atactic polymer, if not properly removed, would impair the mechanical properties of the product. Isotactic polypropylene is treated with isopropanol to remove catalyst residues (de-ashing) and hydrocarbon diluent. Catalysts, when washed with alcohols, are transformed into titanium and aluminium compounds that are soluble in hydrocarbons, alcohol or water. It should be pointed out that a catalyst system is active only in the form of suspension. It is then washed with methanol and dried. The dried polymer flakes are either compounded with suitable stabilizers and palletized or supplied directly to processors. Major fibre manufacturers like to buy virgin polymer and do in-house compounding. In contrast to manufacturers of polyester, nylons, and other synthetic fibres, the polypropylene fibre manufacturers do not carry out the complex polymerization; instead they prefer to obtain pallets or flakes, do the compounding, and spin the fibres.

The rate of polymerization is controlled by temperature, pressure and catalyst concentration. The method of catalyst preparation may also affect the rate. Increase in temperature increases the rate but reduces the stereoregularity of the polymer. The molecular weight, however, can be controlled by feeding hydrogen into the reactor at constant partial pressure.
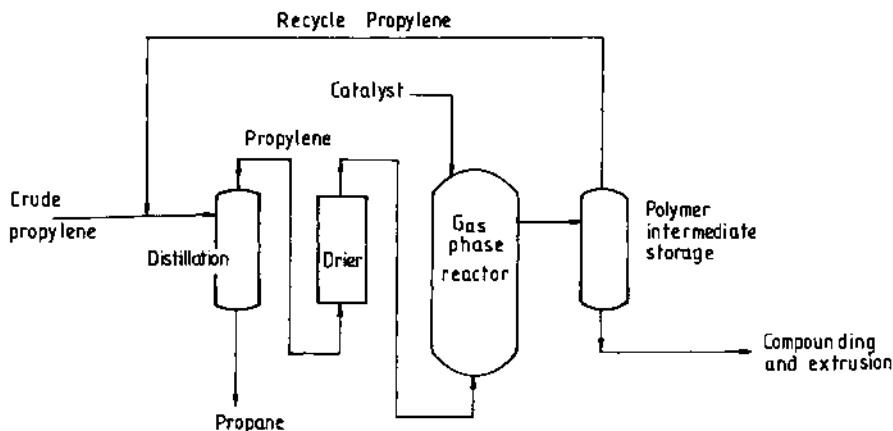
Fig. 16.2 Gas phase polymerization.

The viscosity average molecular weight of the polymer may range from 100 000 to 1 000 000, while the ratio $\bar{M}_w/\bar{M}_n$ ranges from 4 to 15.

(b) Gas phase polymerization process

Polymer made by this process is more suitable for tape yarns but is not recommended for multifilament yarn production. Figure 16.2 is a schematic sketch of a typical gas phase polymerization system for polypropylene. The dried and purified liquid propylene is continuously fed to the bottom of the polymerizer reactor, while a high efficiency Ziegler–Natta catalyst is introduced from the top. A mixture of solid catalyst and up-flowing propylene gas comes in contact and polymerization takes place. The solid catalyst fragments as the polymerization progresses and the size of the polypropylene particles grows. A reaction temperature of 90 °C and pressure of 30–35 atm. is used. Temperature control is accomplished by using liquefied propylene which partially evaporates in the reactor, thereby cooling the system. About 15% of the propylene is in the reactor while 85% is being recycled. Unreacted propylene and the powdered polypropylene are continuously removed from the reactor. The propylene is recycled while the polymer is combined with suitable additives and stored or shipped.

16.3 STABILIZATION AGAINST DEGRADATION

In the absence of oxygen, polypropylene is relatively stable (i.e. stable to pyrolytic degradation even up to 350 °C). However, as-spun polypropylene is unstable to ·both heat and light, particularly in the presence of oxygen. At high temperatures, as used in the melt for extrusion, polymer

molecular weight and melt viscosity change, causing difficulties in processing. Similarly, weathering results in a sharp drop in fibre elongation together with an increase in oxygen uptake. The oxidation resistance of polypropylene is very poor, so much so that it is impossible to process polypropylene under commercial operating conditions without the presence of antioxidants. Attention, therefore, must be paid to improve melt extrusion stability, long-term thermal stability, and UV light stability.

More than any other textile-grade polymer, polypropylene owes its existence to the host of stabilizers that are compounded to restrict degradation. This susceptibility is mainly because of the presence of a tertiary carbon in the chain.

16.3.1 MECHANISM OF THERMO-OXIDATIVE DEGRADATION

Oxidative degradation is a chain reaction; it can be triggered by heat or light and can be accelerated by certain metal catalysts. The generally adopted scheme of simple oxidative degradation under the influence of heat is as follows.

Initiation $\qquad$ $PPH \xrightarrow{\Delta H} PP^{\bullet} + H^{\bullet}$

$\qquad\qquad\qquad PPH \xrightarrow{\Delta H + O_2} PP^{\bullet} + HOO^{\bullet}$

Propagation $\qquad PP^{\bullet} + O_2 \longrightarrow PPOO^{\bullet}$

$\qquad\qquad\qquad PPOO^{\bullet} + PPH \longrightarrow PPOOH + PP^{\bullet}$

$\qquad\qquad\qquad PPOOH \longrightarrow PPO^{\bullet} + O^{\bullet}H$

$\qquad\qquad\qquad O^{\bullet}H + PPH \longrightarrow H_2O + PP^{\bullet}$

Termination $\qquad PP^{\bullet} + PP^{\bullet} \longrightarrow PP{-}PP$

$\qquad\qquad\qquad PP^{\bullet} + PPOO^{\bullet} \longrightarrow PP{-}OO{-}PP$

$\qquad\qquad\qquad PPOO^{\bullet} + PPOO^{\bullet} \longrightarrow PP{-}OO{-}PP + O_2$
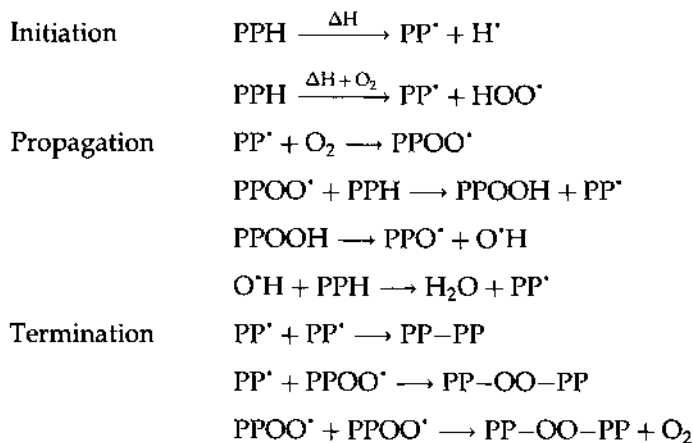
The reaction of free radicals with oxygen is almost instantaneous with practically no activation energy. Termination is possible only by dimerization and disproportionation. However, such reactions occur only when the concentration of such free radicals is very high and degradation is well advanced.

When the concentration of peroxides in the system increases, it begins to decompose. The reaction becomes autocatalytic and the deterioration becomes very rapid.

$$2PPOOH \longrightarrow PP^{\bullet} + PPOO^{\bullet} + H_2O$$

$$PPOOH \longrightarrow PPO^{\bullet} + O^{\bullet}H$$
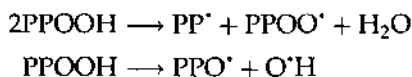
16.3.2 MECHANISM OF PHOTO-OXIDATION

Unprotected polypropylene progressively loses its chemical and physical properties during weathering at ambient temperatures. This is attributed to UV light absorption in the range 3000–4000 Å. Propylene, when pure, does not usually absorb in the spectral region above 3000 Å and should not degrade in sunlight. However, processed PP contains small amounts of carbonyl groups and hydroperoxides – the photoactive species. The alkyl hydroperoxides, for instance, absorb a part of the UV light reaching the substrate and break into free radicals.

$$PPOOH \xrightarrow{h\nu} PPO^{\bullet} + OH^{\bullet}$$
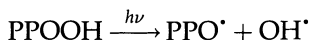
The same applies to carbonyl groups, though the reactions are more complex. Thus, UV degradation differs from thermal oxidation in the nature of the initiation; also in this case the number of oxidation cycles per initiation step is small and the rate of initiation high. Since more keto groups are formed as by-products of degradation, the amount of energy absorbed keeps on increasing with time. Initiation is followed by propagation and termination. The detailed mechanisms are described elsewhere [3].

16.3.3 THE STABILIZERS

Stabilizers are generally classified as heat or light stabilizers. This distinction is, however, superficial. A more appropriate classification would be as follows [3].

1. Free radical scavengers: these have the capacity of terminating the propagating chain by giving inert free radicals, e.g. hindered phenols.
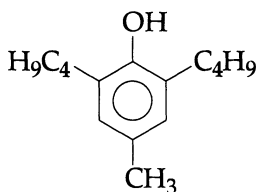
(2,6-di-ter-butyl-p-cresol)

2. Peroxide decomposers: these help to preferentially decompose the alkyl peroxides into non-radical stable products, e.g.

$$(C_{12}H_{25}-O-\overset{\overset{\displaystyle O}{\displaystyle \|}}{C}-CH_2-CH_2)_2S$$

(dilauryl thio dipropionate, DLTDP)
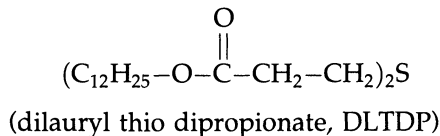
3. UV absorbers: these demonstrate UV screening effects by absorbing the UV radiation. Examples are carbon black and Cyasorb UV 531^{TM}, which is
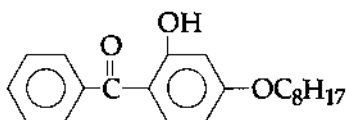
(1-hydroxy, 3-octoxy benzophenone)

4. Energy quenchers: these act by harmless transfer of energy as

$$PPH \xrightarrow{h\nu} PP^{\bullet} \xrightarrow{Q} PPH + Q^{\bullet} \longrightarrow Q + h\nu.$$
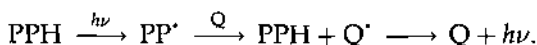
Nickel chelates have proved quite successful in this role, such as
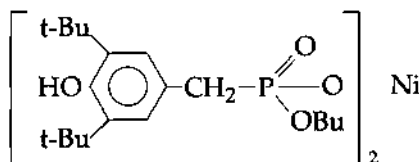
(Irgastab 2002^{TM}, Ciba-Geigy)

5. Metal deactivators: metals, if present, catalyse oxidative degradation. Chelating agents are sometimes added to prevent this.
6. HCl scavengers: the residues of the Ziegler–Natta catalyst, if not removed by thorough extraction, participate in degradative process with the liberation of hydrochloric acid. HCl acceptors such as epoxy compounds, di-butyl tin compounds, etc. are used to prevent this.

A recent addition to the family of stabilizers is the compound commonly known as HALS (hindered amine light stabilizers). These contain a 2,2,6,6-tetramethyl piperidyl group. These are excellent light stabilizers and long-term thermal stabilizers. CR 144^{TM}, a poly(2,2,6,6-tetramethyl-4-piperidyl amino triazine), is one such compound. Strictly speaking, they fall under the class of free radical scavengers.
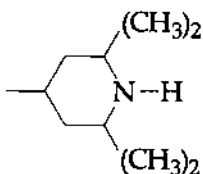
Normally these stabilizers are not used alone but in combination, where their activities are synergized. In addition to these, other additives

such as pigments may also have to be added. The compatibility of additives therefore becomes quite important.

16.4 FIBRE PRODUCTION

16.4.1 THE MATERIAL

Polypropylene (PP) is generally available in the form of chips or granules which are white in colour and are semicrystalline. The polymer is sold in a range of molecular weights, which are characterized by melt flow index (MFI). The MFI for fibre-grade PP is the weight in grams of melt flowing out in 10 min in a melt flow indexer of specified dimensions under a load of 2.16 kg at 230 °C. For textile applications polymers in the medium molecular weight range with MFI of 15–25 g/10 min are used, while for the technical sector polymers with higher molecular weight in the MFI range of 3–5 g/10 min are used.

The molecular weight and molecular weight distribution are important both for the processing of the polymer and the properties of the fibres produced therefrom [6–11]. The polydispersity of commercially available polymer ranges from 2 to 12 or more. The narrower the molecular weight distribution, the easier the control of spinning; a molecular weight distribution of around 3 is considered ideal for high speed spinning. In general changes in molecular weight have the following effects.

- The degree of crystallinity in fibres increases as molecular weight decreases.
- The nucleation rate increases as the molecular weight decreases.
- The crystallization rate increases with increase in polydispersity.
- Optimum spinning temperature increases with increase in molecular weight and with the breadth of the molecular weight distribution. However, the effect of molecular weight distribution is less [8, 9].
- Broad molecular weight distribution demonstrates higher draw resonance and poor spinnability [10].
- Polypropylene with a narrow molecular weight distribution shows higher birefringence at higher spinning speeds, and consequently higher tenacity and lower elongation [11].

In recent years, the production of polymers with narrow molecular weight distribution has increased significantly to give what are known as the controlled rheology (CR) resins. These polymer grades show improved spinning and can be spun at higher speeds and lower temperatures than conventional resins.

Kloos [12] has summarized the influence of polymer characteristics and spinning parameters on the spinnability and mechanical properties of PP fibres. Some of his data are given in Table 16.4.

Table 16.4 Influence of polymer characteristics and spinning parameters

	Spinnability	Fibre properties
Molecular weight distribution (MWD)	Improves with decreasing MWD	Tenacity improves with narrowing of MWD
Homogeneity	Improves with better homogeneity	Uniformity in properties improves with better homogeneity
Spinning temperature	Improves with increase in temperature	Birefringence and tenacity improve at higher value
Draw-down ratio	Improves at lower draw-down ratio	Birefringence and tenacity improve at higher value
Take-up velocity	Improves with lower velocity	Birefringence and tenacity improve at higher value

16.4.2 THE PROCESSES OF FIBRE PRODUCTION

Polypropylene fibres are produced by a larger variety of processes than any other melt-spun fibres. These processes include [1]:

(a) short air-quench melt-spinning (two-stage process);
(b) long air-quench melt-spinning (high speed spinning process);
(c) spin–draw process;
(d) spin–draw texturing process (bulked continuous filament or BCF process);
(e) water-quench melt-spinning process;
(f) tape yarns from slit film.

Before briefly describing the above processes, some general features will be summarized. As stated in Chapter 2, the average molecular weight of fibre-grade polypropylene is relatively high compared with that used in the case of PET and nylon fibre-grade polymers and this results in high melt viscosity. Hence the extrusion temperatures are 65–125 °C above the polymer melting point ($T_m \sim 165$ °C), in the range 230–290 °C. As stated in Chapter 4, the screw lengths are longer for achieving homogenization in the extruder. Alternatively, a large diameter screw with shallow grooves may be used. Because of the high specific heat and low thermal conductivity of polypropylene, the cooling zones must be correspondingly larger than those in the case of PET or nylon [13]. Because PP is difficult to dye, pigmentation is carried out by the use of colour masterbatches which are added during extrusion. Other additives may also be added at this stage. The methods of production will now be described.

(a) Short air-quench melt-spinning

In this case, as the name suggests, the entire system can be located in one floor as the quench zone is not more than 1 m long. The spinning speeds

are therefore low and are generally in the range 100–300 m min^{-1}. The productivity is optimized by using spinnerets with a large number of orifices, say up to 55 000 per spinneret. At the lower speeds used, the tow can be fed continuously to the drawing unit [13].

This method is used for the production of high tenacity polypropylene staple fibres and filament yarns with tenacity up to 10 cN dtex^{-1}; for this appropriate filament cooling and drawing facilities must be used. The short spinning method, which is profitable even when relatively small quantities are involved, is highly flexible as regards colour change.

(b) Long air-quench melt-spinning

This method is also called the long spin, high linear speed technique and a long length of the cooling duct (3–10 m) is needed to ensure that at the high speeds used, the filaments are brought to a low enough temperature before winding. The basic spinning process is similar to that used for producing PET and nylon filaments; however, it is essential that an appropriate grade of PP with a narrow molecular weight distribution is used. Normally this method is used to produce POY which can either be drawn or draw-textured.

(c) Spin–draw process

This integrated process couples spinning and drawing into one continuous operation. Though the actual spinning speed may be 300–700 m min^{-1}, the ultimate winding speeds may be as high as 3000–3500 m min^{-1}. The flexibility of this process is remarkable in that a large range of polymer grades can be used to produce yarns with different mechanical properties. Normally this process is used to produce high tenacity coarser industrial yarns. However, fine denier yarn for texturing can also be produced.

(d) Spin–draw texturing process

Bulked continuous filament (BCF) can be produced using this method. This is a unique process which combines spinning, drawing and texturing in one process. The various steps involved are similar to those used in the spin–draw process; however, after stretching and prior to being wound onto reels, the filament is subjected to a bulking operation by overfeeding the yarn into a hot fluid (steam or hot air). The filaments are not only individualized but also become pliable due to higher temperatures in the jet. They are then thrown onto a cooling drum as they emerge from the fluid jet. These are cooled in tensionless condition on the drum whereby the crimp is stabilized before the final winding (Fig. 16.3).
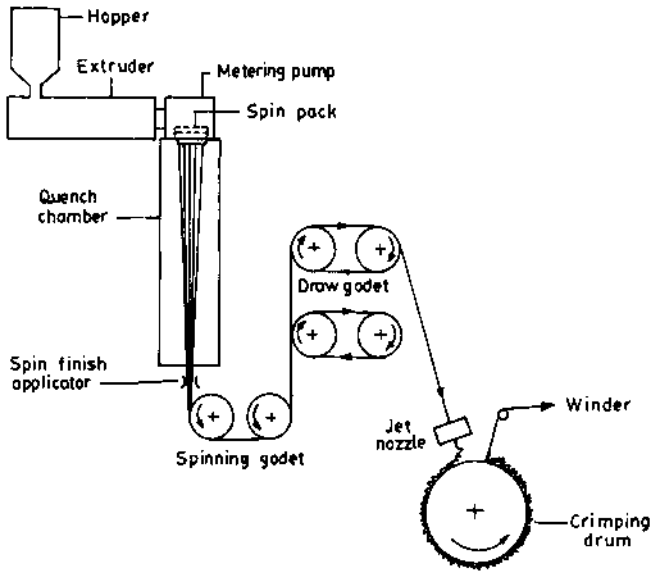
Fig. 16.3 The BCF production sequence.

A large proportion of BCF yarn is used in the carpet industry. It is inexpensive and is available in a wide range of colours.

(e) Water-quench melt-spinning process

The method is used for the manufacture of heavy denier (100 or higher) monofilaments because cooling is more efficient. The basic process is the same as melt-spinning except that after travelling a short distance below the spinneret, the filaments enter a water-quench tank.

(f) Tape yarns from slit film

Coarser filaments can be obtained using this method in which polypropylene is extruded as film. This film is then drawn uniaxially and as it fibrillates it is cut into yarns with knives. It is, however, also possible to extrude a profiled film which fibrillates automatically during drawing. The yarns produced from film have higher tenacity levels (4.5–6.5 cN dtex^{-1}) due to the high orientation of macromolecules and they are particularly suitable for use in packing materials or industrial textiles.

In addition to these, the spun-bonding and melt-blowing techniques are also used to produce spun-bonded non-wovens. These techniques

Table 16.5 Comparison of various PP filament yarn manufacturing processes

Techniques	Merits	Demerits
Conventional (two-stage) process	Cover wide denier range	Higher wastage than one step process
	Suitable for various grades of polymers	Higher space requirement
	Technology simple to adopt	
High speed POY spinning process	Suitable for making finer denier feeder materials for draw-twisting and draw texturing	High capital cost
	Better quality	
	Cost effective	
	High production	
Spin–draw process	Cost effective for deniers above 420 due to lower wastage and higher productivity	High capital cost
	Suitable for various grades of polymer	
Spin draw texturing process	Can produce high quality carpet yarns	High capital cost

are described in Chapter 19. Some of the important processes for the manufacture of PP yarns are compared in Table 16.5. The typical requirements for some of the common applications of polypropylene fibres are summarized in Table 16.6.

The high melt elasticity and the phenomenon of draw resonance have to be taken into consideration before the fibre can be spun efficiently

Table 16.6 Typical requirements for some common applications

Denier per filament	Product and application	Stretch ratio	Spinning speed (m min^{-1})	Melt flow index (g/10 min)
20–40	Multifilament CF, BCF (carpet yarn)	2.5–4	500–1500	10–20
6–20	Multifilament CF, BCF (upholstery)	3–4	500–1500	20–40
3–10	Multifilament, staple (heavy duty fabrics)	2–4	100–300[a] & 300–1000[b]	10–20
1–3	Multifilament, staple (light-weight apparel)	1.3–4	100–100[a] & 1000–4000[b]	18–40 20–40

[a] Short spin.
[b] Long spin.

without many breaks. These two features, which are prominent in polypropylene, have already been discussed in Chapter 3.

16.5 STRUCTURE DEVELOPMENT DURING SOLIDIFICATION

The rate of crystallization of polypropylene is high. As the molten fluid emerges from the spinneret, it cools as it is being attenuated and develops molecular orientation as well as morphological order. Figure 16.4 shows how surface temperature, filament diameter and birefringence change along the spinline for a wind-up speed of $150\,\mathrm{m\,min^{-1}}$ [14]. Crystallization commences around 24 cm below the spinneret exit when the temperature reaches a value of around $100\,°C$. A dramatic improvement in orientation occurs at this stage. As discussed in earlier chapters, amongst the factors which affect the structure and morphology, spinline stress is very important and it depends on the molecular weight of the polymer, the extrusion temperature, the temperature and cross-flow rate of the cooling air, and the take-up velocity. The spinline stress may increase from $10^5\,\mathrm{dyn\,cm^{-2}}$ at a take-up value of $50\,\mathrm{m\,min^{-1}}$ to greater than $10^7\,\mathrm{dyn\,cm^{-2}}$ for a take-up value of $600\,\mathrm{m\,min^{-1}}$; the corresponding increase in birefringence is five-fold. The overall crystallinity also increases as the spinline stress increases due to an increase in speed.

The spun fibres exhibit a skin–core effect with the skin having higher orientation than the core, as shown in Fig. 16.5 [15]. When crystallized from the melt, isotactic polypropylene molecules adopt a 3_1 helical conformation. Depending on the crystallization conditions, these helices pack in different geometries [16] giving rise to the three well-known polymorphs, namely the α-monoclinic, the β-hexagonal and the γ-triclinic crystal forms which exist in conjunction with an amorphous phase. In addition to these, a phase possessing order intermediate between the
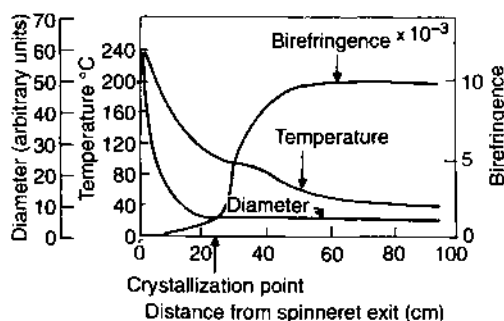
Fig. 16.4 Changes in diameter, temperature and birefringence along the spinline during melt-spinning of polypropylene. Melt temperature $260\,°C$, throughput = $0.3\,\mathrm{g\,min^{-1}}$ [14].
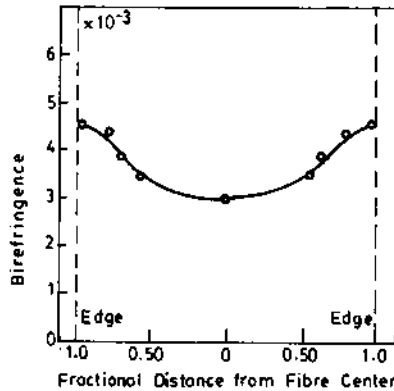
Fig. 16.5 Difference in orientation between skin and core of a typical polypropylene filament [15].

amorphous (atactic) and crystalline states can be obtained by quench cooling and is referred to as the 'smectic' phase. Because of its relatively higher crystallizability, the as-spun polypropylene fibre is significantly crystalline; however, the crystallites may be in the paracrystalline,
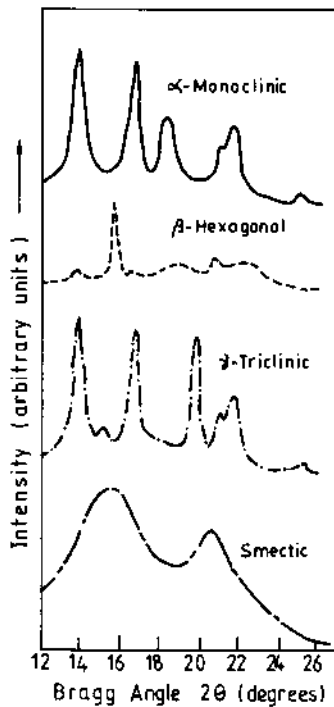
Fig. 16.6 X-ray scattered intensity profiles for various crystalline forms of polypropylene.

smectic form. When drawn and/or annealed they move towards the more stable α form [17–22]. Figure 16.6 shows the wide angle X-ray diffractograms of various forms. An increase in spinning speed increases the spinline stress even at similar draw-down ratios. This changes the crystal structure from smectic to α form as depicted in Fig. 16.7. In fact the draw-texturing of POY polypropylene at relatively high speeds has been made possible despite high crystallinity of feeder yarn because of the presence of part smectic structure. This can quickly and easily get transformed to a more stable α form during draw-texturing to give stable texture and crimp properties. The increase in spinning speed increases tenacity and decreases elongation to break, giving flexibility for manipulation of product properties (Fig. 16.8). Because of its metastable structure and the fact that its glass transition temperature is below room temperature, polypropylene fibres may show physical ageing at room temperature. They also show higher creep.

An interesting feature is observed when the density of as-spun polypropylene fibres is plotted as a function of take-up velocity. For samples spun at 290 °C with a high throughput rate, a minimum in density occurs at around 800–1000 m min^{-1} [23, 24]. The location of the minimum can vary depending on the spinning temperature and the actual throughput rates. Using a steady-state model that includes crystallization in the spinline and the effect of crystallization on the extensional viscosity and other physical characteristics of polypropylene [24], it has
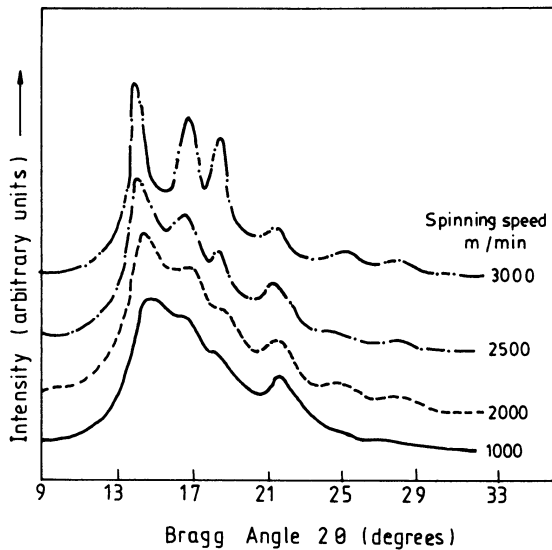
Fig. 16.7 Effect of spinning speed on crystallographic transition in polypropylene (MFI 24) fibre from smectic to α-monoclinic structure (at the same draw-down ratio).
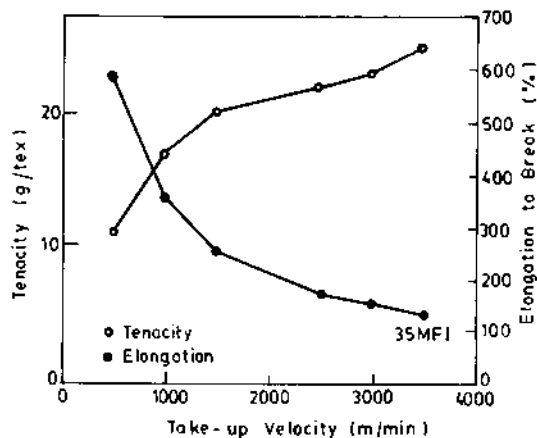
Fig. 16.8 Effect of spinning speed on tenacity and elongation of polypropylene (MFI 35) yarn spun at 205 °C [adapted from reference 1].

been shown that the reduction in density is possible if the quench rate of the extruded filaments is higher and the contribution to crystallinity from the orientation effects is not substantial. In addition, the formation of different crystalline forms during crystallization can also lead to a drop in density, although this latter feature is not reflected in the model used for simulation.

16.6 FIBRE PROPERTIES

Some typical properties of polypropylene fibre are summarized in Table 16.7. The low temperature softening and melting behaviour of polypropylene fibre limits its use to areas where heat resistance is not of

Table 16.7 Typical properties of textile-grade polypropylene fibre

Tensile strength (gf den^{-1})	3.5–5.5
Elongation (%)	40–100
Abrasion resistance	Good
Moisture absorption (%)	0–0.05
Elastic recovery (after 30 s at 2% elongation)	
Immediate (%)	91
Delayed (%)	9
Softening point (°C)	140
Melting point (°C)	165
Chemical resistance	Generally excellent
Relative density	0.91
Thermal conductivity	6.0 (with air as 1.0)
Electric insulation	Excellent
Resistance to mildew, moth	Excellent

prime importance, and hot wet processes or hot washing are avoided. An area in which polypropylene fibre is outstanding is as an industrial fibre in applications as diverse as geotextiles, fishnets, cordage, marine ropes, agricultural twine, conveyor belting, tenting material, support fabrics, etc. Through the employment of suitable polymer and processing conditions, yarns with high modulus and high tenacity can be produced. These properties, added to its high toughness, impact resistance, low density and resistance to moisture and chemical environment, make it the ideal choice for geotextiles, for example. Generally fibres spun with low spin orientation are capable of attaining a higher degree of total orientation on cold drawing, and thus have superior mechanical properties, compared with fibres with higher spin orientation. Similarly, rapidly quenched polypropylene fibres allow much higher total orientation on cold drawing than the slowly cooled fibres, as stated earlier. Requirements for routes leading to high tenacity polypropylene yarns have been summarized by Ahmed [3]. It has recently been shown [25] that as-spun fibres produced from a low molecular weight controlled rheology-grade polymer (MFI 35 g/10 min), extruded at 280 °C with a winding speed of 200 m min^{-1}, give rise to paracrystalline fibres of low orientation which, on being subjected to a two-stage drawing process at 60 and 140 °C, respectively, are transformed into high oriented monoclinic fibres with tenacity of 85 cN tex^{-1}.

Some of the advantages and shortcomings of polypropylene fibres based on their properties are summarized below.

1. Polypropylene is a light fibre; its density (0.91 g cm^{-3}) is the lowest of all synthetic fibres.
2. It does not absorb moisture. This means that the wet and dry properties of the fibre are identical. Low moisture regain is not considered a disadvantage because it helps in quick transport of moisture as is required in special applications like babies' ever-dry nappies.
3. Its colours do not fade/or bleed because the dyeing is done by blending colour pigments/master batch with the resin itself prior to fibre extrusion.
4. It has excellent chemical resistance. Polypropylene fibres are very resistant to most acids and alkalis.
5. Polypropylene fibres neither support the growth of mildew/fungi nor are attacked by insects and pests.
6. It is easy to process and ensures high processing yields and profitability. Its cost is lower than that of polyester and nylon fibres.
7. The thermal conductivity of PP fibre is lower than that of other fibres and may be used in applications as thermal wear.

The fibre, however, has certain limitations; these are listed below.

1. It has a low melting temperature, and so requires extra care during ironing.
2. It cannot be dyed after manufacture. Polypropylene is normally mass-coloured before fibre extrusion; a major limitation is the lack of a wide range of shades.
3. Polypropylene has low UV and thermal stability; it requires the addition of expensive UV stabilizers and antioxidants to overcome the problem.
4. Polypropylene has poor resilience compared with polyester or nylon; higher denier fibre is, therefore, desirable to overcome this problem.
5. Polypropylene undergoes creep due to its low T_g (-15 to $-20\,^\circ$C).
6. It melts and burns like wax and is flammable; flame retardants may be added together with stabilizers.

16.7 APPLICATION AREAS

Polypropylene has established itself as a very useful industrial and household fibre. However, it has not made a very significant impact in the apparel sector mainly due to its hydrophobicity, lack of dyeability and a slightly waxy handle. Of late, however, due to the production of fine denier filaments and textured yarns, it is making in-roads into this sector as well.

Carpets remain one of the major application areas where PP is used as both backing and pile component. However, consumption as backing material is higher. Industrial applications include ropes, woven sacks, geotextiles, polygrass, medical and surgical disposables, tarpaulins, etc. It is increasingly being used in woven sacks and also in soft luggage. Air-jet textured blended and fancy yarns are used to produce attractive but cheap and durable upholstery fabrics. Polypropylene non-wovens are increasingly being used as filter fabrics for wet filtration in the chemical and pharmaceutical industries. Polypropylene blankets are also in use along with acrylic ones.

As for the apparel sector, textured polypropylene is finding its way into the hosiery industry, e.g. in undergarments, swim suits, sports wear, socks, etc. Fashioned outerwear is still not its forte. However, blended yarns with acrylic are now being used to produce hand/machine knitting yarns to give 'melange' effects.

REFERENCES

1. Wishman, M. and Hagler, G.E. (1985) Polypropylene fibres, in *Handbook of Fiber Science and Technology*, Vol. IV: *Fibre Chemistry* (eds M. Lewin and Eli M. Pearce), Marcel Dekker, New York, pp. 371–502.
2. US Patent 3 235 623, Soc. Rhodiaceta (1966).

3. Ahmed, M. (1982) *Polypropylene Fibres – Science and Technology*, Elsevier Scientific Publishing Co., New York.
4. Chalk, A.J. (1957) *Trans. Faraday Soc.*, **53**, 1214.
5. Anon. (1987) *Catalysts for Polypropylene*, Information Brochure, Himont Inc., Wilmington, USA.
6. Griffith, J.H. (1959) *J. Polym. Sci.*, **38**, 107.
7. Parrini, P. (1963) *Macromol. Chem.*, **62**, 83.
8. Kamide, K. and Inamoto, Y. (1967) *Sen-i-Gakkaishi*, **23**, 79.
9. Kamide, K. and Inamoto, Y. (1967) *Sen-i-Gakkaishi*, **23**, 578.
10. Minoshima, W., White, J.L. and Spruiell, J.E. (1980) *J. App. Polym. Sci.*, **25**, 287.
11. Lu, F.M. and Spruiell, J.E. (1987) *J. Appl. Polym. Sci.*, **34**, 1521.
12. Kloos, E. (1987) 4th International Conference on PP Fibres and Textiles, University of Nottingham, September.
13. Wulfhorst, B. and Meier, K. (1989) *Chemifasern Textilindustrie*, **39/91**.
14. Katayama, K., Amano, T. and Nakamura, K. (1968) *Kolloid Z.*, **226**, 125.
15. Fung, P.Y.F., Orlando, E. and Carr, S.H. (1973) *Polymer Eng. Sci.*, **13**, 295.
16. Caldas, V., Brown, G.R., Nohr, R.S., MacDonald, J.G. and Raboin, L.E. (1994) *Polymer*, **35**, 899.
17. Nadella, H.P., Henson, H.M., Spruiell, J.E. and White, J.L. (1977) *J. Appl. Polym. Sci.*, **21**, 3003.
18. Addink, E.J. and Beintena, J. (1961) *Polymer*, **2**(1), 185.
19. Morrow, D.R. (1968) *Am. Chem. Soc. Polym. Preprints*, **9**(2), 1192.
20. Gailey, J.A. and Ralston, R.H. (1964) *Soc. Plast. Eng. Trans.*, **4**, 29.
21. Samuels, R.J. and Yee, R.Y. (1972) *Polym. Sci.*, **10**, A-2, 385.
22. Natta, G. (1959) *Soc. Plast. Eng. J.*, **15**, 373.
23. Jinan, C., Kikutani, T., Takaku, A. and Shimiju, J. (1989) *J. Appl. Polym. Sci.*, **37**, 2683.
24. Bhuvanesh, Y.C. and Gupta, V.B. (1995) *J. Appl. Polym. Sci.*, **58**, 663.
25. Wang, I.-C., Dobb, M.G. and Tomka, J.G. (1995) *J. Textile Inst.*, **86**, 383.

Rayon fibres

<p style="text-align:right; font-size:3em; font-weight:bold">17</p>

A.K. Sengupta

17.1 INTRODUCTION

Rayon, which is one of the oldest manufactured fibres, is a regenerated cellulose fibre with a wide spectrum of properties. Historically, rayon faced a strong challenge from synthetic fibres like nylon, polyester and acrylics, which came much later, but in spite of this competition it has retained its place as a major textile fibre. The important considerations in favour of rayon are that the essential raw material for its production, namely cellulose, is abundantly available and a renewable source. Moreover, its hygroscopicity and easy dyeability are additional assets. Furthermore, rayon fibres can be produced with a wide range of properties, particularly mechanical properties, so far unmatched by any other fibre, natural or manufactured.

Methods of dissolving cellulose were first discovered in the late nineteenth century and the first fibres were made by dissolving cellulose in cuprammonium hydroxide and then forcing the solution through tiny orifices into a bath containing reagents to remove solvent to regenerate cellulose in filament form. Problems associated with lack of stability and considerations of cost competitiveness soon pushed this method into the background. With the discovery of the viscose process the cellulosics have been, and still are, predominantly produced by this process.

17.2 THE VISCOSE PROCESS

The viscose process resulted from research in the UK by Cross, Bevan and Beadle during the 1880s. By 1905 the Samuel Courtauld Company (UK) was in serious production of viscose yarn by a process fundamentally similar to that of today [1]. Events in the further development of the viscose process were [1]: colour pigmentation (1926), production of cut staple fibre (1934), tyre reinforcement yarn (1935), improved tyre yarn (1956), crimped fibre (1957), high wet-modulus fibre (1965) and hollow fibre (1976).

17.2.1 CHEMISTRY OF THE VISCOSE PROCESS

The chemistry of the viscose process consists of first forcing the cellulose I chains apart in both amorphous and crystalline areas by swelling with hydrates of sodium hydroxide, xanthating some of the hydroxyl groups so that the derivative may be soluble in water or dilute sodium hydroxide, and then reversing the process in spinning by removing the solvent water, sodium ions and xanthate groups, so that the cellulose hydroxyl groups may draw the chains together first through van der Waals forces and then through hydrogen bonding to obtain a cellulose II network [2].

A number of important chemical and physical processes start simultaneously when the liquid viscose enters the spinning bath. These are:

1. coagulation of liquid filament to xanthate gel filament;
2. neutralization and acidification of the gel filament;
3. deswelling of the gel filament;
4. dexanthation of the gel filament.

The speed, interaction, and permitted extent of these mechanisms determine the plasticity, stretchability and orientability of the gel filament. The rates of the above four mechanisms determine the morphological order and the rates can be varied to obtain a wide spectrum of submicroscopic order ranging from highly amorphous to highly crystalline. Thus, although the chemistry of the viscose rayon process is basically simple, the succession of chemical reactions is quite complex and the way in which this complicated sequence is carried out determines the fine structural parameters of the rayon fibre and, hence, their physical properties.

17.2.2 MANUFACTURE OF VISCOSE RAYON

The basic steps in the manufacture of viscose rayon fibre and filament are presented schematically in Figs 17.1(a) and (b), respectively. Several

Cellulose wood pulp   Steeping

Carbon disulphide
added

Shredding/grinding   Ageing   Xanthation

Caustic soda
added

Dissolving   Ripening   Filtration

Extrusion & stretching

Cutting

wet processing   drying

Bale
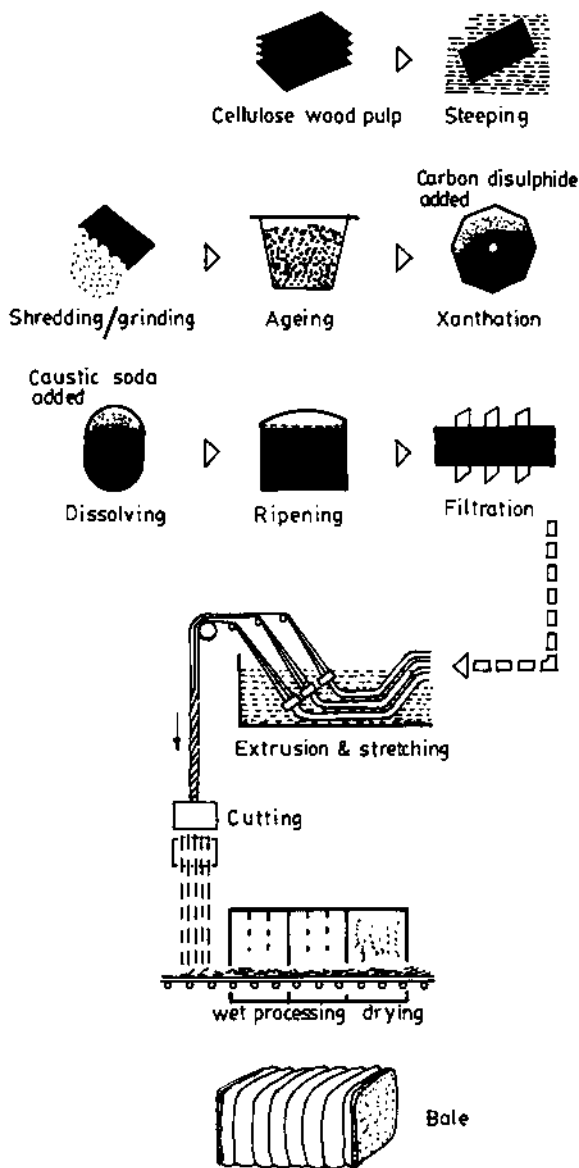
Fig. 17.1 (a) Flow diagram of production of viscose fibre [1].

important chemical reactions with multitudes of side reactions take place during the process. The most important chemical reactions essential for the manufacture of viscose rayon are presented in Table 17.1.

A brief description of the various operations is given below.

Wood pulp (87 to 98 % ⍺-cellulose)

```
┌─────────────────┐     Sodium hydroxide solution (17-19 %)
│   Steeping      │──── Wetting agent  catalyst
│ (alkali cellulose)
└─────────────────┘
        │
        ▼
┌─────────────────┐     Surfactant
│   Shredding     │────
└─────────────────┘
        │
        ▼
┌─────────────────┐
│     Ageing      │
│ (depolymerization)
└─────────────────┘
        │
        ▼
┌─────────────────┐     Carbon  disulfide
│   Xanthation    │──── (wet  churn)
└─────────────────┘
        │
        ▼
┌─────────────────┐     Sodium  hydroxide  solution
│   Dissolution   │────
└─────────────────┘
        │                Viscose  composition :
        ▼                   Cellulose  6.5 to 9 %
┌─────────────────┐          Sodium hydroxide  5.5 to 6.5 %
│ Blending, ripening        Total  sulfur  2.0 to 2.5 %
│ filtration, deaeration
└─────────────────┘
        │ Pigments, delusterant
        ▼
┌─────────────────┐     Coagulation bath
│                 │──── Carbon  disulfide
│    Spinning     │──── Glauber's  salt
└─────────────────┘
        │
        ▼
┌─────────────────┐     Wash  solution
│ Neutralization, │────
│Purification, Finishing
└─────────────────┘
        │
        ▼
┌─────────────────┐
│     Drying      │
└─────────────────┘
        │
        ▼
┌─────────────────┐
│     Winding     │
└─────────────────┘
```

Fig. 17.1 (b) Flow diagram of production of viscose filament [3].

(a) Steeping

Cellulose pulp boards (13 in × 18 in or 20 in × 30 in) containing cellulose between 87 and 98% are stacked vertically 3–6 in apart (separated by perforated spacers) in a steeping tank containing 17.5–18% NaOH. The steeping operation which converts cellulose into alkali cellulose and also

Table 17.1 Sequence of reactions in the viscose process [4]

1. Steeping	$C_6H_9O_4OH + NaOH$ (Cellulose)	$\rightarrow C_6H_9O_4 . ONa + H_2O$
2. Xanthation	$C_6H_9O_4ONa + CS_2$	$\rightarrow C_6H_9O_4OCSSNa \quad + \quad Na_2CS_3$ (Sodium cellulose (Sodium xanthate) trithiocarbamate)
3. Mixing	$C_6H_9O_4 . OCSSNa + NaOH$	$\rightarrow$ Viscose solution
4. Ripening	$C_6H_9O_4 . OCSSNa + H_2O$	$\rightarrow C_6H_9O_4OH + CS_2 + NaOH$
5. Spinning	$C_6H_9O_4 . OCSSNa + H_2SO_4$	$\rightarrow C_6H_9O_4 . OH + CS_2 + Na_2SO_4$

Table 17.2 Constitution of alkali cellulose under varying press-weight ratios

Press-weight ratio	Cellulose	NaOH (%)	H_2O (%)
3.0	29.8	15.2	55
2.5	35.0	15.0	50

removes hemicelluloses and resinous impurities is carried out for 30–60 min, preferably at a temperature of 18 °C. Although it has not been firmly established whether a true sodium salt of cellulose is formed in this operation or whether the product is a hydrated adduct between NaOH and cellulose, the alkali cellulose is highly reactive and behaves as a sodium salt of cellulose in many reactions. After the stipulated period of immersion in NaOH solution, the pulp boards are pressed by a hydraulic ram fitted to the steeping tank to remove the excess alkali. The press-weight ratio, which is defined as the ratio between the weight of the pressed alkali cellulose sheet and the weight of the air-dried pulp, needs to be carefully controlled and is preferably adjusted to 2.7–3. The composition of constituents for press-weight ratios of 2.5 and 3 are given in Table 17.2.

Although the variation in press-weight ratio does not change the NaOH content in alkali cellulose, both cellulose and water content are changed. Batch-to-batch variation in press-weight ratio could cause serious problems in maintaining the quality of the product as press-weight ratio influences the success of subsequent operations like shredding, xanthation and filterability.

(b) Shredding

This is a mechanical operation where the alkali cellulose boards are shredded into fluffy crumbs. Shredding is accomplished through rotating serrated blades and the operation is carried out for 1–3 h at 25–35 °C. Occasionally surfactants like polyethylene glycol are added at this stage. Surfactants decrease surface tension; this improves the dispersion of carbon disulphide, resulting in an overall increase in the degree of xanthate substitution.

(c) Ageing

This is an oxidative depolymerization step and needs to be carefully controlled to obtain the desired degree of depolymerization. The shredded crumbs are stored in rectangular galvanized steel containers and covered with lids. The oxygen available from the air within the

fluffy crumbs is sufficient and exposure to outside air is avoided as otherwise the crumbs dry out and carbon dioxide from air produces carbonates which affect xanthation and filterability. Ageing is carried out for 1–3 days at a temperature of 25–30 °C. The ageing process can be accelerated considerably with the use of higher temperatures and catalysts in the form of heavy metal salts such as manganese or cobalt. The ageing step can be avoided if the degree of polymerization required is high, e.g. in the case of polynosics. Occasionally ageing is referred to as a mercerization step. It is to be clearly understood that ageing and mercerization are distinctly different. During mercerization reactivity increases but there is no loss in the degree of polymerization (DP). During ageing chemical reactivity as measured by rate of hydrolysis or xanthate formation does not increase, but the solution viscosity is greatly affected.

(d) Xanthation

Aged alkali cellulose is transferred into hermetically sealed churns or barrates where carbon disulphide is introduced in a weight proportion of 32–35% of the weight of cellulose in alkali cellulose. The churn is slowly rotated at 1–4 rev min^{-1} for a period of 1–3 h at a temperature of 20–30 °C. Approximately 65% of CS_2 reacts with cellulose while the remainder goes into other reactions, the prominent reaction being formation of Na_2CS_3, which is responsible for the orange coloration of the flake. The xanthation ratio or the degree of substitution (the gamma or γ value) can be increased by increasing the CS_2 content and increasing the xanthation time. Although this does not improve solubility, a higher γ value is required for the manufacture of high performance rayons and polynosics. The ratio of total sulphur to the xanthate sulphur is an important variable during coagulation and regeneration.

(e) Dissolution

Dissolution of cellulose xanthate takes place in cylindrical vessels equipped with agitators. A 4–6% solution of NaOH is used. During dissolution, a considerable amount of air is whipped into solution which is removed by evacuation.

(f) Filtration

Viscose solution is filtered through a filter cloth and other filter aids to remove impurities and undissolved cellulose particles. Filtration is done in several stages, the last stage being as close to the spinneret as possible.

(g) Blending

Viscose solutions from several dissolving tanks are blended in a large vessel to homogenize and remove batch-to-batch variations.

(h) Ripening

As initially produced viscose is relatively difficult to coagulate, it is therefore not suitable for industrial use. After blending, the viscose solution is transferred to large tanks in a constant temperature room where it is kept for 1–3 days at a temperature of 15–25 °C. Ripening is basically storage at controlled temperature. During this period various changes occur, the most important of which is spontaneous decomposition of xanthate coupled with changes in the distribution of the xanthate groups, both within the cellulose chain as well as among cellulose chains. The viscosity of the xanthate solution initially drops as redistribution of xanthate groups increases the dispersion, and then increases as dexanthation and agglomeration of cellulose molecules gradually reduce solubility. As coagulability is the index of ripeness, the progress of ripeness is followed by determining the readiness to coagulate in standard salt solutions. The two tests used for measurement of ripeness are Hottenroth number or Hottenroth index and salt index or point index.

- Hottenroth number: this gives the volume in ml of a 10% ammonium chloride solution which is needed to coagulate 20 g of viscose solution diluted with 30 ml of water.
- Salt index: this gives the concentration of sodium chloride solution at 15 °C needed to coagulate one drop of viscose solution from a glass rod of 3/16 in diameter.

Each type of viscose requires a certain time of ripening to make it spinnable. Amongst the variables for controlling ripening, temperature is the most convenient for obtaining the proper degree of ripening in the desired time. Therefore, precise temperature control is necessary during ripening.

(i) Spinning

The spinning of viscose into a fibre involves the basic reaction of regeneration and is simply the recovery of cellulose from cellulose xanthate by an acid decomposition reaction. Upon entering the bath the viscose filament is coagulated and acid diffuses into the filament, regenerating cellulose. During this time the viscose fibre is also stretched to orient the cellulose molecules in the direction of the fibre axis.

The conventional viscose bath for standard rayon contains the following ingredients:

1. a salting-out agent, e.g. Na_2SO_4;
2. a regenerating agent, e.g. H_2SO_4;
3. a compound-forming agent, e.g. $ZnSO_4$.

In standard viscose rayon spinning, viscose of 30–50 poise viscosity made with 32% CS_2 (on weight of cellulose) is spun into an aqueous acid salt spin bath of the following type at a temperature of 45–50 °C.

H_2SO_4	8–10%
Na_2SO_4	16–24%
$ZnSO_4$	1–2%

Spinning speeds may be as high as $120 \, \text{m min}^{-1}$.

When the filaments are being formed in the bath, simultaneous processes take place during which sulphur is evolved and deposited on the surface of the filaments. During subsequent finishing, the filaments are subjected to washing and desulphurization, i.e. to a treatment with a solution of sodium sulphide or sulphite for dissolving the sulphur deposited on the filaments. Furthermore, the following operations are carried out: bleaching (with hypochlorite, hydrogen peroxide or sodium chlorite), soaping or oiling to soften the filaments and final drying.

Modern spinning bath systems may be described as (1) the zinc-based spinning bath, and (2) the non-zinc spinning bath. Systems which use zinc are employed in the production of regular and crimped rayon, rayon tyre yarn, and modified high wet-modulus rayon or high performance rayon. The non-zinc spin bath is used in the spinning of polynosic. Considering that over 95% of the rayon produced today is spun with zinc in the spin bath, the role of zinc in the structural regulation of viscose fibre is of paramount importance and needs to be clearly understood.

17.2.3 ROLE OF ZINC IN SPINNING BATH

The viscose reaction sequence in the presence and absence of zinc is presented in Fig. 17.2.

In the non-zinc spinning process under normal conditions of acid concentration in the spinning bath, cellulose xanthate gel is converted into cellulose xanthic acid and then to cellulose. The process is rapid and regeneration takes place before the cellulose molecules can be properly oriented. This results in a rather disoriented matrix with poor crystalline organization. The net result is a regenerated cellulose filament with poor dry strength and a very inferior wet strength.
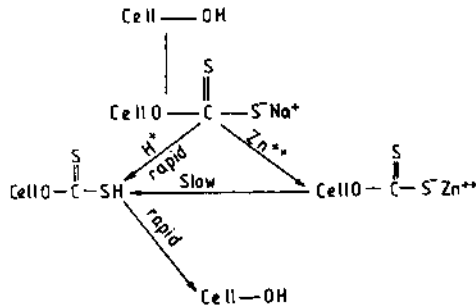
Fig. 17.2 Viscose reaction sequence. Cell—OH represents $C_6H_9O_4OH$ [5].
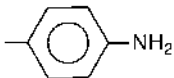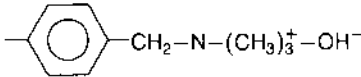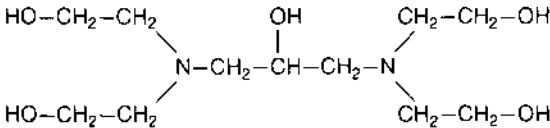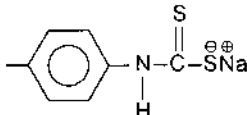
The presence of zinc, however, results in a transient zinc cellulose xanthate complex which is more stable against acid-induced regeneration. Zinc, being bivalent, forms transient crosslinks between adjacent xanthate groups. Coupled with this crosslinking, the strong deswelling action of zinc results in a tough shrunken zinc xanthate gel which can be stretched to a high degree before regeneration, resulting in a highly oriented structure with small crystal sizes and a relatively larger number of crystals.

The formation of zinc xanthate is dependent on the $H^+-OH^--Zn^{2+}$ diffusion balance and therefore the concentration of acid in the bath markedly influences the activity of zinc. The activity of zinc with the formation of zinc xanthate is manifest only over a specific range of acid concentration, generally between 2.5 and 7% H_2SO_4 concentration in the bath. In a very weak acid bath the transport of Zn ions is hindered due to $Zn(OH)_2$ precipitates which effectively block the diffusion of Zn ions into the filament. At high acid concentration, the protons move faster than Zn ions and cellulose is regenerated without passing through the zinc xanthate state. Thus, the strong deswelling action of zinc, concomitant with the formation of zinc xanthate, is evident only at a specific range of acid concentration.

It has been suggested that the increase in gel plasticity associated with retardation of regeneration allows the molecular chains to be aligned in the direction of the fibre axis through orientation stretching. Thus improvement in gel plasticity is a basic step in the manufacture of high strength regenerated cellulose fibres. There are three practical ways to improve gel plasticity. These and the resultant fibres are:

1. addition of chemical modifiers to viscose:
   - tyre yarn
   - high wet-modulus (HWM) yarn (modified)
2. low acid, low salt, low temperature spin bath:
   - polynosic (Toramomen process)

Table 17.3 The five main types of modifiers for viscose

Chemical type	Example
Tertiary amines	$-\!\!\langle\bigcirc\rangle\!\!-NH_2$
Quaternary ammonium salts	$-\!\!\langle\bigcirc\rangle\!\!-CH_2-N-(CH_3)_3^+-OH^-$
Polyoxyalkylene derivatives	$HOCH_2CH_2-(OCH_2CH_2)_x-OCH_2CH_2OH$
Polyoxyhydroxypolyamines	$\begin{array}{c} HO-CH_2-CH_2 \\ \diagdown \\ \qquad\qquad N-CH_2-CH-CH_2-N \\ \diagup \qquad\qquad\quad | \\ HO-CH_2-CH_2 \qquad OH \end{array}$ with CH_2-CH_2-OH and CH_2-CH_2-OH
Dithiocarbamates	$\begin{array}{c} \qquad\quad S \\ \qquad\quad || \\ -\!\!\langle\bigcirc\rangle\!\!-N-C-\overset{\ominus\oplus}{S}Na \\ \qquad\quad | \\ \qquad\quad H \end{array}$

3. addition of formaldehyde to the spin bath:
   - Super HWM or Ten X yarn.

17.2.4 SPINNING WITH MODIFIERS

Perhaps the most important factor leading to the improved technology is the recognition that certain chemicals added to viscose serve to stabilize xanthate decomposition, thereby prolonging the period during which effective stretch may be applied. While hundreds of chemical compounds have capabilities to act as retardants, the most widely known fall into the five general chemical classes listed in Table 17.3.

(a) Action of modifiers

It should be recognized that modifiers by themselves do not have any effect on viscose. They are only effective in the presence of zinc. In fact, they greatly enhance the role of zinc in the spinning bath.

Modifiers, also known as dopes, are used in weight proportions of 1–3% by weight of cellulose and are mixed with the viscose solution prior to spinning. They are also sometimes used in the spinning bath and the desired effect is the same. Sometimes, modifiers of different chemical types are used in combination. In a dope-free spinning bath an increase in zinc concentration in a low acid spinning bath increases

Table 17.4 Characteristics of skin and core

Characteristics	Skin	Core
Crystalline length (Å)	104	206
Swelling in water (%)	55–65	75–85
Hygroscopicity (%)	13–14	11–12
Loss of strength in the wet state (%)	20	50

the extent of skin formation, but an all-skin rayon can only be obtained in the presence of dope. Skin is the portion which has passed through the zinc xanthate state before acid decomposition and its structure and properties are different from the core. Table 17.4 lists the differences in the properties of skin and core. An all-skin rayon is the requirement for tyre yarns and modified high wet-modulus rayon.

There is still speculation about the way the modifiers act in a zinc-containing bath. The most probable mechanism is the formation of a semipermeable membrane by the combined action of zinc ions, by-product trithiocarbamate ions from the viscose and the modifier. This semipermeable membrane retards the diffusion of both Zn^+ and H^+ ions in the filament, but the actual ratio of Zn^+ to H^+ ion penetration is markedly increased in the presence of a modifier.

Thus the time for zinc xanthate formation is prolonged due to the semipermeable membrane acting as a barrier for proton diffusion; hence the acidification boundary is shifted further away from the spinning nozzle in the presence of a modifier.

Schematic representations of diffusion boundaries under varying spinning conditions are presented in Fig. 17.3. These are:

(A) schematic representation of viscose spinning into an acid bath without Zn salt;

(B) schematic representation of viscose spinning into a normal bath. The skin area on the filament surface at the right side denotes a zone having gone through the Zn xanthate state;

(C) schematic representation of 'modified' viscose spinning. The break in the filament in the plastic–gel area may extend for a distance of a few inches or with certain good retardants up to several feet.

In Fig. 17.3, each boundary represents a change in the pH value which is observed by introducing selective pH indicators in the viscose solution.

(b) Tyre yarn

A viscose solution of viscosity 100 poise containing modifier 1–3% by weight of cellulose and with a CS_2 content of 40% is spun underripe
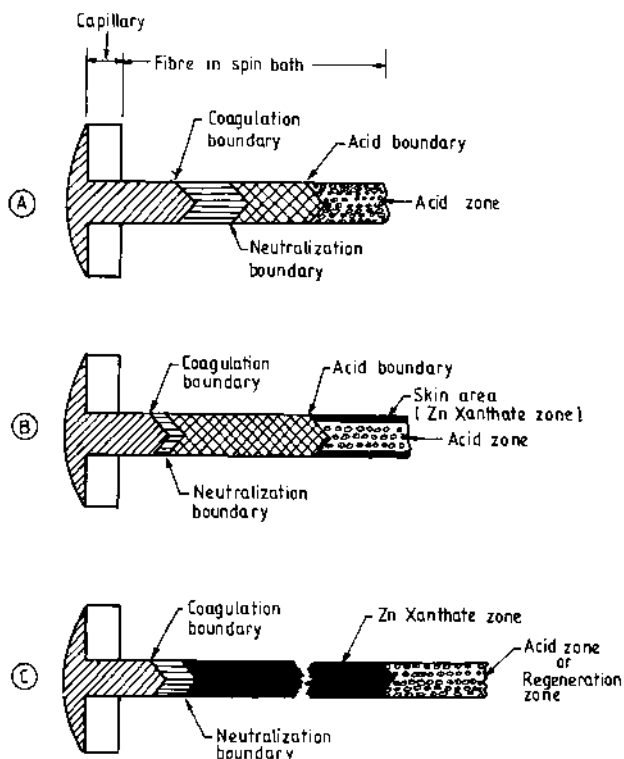
Fig. 17.3 Diffusion boundaries for various spinning baths [5].

(salt index 6–15) into an aqueous spinning bath containing:

H_2SO_4	8–10%
Na_2SO_4	16–24%
$ZnSO_4$	6%

The spin bath temperature is kept around 55 °C and the spinning speed is between 40 and 60 m min^{-1}. The stretch applied is 75–125%.

(c) Modified high wet-modulus yarns

The conditions of viscose solution and spinning bath composition are generally similar to those of tyre yarns. The spin bath temperature is kept lower (35 °C). The lower bath temperature than tyre yarn gives a more deformable gel necessitating a slower spinning speed (20–40 m min^{-1}). The result is that gel fibres are stretched at an earlier state of the gel dehydration and decomposition when the gel is more plastic and can be stretched more (125–150%).

17.2.5 POLYNOSIC FIBRE

The term 'polynosique' was coined in 1959 to stress the high polymeric nature of the material. The typical polynosic fibre is a viscose fibre extruded on the lines of the Tachikawa patent and possessing a higher wet modulus than ordinary rayon, the extension at $0.5\,\mathrm{gf\,den^{-1}}$ load being not more than 3.5% in water. The situation in the 1990s is, however, complicated by the use of the term polynosic for fibres extruded by different methods which fail the tensile test. All that can be said is that polynosics are high strength viscose rayon fibres with particularly higher wet strength.

The early research on the viscose process aimed at rapid coagulation and regeneration following extrusion, but the typical polynosics reverse this trend and employ a weak spinning bath containing rather dilute acid and sodium sulphate and omit the usual zinc sulphate. This situation allows slow xanthate decomposition while appreciable stretch is applied before complete regeneration. A structure that is more highly crystalline and oriented is developed with higher modulus characteristics, both wet and dry. A comparison of crystallinity and orientation of polynosic fibre with those of standard viscose and tyre yarn is given below:

	Crystallinity (%)	Birefringence
Standard viscose	45.2	0.027
Tyre yarn	41.5	0.037
Polynosic	55.5	0.046

The absence of zinc ions coincides with an absence of skin structure. The degree of polymerization is maintained at about twice the level of ordinary rayon, through the elimination of ageing stage and through the elimination of ripening of the cellulose xanthate which is dissolved in water instead of alkali. Some typical parameters of viscose solution and spinning bath are given below:

Viscose solution:		6.0% cellulose
		4.4% NaOH
		65 γ value
		500–600 DP
		500 poise viscosity
Spinning bath:	H_2SO_4	2–3%
	Na_2SO_4	4–6%
	Temperature	25 °C
	Spinning speed	20–30 m min^{-1}
	Stretch	150–300%

In recent years, high speed spinning of polynosic with take-up speed of $100\,\mathrm{m\,min^{-1}}$ has been possible.

17.2.6 SUPER HIGH WET-MODULUS RAYON [2]

It has been reported that addition of about 1% formaldehyde to the spin bath or to the viscose substantially increases the toughness and plasticity of viscose gel, permitting stretch of up to 500–600%. It is suggested that formaldehyde forms an addition compound with cellulose xanthic acid gel filament that is stable to H_2SO_4 in the presence of excess formaldehyde. The reaction sequence in the spin bath is on the lines suggested below:

$$\text{Cell OC}\underset{\text{SNa}}{\overset{S}{\Big\langle}} + H_2SO_4 \rightarrow \text{Cell OC}\underset{\text{SH}}{\overset{S}{\Big\langle}} + Na\,HSO_4$$

Sodium cellulose
xanthate

$$\text{Cell OC}\underset{\text{SH}}{\overset{S}{\Big\langle}} + CH_2O \rightarrow \text{Cell OC}\underset{\text{SCH}_2\text{OH}}{\overset{S}{\Big\langle}}$$

Cellulose xanthic acid   Formaldehyde derivative
of cellulose xanthic acid
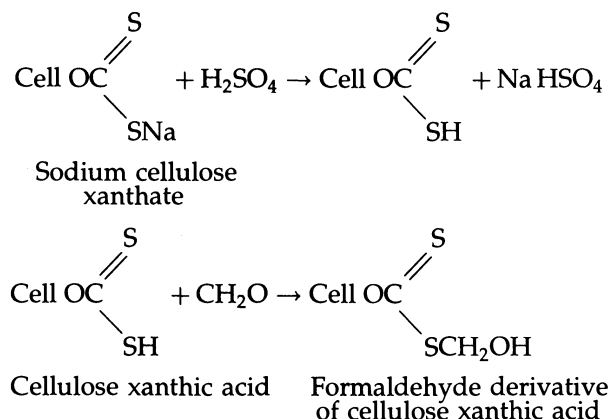
The bulky formaldehyde derivative groups (more bulky than the xanthate group) keep the chains mobile and free to move relative to one another, while transient formaldehyde crosslinking between OH groups and possibly physical entanglement of the bulky substituent groups give the gel filament the requisite toughness to withstand such a high level of stretch. In the absence of formaldehyde in the bath, the formaldehyde derivative reverts back to cellulose xanthic acid and then to cellulose. Hence, a multiple bath is used where the last bath, used for regeneration, contains no formaldehyde. Fibres with tenacity of $10\,gf\,den^{-1}$ and 6% elongation have been produced using this process. In spite of such excellent tensile properties, the toxic nature of formaldehyde and difficulties in its use have prevented any significant commercial exploitation of this process. A comparison of the properties of various cellulosic fibres is given in Table 17.5 [2].

17.3 ADVANCES IN VISCOSE RAYON TECHNOLOGY

The survival of viscose rayon over such a long period has been due to a concerted effort to reduce production costs and improve quality on the one hand, and the introduction of new variants through alteration of the process chemistry to meet the demands for more versatile products in newer applications on the other.

Table 17.5 Properties of various cellulosic fibres

Property	Standard rayon	Tyre yarn	Modified HWM	Polynosic HWM	Ten-X type HWM	Cotton
Tenacity (gf den^{-1}) (conditioned)	2.0–3.0	4.5–6.5	4.0–6.0	4.0–7.5	9.0–10.0	–
Tenacity (gf den^{-1}) (wet)	1.3–2.2	3.2–4.8	2.7–4.6	2.7–6.0	7.7–8.0	–
Elongation (%) (conditioned)	15–30	18–22	8–16	6–12	5–7	7–12
Moisture regain (%)	11–13	11–13	10–12	9–11	9–11	7–7.5
Secondary swelling (%)	80–120	60–80	60–75	55–70	65	40
Crystallinity (%)	33–42	29–45	37–42	39–47	46–52	50–70

17.3.1 DEVELOPMENTS IN PROCESS TECHNOLOGY [6]

One of the fundamental changes in the viscose process has been the conversion from the old batchwise process to continuous or semicontinuous systems. In the original batch process, the sequence of steeping, pressing and ageing took up to 40 h to produce alkali cellulose. Moreover, difficulties in ensuring constant temperature and equal ageing time, because of a large number of bins involved, frequently resulted in a variable degree of polymerization in the resultant viscose. In modern plants bales of wood pulp are automatically fed into continuous slurry steeping units in which the pulp is simultaneously disintegrated and steeped before passing on to continuous slurry presses where the slurry is first dewatered and then pressed. Subsequently, ageing is carried out in drums, silos or slow-moving conveyors under controlled temperature and humidity conditions. The use of catalysts and elevated temperatures during ageing have reduced the ageing time to 4–5 h.

The xanthation process has been improved with the use of wet churns in which both xanthation and mixing are carried out. Ripening is now generally carried out continuously in large tanks which also act as buffers for filtration and spinning.

One thrust area of development has been the improvement in filtration to give a product with a low level of particulate contamination. The purity requirements of viscose are different for each product with the viscose destined for finer denier requiring more stringent filtration. Traditionally a filter press has been used for viscose filtration. Materials used as a filter are nylon non-woven fabric, cotton flannel or cotton cloth. More recently the introduction of backflush filters with non-woven metal screens has improved the filtration efficiency phenomenally. With the new non-woven metal screen the filtration amount has increased 50-fold (Table 17.6). Thus the filter's size could be decreased to one-fiftieth of the former filter press to maintain the same filtration amount.

Table 17.6 Comparison of performance between a backflush filter and a filter press [7]

Filter		Filtration amount ($l\,m^{-2}\,h^{-1}$)	Particle number (particles cm^{-3})						
			3–10 μm	10–20 μm	20–30 μm	30–40 μm	40–50 μm	50–60 μm	>60 μm
No filtration		–	5500	260	60	15	5	4	21
Filter press	Non-woven fabric Cotton flannel Cotton cloth	30	1560	40	0	0	0	0	0
Backflush filter	40 μm non-woven metal screen	1500	1430	30	1	0	0	0	0
	20 μm non-woven metal screen	1500	950	10	0	0	0	0	0

One striking feature in the development of process technology for the manufacture of viscose rayon has been the increase in the level of automation to improve process continuity and fibre quality through improved process control. Automatic analysis and control of spin bath and wash liquors has been introduced and drying is frequently computer controlled using both feedback and feed-forward control loops, coupled in some cases with fibre conditioning systems.

17.3.2 DEVELOPMENTS IN PROCESS CHEMISTRY [8]

Reduction in consumption of the chemicals used, e.g. CS_2, NaOH and H_2SO_4, has been a principal objective of research in the past. Improved economy can be derived by any step which leads to a lowering of consumption of CS_2 or caustic or achieving higher cellulose content in the viscose or any combination of these factors.

There are a number of ways to achieve reduction in the amount of CS_2 used in viscose. The most attractive of these is the SINI™ process [8], which also allows a substantial reduction in viscose alkali content. The process, known as the double-steeping process, uses a second steeping operation of aged alkali cellulose at a lower alkali concentration (10–12%). A second steeping after ageing reduces the amount of free alkali in the crumb without changing the bound alkali. This reduces the formation of by-products and improves the distribution of xanthate groups to get a stable viscose. The SINI process can yield a 30% reduction in CS_2 usage, thus substantially reducing CS_2 emission. A viscose with acceptable filterability levels could be prepared using CS_2 at a much lower level (16–24%) than in the normal process (28–34% on cellulose). It is claimed that even inferior-grade pulp can be used with this process to yield good quality viscose fibre. This could possibly be due to the removal of low molecular weight fractions in the second steep as well as the increased rate of swelling of alkali cellulose which increases its reactivity to CS_2 during xanthation. With the SINI process, a higher CS_2:NaOH ratio (9:4.5) can be used in the viscose solution which results in a substantial reduction in H_2SO_4 consumption during spinning.

Activation of cellulose with liquid ammonia prior to xanthation also reduces CS_2 consumption by as much as 33%. Use of ammonium hydroxide also increases reactivity but its effect is much less pronounced than that of liquid ammonia. Xanthation in the presence of surfactants like Berol Spin 641™ decreases CS_2 consumption without affecting the quality of rayon produced. The addition of urea to the steeping solution results in substantial changes in the viscose; its viscosity is reduced, the ripening time is increased, and a higher degree of xanthate substitution is obtained [9]. It is presumed that a complex of the urea with the alkali cellulose is formed which limits side reactions occurring during

xanthation, thereby increasing the xanthate substitution. A reduction of viscose viscosity allows for an increase in α-cellulose content in the viscose and also an increase in the ratio of α-cellulose to NaOH in the viscose which leads to a reduction in the consumption of sulphuric acid. The production of viscose with an increased concentration of α-cellulose results in a reduction in the amount of energy required in the transport, filtration and deaeration of more concentrated viscose solutions.

17.4 VISCOSE FIBRE VARIANTS

Over the years, viscose rayon has moved with the times to meet the changing demands of the textile market. While the use of continuous filament has shrunk, the staple fibre market has increased with the variety of end uses encompassing both the original conventional textile products and a growing number of non-wovens. There is now a more diverse range of staple fibre products than ever before which have been produced by either modification of process chemistry, alteration of the viscose or the regeneration conditions, or by modification of the washing or drying conditions. Details of typical properties for common viscose staple fibre types are given in Table 17.7 [6].

17.4.1 FIBRE VARIANTS FOR IMPROVED BULK AND HANDLE

The desire to improve the aesthetic properties of viscose rayon has led to two diverse approaches to the production of fibres with improved bulk and handle. One approach has been to produce high performance crimped fibres where the bulk is due to the interaction between fibres, creating bulk in the resultant yarns and fabrics. The second approach has

Table 17.7 Typical properties of viscose staple variants [6]

Fibre	Conditioned		Wet		Water imbibition (%)
	Tenacity (gf den^{-1})	Extension (%)	Tenacity (gf den^{-1})	Extension (%)	
Standard	2.0–2.5	19–25	1.0–1.3	28–33	90–100
High strength	2.6–3.0	16–20	1.5–1.7	20–25	85–95
Standard crimped	1.8–2.3	20–28	0.9–1.2	30–35	90–100
High performance crimped	3.0–3.5	14–18	1.8–2.2	17–22	75–85
Polynosic	3.0–5.0	6–12	2.0–4.0	9–15	55–75
Modal	3.5–4.5	12–15	2.2–3.2	17–21	70–80
Tubular inflated	2.3–2.7	14–16	1.2–1.5	18–20	120–140
Super inflated	1.0–1.2	26–32	0.5–0.7	38–46	250–300
Alloy	1.6–1.9	14–18	0.8–1.0	18–22	160–180

Table 17.8 Composition for producing high performance fibres [10]

Composition	Typical range (%)
Cellulose	7.0–7.5
NaOH	6.0–7.5
CS_2 (on cellulose)	30–32
Modifiers: Dimethylamine	0.8–1.5
Polyethylene glycol	0.8–1.5

been to produce an inherently bulky fibre using an inflation technique during fibre production.

(a) High performance crimped fibres

For many years standard crimped fibres have been available which are produced by altering the regeneration condition so that the skin of the fibre bursts while still in the spin bath. The liquid viscose thus processed is regenerated under slightly different conditions and a bicomponent structure results. The two parts of the fibre shrink differently in the subsequent washing and drying processes and the fibre develops a permanent crimp as a result. More recently crimped high wet modulus fibres have been produced which give improved hand and cover compared with uncrimped high wet modulus fibres, and the loss in mechanical properties normally associated with the crimping process is minimized. Courtauld's Vincel™ and ITT Rayonier's Prima™ are two such products. Some typical conditions [10] for producing high performance crimped fibres are given in Tables 17.8, 17.9 and 17.10 [10].

(b) Inflated fibres

An inherently bulky fibre is produced using a technique in which the fibre is inflated during regeneration. A range of fibre cross-sections can be produced, but a tubular structure provides the best combination of bulk and handle while still retaining the physical properties and processing performance of standard viscose rayon.

Table 17.9 Spinning specifications [10]

Xanthate sulphur (%)	0.8–1.2
Viscosity (poise)	80–100
Salt index (NaCl)	4–6
DP (fibre)	400–600

Table 17.10 Spinning conditions [10]

	Primary bath	Secondary bath
H_2SO_4 (%)	5.0–5.5	2.5–4.5
Na_2SO_4 (%)	15.0	–
$ZnSO_4$ (%)	2.0–3.0	–
Temperature (°C)	35–45	95+
Stretch (%)	90–100	25–30
Take-up speed (m min^{-1})	30–50	30–50

In the inflation process sodium carbonate is added to the viscose solution and, on contact with the acidic spinning bath, gaseous carbon dioxide is evolved. Coupled with the normal spinning gases liberated in the process, this generates sufficient pressure to inflate the fibre. The mechanism involves the formation of a stationary bubble of gas inside the skin of the partly formed fibre, and this acts as a former over which the still liquid viscose is pulled. The size of the bubble and, hence, the wall thickness of the fibre depends on how effectively the gas is retained within the skin during regeneration. This degree of retention depends on the relative rates of regeneration, gas evolution and gas loss. By accurately controlling the viscose and regenerating conditions, this complex process can be adjusted to consistently produce a fibre with the desired cross-section. A typical example of an inflated rayon fibre is the fibre Courcel^{TM} made by Courtaulds. Courcel is a fibre with significantly greater bulk and absorbency than ordinary rayon and with improved handle in fabric form.

A recent addition is the SI Fibre^{TM}, which is another of the inflated fibre products in which the structure of the fibre is physically altered to give a higher surface area. SI Fibre is produced in the same way as Courcel, but in this case the regenerating conditions are controlled so as to produce a very thin-walled tube which then collapses to give a fibre with longitudinal cells and a multilimbed cross-section.

17.4.2 SUPER ABSORBENT FIBRES [6]

A major market for viscose rayon is in sanitary protection and in surgical dressings and swabs. For these end uses high absorbency and purity are the key requirements. Development work to produce higher absorbency fibres has resulted in the production of 'alloy' rayon fibres. For these fibres highly hydrophilic polymers that are also compatible with viscose are added to the spinning solution. Chemicals such as sodium polyacrylate, carboxymethyl cellulose, acrylamido-2-methylpropane

sulphonic acid, polyethylene glycol, sodium alginate, etc. are added to make alloy fibres.

Enka has developed highly absorbent fibres using polymers of sodium salts of substituted and unsubstituted acrylic acids and copolymers of alkyl vinyl ether and ethylene dicarboxylic acid. Of these, the fibres incorporating sodium polyacrylate and copolymers of the sodium salts of acrylic acid and methacrylic acid are most important commercially. More sodium hydroxide is added to the viscose than is usually required to compensate for dilution and for neutralization by the alloying polymer.

The alloy fibres which have been extensively used in tampons for several years are declining in popularity and are being replaced by crimped variants of hollow fibres. The reasons for the decline in the use of alloy fibres are two-fold. Firstly, the high moisture affinity of alloy fibres is a deterrent to processability as hydrogen bonding makes the fibres more difficult to open when going from the bale to random laid or carded webs. Moreover, high fibre absorbency alone is not necessarily indicative of high tampon absorbency, as absorbency in a tampon is as much due to fluid retention in the open structure between the fibres as the fluid retention within or on the fibres. It is for this reason that the crimped fibre variants are generally used in tampons as the crimp generates greater interstitial space in the compressed structure and hence greater overall absorbency. A more recent alternative in the use of tampons is Courtauld's super inflated fibre (SI Fibre) made from 100% cellulose. This fibre has a multilobed cross-section and its chain structure is less ordered than regular rayon and therefore more accessible to water. Wet collapse is less because the hollow tube opens when wet. The high surface area makes for more effective hydrogen bonding to give better inherent web strength. Crimp, crenulation and hollows all contribute to absorbency, web integrity and cotton-like handle. In tampons, SI Fibre gives approximately a 30% improvement in absorbency over standard rayon, which is comparable to the performance of alloy fibres. The self-bonding problem which makes a highly absorbent rayon difficult to process has not been entirely eliminated with hollow fibres.

For use of viscose in surgical dressings and swabs, while the general properties of standard or crimped rayon are suitable, the fibre must be modified to meet the sterilizing requirements of the dressings' manufacturers or users. Regenerated cellulose has a tendency to yellow when subjected to a hot, humid environment such as is encountered during steam sterilization. This yellowing is clearly unattractive, particularly for surgical products. New products have been developed through modifications in the manufacturing conditions that do not turn yellow following steam autoclaving.
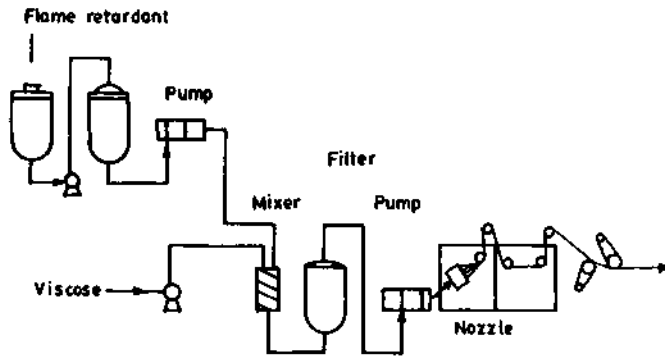
Fig. 17.4 The Tufban production process [7].

17.4.3 FLAME RETARDANT FIBRES

Flame retardant additives are incorporated in the viscose dope prior to spinning. Some of the compounds used are halogenized triaryl phosphate, halogenized alkyl thiophosphate, aloxyphospazenes, etc. F.M.C. Corporation, USA, have developed a phosphonitrilic chloride-based flame retardant additive while Courtaulds, UK, have developed a liquid additive based on brominated or chlorinated alkyl phosphate ester and produced a flame retardant viscose rayon called Darelle™. Toyobo Co., Japan, produces Tufban™, a flame retardant fibre, using a flame retardant compound whose main component is phosphorous. The flame retardant compound is mixed with viscose solution prior to spinning, as shown in Fig. 17.4.

As a limiting oxygen index (LOI) of more than 26% qualifies a material for flame retardancy, Tufban's LOI value of 30–32% (Table 17.11) makes it an excellent fire resistant material. It is claimed that normal washing and dry-cleaning do not affect its flame retardant characteristics.

Table 17.11 LOI (limiting oxygen index) of Tufban™ and some other fibres [7]

Material	LOI (%)
Tufban	30–32
Cotton, rayon, and polynosic	18–20
Polyester	20–22
Acrylic	19–20
Nylon	20–22

17.4.4 INCORPORATION OF CARBON IN VISCOSE FIBRES [11]

(a) Incorporation of carbon black for antistatic properties

Electrically conductive carbon is used for the production of electrically conductive viscose fibre. The conductivity increases with decreasing particle size of the carbon. For the production of electrically conductive viscose fibres, a slightly alkaline, electric conductive carbon black with a particle size of 20 nm is dispersed in water and mixed in viscose solution prior to spinning. The conductive viscose fibre Viscostat^{TM}, a product of Lenzing AG, contains 30% electrically conductive carbon black. There is a loss of about 50% in the tenacity of this fibre compared with the tenacity of regular viscose fibre. On the other hand, electrical conductivity is increased by five orders of magnitude. Blends of Viscostat with synthetic fibres such as polyester, nylon and polypropylene are used for protective clothing and floor covering applications in hazardous environments involving inflammable liquids and gases. It may also be used to prevent generation of sparks as a result of friction-induced electrostatic charging. It is also used in the electronics industry where high voltage charge generated by friction can cause damage to semiconductive components and breakdown in data processing plants.

(b) Incorporation of activated carbon

Viscarbon^{TM} of Lenzing AG is an activated-carbon-containing fibre with outstanding adsorption properties. For the production of activated-carbon-containing viscose fibres, activated carbon from coconut with very fine pores is used. This activated carbon has to be ground to a very fine particle size and thoroughly dispersed in water in order to be incorporated in viscose fibres in a satisfactory way. Fabrics made using activated-carbon-containing viscose fibres are used in applications such as protective clothing against gases, flat structures for industrial gas adsorption, shoe insoles, odour-absorbing and antimicrobial wound dressings, etc.

(c) Incorporation of graphite

The outstanding sliding and lubricating ability of natural graphite is well known. Incorporating 40% of lubricating graphite with a purity of 99.5% into viscose yields fibres with excellent lubricating properties which are used as packings and sealings for crankshafts. Packings from graphite-containing viscose fibres may be used up to a temperature of 180–200 °C. They are stable in the pH range 5–9 and are predominantly used to seal pumps and fittings for water, salt solutions, weak organic and inorganic

acids, weak alkaline solutions, molasses, vegetable oils, etc. Graphite-containing viscose fibres have also been successfully used as sealings against gases like carbon dioxide, nitrogen and hydrogen. Sealings for crankshafts from graphite-containing viscose fibres have high abrasion resistance for long life duty and can be used with pressures up to 50 bars and gliding velocities up to $15\,\mathrm{m\,s}^{-1}$.

17.5 ALTERNATIVES TO THE VISCOSE PROCESS

The 'viscose process' has been largely given up in many of the more developed countries during the last two decades. While the viscose process provides an inexpensive route to regenerate cellulose in fibrous form, it constitutes a health hazard due to toxic pollutants. Significant pollution control regulations have reduced the cost-effectiveness of this process, particularly in the countries where regulations are strict and, more importantly, are strictly enforced. There has, thus, been an intense search throughout the world since the end of the 1960s to replace the viscose process by some other route. In recent years, several solvents have been revealed in patents and some of these have been used to produce cellulose on a commercial scale. Two major routes which are much easier and less polluting than the old viscose process are now available. These are:

1. spinning of solutions of cellulose derivatives with a subsequent saponification to yield 'true' cellulose fibre;
2. direct spinning of cellulose from 'new' organic solvents.

17.5.1 SPINNING OF SOLUTIONS OF CELLULOSE DERIVATIVES

The solvent class of cellulose derivatives encompasses two basic systems [12]:

1. in which dissolution involves nearly simultaneous derivative formation, e.g. metal–amine solvents, N_2O_4–DMF, DMSO–PF solvent systems;
2. that produce a derivative from which cellulose can be easily generated, e.g. liquid ammonia–salt system.

(a) Metal–amine solvent

The best known solvent in this group is the cuprammonium hydroxide system in which cellulose forms a coordinated complex with the copper ion. The glycol group of 1,4-anhydroglucose unit chelates to occupy two of the coordinating sites of the copper(II) ion, displacing two ammonia molecules. Regeneration of fibres from cuprammonium hydroxide

solution has been the basis for commercial production of cuprammonium rayon. The cuprammonium process [13] will now be briefly described.

The cuprammonium process is the original solvent spinning process. Compared with the viscose process, the cuprammonium process produces a much lower quantity of harmful secondary substance; no noxious gases are formed and the effluent is less polluted.

The starting material is, usually, bleached cotton linter, sometimes also rayon pulp. In contrast to the viscose process, there is no hemicellulose extraction possibility in this system. Rayon pulp for the cuprammonium process should therefore contain less than 4% hemicellulose.

In this process, the cellulose is opened up, mixed with copper hydroxide or a basic copper salt in the presence of a concentrated aqueous ammonia solution at 20 °C, and the solution is filtered and deaerated. During deaeration ammonia is also extracted. The spinning solution, depending on spinning conditions, contains 4–11% cellulose, 4–6% Cu and 6–10% NH_3.

Cuprammonium fibres are spun usually by the two-bath process. In the first bath the complex of cellulose and ammonium copper(II) hydroxide hydrate is precipitated with water and in the second bath the cellulose is regenerated with dilute sulphuric acid (1.5–2% solution at 20–24 °C). The after-treatment of cuprammonium fibres includes washing out the acid and salts, the removal and recovery of copper as well as spin finishing and drying.

(b) N_2O_4–DMF solvent system

An example of a cellulose solvent which involves formation of a chemical derivative as part of the dissolution mechanism is the dinitrogen tetroxide–dimethyl formamide system (N_2O_4–DMF). The derivative formed is cellulose nitrile, which is reasonably stable in the polar DMF solvent but is readily decomposed by hydrolysis when added to aqueous regeneration media. Other polar aprotic solvents such as dimethyl sulphoxide and dimethylacetamide can be used in place of DMF. The Camilon process [14] represents one such process and is briefly described below.

The process uses dimethyl formamide with 15–17% dinitrogen tetroxide as a solvent. Cellulose is dissolved at 20 °C under normal pressure to give a stable solution whose storage stability is 10–15 days, in contrast to viscose solution whose storage stability is only 1–2 days. The solution is then extruded into a spinning bath (at 20 °C) consisting of dimethyl formamide, water and an inorganic salt. The Camilon process is much shorter than the standard viscose process since ageing, xanthation and ripening are not required in this process. Moreover, since the solution is

Table 17.12 Fibre properties [14]

Property	Viscose	Camilon
Strength ($cN\,tex^{-1}$)	15–25	15–25
Elongation (%)	15–25	15–20
Modulus ($kgf\,mm^{-2}$)	200–300	400–500
Wet strength (%)	45–55	40–50
Wet modulus ($kgf\,mm^{-2}$)	50–70	60–80
Recovery angle (degrees)	50–60	100–120

homogeneous, containing practically no gels, the number of filtrations required is reduced to one. At the post-spinning stage, steps such as desulphurization, bleaching and acidification are also absent. The properties of Camilon fibres (Table 17.12) compare favourably with the properties of standard viscose rayon. While the strength and elongation percentage values of both are similar, the Camilon fibre has higher modulus and recovery angle. Camilon fibres are reported to have better dyeability than viscose.

(c) DMSO–PF system

Like N_2O_4–DMF, the dimethyl sulphoxide–paraformaldehyde (DMSO–PF) solvent system also involves formation of a derivative. The mechanism of dissolution involves the formation of methylol cellulose. This derivative is soluble and stable in the dissolving system but is easily converted back to cellulose upon regeneration in protic solvents.

Preliminary investigations on fibre formation using this system have been reported [15] but the process has yet to be commercialized.

(d) Liquid ammonia/salt system: the Celca process

This process was invented by Neste Oy in Finland [16]. Cellulose is opened and activated in liquid ammonia containing urea. After evaporation of the ammonia, the intimate mixture is heated to 135 °C, at which temperature cellulose carbamate is produced:

$$Cell\text{–}OH + H_2N\text{–}\overset{\displaystyle O}{\overset{\displaystyle \|}{C}}\text{–}NH_2 \rightarrow Cell\text{–}O\text{–}\overset{\displaystyle O}{\overset{\displaystyle /\!/}{\underset{\displaystyle \diagdown NH_2}{C}}} + NH_3$$

(cellulose
carbamate)
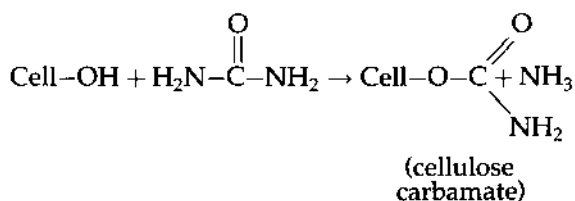
After the reaction the cellulose is washed with hot water to remove unreacted urea and by-products. The dried carbamate is stable, making

subsequent handling and use easy. Cellulose carbamate is dissolved in 8% sodium hydroxide to a content of 7–10%. As the carbamate groups hydrolyse in alkaline media, the dissolution is best done at temperatures around or below 0 °C. The solution obtained is spun into a sulphuric acid bath where the unstable carbamate decomposes and cellulose is regenerated:

$$2\,Cell-O-\overset{\overset{\displaystyle O}{\|}}{\underset{\underset{\displaystyle NH_2}{\diagdown}}{C}} + 2H_2O + H_2SO_4 \rightarrow 2\,Cell-OH + (HN_4)_2SO_4 + 2CO_2$$
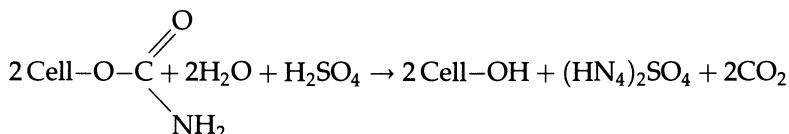
The Celca process resembles the viscose rayon process. The fibres obtained, however, are more brittle than rayon fibres and the production process is more expensive.

17.5.2 SPINNING WITH DIRECT SOLVENTS [17]

Since the 1970s a number of scientific reports and patents have focused on the development of new organic solvents which would dissolve cellulose directly without the formation of a derivative during dissolution. Several such solvents have now been identified, the prominent ones being:

(a) calcium thiocyanate–water, $Ca(SCN)_2 . H_2O$;
(b) ammonia–ammonium thiocyanate, NH_3–NH_4 SCN;
(c) lithium chloride–dimethylacetamide, LiCl–DMAc;
(d) N-methylmorpholine–oxide, $MMNO$–H_2O.

(a) Calcium thiocyanate–water

Dried cellulose is added to calcium thiocyanate, i.e. $Ca(SCN)_2 . 3H_2O$, which is then evacuated to allow the penetration of the solvent. The mixture is then heated to temperatures between 120 and 140 °C. As dissolution proceeds on heating, the solution becomes viscous. The viscous solution is extruded and then a water wash is given to produce the cellulose fibre.

The physical properties of rayon fibre produced using this system are poor and, as yet, the fibre is of no commercial interest. A tenacity of only $0.8\,gf\,den^{-1}$ has been reported so far.

(b) Ammonia–ammonium thiocyanate

The solvent is prepared by condensing NH_3 to a predetermined weight with a known amount of NH_4SCN. Solutions of cellulose in NH_3–NH_4SCN are prepared by making a slurry of cellulose and solvent and
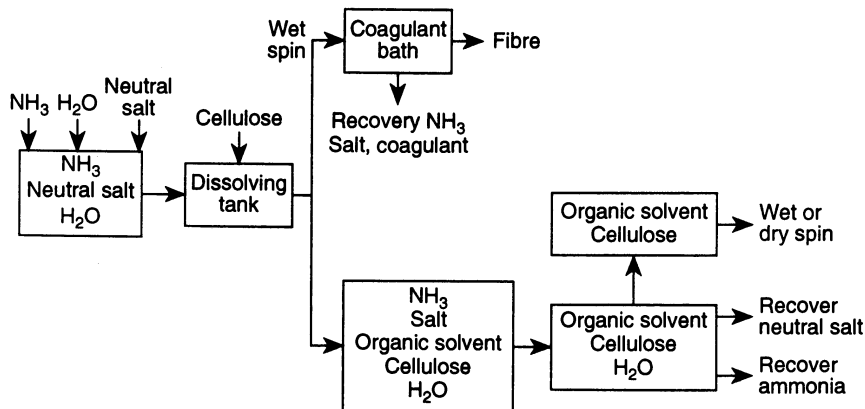
Fig. 17.5 Flow diagram utilizing NH_3–NH_4SCN solutions for cellulose fibre production [17].

stirring at $-10\,°C$. Fibres have been spun using wet-spinning, dry-spinning and dry-jet wet-spinning. The best fibre properties have been obtained with dry-jet wet-spinning using solutions containing 14% cellulose at a solvent composition of 24.5:75.5 (wt%) NH_3:NH_4SCN. A tensile strength (conditioned) of $3.0\,gf\,den^{-1}$ with an elongation of 8%, and a modulus of $167\,gf\,den^{-1}$ have been reported. A flow diagram for the manufacture of rayon fibre using NH_3–NH_4SCN solvent is given in Fig. 17.5 [17].

(c) Lithium chloride–dimethyl acetamide [18]

Lithium chloride–dimethyl acetamide, LiCl–DMAc, is a cellulose complexing solvent, where the lithium cation (Li^+) is believed to complex with the carbonyl oxygen of DMAc leaving the chloride ion free to hydrogen bond with the cellulose hydroxyl groups. Interaction of Cl^- with the cellulose hydroxyl protons apparently results in competitive hydrogen bond formation and disruption of the existing intermolecular hydrogen bonded structure. Accumulated association of Cl^- along the cellulose chain can be viewed as producing an anionically charged polymer with the macrocation, $(Li–DMAc)^+$, as the counterion. The polymer molecules are forced apart by the ensuing charge–charge repulsion and bulking effects. A continuous influx of solvent results in further disruption of the cellulose binding forces until the polymer is totally solvated.

Manufacture of cellulose rayon using LiCl–DMAc as a solvent has been reported by Turbak [19]. Cellulose solutions of 6–14% in LiCl–DMAc were used to spin fibres via wet, dry-jet/wet- and dry-spinning techniques. It was observed that fibres from the wet-spinning process exhibited superior properties. Different coagulating baths including

Table 17.13 Rayon fibre properties [18]

	Regular	Intermediate wet modulus	High wet modulus	LiCl–DMAc
Tenacity (gf den^{-1})				
Conditioned	1.5–2.8	3.5–5.0	3.5–6.0	1.7–3.7
Wet	1.0–1.8	2.5–3.5	2.5–4.5	0.6–2.6
Elongation (%)				
Conditioned	14–25	12–19	6–14	6–12
Wet	18–35	18–24	9–18	8–18
Wet modulus (gf den^{-1})	0.2–0.3	0.4–0.6	0.7–3.0	0.5–1.4

water, acetone, acrylonitrile and acetone were tried and it was reported that the viscose-type spin system using an acrylonitrile bath produced high wet modulus rayon fibres at speeds up to 150 m min^{-1}. Table 17.13 compares LiCl–DMAc fibre spun into acrylonitrile with typical viscose rayon fibres.

A flow diagram for cellulose fibre production using LiCl–DMAc solution is shown in Fig. 17.6 [17].

(d) *N*-Methylmorpholine–*N*-oxide

Of the direct solvents for cellulose, the tertiary amine oxides have probably received the greatest amount of attention. The first indication that tertiary amine oxides might provide useful solvents for cellulose was obtained in 1939. However, little was done to develop this for more than three decades until it was reported that certain cyclic tertiary amine oxides were excellent solvents for cellulose [12]. A high structural
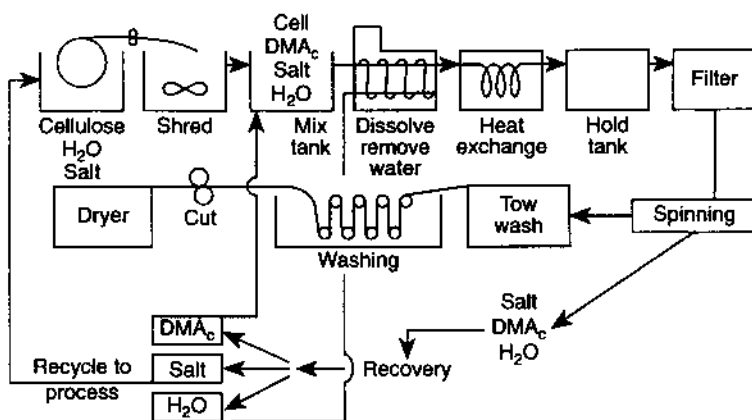
Fig. 17.6 Flow diagram utilizing LiCl–DMAc solutions for cellulose fibre production [17].
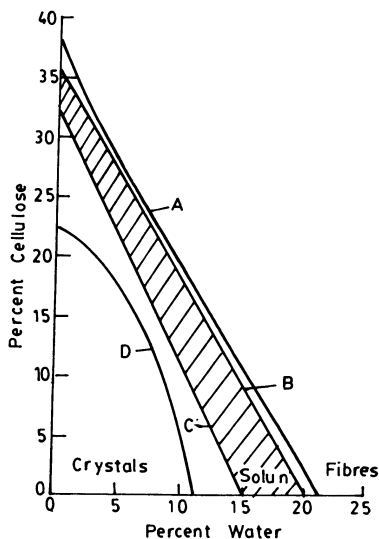
Fig. 17.7 The solubility of cellulose in the MMNO–H_2O system [17].

specificity with a group of solvents was noted. It was emphasized that the amine oxide should preferably be in a cyclic structure such as N-methylmorpholine-N-oxide, N-methylpiperidine-N-oxide, or N-methyl-pyrrolidine-N-oxide. Of these, N-methylmorpholine-N-oxide, MMNO, has proved to be an excellent solvent of cellulose for commercial exploitation.

N-Methylmorpholine-N-oxide occurs in the form of several hydrates with melting point inversely related to the water content. The mono-hydrate is 13.3% (w/w) water and has proved to be an excellent material for dissolving cellulose. The solubility of cellulose in the MMNO–H_2O system is shown in Fig. 17.7 [17].

N-Methylmorpholine-N-oxide is commercially available in the form of several hydrates. The active solvent moiety of MMNO is its N—O appendage with its strong dipolar character. The oxygen of this group is able to form one or two hydrogen bonds with hydroxylated substances such as water and alcohols. Similar hydrogen bonding is also believed to occur with cellulose. When the dissolution of cellulose occurs in the presence of water, there is a competition between water and cellulose for the MMNO molecules which seem to prefer water to cellulose. This explains why cellulose solutions can be prepared only with compositions poor in water. Thus with 13.3% water, MMNO forms a monohydrate that readily dissolves cellulose; with 23.5% water it forms a dihydrate that will not dissolve cellulose. Apparently, some water is needed to open the internal pores of cellulose; but too much water gets between the N—O bond of amine oxide and cellulose, thereby preventing solution.

The manufacture of cellulose fibres using *N*-methylmorpholine-*N*-oxide will now be described.

Several methods are available for the manufacture of cellulose fibres using MMNO as a solvent. These fibres are generically classified as 'Lyocell' and defined as cellulose fibre obtained by an organic solvent spinning process. Two of these are briefly described below:

The ITF-Lyon process [20]

Institute Textile de France and Centre Technique du Papier have jointly developed a technology for producing cellulose filaments using MMNO as a solvent. The steps in the preparation of cellulose by this novel solvent spinning method are given below:

1. *Swelling*: the solvent is used in a highly hydrated form. The Texaco Company markets it with a water content of 40% at which concentration MMNO is quite stable and can be stored without any problem. The initially fluffy cellulose is introduced into the solvent at high water content and the cellulose–solvent mixture is thermally dehydrated till the concentration of water corresponds to a monohydrate, when the cellulose undergoes swelling. This operation is carried out in a mixer with double spiral heating. The mixing step is performed under vacuum.
2. *Gelling*: this occurs at a water content close to that of monohydrate, approximately 13%, as is indicated in the phase diagram of Fig. 17.8.
3. *Dissolution*: this operation requires mechanical agitation as well as maintenance of temperature around 100–120 °C. A twin screw extruder equipped with a degassing zone is used. A 10–15% solids content (cellulose) produces a good spinnable fibre. The high temperature needed for dissolution causes polymer degradation which can be checked effectively by the use of antioxidants. As shown in Fig. 17.9, at 90 °C the sample without antioxidant shows considerable polymer degradation which becomes still higher at higher temperatures. The data for samples containing antioxidants show that at 90 °C the loss in DP is considerably reduced. At higher temperatures a similar advantage would be obtained.
4. *Spinning*: spinning is carried out continuously after dissolution in the twin screw extruder. The cellulose solution is pumped through a filter with sand bed and a multihole circular spinneret. The filaments undergo stretching during their passage in air and then enter into a water bath where the cellulose is generated by phase separation. The separation is rapid and a production speed of $150 \, \text{m} \, \text{min}^{-1}$ is shown to be possible.

The possibility of adjusting the modulus by means of the degree of drawing gives this new product a vast domain of applications.
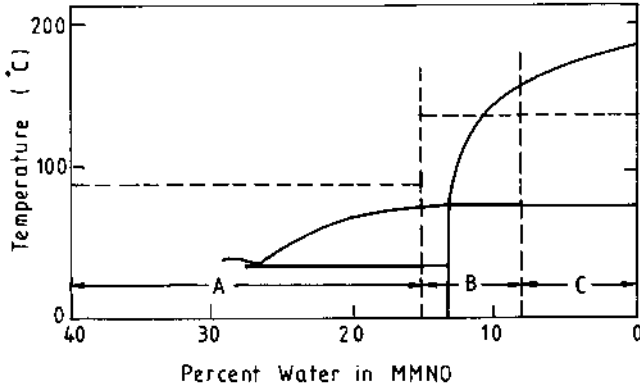
Fig. 17.8 Phase diagram during gelification. Key: A = zone of work at mixer (dehydration); B = zone of work in twin screw extruder (dissolution of cellulose); C = domain of instability.

Courtauld's Tencel^{TM}

In the late 1980s Courtaulds introduced Tencel^{TM} fibre, which is also a solvent spun fibre using amine oxide (MMNO) as the solvent. In the process, amine oxide is heated and is then used to dissolve wood pulp. A very clear but very viscous solution is obtained which is filtered and then spun into a bath containing a dilute aqueous solution of the solvent.
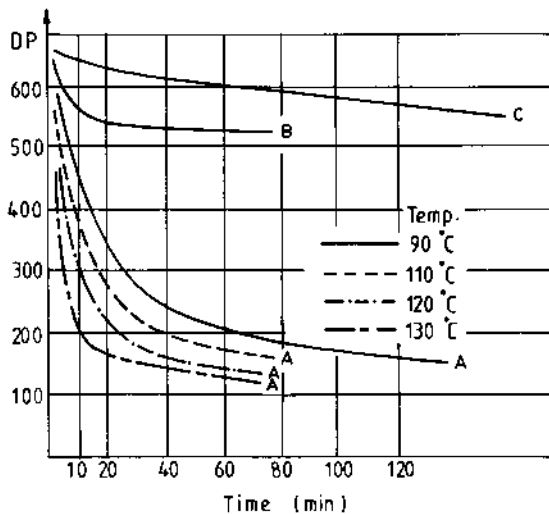
Fig. 17.9 Comparative curves of the fall of DP as a function of time and temperature (A) without antioxidant, (B) with antioxidant 1, (C) with antioxidant 2.
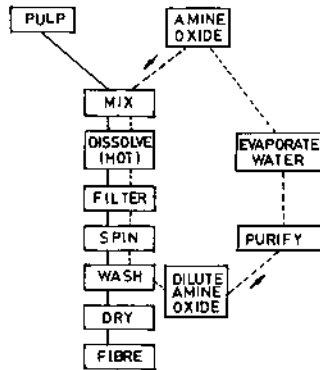
Fig. 17.10 The Tencel solvent spinning process [21].

The bath removes the amine oxide from the fibres. The fibres are then washed and dried. The removed solvent is reclaimed for further use. A line diagram of the Tencel solvent route along with solvent recovery for re-use is presented in Fig. 17.10 [21].

The actual degree of polymerization in the Tencel fibres is higher than for standard viscose, modal (HWM) or polynosics and the fibre strength is higher than previous cellulosic fibres. Tencel fibres have excellent wet strength and wet modulus. The fibre is round in cross-section and has a natural high lustre. Some properties of Tencel fibre are compared with those of some other fibres in Table 17.14. The high wet modulus of the fibre is an important attribute as it imparts Tencel fabrics with very low potential shrinkage in the wet state. X-ray studies of the fibre have shown the cellulose crystals to be highly parallel in the longitudinal direction of the fibre. This no doubt contributes significantly to the high tensile strength of the fibre, and it also leads to the propensity for some degree of fibrillation, for example, during abrasion in the wet state [22].

Table 17.14 A comparison of Tencel fibre properties [21]

	Tencel	Polyester	Cotton	Viscose
Linear density (dtex)	1.7	1.7	-	1.7
Tenacity (cN tex^{-1})	42–44	42–52	23–25	23–25
Elongation (%)	14–16	25–35	7–9	20–25
Wet tenacity (cN tex $^{-1}$)	37–41	42–52	27–31	10–12
Wet elongation (%)	16–18	25–35	12–14	25–30
Wet modulus (@ 5% extension) (cN tex^{-1})	270	210	100	50
Water imbibition (%)	65	3	50	90

REFERENCES

1. Ford, J.E. (1991) *Textiles*, **3**, 4–5.
2. Charles, F.R. (1966) *Can. Textile J.*, August, pp. 37–49.
3. Peter Von Bucher, H. (1968) Viscose rayon textile fibers, in *Man-Made Fibers: Science and Technology*, Vol. 2 (eds H.F. Mark, S.M. Atlas and E. Cernia), Interscience Publishers, New York, p. 10.
4. Sisson, Wayne A. (1960) *Textile Res. J.*, **30**, 3, 153–170.
5. Smith, D.K. (1959) *Textile Res. J.*, **29**, 1, 32–40.
6. Aitken, R.A., Hopkins, A.S., Hoyland, D.A. and Smith, R.J. (1984) *Fiber Producer*, August, pp. 23–32.
7. Nagata, T. (1990) *Textile Asia*, May, pp. 66–70.
8. Daul, G.C. (1981) *Ind. Eng. Chem. Prod. Res. Dev.*, **20**, 222–230.
9. Laszkiewicz, B., Weislo, P. and Cuculo, J.A. (1992) *J. Appl. Polym. Sci.*, **46**, 445–448.
10. Müller, T.E., Barch, F.P. and Daul, G.C. (1976) *Textile Res. J.*, **46**, 3, 184–194.
11. Martini, J., Rüf, H. and Wimmer, A. (1987) *Chemiefasern Textilindustrie*, **37/89**, June, pp. 66–70.
12. Dutta, P.K. (1995) *Asian Textile J.*, January, pp. 54–56.
13. Koch, P.A. (1991) *Chemiefasern Textilindustrie*, **41/93**, February, pp. E11–E21.
14. Chegolya, A.S., Gruishpan, D.D. and Burd, E.Z. (1989) *Textile Res. J.*, **59**, 9, 501.
15. Kalb, B., Cox, R.G. and St. John Manley, R. (1982) *J. Polym. Sci., Polym. Phys. Ed.*, **20**, 1207.
16. Volbracht, L. (1989) *Man-Made Fiber Year Book*, Chemiefasern & Textilindustrie, Frankfurt, pp. 32–36.
17. Cuculo, J.A., Hudson, S.M. and Wilson, A.V. (1993) *Int. Fiber J.*, June, pp. 50–57.
18. Dawsey, T.R. and McCormick, C.L. (1990) *J. Macromol. Sci., Rev. Macromol. Chem. Phys.*, **C30**(3&4), 405–440.
19. Turbak, A.F. (1984) *TAPPI*, **67**, 94.
20. Loubinoux, D. and Chavnis, S. (1984) *L' Industries Textile*, No. 1140, January.
21. Anon. (1993) *Textile Month*, February, p. 43.
22. Cole, D.J. (1992) In *Advances in Fibre Science* (ed. S.K. Mukhopadhyay), Textile Institute, Manchester, p. 28.

Manufactured fibres for high performance, industrial and non-conventional applications

18

Satish Kumar and V.B. Gupta

18.1 INTRODUCTION

The emphasis in this book has up till now been on manufactured commodity fibres, like poly(ethylene terephthalate), nylon 6, nylon 66, polyacrylonitrile, polypropylene and viscose rayon, which have been described individually in separate chapters. While describing these fibres, it was emphasized that they are used not only as apparel and household textiles but also as industrial fibres or technical textiles. Taking polyester, which is a well-known apparel and household textile fibre, as an example, it is interesting to note that, in the USA, industrial polyester yarn consumption in 1991 was over 50% of the total polyester filament yarn consumption [1], with tyre cord alone accounting for 38%, the rest being used in seat belts, V belts, coated fabrics, cordage, hoses and other applications. In the recent past, the pattern for fibre production has shown significant changes, with the industrial nations moving towards lower volume but much higher value-added products for industrial markets, while the developing countries are expanding their production capacities for commodity fibres [2].

This chapter has been designed to cover those fibres which are manu-factured for industrial/technical end uses, for which the terms 'indus-trial textiles' or 'technical textiles' are often used. However, a different title has been selected for this chapter in spite of a certain degree of ambiguity in that both high performance and non-conventional applica-tions come within the wider framework of technical or industrial applications. The justification for the present title is two-fold: first, it conforms with terminology that is widely accepted, and second, it emphasizes that the focus of this chapter is on high performance fibres which form a small but important part of the total gamut of industrial fibres.

In dealing with such a broad range of products, it is essential to define the scope of the chapter and to put its contents in the correct perspective. To facilitate this, the manufactured fibres need to be classified appro-priately. Industrial fibres are used on the basis of a combination of properties; these include mechanical properties, temperature resistance, chemical resistance, flame resistance, etc. The widely followed practice of using mechanical properties as the basis of classification leads to the following four categories of fibres.

1. *Fibres with average mechanical properties.* Standard textile fibres belong to this category for which Atlas and Mark [3] have laid down the following mechanical property requirements: tenacity, 3–5 gf den^{-1}; elongation to break, 35%; modulus of elasticity, 30–60 gf den^{-1}; and completely reversible elongation up to 5% strain. These fibres also find uses in the industrial sector, e.g. as non-wovens.
2. *Fibres with above average mechanical properties.* Industrial fibres like tyre cords belong to this category for which Atlas and Mark [3] have laid down the following mechanical property requirements: tenacity, 7–8 gf den^{-1}; elongation to break, 8–15%; modulus of elasticity, 50–80 gf den^{-1}; and a high degree of toughness.
3. *Fibres with superior mechanical properties.* These fibres would also come under the general umbrella of industrial fibres and will have a tenacity of 8–20 gf den^{-1}, elongation to break of 5–15%, and modulus of elasticity of 80–250 gf den^{-1}. The development of such fibres is a subject of intense research aimed at bridging the gap in properties between fibres belonging to categories 2 and 4.
4. *Fibres with outstanding mechanical properties.* High performance fibres belong to this category and, unlike the polymeric fibres belonging to the above three categories, they can also be inorganic or metallic. The polymeric high performance fibres have a tenacity of 15–50 gf den^{-1}, elongation to break of 0.5–5% and modulus of elasticity of 250–4000 gf den^{-1}. The strength and modulus of the non-polymeric high performance fibres are also very high though, because of their high

density, the specific strength and specific modulus will not be as high as for polymeric high performance fibres.

Fibres belonging to categories 1, 2 and 3, which will be discussed only briefly, are the well-known commodity fibres like polyesters, polyamides, polypropylene, viscose rayon and polyacrylonitrile or high tenacity variants of these commodity fibres. Small quantities of many other fibres are also used for industrial applications coming within the purview of these categories and these include, amongst others, poly(phenylene sulphide), poly(ether ether ketone), poly(tetrafluoroethylene), etc., which will be briefly considered. Fibres belonging to category 4, i.e. the high performance fibres, include aramids, ordered polymeric fibres, aromatic polyesters, extended chain polyethylene, carbon fibres, glass fibres, boron fibre, silicon carbide and alumina fibres, etc. The main thrust of this chapter will be on these high performance fibres. Finally, some speciality fibres such as electrically conducting polymeric fibres, optical fibres, fibres for medical applications and elastomeric fibres will also be considered. One important statement regarding the actual values of fibre properties, particularly their mechanical properties, needs to be made. A wide variety of values has been published for a particular fibre type and also appears in manufacturers' data sheets. The information provided in the text and the tables should therefore be taken only as a rough guide.

18.2 FIBRES FOR INDUSTRIAL APPLICATIONS

18.2.1 FIBRES WITH AVERAGE MECHANICAL PROPERTIES

These fibres have already been described in detail in the earlier chapters. Although the bulk of fibres belonging to this category are used for standard textile uses, a number of non-woven products and also a variety of industrial fabrics are produced from standard textile fibres with average mechanical properties. Two processes for producing non-woven fabrics are described in Chapter 19.

18.2.2 FIBRES WITH ABOVE-AVERAGE MECHANICAL PROPERTIES

The industrial fibres with above-average mechanical properties are produced by techniques similar to those used for producing fibres for apparel and household textiles, namely melt-spinning in the case of polyester, polyamides and polyolefins, and wet-spinning for viscose and acrylics. Of course, there are some important differences in both the starting material and the process. For example, while for apparel use, polyamides have a number average molecular weight of $18\,000\,\mathrm{g\,mol^{-1}}$ or

so, for industrial applications the number average molecular weight would preferably be in the range of 25 000–35 000 g mol^{-1}. Furthermore, additives to stabilize the material against thermal and UV degradation are generally added. The draw ratio may be in the range 3.5–4.5 instead of the usual 2.6–3.6 for apparel-grade fibre. The industrial filaments are coarser and for drawing them to the higher draw ratios that are necessary relatively higher temperatures of drawing have to be used. For producing these filaments, the integrated spin–draw process is often used instead of the conventional two-stage spinning followed by drawing. This process has already been described in Chapter 4.

18.2.3 FIBRES WITH SUPERIOR MECHANICAL PROPERTIES

The industrial fibres with superior mechanical properties can be produced by the solution and/or gel-spinning technique using solutions with a range of polymer concentration. By gel-spinning of high molecular weight poly(ethylene terephthalate), fibres with elastic modulus of 30 GPa [4] and tensile strength of 1.9 GPa (15 gf den^{-1}) [5] have been produced. The gel-spinning technique is described later. However, fibres belonging to this category can also be produced through the simpler melt-spinning route using special drawing and annealing procedures. The first such method makes use of the zone drawing and zone annealing techniques [6]. An amorphous or very low crystalline as-spun PET fibre forms the starting material. It is drawn at a relatively low temperature to give a fibre of low crystallinity which is converted by zone annealing at a high tension into a highly oriented, highly crystalline fibre with less chain folding. A fibre with a modulus of 21.5 GPa has been produced by this technique. A second method uses two-stage drawing of a conventional melt-spun PET yarn, each stage being followed by an annealing step [7]. In these fibres, crystalline order is reported to occur over longer lengths and a modulus of 18.6 GPa has been obtained at a draw ratio of 20.

18.2.4 SOME OTHER FIBRES OF CATEGORIES 2 AND 3

Poly(phenylene sulphide) (PPS) and poly(ether ether ketone) (PEEK) are new entrants to the fibre field with promise of good potential. They are melt-spun at quite high temperatures of about 300 and 360 °C, respectively, have high thermal stability and possess almost total resistance to hydrolysis and high resistance to chemical attack. These fibres can be commingled with carbon and other reinforcing fibres which can be used to make preforms for complex composite structures. PEEK monofilaments are used as tennis racquet strings because of their high work recovery.

Poly(tetrafluoroethylene) (PTFE) fibres have the lowest coefficient of friction of around 0.05 and are extremely inert to virtually all chemical and thermal treatments until they begin to decompose at about 400 °C. The main limitations to their use are somewhat poorer tensile properties and their high cost.

18.3 FIBRES FOR HIGH PERFORMANCE APPLICATIONS

Far-reaching developments have taken place in the growth of high performance fibres through technological innovations [8–12]. These include: polymeric fibres (aramids, ordered polymeric fibres, aromatic copolyesters, and extended chain flexible polyolefin fibres); carbon fibre; glass fibre; boron fibre; ceramic fibres like silicon carbide and alumina; and metallic fibres. But before describing these fibres, it is worth recalling some points made in Chapter 2, which dealt with the structural and morphological basis of fibrous structures. By examining the structures of fibres made through different processing routes, it was concluded that a high density of extended molecules gives rise to extensive chain continuity along the fibre axis direction and this results in high modulus and high strength. However, if the chains are flexible, the melting points are low and thermal resistance is a limitation. On the other hand, well-oriented rigid chains, generally based on aromatic structures, give fibres in which both mechanical properties and thermal resistance are excellent. Thus high performance polymeric fibres, defined on the basis of mechanical properties, may be based on highly oriented linear aliphatic or aromatic molecules. Carbon fibres, on the other hand, are planar graphitic structures with excellent mechanical properties. However, they are expensive (the approximate 1994 cost of carbon fibres in the USA was US$15–100 per lb as opposed to the cost of polymeric high performance fibres which was in the US$10–50 per lb range). The inorganic fibres have a three-dimensional structure in contrast to the one-dimensional structure of polymeric fibres and two-dimensional structure of carbon fibres. They have the highest thermal resistance and good mechanical properties though they are brittle. However, while glass fibres are relatively inexpensive (E- and S-glass fibre costs are US$1 per lb and US$5 per lb, respectively), the other inorganic fibres are very expensive; their approximate cost in the USA in 1992 was US$100–4000 per lb. Also, while glass fibres are produced by the melt-spinning route, special processing techniques, which are different from those used for textile-grade fibres described earlier, become necessary to produce the other inorganic fibres and will be briefly considered in what follows. One of the principal high performance applications for these fibres is in their use as reinforcements for composite materials.

18.3.1 POLYMERIC FIBRES

(a) Aramid fibres

Amongst aramids, poly(p-phenylene terephthalamide) is the most successful high performance fibre. However, historically it was preceded by poly(m-phenylene isophthalamide) fibre, which is not a high performance fibre of category 4, and poly(p-benzamide) fibre, which was a high performance fibre but is no longer commercially produced. These two fibres will be described briefly as the knowledge gained from processing these materials and from the structure–property relationships for these fibres was to a large extent responsible for the development by Du Pont, USA, of poly(p-phenylene terephthalamide) in the form of Kevlar^{TM} fibre.

The initial motivation for development of high performance fibres came from the aerospace industry seeking fibres for use in light but stiff, strong and tough composite structural parts. Following the success of nylon 66 fibre, the choice of Du Pont scientists naturally fell on aromatic polyamides of this type, which have a relatively more rigid backbone.

Nomex^{TM} fibre

The first all-aromatic polyamide, which was commercially released by Du Pont in 1961, was Nomex^{TM}. This was produced using the following reaction:

| m-Phenylene diamine | Dichloride of m-isophthalic acid |

Poly(m-phenylene isophthalamide) or Nomex
(repeat unit)
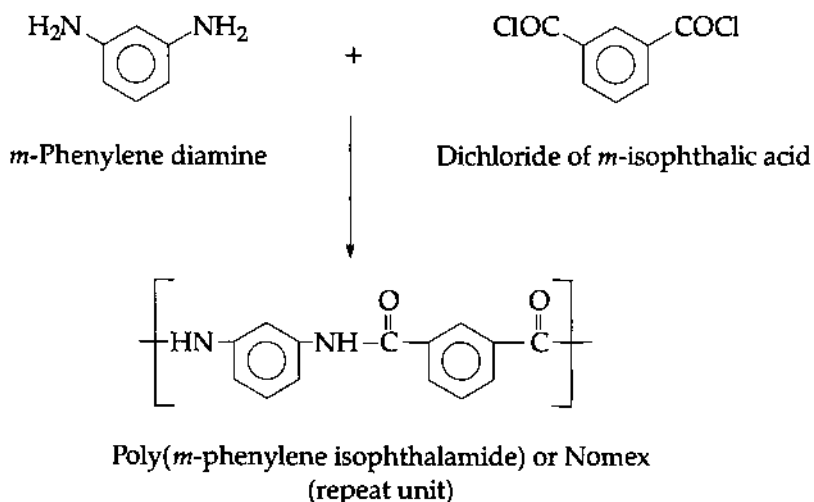
The polymer of inherent viscosity $1.65\,dl\,g^{-1}$ was dissolved in dimethyl formamide (DMF, boiling point 165 °C) to give a stock solution

of 20% polymer to which 4.5% lithium chloride (LiCl) was added to improve solvent power. The solution was dry-spun through orifices of 0.13 mm diameter into hot air at 200–210 °C and wound up at speeds of 125 m min^{-1}. Alternatively it could be wet-spun by coagulating in water. Then the wound-up fibre was extracted in cold water for 64 h to remove LiCl–inorganic salt and finally drawn 5.5 times its original length in steam at 56 psi pressure. Yarn so obtained had a tenacity of 3.6 gf den^{-1} and 23% elongation to break. However, its strength retention at high temperatures was excellent; it retained almost half its tenacity at a temperature of 250 °C. Thus Nomex is a fibre with excellent thermal resistance but rather poor mechanical properties for a high performance fibre. Protective clothing in hostile environments where heat, chemicals and radiation are present, furnishings in public places because of its excellent flame resistance, industrial filters and hollow fibres for desalination by reverse osmosis are some of its applications. Around 10 000 t yr^{-1} of Nomex is produced by Du Pont in USA and 1000 t yr^{-1} of Conex^{TM} [13], which is similar to Nomex [14] but with a slightly different structure (described in Section 14.4.2), by Teijin in Japan [13].

The *meta*-oriented aromatic rings were no doubt useful as they facilitated the processing of Nomex on conventional processing equipment. However, the mechanical properties of the fibre were rather poor as compact packing of molecules was not possible. Replacement of *meta*-oriented aromatic rings with *para*-oriented rings would be expected to allow better intermolecular registration of amide groups and make it more crystallizable. This would stiffen the structure but at the same time make it difficult to dissolve. The development of poly(*p*-benzamide) or Fibre B, which was released as an experimental fibre by Du Pont in 1970 [14], fulfilled these expectations.

Fibre B

The starting material for fibre B was *p*-aminobenzoic acid,

$$H_2N \;-\!\!\left\langle\bigcirc\right\rangle\!\!-\; COOH$$
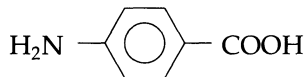
which was converted to poly(*p*-benzamide),

$$\left[HN \;-\!\!\left\langle\bigcirc\right\rangle\!\!-\; CO\right]_n$$

to form *in situ* spinning solution in lithium chloride–dimethyl acetamide (LiCl–DMA) solvent system. The phase diagram for such solutions, with respect to the polymer and lithium chloride concentrations, defining the regions containing solid, isotropic and anisotropic solutions, is shown in
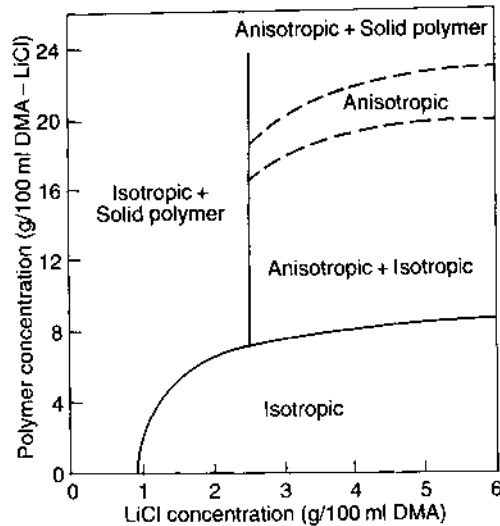
Fig. 18.1 Phase diagram for poly(p-benzamide) of intrinsic viscosity 1.18 dl/g in DMA–LiCl [15].

Fig. 18.1 [14, 15]. The solution viscosity data for solutions of Fibre B of four different intrinsic viscosities is shown in Fig. 18.2 [15]. It is observed that at low polymer concentrations up to the point of maximum solution viscosity, the solution behaves as a normal isotropic one, the solution viscosity increasing with polymer concentration. However, as the polymer concentration is increased beyond this 'critical concentration', the solution viscosity decreases as the solution undergoes a transition from an isotropic to a partially anisotropic liquid crystal state. The maximum degree of anisotropy at the new minimum solution viscosity corresponds to a state in which the molecules are mostly free from chain entanglements. Groups of such molecules can thus aggregate, while still keeping a safe distance from one another to avoid precipitation, into rod-like parallel chains, which form the anisotropic regions of the solution [14]. These regions have sufficient difference in density from the isotropic regions for partial separation by centrifuge to be achieved. The Fibre B solutions in DMA–LiCl were wet- or dry-spun and the fibres were then washed and dried. The as-spun fibres were then heat-treated in a nitrogen atmosphere to achieve improvements in tensile properties, mainly through an increase in molecular weight and to some extent orientation that follows heat treatment [14].

The liquid crystalline state has been known for over 100 years. Flory predicted in 1956 [16] that as the molecular chain becomes more rod-like, a critical aspect ratio is reached above which the molecules would line up to pack as a three-dimensional aggregate; the requirement for liquid
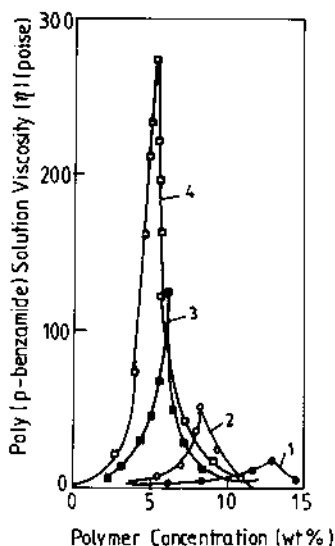
Fig. 18.2 Viscosity of poly(p-benzamide) solution as a function of polymer concentration in DMA–LiCl for polymers of intrinsic viscosities: (1) 0.47, (2) 1.12, (3) 1.68 and (4) 2.96 dl/g [15].

crystal formation thus being elongated (minimum length-to-diameter ratio 6.4) rigid, rod-shaped molecules. They may be either thermotropic, which change phase with temperature and can be melt-spun, or lyotropic, which form in solutions and change phase with change in concentration, and sometimes also with temperature.

Production of Fibre B was halted by Du Pont due to high monomer cost and limited storage stability of the spinning solution. By this time it was realized that spinning from strong acids was feasible and attention was paid to other all *para* types; the major breakthrough came with Kevlar, which had been synthesized as early as 1958 [17], but not pursued due to problems relating to dissolution and spinning. Now with the experience gained during manufacture and marketing of Fibre B, Du Pont was in a position to revive their interest in Kevlar.

Kevlar fibre

The poly(p-phenylene terephthalamide) fibre (PPTA) was commercially released by Du Pont in 1972 under the trade name Kevlar^{TM}, and it immediately established itself because of its outstanding modulus, strength, toughness and temperature resistance.

PPTA is synthesized by the condensation of terephthaloyl chloride (TCl) and p-phenylene diamine (PPD) in a mixture of hexamethyl

phosphoramide (HMPD) and n-methyl pyrrolidone (NMP) solvents, as follows:

$$H_2N-\langle\bigcirc\rangle-NH_2 \quad + \quad Cl-\overset{\overset{O}{\|}}{C}-\langle\bigcirc\rangle-\overset{\overset{O}{\|}}{C}-Cl$$

PPD   TCl

Polymerization in solvent

$$\left[-NH-\langle\bigcirc\rangle-NH-\overset{\overset{O}{\|}}{C}-\langle\bigcirc\rangle-\overset{\overset{O}{\|}}{C}-\right]$$

PPTA or Kevlar: repeat unit
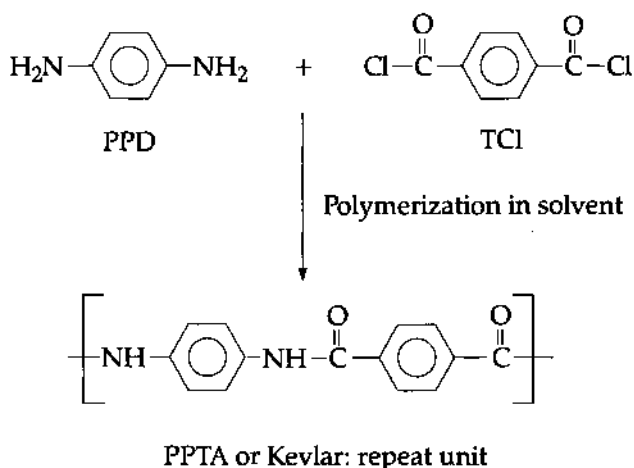
The polycondensation reaction is normally carried out at 10–20 °C to avoid degradation and to minimize the side reactions. The reactants are vigorously stirred and the products are subsequently ground in water, filtered, and the resulting solid polymer thoroughly washed. A polymer of minimum intrinsic viscosity of $4 \, dl \, g^{-1}$, measured in sulphuric acid, is preferred for satisfactory fibres. Some characteristics of PPTA are compared with fibre-grade nylon 66 in Table 18.1 [18]. PPTA forms liquid crystal solution under certain conditions of concentration, temperature, solvent and molecular weight. The effect of polymer concentration on solution viscosity is shown in Fig. 18.3 [19]. As in the case of Fibre B (Fig. 18.2), the initial increase of viscosity with increasing polymer

Table 18.1 Some characteristics of PPTA and nylon 66 polymers [18]

Parameter	PPTA (powder polymer)	Nylon 66 (chips)
$\bar{M}_w$	50 000	40 000
$\bar{M}_n$	20 000	20 000
Polydispersity	2.5	2.0
DP	84	93
Average chain length (Å)	1080	1600
Persistence length[a] (Å)	200	5.4

[a] Persistence length is a measure of chain rigidity and is related to the degree of straightness of the chain.
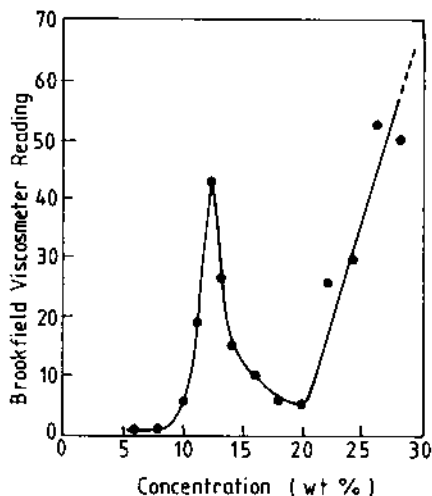
Fig. 18.3 Effect of polymer concentration on viscosity of PPTA–H_2SO_4 solution [19].

concentration is followed by a steady drop after a critical concentration. The 100% liquid crystalline state is achieved at a polymer concentration of 20% in 100% H_2SO_4.

The polymer is added to concentrated sulphuric acid to prepare a 20% solution and extruded through a spinneret (typical hole diameter 0.05–0.10 mm) at about 100 °C for standard fibre and 70–90 °C for high tenacity fibre through about 1.0 cm or 0.5 cm of air gap into cold water maintained between 0 and 5 °C, as shown in Fig. 18.4 [20].

In addition to variation in the coagulation conditions, the properties of the fibre can be diversified by variation in the spin stretch factor (SSF),
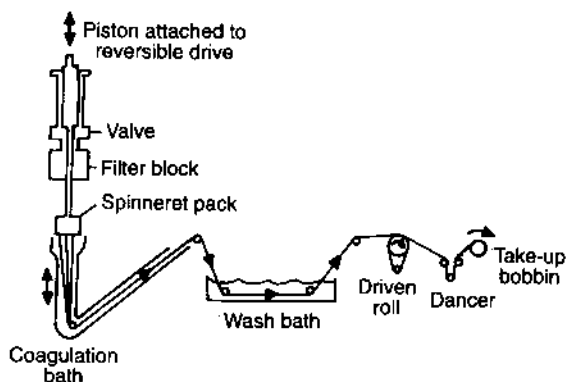
Fig. 18.4 A dry-jet wet-spinning process for PPTA fibre [20].

which is the ratio of the fibre velocity leaving the coagulating bath to the dope velocity emerging from the spinneret. As the SSF increases, the tenacity and modulus both increase at the expense of extension to break, while a limiting SSF (usually less than 10) is reached where frequent filament breaks make the process uneconomic. Fibre precipitation starts in the air gap itself as the temperature in the gap is lower than that of the dope and the acid is removed in the coagulation bath. The spinning speeds are generally around $50 \, \text{m} \, \text{min}^{-1}$.

Following washing and drying, the yarn is collected on a take-up bobbin. The properties of the fibre can be enhanced by heat treatment under tension, using temperatures in the range 450–550 °C for a few seconds.

The process of spinning involving wet-spinning with a small air gap is called dry-jet wet-spinning. This process represented a major breakthrough – in comparison with wet-spinning the air gap method allows the use of low temperature coagulation without freezing the spin solution. The air gap keeps the spin dope at a higher temperature (70–100 °C) than that of the coagulation bath for some time, making possible higher concentration of around 20% to be maintained in the air gap. This is the 100% liquid crystalline state when the maximum anisotropy occurs, leading to good molecular orientation in the spinline. This also allows higher stretch to be given in the air gap; in fact, a ten-fold attenuation occurs in dry-jet wet-spinning compared with three-fold in conventional wet-spinning, again leading to higher orientation. The alignment of liquid crystal domains in dry-jet wet-spinning is shown schematically in Fig. 18.5 [21]. As opposed to a fibre with tenacity of $12 \, \text{gf} \, \text{den}^{-1}$, modulus of $100–500 \, \text{gf} \, \text{den}^{-1}$ and elongation to break of 10% which is obtained by wet-spinning of PPTA, dry-jet wet-spinning results in a
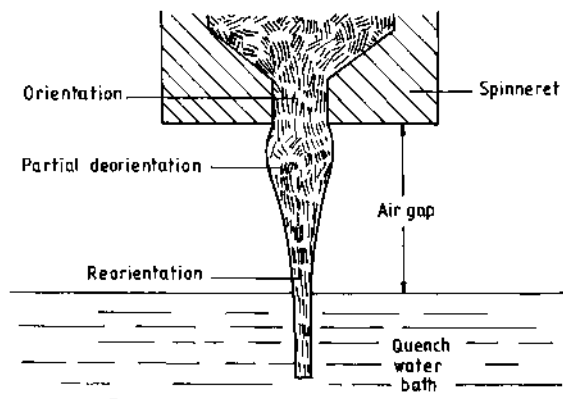
Fig. 18.5 Alignment of liquid crystalline domains in dry-jet wet-spinning [21].
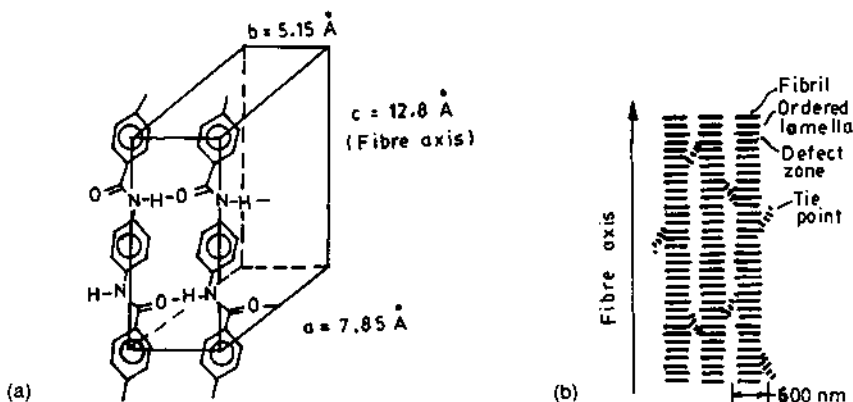
Fig. 18.6 (a) The unit cell of PPTA crystal. (b) Fibrillar morphology of PPTA fibre [22].

tenacity of $15–30\,\text{gf den}^{-1}$, modulus of $200–1000\,\text{gf den}^{-1}$ and elongation to break of less than 5% [14].

Kevlar fibres have extended chains, are highly oriented and are almost completely crystalline; the ordered structure along the fibre axis is in the form of a highly ordered fibrillar structure. The molecules form rigid planar sheets with the aligned molecules hydrogen-bonded together (Fig. 18.6(a)). There are levels of structural features of these aramid fibres which are different than those for the conventional fibres. For example, a pleated structure is observed in Kevlar 49 fibre by optical and electron microscopy; the pleats are around 500 nm long with the adjacent components of pleat being at approximately equal but opposite angles of 170 °C. The fibrillar columns, which are aggregates of elongated, oriented liquid crystalline domains (Fig. 18.6(b)) [22], lie along the axial pleats.

Kevlar has been produced by Du Pont in two grades, 29 and 49, for over 20 years and successfully used in a wide range of manufacturing processes as a textile fibre and as a reinforcing material. The range was later extended by the addition of two new Kevlar grades, 149 and 981, and by two competitive fibres Twaron™, from Akzo, Holland and Technora™ from Teijin Co., Japan [9, 20].

Some characteristic properties of some PPTA fibres are summarized in Table 18.2 in which the properties of Nomex fibre and Fibre B are also included for comparison. Kevlar 29 is mainly used as belting in radial tyres and as cord in heavy duty truck tyres and aircraft tyres, where its advantages of light weight, greater durability, low resistance to rolling and lower cost than steel are advantageous. The other three Kevlar grades are used for composite applications in civilian and military aircraft, helicopter parts, protective apparel, ropes and cables, industrial fabrics and pressure vessels.

Table 18.2 Properties of some aromatic polyamide fibres

Fibre	Modulus (GPa)[a]	Tensile strength (GPa)[a]	Extension to break (%)	Relative Density (g cm^{-3})
Nomex™	(150)	(5)	20	1.38
Fibre B	(1000)	(22)	5	1.45
Kevlar 29™	58	2.76	3.7	1.44
	(457)	(21.7)		
Kevlar 49™	120	2.76[b]	1.9	1.45
	(938)	(21.6)		
Kevlar 149™	166	2.2[b]	1.2	1.47
Kevlar 981™	120	3.5	2.8	–
Twaron™	79	3.0	3.3	1.44

[a] Values in parentheses are given in units of gf den^{-1}.
[b] 3.4–3.5 GPa as per current Du Pont literature.

(b) Ordered polymeric fibres

Two polymeric fibres which form lyotropic liquid crystalline solutions under suitable conditions and have gained importance in the recent past due to their excellent mechanical properties and thermal resistance are poly(p-phenylene benzobisthiazole) (PBZT) and poly(p-phenylene benzobisoxazole) (PBZO or PBO). They are called 'ordered polymers' because of their ability to form highly ordered structures in the solid state [8, 11]. Trans-PBZT is polymerized from 2,5-diamino-1,4-benzene-dithiol dihydrochloride (DABDT) and terephthalic acid while cis-PBZO is based on 4,6-diamino-1,3-benzenediol dihydrochloride (DABDO) and terephthalic acid (TA), as shown below:

DABDT   TA

PBZT
(repeat unit)

PBZO or PBO
(repeat unit)
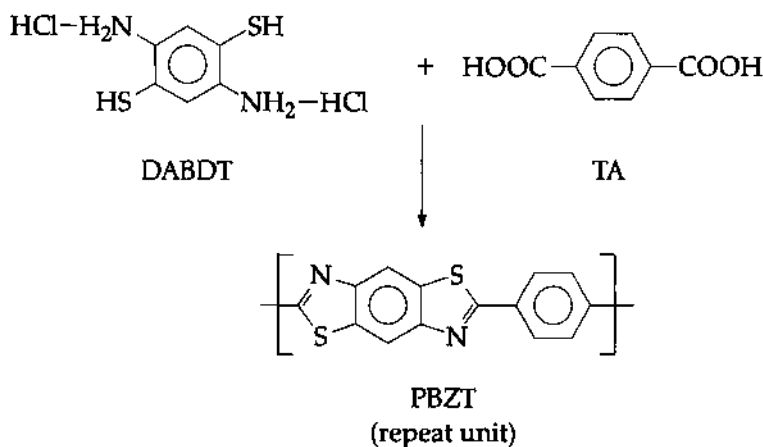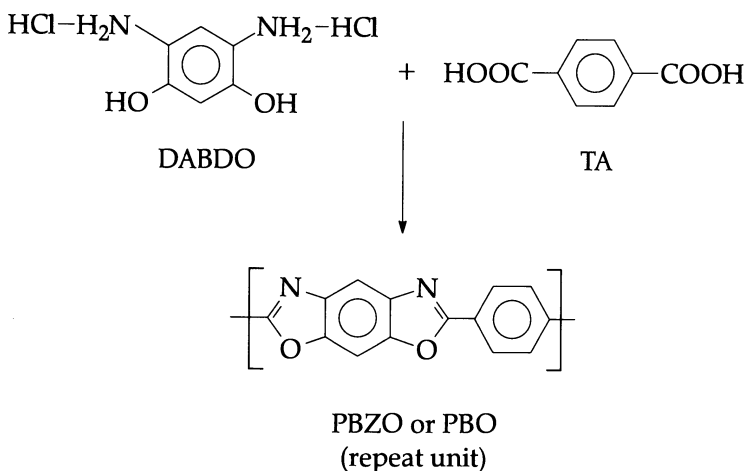
Both reactions are carried out in polyphosphoric acid (PPA) solvent and molecular weights of $50\,000$–$100\,000\,\mathrm{g\,mol^{-1}}$ are obtained, corresponding to about 200–400 repeat units per chain. The persistence length of *trans*-PBZT is around $500\,\mathrm{\mathring{A}}$ and of *cis*-PBO around $640\,\mathrm{\mathring{A}}$, much higher than that of PPTA ($200\,\mathrm{\mathring{A}}$) or of polyethylene ($5.7\,\mathrm{\mathring{A}}$), consistent with the high rigidity of the chain. The Mark–Houwink relationship for PBO is $[\eta] = 2.77 \times 10^{-7} M_w^{1.8}$ in methanesulphonic acid (MSA); the very high Mark–Houwink exponent of 1.8 also signifies high chain rigidity of the molecule. Their dissolution requires the use of strong, protonating acids such as PPA, MSA, etc. The critical concentration curve for PBO is given in Fig. 18.7 [23].

These polymers are spun using the dry-jet wet-spinning technique from a liquid crystalline solution in PPA or MSA. Water is used as the coagulant in the case of PBO/PPA solutions. Following washing and drying, the fibres are heat-treated under tension in an inert atmosphere. For the PBO fibre, heat treatment temperatures of 500–700 °C with a residence time of a few seconds to several minutes is typically used. In these fibres, the amorphous phase, as commonly understood in flexible chain polymers, does not exist. While PBZT is axially disordered, PBO has three-dimensional order. Some properties of these two fibres are summarized in Table 18.3. The poor compressive strength limits their use to those applications where axial compression loading does not occur. These fibres can be used as reinforcements in composites, multilayer circuit boards, athletic equipment and for marine applications and cables. Because of their excellent thermal and flame resistance, they can be used as fire protection fabrics. Fabrics made from these fibres are also excellent for ballistic protection. The thermal resistance of the PBO fibre
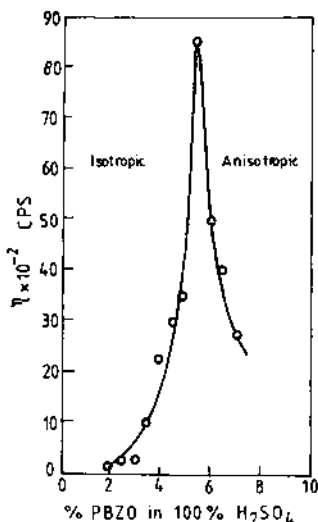
Fig. 18.7 Viscosity vs. concentration curve for PBZO of inherent viscosity 2.1 at 70 °C [23].

is outstanding; there is only 10% weight loss after heating in air at 300 °C for 200 h.

(c) Aromatic polyesters

The polyester fibre, poly(ethylene terephthalate) (PET), has been extensively discussed earlier as a very successful fibre. It is an aliphatic–aromatic polyester to which the aromatic terephthalic acid residue confers rigidity while the glycol residue is responsible for flexibility. However, it has still not been possible to make high performance fibres of PET, even when high molecular weight polymer is used. Wholly aromatic polyesters overcome this shortcoming; they form a liquid crystalline phase over a certain temperature range in the melt. Such polymers are called thermotropic liquid crystalline polymers. Unfortunately, very few of the aromatic polyesters are suitable for fibre-making because of their tendency to degrade at higher temperatures and the poor tractability of the polymer melts [21].

Table 18.3 Some properties of PBZT and PBO fibres

Fibre	Modulus (GPa)	Tensile strength (GPa)	Compressive strength (GPa)	Relative Density (g cm^{-3})
PBZT	325	4.1	0.3–0.4	1.58
PBO	360	5.7	0.2–0.4	1.58

A two-component wholly aromatic thermotropic polyester is made by melt synthesis from *p*-hydroxy benzoic acid (HBA) and 2,6-hydroxy naphthoic acid (HNA); the hydroxyl groups are acetylated to facilitate polymerization. As a result HBA is converted to *p*-acetoxy benzoic acid (ABA) with a melting temperature of 230 °C, while HNA is converted to acetoxy naphthoic acid (ANA) as shown below:

HBA   Converted to   ABA

HNA   Converted to   ANA
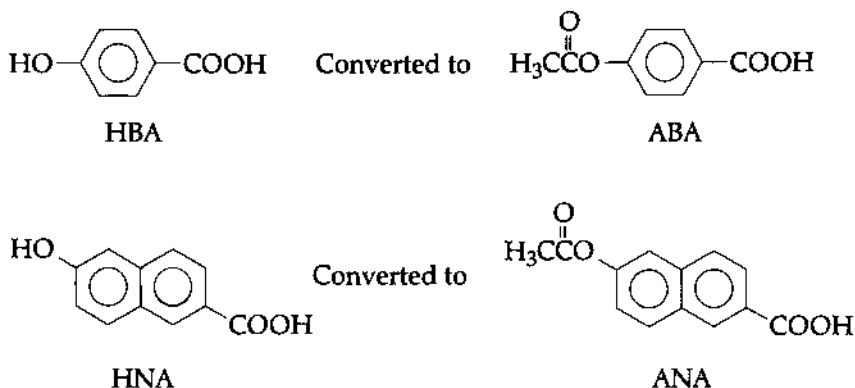
The components are taken in the desired ratio and polymerized through condensation to yield the polymer which has a random sequence distribution of the two components, as shown below:
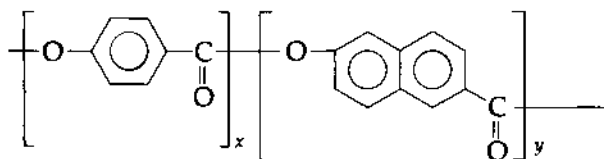
Vectran^{TM} fibre, marketed by Hoechst Celanese Co., is synthesized with a comonomer ratio of ANA:ABA as 30:70 and has a thermal distortion temperature of 180–240 °C and a melting point of 270 °C.

In these fibres, as in the case of Kevlar, the link between the aromatic rings offers some possibility of rotation and consequent structural flexibility. In PBZO, on the other hand, the link itself is a ring as shown earlier, and therefore we may expect a more rigid and therefore a stiffer fibre, as was found to be the case.

The spinning process is similar to conventional PET melt-spinning. The thermotropic liquid crystalline spinning melt with a typical intrinsic viscosity of 1.5–3 dl g^{-1} is extruded at 280–350 °C through spinneret holes to form the yarn at wind-up speeds approaching several thousand metres per minute. The as-spun fibres, which are 10% crystalline after quenching, are heat-treated at temperatures of 250–300 °C for several hours during which crystallinity increases to 20%, solid state polymerization

occurs (M_n increases by three times) and fibre strength increases. Fibres of tensile strength 2.5–3.1 GPa (20–25 gf den^{-1}), tensile moduli 62–86 GPa (500–700 gf den^{-1}) and elongation to break of 2.2–2.5% are obtained.

The principal applications for this fibre are as ropes and cables, because of their high strength, good abrasion resistance and negligible creep; other applications are as bow strings, bicycle frames and sail cloth mainly because of excellent vibration-damping capability.

(d) High modulus flexible chain fibres

The only flexible chain fibre which has been commercialized as high performance fibre is polyethylene [24, 25]; the repeat unit is:

$$
\left[\begin{array}{c} \begin{matrix} H & H \\ | & | \\ C\!-\!C \\ | & | \\ H & H \end{matrix} \end{array}\right]
$$
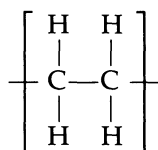
The backbone is highly flexible because of the possibility of rotation around C–C bonds and because the only other element present is light hydrogen. The estimated crystal modulus of polyethylene along the molecular chain is over 300 GPa [24], whereas for Kevlar it is in the range 200–250 GPa [11, 26]. An elegant explanation of the physical basis for this high modulus was offered by Frank [27] as follows:

> The Young's modulus for diamond in the [110] direction is 1160 GPa. In the [110] direction, diamond is composed of fully aligned zig-zag chains of carbon just like those in polyethylene, utilizing half the neighbor-to-neighbor bonds in the crystal, while the other half of the bonds are at right angles to this direction, contributing nothing to the Young's modulus in this direction, just as the carbon-to-hydrogen bonds in fully aligned polyethylene contribute nothing to its longitudinal Young's modulus. The cross-sectional area per chain in diamond is 0.0488 nm^2, four times smaller than polyethylene, 0.182 nm^2. Hence, from this analogy, we could expect a modulus of 285 GPa for fully aligned polyethylene, well above that of steel.

Thus the small cross-sectional area of polyethylene chain (Kevlar chain has a cross-sectional area of 0.205 nm^2) contributes to its high crystal modulus in the chain direction as it ensures that a relatively large number of chains per unit cross-sectional area take the load.

It is worthwhile pointing out at this stage that the measured modulus of melt-spun high density polyethylene (HDPE) is 5 GPa. As discussed

in Chapter 2, this can be explained in terms of lack of chain continuity in the axial direction due to chain folding. Obviously if chain folding can be avoided, high modulus fibres can be produced. The fibres produced by Pennings and co-workers [28, 29], when dilute solutions of polyethylene were cooled under conditions of continuous stirring, had the shish kebab structure as shown in Chapter 2 in Fig. 2.8(a) with extensive chain folding. It was pointed out by Frank [27] that absence of extensional deformation during stirring of a dilute solution did not allow molecular extension to take place.

The early work on developing high modulus HDPE fibre followed different routes. These included extension of polyethylene in an Instron capillary rheometer [30, 31], which did not lead to a commercial process. The work progressed in two directions. The first was the well-known melt-spinning and hot drawing route followed for polyester, polyamides and other melt-spun fibres [24]. High modulus, high strength fibres could be obtained by processing HDPE polymer of $\bar{M}_w$ less than $300\,000\,g\,mol^{-1}$ at elevated temperatures (of the order of 250 °C) and then rapidly cooling the filament to give an essentially isotropic polymer. The fibre is then subsequently drawn in the temperature range 80–125 °C and draw ratios of 30 or higher can be achieved to give fibres of Young's modulus 60 GPa, breaking stress of 1.3 GPa and elongation to break of 5%. The second direction was the solution-spinning of HDPE, starting from the ideas developed by Pennings and co-workers [28, 29]. By 1980 improvements made by Smith and Lemstra [32] led to gel-spinning and drawing, by which technique fibres of tensile strength 7 GPa and modulus of 200 GPa could be produced [24].

The industrialization of gel-spinning soon followed and these extended chain HDPE fibres are now commercially available: Spectra™ manufactured by Allied Signal in the USA, Dyneema™ by DSM/Toyobo in Holland and Japan, and Tekmilon™ by Mitsui in Japan [9].

Melt-spinning of very fine HDPE filaments is restricted from a practical viewpoint to relatively low molecular weight polymers because of the requirement of a comparatively low melt viscosity giving rise to fibres with tenacity of 1.3 GPa. This disadvantage has been overcome by using the solution process which involves the hot drawing of gel-spun fibres prepared by spinning of approximately 5% solution of high molecular weight (approximate $\bar{M}_w$ 10^6) in decalin or paraffin oil into a small air gap before entering a water bath at room temperature to form a gel fibre with nearly all the solvent in the fibre and then drawing to draw ratios of 30–100 at 100–150 °C, as the solvent leaves the fibre. It is interesting that even after removal of the solvent, the gel can still be highly drawn. This is because the as-spun fibre has a swollen network in which chain-folded lamellae form the junctions, allowing the as-spun fibre to be drawn to over 200 times [8].
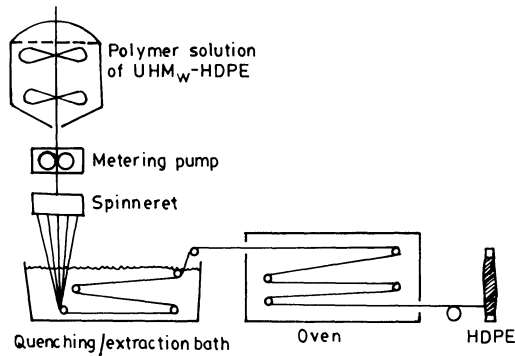
Fig. 18.8 The gel-spinning process [25].

The gel-spinning and drawing process is schematically shown in Fig. 18.8 [25] and may be considered under the following three heads.

1. *Dissolution*: a homogeneous solution of ultra high molecular weight HDPE is prepared at elevated temperatures with stirring. This forms a solution with minimum chain ends which is capable of gelation with optimum number of entanglements.
2. *Spinning*: a gel-like, as-spun fibre is obtained by spinning the solution at 130–140 °C with controlled crystallization and minimum number of entanglements.
3. *Drawing*: high draw ratios can be achieved with minimum amorphous phase.

In a set of elegant experiments, Matsuo and Ogita [33] took HDPE of molecular weights of 1×10^6, 3×10^6 and 6×10^6, respectively, and studied the concentration dependence of draw ratio for the three dried gel films. To obtain a draw ratio of 350–400, the concentrations had to be maintained at 1.6 g/100 ml for $\bar{M}_w$ of 1×10^6 at 0.65 g/100 ml for $\bar{M}_w$ of 3×10^6 and at 0.4 g/100 ml for $\bar{M}_w$ of 6×10^6. Higher and lower concentration than these optimum levels were found to lead to lower draw ratios and, therefore, inferior mechanical properties. The authors concluded that most of the chain molecules in the regime of low concentration are random coils having coupling entanglements that will be predominantly intramolecular in nature. On the other hand, solutions corresponding to the regime of high concentration are thought to consist of interpenetrating random coils which form a large number of coupling entanglements that are both intra- and intermolecular. For specimens prepared from solutions with critical concentration, which is different for different molecular weights, it may be expected that there exists a suitable level of entangled meshes that act as interlamellar crosslinks and effectively transmit the drawing force, and therefore the possibility

of polymer chains slipping past each other without interconnection is very low. The shift of the critical concentration to lower values with increasing molecular weight is probably due to the fact that the number of coupling entanglement meshes of HDPE with very high molecular weight (say 6×10^6) increases drastically with increasing concentration. This may be expressed in terms of the following relationship [34]:

$$\lambda_{\max} = K/(\bar{M}_w C)^{1/2}$$

where $\lambda_{\max}$ is the maximum draw ratio, K is a constant, $\bar{M}_w$ the weight average molecular weight and C the concentration of the solution. Mackley and Sapsford [35] have made an interesting observation, which provides a bridge between the melt-spinning approach of Ward and co-workers and the gel-spinning technique of Smith and Lemstra, by postulating that the processing conditions in both cases result in an entanglement concentration high enough to ensure a connected network, yet sufficiently low to enable high draw ratios to be obtained while increased molecular weight provides strength. A model of UHMWHDPE gel-spun and drawn fibre was presented in Chapter 2 (Fig. 2.8) which is in accordance with this concept.

The cost of solvent recovery and the controlled low speed spinning and drawing increase the cost of the fibre to a level comparable with that of other high performance polymeric fibres. This lightweight, high strength, high modulus fibre has high toughness but a low melting point. Some of its applications are as marine ropes and cables, sail cloth, concrete reinforcement, fish netting, sports equipment and medical implants.

18.3.2 CARBON FIBRES

In 1879 Swan and Edison used carbonized cotton yarns as electric lamp filament. However, these carbonized fibres did not have the mechanical properties expected of a high performance fibre.

It was not until the late 1950s and early 1960s that serious efforts were made to produce high strength carbon fibres. Three groups were involved in this search: Wright Patterson Air Force Base in Dayton, Ohio, USA, using viscose rayon as the precursor; Shindo in the Industrial Research Institute in Osaka, Japan, using polyacrylonitrile (PAN) as the precursor; and Watt, Johnson and Phillips in the Royal Aircrafts Establishment in Farnborough, England, again using PAN fibre as the precursor.

(a) Production of carbon fibres

The three stages involved in the production of carbon fibres from rayon, which came out of the work of the US group, are oxidative stabilization

at temperatures up to 400 °C, carbonization at temperatures up to 1500 °C, and graphitization above 2500 °C. It is in the carbonization stage that graphite-like layers start forming; however, during this process the original preferred orientation of the cellulose structure is lost. Therefore, unless a stretch of up to 50% is applied at higher temperatures, particularly during graphitization, a high modulus fibre is not obtained, making it a rather difficult technique.

The production of PAN-based carbon fibres also involves three stages, namely oxidative stabilization at 200–300 °C, carbonization up to about 1500 °C and graphitization between 1500 and 2700 °C, according to the type of fibre required.

Shindo was the first to use PAN precursors but the carbon fibres he made from them did not have the strength and stiffness required of a high performance fibre. The group at Farnborough made this possible by applying tension to the fibre during oxidative stabilization in the 200–300 °C temperature range; disorientation was prevented as a result and in fact improvement in orientation was obtained.

The first stage in the conversion of PAN to carbon fibre is one of oxidation when the PAN fibres are heated in air between 200 and 300 °C; controlled shrinkage is allowed during this treatment to ensure that no disorientation occurs. PAN, with a highly polar nitrile ($-C{\equiv}N$) group on every second carbon atom, is unique among the commodity fibres in forming a ladder polymer when heated to 200–220 °C (Fig. 18.9(a)) [36]; this consists of linked hydrogenated naphthylpyridine rings and increases the thermal stability of the polymer since it prevents the easy formation of small volatile fragments [37]. When the fibres are heated in air at 220 °C, ketonic groups are formed by oxidation of the $+CH_2+$ groups (Fig. 18.9(a)). It was at one time thought that the oxidation stage in the preparation of high modulus carbon fibres for PAN led to ($-O-$) links between chains, but doubts have been expressed about this mechanism.

After the oxidative treatment, the fibre is now ready to undergo processing at higher temperatures. When the black, oxidized fibre is heated slowly to a higher temperature (1000–1500 °C) in an inert atmosphere, intermolecular reactions occur giving crosslinking. Carbonization, as it is called, is done under tension but no stretch and it proceeds by elimination of a number of low molecular weight gaseous products (mainly HCN, NH_3, H_2, CO and CO_2), a process which is time and temperature dependent. The yield of carbon fibres is about 50% of the mass of original PAN. Most of the volatiles are produced below 1000 °C. At this stage the filaments contain mostly carbon and some nitrogen atoms (Figs 18.9(b)) [36], arranged in aromatic ring patterns in parallel planes. However, the carbon atoms in the neighbouring planes are not yet perfectly ordered, and the filaments have a relatively low tensile modulus.
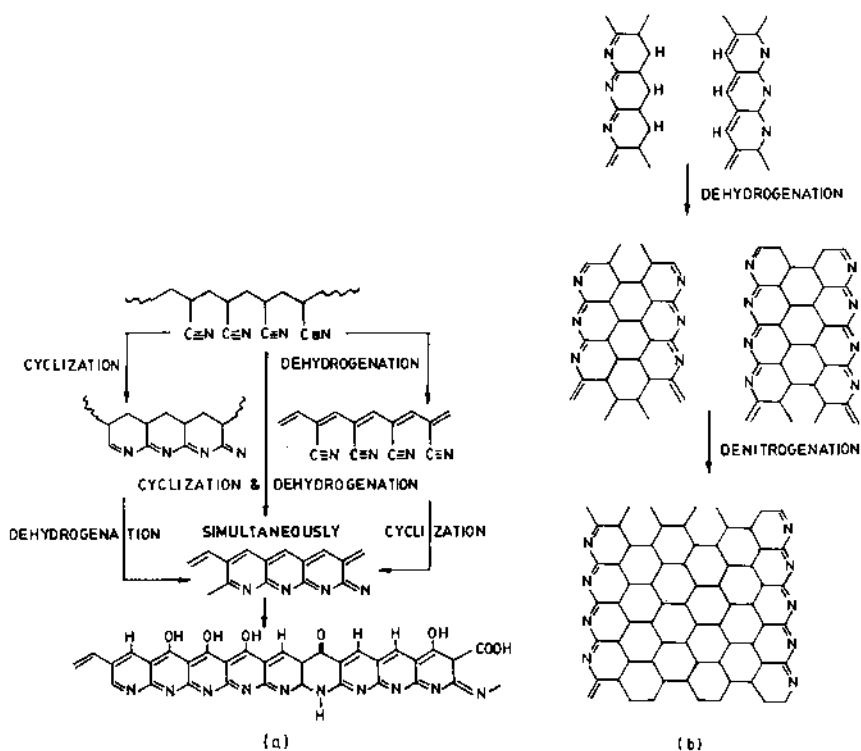
Fig. 18.9 Chemical changes during (a) oxidative stabilization and (b) carbonization of PAN fibres [36].

The carbonized filaments are subsequently heat treated at temperatures in the 1500–2700 °C range, the process being called graphitization. During this treatment, their structure becomes more ordered and turns towards a true graphitic form with increasing heat treatment temperature. The graphitized filaments attain a high tensile modulus but their tensile strength may be relatively low (Fig. 18.10) [38]. The structural origin of the decrease in strength at higher heat treatment temperatures is not well understood. The tensile strength can be increased by hot stretching them above 2000 °C during which the graphitic planes are aligned in the filament direction. Moduli of 700 GPa may be obtained with a stretch of 30% at this stage. The extension required for viscose rayon fibres to achieve higher modulus during graphitization is around 300% and correspondingly more difficult to produce [37]. Other physical properties of carbon fibres such as electrical and thermal conductivities, longitudinal coefficients of thermal expansion and oxidation resistance can be improved by controlling the order and by eliminating the defects,

Heat Treatment Temperature (°C)
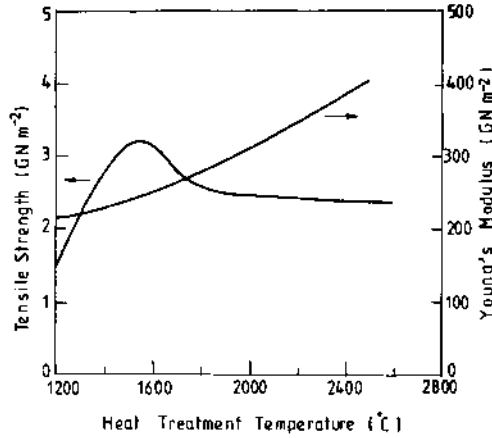
Fig. 18.10 Strength and elastic modulus of PAN-based carbon fibre as a function of final heat treatment temperature [38].

for example vacant carbon sites or catalyst impurities. A line sketch of a continuous carbon fibre-producing plant is shown in Fig. 18.11 [39].

Pitch is another important source of carbon fibres. It is a by-product of petroleum refining or coal coking. The carbon atoms in pitch are arranged in low molecular weight aromatic ring patterns. Heating to temperatures above 350 °C joins these molecules into long, two-dimensional sheet-like structures, referred to as mesophase pitch, which contain both isotropic and anisotropic (liquid crystal) material. The mesophase pitch is melt-spun through a multihole spinneret, causing the molecules to become aligned in the direction of extension, and 'green yarn' is produced. Then the yarn is cooled and subsequently
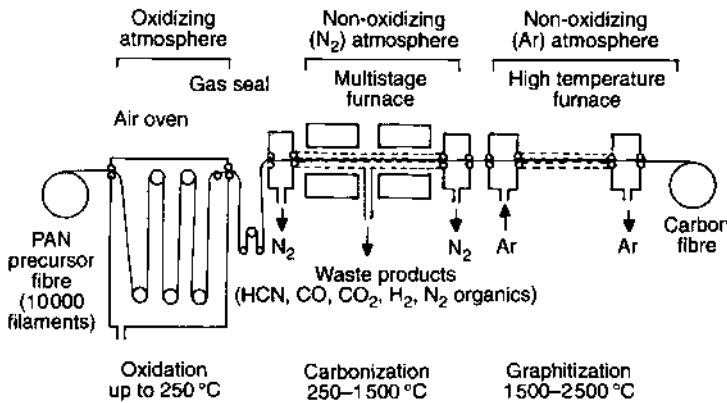
Fig. 18.11 A PAN-based carbon fibre production unit [39].
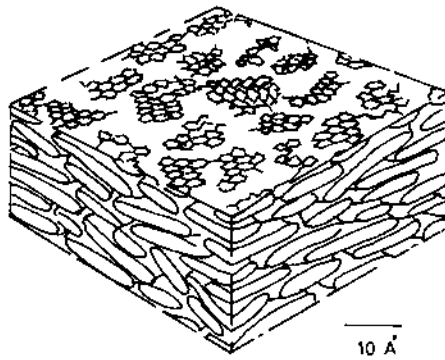
Fig. 18.12 Arrangement of graphite layers in the mesophase lamellar model of carbon fibre [40].

subjected to heat treatment below its softening point (250–400 °C) in an oxygen-containing atmosphere and made infusible by oxidation to avoid fusing together of the filaments. The yarn is then carbonized at temperatures around 2000 °C. The main advantage of this process over the rayon or PAN process is that no tension is required during processing in order to develop or maintain the molecular orientation necessary to achieve high modulus and high strength [37]. Graphitization in the temperature range 2500–3000 °C further improves the properties. Because of the liquid crystal nature of the pitch, molecular orientation is achieved in the spinning process and is preserved or enhanced on processing without the use of tension. The arrangement of the molecules in pitch-based carbon fibres is lamellar in nature and is shown schematically in Fig. 18.12 [40].

The pitch-based carbon fibres are not inexpensive in spite of petroleum pitch being a readily available, low cost material. Currently available pitch-based carbon fibres exhibit much lower elongation to break at equal modulus than do PAN-based carbon fibres.

(b) Surface treatment of carbon fibres

Carbon fibres are rarely, if ever, used alone. Their major use is as a reinforcement in composites. If the surface of the carbon fibres is not given any treatment, the composites produced have low interlaminar shear strength (ILSS) with the result that the full potential of the fibres is not realized. This is attributed largely to weak bonding between the fibre and the matrix.

The surface treatments may be classified under two categories:

1. *Oxidative*: these include gaseous oxidation (in air, in oxygen or catalytic) and liquid phase oxidation (chemical in nitric acid, hydrogen

peroxide, etc. or electrochemical using nitric acid or sodium hydroxide). The improvement in ILSS is 10–55% with gaseous oxidation and 100–200% with liquid phase oxidation [41].

2. *Non-oxidative*: these include whiskerization, polymer grafting or pyrolytic carbon deposition. The improvement in ILSS is 200–300% with whiskerization, 60–100% with pyrolytic carbon coating and 80–100% with polymer grafting.

The two factors which contribute to the improvement in ILSS and consequent enhancement of mechanical properties are the surface acidic functional groups and the increase in specific surface caused by the various treatments; both these improve the bonding between the fibre and the matrix.

(c) Structure and morphology of carbon fibres

Diamond and graphite are crystalline forms of carbon. In graphite each carbon atom is linked with three other carbon atoms to form a layered structure with the layers being stacked with the typical van der Waals distance between them (Fig. 18.13) [13]. In diamond, each carbon atom is covalently linked with four other neighbouring carbon atoms. Most graphite samples seem to be a mixture of two forms with the hexagonal form predominating in the ratio of 4 or 5:1 over the rhombohedral. The layered structure of graphite has been conceived [42] to be in the form of ribbons of Sp^2 type (planar) carbon. The ribbons are undulating and their dimensions depend on heat treatment conditions. They contain straight parts with lengths in the 60–600 Å range depending on orientation, the heat treatment temperature and the precursor; the width varies
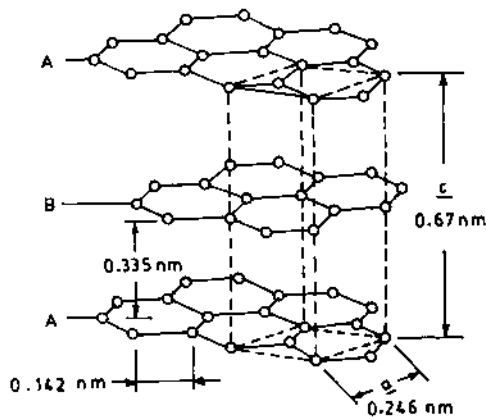
Fig. 18.13 Structure of hexagonal graphite [13].
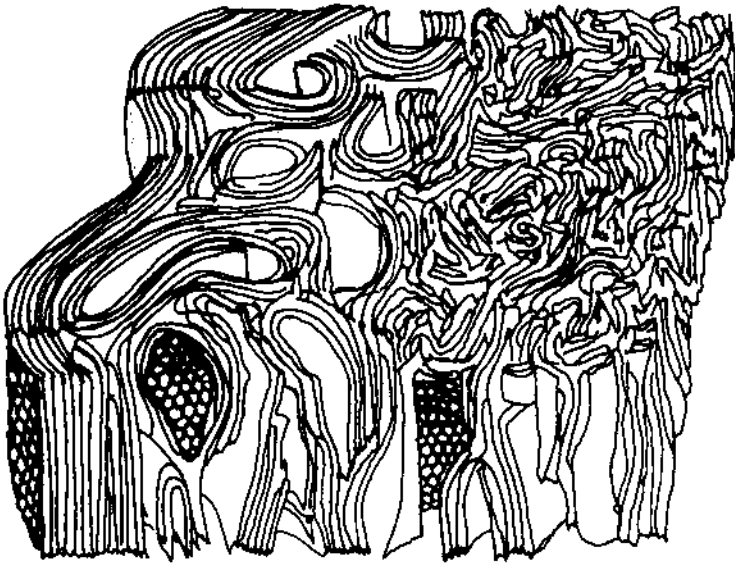
Fig. 18.14 Structure of carbon fibre [43].

between 50 and 1000 Å. The space between the ribbons gives rise to needle-shaped pores or voids. A three-dimensional arrangement of the layer planes in carbon fibre has been conceived as shown schematically in Fig. 18.14 on the basis of comprehensive high resolution electron microscopy [43], which included dark- and bright-field image analysis and specimen tilting procedures.

The arrangement of the layer planes in the cross-section of the fibre is important since it affects the transverse and shear properties of the fibre. The cross-section arrangement is a function of processing conditions but believed to be independent of heat treatment temperature. The PAN-based high modulus carbon fibres have a thin skin of circumferential layer planes and a core with the layer planes along the fibre axis having random orientation. In contrast the mesophase pitch-based fibres exhibit radially oriented layer structures in the core and circumferential layer planes. In some cases all the layer planes may lie as annular rings. While the concept of basal planes forming ribbons or sheets, arranged parallel to the fibre axis direction, has been well substantiated from X-ray and electron microscopic studies, a sheath–core structure having different arrangements of these basal planes in the skin and the core, as described above, seems possible with certain precursors and processing conditions, while some other precursor and processing conditions could as well result in an isotropic cross-section of the carbon fibres [44].

Table 18.4 Some properties of PAN-based carbon fibres

Parameter	High strength	High modulus	Ultra high modulus	Single crystal graphite
Carbon component weight (%)	92–94	>99	>99.9	100
Density (g cm^{-3})	1.7–1.8	1.8–1.9	1.9–2.1	2.25
Filament diameter (μm)	5–8	5–8	6–8	–
Tensile modulus (GPa)	220–250	340–380	520–550	1000
Tensile elongation (%)	1.2–1.4	0.6–0.7	0.3–0.4	2.0
Tensile strength (GPa)	2.5–7.0	2.2–2.4	1.8–1.9	–
Electrical resistivity (10^{-4} Ω cm)	15–18	9–10	6–7	0.40

(d) Properties of carbon fibres

The PAN-based carbon fibres are produced in three grades, namely high strength, high modulus and ultra high modulus. Some of their properties are summarized in Table 18.4, in which some properties of single crystal graphite have also been included for reference. It is of interest to compare the properties of PAN-based carbon fibres with those obtained from pitch and rayon: Table 18.5 summarizes the range of properties that are currently available.

Some noteworthy observations are as follows.

• The density of carbon fibre is highly variable and has a range of 1.7–2.2 g cm^{-3}, depending on the precursor, the processing conditions and the heat treatment temperature. It may, however, be noted that the density values for the carbon fibre are appreciably higher than those of the precursor fibre; the density of the PAN precursor fibres is generally between 1.14 and 1.19 g cm^{-3}.

• The achievement of higher modulus is at the cost of toughness. The modulus in the fibre axis direction is highly orientation-dependent. In PAN-based fibres the degree of order and the modulus increase with

Table 18.5 Comparison of some properties of carbon fibres produced from different precursors

	From rayon	From mesophase pitch	From PAN
Density (g cm^{-3})	1.66	1.9–2.2	1.81
Tensile modulus (GPa)	393–524	195–900	222–533
Tensile strength (GPa)	2.2–2.65	2.1	1.8–7.1
Tensile elongation (%) at failure	1.67–1.82	0.4–0.5	0.5–2.4
Electrical resistivity (10^{-4} Ω cm)	10	1.8	10

increase in graphitization temperature, while the tensile elongation decreases significantly.

- The mesophase pitch-based carbon fibres can be produced with high modulus.
- The carbon fibres produced from various precursor materials are electrical conductors. However, their ability to conduct electricity has one potential hazard, namely that if they become airborne during manufacture or service, they can settle on electrical equipment and cause short circuiting.

It may also be added that carbon fibres, like the polymeric fibres, are highly anisotropic and this has important consequences, e.g. the in-plane properties will be very different from the properties perpendicular to the graphite planes. For example, the principal coefficient of thermal expansion perpendicular to the fibre axis lies between 7×10^{-6} and $12 \times 10^{-6} \, \text{K}^{-1}$, whereas it is between -0.5×10^{-6} and $-1.2 \times 10^{-6} \, \text{K}^{-1}$ in the fibre axis direction. Similarly the modulus perpendicular to the fibre axis is in the range 12–20 GPa, as opposed to the axial modulus being in the range 250–390 GPa [45].

(e) Applications

The high specific strength and stiffness of carbon fibres are the basic characteristics which are useful in almost all applications of these fibres. The other properties such as temperature resistance, chemical and biological inertness, electrical conductivity, good vibration damping ability and fatigue resistance may be useful in specific applications. The main shortcomings of carbon fibres are: (1) they have a low impact strength, and (2) they are expensive.

The two main sectors of carbon fibre applications are the high technology sector, which includes aerospace and nuclear engineering, and the general engineering, transportation and sports sectors, which include engineering components such as bearings, gears, cams, fan blades, etc., automobile bodies and sports equipment [41]. The requirements of the two sectors are different because while the aircraft and aerospace sectors lay emphasis on maximum performance and fuel efficiency, the engineering and surface transportation uses with less critical performance needs are dominated by cost constraints and high production rate requirements. More specifically the following applications deserve mention.

- The cargo bay doors and booster rocket casings in the US Space Shuttles are made of carbon fibre-reinforced composites.
- Modern fighter and commercial aircraft have a number of components containing carbon fibre-based composites.

- Machinery items such as turbine, compressor, helicopter and windmill blades; fly wheels, moving parts and shuttles in textile machinery.
- Ligament and hip joint replacement and heart valves and other surgical implants.
- Sporting equipment such as racing car components, tennis racquet handles, pole vaulting pole and rowing oars.

As stated earlier, the highly anisotropic nature of the fibre results in low stiffness and strength perpendicular to the fibre axis and, coupled with the low extensibility, the strength of a composite with a planar arrangement of fibres is very low when the impact is perpendicular to the fibre. A bird hitting the blades of an aircraft engine can result in impact failure and considerable efforts are being made to remove this shortcoming.

18.3.3 GLASS FIBRES

Glass fibres represent an important category of manufactured high performance fibres as they are widely used because of their useful properties, i.e. incombustibility, corrosion resistance, high strength, moderate density, good thermal and sound insulation and electrical properties. There is also a practically inexhaustible supply of raw material for their production and the fibres are inexpensive [46]. The most frequently used definition of glass is that adopted by the American Society for Testing and Materials (ASTM) which states that 'a glass is an inorganic product of fusion which has cooled to a rigid condition without crystallizing'. Unlike the fibres considered up till now, glass fibre is neither crystalline nor are its molecules in an oriented state; its isotropic three-dimensional network gives it the unique property of having comparable properties along and perpendicular to the fibre axis direction.

One of the main constituents of glass is silica (SiO_2). Atoms of crystalline silica form a lattice; it melts at 1713 °C when groups of atoms become detached and can move freely. As the molten material cools, the atoms try to form an ordered structure. However, if cooled rapidly, the melt thickens and is fixed in a random structure, which is typical of a fluid, before regular arrangement can take place. The very high temperature at which the transition from a solid state to a workable molten condition is achieved is still a problem for the glass-maker; its origin has a thermodynamic basis [47]. The ordering of atoms or molecules into a crystalline array is an exothermic process as a result of which a quantity of heat, ΔH, is evolved and transferred, say at a temperature T. The ratio $\Delta H/T$ equals the entropy change, ΔS. If foreign atoms are added to the liquid during freezing, disorder increases (ΔS becomes large) while ΔH is unchanged; thus the transfer temperature, $T = \Delta H/\Delta S$, comes down.

Table 18.6 Typical composition of glass fibres (in wt %)

Glass type	SiO_2	Al_2O_3	CaO	MgO	B_2O_3	Na_2O	K_2O
Soda–lime glass	72	0.6	10	2.5	–	14.2	–
E-glass	54.4	14.4	17.5	4.5	8.0	–	0.5
S-glass	65.0	25.0	–	10.0	–	–	–

The glass-maker has been making use of this concept since prehistoric times by selecting complex or impure solutions; for example, addition of 25% soda (Na_2O) to SiO_2 lowers the melting temperature to 793 °C (from 1713 °C). Another important advantage is that introduction of elements such as sodium or potassium, which shed electrons easily and form weak ionic bonds with oxygen, lowers the number crosslinks and results in the formation of a more mobile network; a typical network of soda–lime glass is shown in Fig. 18.15 [45]. A molecular network gives rise to high viscosity, which is useful for glass formation in that the frictional forces inhibiting the formation of new molecular configuration in the liquid are high, thus promoting the formation of a random glass-like structure.

(a) Chemical composition of glass

The chemical compositions of soda–lime glass, which is extensively used for window glass and other commodity applications like container glass, together with that of E-glass, which finds extensive use in the form of fibres in composites and of S-glass, a source of high strength glass fibre, are given in Table 18.6.

It is worth pointing out that, unlike soda–lime glass, the total alkali content in E- and S-glass fibre is kept below 2% to ensure good corrosion resistance and a high electrical surface resistivity. Addition of B_2O_3 decreases the liquidus temperature and provides a larger temperature range over which a glass may be worked without devitrification.

(b) Manufacturing process

There are four steps involved in the manufacture of E-glass fibre. First the various ingredients listed in Table 18.6 are dry-mixed. Then they are melted in a refractory furnace at 1370 °C. The molten glass is extruded through a number of orifices, usually 200 or its multiples, in an electrically heated platinum bushing, and 0.5–2.0% by weight of size or binder is applied to the strand on solidification but before winding them on a bobbin at $1000 \, m \, min^{-1}$ with the help of a traversing machine; the winder also draws them from the molten state and attenuates the

diameter of the filament. The size is a mixture of lubricants which prevents abrasion between the filaments, antistatic agents, a binder which packs the filaments into a strand and gives them cohesion and a coupling agent which promotes adhesion between fibres and the specific matrix for which it is formulated [48].

Some glass fibre manufacturers use marbles or batch as the starting material for fibre manufacture. Glass fibres are produced in various forms:

- strands, as described above;
- roving, which is an aggregate of parallel strands wound in a cylindrical forming package and is used in filament winding and pultrusion processes of composite fabrication;
- chopped strands produced by cutting a continuous strand into short (3–12 mm) lengths;
- milled fibres produced by grinding a continuous strand in a hammer mill (0.8–3.2 mm).

The other forms include woven roving or woven cloth and are used for a number of applications including textile-based composites.

(c) Structure

Figure 18.15 [45] is a two-dimensional representation of a three-dimensional network of linked polyhedron units in a simple sodium silicate glass. Each polyhedron is a combination of oxygen atoms around a silicon atom and they are bonded to each other by strong covalent bonds. If regularly attached, they form an ordered crystalline solid; glass, which is amorphous, is an antithesis of regular polyhedron

- Silicone atom
- ○ Oxygen atom
- Sodium ion
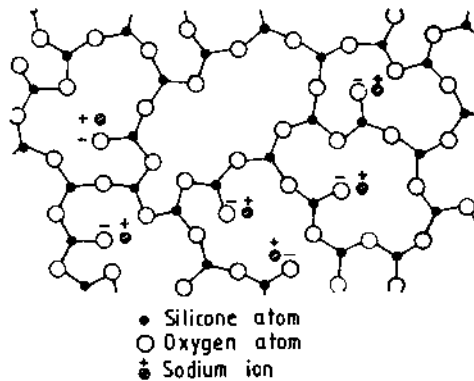
Fig. 18.15 Two-dimensional representation of network structure of sodium silicate glass [45].

Table 18.7 Some characteristics and fracture energy
of fibre made from E-glass

Characteristic/property	Values
Diameter	8–14 µm
Density	2.56 g cm^{-3}
Young's modulus (tensile)	76 GPa
Modulus (transverse) [45]	76 GPa
Tensile strength (typical)	1.4–2.5 GPa
Tensile strength (freshly spun)	3.5 GPa
Elongation to break (typical)	1.8–3.2%

crystals. The sodium ions form ionic bonds with oxygen atoms and are linked directly to the network. The structure of the network and the strength of the individual bonds can be varied by the addition of other metal oxides and so it is possible to produce glass fibres with different chemical and physical properties. The flux atoms such as sodium in Fig. 18.15 reduce the amount of crosslinking as some oxygen atoms are now strongly bonded only to a single atom and have weaker ties (not shown in the figure) with one or more flux atoms. This results in lowering the melting point of glass (it must be emphasized that an amorphous solid does not have a melting point; it just softens to give a melt-like consistency).

(d) Properties

Some characteristic properties of filaments made from E-glass are shown in Table 18.7. The strength and modulus of glass is determined primarily by the three-dimensional structure of the constituent oxides; an important consequence of this is that the mechanical properties along the fibre axis are the same as transverse to the axis. The elongation to break of glass fibres is higher than that of carbon fibres. However, the strength of glass fibres is very sensitive to surface cracks and freshly spun thin fibres are the strongest. According to Gordon [49] the high strength of thin fibres may be due in part to the fact that such fibres are easily bent and it is therefore easier to bend them than to scratch them.

(e) Applications

An important application for glass fibre is as a reinforcement for polymeric materials; reinforced plastics are extensively used in industrial (appliances and equipment) and automotive applications, in sports and leisure activities, and also in various components of lightweight aircraft. E-glass has the lowest cost of all commercially available reinforcing

fibres, which is the reason for its widespread use in the fibre-reinforced plastics industry.

18.3.4 BORON FIBRE

An important shortcoming of glass fibres is their low stiffness (76 GPa). This, combined with their inability to withstand high temperatures, limits their applications as a high performance fibre. Boron fibres have a modulus of 379–414 GPa and this, coupled with their relatively large diameter (100 μm) because they have to be made by deposition on a filament substrate (say of tungsten), offers excellent resistance to buckling. Boron fibre-reinforced composites have high compressive strength. Boron fibre has the added advantage, which it shares with carbon fibres, that its strength is not as sensitive to surface damage as that of glass fibres [37]. The principal disadvantage of boron fibre is its high cost.

  Boron fibres are manufactured by chemical vapour deposition (CVD) of boron on a heated substrate, using a process shown schematically in Fig. 18.16 [50, 51]. Tungsten filament of 12.5 μm diameter has been found to be an appropriate substrate though carbon fibre substrate has also been tried. A gaseous mixture of boron chloride and hydrogen is used for the production of boron vapours through the following reactions:

$$2BCl_3 + 3H_2 \rightarrow 2B + 6HCl.$$
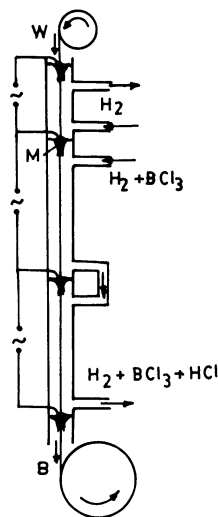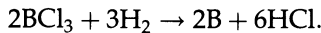
Fig. 18.16 A CVD unit used to produce boron (B) on a tungsten (W) substrate [50].

The electrically heated tungsten filament (to a temperature of 1100–1300 °C) is continuously pulled through the reaction chamber. The temperature of deposition is critical. If it is too low, the rate of deposition is slow; if too high, large crystals are produced and this leads to low strength. The residence time in the reaction chamber is 1–2 min. During deposition, part of the tungsten (W) substrate is converted into various tungsten borides, WB, W_2B_5 and WB_4. A cross-section of the boron fibres shows three regions: an outer layer of boron; a transition layer between tungsten and boron, which is tungsten boride; and a central tungsten core. Boron deposited using this process is polycrystalline, the likely structure being β-rhombohedral. The crystalline grains are of 2 nm size and the fibre is therefore generally regarded as amorphous. The boron fibre shows a 'corn on the cob' structure. Since boron reacts with typical matrix materials such as aluminium and titanium, these fibres are coated with SiC and/or B_4C, the barrier layer being vapour deposited onto boron, using, for example, a mixture of hydrogen and methyl dichlorosilane.

Due to the composite nature of the boron fibre, complex internal stresses and defects such as voids and structural discontinuities result from the presence of a core and the deposition process [51]. The average tensile strength of boron fibre is 3–4 GPa while its Young's modulus is around 390 GPa; the properties can be improved by heat treatment and/or chemical polishing, as shown in Table 18.8 [51, 52]. Boron has a density of 2.34 g cm^{-3}, about 15% less than aluminium. Boron fibre with the tungsten core has a density of 2.6 g cm^{-3} for a fibre of 100 μm diameter. Its melting point is 2040 °C. The fibres can be used up to 500 °C; the change in strength above 500 °C is large due to oxidation. The high price of boron fibre, mainly due to the high cost of tungsten substrate, has restricted its use to military aircraft and space shuttles, where it acts as a reinforcement fibre generally in aluminium-based composites. However, small quantities of this fibre are used for sports goods such as golf clubs [51]; the high modulus of boron fibre contributes predominantly

Table 18.8 Strength properties of improved large diameter boron fibres [51, 52]

Diameter (μm)	Treatment	Strength		Relative fracture energy
		Average (GPa)	Coefficient of variation (%)	
142	As-produced	3.8	10	1.0
406	As-produced	2.1	14	0.3
382	Chemical polish	4.6	4	1.4
382	Heat treatment plus polish	5.7	4	2.2

to the outstanding mechanical properties of the reinforced plastics components.

18.3.5 CERAMIC FIBRES

Technological developments in the aerospace and some other engineering industries (e.g. nuclear, metallurgical and chemical) have created very stringent demands for materials having combinations of outstanding properties such as high stiffness and strength, high temperature performance, low density, unique electrical properties and interaction with electromagnetic radiation. Ceramic fibres, which are polycrystalline refractory fibres composed of metal oxide, metal carbide, metal nitride or other mixtures, meet these requirements to a very significant extent. They are notable for their high temperature performance, and are particularly useful as reinforcement in metal and ceramic matrix composites. Ceramic reinforcement fibre structures such as silicon carbide (SiC) and aluminium oxide or alumina (Al_2O_3) are in commercial production; other ceramic fibres are either being produced on a pilot scale or are in their early stage of development. Silicon carbide retains its strength well above 650 °C, and Al_2O_3 has excellent strength retention up to about 1370 °C. Both fibres are suitable for reinforcing metal matrices in which carbon and boron fibres exhibit adverse reactivities.

There are two standard routes for manufacturing ceramic fibres – chemical vapour deposition and spinning. Chemical vapour deposition makes use of a substrate like tungsten or carbon filament. The ceramic is then vapour deposited on the heated precursor; the technique is similar to that described earlier for the manufacture of boron fibres. For spinning of ceramic fibres, in analogy with the highly successful technique of carbon fibre manufacture, the precursor polymer is synthesized with the potential for yielding fluids. It is then spun to a precursor filament using conventional techniques of fibre formation like melt-, dry- or wet-spinning or the sol-gel method. The filament is finally converted cohesively to the desired ceramic structure through controlled pyrolysis [53].

(a) Silicon carbide fibres

Silicon carbide fibres can be produced using three different routes [48, 54].

Chemical vapour deposition (CVD)

Silicon carbide monofilaments can be produced using the CVD technique on tungsten or carbon substrate filament in a tubular glass reactor in which silane and hydrogen gases are made to react at about 1300 °C to produce β-SiC vapours which deposit on the substrate.

Table 18.9 The properties of some ceramic fibres

Fibre	Density $(g\,cm^{-3})$	Modulus (GPa)	Tensile strength (GPa)	Compressive strength (GPa)	Coefficient of thermal expansion $(10^{-6}\,K^{-1})$
SiC (CVD) (Textron, USA)	3.00	400	3.45	–	5.7
Nicalon^{TM}	2.80	200	2.80	3.10	3.1
Nextel 440^{TM} (Al_2O_3, B_2O_3, SiO_2)	3.05	186	2.10	–	5.0
Al_2O_3 (Fibre FP)	3.70	350–380	1.70	6.90	6.8

Textron Speciality Materials, USA, has developed an SiC filament, whose properties are listed in Table 18.9, on a pitch-based carbon monofilament substrate of about 38 μm diameter. The process is carried out in two stages. First, approximately 1 μm thick pyrolytic graphite is deposited to render the substrate fibre smooth and enhance its electrical and thermal conductivity. In the second step, the coated substrate fibre is exposed to silicon and hydrogen gases at a peak temperature of 1300 °C which react to form β-SiC on the substrate. The final fibre has a diameter of about 140 μm.

Spinning and heat treatment

Silicon carbide multifilament tows are commercially produced, for example under the trade name Nicalon^{TM}, by melt-spinning of a polymer precursor, such as polydimethyl silane, which is previously distilled to remove the low molecular weight components to give a polymer of average molecular weight of 1500. It is melt-spun at 280 °C in nitrogen gas. The resulting filament is first heated in air to 190 °C for 30 min to crosslink the polydimethyl silane molecules by oxygen and then heat-treated at 800–1500 °C in nitrogen or vacuum to form a crystalline structure. During heat treatment, hydrogen and methane gases are released at about 700 °C and a significant amount of additional hydrogen is released at 1200 °C. This is probably due to the presence of excess carbon in the fibre, as can be seen from the following reaction.

$$\left[\begin{array}{c} CH_3 \\ | \\ \text{—}\!\!\!-\!\! Si -\!\!\!-\!\!\text{—} \\ | \\ CH_3 \end{array}\right]_n \longrightarrow n[SiC + CH_4 + H_2]$$
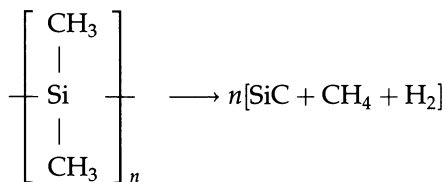
Polydimethyl silane

The amorphous to crystalline transition occurs at about 1100 °C. The crystal grain size of the fibre heat-treated at 1500 °C is about 10 nm. The fibre heat-treated at about 1250 °C has very small β-SiC crystals and has the optimum mechanical properties. The Nicalon yarn has around 500 filaments, each with an average diameter of around 10–20 µm. The properties of Nicalon fibre are shown in Table 18.9. It is worth pointing out that this fibre is not pure SiC but contains some carbon and SiO_2.

Whiskers from rice hull

Whiskers are normally obtained by vapour phase growth as short fibres with non-uniform dimensions but with extremely high strength. Silicon carbide whiskers of diameter 0.1–1 µm and length of around 50 µm are produced from rice hull which contains 10–20% SiO_2, cellulose and other organic and inorganic materials. Rice hull, which is a waste product of rice milling, is first heated in an oxygen-free atmosphere to 700–900 °C to remove the volatiles and then to 1500–1600 °C for 1 h to produce SiC whiskers. A final heat treatment at 800 °C in air removes free carbon and the resulting SiC whiskers contain 10 wt % SiO_2 and up to 10 wt % silicon nitride (Si_3N_4). The modulus of SiC whiskers is 700 GPa and their strength 13 GPa.

(b) Aluminium oxide or alumina fibres

The alumina fibre is manufactured by the spinning and heat treatment route. One method that has been used for the production of alumina fibre is to extrude an aqueous solution of aluminium oxychloride [$Al_2(OH)_5Cl$] with rheological aids being added to the solution to ensure continuous extrusion of the filament. The syrupy solution is extruded into dry air when loss of water leads to a rapid increase in viscosity. The fibre is then subjected to progressive increase in temperature to remove chlorine and organic matter and to form an anhydrous alumina phase. With some silica remaining in the fibre, fibres of diameter 3 µm containing predominantly η-alumina and a high porosity are obtained and have a modulus of 100 GPa [37].

An alternative process is the one used by Du Pont to produce fibre FP (not in production now), a high purity polycrystalline α-Al_2O_3 fibre. An aqueous slurry mix of alumina and proprietary spinning additives is first prepared and its viscosity is then carefully controlled by removing water to produce a mix suitable for dry-spinning to a fibre. The spun fibre is fired in two stages, low firing to control shrinkage and flame firing to produce a suitably dense α-Al_2O_3. The resultant fibre is then coated with a thin layer of silica of thickness 4–5 nm to heal the surface flaws and thus increase the strength; the wettability of the fibre with the matrix also

improves as a result. There are 210 filaments in the yarn, the average diameter of each filament being 20 μm. The properties of alumina fibres are given in Table 18.9; the fibre retains almost all its tensile strength after 300 h exposure in air at 1000 °C. The fibre has a high compressive strength estimated to be about 6.9 GPa.

Continuous alumina fibres have also been manufactured by Sumitomo, Japan, under the trade name Altex™ with a diameter of 8–10 μm. Staple alumina fibres are manufactured by ICI (fibre trade name Saffil™) with diameter in the 3–5 μm range. Alumina fibres may be coated with SiC for use in some metal matrix composites.

A number of other ceramic fibres have been made or developed. These include silicon nitride (Si_3N_4), boron carbide (B_4C), boron nitride (BN), fused silica (SiO_2), etc.

18.3.6 METALLIC FIBRES

Strong metal wires or filaments are useful reinforcing materials. Fine steel wire, for example, has been well-known for radial tyre reinforcement. Metallic fibres are known more for reinforcement of concrete than of soft metals or polymers [51]. Two routes are normally followed to manufacture fine metal wires or ribbons for reinforcement purposes. The first is by cold drawing; the strength develops due to cold work. This has been explained in terms of the microstructure for a carbon steel wire as follows [37]. The pearlite platelets, which are unaligned before cold drawing, undergo slip and alignment occurs parallel to the drawing direction. A cell-like structure is formed with cell wall spacing normal to the wire axis being continuously reduced with enhancement of the strength as a consequence. The second route for forming a very strong filamentary form of metal is the rapidly quenched ribbon. Wires from metallic glass of diameter as small as 0.05 μm can be made though the normal diameter range is 25–150 μm.

Fine metal wires can also be produced by drawing a hollow silica tube containing molten metal [37]; these are called Taylor wires. Metal filaments of 10 μm diameter can be produced and are strong because the rates of cooling are sufficient to induce glass formation. Metal filaments of diameter of 100 μm can also be made by extrusion of a melt, as in the case of oxide ceramics, if attention is paid to the form of the orifice and speed of extrusion [37].

The properties of some metal wires are shown in Table 18.10.

18.3.7 THE OVERALL SCENARIO

A consideration of the various high performance fibres of different types has clearly shown that there has been a phenomenal growth in this area

Table 18.10 The properties of some metallic fibres [51]

Metal wire	Density $(g\,cm^{-3})$	Modulus (GPa)	Tensile strength (GPa)	Coefficient of thermal expansion $(10^{-6}\,K^{-1})$
Stainless steel (18.8) (50–250 µm diameter)	8.0	198	1.0–1.4	18
Tungsten (<25 µm diameter)	19.3	360	5.5	4.5
Beryllium	1.85	300	1.8	11.6

since the 1970s. The modulus–strength maps for these fibres are presented in two different units in Figs 18.17(a) and (b), respectively, as they help in highlighting the advantage of polymer-based fibres over the ceramic fibres (and also metallic fibres) due to their relatively lower density as far as the specific stiffness and specific strength are concerned. However, for high temperature applications, the superiority of fibres of other types, particularly the ceramic fibres and ceramic whiskers, is unquestioned.

18.4 FIBRES FOR NON-CONVENTIONAL APPLICATIONS

18.4.1 ELECTRICALLY CONDUCTING POLYMERIC FIBRES

As a consequence of covalently bonded molecular structure, polymers are strong electrical insulators and have been widely used for applications in which insulation and low electrical loss are important considerations. For certain applications which require shielding to electromagnetic interference (moulded instrument housings) or antistatic products (floor coverings), the addition of carbon black powder or metallic (typically aluminium) fillers in the form of powder, flakes or fibres renders the polymer conductive. In this context, it is worth pointing out that for some special applications PBZT and PPTA fibres have been spun from spinning dopes containing metallophthalocyanine for making them conducting.

Considerable efforts are now being made to develop polymers with intrinsic electrical conduction characteristics which are brought about by chain unsaturation (the presence of conjugated bonds) and electron delocalization (by doping) effects. Due to high conjugation, which appears to be a prerequisite for a conducting polymer, most conducting polymers are difficult to process. A three-step method has been suggested [55], which involves the use of a soluble polymer precursor to produce fibres followed by the conversion of the fibre into conjugated polymer, which is finally doped for conductivity. However, all the precursor routes lead to
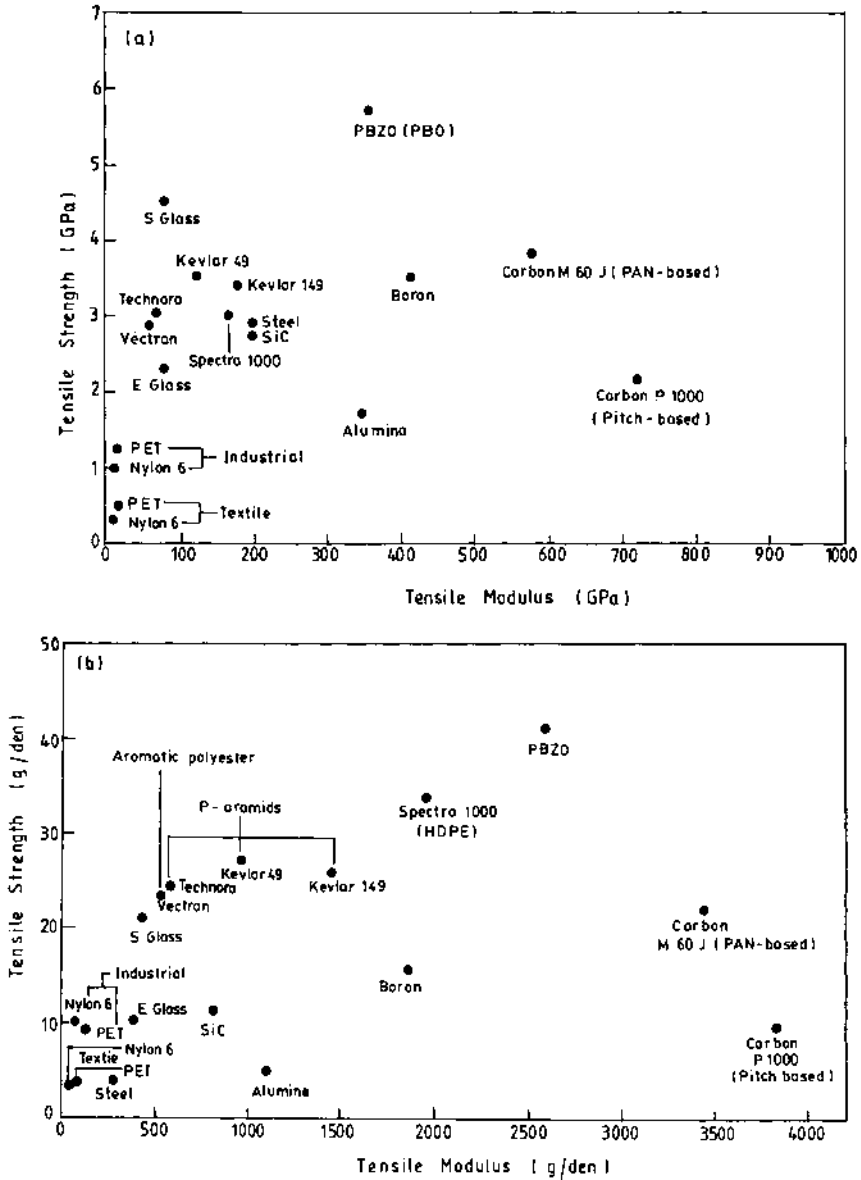
Fig. 18.17 Strength–modulus maps for a wide range of fibres in units of (a) GPa, and (b) gf den^{-1} and N tex^{-1}.

a polymer which cannot be reprocessed. Pyrolysis of PAN fibres has been shown to lead to graphitic structures which conduct electricity. Some ladder polymers produced by solution spinning have also been shown to have potential as electric conductors [56].

Predictions of superconductivity in polymers were made in the 1960s [57]; however, no such polymeric materials have been synthesized and/or processed. There is considerable activity [58] in making conducting fibres from mixtures of superconducting oxides and poly(vinyl alcohol) (PVA) using the suspension–solution spinning method. Powders of the oxides and dispersers are put into a PVA solution to make a spinning dope, which is extruded through spinnerets into a coagulation bath. The as-spun fibres are heat-treated to produce superconducting fibres which have still to reach the expected practical requirements.

18.4.2 OPTICAL FIBRES

The use of light in transmitting a telephone signal over a distance of 200 m was demonstrated by Alexander Graham Bell in 1880 almost immediately after the invention of the telephone [59]. However, this invention was not commercialized because of the non-availability of high intensity light and the low transmission efficiency of glass. High intensity light sources (lasers) became available in the 1960s and, at about the same time, research in manufacturing technology of glass fibres led to a significant increase in the transmission of light through the fibre. This led to the realization that the use of glass fibre offers considerable advantage over copper wires as a communication medium at optical frequencies. This unique property is based on the principle of total internal reflection. For smooth surfaces there is little loss of light at the repeated reflections and for some materials little absorption so that light can be transmitted over long distances with little loss in intensity.

Optical fibres are bundles of small diameter, flexible light pipes and comprise a fibre of transparent material of relatively higher refractive index coated with material of lower refractive index to achieve total internal reflection. Alternatively, optical fibres can also be made with gradually decreasing refractive index from fibre core to the fibre surface. The fibres belonging to the first category are called step index optical fibres and those belonging to the second category are called graded index optical fibres. At present, glass is the common material for optical fibre; however, some polymers are being studied for this purpose and their production and properties are described in reference [60]. Extremely sophisticated compositions of silica-based fibres with close control over the defects in them and the radial variation of composition are now produced, with a double crucible apparatus, for example [59], with diameters of around 0.1 mm in very long lengths for optical communication. The absorption loss has been substantially reduced by decreasing the low concentration of optically absorbing impurities to below one part per billion. Propagation losses of fused silica fibres are

now as small as $0.1\,\mathrm{dB\,km^{-1}}$, which is the intrinsic minimum value [37]. A bundle of optical fibres protected by a plastic jacket forms the optical cable and is fast replacing the conventional systems used for most long distance communication systems all over the world. Vapour deposition methods have been developed to produce optical fibres with very low losses. Detailed information on optical fibres appears in the literature [59–61].

18.4.3 MEDICAL APPLICATIONS

The medical applications include the use of polymeric materials in surgery in the form of fibres (suture threads, artificial skin and tendon, etc.), as biomembranes and chemical membranes with the functions of separation, condensation and purification (artificial kidney and lung), etc. [8].

Compared with natural sutures (silk, catgut, cotton), polymer fibres (PET, nylon, PP) possess greater mechanical strength, uniformity and resistance to microorganisms. Artificial skins are usually non-woven fibre products made from polysaccharides, while artificial tendons are based on PP, PET, Kevlar and carbon fibre composites.

Amongst the biological and chemical membrane fibres, while hollow fibre membranes based on cellulose and regenerated cellulose fibres are mostly used, new manufactured hollow fibres made from polysulphone and polyacrylonitrile have also been commercialized to provide adequate clearance for molecules of low hydrophilicity [8]. The use of microporous polypropylene hollow fibres and PTFE membranes for artificial lungs is another interesting development. Hollow fibres or woven tubes made from PTFE and PET are two well-known artificial blood vessels. Numerous other applications of fibrous polymeric materials as healthcare and hygiene products and detailed information on the applications described above appear in reference [62].

18.4.4 ELASTOMERIC FIBRES

Elastomeric fibres are made from natural or synthetic polymers having high elongation (300% or higher) and good recovery. Natural rubber and polyurethane are commercially used for this purpose. Natural rubber thread can be made by slitting a rubber sheet or by extruding a natural latex in filament form into an acid coagulation bath, followed by washing, drying and curing. The mechanical properties of the thread can be varied by making changes in the degree of crosslinking.

The elastomeric polyurethane fibres have been given a generic designation 'Spandex' and comprise hard and soft segments with an appropriate crosslink density. The number of polymers with this classification

is large as a number of structures exist with a urethane linkage,

$$-O-\overset{\overset{\displaystyle O}{\|}}{C}-\overset{\overset{\displaystyle H}{|}}{N}-$$
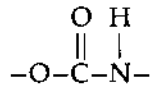
in them. They are produced typically through the reaction of a diisocyanate and a glycol:

$$HO-R-OH + OCN-R'-NCO \rightarrow \{O-R-O-\overset{\overset{\displaystyle O}{\|}}{C}-\overset{\overset{\displaystyle H}{|}}{N}-R'-\overset{\overset{\displaystyle H}{|}}{N}-\overset{\overset{\displaystyle O}{\|}}{C}\}$$
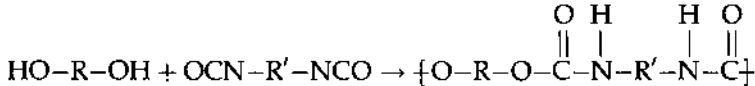
Various techniques and modifications exist to produce products with enhanced elasticity [63]. Lycra^{TM} was the first commercial polyurethane elastomer fibre marketed by Du Pont and was based on polyethylene glycol and toluene-2,4-diisocyanate [14]. Polyurethane fibres, also known as Spandex^{TM}, can be commercially produced by four processes: melt extrusion, solution dry-spinning, solution wet-spinning, and reaction spinning. The first three methods have been described in the earlier chapters. In reaction spinning, a 1000–3000 molecular weight polyester or polyether glycol reacts with a diisocyanate at a molar ratio of about 1 : 2 to produce isocyanate-terminated prepolymer. The prepolymer is extruded into a diamine bath where the diamine and the isocyanate react and a polyurethane filament is formed. A typical polyurethane filament has elongation to break of 300% in the first loading cycle, a tenacity of 0.05–0.09 N tex^{-1} and a modulus of 0.013–0.022 N tex^{-1} [14]. The finer the fibre, the higher its price. The fibres are used in swimwear, stretch fabrics, hosiery, belts, girdles, etc.

REFERENCES

1. Schiffler, D.A. (1993) In *Polyester: 50 Years of Achievement* (eds D. Brunschweiler and J.W.S. Hearle), The Textile Institute, Manchester, UK, p. 102.
2. McIntyre, J.E. (1985) In *Handbook of Fibre Science and Technology: Fibre Chemistry*, Vol. IV (eds M. Lewin and Eli M. Pearce), Marcel Dekker, New York, pp. 1–71.
3. Atlas, S.M. and Mark, H.F. (1967) In *Man-made Fibres: Science and Technology*, Vol. I (eds H.F. Mark, S.M. Atlas and E. Cernia), Wiley-Interscience, New York, pp. 1–11.
4. Ito, M., Takahashi, K. and Kanamoto, T. (1990) *Polymer*, **31**, 58.
5. Ito, M., Takahasi, K. and Kanamoto, T. (1990) *J. Appl. Polym. Sci.*, **40**, 1257.
6. Kunugi, T., Suzuki, A. and Hashimoto, M. (1981) *J. Appl. Polym. Sci.*, **26**, 1951.
7. Fakirov, S. and Evstatiev, M. (1990) *Polymer*, **31**, 431.
8. Jiang, H., Adams, W.W. and Eby, R.K. (1993) High performance polymer fibres, in *Materials Science and Technology*, Vol. 12 (ed. E.L. Thomas), VCH Publishers, Weinheim.
9. Hongu, T. and Phillips, G.O. (1990) *New Fibres*, Ellis J. Horwood, Chichester, UK.

10. Mukhopadhyay, S.K. (1993) *High Performance Fibres, Textile Progress*, Vol. 25, No. 3/4, The Textile Institute, Manchester.
11. Kumar, S. (1990) In *International Encyclopedia of Composites*, Vol. 4 (ed. S. Lee), VCH Publishers, Weinheim.
12. Bunsell, A.R. (ed.) (1988) *Fibre Reinforcements for Composite Materials*, Elsevier Science Publishers, Amsterdam.
13. Wulfhorst, B. and Busgen, A. (1989) *Chemiefasern Textilindustrie*, **39/91**, December.
14. Hughes, A.J., McIntyre, J.E., Clayton, G., Wright, P., Poynton, D.J., Atkinson, J., Morgan, P.E., Rose, L., Stevenson, P.A., Mohajer, A.A. and Ferguson, W.J. (1976) *The Production of Man-made Fibres, Textile Progress*, Vol. 8, No. 1, The Textile Institute, Manchester, UK.
15. Du Pont, British Patent 1 262 002 (USA, 15 May 1969).
16. Flory, P.J. (1956) *Proc. Roy. Soc. (Lond.)*, **A234**, 73.
17. Du Pont, British Patent 871 578 (USA, 5 February 1958).
18. Data given by Dr R.S. Irwin of Du Pont, USA, in a lecture at IIT Delhi, on 20 March 1985.
19. Blair, T.I. and Morgan, P.W. (to Du Pont), US Patent 3 673 143 (1972); US Patent 3 817 941 (1974).
20. Ward, I.M. and Cansfield, D.L.M. (1992) High performance fibres, in *Advances in Fibre Science* (ed. S.K. Mukhopadhyay), The Textile Institute, Manchester, pp. 1–24.
21. Yang, H.H. (1989) *Aromatic High Strength Fibres*, Wiley, New York.
22. Panar, M., Avakian, P., Blume, R.C., Gardner, K.H., Gierke, T.D. and Yang, H.H. (1983) *J. Polym. Sci., Polym. Phys. Ed.*, **21**, 1955.
23. Won Choe, E.W. and Kim, S.N. (1981) *Macromolecules*, **14**, 920.
24. Ward, I.M. (1985) *Adv. Polym. Sci.*, **70**, 1.
25. Lemstra, P., Kirshbaum, R., Ohta, T. and Yasuda, H. (1987) In *Developments in Oriented Polymers*, Vol. 2 (ed. I.M. Ward), Elsevier Applied Sciences, Amsterdam, p. 37.
26. Tashiro, K., Kobayashi, M. and Tadokoro, H. (1977) *Macromolecules*, **10**, 413.
27. Frank, F.C. (1970) *Proc. Roy. Soc.*, **A319**, 127.
28. Pennings, A.J. and Kiel, A.M. (1965) *Kolloid Z.*, **205**, 160.
29. Pennings, A.J., Mark, J.M.A.A. and Kiel, A.K. (1970) *Kolloid Z.*, **237**, 336.
30. Southern, J.H. and Porter, R.S. (1970) *J. Appl. Polym. Sci.*, **14**, 2305.
31. Odell, J.A., Grubb, D.T. and Keller, A. (1978) *Polymer*, **19**, 617.
32. Smith, P. and Lemstra, P.J. (1980) *J. Mater. Sci.*, **15**, 505.
33. Matsuo, H. and Ogita, T. (1991) High modulus and high strength fibres, in *Book of Papers, First Asian Textile Conference on Opportunity, Trends and Developments in Textile Industries of the Asian Region in 2000* (ed. M.L. Gulrajani), Textile Association, India, pp. 178–218.
34. Bastiaansen, C.W.M. (1990) *J. Polym. Sci., Polym. Phys. Ed.*, **28**, 1475.
35. Mackley, M.R. and Sapsford, G.S. (1982) In *Developments in Oriented Polymers – I* (ed. I.M. Ward), Applied Science Publishers, London, pp. 201–224.
36. Gupta, A.K., Paliwal, D.K. and Bajaj, P. (1991) *J. Macromol. Sci., Rev. Macromol. Chem. Phys.*, **C31(1)**, 48.
37. Kelly, A. and Macmillan, N.H. (1986) *Strong Solids*, Clarendon Press, Oxford, p. 347.
38. Moreton, R., Watt, W. and Johnson, W. (1967) *Nature*, **213**, 690.
39. Baker, A.A. (1983) *Metals Forum*, **6**, 81.

40. Zimmer, J.E. and White, J.L. (1983) In *Advances in Liquid Crystals*, Vol. 5 (ed. G. Brown), Academic Press, Inc., Orlando, Florida.
41. Donnet, J.B. and Bansal, R.C. (1990) *Carbon Fibres*, 2nd edn, Marcel Dekker, New York.
42. Perret, R. and Ruland, W. (1970) *J. Appl. Cryst.*, **3**, 525.
43. Bennett, S.C. and Johnson, D.J. (1978) In *Proceedings of the 5th International Conference on Carbon and Graphite*, Society Chem. Ind., London, p. 377.
44. Jain, M.K. and Abhiraman, A.S. (1987) *J. Mater. Sci.*, **22**, 278–300.
45. Hull, D. (1981) *An Introduction to Composite Materials*, Cambridge University Press, Cambridge.
46. Khazanov, V.E., Kolesov, Yu I. and Trofimov, N.N. (1995) Glass fibres, in *Fibre Science and Technology* (ed. V.L. Koshkov), Chapman & Hall, London, pp. 15–230.
47. Charles, R.J. (1967) The nature of glasses, in *Scientific American*, September.
48. Mallik, P.K. (1993) *Fibre-reinforced Composites: Materials, Manufacturing and Design*, 2nd edn, Marcel Dekker, New York.
49. Gordon, J.E. (1968) *The New Science of Strong Materials or Why You Don't Fall Through the Floor*, Penguin Books, Harmondsworth, UK.
50. Van Maaven, A.C., Schob, O. and Westerveld, W. (1975) *Philips Tech. Rev.*, **35**, 125.
51. Chawla, K.K. (1987) *Composite Material Science and Engineering*, Springer-Verlag.
52. Dicarlo, J.A. (1985) *J. Metals*, **37**, 44.
53. Varaprasad, D.V., Wade, B., Venkatasubramanian, N., Desai, P. and Abhiraman, A.S. (1991) *Ind. J. Fibre Textile Res.*, **16**, 73.
54. Andersson, C.H. and Warren, R. (1984) *Composites*, **15**, 16.
55. Feast, W.J. and Winter, J. (1985) *J. Chem. Soc., Chem. Commun.*, 202.
56. Wynne, K.J., Zachariades, A.E., Inabe, T. and Marks, T.J. (1985) *Polym. Commun.*, **26**, 162.
57. Little, W.A. (1964) *Phys. Rev.*, **134**(6A), A1416.
58. Goto, T. (1987) *Japanese J. Appl. Phys.*, **26**, L1527.
59. Pal, B.P. (ed.) (1992) *Fundamentals of Fibre Optics in Telecommunication and Sensor Systems*, Wiley Eastern Ltd, New Delhi.
60. Kajiwara, K. and McIntyre, J.E. (eds) (1994) *Advanced Fibre Spinning Technology*, Woodhead Publishing Ltd., Cambridge, UK, pp. 208–224.
61. Levy, A.C. and Taylor, C.R. (1988) In *Encylopedia of Polymer Science and Engineering* (eds H.F. Mark, H.M. Bikales, C.G. Overberger and G. Menges), Wiley-Interscience, New York, Vol. 7, p. 1.
62. Adanur, S. (1995) Medical textiles, in *Wellington Sears Handbook of Industrial Textiles* (ed. S. Adanur), Technomic Publishing Co. Inc., Lancaster, USA, pp. 329–355.
63. Datye, K.V. and Vaidya, A.A. (1984) *Chemical Processing of Synthetic Fibres and Blends*, John Wiley & Sons, New York.

Spunbonding and melt-blowing processes   **19**

B.C. Goswami

19.1 INTRODUCTION

The Textile Institute defines a fabric as 'a manufactured assembly of fibres and/or yarns, which has substantial area in relation to its thickness and sufficient mechanical strength to give the assembly inherent cohesion'. Fabrics are most commonly woven or knitted, but the term includes assemblies produced by lace-making, tufting, felting, netmaking and the so-called non-woven processes. The distinctive characteristics of the 'sheet material' (fabric) arise from the manner in which the fibres are arranged in the planar structure. Woven and knitted fabrics are made by interlacing and interlooping of linear assemblies of filaments and fibres; non-wovens are made by bonding of web-like arrays of fibres or filaments. The webs may be made from fibres of discrete lengths (ranging from a few millimetres to a few metres) by the carding or wet-laying process, or they may be produced by laying or blowing filaments as they are being melt-extruded. The fabrics made by these latter processes are commonly known as spunbonded or spunlaid and melt-blown non-woven fabrics.

Spunbonded fabrics may be defined generically as continuous filament fibrous structures which are made in the form of fabrics, sheets or tapes and are prepared from synthetic polymers in a process integrated with fibre manufacture. Melt-blown fabrics are fibrous structures produced by extruding a polymer melt through a die into a high velocity stream of hot air to produce fine or super fine fibres which are deposited on a moving screen after quenching.

19.2 SPUNBONDED FABRICS

19.2.1 INTRODUCTION

The earlier development of spunbonded structures dates back to the 1940s [1] and was primarily confined to Europe and North America. However, the introduction of the fabrics in the Western industrial countries and Japan dates back to the mid 1960s. Since then, a number of publications have appeared in the trade literature that describe their development, profitability, end use applications and potential growth [2–4]. The process of making spunbonded fabrics combined the production of fabrics or webs with the production of fibres (filaments), i.e. the whole sequence of operations from extrusion of basic polymer to the fabric is carried out in one single step. Hartmann [5] has discussed the factors that led to the development of spunbonded fabrics. The development and introduction of commercial spunbonded fabrics by the Du Pont company in the USA and Freudenberg in Western Europe opened the flood gates, which is evident from the number of patents filed since then. Most of the published work in the field of spunbonds is in the patent literature and it deals with the process of manufacturing spunbonds from various polymeric systems.

19.2.2 RAW MATERIALS

Due to the very nature of the process, i.e. the combining of the extrusion and the web (fibrous sheet or mat) making, it is convenient to use those fibres that can be melt- or dry-extruded (spun). This obviously does not exclude the viscose rayon filament fabrics that have been reportedly used by Courtaulds and American Enka Co., but this was done after the fibres were extruded (wet-spinning), wound on cakes and then reprocessed into webs. However, most of the polymers and consequently the spunbonded fabrics are made from polymers that can be melt-extruded. And those that are commercially processed include such fibre-forming polymers as polyamides (nylon 4, nylon 6, nylon 66, nylon 7, nylon 11), polyesters, isotactic polypropylene and polyethylene. Most of the earlier spunbonds were produced from homopolymers but lately copolymers extruded either in the side-by-side or sheath–core configurations have been used.

Nylon 66 is the most commonly used polyamide; however, nylon 6 is also finding its uses in certain spunbonded fabrics. Sometimes both polymer types are used, which enables thermal bonding to be accomplished owing to differentials in the softening and the melting points of the two polymers. There are certain advantages in using nylons; these include ease of bonding, lower rigidity and dyeability. However, the nylons are not cost-effective from the point of view of production cost as compared

with, say, polyesters or polyolefins. Nylon spunbonded fabrics do offer relatively better extensibility and resiliency characteristics.

On the other hand, poly(ethylene terephthalate) fibres, even though they have excellent characteristics like better dimensional stability and lower shrinkage at elevated use temperatures and have found uses in spunbond applications, have lagged in their popularity due to economics and some processing concerns. Polyester fibres are extruded at a relatively higher temperature and the resin has to be dry before melting and extrusion. Obviously, the spunlaid webs can be bonded thermally, but in these processes the melting point of the bonding filaments is lowered by leaving a certain amount of filaments undrawn (amorphous in nature) or extruding a copolymer along with the other filaments. In recent years, copolymers have been developed that soften and melt at much lower temperatures than fibre-grade molecular weight polymers. This may be accomplished by incorporating a small amount of isophthalic acid in place of terephthalic acid.

There are only half a dozen manufacturers of polyester spunbonded fabrics in the world and the bulk of such fabrics is made from both isotactic polypropylene and polyethylene polymers [6], of which the former accounts for by far the major share. This is governed by the cost and the ease of processing of polypropylene. Because of its low density, polypropylene yields 45% more fabric volume compared with polyester. The lowest cost, low density (lower than water), no moisture sorption and a fairly wide range of physical properties make the polypropylene spunbonded fabric useful in a variety of end uses including diaper cover stock and medical and geotechnical applications. Polyethylene and polypropylene are used extensively in sheath–core configuration to take advantage of the lower melting point of the former in thermally bonded spunbonds; the polypropylene core fibre retains its fibrous character and excellent physical properties. Even though there is only a very small window of temperature at which polypropylene will melt for bonding purposes, the fabrics made in this manner do not suffer any appreciable loss of fibre properties [7]. Polyolefin resins used for fibre- or film-forming applications are equally suitable for spunbonding applications. In spunbonding applications, extruded filaments with a variety of morphological characteristics (highly amorphous to highly oriented and crystalline form) may be used. The morphology will have a fundamental effect on the mechanical and thermal characteristics of the fabrics. The polymer may be pigmented or extruded in the unadulterated form in which case the fabrics are highly lustrous. In the case of polyolefins the almost negligible amount of waste during processing makes the use of these polymers much more attractive. Polyethylene filaments have comparatively lower tensile strength, but the lower processing temperature makes it cost-effective.

19.2.3 MANUFACTURING PROCESSES

The steps involved in the making of a spunbonded fabric are: (a) extrusion and web formation, (b) bonding to achieve cohesiveness and structural integrity, and (c) finishing. The equipment and the process of extrusion of filaments are similar to those used for making filament yarns and tows, but the subsequent processes of drawing and handling the filaments for spreading diverge from the traditional spinning processes. It is here where the spunbonding process takes over. There are other ways of combining polymer extrusion (for yarn or filament or fibrillar formation) and web formation for the sake of making planar fibrous sheet material. These are classified according to the process of manufacturing for want of any other way of categorizing them as: (1) filament to spunbond; (2) melt-blown; (3) flash spinning; (4) foam spinning; (5) fibrillated nets; (6) monofilament extrusion; (7) extruded nets; (8) tack spun; and (9) fabrics from yarns and tows. The first two processes are the well-known manufacturing techniques which will be discussed in detail in the text; the other processes are described in the published literature.

The developments in the manufacturing technologies of spunbonded or spunlaid fabrics, as they are sometimes called, have been summarized in a number of publications [8–11]. Most of the literature pertains to patents from where the material on the technologies is extracted and summarized.

Du Pont was the first company to introduce spunbonded fabrics based on the melt-extrusion of polyester trade mark fabric Reemay[TM] in 1965 [12]. Some of the early patents [13–23] on the manufacturing technologies were issued to Du Pont and Freudenberg and others. A typical spunbond line for the filament to fabric system is shown in Fig. 19.1.

Polymer melt is extruded through spinnerets in a manner similar to that used for the spinning of continuous filaments of polyester, nylon, polypropylene or polyethylene. The pressure and temperature during extrusion and metering of the polymer are also essentially similar, as are the spin packs including the filter types. However, the stainless steel spinnerets may contain few to several hundred holes of suitable diameter. The extruded bundle of filaments is quenched below the extrusion point and the solidified filaments are drawn and hauled off to be deposited onto a perforated screen. The operation beyond quenching is where the spunbonding process differs from the traditional spinning processes.

In the traditional spinning processes the threadline speed was generally limited to 1000–1500 m min^{-1}. This was decided by the design of the winding unit. However, if the drawing step is combined with the spinning part then the speed reduces even further by virtue of the draw
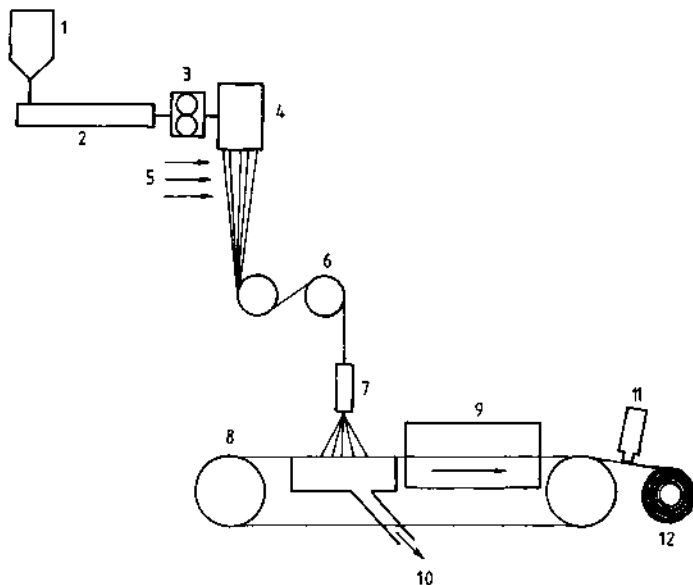
Fig. 19.1 Typical spunbonding line. Key: 1 = feed hopper; 2 = extruder; 3 = gear pump; 4 = spinneret; 5 = cooling air; 6 = draw roll; 7 = air gun; 8 = porous belt; 9 = bonding oven; 10 = vacuum exhaust; 11 = fabric inspection; 12 = wind-up.

ratio effect (draw ratio ~4.00 in most cases). Developments in the design of winders have allowed spinning speeds of up to 8000 m min^{-1} (6000–7000 m min^{-1} commercial speeds) to be successfully used. The concomitant effect of increase in threadline speed is the drawing of the filament which culminates in the development of partially oriented yarns (POY). These yarns can then be oriented in a subsequent step or drawn and textured, bulked or passed through an aspirator for making a web. The POY yarns (filaments) usually produced by this route have tenacities (especially polyester) that are approximately 60% and extensibilities that are 140% of those processed through the traditional route of drawing. Consequently, depending upon the desired economics and required fabric characteristics, any combination of processing steps may be adopted. The wide choices are reflected in the world patents filed in this particular area.

The limiting factor in the production of spunbonds by this route is not necessarily the threadline speed, but the filament handling or filament forwarding-jet device, the number of filaments per jet and the ratio of the filament forwarding speed to the speed of collecting surface – that is the web-making process. The ratio of filament forwarding speed to the speed of the collecting surface may vary anywhere from 5:1 to 15:1 and greater. It is, therefore, the filament forwarding-jet device or the haul-off gun that is the controlling element and consequently the process that has
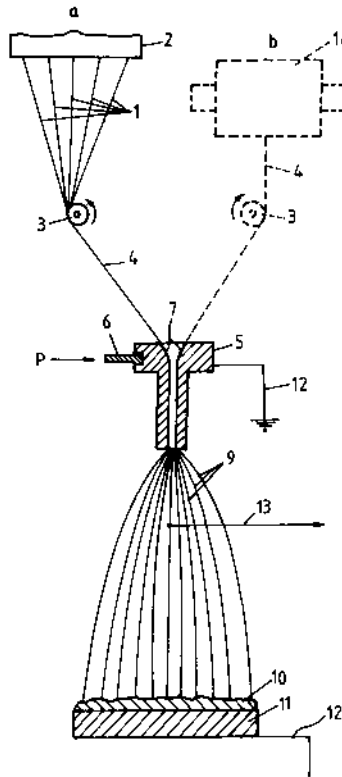
Fig. 19.2 Kinney's apparatus for hauling off (a) as-spun and (b) lagged filaments [16].

received the maximum attention in the spunbonding process. A line diagram of Kinney's [16] apparatus for hauling off freshly spun (as-spun) and lagged yarn is shown in Fig. 19.2, while Fig. 19.3 shows a cross-section of the jet assembly. Figures 19.4 and 19.5 show schematically two different arrangements for carrying out the process of charging polymer filaments that exhibit specific resistivity of below $10^{10} \, \Omega\,cm$ at 200 °C. Figure 19.5 shows the arrangement where extruded filaments from two separate spinnerets are fed into the charging and the jet assembly. The filaments from one spinneret pass through a heated drawing godets assembly while those from the other spinneret (shown dashed) are fed undrawn; the entire bundle of filaments then passes through an oscillating gun and is deposited on a porous conveyor belt. The filaments may be charged triboelectrically and simultaneously oriented with a pneumatic jet which helps to propel the charged filaments forward, or the filament bundle may be charged by a continuous corona discharge upstream from the aspiration jet. The fibre-forming polymeric materials
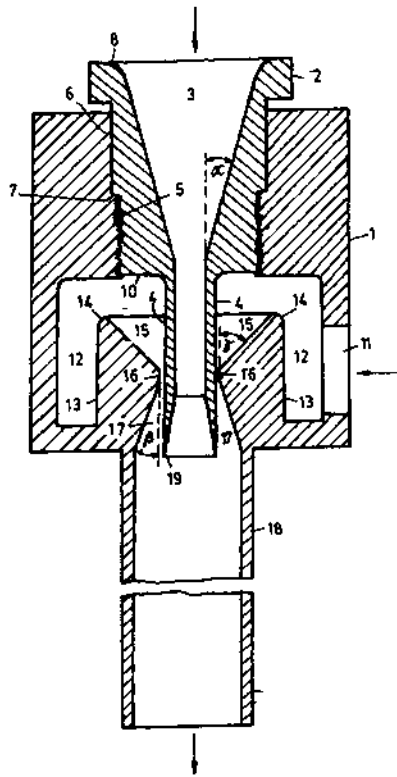
Fig. 19.3 Cross-section of a jet assembly [17].

that are capable of holding an electrostatic charge sufficient to separate filaments from each other include polyamides, polyesters, polyolefins, polyurethanes, polycarbonates and polyacetals, to name a few. Other considerations that account for the uniformity of the deposition of filaments in the web are the release of tension, induced by pneumatic jets, which permits the separation of the filaments (due to charge) and their subsequent deposition in a random manner. It is suggested that a level of electrostatic charge of more than 30 000 e.s.u. per square metre of filament surface is required ($1 \, C \, m^{-2} = 3 \times 10^{9}$ e.s.u.). In other words, it is a function of the volume of linear density of the filament. The charge level mentioned above is applicable to continuous filaments of linear density from 0.1 to 30 denier having a volume density of $0.8–1.5 \, g \, cm^{-3}$. These specifications apply to polyolefins, polyamides and poly(ethylene terephthalate) fibres.

On the other hand, in a system that utilizes oscillating multiple guns placed side by side, the deposition of the filament loops on the screen occurs in such a way that the adjacent sections overlap [17]. This ensures
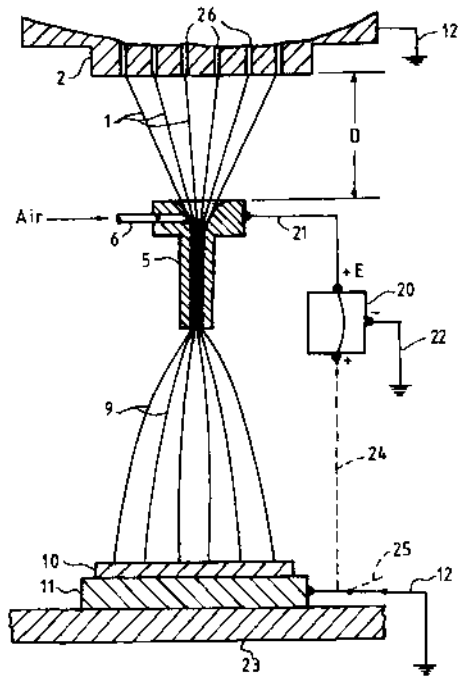
Fig. 19.4 Arrangement for charging of filaments [16].

that the swirls of one section randomly intermingle with the overlapping portion of the other and thus produce a uniform fabric. The web is held on to a moving perforated belt by a suction system as shown in Fig. 19.6. The consolidation and web disturbance after deposition on the conveyor belt are minimized. This type of arrangement is used by practically all the equipment manufacturers.

In another technique [16,24] the filaments are spontaneously bonded after they are collected on the forming belt. This is possible with webs made from certain nylons and nylon copolymers, but polymers such as polyester and polypropylene do not exhibit tackiness soon after they have solidified. In such cases the web is tacked lightly by the application of heat ($\sim$120 °C) and pressure to achieve enough cohesion for further handling and processing. In yet another technique [25] the drawn filaments are deposited on a conveyor after hitting a vibrating deflector plate which is claimed to produce a uniform web.

Figures 19.7(a) and 19.7(b) show the jet design from two different patents [16,26]. The primary function of a gun is to forward the filament bundle in the jet through a high velocity point and a low pressure zone where the air is entrained with the filaments. The filaments then move with the expanding air supply and spread into a cone shape which
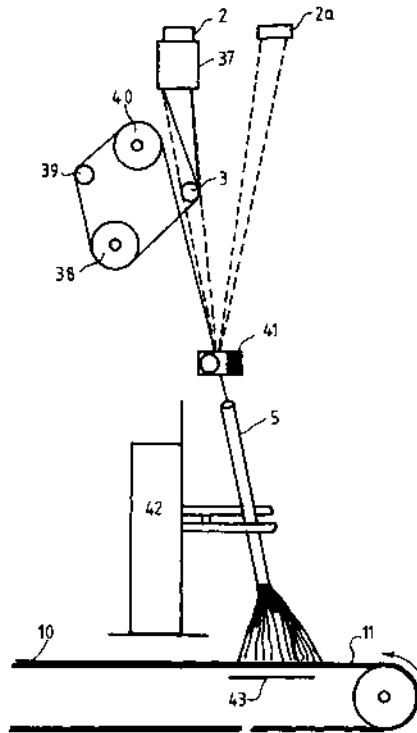
Fig. 19.5 Filaments from two separate spinnerets.

causes the filaments to separate. The amount of separation and accelera-tion will depend on the gun design. The air pressure in the gun ranges anywhere from hundreds to thousands of kilopascals and the air velocity is extremely high – many times the supersonic. The air velocity is always greater than the filament's velocity which helps to generate tension in the filament bundle as a consequence of skin friction (aero-dynamic drag). Better separation between the filaments (important for producing a uniform web) is achieved by charging the filament bundle electrostatically prior to entering the gun. The best separation of fila-ments depends on a number of gun design parameters and the supply of air. Low air supply may cause the bundle to rope up. On the other hand the gun geometry should be such that maximum productivity is achieved at maximum air pressure at a minimum consumption of air. The gun described by Brock [26] claims such performance where a sig-nificant improvement of separation of filaments is achieved without affecting the entrainment and increasing the air consumption over the existing guns. In another method [27] the air used for quenching the filaments is utilized to draw the filaments through a two-dimensional
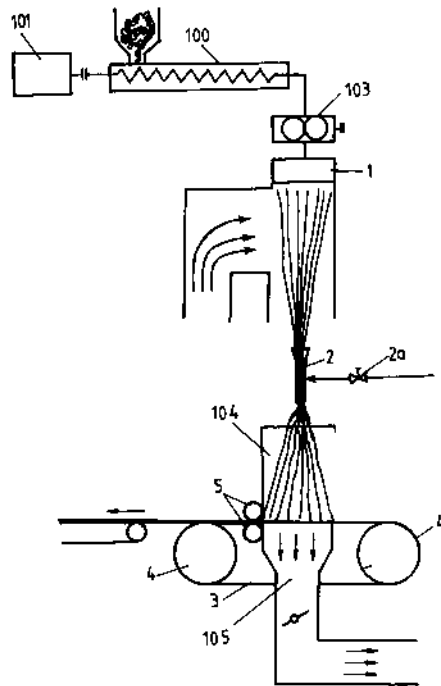
Fig. 19.6 Suction and conveyor belt assembly [17].

nozzle spanning the full width of the machine, as shown in Fig. 19.8. Because no air is inducted into the system, the quench air attains uniform acceleration into the nozzle, thus developing the drawing force (tension) without causing undue turbulence. This double use of the air makes the process more economical. The quench air is generally introduced at a temperature that may vary from 5 to 55 °C (~40–130 °F) at a rate of 17–70 m^3 min^{-1} per metre (~20–80 standard cubic feet min^{-1} per inch) of machine with nozzle opening from about 3 to 25 mm (~1/8–1 in). Suitable drawing tension is obtained with air speeds of 1.5–4 times the filament velocity; this will depend on the length and the design of the nozzle. The fineness of the filaments (length per unit weight) can be varied (increased) by changing the following parameters in the process [27]: (a) enlarging the nozzle opening, (b) reducing air flow, (c) increasing the exhaust flow rate, (d) lowering quench air temperature, (e) decreasing polymer temperature, (f) increasing the molecular weight of the polymer, and (g) increasing the polymer throughput rate per hole.

After the filaments (either bundle or sheet) exit the gun nozzle, they are collected on a moving porous belt to form a non-woven web. The filaments that are moving at a speed of 3500–8000 m min^{-1} are
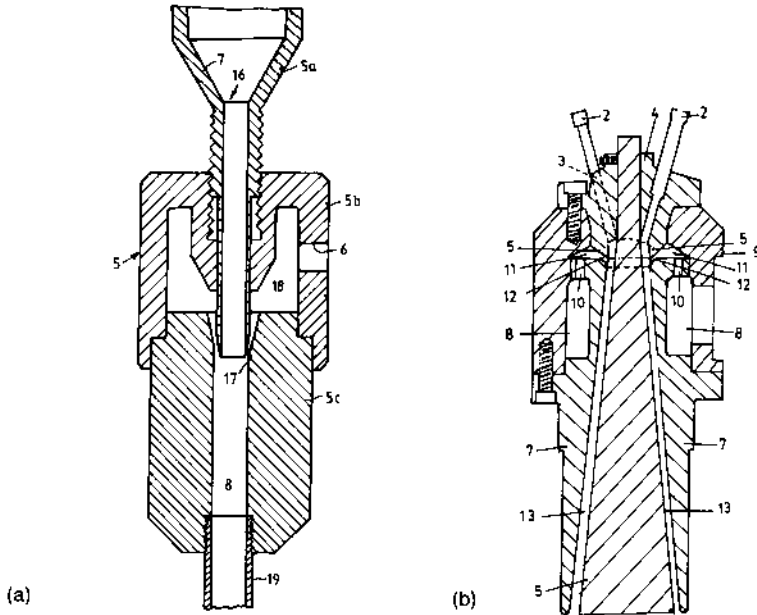
Fig. 19.7 (a) Kinney's JET [16]; (b) Jet design [26].

surrounded by air that is moving even faster. They hit the screen (conveyor belt) and are laid down in loop-like arrangement. The loop shape and the laydown arrangement will depend strongly on the manner in which the filaments impinge upon the screen and the dissipation of the air. At the exit end of the nozzle the flow becomes a free jet which may become turbulent during the process of diffusion. The velocity of the jet decreases, the tension in the filaments falls to practically zero and the local turbulent eddies displace the filaments into loops. The arrangement of the nozzle and the spraying of the filament will determine the uniformity of laydown and consequently the uniformity of web thickness and weight in the transverse direction.

The level of charge, size of jet, the air velocity and the jet-to-laydown distance have an important influence on the uniformity of laydown. The charge helps to spread uniformly that bundle of filaments after the tension on the filaments impacted by the moving air-jet has dissipated to zero. In other words, increasing the distance from the jet to the laydown and decreasing the air velocity increases the time available for the charge to spread the filaments, thus helping uniformity and preventing bunching.

A number of different arrangements of the nozzles (guns), e.g. linear or side-by-side, have been suggested in various patents. The arrangement and the manner in which the gun(s) are moved relative to the
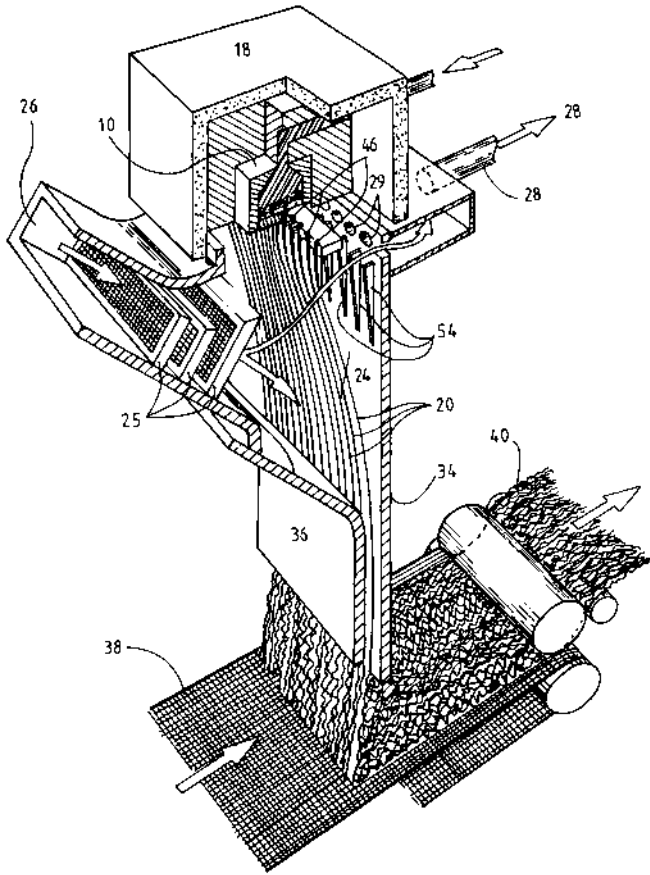
Fig. 19.8 Nozzle spanning the full width of the machine [27].

moving conveyor (porous) belt will determine the weight uniformity of the final web. Weight variation in the web, both in the long and transverse direction, may occur due to the overlapping of the laydown and at the reversal points at the edges. There are a number of possible arrangements of spray guns, gun scanning rate and the use of multiple guns; these are referred to in patents too numerous to cite. Some processes use either slowly oscillating jets and blades [16, 18] or elliptic oscillators [28], while others use multilaying systems with cross-moving directions [29]. However, it is not the geometric arrangement of the spinneret and the jets but an interactive dynamic process amongst all the processing points along the threadline that governs the arrangement (orientation) of fibres in the web. This is further compounded by the web weight being produced. Gerkin [30] analysed the arrangement of fibres in a web and came to the conclusion that with the aid of a CAD system it is

Table 19.1 Web structure variables determining spunbonded properties [31]

Filament variables
  Denier
  Tenacity
  Modulus
  Elongation
  Cross-section
  Crimp
  Micromorphology
Bonding variables
  Binder nature
  Binder concentration
  Binder distribution
  Self-bonding
Filament arrangement variables
  Fabric weight uniformity
  Filament separation
  Random vs. directional

possible to develop a filament arrangement which can help predict the properties of spunbonded fabrics.

The web made by the spunbonding process does not have integrity and lacks mechanical characteristics for further handling. Consequently, the web is bonded by the well-known methods used in the bonding of staple fibre non-wovens which include chemical or adhesive bonding, thermal bonding, needle punching, and hydroentanglement. The various bonding processes have been described in numerous texts on non-wovens. The structure and properties of spunbonded fabrics are influenced by three groups of parameters [31], as shown in Table 19.1. It is obvious that properties of the filaments play an important role in determining the physical and mechanical properties of a web. The type, nature and concentration of binder superpose their influence on the filament orientation distribution in the web. The former is easily controlled while the latter depends on the type of gun and the filament spreading and collecting process. There is not much published in the open literature on the development of fine structure in the filament during the spunbonding process and the filament orientation achieved in the web as a function of the web processing parameters that control the formation of a web. Most of the published work deals with the properties of spunbonded fabrics in terms of the type of polymer, degree and type of bonding, and with some reference to the filament orientation distribution in the web. It is extremely difficult to extract filaments from the bonded spunbonded web without causing damage to the filament.

19.2.4 DYNAMICS OF THE SPUNBONDING PROCESS

Chen *et al.* [32] were the first to attempt to relate the development in fibre structure to the process of spunbonding. They designed an experiment that simulated the spunbonding process and developed the theory of the force balance and the dynamics of spunbonding. They suggested that the dynamics are determined by the magnitude of the aspirator (air-jet) air drag and its relationship to the velocity of air blown along the fibres. The study characterized the air drag and related the orientation in the fibre to process conditions, notably the aspirator air drag. In the experimental setup a filament is allowed to hang freely (with the top end tied to a tension meter) through the aspirator. The tension is measured in the filament as a function of the length of the filament in (penetrating) the aspirator. The theoretical analysis has been carried out to reduce the problem of the dynamics of spunbonding in terms of the friction factor–Reynold's number relationship for the air drag in the aspirator. This relationship is given by:

$$C_f = 0.91(N_{Re})^{-0.61}$$

where

$$N_{Re} = \frac{dv\rho_a}{\eta_a}.$$

Here C_f is the friction factor, d is the filament diameter, v is the air velocity, ρ_a is the density of the air, η_a is the viscosity of the air and N_{Re} is the Reynold's number of the air relative to the fibre.

The tension generated in the freely hanging filament is measured as the air is passed through the aspirator, as shown in Fig. 19.9. The development of tension as a function of filament length in the aspirator at various air pressures (air velocities) is plotted in Fig. 19.10. Figure 19.11 shows the relationship between the friction factor C_f and the Reynold's number where the results of various studies are compared. All studies except that reported by Chen *et al.* [32] were carried out on taut filaments (held at both ends). Table 19.2 shows the fibre air drag correlations from various studies [32–38]. It is clear from the results that there is an extremely good correlation between this study and those reported by Anderson and Stubbs [33] and Andrews and Cansfield [34]. Chen *et al.* [32] have also reported the results of the calculations of the contributions of individual forces, i.e. F_{grav}, F_{drag} and F_{asp}, in the spinline. The filaments produced by the spunbonding process were characterized for birefringence and crystalline orientation; the data are shown in Figs 19.12 and 19.13, respectively. There is an extremely good agreement between the data for melt-spun fibres and the spunbonded fibres. In other words the orientation and morphology of fibres drawn
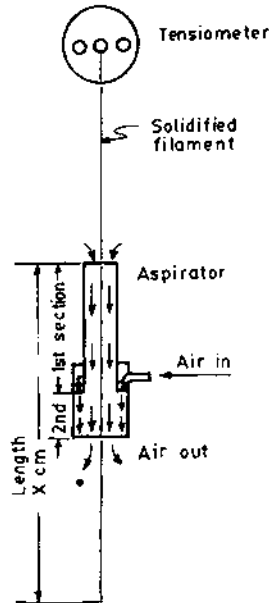
Fig. 19.9 Measurement of tension in a freely hanging filament as air is passed through the aspirator.

down during melt-spinning by applied tension and by air drag are the same.

A study reported by Hajji *et al.* [39] has discussed the results of the modelling of the commercial Reicofil™ spunbonding (developed by
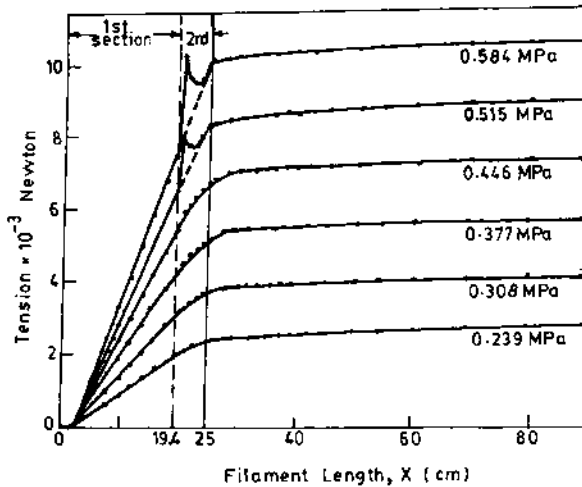
Fig. 19.10 Aspirator drag force as a function of filament length [32].

1. Andrews and Cansfield
2. Anderson and Stubb
3. Chen *et al.*
4. Selwood
5. Gould and Smith
6. Matsui
7. Hamana *et al.*
8. Sano and Orii
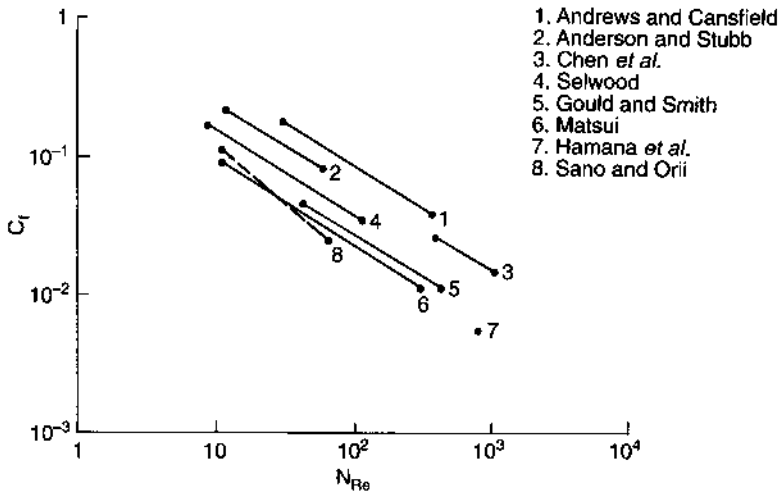
Fig. 19.11 Friction factor Reynolds number relation for air drag on filaments [32].

Reifenhauser GmbH, Troisdorf, Germany) process. The model for melt-spinning of a single filament is modified and applied to the spun-bonding process. This model includes the solution of a system of four first-order differential equations that represent (a) momentum balance, (b) energy balance, (c) rheological constitutive equations, and (d) crystallization kinetics. Hajji *et al.* found that there was a good agreement between the predicted final fibre diameter and crystallinity as obtained from the model and the experimental results obtained from the fibres extruded on the line. However, they observed that the birefringence measurements did not agree with the predicted trends, even though the

Table 19.2 Fibre air drag correlations [32]

Friction factor/ Reynolds number relationship	Investigators
$C_f = 0.9N_{Re}^{-0.61}$ [a]	Anderson and Stubbs [33]
$C_f = 1.3N_{Re}^{-0.61}$ [a]	Andrews and Cansfield [34]
$C_f = 0.58N_{Re}^{-0.61}$ [b]	Selwood [35]
$C_f = 0.68N_{Re}^{-0.8}$	Sano and Orii [36]
$C_f = 0.37N_{Re}^{-0.61}$	Hamana, Matsui and Kato [37] Matsui [65]
$C_f = 0.43N_{Re}^{-0.61}$	Gould and Smith [38]
$C_f = 0.91N_{Re}^{-0.61}$	Chen *et al.* [32]

[a] Recalculation according to Matsui [65].
[b] Recalculation according to Gould and Smith [38].
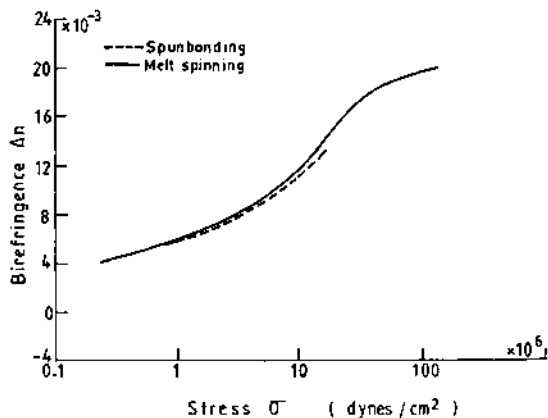
Fig. 19.12 Birefringence as a function of spinline stress [32].

predictions were roughly within the same range of the experimental data. The authors are uncertain whether the explanation for the differences lie in the model or the on-line experimental data obtained from the spunbonding process.

Other studies reported in the literature deal with the properties of fabrics made by the spunbonding process [40] and orientation of fibres in the web [41–42]. The mechanical and the physical properties of spunbond fabrics are determined by a number of fibre, web and bonding parameters and it is very difficult to compare properties reported from various sources as the structural data differ between various manufacturers.
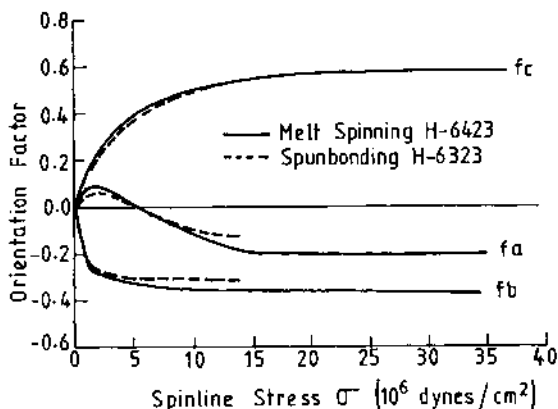
Fig. 19.13 Crystalline orientation factors as a function of spinline stress [32].

19.3 MELT-BLOWN FABRICS

19.3.1 INTRODUCTION

Melt-blown fabrics are defined by the process by which extremely fine or 'super fine' fibres are extruded and collected into a matt to form a fabric. In 1951 a research project was initiated by the Naval Research Laboratory in Washington, DC, USA, to produce very fine organic fibres. The idea behind the concept was to develop a face mask (for filtration of microorganisms and gases) for the protection of soldiers in adverse environmental conditions. Subsequently two reports [43,44] were published by the laboratory that described in detail the development of an apparatus primarily consisting of a ram-style extruder in which thermoplastic polymer is extruded through a row of orifices in a slit die. As the polymer emerged from the orifice, it was blown and attenuated by two converging hot air streams at the tip of the die, before being deposited on a collection screen. This technique demonstrated the feasibility of producing non-woven fabrics made up of 'super fine fibres' – fibres much finer than those that could be produced by the known techniques of melt-spinning. Just about the same time, Wente [45] published a paper describing the formation of 'super fine' fibres from low viscosity polymers such as linear polyamides, polystyrene and others. The melt-blowing process was further developed and commercialized by Exxon Corporation in the 1960s and 1970s. Most of the published material up until the late 1980s was primarily in the patent literature. Moore [46] has given a list of patents published on the melt-blowing technology. He cites over 400 patents that have been published in the literature on melt-blowing technology and products made from melt-blown fibres. Initially the Exxon Chemical Company in the USA held most of the patents (especially between 1971 and 1975) on the melt-blowing process which they later licensed to others involved in this field. Later the Europeans, especially the Germans and the British, and also the Japanese got into the act along with other US companies such as Kimberly Clark, which dominates the field. Some of the other companies are 3M Company (USA), Biax-Fiber Film (USA), Freudenberg Nonwovens (Germany), Asalin (France) and Toray (Japan).

19.3.2 MANUFACTURING PROCESS

The manufacturing process for the melt-blown fibres (fabrics) is shown schematically in Fig. 19.14. A typical process line includes an extruder fitted with a metering pump, a die assembly and a collecting screen followed by a winding unit. The extruder, including the screen pack for the filtration of polymer, has a design essentially similar to that
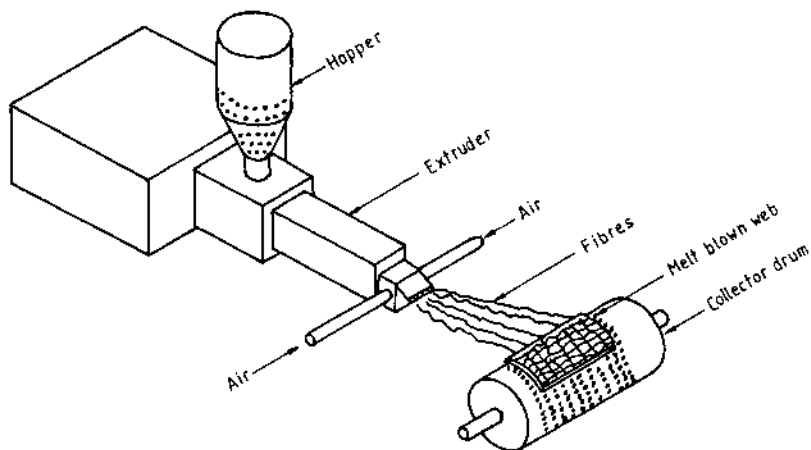
Fig. 19.14 A melt-blowing process.

used in the extrusion of films and tapes. However, the melt-blowing process uses a special die which has three distinct components, namely a polymer distribution system, a die nosepiece and an air delivery system. The melt-blowing process is generally carried out at temperatures that are normally higher than the corresponding melt-spinning or the film extrusion process. In addition, the polymer is extruded through individual holes of approximately 0.4 mm in diameter that are spaced at 8–15 holes per cm and a die that may vary from 25 to 100 cm in width. The polymer is generally extruded at a rate of $1 \text{ g min}^{-1} \text{ hole}^{-1}$. All these requirements make the distribution of the polymer and obviously the design of the die relatively more critical than that used in film extrusion. The polymer distribution which includes the flow and the dwell time across the die width are the considerations that need to be taken into account in the design of the die. There are basically two types of polymer distribution systems used in the melt-blowing process. These include the T-type (both tapered and untapered) and the coat-hanger type. Matsubara [47–50] has published a series of papers on the design of the distribution system and has provided a geometric design of a coat-hanger and a T-type die for extruding polymer films. The geometric considerations in the design of a die are critical when processing heat-sensitive resins or extruding melt-blown fibres at relatively higher temperatures than are normally employed in extrusion of such materials as polyethylene and polypropylene. The analysis given by Matsubara is an extension of the work reported by McKelvey [51]. The designs of the coat-hanger die, the modified coat-hanger die and the T-type die are shown in Figs 19.15, 19.16 and 19.17, respectively.
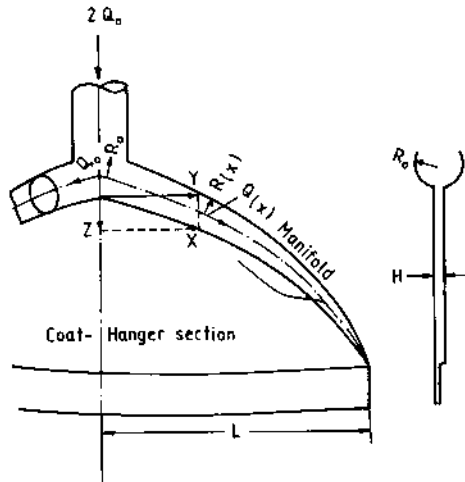
Fig. 19.15 A coat-hanger die [47].

The die nosepiece design has an extremely important influence on the uniformity of the fibres being extruded. The polymer melt passes from the feed distribution channel to the nosepiece. Because of the size of the filaments being extruded (a few μm in diameter), the tolerance in the size of the channels and the orifices needs to be extremely close. The nosepiece, which is synonymous with the spinneret in fibre spinning, consists of a hollow, wide tapered metal piece with several holes across the width of the die. The orifice or hole diameter is of the order of 0.4 mm and there are approximately 1 to 15 holes per centimetre. The holes may be drilled through a solid piece or formed into a capillary by milling and matching two flat pieces, as shown in Fig. 19.18. The air manifolds
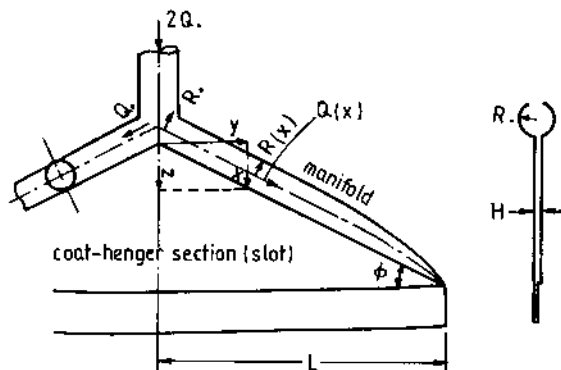
Fig. 19.16 A linearly tapered coat-hanger die [50].
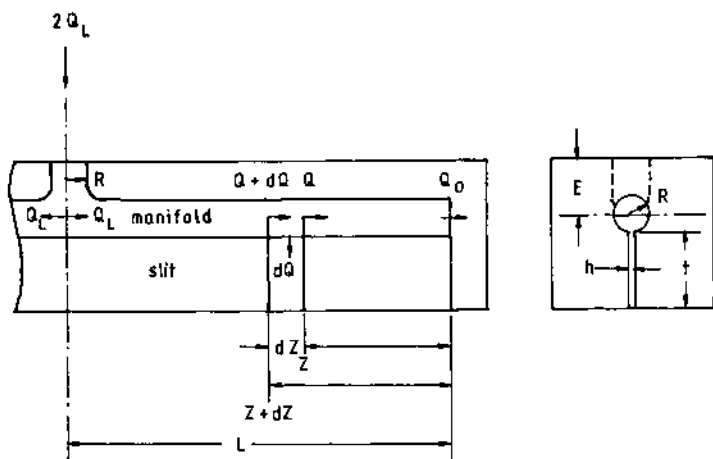
Fig. 19.17 A T-die [49].

through which the hot air is supplied are placed on the top and bottom of the nosepiece, as shown in Fig. 19.19. The air supplied by a compressor may vary in velocity from 0.5 to 0.8 times the speed of sound and the air temperature may be in the range 230–360 °C. As the polymer is
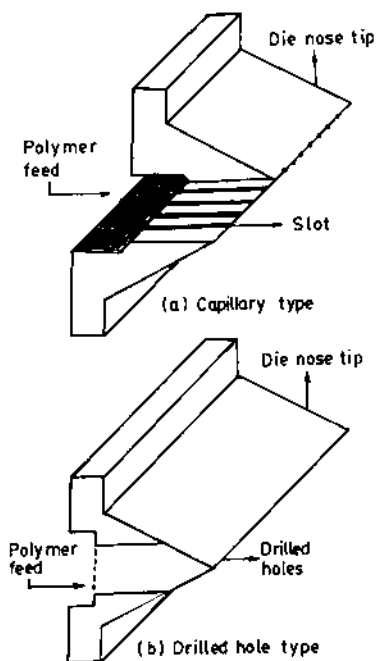
Fig. 19.18 A die nosepiece [68].
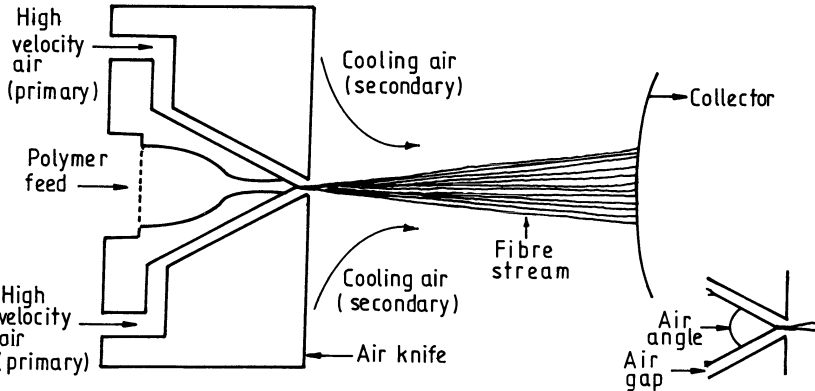
Fig. 19.19 Primary and secondary air flow and web formation [68].

extruded through the orifices (holes in the die) the hot air streams emerging from the top and bottom part of the nosepiece attenuate the extrudate. The size of the filaments obtained will depend on a number of resin and processing factors which will be discussed later. The attenuated and blown filament sheet cools down as it is being carried by the air stream away from the die and is deposited on a collector. The melt-blown fibres lie in a random orientation on the collector and the collected web can attain the form and shape of the collecting surface. This may be flat, cylindrical or any other tortuous shaped form. The web will show some bonding provided it is collected on a surface that is placed closer to the die and the polymer has a chance to cool down and solidify but the fibres are still tacky. The web flat sheet can then be wound on a suitable package for further processing.

The process, the raw material and consequently the web structure and properties have gone through a tremendous development ever since melt-blown fabrics were introduced in the early 1970s. The developments in processing have been in the die design, air throughput, air temperature, die-to-collector distance and the quenching environment. The die design includes the hole size, die set back, air gap, air angle and air flow pattern. The polymer flow rate and air temperature basically determine the fineness of the filaments produced and the entanglement (orientation) in the web. The turbulence in the air flow has a great influence on the ropiness of the bundles of filaments on the collector surface. Air angles varying from 30° to 90° have been studied; however, an angle of 60° gives a satisfactory web. Air pressure is generally in the range of 69–172 Pa (10–25 psi). The polymer viscosity has a very significant influence on the orientation and the size of the filaments obtained. Resins with melt flow rate of 1500 with very low polydispersity have been developed for this process. Earlier processes used the regular

Table 19.3 Processing parameters for producing melt-blown fabrics

	Earlier example	Current conditions
Polymer melt flow index (g/10 min)	33	450–1500
Extruder temperature (°C)	~275	~205
Die temperature (°C)	~315	~230
Air flow rate (m s^{-1})	~12[a]	~26[a]
Throughput (g min^{-1} hole^{-1})	0.5	~1.00

[a] Will depend on the gap size and air pressure.

fibre-grade resin, e.g. MFI 12–35 for polypropylene (the most commonly used polymer). Obviously, any polymer that can be spun into a fibre may be used in the melt-blowing process. Data on an earlier melt-blown fabric made from polypropylene are compared with the current resin and processing parameters in Table 19.3.

Fabric width may vary up to 5 m. The polymers that have been commercially used in the melt-blowing process include low and high density polyethylene, ethylene copolymers, polypropylene, polyamides, polyesters, polystyrene, poly-4-methylpentene-1, polymethyl methacrylates, polytetrafluoroethylene, polycarbonates, polyurethanes, silicones, pitch and blends of various resins. The factors that influence the fibre and web properties are given in Table 19.4.

Since the first published report by Wente and his co-workers, perhaps millions of square metres of melt-blown fabrics have been produced. Melt-blown fabrics have been produced from different types of polymers and have been used in a number of end use applications of which the most important are in filtration, as surgical face masks and in clean-up of oil spills. It was not until the early 1970s that systematic studies on the effects of processing parameters and resin characteristics started appearing in the literature [52–68]. Some of the important experimental and analytical studies on all aspects of the melt-blowing process are listed in Table 19.5. This is not to discount the initial work by Wente, which was quite thorough, that established the basic relationship between the process and the characteristics of fibres produced.

19.3.3 DYNAMICS OF THE MELT-BLOWING PROCESS

The ultimate aim in the melt-blowing process is to produce fibres of extremely small diameters. Air drag is the most important parameter that determines the final diameter of the fibre. The role of air drag on filaments during melt-spinning has been studied extensively and the results have been reported in numerous publications. Narasimhan and Shambaugh [56] applied the relationship reported by Matsui [65] for

Table 19.4 Polymer and process characteristics affecting web quality

Parameter	Web quality
Resin MFR	Fibre diameter
	Throughput
	Shots
	Fibre length
Air temperature	Fibre diameter
	Ropiness
Resin temperature	Fibre diameter
Resin molecular weight	Shots
	Molecular orientation
Air angle	Shots
	Fibre fineness
	Distribution
	Fibre entanglement
	Web uniformity
Air flow rate	Fibre diameter
	Filament length
	Fibre fragment (fly)
	Web bulk
	Web permeability
Quenching rate	Web tear strength
	Web softness
Collector speed	Fabric (web) weight

conventional melt-spinning speed of up to $6000\,\mathrm{m\,min^{-1}}$ to the air drag conditions under which melt filaments are attenuated. They considered speeds of up to $762\,\mathrm{m\,min^{-1}}$ and gas temperature in excess of $400\,°\mathrm{C}$. The model for determining the filament characteristics is based on the development of tension resulting due to skin friction between filament surface and moving gas. To apply the Matsui model the authors assumed that the gas velocity falls to zero at a certain distance (15 cm in this case) from the nozzle exit. Their relationship is expressed as follows:

$$C_f = 0.37 \times N_{Re}^{-0.61}$$

where C_f is the air drag coefficient, N_{Re} is the Reynolds number $(= DV\rho/\eta)$, D is the filament diameter, V is the gas velocity, ρ is the air density and η is the dynamic viscosity.

Figures 19.20 and 19.21 show the plots developed by these authors and the prediction made from Matsui's equation. The authors used a stationary ersatz metal filament mounted on a sensitive transducer to determine the stress developed when the gas is passed over the filament. The plots suggest a fair agreement between the theoretical model and the experimental results. The differences may be attributed to a number

Table 19.5 Studies of melt-blowing technology

Reference	Notes
[45] Wente (1956)	Equipment design, single fibre and fabric properties
[52] Buntin and Lohkamp (1973)	Use of multiple dies and a circular die for producing melt-blown fabrics
[53] Jones (1987)	Effect of resin melt flow rate, polydispersity, extruder temperature and throughput rate on the properties of melt-blown fabrics
[54] Eaton et al. (1987)	Effects of pigments in the melt and melt flow rate on properties of webs
[55] Wadsworth and Muschelewicz (1987)	Effect of diameter of orifice (0.2, 0.4 mm) and melt flow index on the diameter of melt-blown fibre
[56] Narasimhan and Shambaugh (1987)	Effect of air drag on the structure development in melt-blown fibres
[57] Choi (1988)	Strength of melt-blown fibres and fabrics
[58] Bodaghi (1989)	Structure–property relationship in melt-blown air- and water-quenched melt-blown fibres
[59] Malkan (1990)	Effect of MFI (300 and 1400) and polymer flow rate on structure and properties of melt-blown fibres
[60] Shambaugh (1988)	Die geometry and fibre formation and properties
[61] Mulligan and Haynes (1989)	Air drag on monofilament in the melt-blowing process
[62] Uyttendaele and Shambaugh (1990)	Dynamics of the melt-blowing process
[63] Majumdar and Shambaugh (1990)	Air drag in melt-blowing process
[64] Straeffer and Goswami (1990)	Effect of melt flow index and polydispersity on the geometric and mechanical properties of melt-blown fibres

of factors under which the melt-blowing process is carried out. Mulligan and Haynes [61] modelled their experimental setup to simulate the melt-blowing process as closely as possible (similar to that used by Chen et al. [32]) and found a good agreement between the predicted drag force and the actual tension measured on a free fluttering filament. Straeffer and Goswami [64] have reported that the models suggested by Kase and Matsuo [66], Chen et al. [32] and Andrews and Cansfield [34] all predicted similar fibre diameters but none agree with the actual diameters obtained during melt-spinning.

At an air velocity of $3000 \, m \, min^{-1}$ and polymer flow rate of $0.5 \, g \, min^{-1} \, hole^{-1}$, the smallest diameter predicted was $22 \, \mu m$ while
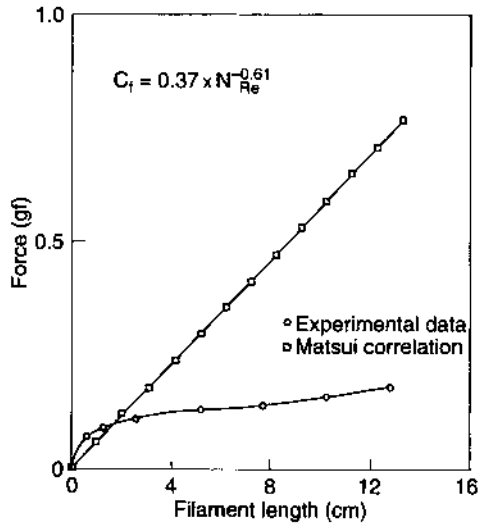
Fig. 19.20 Drag force on a filament (gas temperature, 50 °C; filament diameter, 0.13 mm; gas velocity, 268.1 m s^{-1}) [56].

actual fibre diameters were in the range 2–10 μm. The disagreement may be attributed to the fact that all the models were developed for low air velocities using solid filaments when held taut or allowing one end to flutter freely. All the models ignored viscous forces which are important
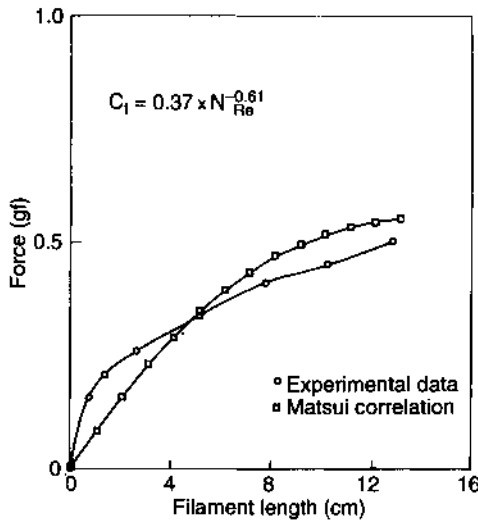
Fig. 19.21 Matsui correlation with linearly decreasing velocity (gas temperature, 385 °C; filament diameter, 0.13 mm; initial velocity, 268.1 m s^{-1}; gas velocity 0 at 15 cm distance) [56].

in the melt-blowing process where the fibre is drawn by the air immediately after leaving the die and while it is still molten. Consequently the surface characteristics of the fibres are different.

The fibres made during the melt-blowing process exhibit a wide variation in fibre size. Bodaghi [58] and Straeffer and Goswami [64] have reported studied that deal with the development of shape, morphology and the physical properties of fibres made from polypropylene resins of different melt flow index. The experimental polymers and the processing conditions used in the two studies are given in Table 19.6. Most of the

Table 19.6 Melt-blown processing conditions

(a) Polypropylene resin [64]

Condition	UHF-300	PF-011	UHF-1100
Extruder temperature (°C)	204	193	177
Die temperature (°C)	274	246	232
Air temperature (°C)	296	271	249
Melt temperature (°C)	232	210	188
Ambient temperature (°C)	27	27	27

(b) Polypropylene and polyester resins [58]

	PP (HIMONT)	PP (EXXON)	PET (3M)
BTF			
Polymer flow rate (kg h^{-1} cm^{-1})	0.089	0.089	0.178
	0.178	0.178	–
Melt temperature (°C)	205	205	300
Die temperature (°C)	260	283	300
Air temperature (°C)	260	310	316
Air pressure (Pa)	69	69	69
	206	206	–
Orifice size (cm)	0.064	0.064	0.064
Air gap (cm)	0.038	0.038	0.038
BMF			
Polymer flow rate (kg h^{-1} cm^{-1})	0.089	0.089	0.178
	0.178	0.178	–
Melt temperature (°C)	205	205	316
Die temperature (°C)	275	293	316
Air temperature (°C)	275	316	316
Air pressure (Pa)	206	206	206
	483	483	483
	618	618	618
Orifice size (cm)	0.025	0.025	0.025
Air gap (cm)	0.038	0.038	0.038

BTF = blown microfibres > 10 µm; BMF = blown microfibres < 10 µm.

Table 19.7 Degradation of the polymers upon processing, at a polymer flow rate of 0.6 g min hole^{-1} and an air pressure of 26 psi [64]

Physical property	UHF-300		PF-011		UHF-1100	
	Before	After	Before	After	Before	After
Density (g cm^{-3})	0.9017	0.8934	0.9016	0.8914	0.9012	0.8912
$\bar{M}_n$	14 900	12 500	14 100	10 600	11 300	11 300
$\bar{M}_w$	53 500	41 200	60 100	39 400	54 000	30 800
Polydispersity	3.59	3.32	4.26	3.73	4.77	2.73

studies reported in the literature deal with the processing and properties of polypropylene fibres. Haile and Meyer [67] have dealt with the processing of polyester resin on the melt-blowing system.

Because of the high temperature at which the polymers are generally extruded in the melt-blowing process, the polymers do suffer some degradation (Table 19.7). It has also been demonstrated that the polymers with higher molecular weight and lower polydispersity produce stronger fibres. Table 19.7 shows resin properties before and after processing. A typical shear stress–shear rate curve is shown in Fig. 19.22. Results reported in the literature on the degradation of polymer during melt-blowing by various groups agree with each other. There are various reasons which account for the degradation phenomenon in polypropylene resins. In addition to the high temperature, other factors that contribute to the degradation are the process of manufacture of high MFI from low MFI resin, stabilization treatments for both thermal and ultraviolet degradation, and the addition of peroxides in the resin.
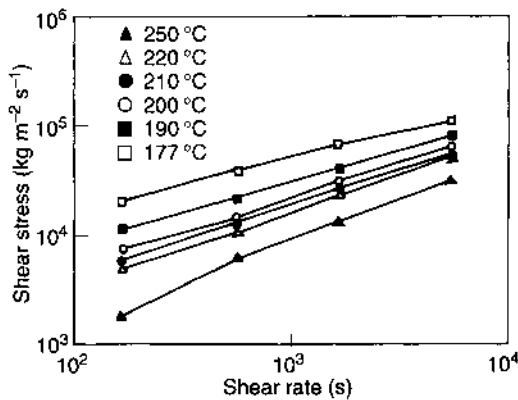
Fig. 19.22 Shear data for UHF-30 [64].

19.3.4 STRUCTURE AND MECHANICAL PROPERTIES

(a) Structure

Scanning electron micrographs of the fibres collected during melt-blowing show a variety of fibre diameters in the web. Within a sample the fibre diameters may vary from 1 to 10 μm, depending on the resin and processing conditions. All the studies indicate that the average fibre diameter decreases with increasing air velocity and polymer flow rate, but the resin MFI does not have a significant effect on fibre diameter. However, the resin flow rate and air pressure and air turbulence do cause a change in the distribution of fibre diameters. Similar fibre diameter distributions have been reported by Narasimahan and Shambaugh [56], Choi [57] and Bodaghi [58]. The fibre diameter and diameter distribution will be strongly influenced by the viscosity of the polymer at the die tip.

The processing conditions or the resin characteristics do not appear to affect the density of fibres melt-blown from polypropylene. However, DSC data reported by Bodaghi [58] and Straeffer and Goswami [64] indicate small changes in the heat of fusion and the melting point of fibres. Bodaghi has also reported wide angle and small angle X-ray data on the polypropylene resins. He suggests that conventional melt-blown fibres do not show any crystalline orientation.

The melt blown fibres exhibit a much lower level of birefringence than the corresponding melt-spun or spunbonded fibres. The only stress developed in the fibres is due to skin friction between the fibre surface

Table 19.8 Birefringence of melt-blown fibres [58]

	Air pressure (kPa)	Average fibre diameter (μm)	Average birefringence
BTF			
PP (Himont)	69	38.7	0.00024
	206	22.2	0.0095
PP (Exxon)	69	42.2	Not measured
	206	27.0	0.0087
PET (3M)	69	44.1	0.00036
BMF			
PP (Himont)	206	7.4	0.0091
	618	2.0	0.0123
PP (Exxon)	206	8.8	0.0089
	618	4.4	0.0133
PET (3M)	206	9.8	0.0095
	618	6.7	0.0162
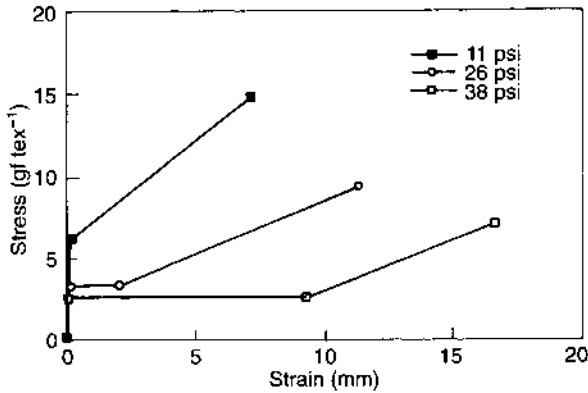
Fig. 19.23 Average stress–strain plot for UHF-300 at a polymer flow rate of 1 g min^{-1} per hole [64].

and the blowing gas. Birefringence shows an increasing trend with increasing gas flow rate and is highly influenced by the final fibre diameter. Birefringence values also show a very wide distribution (standard deviations are often larger than the Δn values). The high MFI resins generally exhibit a wider range for Δn at both low air pressure and lower flow rate. The average birefringence values of melt-blown fibres generally fall within the range of 0.005 to 0.009 for polypropylene resins as reported by Straeffer and Goswami [64]; these values agree with other studies [58]. A general comparison of birefringence values of fibres obtained from various processes is shown in Table 19.8.
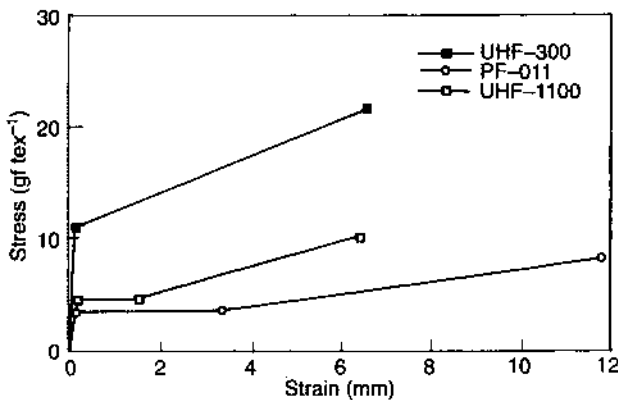
Fig. 19.24 Average stress–strain plot for a polymer flow rate of 0.6 g min^{-1} per hole and air pressure of 26 psi [64].
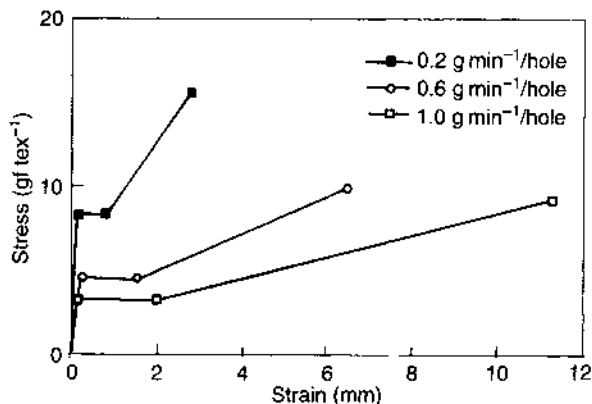
Fig. 19.25 Average stress–strain plot for UHF-300 at an air pressure of 26 psi [64].

(b) Mechanical properties

The fibres produced by the melt-blowing process are very delicate and are relatively weaker than the fibres produced by other processes, e.g. melt-spinning or spunbonding from the same resins. Figures 19.23, 19.24 and 19.25 show the stress–strain curves of typical melt-blown fibres and show the effect of air flow rate, resin MFI and resin flow rate (shear rate). The tenacity of the fibres increases with increasing air flow and decreasing polymer flow rate. This trend coincides with the effect of these processing factors on the fibre diameter. The average fibre diameter produced usually determines its average tenacity. The melt-blown fibres have tenacity which varies anywhere from 3 to $30 \, \mathrm{gf \, tex^{-1}}$; elongation varies anywhere from 150 to 1400%. A comparison of the tenacity, initial modulus, elongation and the average diameter of fibres between various processes is shown in Table 19.9.

The air flow rate significantly affects the tenacity, yield stress, initial modulus, post-yield modulus and breaking elongation; higher air velocity

Table 19.9 Comparisons of tenacity, initial modulus and breaking elongation [64]

Resin	Tenacity $(10^3 \, \mathrm{psi})$	Initial modulus $(10^4 \, \mathrm{psi})$	Elongation (%)	Average diameter (μm)
UHF-300	8.6	2.4	1400	23.2
PF-011	7.0	2.0	1400	28.7
UHF-1100	13.5	6.0	990	15.8
PP-3085	8.3	4.2	290	20 +
PP-3085 (Bodaghi)	4.0	2.8	318	20 +
Unspecified (Choi)	7.8	–	130	3.4

Table 19.10 Mechanical properties of webs made under different conditions [58]

	MD[a]			TD[b]		
	Strength $(10^7 \, dyn\,cm^{-2})$	Modulus $(10^7 \, dyn\,cm^{-2})$	Elongation (%)	Strength $(10^7 \, dyn\,cm^{-2})$	Modulus $(10^7 \, dyn\,cm^{-2})$	Elongation (%)
BTF						
PP (Exxon) $d = 8$ in, air quench	0.7	7.4	178	0.60	4.3	180
PP (Exxon) $d = 8$ in, water quench	0.59	2.2	199	0.42	1.8	190
PP (Exxon) $d = 36$ in, air quench	0.67	7.1	171	0.10	1.1	86
BMF						
PP (Himont) $d = 8$ in, water quench	1.9	55	123	0.99	40	110
PP (Himont) $d = 8$ in, water quench	0.9	35	170	0.9	34	171
PP (Exxon) $d = 8$ in, air quench	2.9	62	87	2.0	51	96

[a] MD = machine direction.
[b] TD = transverse direction.
d = die collector distance.

increases the values of all the properties except the elongation which shows a decrease. The increasing air flow rate increases the draw in the fibre, thus causing higher molecular orientation. A necking region in the stress–strain curve was more prevalent at lower air flow rates.

Melt flow index also has a significant effect on the mechanical properties of fibres. Higher MFI resins usually produce fibres with higher tenacity, higher modulus and lower elongation.

The webs made from melt-blown fibres usually show tenacity, modulus and breaking elongation values that are lower than those of the corresponding fibres, as shown in Table 19.10. Bodaghi [58] has shown that the water-quenched webs generally show lower tensile strength and initial modulus than the corresponding air-quenched webs. However, elongation to break is higher for water-quenched than for air-quenched fabrics. This is directly influenced by the degree of orientation and the fibre diameters achieved in the respective processes. Higher molecular weight resins produce fabrics with higher tensile strength, higher initial modulus and lower elongation to break than the comparable fabrics produced from lower molecular weight resins as reported by Bodaghi [58]. Eaton [54] has reported a study on the effect of pigments in the melt on the properties of melt-blown fibres made from polypropylene resins. The pigment particles in the melt act as nucleating agents, thus affecting the crystallinity and the rate of crystallization in the fibres. The effect is pronounced for higher melt flow index resins.

REFERENCES

1. Slaytor, G. and Thomas, J.H. (1940) US Patent 2 206 058.
2. Mansfield, R.G. (1977) *Textile World*, **127**, September, 81.
3. Mansfield, R.G. (1979) *Textile World*, **129**, February, 83.
4. Hartmann, L. (1974) *Textile Manufacturer*, **101**, September, 26.
5. Hartmann, L. (1973) *Melliand Textilber.*, **54**, 460.
6. Newton, A. and Ford, J.E. (1973) *Textile Prog.*, **5**(3), 1.
7. Wei, K.Y., Vigo, T.L. and Goswami, Bhuevenesh C. (1985) *J. Appl. Polym. Sci.*, 1523–1534.
8. Burnip, M.S. and Newton, A. (1970) *Textile Prog.*, **2**(3).
9. Newton, A. and Ford, J.E. (1973) *Textile Prog.*, **5**(3).
10. Purdy, A.T. (1983) *Textile Prog.*, **12**(4).
11. Goswami, B.C. (1986) *Encyclopedia of Materials Science and Engineering* (ed.-in-chief, M.B. Bever), Pergamon Press, Oxford.
12. Shealey, O.L. (1965) *Textile Res. J.*, **35**, 322.
13. Callander, M.E., US Patent 2 382 290 (1945).
14. Carl Freudenberg KG, British Patent 1 064 847 (18 November 1963).
15. Guandique, E. and Katz, N., US Patent 2 810 426 (1957).
16. Kinney, G.A. (to Du Pont), US Patent, 3 338 992 (29 August 1967).
17. Osker Dorschner *et al.* (to Messalgesellschaft AG, Frankfurt, Germany), US Patent 3 692 618 (9 October 1972).

18. Carl Freudenberg, US Patent 3 565 729 (Germany, 3 February 1962).
19. Farbenfabriken Bayer A.G., British Patent 1 215 679 (Germany, 22 June 1968).
20. Monsanto Co., British Patent 1 219 921 (USA, 27 January 1967).
21. Allied Chemical Corpn., US Patent 3 734 803 (28 September 1971).
22. I.C.I. Ltd, US Patent 3 708 365 (UK, 17 February 1967).
23. Celanese Corpn., US Patent 3 689 324 (8 December 1970).
24. Hartman, L. (1974) *Textile Manufacturer*, **101**, 26.
25. Pierre Porte (to Rhone-Poulenc Textiles, Paris, France), US Patent 3 923 587 (2 December 1975).
26. James Brock (to Imperial Chemical Industries Ltd, London, England), British Patent 1 436 545 (19 May 1976).
27. David, W. and Mormon, M.T., US Patent 4 405 297 (20 September 1983).
28. Du Pont Co., US Patent 3 293 718 (1 July 1963).
29. Hartman, L., US Patent 3 554 854 (7 February 1969).
30. Gerkin, L. (1987) *Man-made Fiber Yearbook*, Chemifasern Textilindustrie.
31. Ericson, C.W. and Baxter, J.F. (1973) *Textile Res. J.*, **43**, 371–378.
32. Chen, C.H., White, J.L., Spruiell, J.E. and Goswami, B.C. (1983) *Textile Res. J.*, **53**, 44–51
33. Anderson, S.L. and Stubbs, R. (1958) *J. Textile Inst.*, **49**, T53–T57.
34. Andrews, E.H. and Cansfield, D.L.M. (1963) cited by A.B. Thompson in *Fiber Structure* (eds J.W.S. Hearle and R.H. Peters), Textile Institute, Butterworth, Manchester.
35. Selwood, A. (1962) *J. Textile Inst.*, **53**, T576.
36. Sano, Y. and Orii, K. (1968) *Sen-i-Gakkaishi*, **29**, 212–218.
37. Hamana, I., Matsui, M. and Kato, S. (1969) *Melliand Textilber.*, **4**, 382–388.
38. Gould, J. and Smith, F.S. (1980) *J. Textile Inst.*, **71**, 38–49.
39. Hajji, N., Spruiell, J.E., Lu, F.M., Malkan, S. and Richardson, G.C. (1992) *J. Nonwoven Res.*, **4**, 16.
40. Shealy, O.L. and Hentschel, R.A.A. (1968) *Textile Res. J.*, **38**, 7–15.
41. Gerking, L. (1987) *Man-man Fiber Yearbook*, Chemifasern Textilindustrie.
42. Mehrotra, S. (1989) *The effect of web formation parameters on the orientation distribution of fibers in spunbonded fabrics*, Thesis Clemson University, Clemson, South Carolina, USA.
43. Report Number 4364, *Manufacture of superfine organic fibers*, Naval Research Laboratory, 15 April 1954.
44. Report Number 5265, *An improved device for the formation of super-fine organic fibers*, Naval Research Laboratory, 11 February 1959.
45. Wente, V.A. (1956) *Ind. Eng. Chem.*, **48**(8), 1342–1346.
46. Moore, G.K. (1989) *Meltblown Technology Today*, Miller Freeman Publications, San Francisco, pp. 150–158.
47. Mastubara, Y. (1979) *Polym. Eng. Sci.*, **19**(3), 169–172.
48. Mastubara, Y. (1980) *Polym. Eng. Sci.*, **20**(3), 212–214.
49. Mastubara, Y. (1980) *Polym. Eng. Sci.*, **20**(11), 716–719.
50. Mastubara, Y. (1983) *Polym. Eng. Sci.*, **23**(1), 17–19.
51. McKelvey, J.M. (1962) *Polymer Processing*, John Wiley, New York.
52. Buntin, R.R. and Lohkamp, D.T. (1973) Melt-blowing – a one-step web process for new nonwoven production, *TAPPI*, **56**(4), 74–77.
53. Jones, A.M. (1987) Proceedings of the 4th International Conference on Polypropylene Fibres and Textiles, 23–25 September, Nottingham, UK, pp. 47.1–47.10.

54. Eaton, G.M., Wadsworth, L.C., Cheng, C.Y. and Bennett, D.S. (1987) Proceedings of the INDA-TEC Conference, 18–21 May, Hilton Head, SC, USA, pp. 221–231.

55. Wadsworth, L.C. and Muschelewicz, A.O. (1987) Proceedings of the 4th International Conference on Polypropylene Fibres and Textiles, 23–25 September, Nottingham, UK, pp. 47.11–47.20.

56. Narasimhan, K.M. and Shambaugh, R.L. (1987) *The process of melt blowing*, Proceedings of the INDA-TEC Conference, 18–21 May, Hilton Head, SC, USA, pp. 189–205.

57. Choi, K.J. (1988) *Polym. Eng. Sci.*, **28**(2), 81–89.

58. Bodaghi, H. (1989) *Melt blown microfiber characterization*, Proceedings of the INDA-TEC Conference, 30 May–2 June, Philadelphia, PA, USA, pp. 535–571; INDA (1989) *J. Nonwoven Res.*, **1**, 1.

59. Malkan, S.R. (1990) *Process–structure–property relationships in melt blowing of different molecular weight polypropylene resins*, PhD Dissertation, The University of Tennessee, Knoxville.

60. Shambaugh, R.L. (1988) *Ind. Eng. Chem. Res.*, **27**(12), 2363–2372.

61. Mulligan, M.W. and Haynes, B. (1990) *Am. Soc. Mech. Eng.*, **54**, 47–50.

62. Uyttendaele, M.A. and Shambaugh, R.L. (1990) *Am. Inst. Chem. Eng.*, **36**(2), 175–186.

63. Majumdar, B. and Shambaugh, R.L. (1990) *J. Rheol.*, **34**(4), 591–601.

64. Straeffer, G. and Goswami, B.C. (1990) Proceedings of the INDA-TEC Conference, 5–8 June, Baltimore, MD, USA, pp. 385–419.

65. Matsui, M. (1976) *Trans. Soc. Rheol.*, **26**, 465–473.

66. Kase, S. and Matsuo, T. (1965) *J. Polym. Sci.*, **A3**, 2541–2559.

67. Haile, W.A. and Meyer, M.F. (1987) New developments in polyester melt-blown fabrics, Proceedings of the INDA-TEC Conference, 18–21 May, Hilton Head, SC, USA, p. 238.

68. Malkan, S.R. and Wadsworth, L.C. (1991) *Int. Nonwovens Bull.*, No. 3.

Reuse of polymer and fibre waste

20

P. Bajaj and N.D. Sharma

20.1 INTRODUCTION

During the production of fibres, a certain amount of waste is generated in pre- and post-spinning operations. Since almost all synthetic fibres are non-biodegradable, their disposal poses serious problems. Recycling of thermoplastics (polymers and fibres) has therefore become a subject of vital importance, keeping in view the long-term environmental effects of waste disposal. The current concern regarding the disposal of industrial and post-consumer waste in diminishing landfill sites and the general impact of wastage on the environment have focused attention on developing effective reclamation and recycling policies. More and more fibre producers are therefore establishing corporate recycling policies for various polymers and fibre wastes created during manufacturing or post-consumer waste [1–18]. In this chapter, various aspects relating to the reuse of PET, nylon 6, nylon 66, polypropylene and acrylic fibre waste will be considered.

Recycling is the most viable approach to reduce the solid waste. The main objective of textile recycling efforts is to reprocess the by-products of textile and fibre industries back into the original stream or into useful end products [19]. Putting the waste back into the original system in the form of monomers has the greatest economic value. Thermoplastic waste could be diverted to less critical end uses such as fibrefill, melt-blown products or spunbonded products. Injection moulding is also another possibility for the textile waste.

Table 20.1 Commercial products from fibre and polymer waste [20]

Manufacturer	Nature of the waste used	Product developed	End use
Wellman Inc. (USA and Europe)	Fibre waste, post-consumer PET soft drink bottles, PET film, and plant scrap	Fortel Ecospun	Fibre fill, fleece, carpet, T-shirts, shoe-laces, knitwear, home furnishings
Hoechst Celanese Corp.	Post-industrial and post-consumer PET wastes	Trevira-II	Sleeping bags, insulated apparel
Malden Mills Ind.	PET waste	Polartec recycled series	Skiwear fabrics
Roffe, Inc.	Plastics waste	Ecotherm (recycled 30%; virgin 70%)	Insulation materials
Roffe, Inc.	Post-consumer plastics waste	Ecostate 4 and 6	Jacket liners, lightweight outer layers
Roffe, Inc.	Post-consumer PET waste	Ecotec-200	Dense soft double side fleece
Dyersburg Fabrics, Patagonia	PET waste	Dyers port-Eco, PET filament (30%) plus Ecospun fibre (70%)	Fleece used in outerwear
Deja, Inc.	Trim waste, paper bags, plastic bottles	Ecosneakers and Envirolites	Footwear for casual wear
Hills, Inc.	PET waste, beverage bottles rejected preforms or mouldings	–	Carpet face fibres
Image Industries, Inc.	Baled post-consumer bottles, post-industrial waste pregranulated and flakes	–	Carpet manufacture
Du Pont, Virginia	Milk and water jugs	Tyvek 25% (post-consumer recycled HDPE)	Protective garments and envelopes
Pure Tech. Intern, Inc., NY, licensed its technology to Taiwan Recycling Corpn.	Plastics, PET bottles, PVC labels and bottles, PP caps, HDPE milk and water bottles	RPETcMF, RPETgMF, RETgMF and RHDPEb	Fibre application
FARE S.p.a., Italy	PET waste and polypropylene materials	–	Staple fibres

Table 20.1 Continued

Manufacturer	Nature of the waste used	Product developed	End use
Tex America, Inc.	Polyester waste	–	Fibres for carpets and non-wovens
Zimmer AG	Recycling nylon carpet	–	Nylon 6 for engineering plastics
Napcar, USA	PET bottles	–	Fibrefil for skiwear, sleeping bags, and carpets
Bartex Corpn.	Thermoplastic waste – except PVC	–	Pellets
Fleissner GmbH and Co.	PET bottles	–	Finished carpets with better dyeability

The key objective for any recycling system used by the fibre producers is the conversion of the normally low bulk density wastes into high bulk density, free flowing granules. There are two methods [8] for converting the fibre waste into high bulk density: agglomeration (densification) and re-extrusion. During the conversion process, it is necessary to exert as little stress on the polymeric materials as possible to prevent any change in the material properties.

The world's most recyclable polymer is polyester. Some of the products in which recycled polyester (polyethylene terephthalate) is used are: fibres, films, strapping, foams, sheeting, food and non-food contact bottles by direct extrusion [8]. Hoechst Celanese [9], the major producer of polyester products, is now concentrating on manufacturing processes which minimize the generation of solid waste as well as reclamation, recycling or disposal of such materials by environmentally appropriate means.

Wellman, Inc. [12] is another major producer of polyester staple and partially oriented yarn products. This company is also the largest plastics recycler. Wellman utilizes the recycled PET bottles and other wastes to manufacture polyester fibres, which are used in making pillows, furniture cushions, carpets and rugs. The success story of Image industries [11] also lies in its sourcing of raw materials derived from baled bottles, granulated flakes, and post-industrial waste. It is claimed that in 1994, over 500 million plastic containers were converted into over 45 million pounds of polyester fibre for carpets and home furnishings. A list of the major companies using polymer and fibre waste for the production of various products is given in Table 20.1 [20].

Depending on the source and morphology of the polymer and fibre waste, recycling is generally done so that the waste is converted into a polymer or as monomers which can be reused in the same plant for fibre production or in the production of value-added products like resins, adhesives, thickeners, etc. Various processes and technologies adopted for recycling and reuse of thermoplastics (polymers and fibres) are discussed in this chapter.

20.2 UTILIZATION OF PET WASTE

In the manufacture of polyethylene terephthalate (PET), polybutylene terephthalate (PBT) and copolymers of PET, a significant amount of waste is generated. The polyester waste from the fibre and textile industry consists of chips, continuous filaments, staple fibres and polymeric lumps. The waste is usually contaminated with dyes, finishes, knitting oils and other fibres such as cotton, wool, rayon, nylon and acrylic. The waste may also be contaminated with paper (labels), metal and pigments, which are present because of the mixing of waste with moulded articles. At times polyester waste is also contaminated with polyester films, magnetic recording tapes, graphic art materials and electrical insulation. In some of the applications, polyester fibre is coated with binders, adhesives, other polymeric materials and metal compounds. The selection of a suitable process thus depends upon the quality of the waste, degree of chemical/mechanical damage, economy of the process used, and mode of disposal of secondary waste. Michels [3] reviewed the production of secondary products from PET waste and their utilization. Petrov *et al.* [21–23] have reported the various processes for the recovery of monomers from polyester waste. Wagner [4] has discussed the re-extrusion process while Liedner [2] has reported the recovery of economic value of plastic waste involving reinforced thermoplastic polyesters and their end uses. Sharma and co-workers [24, 25] have documented the recovery of DMT and the process of glycolysis using PET waste. Recovery of PET from the waste in different forms, i.e. as granulates, powder, fibre or as monomer, is described below.

20.2.1 RECOVERY AS POLYMER

Spinnable polymer can be recovered from the low-damaged, clean filaments or fibre waste, either by re-extrusion followed by granulation or by dissolution in a suitable non-depolymerizing solvent and precipitating out the polymer in the powder form. Tamazina *et al.* [26] have shown that the physico-chemical properties of the fibre obtained by repeated extrusion and spinning are satisfactory up to three recyclings. However, during the extrusion–melting of the fibrous waste, the
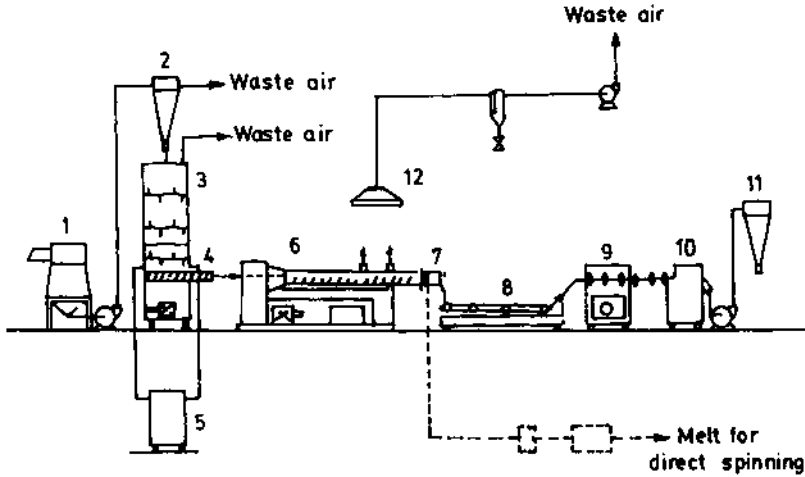
Fig. 20.1 Syntex process. Key: 1 = cutting mill; 2 = cyclone separator; 3 = feeding silo; 4 = force feeder; 5 = hot air system; 6 = extruder; 7 = filtering system and die; 8 = cooling tank; 9 = drying tower; 10 = granulator; 11 = cyclone; 12 = fume removal [4, 11, 20].

polymer undergoes significant thermal, thermo-oxidative and mechanical degradation as a result of uneven heat transfer due to the high heat insulation property of the fibrous mass. By heating the fibrous waste below its melting point in an inert medium, the drop in molecular weight which occurs during re-extrusion can be compensated [27]. A schematic diagram of the re-extrusion process developed by Syntex Chemie GmbH [11] is shown in Fig. 20.1.

The fibre waste is cut to a standard size and continuously delivered to a forced feed which also acts as a drying unit. By optimum drying of the waste prior to re-extrusion, hydrolytic degradation is reduced. The extruder is equipped with one or two degassing zones to remove low-boiling impurities and part of the finish oils present on the surface of waste. The molten, degassed, and homogeneous filtered mass is cast as a sheet, cooled in a water bath, and granulated. These granules may be blended with virgin granules to produce staple fibres. The granulation process can be bypassed by feeding the melt from the extruder directly to a spinning system. Alternatively, the compressed fibre waste is introduced into a twin screw extruder and the molten material thus obtained is subjected to reduced pressure at 260–290 °C to produce polyester with an improved degree of polymerization [28,29]. This process gives polyester which can be spun into fibres used for non-wovens and fibrefill applications. Such products are comparable to those produced from virgin polymer.

(a) Recovery as moulding-grade polymer

Polyester bottles and scrap need purification and/or separation from their contaminants before they can be melt-granulated. The apparatus which carries out this scrap recovery comprises a hammer mill for breaking the scrap articles into chips and a combination of separator and sorter for separating contaminants from the chips and for sorting out the different materials. The chips are electrostatically charged and heated by radiofrequency, causing them to become differentially heated according to their dielectric constants. The separation is a result of differential loss of electrostatic charges impressed upon the different types of materials. The electrostatically charged particles adhere to the conducting conveyor belt. When the particles are heated by the radiofrequency field, they lose the charge at different rates and lose their adherence to the conveyor belt, falling off successively according to their intrinsic dielectric characteristics [30]. The purified polyester chips are melted and granulated. Such granules are suitable for processing into non-food contact products [31]. In the case of films, the surface coating is removed before the scrap is melted for granulation. Small pieces of polyester films are treated with sodium hydroxide solution [32]. Aqueous monoethanolamine solution (2–15%) is also effective at 100–170 °C in removing the coatings on the film [33]. Non-aqueous alkaline solutions have been used to clean magnetic recording tapes [34]. Thus, a treatment with ethylene glycol containing 0.1% sodium hydroxide at 150 °C for 15 min, followed by washing with dichloromethane, gives a polyester film free from coatings.

(b) Recovery as powder by dissolution

Spinnable polymer from polyester waste is obtained by dissolving the waste in a suitable solvent and then precipitating the polymer. The solvent selected for this purpose should satisfy two requirements: (1) the polymer should not undergo depolymerization in the solvent, and (2) the polymer must be rapidly and efficiently recovered from the solution. Polyester waste and scrap can be dissolved in hot polar solvents, and the solution then cooled at a constant rate to precipitate polyester particles of desired size which are recovered by filtration [35]. It is also possible to recover polyester in powder or flocculate form by shock quenching the polyester waste solution [36]. The solvents used for the dissolution are listed in Table 20.2.

Solvents having carbocyclic rings are suitable for dissolving polyester, for example biphenyl, biphenyl ether, naphthalene, acenaphthene, phenanthrene, etc. These solvents dissolve polyester at 160–240 °C in a concentration of 10–40% by weight of the polymer in solution. The polymer precipitates as amorphous gel or paste when the polymer solution is

Table 20.2 Solvents for polyester waste

Chemical class	Typical solvents
Aromatic ether	Anisole, dibenzyl ether, diphenylether
Aromatic alcohol	Benzyl alcohol
Ester	Dibutyl phthalate, bis(2-ethyhexyl)-phthalate
Ketone	Acetophenone
Sulphide	Dibutyl sulphide, diisoamyl sulphide, diphenyl sulphide, dihexyl sulphide
Sulphoxide	Dimethyl sulphoxide, diethyl sulphoxide, tetramethylene sulphoxide
Piperidone	N-Formyl piperidone
Lactam	2-Pyrrolidone, N-methyl-2-pyrrolidone, N-butyl-2-pyrrolidone
Lactone	γ-Butyrolactone
Pyrrole	N-Benzyl pyrrole, N-butyl pyrrole, 2,4-dimethyl pyrrole
Amide	N,N-Dimethylformamide, N-methylformamide, N,N-dimethyl acetamide
Nitroaryl	Nitrobenzene, 1-methoxy-2-nitrobenzene

gradually cooled to about 100 °C. Shock quenching is accomplished by the addition of a liquid quenching medium which is preferably miscible with the solvent. Such a medium keeps the solvent in liquid form even below its freezing point. Alternatively, the polyester solution can be wet-spun or dry-spun into an inert gaseous quenching medium (N_2, CO_2, etc.) and the residual solvent in the polymer can be removed by extraction with a suitable solvent. The preferred quenching media for the polyester solution in naphthalene include dimethyl formamide, acetone, dichloromethane, 1,1,1-trichloroethane, 2-butanone, dimethyl acetamide, benzene, toluene, xylene, ethanol and methanol.

A flow diagram of a typical process for recovering polyester powder from scrap containing contaminants such as dyestuffs, finish oils and tints is shown in Fig. 20.2 [37]. The scrap is treated with naphthalene at 165 °C to remove finish oil and most of the dye present on the scrap. The moisture present in the scrap is also evaporated. The dirty naphthalene is removed and the clean waste is dissolved in fresh pure naphthalene at 190–210 °C. The hot polyester solution is filtered and mixed with the quenching medium, when the polyester powder precipitates. Although the dissolution procedure provides polyester in powder form, it uses expensive, toxic and hazardous chemicals and requires a lot of equipment to process the waste and recover the solvents. This process is therefore only feasible when operated continuously on a large scale.

20.2.2 MANUFACTURE OF CARPET FIBRES

A recycling process that is becoming very popular is based on the use of PET bottles to manufacture high quality carpet fibres. The Fleissner
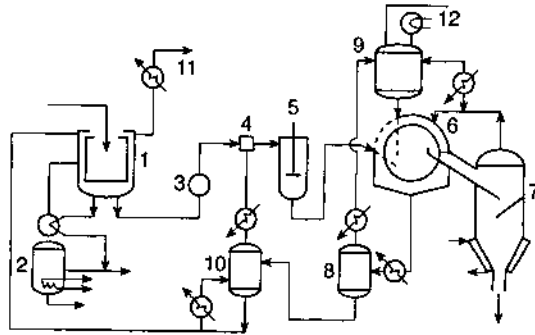
Fig. 20.2 Recovery of polyester in powder form. Key: 1 = washer–dissolver; 2 = purification column; 3 = filter; 4 = nozzle; 5 = slurry tank; 6 = centrifuge bin; 7 = drying bin; 8 = dichloromethane recovery column; 9 = dichloromethane tank; 10 = dichloromethane column; 11 and 12 = condensers [37].

Company of Germany has designed a fibre draw line which is installed behind a spinning system manufactured by M/s Automatik. The unit operates at 100% capacity and cleaned soft drink bottle waste is used to produce carpet fibres. The plant produces 70 t day^{-1} of the carpet fibre through 32 spinning positions having rectangular-type spinnerets. The spun tow is drawn in a single step and passes through a steam duct. The temperature in the fibre line is precisely controlled to get a uniform product. The best parameters for the fibre line are achieved by experience depending upon the quality of the waste. The equipment is versatile; it can produce staple fibres of 6–20 denier.

The uniformity in the tow and precise stacking unit are essential for good crimp rigidity. Higher numbers of crimps are observed in the thick portion of the drawn fibre. A crimper with 350 mm working width is used with the well-known stuffer box principle to provide two-dimensional crimping. The crimped tow is heat-set just after crimping to ensure good rigidity and resilience. The optimum utilization of process parameters provides the carpet fibres with the same physico-mechanical properties as those obtained with the virgin PET polymer. The tow is cut to staple fibres, and spun into yarn. The finished carpets show better dyeing properties than those of the carpets produced from virgin PET staple fibres. Compact and large units are producing large volumes of carpet fibres by this process and the process of mass coloration is being practised by some of the producers to produce coloured fibre. This product is used in the automobile sector where light fastness and UV stability of coloured material are of high importance.

A polyester recycling system with enhanced efficiency has been developed by Erema North America Inc. of the USA. The Erema model RGA-80 extrusion system (Fig. 20.3) reprocesses clean polyester scrap
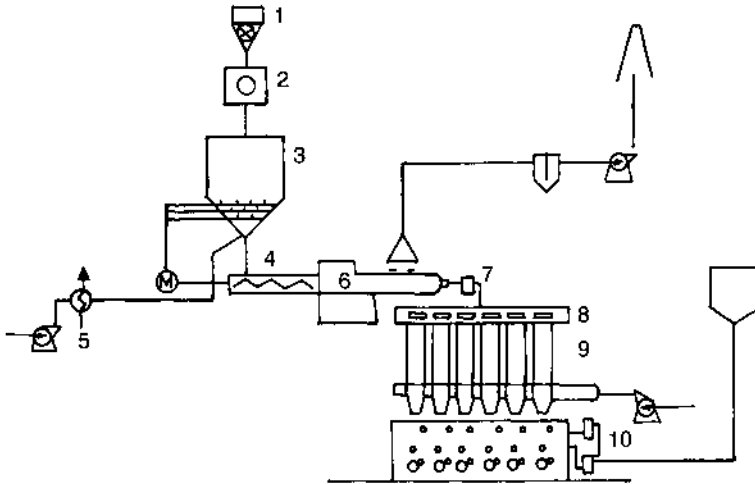
Fig. 20.3 Manufacture of staple fibre. Key: 1 = cutting mill; 2 = cyclone; 3 = feeding silo; 4 = force feeder; 5 = hot air system; 6 = extruder; 7 = filter with pump; 8 = spinbeam; 9 = quenching; 10 = take-up [4, 20].

and fibres into a product of near virgin quality. The material is densified and fed into the extrusion screw. The process of compression and melting occurs gradually at a precisely controlled temperature with minimum heat requirement. The extrusion system does not have a grinder and thus provides a noise-free environment. The best part of the system is the Erema RTF screen changer with two pistons and four large melt filtration screens. The contaminated screens are back-flushed in sequence, one at a time. In the process of cleaning, 75% of the surface remains always active. The screens may be changed manually without stopping the process. When the piston is used to change the screen, the stand-by piston with two screens attached runs the operation. The overall operation is highly efficient and units capable of handling from 600 to 1500 kg waste per hour are under operation.

20.2.3 RECOVERY AS MONOMERS

Fibrous waste has a very low bulk density and is therefore difficult to handle. It is, therefore, compacted before cracking it down to monomers. A method has been described which comprises melt- or pressure-bonding the surface of the fibrous waste to form discrete compressed shapes with increased bulk density. This polyester fibre waste is continuously fed into a wedge-like space between a rotating cylinder and a pair of rollers. The waste is crushed in this space and is extruded from the peripheral surface of the cylinder. It is then cut into chips. Alternatively, the fibrous waste is treated with a counter-current of superheated steam

at 300–400 °C in a tower. The finish oils and other volatile impurities are steam-distilled and the molten hydrated polymer is collected at the bottom of the tower. The melt solidifies and is then ground to the desired particle size.

The chemical processing of the compacted waste can be carried out by three methods: (a) methanolysis, (b) glycolysis, and (c) hydrolysis.

(a) Methanolysis

This process permits post-consumer soft drink bottles to be recycled back into soft drink bottles and other food contact containers. This is the most popular recycling approach at Hoechst Celanese, USA. The waste is treated with methanol under pressure to recover dimethyl terephthalate (DMT) and ethylene glycol (EG). At 185 °C, the reaction is complete in 3 h. The reaction is catalysed by transesterification catalysts such as zinc acetate, manganese acetate, cobalt acetate, lead oxide, etc., of which zinc acetate is the most commonly used [38,39]. Arylsulphonic acids such as benzene sulphonic acid, naphthalene sulphonic acid, p-toluene sulphonic acid, etc., can be used as depolymerization catalysts [40]. The ratio of waste to methanol (by weight) is an important factor affecting the yield of the reaction and is varied from 1:2 to 1:10, the optimum being 1:4 [41].

During subsequent processing of the reaction product, the catalyst pushes the equilibrium towards the formation of diglycol terephthalate and transesterification takes place. It is important to deactivate the catalyst in the reaction mixture before the recovery of DMT. It has been reported that the addition of a phosphorus-containing compound such as phosphoric acid, triphenyl phosphate, trioctyl phosphate, etc., would deactivate the ester interchange catalyst in the reaction mixture and thereby minimize the transesterification reaction [42–44].

A flow diagram of the high pressure methanolysis process is shown in Fig. 20.4 [45]. The polyester waste in powder form is charged into the reactor along with the calculated amounts of methanol and catalyst. The reactants are heated to a temperature of 180–210 °C at 2–4 MPa pressure. Depolymerization of the polyester takes place with the liberation of ethylene glycol. Once the reaction is over, the mass in the reactor is cooled and fed to a crystallizer where the DMT crystallizes out from the solution. The crystals are then melted and distilled to obtain pure DMT suitable for polymerization. The mother liquor from the centrifuge is distilled to recover ethylene glycol and methanol. As continuous feeding of the waste into the high pressure reaction vessel is difficult, this process is carried out in batches. Dimethyl terephthalate is recovered in an improved yield by adding sodium carbonate to the mother liquor and refluxing for 2 h to convert monomethyl hydroxyethyl-terephthalate into DMT [45].
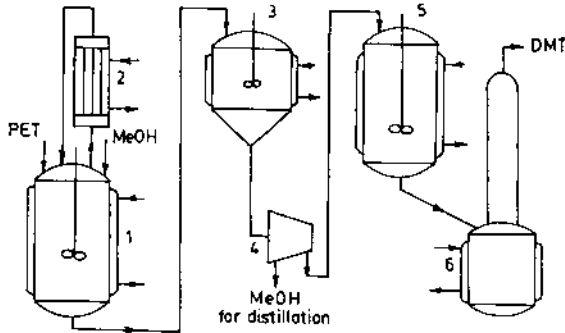
Fig. 20.4 High pressure methanolysis (batch process). Key: 1 = autoclave; 2 = reflux condenser; 3 = crystallizer; 4 = centrifuge; 5 = melter; 6 = distillation column [45].

A schematic diagram of a two-stage continuous process for the recovery of DMT is presented in Fig. 20.5 [41]. The polyester waste is fed into a melter in the temperature range 265–285 °C, and is collected in a reservoir. The reservoir compensates for the variation in the supply of the polyester waste. From the reservoir, the melt flows to the first autoclave fitted with an agitator into which methanol, preheated to the reaction temperature, also flows. The optimum ratio by weight of polyester waste to methanol is 1:4. The autoclave is maintained at a temperature of 190–210 °C and a pressure of 3–4 MPa. The flow rates of the two streams are adjusted so as to provide an average residence time of 7–13 min. The partially reacted mixture then flows through the
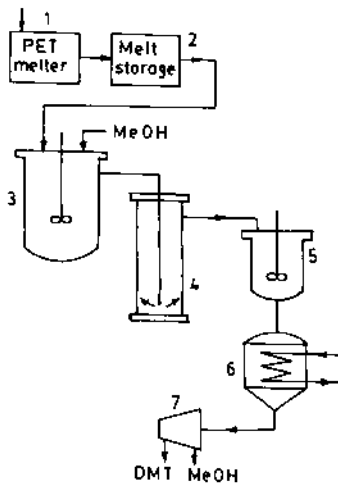
Fig. 20.5 Continuous methanolysis. Key: 1 = melter; 2 = melt storage; 3 = first autoclave; 4 = second autoclave; 5 = mixer; 6 = crystallizer; 7 = centrifuge [41].

immersion tube and enters the bottom of the second autoclave. It slowly ascends in the second autoclave at a rate of 5–10 cm min^{-1} without mixing. Impurities which have a higher relative density than the reaction mixture are collected at the bottom of the autoclave and may be drawn off. The pressure in the second autoclave is as high as that in the first autoclave but the temperature in the second autoclave is slightly lower than that in the first. The reaction product then flows through a relief valve which reduces the pressure to 0.3 MPa and enters into a stirred vessel where it is cooled to about 100 °C. At this temperature, DMT does not precipitate from the solution. The pressure is further released and the solution is cooled to precipitate DMT. The precipitated DMT is removed by filtration. The DMT is washed with methanol and separated by centrifugation. It is further purified by distillation.

In another continuous process of methanolysis [46], the polyester scrap is treated with superheated steam and after the molten polyester solidifies, it is ground in a micro cyclone mill into particles having a mean size of 1 μm. The polyester powder is atomized with an inert gas (nitrogen) and methanol vapours to form an aerosol. This is passed through a reaction tube maintained at 250–300 °C in turbulent flow. The effluent is cooled to remove unreacted materials and DMT is then recovered by further cooling followed by fractional crystallization. The aerosol can be produced by a number of methods, using flowing inert gas or flowing methanol vapours or a mixture. It is necessary to pass the aerosol through the reaction zone in turbulent flow. The ratio of polyester powder to methanol (by weight) is maintained at between 2.5 and 5. It is reported that the depolymerization takes place at a very high rate and further side reactions are practically negligible. It is important to carry out this reaction in an oxygen-free atmosphere.

It has also been suggested that the high pressure methanolysis of the polyester waste be combined with the esterification of TPA with methanol. When polyester waste is added to a mixture of TPA and methanol and the reaction is carried out, both the polyester and TPA are converted to DMT. The TPA used in the commercial production of DMT is in the form of a crude oxidation product of methyl *p*-toluate or *p*-xylene, and hence can be mixed with the polyester waste. The weight of polyester to TPA may range from 20 to 30%.

The colour of the reaction mass of the methanolysis of polyester waste can be substantially reduced by selective catalytic hydrogenation of unsaturated colour-forming impurities. The hydrogenation is carried out at 100–150 °C under pressure of 7.5–15 MPa for 1–6 h, using palladium, platinum or ruthenium on carbon, Kieselguhr or alumina [47].

The so-called EG distillation residue, obtained during the cleavage of PET waste and subsequent recovery, still contains a considerable amount of ethylene glycol along with some diethylene glycol on heating

at high temperature. It has been difficult to recover the remaining EG from the residue, but the distillation in the presence of 0.005–2% (based on glycol) nitrilotrialkanol, such as $N(CH_2CH_2OH)_3$, at 200 °C gives increased recovery of EG of polymerization grade. The use of ammonia in place of nitrilotrialkanol is also effective but the product requires further purification.

(b) Glycolysis

Poly(ethylene terephthalate) dissolves in boiling glycol under atmospheric pressure and more rapidly when heated under pressure. On cooling the solution, oligomers of ethylene terephthalate are obtained. There is an equilibrium between the monomeric ethylene terephthalate, diglycol terephthalate and low oligomers. The equilibrium can be shifted to the left by the addition of glycol to the glycolysis product. On cooling the solution, crystals of diglycol terephthalate (DGT) separate out. The ratio of glycol to polyester waste varies from 1 to 10. The reaction is catalysed by transesterification catalysts such as acetate of manganese, cobalt, sodium, calcium, etc. [48]. The amount of catalyst used is between 0.1 and 1% by weight. Petrov and Aizenshtein [48,49] have investigated the kinetics of glycolysis of polyester waste obtained from the spinneret face and that of stretched monofilaments using zinc acetate as the catalyst. The unstretched waste from the spinneret face is normally amorphous and of low orientation while the stretched monofilaments are crystalline and highly oriented. The kinetic study clearly brings out the influence of crystallinity and orientation on the rate of glycolysis of the above-mentioned two types of polyester waste.

A flow diagram of the glycolysis process is shown in Fig. 20.6 [50]. Polyester waste, along with ethylene glycol and catalyst, are charged
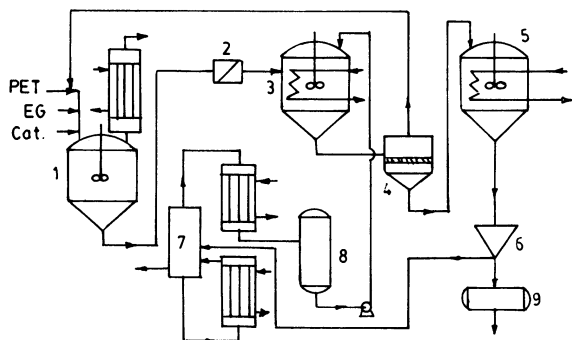
Fig. 20.6 Glycolysis process. Key: 1 = tank with agitator; 2 = filter; 3 = mixing vessel; 4 = oligomer filter; 5 = mixer; 6 = crystallizer; 7 = centrifuge [48].
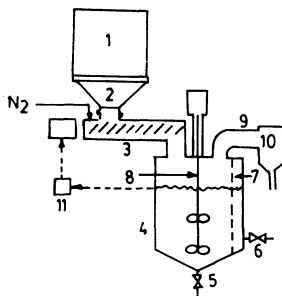
Fig. 20.7 Continuous atmospheric depolymerization of polyester. Key: 1 = storage hopper; 2 = vibrating chamber; 3 = screw feeder; 4 = depolymerizer; 5 = bottom drain; 6 = side outlet; 7 = vertical screen of 10–15 mesh; 8 = agitator; 9 = vapour removal conduit; 10 = spray condenser; 11 = level-control device [51].

into an agitated vessel fitted with a reflux condenser and the contents are heated to the boiling point of the mixture. The reaction product is filtered and fed to a mixing vessel where it is mixed with water. The oligomers are separated by filtration and returned to the reaction vessel. The filtrate containing DGT, EG and water is fed to a crystallizer. The crystals of DGT separate out from the solution and are removed by centrifuging. The cake of DGT is dried and purified by recrystallization from water. Ethylene glycol can be recovered from the filtrate by distillation.

Fibre Industries Inc. [51] has developed a process for continuous atmospheric pressure glycolysis of polyester waste to either DGT or to low molecular weight depolymerizates suitable for direct introduction into a polymerization system. The process is illustrated in Fig. 20.7. The particulate polyester waste and glycol are fed to an agitated depolymerizer. After passing through a fine mesh vertical screen, the depolymerized product is added to the first-stage polymerizer. A level-control device monitors the liquid level in the depolymerizer, adjusting the flow of waste from the feeder accordingly. The agitation prevents oligomer freezing in localized areas upon injection of glycol into the system.

The oligomer from the depolymerizer, preferably filtered, may be directly added to the first-stage polymerizer as a sole feed or may be mixed with virgin monomer in any desired ratio – preferably 1–25 parts reconstituted oligomer to 99–75 parts virgin monomer. The glycolysed product, however, interferes with the normal polycondensation process and the viscosity build-up is poor. Addition of a small quantity of 5-sulphoisophthalic acid sodium salt or its dimethyl ester (0.02–0.15%) along with the glycolysed product helps in polymerization and build-up of viscosity [50–52].

During the glycolysis of polyester waste, diethylene glycol (glycol ether) is formed and the DGT is contaminated with this product. When this DGT is used for polyester manufacture, the glycol ether copolymerizes with DGT to form polyester having a low melting point, reduced wrinkle resistance, and low light fastness. Attempts have been made to minimize the formation of glycol ether during the glycolysis process. It has been reported [53] that the use of sodium acetate dihydrate as a catalyst, the continuous introduction of water into the reaction mixture, and the use of DGT as a solvent for depolymerization, all suppress the formation of glycol ether. The ratio of DGT to polyester waste is about $3:1$. The reaction is carried out at 225–235 °C. The amount of water introduced into the reaction mixture is about 0.01–0.03 times the weight of polyester waste.

The DGT obtained from polyester waste is usually impure, containing colouring impurities, and its purification is very difficult. It can be crystallized from various solvents such as water, ethylene dichloride, tetrachloroethane, 1,2-propyl dichloride or butyl acetate. Activated carbon is used to remove the colouring impurities. However, even after repeated crystallizations the product obtained is not of polymer grade. The distillation of DGT is not possible because it polymerizes at the distillation temperature.

In order to overcome these difficulties, DGT may be converted into DMT which can be easily purified by distillation. The ester interchange is an equilibrium reaction, and the presence of excess glycol in the mixture affects the yield of DMT. Therefore, excess glycol in the glycolysis product must be removed by vacuum distillation. The ester interchange can be catalysed by sodium carbonate, calcium hydroxide, magnesium methoxide, etc. [54]. The amount of methanol needed for the ester interchange reaction is between 1 and 2 times the amount of polyester waste originally taken. It is necessary to maintain the pH of the solution around 10–12 during the process of ester interchange. If the pH of the solution is less than 9, the reaction does not take place.

After the glycolysis of polyester is over, and excess glycol is removed by vacuum distillation, the DGT is added to methanol containing a catalyst and the mixture is heated to a temperature below its boiling point. After a period of 30 min to 1 h, DMT crystallizes out from the solution and is removed by filtration and purified by distillation. If methanol is added to the glycolysis product, 1 or 2 hours are needed for the crystals to appear and they appear suddenly, releasing a great deal of heat and forming blocks. Thus it becomes difficult to remove the crystals. For this reason, the glycolysis product should be added to methanol [51]. Recycled polyester made from glycolysis has a very high quality; in fact, it is almost equivalent to virgin material.

(c) Hydrolysis

Hydrolysis with water

Polyester waste can be hydrolysed with water at 150–250 °C under pressure [55]. The amount of water used is about 2–4 times the weight of waste. The hydrolysis is catalysed by transesterification catalysts such as sodium acetate. The reaction is completed in 4 h at 220 °C and in 1.5 h at 245 °C. The crude terephthalic acid is filtered off from the reaction mixture and dried. The filtrate contains ethylene glycol which may be recovered after concentration. This process is economical; however, the acid requires further purification to remove TiO_2, dyes and other additives present in the waste. The crude terephthalic acid can be purified by converting it into disodium salt, treating the solution with carbon and passing it through ion-exchange resin before acidifying with sulphuric acid to recover pure terephthalic acid.

Hydrolysis with acids

Polyester waste can be hydrolysed with a strong acid such as sulphuric acid, nitric acid and phosphoric acid to produce terephthalic acid in good yield without the use of elevated pressure and temperatures. At low temperatures and low concentrations the reaction is too slow to be practical. However, when sulphuric acid of 87% concentration is used at 60–95 °C, the reaction is complete within several minutes. The mechanism of depolymerization by sulphuric acid is shown in Fig. 20.8. The sulphuric acid reacts with the polyester chain by addition to the carboxylic carbon of the ester linkage. This intermediate compound reacts with water and substitutes hydroxyl groups to re-form sulphuric acid. The presence of two hydroxyl groups on the same carbon being chemically unstable, the product undergoes simultaneous rearrangement with splitting of water. The amount of acid employed is preferably about 1.2 times the weight of the polyester. Concentrated sulphuric acid is taken in an agitated vessel and is heated to 60–65 °C. Polyester scrap is added to the acid and the mixture is thoroughly agitated. Once the dissolution is over, a syrup is obtained. If the polyester is free from pigments or dyes, the syrup liquid can be poured into water to precipitate terephthalic acid (TPA). In most cases, the polyester is contaminated with dyes and pigments, so the syrup is neutralized with alkali. The amount of alkali must be sufficient to neutralize both the mineral acid and the TPA. The deeply coloured solution containing insoluble impurities is filtered and the filtrate, with a pH between 7.5 and 9, is passed through an ion-exchange column to remove the remaining coloured impurities. Alternatively, the solution can be treated with adsorbents like activated charcoal. The clear solution is then acidified with sulphuric
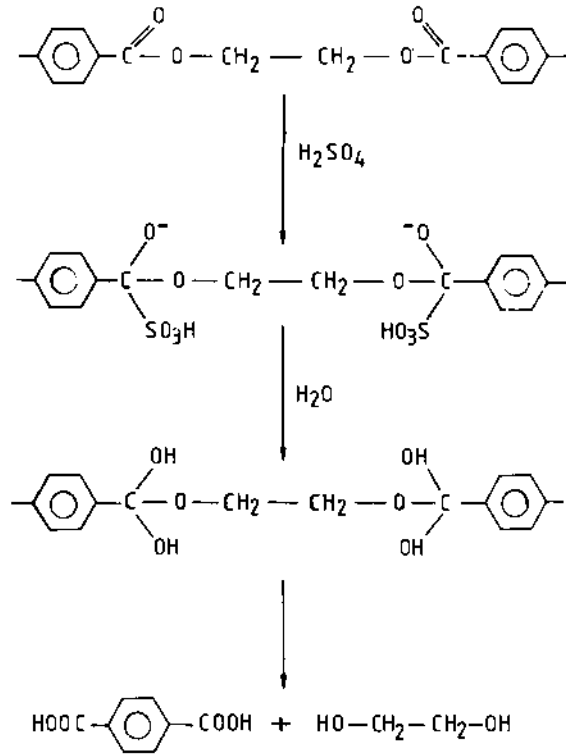
Fig. 20.8 Mechanism of depolymerization of PET by sulphuric acid.

acid to lower the pH to about 2.5–3; the precipitated TPA is then removed by centrifuging. The cake is dried to get TPA of fibre grade.

Glycol is recovered from the mother liquor by extracting it with trichloroethylene. The two phases separate out and the organic phase is distilled to recover the ethylene glycol. The water phase containing sulphuric acid and sodium sulphate may be treated with lime to precipitate calcium sulphate. The precipitate is then removed by filtration and the filtrate containing sodium hydride can be recycled. Alternatively, ethylene glycol can be recovered from the mother liquor by the 'salting out' process. Recently, Yoshioka, Sato and Okuwaki [56] have shown the effect of reaction time on the depolymerization of PET in 7M H_2SO_4 at 150 °C (Fig. 20.9). The depolymerization seems to be accelerated after 3 h of reaction time.

Hydrolysis with caustic soda lye

Caustic soda lye (4–20%) cleaves the ester groups in polyester [57, 58]. The saponification causes a gradual inward peeling or etching of the
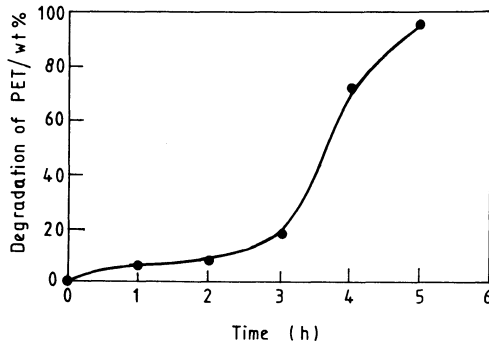
Fig. 20.9 Effect of reaction time on the degradation of PET at 150 °C in 7 M H_2SO_4 [56].

polyester material beginning from the surface. This process is utilized for reducing the linear density of polyester fibres to produce silk-like polyester. The rate of saponification of polyester is reduced after drawing and heat-setting of the fibres. The rate of saponification, however, is enhanced by the presence of amines with a dissociation constant larger than 10^{-5}. The waste is treated with alkali in an autoclave at 210–250 °C at a pressure of 1.4–2 MPa for a period of 3–5 h. The concentration of alkali in the solution is 8–10% by weight. The ratio of alkali to waste in the solution should be 2 : 3. Once the reaction is over, the solution is filtered to remove the insoluble impurities and is acidified with sulphuric or phosphoric acid to liberate TPA [58]. The precipitated TPA is recovered by filtration and is then washed with fresh water and dried. The filtrate is then adjusted to a pH of 7 and is saturated with an inorganic salt such as NaCl or Na_2SO_4 at 45–55 °C. Ethylene glycol separates out as a single phase. The alkali hydrolysis of polyester waste is practicable [59] but its profitability is greatly affected by the higher cost involved in filtration and precipitation operations.

Hydrolysis with ammonium hydroxide

The polyester waste is heated with ammonium hydroxide at 200 °C by direct injection of high pressure steam to yield diammonium terephthalate and EG. The reaction mass is cooled, and then filtered on a rotary drum filter where insoluble impurities are removed. The filtrate is acidified with sulphuric acid to precipitate TPA (99% pure). About 40% of the liquid stream leaving the TPA filter is recycled to the hydrolysing PET reactor; the rest enters the ammonia stripper where lime reacts with ammonium sulphate to form gypsum. On heating, ammonia is driven off to be recycled to the hydrolysing PET reactor. The gypsum
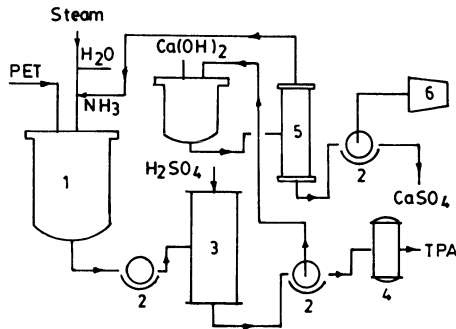
Fig. 20.10 Hydrolysis of polyester waste with ammonia. Key: 1 = PET reactor; 2 = rotary vacuum pump; 3 = acidification reactor; 4 = drier; 5 = ammonia stripper; 6 = ethylene glycol recovery unit.

is removed by filtration. The remaining liquid is distilled to recover EG. The flow diagram is given in Fig. 20.10.

20.2.4 MANUFACTURE OF ALKYD RESINS

By depolymerizing the waste with a polyol and subsequently polycondensing the oligomeric product with a polycarboxylic acid or its anhydride, polyester resins can be produced which have wide industrial applications. Depending on the type of polyol used for depolymerizing the waste and the type of polycarboxylic acid used for subsequent polycondensation, the polyester resin obtained will be either a saturated resin, an alkyd resin or an unsaturated resin (Table 20.3). If the polyol and the polycarboxylic acid used for depolymerization and polycondensation are bifunctional, a saturated resin is obtained [60]. If the polyol or the polycarboxylic acid is trifunctional or polyfunctional, alkyd resin is obtained, but if either of them is unsaturated, an unsaturated resin is obtained [60]. The mole ratio of polyol and polyester waste is controlled between 1 and 2. For producing unsaturated resin, the depolymerized product may be polycondensed with fumaric acid, maleic acid or its anhydride, citraconic or itaconic acid. The unsaturated polyester thus obtained is mixed with at least one vinyl monomer or allyl monomer to give the unsaturated resin. The depolymerization of polyester waste with a polyol is carried out at 200–240 °C in the presence of a catalyst. At higher temperatures, gelation of the product occurs and the product becomes coloured because of the side reactions. Compounds of lead, zinc, magnesium, cadmium, cobalt, antimony, etc., have been tried as catalyst, but they are not very effective. When tetra-alkyl titanate is used as the catalyst, the reaction is three times faster than in the absence of a catalyst. However, this catalyst is insoluble and it has to be

Table 20.3 Alcohols and acids for the preparation of different end products from polyester waste

Alcohols	Acids	End products
Bifunctional	Bifunctional	
Ethylene glycol	Phthalic acid	Saturated resin
1,4-Butanediol	Isophthalic acid	
1,6-Hexanediol	Terephthalic acid	
Neopentyl alcohol	Naphthalene dicarboxylic acid	
Diethylene glycol	Succinic acid	
Propylene glycol	Sebacic acid or its anhydride	
Polyethylene glycol	Adipic acid	
Cyclohexanediol		
Hydrogenated bisphenol		
Trimethylolethane	Benzene–tricarboxylic acid	Alkyd resins
Trimethylolpropane	Benzene–tetracarboxylic acid	
Trimethylolbenzene	(Pyromelletic acid	
	or its anhydride)	
Pentaerythritol		
1,2-Propylene glycol	Fumaric acid	
1,3-Butylene glycol	Maleic acid	
Trimethylene glycol	Citraconic acid	Unsaturated resins
Pentamethylene glycol	Itaconic acid	

dispersed in the reaction mixture. The amount of catalyst needed is about 1 part per 100 parts of polyester waste, which is quite high. It has been reported [61] that the use of soluble catalyst reduces the reaction time substantially even at low concentrations (0.01–0.2% by weight). Such catalysts are listed in Table 20.4. Mixed oxalates and tartrates of titanium and potassium, sodium, ammonium, or calcium are effective catalysts, thereby reducing the depolymerization time to between 1/5 and 1/10 of that required in the absence of a catalyst.

Table 20.4 Soluble catalyst for depolymerization of polyester waste

Catalyst	Amount (wt %)	Temperature (°C)	Time (min)	DP
Potassium	0.05	210	30	1.6
titanyloxalate	0	210	500	Partial depolymerization
	0.04	230	30	1.2
	0	230	30	3.5
	0	230	150	1.8
Ammonium	0.05	220	30	1.8
titanyloxalate	0	220	120	2.4
Potassium titanium	0.04	220	30	1.8
tartarate	0	220	150	2.4

The subsequent polycondensation of the oligomeric product with the polycarboxylic acid is usually carried out at 150–290 °C and an inert gas is purged to remove the by-product. Initially the reaction is carried out at atmospheric pressure or under pressure but, as the reaction proceeds, the pressure is reduced to below 1.3×10^2 Pa. The final polyester resin thus obtained may be coloured, depending upon the quality of the polyester waste. If a colourless product is desired, it can be achieved by the addition of a phosphorus compound such as phosphorus acid, phosphoric acid or triphenyl phosphate during polycondensation. The amount of such compounds varies from 0.001 to 0.05% by weight (calculated as phosphorus atom), based on the weight of the oligomeric product. The polyester resin produced from the waste can be used for the preparation of moulding materials, films, adhesives, coating materials, varnishes, plasticizers, fibre-reinforced plastics, composites, sheets moulding compounds, bulk moulding compounds, premix moulding compounds, etc.

The polyester waste (or the dimethyl terephthalate distillation residue) is reacted with propylene glycol at 185 °C, using zinc acetate as the catalyst. The product is subsequently further reacted with maleic anhydride to get unsaturated resin which is soluble in styrene. The resin is cross-linked in the presence of benzoyl peroxide at 120 °C to give a product having good heat resistance and high impact strength [62]. Such resins can be reinforced with glass fibres to give materials having high chemical resistance [63]. The polyester waste is treated with monoglycerides of linseed oil and the product is polycondensed with phthalic anhydride at 200–225 °C to get alkyd resins having good coating properties. Similar products are used as varnishes either alone or in combination with soluble alkyd resin [64]. Polyester waste, polyethylene oxybenzoate, and a polymer of terephthalic acid, 4-hydroxy benzoic acid, ethylene glycol, and neopentyl glycol are first heated at 230 °C to depolymerize, which on further heating at 270 °C under reduced pressure gave a copolymer [65].

20.3 RECOVERY FROM NYLON 6 WASTE

In the production of nylon 6 materials such as yarn, cord, rod, blocks and moulded articles, a large amount of waste is generated. In a typical industrial situation the waste is obtained at different stages, as shown in Table 20.5. The waste includes polymeric lumps, cables, entangled masses of filaments, drawn fibres with or without finish, rejected bobbins and abnormal batches of polymers besides 10% of the low molecular weight oligomers produced during polymerization. Nylon 6 waste is broadly considered under two categories [66]: (1) liquid waste, which is composed of water extractable from various points of the polymerization

Table 20.5 Waste generated at different stages in the polycaproamide industry

Type of waste	Source	Amount based on total production (%)
Caprolactam	Godowns, transport, charging to melters, loose bags	0–0.2
	Recovery of caprolactam from wash liquor during production	7.5
Polymer	Autoclave, VK tubes, cutters, chips collecting tanks, abnormal batches, during maintenance of equipment	0.8
Platform	Power failure, jet change, maintenance of equipment	2.5
Fibre waste	Stretching, texturing, packing, winding, rewinding, dyeing	DT 1.8 FT 1.17 Coning 1.5 Pkg 0.3
Oligomeric	Recovery of caprolactam from wash liquor	2.5

DT = draw twisting; FT = false twist texturing; Coning = winding of packages; Pkg = at the time of packaging.

and caprolactam recovery processes; and (2) polymer fibre waste (solid waste), which is obtained during polymerization, spinning and take-up, including that obtained during textile processing.

20.3.1 LIQUID WASTE

A conventional process used for the recovery of caprolactam leaves behind 20–25% oligomers together with organic and inorganic compounds as impurities. The residue obtained after the distillation of caprolactam, under reduced pressure, is invariably contaminated with inorganic substances such as MnO_2, $KHSO_4$, K_2SO_4, $NaHPO_4$, Na_2HPO_4 and Na_3PO_4. The major part of the residue contains cyclic and open chain oligomers besides 8–10% of caprolactam [67]. The nature and amount of impurities depends on the process used for the purification and distillation of caprolactam [68].

(a) Recovery of oligomers

The cyclic oligomers have very little solubility in water and dilute solution of caprolactam [69]. They have a tendency to separate out from the extracted liquor during the process of concentration and chemical purification. The cyclic oligomers, in the form of colourless crystals, are found deposited on the walls of the equipment used for the purpose

[70,71]. The presence of 6-aminocaproic acid or its sodium salt cannot be ruled out in the oligomeric waste, especially when sodium hydroxide is used during the process of distillation of caprolactam. A typical composition of distillation residue is:

- open chain oligomers   60–65 parts
- cyclic oligomers   15–20 parts
- inorganic substance   10 parts
- caprolactam   5–10 parts

20.3.2 SOLID WASTE

The solid waste generated in a typical nylon 6 filament plant is around 8–10%. Nylon 6 solid waste can be converted to caprolactam or 6-aminocaproic acid. The regeneration of caprolactam involves two different stages, namely depolymerization of polymeric waste and purification of the recovered products (oligomers and caprolactam). These stages are briefly described.

(a) Depolymerization of nylon 6 waste

The most commonly known process for the recovery of caprolactam is the depolymerization of waste with superheated steam in the presence of inorganic or organic acids such as nitric acid, formic acid, benzoic and hydrochloric acid [69]. The catalytic depolymerization with superheated steam in the presence of phosphoric acid has attained significance on a commercial scale. In a conventional process, superheated steam is passed through a molten mass at 250–300 °C to produce a 10–50% aqueous solution of caprolactam. The solution is subjected to multistage purification by chemical means before concentrating it to a 70% liquor, which is fractionally distilled in the presence of suitable alkali to recover pure caprolactam [70]. The presence of terminating agents, catalysts, antioxidants and additives does not significantly affect the process of depolymerization. The depolymerization of cyclic oligomers and polymer follows the same sequence. However, the cyclic dimer, which is highly stable because of conformational stability of the ring and closely located amide groups, is an exception. The rate of depolymerization of nylon 6 increases considerably with a decrease in molecular weight of the polymer. The caprolactam formed during depolymerization must be efficiently removed from the reaction zone to displace the equilibrium towards the monomer side.

The process of depolymerization of nylon 6 may also be carried out under reduced pressure in the presence of catalysts such as alkali, metallic sodium and phosphoric acid and its salts [71]. In the initial stage, the

depolymerization is very fast, specially in the presence of phosphoric acid; however, the recovered caprolactam is not pure. In the presence of sodium carbonate, however, the problem of dispersing the sodium carbonate into the molten polymer is invariably observed. The process of depolymerization under vacuum in the presence of acid catalysts provides a high yield of caprolactam. In such a process, an adduct of caprolactam with terephthalic acid, isophthalic acid or adipic acid is used to recover 92% of the caprolactam. The yield is further improved in the presence of phosphoric acid.

The depolymerization of cyclic oligomers has been possible by using a heterogeneous catalyst system, wherein oligomers are heated in the presence of metal oxide at 215–260 °C under pressure. However, this process requires frequent regeneration of catalyst which is usually accomplished by heating the catalyst at 400 °C for a period of 8–10 h. Zimmer AG [72] has reported the recovery of caprolactam from nylon 6 carpet (Fig. 20.11).
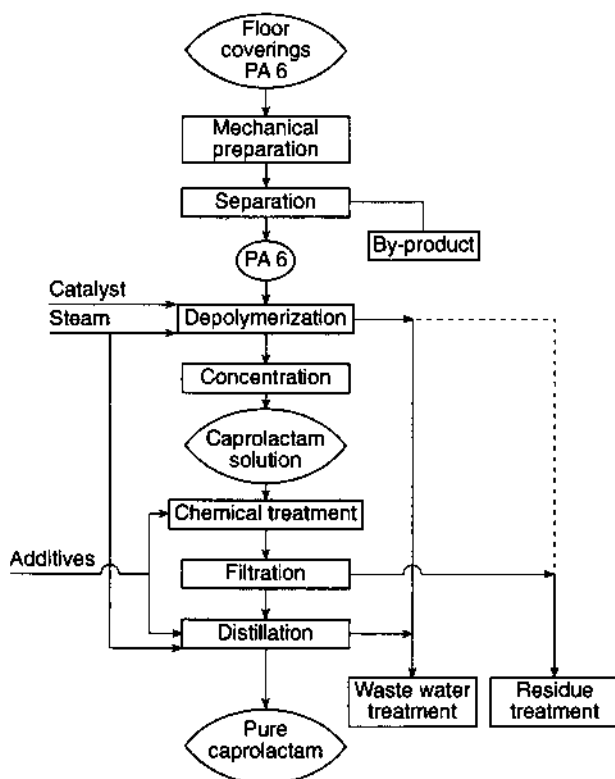
Fig. 20.11 Caprolactam recovery from nylon 6 carpet [72].

(b) Purification of caprolactam

The recovered caprolactam must meet the specification of permanganate number (Pm no.), volatile bases (VB), hazen colour, UV transmittance, solidification point and turbidity, so that it can be used either alone or in combination with virgin caprolactam to produce a polymer of good quality [71]. Aqueous solution of caprolactam obtained after the extraction of nylon 6 polymer is pure enough for reuse without any purification treatment. However, it is usually mixed with cracked liquor obtained by the depolymerization of nylon 6 waste. The liquor requires purification treatment before the recovery of pure caprolactam. In the process of cracking of nylon waste, various acidic impurities are generated due to degradation of polymer and the spin finish present in the system [72]. As the temperature of depolymerization increases, the rate of side reactions is enhanced giving a black tarry oil, volatile bases and other impurities in large amounts.

A number of methods have been reported for purification by recrystallization, solvent extraction and fractional distillation methods. For example, caprolactam can be extracted from its aqueous solution by a membrane solvent extraction process. The solvent extraction technique is being used to purify the aqueous solution of caprolactam, especially the cracked liquor, by extracting the impurity and oily materials. Solvents used for the extraction of impurities must meet some specific requirements. For example, the solvent should be immiscible with water, it should have high dissolving power for impurities and oil, and it should also be a non-solvent for caprolactam, as well as being economical and a non-toxic chemical [73]. A petroleum fraction such as kerosene or diesel is found to meet these specifications and removes all the oily impurities. The solvent enriched with colour and oil impurities is burnt to recover thermal energy. In a conventional process, oil impurities are also removed by separating the layer of such impurities from aqueous solution of caprolactam in a settling tank with high length-to-diameter ratio.

Ion-exchange resins are found to be very effective in the process of purification of aqueous solution of caprolactam [74, 75]. In a conventional process, the aqueous solution of caprolactam is first treated with organic solvents to remove oily impurities followed by treatment with carbon at a temperature of 60–80 °C. The solution obtained after the filtration is sufficiently pure and most suitable for the resin treatment. The presence of oily impurities in the cracked liquor has a tendency to coat the resin surface, thereby making it ineffective. The soiled resins are cleaned by flushing with solvents or emulsifying agent solution in hot water. The cation- and anion-exchange resins are regenerated with a dilute solution of sulphuric acid and an aqueous solution of sodium hydroxide, respectively.

Ion-exchange resins remove all ionic impurities, colloidal and floating particles besides colouring impurities [76]. Alkali metal salts formed in the permanganate oxidative treatment are also removed during ion-exchange treatment. The treatment of aqueous solution of caprolactam with ion-exchange resins helps to facilitate the removal of the distillation residue.

The caprolactam is purified by treating with activated carbon, with the assumption that an equal number of carbonyl and hydroxyl groups are present on the surface of carbon. Thus anionic and cationic impurities are significantly removed on treatment with activated carbon. The removal of carbon by filtration is easier if the solution is acidic in nature. Thus treatment is carried out at pH of 4–6, which is usually maintained by adding a dilute solution of sulphuric acid. Optionally, the carbon residue may be treated with acetone to recover caprolactam from its surface and is treated with preheated steam to reactivate. This process has been used to reduce the concentration of caprolactam in waste water from 500 ppm to 50 ppm.

Impurities in aqueous caprolactam solution are also destroyed by oxidative treatment of liquor with ozone followed by distillation. The process provides a caprolactam with a Pm no. of 3000 compared with a value of zero for the untreated. The caprolactam ozone leaves no ionic impurities and therefore does not burden the ion-exchange resins in the subsequent treatments. The most commonly used oxidizing agents are potassium permanganate, potassium bromide and potassium bromate. The treatment is carried out in neutral medium at 40–60 °C. The strong alkaline or acidic conditions accelerate the oxidation of caprolactam to produce isocyanate, thereby minimizing the yield of recovery. Oxidation reaction is fast above pH 7 because of the rapid saponification of isocyanate, thereby shifting the reaction equilibrium to produce more isocyanate. The incorporation of active carbon containing a substantial amount of Fe^{2+} is highly undesirable since it leads to excessive consumption of potassium permanganate. The caprolactam obtained invariably has an improved Pm no.

In a typical process, $KMnO_4$ treatment is given to the cracked liquor coming out from the depolymerization plant without any pH adjustment [73]. The liquor is usually acidic in nature because of the presence of carry-over phosphoric acid which is a depolymerization catalyst. The $KMnO_4$ treatment is invariably followed by carbon treatment before the process of filtration. The filtered 20–30% aqueous solution of caprolactam is concentrated to 70% and the pH is adjusted to 9–10 by adding sodium hydroxide. The alkaline concentrate of caprolactam is treated with $KMnO_4$ before the removal of water, low boiling impurities and pure caprolactam by the process of distillation under reduced pressure [74]. Since the caprolactam has to be distilled under alkaline conditions, it is not necessary to subject the liquor obtained after second treatment to the process of filtration; it can be taken directly for distillation.

The aqueous solution of caprolactam is reduced by passing hydrogen at 60 °C in the presence of 20% sodium hydroxide and 50% palladium absorbed on carbon [77]. Caprolactam of very high purity having a Pm no. of 18 000 to 21 000 may be obtained by such a process. The treatment with ion-exchange resin before or after the process of hydrogenation or oxidation is always helpful to eliminate most of the impurities and caprolactam with very specific properties may be obtained [78].

Caprolactam is also purified by treating with alkali and formaldehyde solutions followed by fractional distillation to obtain a product free from aromatic amine and other impurities. Its aqueous solution is treated in air in the presence of vanadium pentoxide. The crude caprolactam may also be treated with perboric acid or perborate during or after the process of distillation [79].

(c) Recovery of 6-aminocaproic acid

Nylon 6 waste is subjected to the process of hydrolysis in the presence of aqueous alkali metal hydroxide or acid to produce alkali metal or acid salt of 6-aminocaproic acid (ACA) [80–82]. Being an amino acid, ACA is amphoteric in nature and difficult to prepare in pure form by the process of neutralization. The reaction of nylon waste with dilute hydrochloric acid is very rapid at 90–100 °C and completes within 3–4 h. The reacted mass is poured into water to obtain dilute aqueous solution of ACA salt. The undissolved materials such as pigment, additives and fillers are removed by filtration before passing the acid solution through a strong cation-exchange resin. The cation-exchanger of $-SO_3H^+$ type absorbs ACA and hydrochloric acid is washed away with demineralized water. Washing is extended till the eluent is free of chloride ions. Pure ACA is eluted with ammonium hydroxide to obtain dilute aqueous solution, which is concentrated and allowed to crystallize. A high purity ACA is obtained since most of the ionic impurities are removed over ion-exchange resin and during the process of crystallization. Similarly, nylon 6 waste can be hydrolysed with dilute sulphuric acid. Alternatively, nylon 6 waste can be hydrolysed with sodium hydroxide in the presence of excess of water and the reaction product, i.e. sodium salt of ACA, is converted into pure ACA by using anion-exchange resin [83]. Yet another process to produce ACA is based on the hydrolysis of nylon 6 waste or caprolactam under pressure in the presence of alkali metal hydroxide. In such a process oxalic acid is used to neutralize sodium salt of ACA. The hydrolysis of waste, oligomer and caprolactam may also be carried out at 220 °C in the presence of excess of lime and calcium salt of ACA formed during hydrolysis is converted to pure product by passing carbon dioxide through its aqueous solution, thereby precipitating calcium carbonate as a by-product. This is removed by

filtration to obtain pure ACA. Various processes for reclaiming capro-lactam from nylon 6 waste have been disclosed in patents [83–87].

20.3.3 RE-EXTRUSION OF POLYMERIC WASTE

Remelting or granulation of nylon 6 waste has gained significant impor-tance in the 1990s. Re-extrusion provides the possibility of converting the highly voluminous fibre waste into a compact form to facilitate the process of handling. The process is quite similar to that described for polyester. It has the following advantages:

- the regranulated polymer is free from insoluble impurities when a melt filter is used in the process;
- granules can be produced in standard dimensions and can be added to the virgin material;
- the incorporation of additives such as lubricants, plasticizers and anti-oxidants is possible during extrusion.

The recycled granules are suitable for injection moulding to produce various articles [88,89]. The use of softeners, crystallizers, accelerators and colorants along with the virgin polymer is very common during the course of injection moulding. By using a suitable process, the viscosity of regranulated material can be achieved to a desired level. The viscosity of the material can also be increased by using the process of post-polymer-ization. Detailed analysis of a typical waste is reported in Table 20.6.

The polymer obtained from melting and granulation of waste cannot be spun into a fibre of high quality because the waste suffers thermal degradation besides possessing several impurities in small amounts.

20.3.4 PURIFICATION AND PREPARATION OF POWDER

Nylon 6 waste has a tendency to dissolve in many solvents such as phenol, formic acid, dimethyl formamide and alcoholic solution of calcium

Table 20.6 Typical properties of polycaproamide waste before and after granulation

Properties	Fibre waste		Bristle waste	
	Before	After	Before	After
Viscosity (RV)	2.44	2.32	2.66	2.65
COOH (meq kg^{-1})	56	42	24	30
NH$_2$ (meq kg^{-1})	45	44	–	–
Extractables (%)	2.15	0.9–1.2	1.63	0.3–0.5
Moisture (%)	2.4	1.5	2.5	1.73

chloride or methyl alcohol. For a successful process, it is essential to select a suitable solvent depending upon the end use of the recovered product. A solvent with a high capacity for dissolving the waste with minimum degradation is preferred. The use of methyl alcohol in the presence of chlorides of calcium or manganese has been quite effective. Dimethyl formamide is not used on a commercial scale because of poor solubility of nylon 6 waste in it and problems associated with its recovery process. Formic acid is used in spite of its highly corrosive nature.

The waste is dissolved at elevated temperature and pressure and filtered to remove insoluble materials. The filtrate is pretreated with non-solvent of nylon 6 to obtain the product in powdered form. Technical cresol, i.e. a mixture of *o*-, *p*- and *m*-cresol, is quite an effective solvent for nylon 6 waste because of its less corrosive nature and high dissolution capacity compared with phenol. The dissolved waste can be heated for longer duration at the boiling point of solvent without affecting the quality of the end product. The waste dissolves with a rapid increase in the viscosity of the solution and may be treated with activated carbon and filtered to eliminate coloured impurities. The purified solution is precipitated with a proper solvent preferably in the presence of a dispersing agent to get fine powder of nylon 6 polymer. The solvents are removed by filtration and the residue is washed with alcohol before drying. The powdered polymer can be spun to get fibres/filaments of coarse denier where physico-mechanical properties are not of much importance.

The selection of a particular method used for the recovery of economic value from nylon 6 waste may be decided by keeping in view the various factors listed in Table 20.7.

20.4 NYLON 66 YARN WASTE

Adipic acid and hexamethylene diamine have been recovered from nylon 66 polymer by repeated hydrolysis of the polymer in sulphuric acid, recovering the adipic acid by crystallization after each hydrolysing step and the diamine by distillation after neutralizing the acid.

In this process, the hydrolysis and crystallization of the adipic acid have to be carried out in a step-wise fashion, requiring frequent filtrations and a great deal of time for optimum recovery of the adipic acid. Such a process, therefore, is not efficient for handling high volumes of waste.

The recovery process shown in Fig. 20.12 involves hydrolysing nylon waste with an aqueous mineral acid of 30–70% concentration and feeding the resulting hydrolysate to a crystallization zone. The acid component is crystallized and the crystals removed from the hydrolysate in a continuous process. Calcium hydroxide is added to the resulting mother liquor to substantially neutralize it and to liberate at least 95% (but less

Table 20.7 Methods used for recovery of economic value from polycaproamide

Methods	Process involved	Equipment/ ingredients	Remarks
Recovery of polymer	Mechanical methods	Re-melting	Frequently used; blending up to 30%
		Injection/moulding	Often used; uneven end product
	Solution	H_2SO_4, HCl, $CaCl_2$/MeOH	Used but more expensive Feasible on laboratory scale; cheap but troublesome
		H_2O under pressure	Complicated
		Alcohols under pressure	More efficient than water but expensive
Recovering	Depolymerization to caprolactam	Alkali at high temperature	Complicated
		Water, alkali/acid	Complicated
	Hydrolysis to ACA	Acid hydrolysis	Difficult
		Alkali hydrolysis	Water is preferred
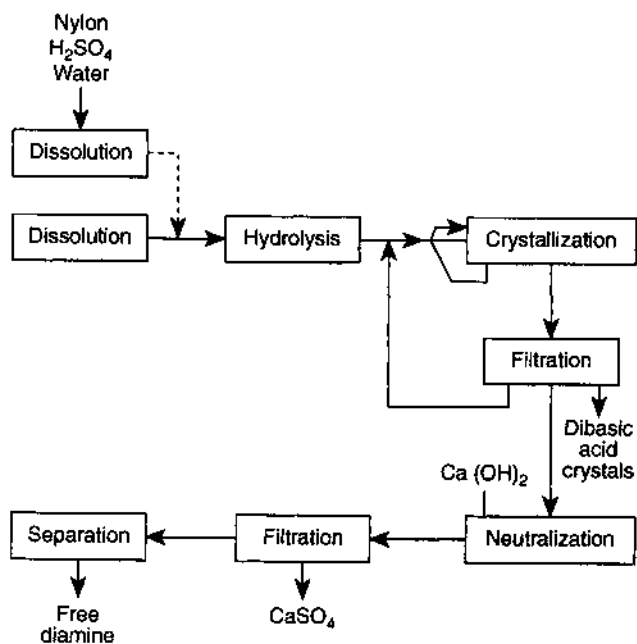
Fig. 20.12 Depolymerization of nylon 66.

than 100%) of the diamine component, separating this from the mother liquor.

To accomplish continuous recovery, adipic acid crystals having an average diameter of about 40–50 nm must be produced. To provide such crystals, the crystallization is effected by continuously introducing the hot hydrolysate containing 10–20% adipic acid into a crystallization vessel, agitating the contents of the vessel while maintaining an average temperature of 20–30 °C, and removing the slurry containing adipic acid crystals from the tank at a rate sufficient to maintain the desired volume in the tank. Usually the hydrolysate from the hydrolysis step contains more than 20% adipic acid. However, optimum crystal size is achieved when the hydrolysate is diluted to 10–20% adipic acid concentration.

The slurry from the crystallization vessel is filtered to remove the adipic acid crystals, the filtrate containing the diamine sulphate being continuously neutralized by the addition of calcium hydroxide. The insoluble calcium sulphate formed in the neutralization reaction is removed by filtration and the diamine is recovered and purified by distillation in the conventional manner. The amount of calcium hydroxide added is preferably such that the diamine sulphate reacts with it to form free diamine; any excess of calcium hydroxide should be avoided to prevent difficulties in filtration.

20.5 POLYPROPYLENE YARN WASTE

The polypropylene (PP) yarn waste is preferably recovered by the same unit where it is being generated. The chopped densified waste is used to produce moulded articles such as toys and household appliances. The addition of waste yarn to an extruder poses a problem and it must be densified in order to eliminate the trapped air and to control the volume. A careful blending of regranulated waste with virgin polymer can produce an end product of required properties.

Warzel [90] developed a process that involves the forced feeding of polypropylene waste into an extruder. In a typical process, a godet roll is used for feeding the yarn at a controlled speed. The wad thus obtained is taken into the pellet mass and is drawn by the extruder screw or by other means before feeding to a moulding machine. The supply of air to the aspirator is shut down in part or totally. In another process, atactic polypropylene waste generated in the order of 5–10% of the total weight of polyropylene is reprocessed at low temperature (−30 °C) before sending it to a crusher to obtain fine particles. The temperature of the atactic PP is raised to room temperature to obtain a free-flowing powder. The reprocressed waste is utilized for various end uses.

Another method used for the disposal of amorphous PP is incineration. Carle and Hann [91] reported a process wherein PP waste is fed to a

catalytic cracking zone together with cycle oil and slurry oil generated in the process to recover propylene. An advantage of this process is that the titanium catalyst residue present in the amorphous polypropylene assists in deactivating the cracking catalyst.

20.5.1   CATALYTIC DEGRADATION OF POLYPROPYLENE WASTE

In a Romanian patent [92], catalytic degradation of polypropylene waste has been disclosed. Mixtures containing 2–25% PP waste with molecular weight 8000–16 000, cooking oil and, optionally, paraffin oil are heated at 400–420 °C and then at 520 °C in the presence of aluminium silicate catalyst, with pore diameter of 120 μm and specific surface area 70–80 m^2 g^{-1}. Processing of PP waste by this method gives 2–4 times the amount of gas as compared with the processes when no catalyst is used.

20.5.2   REUSE OF POLYPROPYLENE OR POLYETHYLENE WASTE AS A SECONDARY SOURCE OF RAW MATERIAL

For certain kinds of waste that neither require extensive cleaning and preparation nor attract prohibitive collection costs, there may be economic advantages if such waste is used to partially replace virgin polymer in the original production cycle.

A number of fibre and tape producers are trying to increase the amount of blended recycled polypropylene they use and even to include polyethylene with virgin polymer during extrusion. Ghosh [93] has investigated the influence of polypropylene waste on the structure–morphology of oriented polypropylene tapes. Horrocks and Richards [94] have also reported the performance of recycled process waste and virgin PP blend geotextile tapes. A significant loss in tape strength occurs when recycled or waste PP is added because of thermo-oxidative degradation. However, useful tapes with acceptable strength can be produced by simultaneous introduction of a specified antioxidant along with the polymer waste.

Hamid and Atiqullah [95] have also recommended the blending technology for the recycling of plastics, particularly polyethylene. However, for the recycling of plastics to succeed, four distinct phases need to be considered, namely collection of post-consumer plastics, sorting out the various plastics from the waste, reclamation (recovery of material into salvaged and usable form), and use of the recovered polymers.

20.5.3   CRITICAL FACTORS IN RECYCLING

In order to recycle PP waste into granules of high quality so that the granules can be blended with virgin material, factors such as change in

melt index, colour, and increase in film gel count are to be kept in mind. The change in melt index during the course of recycling should be as small as possible so that the recycled polymer has melt flow properties very similar to those of the virgin polymer. For better recycling the melt flow index should not increase by more than 10% and 20% in case of extrusion of film and fibre/filament, respectively. The recycled PP should be of light pale colour with a high degree of clarity. The major problem in the recycling of PP is related to the increase in gel particles, which are responsible for the restriction of its use for specific end uses. The gel count range in a film made of virgin PP varies from 20 to 30 while it is not possible to get a reprocessed material with a gel count of less than several hundred. The pale-coloured recycled material is found to have gel counts in the thousands and should not be mixed with virgin resin. The gel formation is attributed to thermal oxidation of the polymer. The presence of traces of water and/or textile lubricants also enhances the gel formation.

20.6 ACRYLIC WASTE

Acrylic waste is generated to the tune of 4–5% based on the production and finished product. The amount of waste depends on the selection of process used to manufacture the acrylic fibre. The waste is composed of polymer powder, dry or wet dope, as-spun or protofibre tow, stretched, crimped and annealed tow and tops, as well as a small amount of staple fibre.

20.6.1 RECOVERY OF MONOMER AND RECYCLING

The polymerization of acrylonitrile to form its copolymers is an equilibrium reaction. Unreacted monomer is separated either from the discharge or the filtrate obtained after polymerization process. The filtrate is subjected to the process of fractional distillation to recover either pure acrylonitrile or a mixture of acrylonitrile with other unreacted monomers. The recovered monomers are fed to the polymerization reactor, ensuring that the concentration of acrylonitrile with respect to other monomers remains constant in the feed. The recycling of unreacted monomers can be efficiently managed in solution polymerization without any intermediate batch storage and analytical computation [96]. In such a process, the polymerization of acrylonitrile with the esters of acrylic acid and/or halogen-containing vinyl monomers is carried out in dimethyl formamide (DMF). The distillate resulting from monomer separation is held to constant minimum amount before adding to the feed to polymerization. The feed is adjusted, on the basis of the amount separated, to obtain a dope of uniform composition. A two-step

distillation process is used to separate the impurities from the DMF and water mixture. The DMF–water mixture is fed into the first column where 70–75% of the water is removed while separating 80% of the solid impurities by crystallization. The discharge of the first column is fed to the second column to eliminate 20–25% of the water and more than 20% of the solid impurities. The heat of vaporization is economically utilized to get pure DMF [97].

A process to remove coloured components from recovered inorganic solvents from the acrylic industry has been developed by Japan Exlan Co. [98]. The process is based on the use of a reverse osmosis membrane whose sodium chloride rejection is in the range of 10–97% under a permeation pressure of 20 kg m^{-2}. The aqueous solution containing sodium thiocyanate is subjected to the process of reverse osmosis to obtain its solution without any appreciable change in the active component.

20.6.2 USE OF SAPONIFIED WASTE

Acrylic waste can be saponified in the presence of sodium hydroxide to produce water-soluble polymer. The kinetics of saponification have been studied in detail [99, 100]. The fibre waste is saponified with an aqueous solution of sodium hydroxide at 80–100 °C over a period of 7–8 h. The transparent light yellow viscous mass is neutralized with dilute sulphuric acid to get a pH of 8–8.5. The reaction mass is diluted and directly used as a printing paste thickener for reactive [101–103] and disperse dyes, and also for pigment printing. The performance of thickener in terms of colour value, brightness, sharpness of prints, and fastness properties justified the potential of saponified acrylic fibre waste as a promising and inexpensive substitute for sodium alginate. The use of saponified material also saves kerosene oil to a significant extent in pigment printing [104, 105].

20.6.3 USE OF CROSSLINKED ACRYLIC FIBRE WASTE

Polyacrylonitrile waste is crosslinked with HCHO, CH$_3$CHO or C$_2$H$_5$CHO to produce water absorbents. A copolymer of acrylonitrile is heated with an aqueous solution of sodium hydroxide and crosslinked with 36% formaldehyde to obtain a water absorbent material. Porous beads are prepared from the solution of polyacrylonitrile waste. The DMF solution of polyacrylonitrile waste containing acid carbonate is added to water or acid and aqueous solvent (but not DMF) to provide porous beads which are coagulated, washed and separated from the reaction mixture. Kravchuk *et al.* [106] have reported the modification of acrylic fibre with 5% of hydrolysed waste. Dyeing behaviour and physico-mechanical properties of acrylic fibres containing hydrolysed

acrylonitrile terpolymer as a dope additive has also been studied [107, 108]. Crosslinked saponified waste has also been used as a thickener for reactive printing [109]. Sizing agents and adhesives have also been developed from acrylic fibre waste.

REFERENCES

1. Sitting, M. (1981) *Organic and Polymer Waste Reclaiming Encyclopedia*, Noyes Data Corpn, NJ.
2. Liedner, J. (1981) *Plastic Waste, Recovery of Economic Value*, Marcel Dekker Inc., New York.
3. Michels, C. (1976) *Textiltechnik*, **26**, 343–346.
4. Wagner, R. (1979) *Fibre Producer*, **7**(2), 34.
5. Milgrom, J. (1982) *Polym. Plast. Technol. Eng.*, **18**(2), 167–178.
6. Darvas, J. (1992) *Int. Polym. Sci. Technol.*, **19**(1), T/40–T/44.
7. Lund, H.F. (1993) *The McGraw Hill Recycling Handbook*, McGraw-Hill, NY, pp. 14.1–14.3.
8. Bassett, J.G. (1992) *Int. Fibre J.*, **7**(5), 28.
9. Webb, J.P. (1992) *Int. Fibre J.*, **7**(5), 8.
10. Wellman, Inc. (1995) *Int. Fibre J.*, **10**(3), 14.
11. Image Industries Inc. (1995) *Int. Fibre J.*, **10**(3), 30.
12. Baker, B. (1995) *Int. Fibre J.*, **10**(3), 34.
13. Keser, D. (1995) *Int. Fibre J.*, **10**(3), 4.
14. Shah, A.H. and Pakurar, T. (1995) *Int. Fibre J.*, **10**(3), 51.
15. Fleissner GmbH (1992) *Canadian Textile J.*, September, pp. 21–22.
16. Engstrom, K. (1992) *Endeavour*, **16**(3), 117–121.
17. Anon. (1993) *Textile Month* (November), pp. 39–40.
18. Stadler, A. (1992) *Kunststoffe*, **82**(10), 911–914 (Germany).
19. Adanur, S. (1995) Textile waste management, in *Wellington Sears Handbook of Industrial Textiles*, Technomic Publishers, Lancaster, PA, USA, p. 713.
20. Sharma, N.D. and Shubhada (1995) *Asian Textile J.*, June, pp. 39–52.
21. Petrov, A.A., Aizenshtein, E.M. and Velikanov, N.N. (1977) *Fibre Chem.*, **9**(6), 584.
22. Petrov, A.A. and Aizenshtein, E.M. (1977) *Khim. Volokna*, **20**(3), 30–35.
23. Petrov, A.A. and Aizenshtein, E.M. (1978) *Khim. Volokna*, **20**(4), 64–68.
24. Sharma, N.D. and Shubhada (1995) *Asian Textile J.*, September, p. 92.
25. Sharma, N.D. and Mathur, V. (1995) *Asian Textile J.*, December, p. 51.
26. Tamazina, V.N., Pleshanova, G.V., Ivanov, Yu.D. and Proshin, S.A. (1976) *Khim. Volokna*, **20**(6), 66–67.
27. Tamazina, V.N., Ozerova, A.I., Alekseeva, G.L. and Sidorov, O.I. (1978) *Khim. Volokna*, **20**(4), 30–31.
28. Regnault, B. and Revol, P. (to Rhone-Poulene Textile, S.A.), German Patent 2 942 248 (30 April 1980).
29. Petrov, A.A., Aizenshtein, E.M. and Tsal, V.A. (to Khim-Volokno Mogilev Industrial Enterprises), USSR Patent 630 267 (30 October 1978).
30. Cobbs, W.H. (Jr) and Stewart, M.J. (to Nordson Corporation), US Patent 4 162 880 (31 July 1979).
31. Clements, J.S. (1980) Recycle polyester bottles, *Plast. Prog. Process*, May, pp. 551–553.

32. Hittel, E.R. and Rennie, F.W. (to E.I. du Pont de Nemours and Co.), US Patent 3 652 466 (28 March 1972).

33. Hornton, J.S. and Glowe, D.E. (to Horizons Inc.), US Patent 3 928 253 (23 December 1975).

34. Miru, S. and Yamamot, N. (to Teijin Ltd), Japanese Patent Kokai Tokkyo Koho 78 94 381 (18 August 1978).

35. Gerber, A.H. and Wainer, E. (to Horizons Research Inc.), German Patent 2 626 358 (23 December 1976).

36. Sidebotham, N.C., Shoemaker, P.D. and Young III, C.W. (to Monsanto Co.), US Patent 4 064 079 (20 December 1977).

37. Sidebotham, N.C., Shoemaker, P.D. and Young III, C.W. (to Monsanto Co.), US Patents 4 003 880 and 4 003 881 (18 January 1977).

38. E.I. du Pont de Nemours and Co., Delaware, British Patent 784 248 (9 October 1957).

39. Dimov, K. and Terlemezyan, E. (1972) *J. Polym. Sci., Part I*, **10**(11), 3133–3141.

40. Vereinigte Glanzstoff Fabriken A.G., British Patent 806 269 (23 December 1958).

41. Grunschke, H., Hammerschick, H. and Naucheim, B. (to Farbwerke Hoechst AG, Meister Locius and Burring), US Patent 3 403 115, Dutch Patent 6 502 050 (24 September 1968).

42. Barkey, K.T., Lefferts, E.B. and May, D.C. (to Eastman Kodak Co.), US Patent 3 488 298 (6 January 1977).

43. Barkey, K.T., Lefferts, E.B. and May, D.C. (to Eastman Kodak Co.), British Patent 1 205 615 (16 September 1970).

44. Currie, R.M., Measamer, S.G. and Miller, D.N. (to E.I. du Pont de Nemours and Co.), US Patent 3 907 868, German Patent 2 506 259 (23 September 1975).

45. Sir Padampat Research Centre, a division of J.K. Synthetics Ltd, Kota, India, British Patent 2 041 916 (8 February 1979).

46. Obernburg, R.L., Gerhard, W. and Leuhaus, C. (to Vereinigte Glenzstoff-Fabriken AG, Germany), US Patent 3 321 510 (23 May 1967).

47. Stevenson, G.M. (to Eastman Kodak Co.), US Patent 3 501 420, German Patent 1 803 929 (1970).

48. Petrov, A.A. and Aizenshtein, E.M. (1979) *Khim. Volokna*, **21**(4), 16–18/*Fiber Chem.*, **11**(4), 277.

49. Petrov, A.A. and Aizenshtein, E.M. (1980) *Khim. Volokna*, **22**(4), 22–23.

50. MacDowell, J.T. and Klusion, N.C. (to E.I. du Pont de Nemours and Co.), US Patent 3 222 299 (7 December 1965).

51. Ostrowski, H.S. (to Fibre Industries Inc.), US Patent 3 884 850, Canadian Patent 960 399 (20 May 1975).

52. Gruntfast, I., Turner, R. and Trenton, N.J. (to Textile Research Institute, Princeton, NJ), US Patent 3 937 675 (10 February 1976).

53. Malik, A. and Most, E.E. (to E.I. du Pont de Nemours and Co.), US Patent 4 078 143 (7 March 1978).

54. Delattre, J., Raynaud, R. and Thomas, C. (to Rhone-Poulene Textile, France), US Patent 4 163 860, German Patent 2 657 044 (7 August 1979).

55. Currie, R.M. and Measamer, S.G. (to E.I. du Pont de Nemours and Co.), US Patent 3 907 868 (23 September 1975).

56. Yoshioka, T., Sato, T. and Okuwaki, A. (1994) *J. Appl. Polym. Sci.*, **52**, 1353.

57. Datye, K.V. and Vaidya, A.A. (1984) *Chemical Processing of Synthetic Fibres and Blends*, John Wiley & Sons, New York, p. 132.
58. Bandyopadhyay, B.N., Pawar, N., Mehta, P.C. and Huddar, S.N. (1991) *Indian J. Fibre Textile Res.*, March, p. 12; Bandyopadhyay, B.N. (1990) *High Performance Textiles*, December, pp. 11–12.
59. Jaroslav, P., Brankovia, C.H. and Black, M. British Patent 8 22 834 (4 November 1959).
60. Datye, K.V. and Vaidya, A.A. (1984) *Chemical Processing of Synthetic Fibres and Blends*, John Wiley & Sons, New York, p. 386; Vaidya, V.R. and Nadkarni, V.M. (1987) *Ind. Eng. Chem. Res.*, **26**, 194.
61. Monsanto Company, British Patent 1 500 856, German Patent 2 607 268 (15 February 1978).
62. Miyake, H., Makimura, O. and Tsuchida, T. (to Toyo Boseki Kabushiki Kaisha, Osaka, Japan), US Patent 3 951 886, German Patent 2 413 717 (20 April 1976).
63. Millivk, W., Newburg, H. and Norman, R. US Patent 4 284 760 (15 August 1981).
64. Duma, V.N., Gaivoronskaya, N.I. and Nazmeyanova, V.N. (1981) *Khim. Promst.*, **1**, 23–26.
65. Rudenko, B.M., Orekov, V.N., Dynin, V.S. and Smirnov, A.A. USSR Patent SU 994 490 (7 February 1983).
66. Sharma, N.D. (1991) *Textile Asia*, June, pp. 66–73.
67. Backer, L. and Kahr, K. (to BASF), German Patent 2 135 085 (1973).
68. Dmirieva, L.A. (1985) *Khim. Volokna*, **4**, 5.
69. BASF AG, German Patent 1 235 924 (1968).
70. Datye, K.V. and Goel, R.H. (1980) *Synthetic Fibres*, **9**, 7.
71. Datye, K.V. (1994) *Synthetic Fibres*, April/June, p. 19.
72. Anon. (1992) *Int. Fiber J.*, October, p. 34.
73. Burel, H.A. and Halaon (to International Inc.), French Patent 1 397 132 (1965).
74. Munayalli, S. and Hans, J. French Patent 1 445 047 (1966).
75. Mikula, F., Petru, K. and Hajas, M. Czech. Patent 120 715 (1968); Petru, K. and Mikula, F. (1974) *Int. Polym. Sci. Tech.*, 1(12), T/57.
76. Vainshtein, G.M. and Ruchinshi, V.R. (1968) *Khim. Prom.*, **48**(8), 572.
77. Mark Borowiak, A. (1972) *Prew. Chem.*, **51**(9), 605–607.
78. Kondo, R. Japanese Patent 71/31 873 (1971).
79. Wagner, K. German (East) Patent 71 112 (1970).
80. Sharma, N.D. and Datye, K.V. (to SPRC), Indian Patent 158 937 (1988).
81. Sharma, N.D. and Datye, K.V. (to SPRC), Indian Patent 158 938 (1987).
82. Sharma, N.D. and Datye, K.V. (to SPRC), Indian Patent 159 116 (1987).
83. Veb Chemiefaserwerk, German Patent 280 102 (1991).
84. Seelig, J. (1994) *Chemiefasern/Textilindustrie*, **44**(1/2), E3–E4.
85. BASF Corp., US Patent 5 169 870 (1993).
86. BASF AG, European Patent 568 882 (1994).
87. BASF Corp., WO 94/06 763 (1994).
88. Polymer Engineering GmbH, German Patent 4 140 857 (1994).
89. Ciba Geigy, European Patent 604 367 (1995).
90. Warzel, F.M. US Patent 4 175 870 (1979).
91. Carle, R.A. and Hann, P.D. US Patent 4 143 086 (1979).
92. Moiceanu, E. and Ocneanu, I. Romanian Patent RO 92 783 (October 1987).

93. Ghosh, S. (1993) *The properties and morphology of oriented polypropylene tapes containing recycled polymers*, PhD thesis, University of Manchester, UK.
94. Horrocks, A.R. and Richards, A.F. (1995) *Textile Res. J.*, **65**, 601–606.
95. Hamid, S.H. and Atiqullah, M. (1995) *J. Macromol. Sci., Rev. Macromol. Chem. Phys.*, **C35**(3), 495–515.
96. Veb Chemiefaserwerk, German Patent 285 788 (1991).
97. Veb Chemiefaserwerk, German Patent 327 326 (1991).
98. Japan Exlan Co. European Patent 556 033 (1994).
99. Bajaj, P., Chavan, R.B. and Manjeet, B. (1985) *J. Macromol. Sci. Chem.*, **A22**(9), 1219.
100. Bajaj, P., Chavan, R.B. and Manjeet, B. (1986) *J. Macromol. Sci. Chem.*, **A23**(3), 335.
101. Bajaj, P., Chavan, R.B. and Manjeet, B. (1984) *Am. Dyestuff Rep.*, **73**(9), 39.
102. Bajaj, P., Chavan, R.B. and Manjeet, B. (1985) *Am. Dyestuff Rep.*, **74**(11), 37.
103. Bhatia, M., Bajaj, P., Chavan, R.B. and Sharma, Y.N. (1987) Proceedings of the ACTI Seminar, Economy, Energy and Environment in Textile Wet Processing, Ahmedabad, p. 72.
104. Bajaj, P., Chavan, R.B. and Manjeet, B. (1987) *Colourage*, June, p. 25.
105. Bajaj, P., Gupta, P.K. and Manjeet, B. (1986) *Colourage*, August, p. 26.
106. Kravchuk, V.M., Zgibneva, Zh.A., Milyavskaya, I.Kh, Ergashev, K.E. and Zakirov, I.Z. (1989) *Khim. Volokna*, **31**(1), 10.
107. Bajaj, P. and Surya Kumari, M. (1989) *Textile Res. J.*, **59**.
108. Bajaj, P. and Surya Kumari, M. (1990) *Textile Res. J.*, **60**, 113.
109. Bajaj, P., Chavan, R.B. and Manjeet, B. (1986) *Textile Res. J.*, **56**, 63.

Index

Page numbers in **bold** refer to figures; page numbers in *italics* refer to tables.